# A METHOD OF PREDICTING CHANGES OF SOIL DRY BULK DENSITY BENEATH AGRICULTURAL WHEELS

PAUL STUART BLACKWELL

Thesis presented for the degree of Doctor of Philosophy
of the University of Edinburgh
Faculty of Science

1979

## DECLARATION

This thesis was composed by the undersigned and is a report of the work undertaken by him on an original line of research.

All sources of information are shown in the text and list of references. All assistance given is indicated and acknowledged.

None of the work reported has been presented for any other degree or professional qualification.

## SUMMARY

Existing research into factors influencing soil compaction and methods of modelling compaction processes have been examined. As the relationships between soil stresses and strains were very complex, simpler interpretations of soil mechanical theories were required for the modelling of soil compaction.

Proposals were made for examination of stress prediction equations developed by Söhne (1953, 1958). Use was also made of the Critical State theory of soil mechanics to describe relationships between soil stresses and strains. Interpretations of this theory were made to derive soil mechanical functions from soil packing state before and after the application of certain levels of stresses. These functions were the apparent virgin compression line ('VCL') and the primary function; soil packing state being expressed as dry bulk density.

Experiments were made to test Söhne's stress prediction equations and identify the 'VCL' and primary function from *in situ* and laboratory measurements of stress and strains of field soils. Stresses were applied to soils in the field by single tractor rear wheels with controlled loads (approx. 1.0 to 2.0 tonnes) and controlled inflation pressures (approx. 80 to 170 kPa). Stresses were measured *in situ* beneath the experimental wheels by deformable spherical transducers. These transducers had been especially developed for this research and could measure combinations of hydrostatic and deviator stresses up to three bar. Two other field experiments, one on a loam, the other on a sandy loam soil, examined the responses of soil of different initial dry bulk

densities (approx. 1.0 to 1.4 $g/cm^3$) at different soil moisture contents (approx. 14 to 28 per cent, w/w) to tractor rear wheels of three different loadings and inflation pressures. Dry bulk density was measured in situ by gamma ray transmission equipment. Measurements of soil strength, soil moisture content and soil moisture tension were also made in situ as well as descriptions of the transverse profiles of the wheel ruts. A soil tank experiment using a sandy loam soil examined relationships between the horizontal projection of the tyre/soil contact area and wheel sinkage. 'Triaxial' equipment was used in the laboratory to measure changes of dry bulk density by different levels of spherical pressure up to five bar. Loose and 'undisturbed' samples of field soils were used at different moisture contents.

Apparent virgin compression lines ('VCL') and primary functions could be derived from the laboratory data. These could be compared to estimations of the 'VCLs' from the field data. The relationships between wheel sinkage and tyre/soil contact area enabled estimation of contact areas by the wheels used in the experiment. These contact areas were used for Söhne's stress prediction equations. Comparison of measured and predicted values of first principal stresses (for soils of different strengths) gave quantitative soil strength limits for the use of each prediction equation. The predicted soil stresses, and measurements of dry bulk density after wheel passage were used to estimate apparent virgin compression lines ('VCL') from the field data.

The differences between the 'VCL' derived from laboratory measurements and those estimated from field data were very similar

to those expected from the differences between the method of stress application used in the field and that used in the laboratory. Therefore it was suggested that the method of identifying 'VCL' had been successful, but further evidence was required for more conclusive proof.

Primary functions were derived from the laboratory tests on loose and 'undisturbed' soil. These were combined with the estimates of apparent virgin compression lines from the field data and Söhne's stress prediction methods to construct a simplified model of soil compaction beneath the centre line of a moving wheel. The applicability of the model was confined to loam or sandy loam soils of cone resistance greater than five bar and initial dry bulk density greater than 1.1 $g/cm^3$ and to beneath the centre line of wheels with less than about five per cent slip or skid.

The compaction model was tested against field measurements of dry bulk density and other soil physical properties, made before and after the passage of suitable agricultural wheels with different loads and contact areas. The field measurements had been made during separate and independent experiments carried out on loam and sandy loam soil. The model was considered a sufficiently accurate method of predicting soil compaction, within the range of applicability mentioned above, since most of the predicted values fell within five per cent of the observed values.

Simulation of soil compaction by the model, and examination of the data from the field experiments suggested that, for soils before ploughing and after sowing operations, increasing tyre/soil contact area and reducing wheel load is the most suitable means of reducing

compaction of 'topsoil'. However reduction of wheel load and not reduction of contact area appeared to reduce compaction of 'subsoil'.

It also seemed that loose soil, below the strength limit of the compaction model, would compact to higher bulk density than firmer soil, with strength above the limit, when run over by the same wheel. Observations of the variation of the apparent virgin compression line with soil moisture content also suggested that soil became more susceptible to compaction at moisture contents above the lower plastic limit, determined by the drop-cone test on soil aggregates similar to those in the field.

ACKNOWLEDGEMENTS

This research was made possible by the availability of considerable assistance and equipment at the Scottish Institute of Agricultural Engineering and the support afforded by an Agricultural Research Council Studentship. I would like to thank all members of the Institute who assisted the project in any way.

In particular it is necessary to mention the following:

- Mr. J.K. Henshall, Mr. N. Turnbull, Mr. J. Kyle, Mr. G. Anderson and Mr. G. West who helped to design, construct, maintain and repair the equipment and machinery;
- Mr. C. Halliday and Mr. A. Cockburn who assisted in the preparation of the sites for the field experiments;
- Mr. J.W. Dickson, Mr. D. Young, Mr. R. Hunter, Mr. P. Johnston, Miss V. Blaire, Miss C. Moar, Mr. K. Johnston, Mr. D. Stobie and Mr. R.G. Clark who were involved in collection of the considerable amount of laboratory and field data;
- Mr. M. Faulds, Miss M. Watson, Mrs. E. McKenzie, Mr. W. Clair, Miss M. Rowlands and Mr. D. Mercer who assisted photographic documentation of the work, processing of the data, preparation of graphs and the design of computer programs;
- Miss F. Kennedy and Mr. M. Januszewicz who helped to obtain and translate various scientific texts;
- Mrs. J. Wood of the Agricultural Research Council, Unit of Statistics who enabled a statistical analysis of much of the data.
- Mr. J. Allison of the Soil Survey of England and Wales for the survey of the experimental site at Lower Terrace field.

- Dr. B.D. Soane, Dr. B. Witney, Professor G.M. Milbourn, the late Professor F.W.H. Elsley, Mr. D.J. Campbell and Dr. J.D. Pidgeon who contributed to much discussion of the research, offered advice and read numerous drafts of the thesis.

- Mrs. I. Meikle for excellent and patient help preparing the typescript.

However, little of this research could have been carried out without the considerable assistance and support I have had from my wife, Glenda.

TABLE OF CONTENTS

## LIST OF FIGURES

## LIST OF TABLES

## INTRODUCTION

Over the past three-quarters of a century there have been fundamental changes in many of the sources of energy used in agriculture. The substitution of animal power by that of fossil fuels has introduced technology often involving large, heavy and powerful machines. Consequently there has been much concern expressed about the effect of such heavy machinery on soil physical conditions (M.A.F.F. (1970), 'Modern farming and the soil'). Despite the increased efficiency of tillage and cultivation equipment for soil loosening, many have noticed the opposite effect caused by the wheels and tracks of vehicles used to carry and operate this equipment. Wheels and tracks of other vehicles and equipment have caused similar concern, especially those carrying the very heavy loads often encountered in agricultural transport. Another change in the sources of energy used in agriculture appears possible during the next half-century. This may offer an opportunity to adopt more rationalised systems of farming, which use a better understanding of soil and plant behaviour than many previous systems. Current agricultural technology could also be improved in the same manner.

The result of wheels and tracks running over the soil is often referred to as soil compaction; any discussion using the term requires a clear definition. Raney and Edminster (1961) considered soil compaction as "the act of moving soil particles closer together". A description more applicable to agricultural soil is given by Soane (1973), "Compaction is a process which causes negative volumetric strain in unsaturated soils. This is

a sufficiently general concept to include many changes of soil physical conditions. However, the term 'packing state' is more precise. This is a generic term for a family of inter-related properties which describe volumetric characteristics of solid gas and liquid phases including bulk density, void ratio, air-filled porosity, specific volume and bulk weight volume. Changes of fluid transmission properties have also been used to describe compaction although they are both principally dependent upon packing state and soil moisture conditions. Therefore a more satisfactory definition of soil compaction would appear to be 'Negative volumetric changes of packing state and associated changes of strength and fluid transmission of unsaturated soil'.

Research into soil compaction has developed over the past forty years, mostly in northerntemperate regions where wet soil conditions combined with intensive agricultural mechanization can cause much soil structural damage. Heavily irrigated tropical areas, growing crops such as sugar cane, have also given rise to compaction problems. Thus a large amount of information is now available about the processes and factors involved in soil compaction. Dunlap and Weber, among others, have recognised that, "As with all scientific study, research into soil compaction aims not just at understanding the process, but also at predicting it", (Dunlap and Weber, 1971). As the understanding of compaction has progressed, so too has the development of prediction methods. However, the rate of development has not always been compatible with that of the simulation of other parts of the agricultural system. Bowen (1975) considered that, "The general utilisation of emergence models, plant growth models and crop models is being

hindered by a lack of a validated vehicular and implement traffic model".

Description of the compaction process in the context of modern agricultural practices enables the more important factors to be identified for use in predictive techniques. The soil compaction process and related causal effects are an interaction of agricultural machinery, soil physical conditions and plant responses. Fig.1 attempts to summarise the causal relationships between those factors of greater importance. Tyre dimensions and forces, as well as the surface soil strength, define the stresses applied at the tyre/soil interface. These interfacial stresses and the strength of the soil beneath the wheel define the extent and magnitude of the stresses applied to each part of the soil. These stresses and the original soil strength control the direction and degree of change of soil structure. The changes are usually increases in strength and bulk density, with corresponding decreases of porosity and number of macropores (negative volumetric change of packing state). Under some conditions, such as extreme wheelslip, the direction of these changes can be reversed. Negative volumetric changes of packing state will usually result in corresponding increases of resistance to tillage, tool wear and resistance to root growth, as well as decreases of the ratesof movement of air and water through the soil.

Under many field conditions these changes will cause a deterioration of the environment for root growth of a crop (Trouse, 1971). However, firming of loose soil by a seed-bed roller may enhance the root growing environment by identical soil physical

Fig.1 CAUSAL RELATIONSHIPS BETWEEN FACTORS INVOLVED IN SOIL COMPACTION

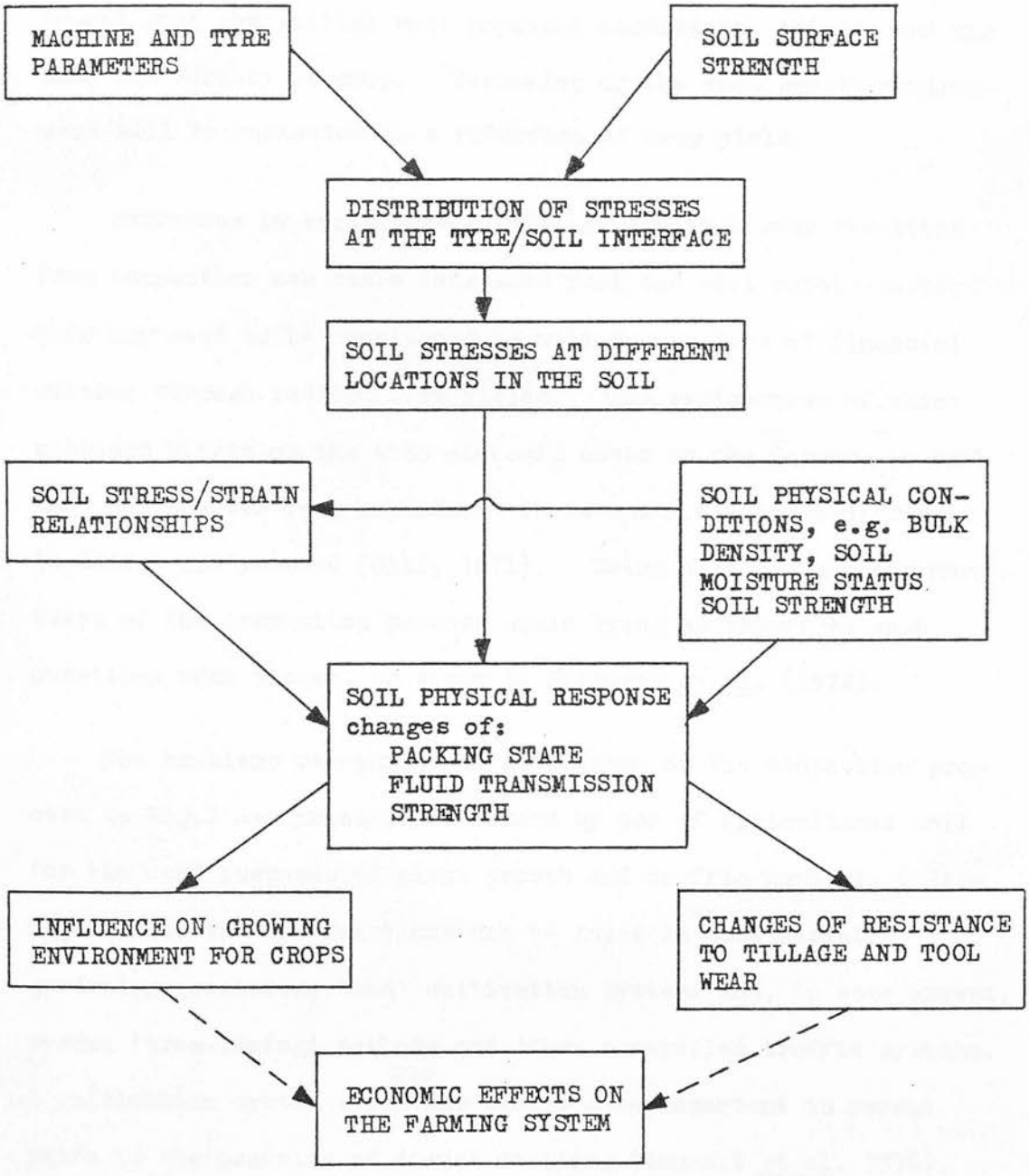

changes. These differences of response can be explained by the parabolic relationships between crop growth and soil physical conditions observed by Håkansson (1973). Whether improvement or deterioration of the root growth environment occurs appears to depend upon the initial soil physical conditions, climate and the kind and variety of crop. Worsening of the root growth environment will be reflected in a reduction of crop yield.

Increases in resistance to tillage and tool wear resulting from compaction can cause increased fuel and tool repair costs; this may need to be considered as well as any loss of financial returns through reduced crop yields. The seriousness of these problems hinges on the true economic costs to the farmer, in both long and shorter term periods. These costs are often difficult to define and measure (Gill, 1971). Being able to quantify more steps of the compaction process would bring an answer to such questions much closer, as shown by Eriksson et al. (1974).

The problems recognised as an outcome of the compaction process in Fig.1 are principally caused by use of agricultural soil for the dual purposes of plant growth and traffic support. Segregation of the two functions can be found in some market gardening practices, 'bed' cultivation systems and, to some extent, recent 'tram-lining' methods and other controlled traffic systems. A cultivation system which has become more important in recent years is the practice of direct drilling (Cannell et al. 1978). Here controlled traffic systems are not often used and compactive effects of traffic are not reversed by periodic primary cultivations. Thus compaction can become cumulative over a number of

seasons. The establishment of a long term 'equilibrium' condition, proposed by Pidgeon and Soane (1978), probably depends on the soil characteristics, traffic systems and wheel systems employed by the vehicles in use. Thus the compaction process may be very important in defining the root growth environment created by such cultivation methods.

The whole soil compaction process and its effects can be divided into a physical part, related to applied stresses and responses of soil physical conditions, and a biological part, related to plant responses to soil physical conditions. This research examines some aspects of the physical part and attempts to develop a method of predicting soil compaction beneath agricultural wheels.

# CHAPTER 1 - REVIEW OF THE LITERATURE

One can distinguish three main groups of materials throughout most research into the mechanical properties of soil. Soil from above approximately half a metre depth, which is usually unsaturated and has high levels of organic matter, is often referred to as 'agricultural soil'. Soil from below approximately half a metre, usually saturated and with low levels of organic matter, is often referred to as 'civil engineering soil'. Other granular materials with similar properties to soil have also been used in some research.

Investigation of the compaction of agricultural soil has examined many different parts of the process; relevant information has also been obtained from research into civil engineering soil and other granular materials with similar properties to soil. Causal relationships between these parts are summarised in Fig.1 and are a guideline for the examination of published research. Existing methods of predicting compaction also require examination. Thus factors of principal influence upon soil compaction can be identified and proposals made for the research of these factors, as well as the development of a suitable method of predicting their effect upon the structure of the soil.

## 1.1 Machinery Characteristics

Soil compaction can result from the passage of agricultural machinery over the soil and principally by the wheels of agricultural vehicles. During the past three-quarters of a century the nature of these vehicles has changed considerably. The trends have mainly been towards larger, heavier and more powerful

vehicles suited to the increasingly large scale of many modern agricultural practices (Soane, 1970). The soil stresses created by the wheels of such vehicles depend partly upon machine parameters and partly upon soil characteristics. The machine parameters are those of vehicle loads, vehicle wheel systems, tyre sizes, construction of tyres and tyre inflation pressures, as well as a component of the tractive or drag forces generated by a driven or towed wheel respectively.

Loads

Tractor units can reach a total weight of six tonnes. Large harvesting equipment can reach 10 tonnes or more, while some recent lime-spreading units weigh 16 tonnes when fully loaded. McKibben (1971) reported a 50 per cent increase of average tractor unit weight over the previous 20 years in Nebraska, U.S.A. More recent statistics of agricultural vehicles in England and Wales (M.A.F.F., 1978) show larger increases of average power and weight of tractors. Vehicles of greater than 60 kW power have increased in number by 18 per cent between 1976 and 1977.

Possible ranges of wheel loadings can be obtained from manufacturers' specifications of agricultural tyres. Table 1a provides examples of ranges of maximum, or 'rated', loadings for tractor and trailer tyres of various sizes for one manufacturer.

TABLE 1a: RANGES OF RECOMMENDED MAXIMUM TYRE LOADS, WITH CORRESPONDING INFLATION PRESSURES AND PLY RATINGS (Size ranges as in Table 2)

| Tyre | Tyre load, kg (ply rating) | Tyre inflation pressure, kPa |
|---|---|---|
| Tractor rear | 1075 (4) to 3190 (10) | 190 to 210 |
| Tractor front | 160 (2) to 885 ( 8) | 175 to 350 |
| Trailer | 1098 (4) to 6340 (12) | 310 to 400 |

These load ranges can be compared to estimates of 'typical' wheel loads by Dwyer (1970) in Table 1b. This reveals tractor wheel loads often to be close to the higher ends of the load ranges, while trailer wheels do not often exploit this very wide range of possible loads.

TABLE 1b: 'TYPICAL VALUES' OF TYRE LOADS (AFTER DWYER, 1970)

| Tyre | Tyre load, kg |
|---|---|
| Tractor rear | 1600 to 2400 |
| Tractor front | 400 to 700 |
| Trailer | 2400 |

Wheel systems

There have often been variations of the conventional four-wheel configurations, twin hubs or twin axles being used to increase the numbers of tyres to six or eight either in tandem or twinned arrangement.

Tyre sizes

Tyre sizes show great variety, from some very small implement tyres to recent innovations of very large 'flotation' tyres (Danfors, 1977). Survey of manufacturers' catalogues reveals the ranges of sizes of agricultural tyres shown in Table 2.

TABLE 2: RANGES OF SIZES OF AGRICULTURAL TYRES

| Tyre | Size code, ins | Overall width, cm | Overall diam, cm |
|---|---|---|---|
| Tractor rear | (11.2/10-28 to 18.4/15-30) | 30 to 44 | 126 to 160 |
| Tractor front | ( 4.0-12 to 7.5-18) | 11 to 21 | 53 to 86 |
| Trailer | ( 4.0-12 to 12-18) | 11 to 53 | 53 to 86 |

These ranges of sizes have been increased by the introduction of low profile tyres, having large section widths ( up to 50 cm) and

similar internal diameters (McLeod et al. 1966; Dwyer, 1970). However, such tyre sizes have become commercially available only recently.

Tyre construction

The structure or ply rating of the tyre indicates the rigidity of the tyre carcass. Common variation of ply rating numbers for agricultural tyres is from 4 to 10. A significant innovation has been the introduction of radial ply tyre construction. Radial ply tyres have been compared to tyres of more conventional cross-ply construction by Thadden (1962); differences of tyre/soil contact area and tyre wall stiffness are most apparent. However, most tyres in common use still appear to be cross-ply rather than radial.

Tyre inflation pressure

Tyre manufacturers' specifications show relationships between tyre load and inflation pressure for various carcass strengths (M.A.F.F., 1976). Examples of such are given in Table 1a. Manufacturers' specifications are not always followed in normal farming practice. It appears that recommended inflation levels may often be exceeded to maintain vehicle stability and reduce tyre damage. Underinflation is also common for combine harvester tyres.

Other forces from the wheel

Tractive forces contributing to the stresses at the tyre/soil interface derive from the reaction of the soil against a component of the tractive torque of the wheel (Vanden Berg et al. 1961). A similar but usually smaller effect can be identified for a towed skidding wheel.

Thus while machinery characteristics are quite variable, they

are well documented (e.g. Inns and Kilgour, 1978) and could be quantified satisfactorily in a general compaction model.

## 1.2 Soil/Tyre Interface Stresses

These stresses can be resolved into two kinds; those normal to the interface (vertical stresses, radial stresses or pressures) and those tangential to it (shearing, slip or skid forces); most research has concentrated upon the former.

The important work of Söhne (1953, 1958) concluded that distributions of vertical stress across tyre/soil interfaces, except for almost rigid soil, were parabolic; largest stresses being found at the tyre centre-line. The power of the parabolic function depended on the firmness or strength of the surface soil. As the soil became softer, the vertical stress would be concentrated more to the centre of the contact area and the distribution became a more accentuated parabola. This process would be accompanied by an increase of the maximum and mean vertical stresses. However, these observations are not firmly based on measurements and assumed a simplified tyre without lugs.

A close examination of the stresses between a smooth, lugless tractor rear tyre and the soil was made by Vanden Berg and Gill (1962). Measurement of vertical contact stresses confirmed Söhne's theories of parabolic distributions on 'soft' and 'firm' soil and very uniform distributions on 'hard' soil; however, a superimposed effect caused by the part of the wheel load carried by the tyre side-walls could also be identified. The effect of such side-wall stresses was most significant for the tyre running on 'hard' soil. Abeels and Declerque (1977) also found influences

of side-wall stresses for very overloaded or under-inflated tyres. Variation of maximum vertical stress with changes of mean vertical stress (computed as the division of wheel load by tyre contact area) was also very similar to what Söhne expected, Vanden Berg and Gill (1962).

Trabbic et al. (1959) examined a tractor rear tyre with lugs. The tyre loads and dimensions were similar to those used by Vanden Berg and Gill (1962). Although only one soil surface strength condition was examined, the distribution of stresses under the tyre carcass surface was close to that observed by Vanden Berg and Gill. Stresses on the faces of the lugs, however, were as much as 50 per cent greater than those expected for a smooth tyre; thus the influence of the lugs appears to be very important to the stress distribution at the tyre/soil interface. There is some evidence that stress variations caused by the lugs may be localised to soil closely adjacent to the tyre/soil interface. Support for the localisation is given by McLeod et al. (1966). Vertical stresses measured 15 cm beneath a lugged tyre were very similar to the inflation pressures of the tyre and corresponded well to the level of vertical stresses expected at the soil/tyre interface of a smooth tyre.

The absolute values of measured stresses in the research described above must be considered cautiously as simple strain-gauged diaphragm stress transducers were used. These devices are sensitive to shearing forces across their faces as well as stresses normal to the diaphragm. Recent improvements in transducer design have been made by Krick (1969) enabling forces on the tyre carcass

surface to be measured in three mutually perpendicular directions.

Revealing work has been done on rigid wheel systems. The rigid body reduces the instrumentation required to measure tangential and radial stresses separately, but is a very simplified concept of conventional pneumatic tyred systems. Early investigations by Hegedus (1965) identified the distribution and scale of radial and tangential stresses. Further work by Onafeko and Reece (1967) and Wong and Reece (1967) has produced the following conclusions about the stresses at the soil/tyre interface of a rigid wheel system:

1) The stress distribution changes according to the amount of slip or skid of the wheel; peak radial stresses move forward of wheel centre for increasing slip and vice versa for skid.
2) The position of the maximum radial stress moves forward of the wheel centre as the strength of the surface soil decreases.
3) Load changes do not produce proportional changes of wheel/soil interface stresses because of alterations of contact area of the wheel.

Work by Kolobov (1966) on pneumatic tyres supports the latter conclusion. Much more work is required on the stress distributions between a moving wheel, with a pneumatic tyre, and the soil to obtain information as satisfactory as that for rigid wheels; examination of the transverse vertical plane as well as the longitudinal one, e.g. Krick (1969), is also valuable.

Reed et al. (1959) have demonstrated that the stress distribution can be altered by using tyres of different sizes and construction ranging from conventional 12.4-36 tractor rear tyres to

'terra' flotation tyres. Effects of radial-ply tyre construction, compared to cross-ply construction, have been examined by Thadden (1962); radial tyres showed greater contact areas when all other factors remained constant. Abeels and Declerque (1977) have shown that the radial construction can alter the distribution of tyre/soil contact stresses in the transverse vertical plane. The stiffer tread of radial tyres seems to generate a stress distribution with two or three peaks of maximum stress. Cross-ply tyres usually have one peak of maximum stress and a more parabolic distribution than that of radial tyres. Relationships between tyre load, inflation pressure and contact pressure for selected tyre sizes have been given by Danfors (1977). Similar figures can be obtained from tyre manufacturers' specifications.

The work described above emphasises that wheel load, tyre inflation pressure, tyre size, tyre construction and soil surface strength are all responsible for controlling the size of the tyre/soil contact area and the distribution of the stresses over it.

## 1.3 Stress Distribution Within the Soil

Stresses applied at the tyre/soil interface are transmitted to other parts of the soil creating a pattern of stresses within the soil. Since the soil stress system is very complex, there has been much discussion about which stresses represent the pattern most satisfactorily.

Any part of the soil beneath or adjacent to a moving wheel can experience a large number of compressive, tensile and shearing forces from a variety of directions. The stress system can be simplified, in isotropic soil with equal strength in all directions,

by considering the three principal stresses (Smith, 1971). Principal stresses can be imagined as acting at right angles to planes in the soil body experiencing no shear stress. Much research has measured only vertical, compressive stresses. This may correspond to the first principal stress, especially beneath the centre of a loaded area. More often other stresses than the vertical compressive stress are required to calculate the principal stresses; this has made much research into soil stress distributions very inadequate.

Computation of all three principal stresses requires simultaneous measurement of stresses in three mutually perpendicular directions, and the associated shear forces. This has been attempted on few occasions, usually by setting three uniaxial strain-gauged diaphragm transducers at right angles to each other, (Reed et al. 1959; Reaves and Cooper, 1960; Ishii and Tokagana, 1972).

However, many of the techniques employed for such stress measurements have suffered from three very severe problems:

1) Interference with the soil: Gill and Reaves (1956) realised that, "a device is not able to measure pressures in the soil due to uncertainties which arise because of arching of the soil when a foreign body is introduced." This 'arching', which tends to transmit stresses around a body instead of through it, is caused by the transducer being less stiff than the surrounding soil; thus the device will tend to detect a stress lower than the real value. Similar soil deformation processes may concentrate soil forces towards

a more rigid body and cause over-registration of stress by a rigid transducer, which is stiffer than the surrounding soil (Frietag, 1971).

2) Unidirectionality: Strain-gauged diaphragms are sensitive to forces from many directions but detect the component of these forces which is perpendicular to the diaphragm plane. Thus if local soil strains cause a rotation of the plane, the direction of detection of the forces also changes. This is mainly evident in soft soils and was overcome by Vanden Berg and Gill (1962) by installing transducers in the tyre carcass instead of the soil; however, this solution is only available at the tyre/soil interface.

3) Installation: Placing a transducer in the soil causes some disturbance which may alter the soil structure and the nature of the stresses being detected. This was partly overcome by Christov (1969) by burying transducers in loose soil which was later packed down to the condition required for the experiment.

Unidirectionality and stiffness problems have largely been avoided by the recent development of omnidirectional sensing rubber ball transducers by Verma and Futral (1975). Unfortunately the interpretation of the signal from these rubber devices is not clear because the same signal can be created from different combinations of stresses on the balls. Satisfactory measurement of soil stresses awaits more suitable devices.

Parallel to research into stress measurement has been the development of methods to predict the distribution of stresses

throughout the soil. Many of these methods have been based on elastic soil responses and originate from Boussinesq (1885). Civil engineering soils have attracted such elastic solutions because of their small plastic responses to stresses, saturated water status, very small strains and isotropic strength. Thus the application of elasticity methods to agricultural soil, which has a much greater plastic response to stresses and must be considered on a smaller scale than civil engineering soil, is probably very limited. A review of a large variety of stress prediction equations derived from the solutions of Boussinesq was made by Poulos and Davies (1974).

Modifications of elasticity solutions were made by Froelich (1934) to account for differences of soil strength and surface stress distributions to predict soil stresses beneath loaded areas. Söhne (1953, 1958) proposed the application of Froelich's equations to agricultural soil beneath loaded tyres. The equations presented by Söhne predicted the vertical stress at different depths beneath a wheel running over soils of different strengths. There has been some comparison of these solutions with measured stresses by Reaves and Cooper (1960). Some correspondence was shown between the predicted and observed levels of stresses, but the measurement techniques suffered from the instrumentation problems already described.

Prediction of horizontal and shearing forces has remained largely unconsidered. However, they are important to compaction behaviour and equations such as those derived by Söhne can be adapted to predict shearing forces from theories of elastic soil

behaviour. Examples of such equations, used in more simplified situations in civil engineering were given by Jurgenson (1934).

Recent research using 'Finite Element' methods has approached the problem of stress prediction from another direction. Instead of the stress/strain behaviour of the soil being assumed, it was measured in laboratory triaxial tests and applied to a Finite Element solution to calculate soil stresses. The Finite Element method employs the mechanical energy balance between work input at the soil surface and work done by the deforming soil. Comparison of Finite Element prediction of soil stresses and prediction from elasticity techniques by Perumpral et al. (1969) showed a close similarity between the two.

## 1.4 Soil Stress/Strain Relationships

A large amount of research has examined the strains of various soils when different combinations and levels of stresses have been applied to them. Laboratory studies have utilised more controlled facilities and more precise measurements, but with the disadvantage of using very simplified, often highly disturbed, soil. Measurements made in the field have been concerned with more realistic soil structural conditions and rates and periods of application of stresses at the disadvantage of using less precise measurements than in the laboratory.

### 1.4.1 Laboratory investigations

Most work has focused on stress/packing state relationships of soil; only recent research by Perdok (1976) has closely examined stress/fluid transmission relationships.

As with the research into soil stress distributions, the research into soil stress/strain relationships has also suffered from the lack of an adequate and commonly accepted theory of the 'effective' soil stress system. Much early work considered vertical stress as the only important force and subjected soil samples to confined, uniaxial stress by a piston in a rigid cylinder, e.g. Day and Holmgren (1952), Reaves and Nichols (1955), Söhne (1958), Kuipers (1959) and Bertilsson (1971). For these uniaxial tests stepwise, or steadily increasing piston loadings have been used. Alternative methods, similar to the 'Proctor' compaction test (Proctor, 1933), where the soil in the cylinder has a series of blows applied to it by a hammer, have been used by Kawano and Holms (1958) and Söhne (1958); the latter referring to the method as 'kneading' compaction.

Koolen (1974) points out that such tests using a rigid cylinder and piston or hammer have inherent problems of cylinder wall/soil friction and variation of stresses across the piston and cylinder surfaces. However, Bertilsson (1971) has demonstrated that errors caused by such problems can be negligible if equipment of an adequately large size is employed.

Improvements of laboratory testing have been made by hydrostatic compression methods, for example McMurdie and Day (1958), Dunlap and Weber (1971) and Davies et al. (1973 b). Here the applied stresses are equal in all directions, hence interpretations of the results are much more simplified than for many uniaxial methods.

Results of both hydrostatic and uniaxial tests (e.g. Bertilsson, 1971) usually show three stages in the process of volumetric soil deformation by compressive stresses. Initially very small elastic deformations occur in response to low levels of stress (between approximately 0 and 0.1 bar). Most of the elastic deformation at this stage is recoverable when stresses return to zero, and the magnitude of the deformation appears to vary little with the initial packing of the soil (i.e. whether dense or loose). Higher levels of stress (between approximately 0.1 bar and 1 to 5 bar) can introduce a second stage of the deformation process. Here strains are more rapid than in the first stage, in response to similar stress increases. More plastic, non-recoverable, strains now occur; in addition to the existing elastic strains. The third stage is an approach to a final, limiting, value of soil deformation, for the system of stresses being applied to the soil. This limit can be considered as the point of minimum air content and maximum structural deformation of the soil. The stages of compression described above correspond well with the observations of Day and Holmgren (1952) and Lambe (1958) of the structural changes occurring during the compression of a soil aggregate.

Thus, for tests on uniform soils in the laboratory using equal values of principal stresses, the nature of the stress/strain relationship is well known, but there has been little systematic quantification of the responses.

The range of possible combinations of applied stresses is considerably extended by methods of 'triaxial' testing (Bishop and Henkel, 1967). Hydrostatic forces can be applied by a pressurised

cell; axial stresses by a loaded piston. When the three principal stresses have different values, Vanden Berg (1966) has shown little correspondence between the largest principal stress and soil strains. However, the comprehensive analyses by Dunlap and Weber (1971) and Bailey (1971) are more satisfactory. They separated the effect of compressive stresses (hydrostatic forces, equal in all directions) from shear stresses (shape changing forces, caused by the deviation of one principal stress from another). Using such ideas, Kumar and Weber (1974) have provided a comprehensive description of the stress/strain relationships of some unsaturated soils. They relate compressive and shear forces to soil strains by a three-dimensional surface in stress/strain space; strains are expressed either as unit volume reduction or bulk density increase. The observations made by Kumar and Weber have begun to correspond with contemporary 'Critical State' theories of stress/strain behaviour derived from saturated civil engineering soils.

Much of the laboratory work described above appears very empirical. However, there are very often common observations of log-linear functions relating soil strain and the logarithm of the stresses. Such log-linear functions have been justified from first principles of particle interaction by Smart (1975).

Roscoe et al. (1958) began the development of the Critical State theory of soil mechanics. The Critical State theory explains the responses of saturated soils to the whole soil stress system by considering more useful resolutions of these stresses than other soil mechanical theories and is able to predict responses

of soils in a wide range of strength conditions. Many previous theories of soil mechanics could only explain behaviour of brittle soils. Critical State theory encompasses very loose 'compressible' soil through to very 'hard', brittle soils. The theory, its development and relevance to agricultural soil are well explained by Kurtay and Reece (1970). In a similar way to Kumar and Weber (1974) the stresses are resolved into a compressive component (spherical pressure) and a shearing component (deviatoric stress). The two stress components are then related to volumetric soil strain by certain functions in three-dimensional stress-strain space. Critical State theory uses changes of specific volume to express soil volumetric strain.

There are some limiting simplifications to the application of Critical State theory to a wide variety of soil conditions and soil stresses. Principal among the simplifications is that of being originally confined to saturated soils. Work by Potamias (1976) has begun to overcome this problem by examining unsaturated remoulded soils. The Critical State theory is also limited to slow deformations, such as expected in civil engineering soils; high stress and strain rates introduce viscous responses of the soil. Chung and Lee (1975) have recently introduced viscous functions into Critical State behaviour. Further limitations are caused by the need to use 'effective' stresses, where effects of pore water stresses are discounted. Pore water stresses in saturated soils are relatively easy to calculate but stresses generated by air/water interfaces in unsaturated soil are more difficult to determine (Fredlund and Morgenstern, 1977). However, despite the current limitations of Critical State theory, it appears to be the

most suitable and comprehensive theory for the stress/strain behaviour of soil.

For any theory of stress/strain relationships of agricultural soil to be sufficiently versatile, a number of factors which influence the relationships must be included, e.g. strain rate, soil moisture conditions, soil organic content and soil texture as well as many other, probably less significant, factors. A large amount of laboratory work has helped to describe the influences of some of these factors on stress/strain relationships of the soil.

The rate of stress application and strain rate have been investigated by Hovanesian and Buchele (1959), Sommer et al. (1972), Dexter and Tanner (1974) and Aref et al. (1974). Exponential curves have been found relating deformation by unit stress and time after stress application. Thus, short periods of stress application, in the order of one second, cause less soil deformation than longer periods. Unfortunately there are problems of measuring high volumetric strain rates of unsaturated soil using laboratory equipment. Unrestricted movement of pore air out of the sample is required during straining. This is very difficult without interfering with the deformation of the sample. Thus, most laboratory investigations have applied high stress rates and short periods of stress to shear well packed soil. This involves very little volume change of the soil compared with other compaction processes.

The influence of soil moisture status (expressed as soil moisture content or soil moisture tension) has received considerable examination due to the extreme influence it has upon soil mechanical behaviour. Most of the laboratory research into stress/strain relationships has examined the effect of soil moisture status, but foremost is work by Stupica (1974), Graecen (1960), Bertilsson (1971) and Söhne (1958). Most of this research has used soil moisture content rather than soil moisture tension, which is more difficult to measure. Results of research into the deformation of soils at different moisture contents for an application of unit stress show characteristic forms for all soils. As soil moisture content increases from lowest levels the amount of soil deformation, expressed as increase of bulk density, increases; this trend is reversed above an 'optimum' moisture content. Beyond the optimum moisture content it appears that the pore volume becomes almost devoid of air and soil deformation is reduced by restricted soil water drainage. The variation in water content of the soil seems to alter the strength of the water films binding the soil particles together, (Baver et al. 1972).

The effect of varying levels of organic matter content on the stress/strain behaviour of soil in confined compression tests has been examined by Free et al. (1947), Soane et al. (1972) and Franklin et al. (1973). Increases of soil organic matter content have generally been found to reduce the deformation of the soil by unit levels of stress. This effect is probably caused by increased levels of organic bonding improving aggregation and increasing soil strength.

Soil textural effects on stress/strain functions have been examined by Chancellor (1971) for a large number of Californian soils, Stupica (1974) for three European soils and Domzal et al. (1975). These results show that sandy loams suffer larger density increases than loams for unit stress at the same moisture content. Domzal et al. (1975) found a rendzina less 'susceptible' to unit stress than a brown earth at the same moisture content. Stupica (1974) also used variations of soil moisture tension and drew similar conclusions to those above. Complementary with this work on real soils Faure and Fies (1972) found that in sand and clay mixtures those with the lowest percentages of clay were most susceptible to compaction. Chancellor (1971) also suggests the clay type has some influence.

Chilingarian and Wolf (1975) emphasise that planar particles can pack together more closely than spherical ones, illustrating the possible effect particle shape may have on soil stress/strain relationships.

Effects of various aspects of soil chemistry on the stress/strain behaviour have also been studied. Pohjakas (1966) found alkaline saline soils 30 per cent to 50 per cent more compactive than the same soil in an unsalinized form. Alternatively, the addition of some chemicals can make soil more resistant to compression. The use of polyelectrolyte on a soil by Taylor and Vomocil (1959) is an example of such improvements of soil strength. Other effects, such as the polar nature of the pore fluid and the species of cation, have also been studied by Chancellor (1971).

The influence of this great variety of factors upon any stress/strain relationships for unsaturated soils is most likely to require the derivation of very empirical solutions; universal functions, derived from first principles of soil behaviour, would need to be extremely comprehensive and complex.

Any research into the mechanical responses of field soils to stresses needs to include the influence of soil structure upon soil strength. This is very difficult, if not impossible using laboratory techniques. Structure is often destroyed and at least disturbed by sampling and handling of the sampled soil in the laboratory. Much of the laboratory work described in this section used remoulded soils, having little relationship to original physical structure of the soil; results of such work have limited application to field soils. More valid conclusions can be drawn from measurements made directly on field soils.. Rates and periods of application of stresses more like those beneath a moving wheel are also required.

### 1.4.2 Field investigations

A large number of experiments have been carried out on field soils examining changes of soil packing state and fluid transmission properties by different combinations and levels of stresses generated by agricultural wheels.

Changes of bulk density and porosity by wheels with different loadings were measured by Fountaine and Payne (1952). Despite the heaviest loading being twice that of the lightest (550 kg) only small bulk density differences were observed in the

upper 4 centimetres. However, the variation may have been disguised by the use of 'undisturbed' core sampling methods. Davies et al.(1973a) used a more detailed experiment examining a larger number of factors. A higher bulk density at 5-10 cm was created by wheels of twice the lowest wheel loading (200 kg) when all other factors remained constant but core sampling methods were also used. Making measurements of soil displacements, proportional to density changes, at different depths in the soil, Danfors (1974) found higher axle loads for the same wheel system were causing larger vertical displacements. However there was some evidence of a 'threshold' stress; little change occurring at 1 m in a dry clay soil until wheel loads reached 6 000 kg. McLeod et al. (1966) provide evidence of greater compaction by tyres using higher inflation pressures (130 kPa) than lower ones (80 kPa) when all other wheel and soil characteristics, other than tyre/soil contact area, remained the same. Fekete (1972) also shows that trailer tyres with higher inflation pressures can cause larger bulk density increases than tractor rear tyres with lower inflation pressures; however changes of tyre dimensions may also influence this.

The observations described above help to support the concepts of 'pressure bulbs' developed by Söhne (1958). The bulbs are defined by isostress lines in the soil. As the wheel load increases and the contact area enlarges and the bulb of stresses can extend deeper and wider into the soil.

Considerable interest has also been shown in the effect of wheel slip on soil packing changes. Weaver and Jamison (1951), Fountaine and Payne (1952) and Vomocil et al. (1958) made measurements after the passages of wheels with different levels of slip. Greater bulk density increases were caused by higher levels of slip, for measurements 'to plough depth', when all other wheel and soil parameters remained constant. Riechmann (1965) found up to 47 per cent greater increases of bulk density at one depth beneath a wheel when the draught force increased from 20 kN to 60 kN. Large horizontal displacements in the top 3 cm of soil beneath a slipping wheel were observed by Khamidov (1960); a drawbar pull of 12 kN caused displacements of one or two centimetres, according to the soil conditions before wheel passage. Work by Raghavan et al. (1977c) revealed that maximum dry bulk density increases under slipping wheels vary according to the level of wheel slip. The increases seem to rise to peak values at about 20 per cent slip, the peak moving according to changes of tyre size, wheel configuration and surface pressure. It is significant that this peak closely corresponds to the same slip level as for maximum traction.

Much of the work described above supports the idea of a combined vertical force (from a loaded wheel) and horizontal force (from a slipping wheel) compacting the soil more than a single vertical force. Reece (1976) explains this as the two forces of reaction and shear at the tyre/soil interface resolving into a larger resultant force; this force will be more effective in compaction than either of the two separate forces.

The initial strength of the soil also influences changes of packing state under agricultural wheels. The effects on soil compaction of the same wheel 'treatment' running over soils of different initial soil strength conditions has been illustrated by Soane et al. (1976); soils with lower original shear strength showed larger bulk density increases.

A small amount of research has examined changes of the fluid transmission characteristics of soils by various stresses applied by agricultural wheels. Vomocil et al. (1958) used large infiltrometers to measure differences in saturated hydraulic conductivity after the passage of various wheels. Largest reductions of infiltrations were observed at highest levels of wheelslip when the original soil moisture content lay between 10 and 18 per cent (w/w); reduction of infiltration also occurred with decrease of forward speed of the wheel. Similar work by Davies et al. (1973a) found a reduction of infiltration rates by a factor of 100 between levels of slip of 0 and 30 per cent. Sack (1962) also reported large reductions of infiltration by tractor wheels running in the furrow during conventional ploughing.

The results described above help to illustrate the effect that shearing and smearing near the soil surface can have on the amount of macropore space and numbers of interconnected pores. A slipping wheel can easily close these very sensitive pore systems and greatly reduce the permeability of the soil. Smaller reductions of infiltration rate have been observed under wheels of different loadings than those using different levels of slip (Davis et al. 1973a).

Few workers have examined the effect of changing rates and periods of stress application but Sitkei and Fekete (1974) show increases of vehicle forward speed will reduce the resultant bulk density of the soil after wheel passage.

In the field work described above comparisons have been made between the effects of a number of different stress treatments to the soil; unfortunately there has not been an intensive systematic study of the soil strains caused by a wide range of stresses. There has also been little attempt to express the soil stresses in more satisfactory ways, such as in the Critical State theory of soil mechanics.

Field evidence of the functions relating soil strains by similar loads at different soil moisture contents is more comprehensive than the fieldwork relating various soil stresses to soil strains. Weaver and Jamison (1951) provided early evidence of the similarity between 'Proctor' curves (Proctor, 1933) and the relationship between soil moisture content and bulk density for different levels of wheel loading. The bulk density/moisture content line for each stress level had the same shape and almost

the same 'optimum' moisture content as the Proctor curve; more detailed results from similar measurements by Raghavan et al. (1976a) provides even more support for the observations of Weaver and Jamison. The shape of the function could be described by empirical mathematical functions and appeared to be influenced by soil textural characteristics in the same way as the Proctor curve. There is also evidence of the importance of soil moisture tension influencing compaction of saturated and near saturated soils (Nagahori and Sato, 1974; Steinhardt, 1974).

Stress/strain relationships are a major cornerstone of the whole compaction process; this is reflected in the amount of research directed towards them. Despite considerable research there have been major shortcomings in the understanding of the nature of the stress/strain functions of soils and in the use of suitable tests to measure these functions, especially for structured field soils and fast rates and short periods of stress application. These shortcomings require solution before soil strains can be satisfactorily predicted.

## 1.5 Strain Distribution within the Soil

In a similar way to the previous classification of soil stresses one can identify two categories of soil strain.

a) Volumetric strain: Only the volume of a soil body changes; its constituent particles move closer together from all directions.

b) Shearing strain: Only the shape of a soil body changes; its volume remains the same. The constituent particles slip over each other.

Reece (1977) illustrated this distinction for a simplified soil system. However, most deformations must be considered as combinations of both categories of strain as particles rearrange themselves in various ways. The work of Day and Holmgren (1952) described this process.

The methods of measuring soil strains can also be classified. At the one extreme there are overall, gross measurements of the total sum of strains; these are measurements of dry bulk density and total porosity. Techniques employed include 'undisturbed' coring and other similar methods of measuring weight and volume of a soil body as described by Freitag (1971). Other direct techniques developed include 'balloon' transducers (Hovanesian and Buchele, 1959). Indirect methods include gamma-ray backscattering, gamma-ray transmission and cone resistance. The latter is handicapped by a poor relationship between cone resistance and bulk density for field soils at one moisture condition. The effects of the structure of undisturbed soil were considered the cause of this problem by Chesness et al. (1970). Gamma-ray transmission techniques were described by Soane (1977) and have been more frequently employed in recent years. These overall measurements of soil strains in terms of dry bulk density and total porosity changes are suitable for measurement of pure volumetric strain, but cannot identify shear strain.

At the other extreme more detailed measurements of strains through the whole soil body have been achieved by soil marking techniques. Chancellor (1966), Reaves and Nichols (1955) and Nichols (1937) used soil markers to measure strains caused by piston sinkage in laboratory soils. Khamidov (1960) used

'X' ray photography of lead balls planted in field soils. Windish & Yong (1970) used the same technique to measure dynamic strains of a laboratory soil beneath a model wheel. Such point marking methods can easily identify shearing strains and often total volumetric strain can also be computed.

Between these extremes of gross packing measurements and detailed observations of soil markers are techniques which attempt to measure uniaxial soil deformations. Selig and Grangaard (1970) and Blackwell and Dexter (1971) have used induction coils to measure uniaxial strains and Spotts and Brown (1975) have developed equipment to install such devices in field soils with minimum interference. Danfors (1974) has also used probes to measure vertical strains in field soils.

Although much information can be obtained from soil marking techniques, they can be very tedious to employ and require considerable disturbance of the soil system before measurements can be made. These problems are reduced by the quicker and less destructive methods of *in situ* soil packing measurements by gamma-ray transmission equipment. More recently proposed double-energy transmission methods (Gardner *et al.* 1972; Soane, 1967) are even less destructive than single energy methods which require simultaneous soil sampling for measurement of soil moisture content. While double-energy methods have been widely used in laboratory conditions, their application in the field presents considerable technical difficulty.

Using the methods described above, a large number of workers

have measured soil deformations caused by wheels running over agricultural soil. The majority of these measurements are of packing state (dry bulk density, total porosity), e.g. Weaver and Jamison (1951); Baganz and Kunath (1963); Fekete et al. (1975); Soane et al. (1976) and Raghavan et al. (1976a). Very little information has been collected using soil markers, most of this being confined to laboratory work.

Results of packing measurements are usually presented as a vertical cross section transverse to the centre line of the wheel rut. On this isolines of equal density or porosity, or density or porosity increases are shown. Occasionally the information is reduced to a single density profile beneath the centre line of the wheel rut. Although a variety of soil and wheel conditions are used to create these results, the following general observations can be made:

1) When 'hard' and 'dry' soil conditions are used, very small density changes are observed, especially for lightly loaded wheels. If the same wheel is run over 'loose' and 'wet' conditions, much greater changes are observed.
2) Very often a zone or zones of maximum density increase are observed.
3) The position of these zones below the tyre/soil interface may vary from next to the surface to various depths below the centre-line of the wheel and to one side.

This last observation has attracted attention from a number of authors, including Chancellor (1966), Reaves and Nichols (1955), Nichols (1937) and Bekker (1961). It is of especial interest

when the position of the zone of maximum density change or 'focus' of compaction occurs below the soil/tyre interface. These authors have proposed theories of failure wedges similar to those described by Hettiaratchi and Reece (1975), beneath the wheel and corresponding wedges to either side. It seems probable that the formation of such wedges is dependent upon the strength of the original soil, as they appear to occur mainly in conditions of low soil strength caused by loose packing conditions, or high soil moisture contents. Evidence of a focus of soil strains by wheel passage is shown in the results of Raghavan et al. (1976a). These foci are mainly observed in soil near saturation, or at high levels of wheel slip.

Further understanding and explanation of these observed soil strain distributions requires more accurate analysis of the responses of field soils to stresses. Methods of predicting these responses when a known set of forces are applied to the soil surface are also needed.

## 1.6 Modelling of Soil Compaction

The development of quantitative models of soil compaction has come from three main fields of study; civil engineering, vehicle mobility and agricultural engineering. Civil engineering has employed large scale models of the behaviour of saturated, inorganic soils in the studies of foundations and the failure of earth structures. Majidzadeh and Guirguis (1973) describe soil compaction models used in the construction of pavements. More recent work using Finite Element methods has provided an analytical framework for modelling the responses of extensive bodies

of soil to various stresses at their boundaries; such techniques are described by Ziencewich (1971). The adaptation of Finite Element methods from mechanical engineering to solve civil engineering and subsequently agricultural engineering soil problems has been a very important step in predicting soil deformation.

Mobility of 'off the road' vehicles is the second field of research contributing to soil compaction models. Vehicle traction studies first developed simple soil sinkage models to account for variations of rolling resistance experienced by a wheel (Bekker, 1956). These methods have been further developed by Kunin and Bushmin (1967) to account for additional soil properties. Analysis has been extended to a moving rigid wheel by Wong and Reece (1967) and Gee-Clough (1976). Recently the analysis of soil stresses and strains generated by a model rigid wheel has been extended, by the Finite Element method, to the whole soil profile by Yong and Fattah (1976). At this point mobility research becomes hybridized with soil compaction models developed from agricultural engineering and civil engineering.

Soil scientists and agricultural engineers have been considering models of soil compaction for a number of years. Early research of Scott-Blair (1938) into surface depression of agricultural soil by loaded areas was intended as an assessment of soil tilth, but can also be interpreted as sinkage measurements for compaction research. More recently wheel sinkage has been related to soil moisture tension by Steinhardt and Trafford (1974). One of the earliest compaction models considering soil deformations other than at the soil surface was that of Nichols

(1937). He considered the soil divided into layers, or zones and examined the stresses and deformations of each zone. A means of approaching a more complete model on this basis was outlined by Bekker (1961) and Söhne (1958). Zonal methods were developed numerically by Chancellor and Schmidt (1961) and Bowen (1975). Good correlation between observed and predicted deformations were often found but zones of maximum deformation were always predicted as nearest the soil surface; real measurements have usually shown greater deformation at some depth below the soil surface. Fekete (1972) attempted to explain the position of these zones of maximum deformation by a model using concepts of failure wedges developed beneath the tyre/soil interface. Unfortunately density changes were considered on a very large scale, all the upper 30 cm depth of soil; this may be too simplified for agricultural purposes. Ishii and Tokugana (1967) have extended ideas of compaction modelling by attempting to predict the number of wheel passes to the resultant dry bulk density.

Zonal methods have also been used in the field by Raghavan et al. (1976b). This work found the observed relationships between surface pressure and resultant dry bulk density at different moisture contents to be similar to the form of the Proctor curve for the same soil. When part of this curve was approximated to a linear function a model relating original soil moisture content to compaction could be constructed. Further developments of this work (Amir et al. 1976 ; Raghavan & McKyes, 1977) created an empirical model relating crop yield to numbers of vehicle passes and soil moisture conditions for a given soil type. Another compaction prediction model extensively developed recently is described by Eriksson

et al.(1974). Much simplified and very empirical stress/strain relationships were used, but some estimate of the economic effects of compaction were achieved.

The use of Finite Element techniques is an improvement of zonal methods. Perumpral et al. (1971) used Finite Element techniques to estimate the compaction of different parts of the topsoil under a moving rigid wheel. The analysis of the soil responses was simplified by ignoring dynamic responses of the soil. Stress-strain relationships were derived from laboratory Triaxial tests and confined to responses to octahedral shearing stress.

Some prediction models developed recently can be considered as hybrids of civil engineering, vehicle mobility and agricultural engineering research. Critical State soil mechanics were incorporated with Finite Element methods by Chung and Lee (1975) to predict soil deformations under a moving rigid wheel. The stresses at the wheel/soil interface were taken from the mobility research of Wong and Reece (1967). Critical State methods were improved by the inclusion of soil viscous and inertial responses; necessary when considering the dynamics of soil behaviour under a moving wheel. Unfortunately, as with much research using Finite Element methods, there was little real data to compare with the predicted soil deformations. The hybrid models represent the current 'state of the art' of more detailed models of soil compaction behaviour. Their predictions of deformation draw attention to dynamic changes under a moving wheel, but when compared to measurements of strain under real, non-rigid wheels there are still some fundamental differences.

Soane et al. (1976), among others, have shown bulk density increases focussing at some depth below the tyre/soil interface while Chung and Lee (1975) and Perumpral (1971) predict maximum changes will be adjacent to the interface. This may be explained by differences between the vertical planes being considered. Most strain measurements for real wheel/soil interactions have been in the vertical plane transverse to the direction of motion whereas all Finite Element studies to date have considered the vertical plane parallel to the direction of motion and through the centre-line of the wheeltrack. Bekker (1961) suggests the width of the wheel will define the form of the soil failure zones below it; this effect may only be able to be identified in the vertical plane transverse to wheel motion. Ziencewich (1971) has applied Finite Element methods to soil strain beneath a rigid footing and identified zones of plastic failure which came to a focus at a point at depth below the footing. This again suggests that application of Finite Element methods to a transverse vertical plane may succeed in modelling real soil strains more closely.

The Finite Element method of predicting stresses and strains of a volume of soil from the stresses and strains of adjacent volumes appears per se to be more similar to the real soil processes of stress and strain than many other prediction techniques.[1] The use of energy balances between external work (boundary stresses and deformations) and internal work (soil stresses and deformations) also seems more realistic than other methods. A more accurate modelling of soil compaction by Finite Element methods requires a better understanding of the stress/strain behaviour of the constituent soil than the approxi-

[1] c.f. Yong et al. (1978)

mations of that behaviour used to date.

Derivation of stress/strain behaviour of soils *in situ*, in field situations is more satisfactory than laboratory techniques; disturbance of the soil before testing can be minimised and the contribution of soil structure be included. Fekete (1972) has approached this on a large scale by relating field measurements of surface sinkage to surface pressure. A more detailed analysis has been made by Fekete *et al.* (1975) using a continuous monitoring of porosity changes under a moving wheel by gamma-ray transmission equipment. The relationships obtained would have been useful if derived in terms of soil stress instead of surface sinkage.

Thus in the past two decades large advances have been made in the development of compaction models. However, many solutions are confined to laboratory situations or are too vague for use with field soils, especially when soil structural effects and fast rates and short periods of stress application need to be included.

## 1.7 Conclusions

The physical process of soil compaction under a wheel is very complex and is dependent upon a large number of variables. Much previous research has examined parts of the system, but few attempts have been made to analyse the whole process.

A constant shortcoming of compaction research has been the lack of a commonly accepted packing state variable to describe the 'compaction' of a soil. For the purposes of this research compaction shall be described as the change of dry bulk density of

soil. This physical property is independent of soil moisture conditions, for soils with insignificant 'shrink and swell' properties. Soil strength and fluid transmission characteristics, both often used to describe compaction , are not independent of soil moisture conditions. Dry bulk density can also be converted to other expressions of packing state, e.g. total porosity, using other simple soil physical measurements. It is more satisfactory to use a non-dimensional quantity to describe packing state. 'Packing density' (Dexter and Tanner, 1971) and 'Materialitet'[1] achieve this by the division of dry bulk density by particle density of the soil solids; unfortunately such non-dimensional terms are not yet in common use.

From the review of previous research the following major factors influencing soil compaction under a wheel have been identified:

1) Soil stresses: These are the forces a volume element of the soil experiences and the rate and period of application of the forces. These in turn are principally dependent upon tyre load, tyre contact area, wheel slip, tyre forward speed and soil strength.

2) The stress/strain functions of the soil: These are the deformation responses of the soil under different combinations of stresses. They are principally determined by the physical constituents of the soil, especially the water phase, and the organisation and structure of these constituents.

---

1 Anderson and Wiklert (1970)

Measurement of these factors for field soils is more satisfactory when soil structural effects and realistic rates and periods of stress application can be included. This demands measurements causing as little soil disturbance as possible, preferably *in situ* methods. Such methods as gamma-ray transmission have been developed and are now in regular use; these can provide quick and accurate measurements of many soil physical conditions. Unfortunately there are currently no adequate means of measuring soil stresses *in situ* .

Techniques have been developed from elasticity theory to predict stresses in soil beneath wheels. However, they have a number of shortcomings.

Understanding of the stress/strain behaviour of field soils has been improved by the Critical State theory of soil mechanics. This theory promises a more coherent explanation of the responses of soil to stresses.

With similar concepts of soil behaviour some soil deformation models, using Finite Element analysis have reached a high level of sophistication, but are limited, as yet, to very simplified field situations.

Working with very simple laboratory equipment in the earlier part of this century, Nichols declared, "Since cohesion can be measured and the relation of pressure to compaction is known and the shear value of soil proportional to pressure, it is possible to determine, with a reasonable degree of accuracy, the amount of force being exerted on different parts of the soil and its direction. It would then seem possible to predict the reaction

of the soil to various force applications." (Nichols, 1937). With the advancement of techniques and understanding since that time, it should now be possible to make predictions for more complex field situations. Unfortunately recent research has fallen short of this aim.

## 1.8 Research Proposals

The need for estimation of soil compaction by agricultural machinery has been restated by the Report of the Ministry of Agriculture, Fisheries and Food, as follows: "The work at present being done to reduce the amount of compaction by machines should continue and methods of cultivation which allow tractors to run on unploughed land should be developed." (M.A.F.F., 1970). Concern for soil structural damage has also been shown by Curtis et al. (1976): "Clearly, knowledge of the load-bearing properties of soil types under different moisture contents is a crucial step in the prevention of structural deterioration."

However, our present 'best estimate' of compaction of field soils is provided by Davies et al. (1972): "Where soil is not saturated and slip is not excessive the depth of the wheel impression is a fairly accurate measure of the amount of compaction taking place."

The following research proposals are now made to improve methods of predicting the compaction of field soils:

1. To appraise the use of prediction methods developed by Söhne (1958) for stresses beneath wheels running over field soils.
2. To appraise the use of Critical State soil mechanics to describe the stress/strain behaviour of field soils.

3. To use 'undisturbed' *in situ* measurements wherever possible to account for the influence of the structure of field soils and realistic rates and periods of stress application.
4. To account for the influence of soil moisture conditions on the stress/strain behaviour of field soils.
5. To develop a method to predict dry bulk density changes of field soils under agricultural wheels from the above measurements.
6. To test the prediction method with suitable field data.
7. To draw conclusions from the experimental results and the performance of the model, which will assist further understanding of compaction processes.

# CHAPTER 2 - DEVELOPMENT OF THE THEORY

In common with many other strain prediction techniques, this method proposes to use knowledge of the stresses experienced by soil under a moving wheel and the stress/strain relationships of the soil to predict the strains the soil undergoes. The theory used to predict the distribution of stresses in the soil is examined in this chapter, as are explanations of soil responses to stresses. The dominating influence of certain soil physical properties upon these responses is also considered.

## 2.1 Predicting Soil Stresses under a Moving Wheel

Concepts of stress distribution under a very slowly moving wheel, developed by Söhne (1958, 1953) from Fröelich (1934), used the following assumptions:

i) Response of the soil to stresses was isotropic, linearly elastic and volumetric soil strains were less than 1 per cent.

ii) The tyre/soil interface was approximated to a flat elipse. The stresses beneath the centre of this elipse were essentially identical to those under the centre of a circular interface of the same area, carrying the same load (see Fig. 2 ).

iii) The distribution of vertical stresses across the tyre/soil interface became more parabolic as the soil became weaker (see Fig.3b).

iv) The isobars of stress under the wheel became more eliptical (the major axis in line with the axis of the contact area) as the soil became weaker. This corresponded to the

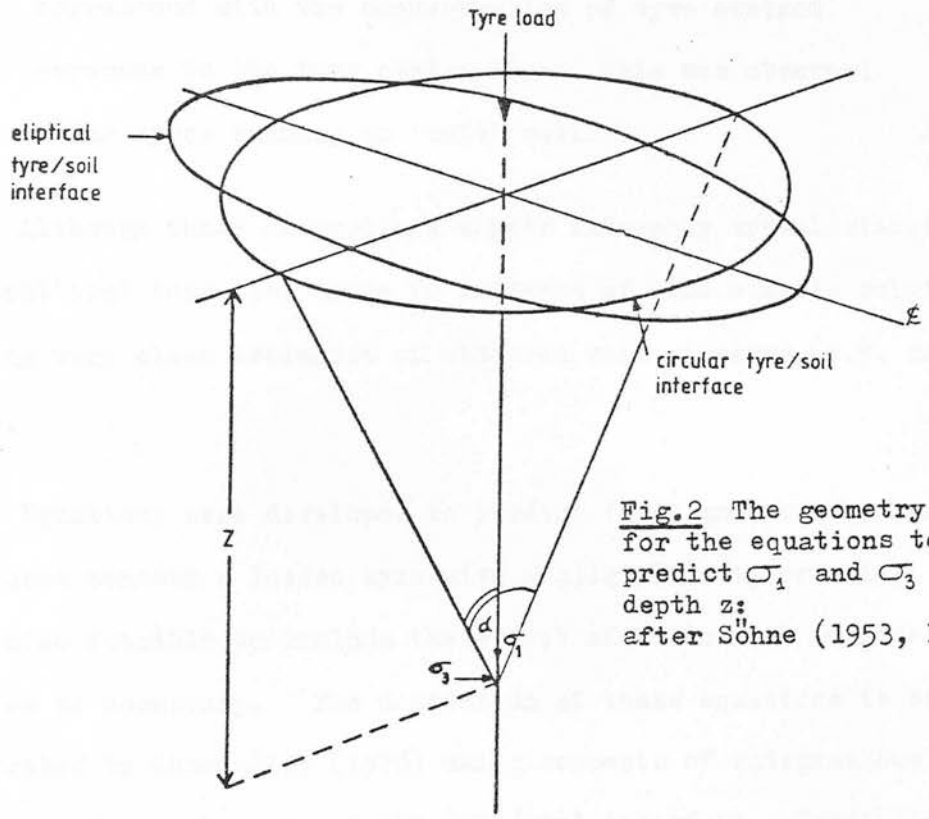


Fig.2 The geometry used for the equations to predict $\sigma_1$ and $\sigma_3$ at depth z: after Söhne (1953, 1958).

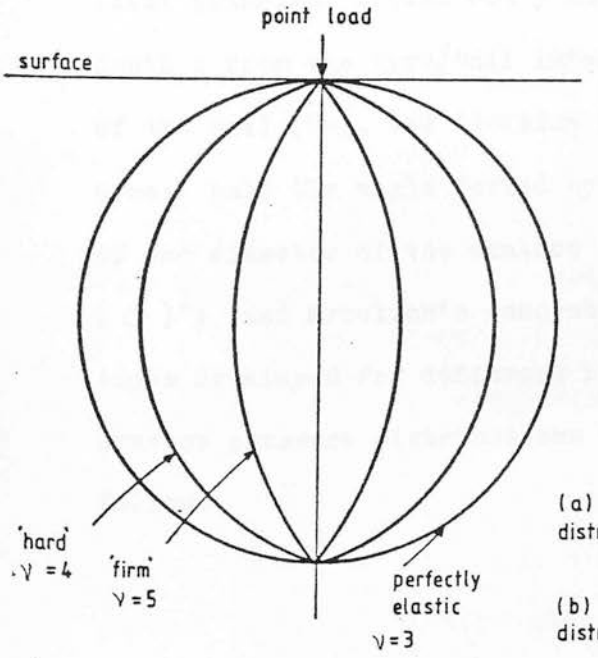


Fig.3a The changes of stress isobars from a point load with variation of the 'concentration' factor ( $\nu$ ); after Froelich (1934).

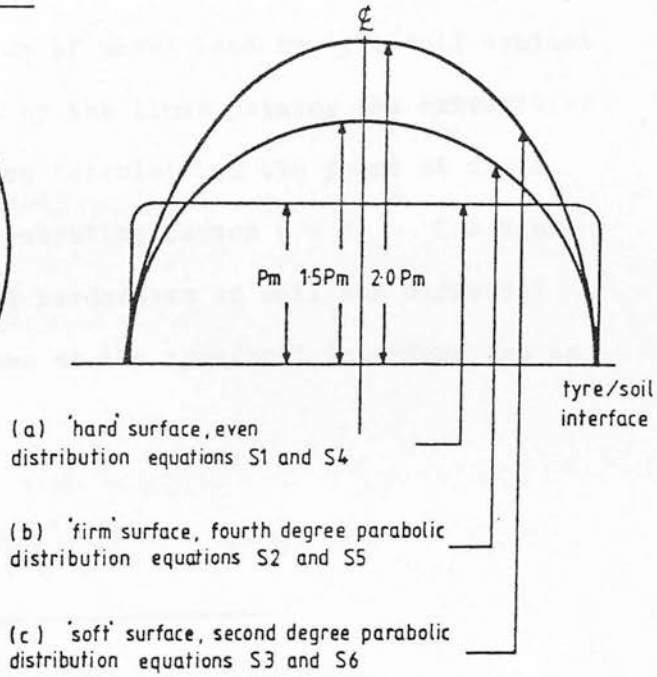


Fig.3b The surface stress distributions for Söhne's equations: Pm = mean surface pressure.

increase of a concentration factor (see Fig.3a). The concentration factor distorted the stress isobars to correspond with the concentration of tyre contact stresses to the tyre centre-line; this was observed under tyres running on 'soft' soil.

Although these assumptions appear extremely unrealistic for agricultural topsoils, there is evidence of such elastic solutions giving very close estimates of observed soil stresses (c.f. section 1.3).

Equations were developed to predict first and third principal stresses beneath a loaded tyre with negligible slip or skid; it was also feasible to include the effect of horizontal surface forces if necessary. The derivation of these equations is broadly described by Chancellor (1976) using concepts of integrations of stresses from sub-areas of the tyre/soil interface. Predictions of first principal stress ($\sigma_1$) and third principal stress ($\sigma_3$) at depth z from the tyre/soil interface use the mean surface pressure of the soil (Pm), the division of wheel load by tyre/soil contact area; half the angle formed by the lines joining the extremities of the diameter of the contact 'circle' and the point at depth ($\alpha$)[1]; and Froelich's concentration factor ($\nu$). The equations developed for different hardnesses of soil and different contact pressure distributions at the tyre/soil interface are as follows:

---

1. See Fig.2.

For first principal stress at depth z

$$\sigma_1 = Pm\ (1 - \cos^4\alpha) \quad (\nu = 4) \ldots \text{S1}$$

$$\sigma_1 = 1.5\ Pm\ (1 - \cos^5\alpha - \cot^4\alpha\ (\tfrac{8}{3} - 5\cos\alpha + \tfrac{10}{3}\cos^3\alpha - \cos^5\alpha)) \quad (\nu = 5) \ldots \text{S2}$$

$$\sigma_1 = 2.0\ Pm\ (1 - \cos^6\alpha - \cot^2\alpha\ (\tfrac{1}{2} - \tfrac{3}{2}\cos^4\alpha + \cos^6\alpha)) \quad (\nu = 6) \ldots \text{S3}$$

For third principal stress at depth z

$$\sigma_3 = {}^{Pm}/_{2}\ (1 - 2\cos^2\alpha + \cos^4\alpha) \quad (\nu = 4) \ldots \text{S4}$$

$$\sigma_3 = {}^{3Pm}/_{4}\ (\tfrac{2}{3} - \tfrac{5}{3}\cos^3\alpha + \cos^5\alpha - \cot^4\alpha\ (5(\cos\alpha)^{-1} - 16 - 5\cos^3\alpha + 15\cos\alpha + \cos^5\alpha)) \quad (\nu = 5) \ldots \text{S5}^1$$

$$\sigma_3 = Pm\ (\cos^6\alpha - \tfrac{3}{2}\cos^4\alpha + \tfrac{1}{2} + \cot^2\alpha\ (\cos^5\alpha - 1 + 3\cos^2\alpha - 3\cos^4\alpha)) \quad (\nu = 6) \ldots \text{S6}^1$$

$\nu$ = Froelich's concentration factor; 4 = 'hard' soil;
5 = 'firm' soil; 6 = 'soft' soil

Estimation of $\sigma_3$ is assisted by assuming a constant value of Poisson's ratio for all depths. This is not done for $\sigma_1$. The surface pressure distributions corresponding to each of the above equations are described in Fig.3b. The distribution becomes more parabolic as the soil becomes weaker. A further equation, $\sigma_1 = Pm\ (1 - \cos^3\alpha)$ is suggested for 'very hard' soil conditions. Inclusion of the effect of horizontal stresses at the soil/tyre interface also requires an assumed value of Poisson's ratio.

Applications of the equations can be made more objective if the soil strength limits for each equation can be quantified. Comparison of predicted and measured values of $\sigma_1$ and $\sigma_3$ in situ and corresponding soil strength measurements would enable this as well as a general assessment of the value of the equations.

1. Derived from Froelich (1934).

Use of the prediction equations requires a measurement of the tyre/soil contact area. This can be directly measured for a stationary tyre, but a moving wheel presents numerous problems. There is evidence that the dynamic and stationary contact areas are not the same (Vanden Berg, 1962) but their differences are proportionally very small. Wheel sinkage is accompanied by an increase of contact area, therefore an empirical relationship was expected between rut depth and contact area; similar to that proposed by Söhne (1958). Such a relationship can assist the estimation of contact area after the passage of a wheel.

## 2.2 Relationships between Stress and Strain

These may be examined using concepts of the Critical State theory of soil mechanics (Roscoe et al. 1958; Schofield and Wroth, (1968); Kurtay and Reece, 1970; Reece, 1976). This is a very coherent theory, able to explain many different soil responses to many different stresses; however, it does not yet incorporate different levels of soil saturation and different rates of strain or different periods of stress application.

Critical State theory simplifies the stresses experienced by a soil body to two components of the effective[1] principal stresses, spherical pressure (P) and deviatoric stress (R). P can be considered as an 'all round' hydrostatic stress while R an axial or shearing stress. The derivation of P and R is explained fully in Kurtay and Reece (1970). Equations relating them to the principal stresses are as follows:

---

1. See section 1.4.1.

$$\text{Spherical pressure } (P) = \frac{\sigma_1 + \sigma_2 + \sigma_3}{\sqrt{3}} \quad . \quad . \quad . \quad (1)$$

$$\text{Deviatoric stress } (R) = \frac{1}{\sqrt{3}} ((\sigma_1 - \sigma_2)^2 + (\sigma_2 - \sigma_3)^2 + (\sigma_3 - \sigma_1)^2)^{1/2} \quad . \quad . \quad . \quad (2)$$

($\sigma_1$, $\sigma_2$ and $\sigma_3$ are the major, intermediate and minor principal stresses respectively.)

Critical State concepts are restricted to isotropic soil conditions which may prevent their application to well structured field soils with different responses to the same stress applied in different directions.

The theory uses a similar simplification to those used for stresses to explain soil strains in terms of volumetric strain and shear strain (Kurtay and Reece, 1970). Dry bulk density is only influenced by volume strain; shear strain is only a change of shape, not of volume. Volumetric strain is expressed as changes of specific volume of soil. Specific volume (v) is the volume of soil occupied by a unit volume of soil solids, i.e. $v = 1 + e$, where e is the void ratio of the soil.

Critical State soil mechanics uses spherical pressure, deviatoric stress and specific volume in three dimensional relationships between soil stresses and strains. The main features of the P, R, v relationships are shown in Fig.4a. The virgin compression line (VCL) and the 'critical state line' (CSL) lie on the curved state boundary surface in P, R, v space. The relationships can be simplified by using logarithmic scales for P and R; then the VCL and CSL become linear and their projections onto the v, ln P plane (Fig.4b) are parallel.

To interpret Critical State theory in terms of dry bulk density (Dbd) the measurement of soil packing must be converted from specific volume to Dbd as follows:

$$v = 1 + e; \quad \therefore v = 1 + \frac{Vv}{Vs}$$ (where Vv = volume of soil voids and Vs = volume of soil solids)

$$\therefore v = \frac{Vs + Vv}{Vs}$$

for unit mass of soil solids $Dbd = \frac{1}{Vv + Vs}$ and

$$\text{particle density } (\rho) = \frac{1}{Vs}$$

$$\therefore v = \frac{\rho}{Dbd} \quad \text{or} \quad \frac{1}{v} = \frac{Dbd}{\rho} \quad [1] \qquad (5)$$

for any one soil $\rho$ is a constant and $Dbd \propto \frac{1}{v}$.

Using this conversion P, R, v can be converted into P, R, Dbd space as in Fig.5.[2]

---

1 Referred to by Dexter and Tanner (1971) as 'packing density' and by Anderson and Wiklet (1970) as 'Materialitet'.

2 ln of P and R are omitted here and subsequently from the text for the sake of convenience.

Fig.4a The main features of Critical State theory. The relationship between spherical pressure (P), deviatoric stress (R) and specific volume (v); after Kurtay and Reece (1970).

Fig.4b Projections of the virgin compression line and critical state line onto the plane relating specific volume (v) to the logarithm of spherical pressure (P).

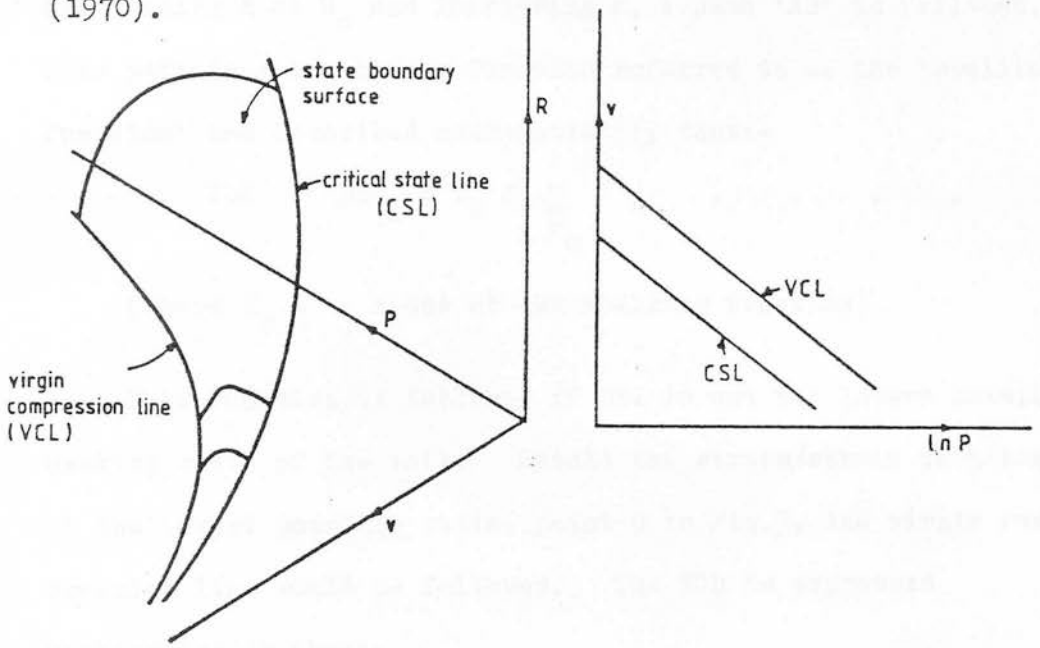


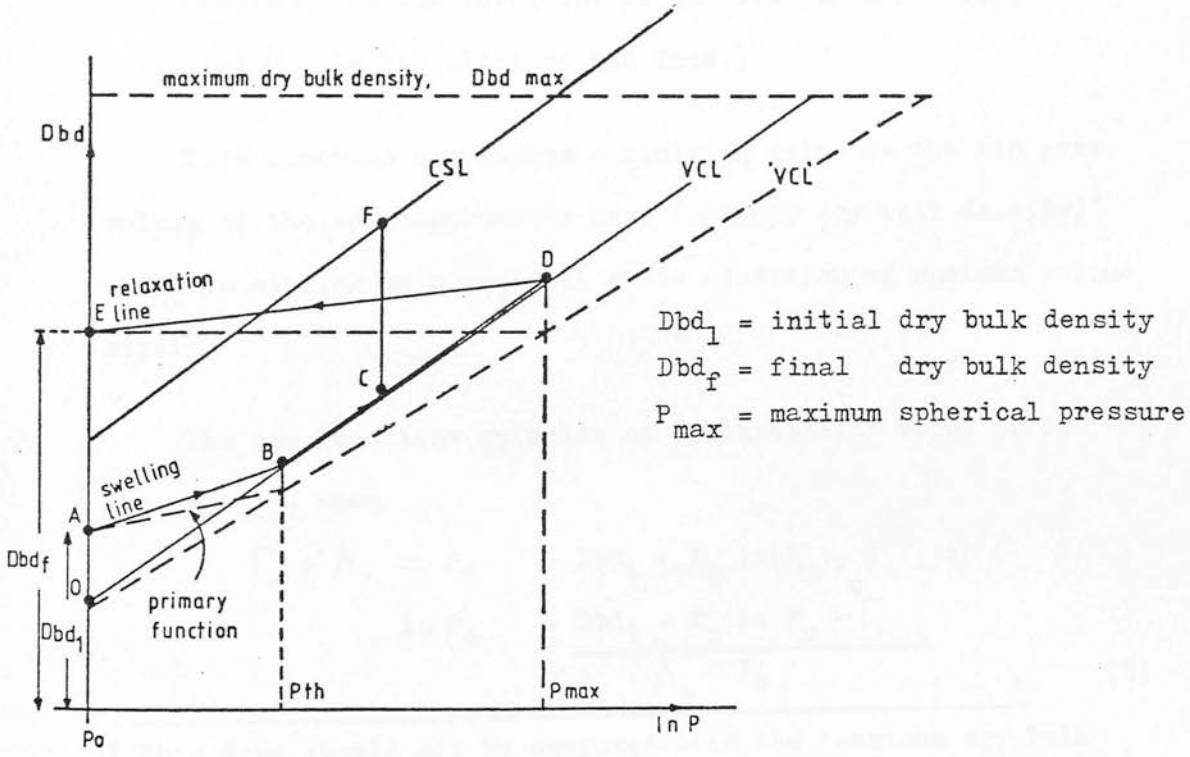


Fig.5 Relationships between dry bulk density (Dbd) and the logarithm of spherical pressure (P). The derivation of the apparent virgin compression line ('VCL'), the primary function and 'threshold' spherical pressure (Pth).

The expected stress/strain path in P, R, Dbd space can then be examined as in Fig.5. At point 'A' P, R and Dbd have values $P_o$, $R_o$ and $Dbd_1$ respectively, where $P_o$ and $R_o$ are very low values. Maintaining R at $R_o$ and increasing P, a path 'AB' is followed. This path is a log-linear function referred to as the 'swelling function' and described mathematically thus:-

$$Dbd = Dbd_1 + K_s \ln \frac{P}{P_o} \quad . \quad . \quad . \quad . \quad . \quad (6)$$

(where $K_s$ = slope of the swelling function)

This function is followed if Dbd is not the lowest possible packing state of the soil. Should the stress/strain path begin at the lowest possible state, point 0 in Fig.5, the virgin compression line would be followed. The VCL is expressed mathematically thus:-

$$Dbd = \Gamma_v + \lambda_v \ln P \quad . \quad . \quad . \quad . \quad . \quad (7)$$

(where $\Gamma_v$ is the intercept of the line when P = 1.0, and $\lambda_v$ is the slope of the line.)

This function approaches a limiting value as the air pore volume of the soil approaches zero (maximum dry bulk density)[1] which is similar to a critical state condition of maximum volume strain.

The two functions coincide at a 'threshold' value of P, i.e. $P_{th}$, when

$$\Gamma_v + \lambda_v \ln P_{th} = Dbd_1 + K_s \ln(P_{th}/P_o) \quad \text{or}$$

$$\ln P_{th} = \frac{Dbd_1 - K_s \ln P_o - \Gamma_v}{\lambda_v - K_s} \quad . \quad . \quad (8)$$

1 This term should not be confused with the 'maximum dry bulk density' of the Proctor test, which is referred to as Proctor maximum dry bulk density.

On reaching a maximum value of spherical pressure (P max) a reduction of P causes path 'DE' to be followed. This path is described by a relaxation function and considered by Critical State theory for saturated soils to have the same slope as the swelling function. The mathematical expression of the relaxation function is as follows:-

$$Dbd = Dbd_f + K_R \ln \frac{P}{P_o} \quad . \quad . \quad . \quad . \quad . \quad (9)$$

(where $Dbd_f$ = final Dbd when P returns to $P_o$

and $K_R$ = slope of the relaxation function)

Observed responses of unsaturated soil to hydrostatic stresses, by Bertilsson (1971) for example, have identified a larger slope of the swelling function than the relaxation function. Thus it is convenient to refer to the former as $K_S$ and the latter as $K_R$.

If R is increased at any point on the stress/strain path 'ABDE', such as point 'C' in Fig.5, a path 'CF' will be followed. This path will be away from the Dbd, lnP plane towards the CSL, and is accompanied by shearing strain. The kind of failure, 'brittle' or 'plastic' depends upon the direction in P, R, Dbd space from which the CSL is approached.

Some reassessment of the stress/strain paths described above is necessary to consider the values of dry bulk density of greatest importance to the compaction of field soils. Initial and final values are of greater importance than the transient values of dry bulk density during wheel passage. This reassessment is assisted if attention is initially confined to the stress/strain

paths in Dbd, lnP space and to soil of 'low' original dry bulk density. Application and removal of a maximum spherical pressure, $P_{max}$, by the passage of a wheel may generate a stress/strain path such as path 'ABDE' in Fig.5. The final dry bulk density after wheel passage, $Dbd_f$, is controlled by $P_{max}$; for any one set of Critical State functions. The number functions can be simplified by ignoring relaxation and correcting the swelling function and VCL to account for this. The VCL and swelling function can then be interpreted in terms of $Dbd_f$ and $P_{max}$. This transposes the VCL to the apparent VCL or 'VCL' and the swelling function to an apparent swelling function, or primary function as in Fig.5.

By applying the same theory to the rest of P, R, Dbd space the CSL can be transposed to an apparent Critical State line ('CSL') and the whole state boundary surface transposed to an apparent form.

Using this interpretation of Critical State soil mechanics the numbers of functions required to predict final dry bulk density values from a known stress history are reduced from 3 to 2 for the Dbd, lnP plane and from 5 to 4 for the whole of P, R, Dbd space.

An important assumption of this interpretation requires the slope of the relaxation function of unsaturated soil to remain constant for all stress/strain paths. Bertilsson (1971) found this for a large range of initial bulk density but some change of slope was evident for initial bulk densities closest to the 'maximum' packing state of the soil for isotropic stress.

2.2.1 Identification of the 'VCL' and 'CSL' by experiment

This can be achieved by applying stress cycles, including such as described above, to a soil of low initial Dbd and monitoring the strains during the cycle by laboratory methods, as proposed by Reece (1977). Alternatively one can subject a number of soil bodies, of a variety of initial dry bulk densities, to a variety of levels of $P_{max}$ (and $R_{max}$) and measuring the resulting final dry bulk densities. If levels of $R_{max}$ are insignificant, a graph relating ln $P_{max}$ to $Dbd_f$ should generate a scatter of points such as in Fig.6a. If adequate ranges of $P_{max}$ and initial dry bulk density are used, the scatter should be spread along the 'VCL' as an elongated linear cluster. Only soil bodies whose stress/strain paths have reached the VCL will contribute to the cluster. Other points in $Dbd_f$, ln $P_{max}$ space will fall short of the cluster and lie above it. A linear regression through the cluster should yield the best estimate of the 'VCL'. This latter method, using measurements of bulk density before and after the passage of a single wheel, appears most suitable for in situ measurements of field soils.

When significant levels of $R_{max}$ are introduced, a different pattern on a $Dbd_f$, ln $P_{max}$ graph must be expected. Increasing R can either increase or decrease Dbd, according to the original packing condition of the soil. Critical State theory predicts that the change of packing state depends on whether the end of the stress/strain path lies above or below the projection of the CSL onto the Dbd, lnP plane before R is applied (see Fig.6b). A stress/strain path on the VCL before R is increased will show increases of Dbd and strain hardening as the stress/strain path

Fig.6a The proposed identification of the apparent virgin compression line ('VCL'). The application of various levels of maximum spherical pressure ($P_{max}$) to various levels of initial dry bulk density ($Dbd_1$) result in various levels of final dry bulk density ($Dbd_f$). A sufficient range of $Dbd_1$ and $P_{max}$ and a sufficient number of observations should develop a linear cluster along the 'VCL'. Each zone above the 'VCL' contains points with different combinations of $Dbd_1$ and $P_{max}$.

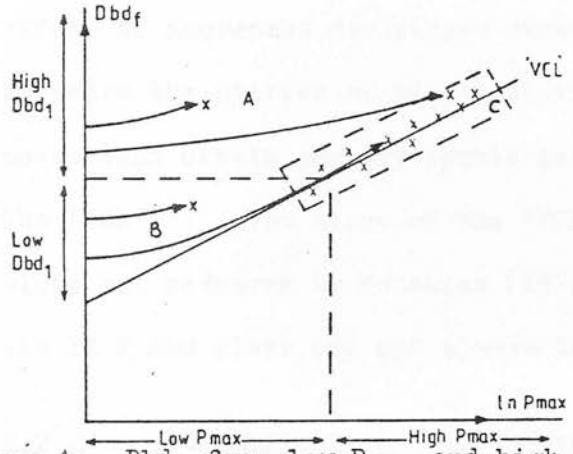


Zone A: $Dbd_f$ from low $P_{max}$ and high $Dbd_1$
Zone B: $Dbd_f$ " low $P_{max}$ " low $Dbd_1$
Zone C: $Dbd_f$ " high $P_{max}$ " low $Dbd_1$

Fig.6b The influence of deviatoric stress upon the stress/strain paths projected onto the $Dbd_f$, $\ln P_{max}$ plane.

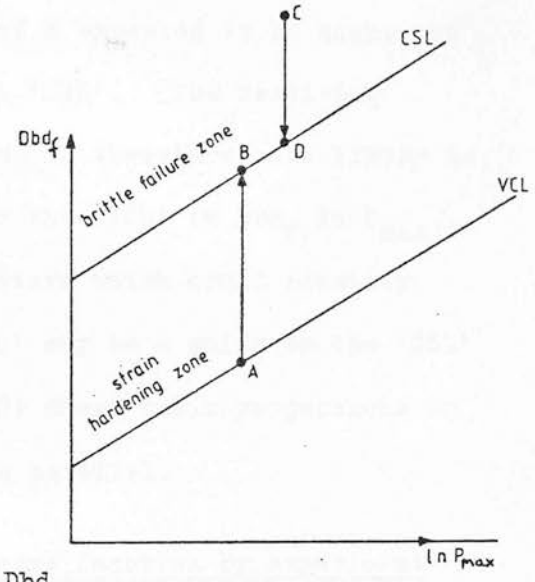


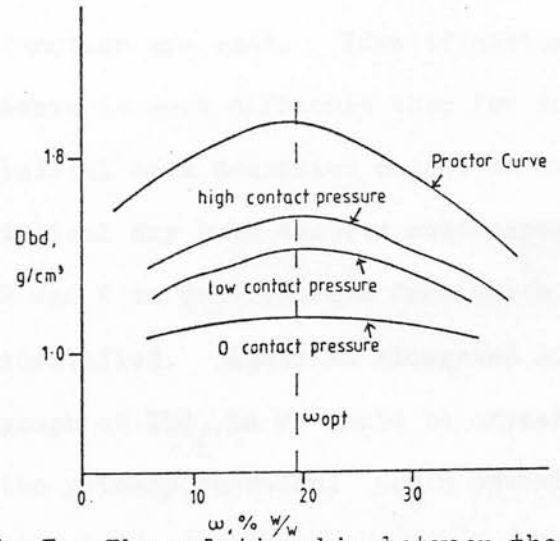


Fig.7a The relationship between the Proctor curve and the responses of a sandy loam to different levels of tyre/soil contact pressure; after Raghavan et al. (1976a). $\omega_{opt}$ is the Proctor 'optimum' moisture content.

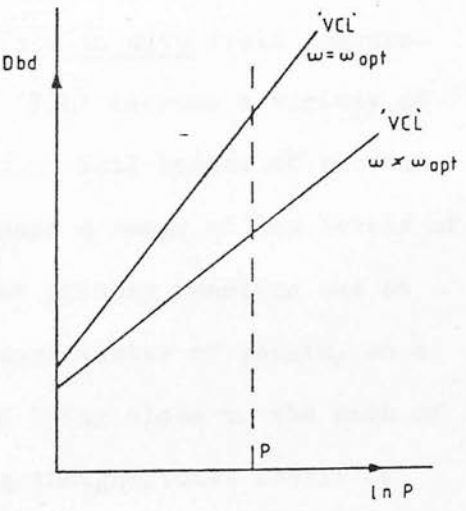


Fig.7b An hypothesis of the effect of soil moisture content variation upon the apparent virgin compression line ('VCL').

approaches the CSL (path 'AB'). A path beginning above the projection of the CSL, in the brittle failure zone, will experience brittle failure and a reduction of bulk density as its stress/strain path approaches the CSL when R is increased (path 'CD'). The former case is more usual for agricultural topsoils. Only when high wheelslip, or very loose initial soil conditions are present, are values of R expected to be high, and the stress/strain paths approach the 'CSL'. The resulting effect of increased deviatoric stress is therefore more likely to increase the scatter of points above the 'VCL' in $Dbd_f$, ln $P_{max}$ space than create any systematic pattern which could identify the 'CSL'. The slope of the 'VCL' may be a guide to the 'CSL' slope but research by Potamias (1976) shows their projections on the ln P, Dbd plane may not always be parallel.

### 2.2.2 Identification of the primary function by experiment

Again laboratory methods may be used to monitor stresses and strains of a soil as the swelling function and relaxation function are used. Identification from in situ field measurements is more difficult than for the 'VCL' because a variety of initial bulk densities cannot be used. Soil bodies of the same initial dry bulk density must experience a range of low levels of P and R to provide data from which the primary function can be identified. Again an elongated linear cluster of points, on a graph of $Dbd_f$, ln P, would be expected lying close to the path of the primary function; again assuming insignificant levels of deviatoric stress.

### 2.2.3 The relative value of in situ and laboratory methods

Although in situ methods may provide more realistic information on the behaviour of undisturbed field soils, methods of measurement in the field are less precise than those used in the laboratory. Assessment of the validity of in situ methods may be assisted by comparing the trends of the results with those from laboratory tests carried out using stresses, stress rates and periods as similar as possible to those in the field. In the laboratory disturbed soils are more conveniently used, but tests on undisturbed cores may give results of greater relevance to in situ conditions.

## 2.3 The Influence of Some Soil Physical Factors upon Critical State Parameters

### 2.3.1 Soil moisture conditions

There is considerable evidence of how soil moisture conditions influence soil strength. Unfortunately little of the research has measured Critical State functions directly but some may be interpreted in terms of Critical State behaviour. Work by Raghavan et al. (1976a) examined large ranges of soil stresses and moisture contentsand found a close correspondence between the form of the Proctor curve and the form of functions derived from 'unit load applications' to soils of different moisture contents, see Fig.7a. Each load application was obtained by different numbers of passes of tractor rear wheels of different loadings. The following function gave a very close fit to experimental observations:

$$Dbd = \begin{matrix} A_1 \\ A_2 \end{matrix} + \begin{matrix} B_1 \\ B_2 \end{matrix} \ln(nP) + \begin{matrix} C_1 \\ C_2 \end{matrix} \ln W, \quad W \leqslant W_{opt} \quad . \quad . \quad (10)$$

(where $A_1$, $A_2$, $B_1$, $B_2$, $C_1$ and $C_2$ are constants used according to the value of W, e.g. $A_1$ for $W > W_{opt}$, $A_2$ for $W \leqslant W_{opt}$,
n = number of passes, P = mean surface pressure,
W = soil moisture content, (% w/w), $W_{opt}$ = optimum soil moisture content from the Proctor test.

Unfortunately the equation is very empirical, which limits its application to soils other than the one for which it was derived. Fig.7b is an hypothesis of the effect of soil moisture content variation upon the 'VCL'. The difficulty of measuring the effective stresses in unsaturated soils requires the use, here and subsequently, of the actual mechanical stresses, uncorrected for the contribution of stresses from the soil moisture phase. An application of spherical pressure P at $W_{opt}$ will generate a point on the 'VCL' ($W_{opt}$). The same level of P at any other value of W will, according to equation (10), produce a lower value of Dbd, hence the 'VCL'$_{(W)}$ will lie below the 'VCL'$_{(W_{opt})}$. The 'VCLs' for different levels of W will probably converge at lower levels of spherical pressure because very low levels of P will have little influence on Dbd, whatever the level of W; this discounts 'shrink and swell' effects of the soil as W changes. Thus alteration of W should alter the slope and intercept of the 'VCL', the slope being a maximum at optimum moisture content. Observations by Bertilsson (1971) have shown changes of slope of virgin compression lines with changes of soil moisture content which follow this expected trend. However the changes of intercept showed a rising, not a 'peaked' trend with changes of soil moisture content.

Although the authors quoted have used W as the parameter describing soil moisture conditions, it is not as well related to soil strength as the soil moisture tension, S. The strength of the soil matrix is influenced by the amount of air/water interfaces (Dexter, 1973), a function of S rather than W . As S depends on W and pore structure, the use of S as a soil moisture parameter may allow soils of different pore structures to be more systematically related. Unfortunately soil moisture tensions are more difficult to measure than soil moisture content, especially in field soils. Further conceptual problems are evident as the pore structure is altered by soil strains, thus S is dependent upon strain and stress of the soil whereas W is much less so.

### 2.3.2 Rate and period of stress application

Soil deformations to applied stresses are not instantaneous especially if the soil stresses are increased from zero over a very short period, as under a vehicle wheel moving over the soil. The rapid increase of stresses beneath a moving wheel can be simplified to an instantaneous change from 0 to a maximum stress level. Such changes of stress and the corresponding volumetric soil deformations were studied by Dexter and Tanner (1974). The exponential functions measured during their work (see Fig.8a) are expressions of the viscous responses of unsaturated soils and can be superimposed onto Critical State theory, as in Fig.8b. If a stress $P_{max}$ is applied instantaneously to a soil body of initial 'low' Dbd and removed after t seconds the stress/strain path will not have travelled as far up the 'VCL' as at 'equilibrium' time, thus the final dry bulk density will be $Dbd_t$, lower than Dbd at equilibrium. If soil stresses and strains are measured simult-

Fig.8a Time dependent responses of dry bulk density (Dbd) to unit applications of maximum spherical pressure ($P_{max}$); adapted from Dexter and Tanner (1974).

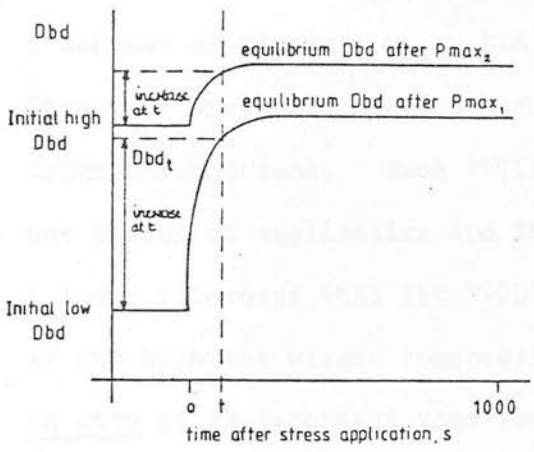


Fig.8b An hypothesis of the effect upon the apparent virgin compression line ('VCL') of the viscous response of soil to the application of spherical pressure for different time periods.

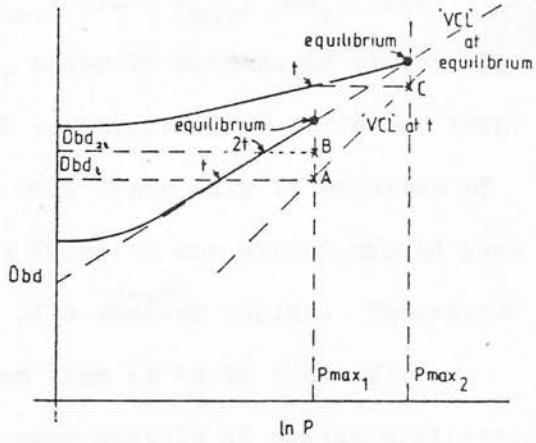


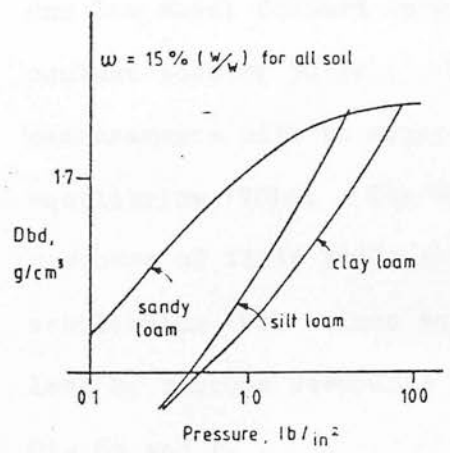


Fig.9 The influence of soil texture upon the response of initially loose soil to confined compression; adapted from Chancellor (1976).

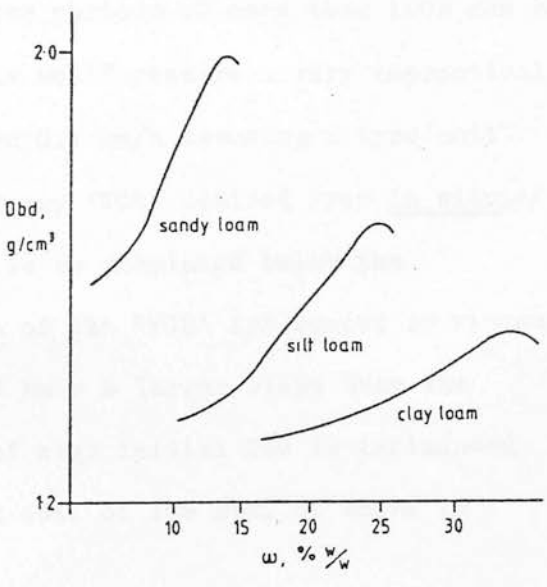


Fig.10 The influence of soil texture upon the response of dry bulk density to confined compression of 2 $kg/cm^3$ at different moisture contents; adapted from Chancellor (1976).

aneously in the laboratory, the identification of the 'VCL' can use an 'equilibrium' period, which is more convenient than shorter times. However, this could present difficulties for the in situ identification techniques described previously. Each period of stress application will generate different points on the graph of final dry bulk density ($Dbd_f$) and ln $P_{max}$; i.e. $P_{max}$, $Dbd_t$, after t seconds of stress; $P_{max}$, $Dbd_{2t}$ after 2t seconds of stress etc. These are shown as points A and B in Fig.8b and a different 'VCL' drawn through each. Each 'VCL' will apply only to stresses of one period of application and the 'VCL' of one period should have a lower intercept than the 'VCL' of a ~~shorter~~ longer period. Therefore if the apparent virgin compression line is to be identified in situ it is important that the same periods of stress application be used, i.e. constant wheel forward speeds and tyre/soil contact lengths are required. The results of Dexter and Tanner (1974), Fig.8a, show that stress periods of more than 100s can be required for equilibrium; this would require a very impractical and low wheel forward speed ( $< 0.1$ km/h assuming a tyre/soil contact zone of 50 cm). Thus any 'VCL' derived from in situ measurements will be expected to be displaced below the equilibrium 'VCL'. The slope of the 'VCL' influenced by viscous response of field soils should have a larger slope than the equilibrium 'VCL' since soil of high initial Dbd is influenced less by viscous responses than soil of low Dbd, as shown in Fig.8a and b.

### 2.3.3 Soil texture

The compressibility of soils of different textures has been examined by Chancellor (1976). A summary of these results is shown in Fig.9. It appears that coarser textured soils have a smaller VCL slope than finer grained soils.

The influence of texture upon the relationship between moisture content and dry bulk density after unit stress application is summarised from Chancellor (1976) in Fig.10. Finer grained soils show an optimum moisture content at higher moisture contents and are less influenced by changes of moisture content than coarser grained soils.

## 2.4 Conclusions and Experimental Aims

Methods of predicting soil stresses beneath wheels have been considered. They have a number of shortcomings, principally the lack of quantitative distinction between 'hard', 'firm' and 'soft' ground. Interpretations of Critical State soil mechanics have been made. Reduction of critical state functions to the apparent virgin compression line and primary function has been suggested when soil packing states before and after the passage of a wheel are measured.

Possible means of identifying these functions from field

and laboratory data have been described. The influence of some dominant soil physical factors (soil moisture conditions and soil texture) as well as the rate and period of stress application have also been examined.

The discussion of soil mechanical behaviour has emphasised the extreme shortcomings of any current laboratory method of applying known stresses to soil, and measuring resulting strains, in a way similar to the processes occurring under a moving agricultural wheel. Therefore the closest simulation of compaction processes appears to require application of stresses from real wheel to field soils in situ. The detailed experimental aims are based upon this concept.

Experimental Aims

A: Investigation of soil stresses *in situ*

1) To use a single tractor rear wheel with known axle load, tyre/soil contact area, tyre inflation pressure and constant, low forward speed ( $\simeq$ 1 km/h), as well as minimum wheelslip, to apply stresses to field soils.

2) To develop and use improved techniques to make *in situ* measurements of stresses beneath these wheels.

3) To derive a relationship between rut depth and stationary contact area to enable the use of Söhne's equations to predict stresses beneath these wheels.

4) To compare the measured and predicted values of stresses beneath the wheels, in relation to the strength of the soil, and assess the usefulness of Söhne's equations.

B: Investigation of soil strains *in situ*

5) To apply a range of soil stresses to field soils of a range of initial dry bulk densities and measure the resulting dry bulk densities after wheel passage.

C: Investigation of *in situ* stress/strain relationships

6) To use the field data from (5) and predicted soil stresses to identify the apparent virgin compression lines and primary functions for field soils at different moisture conditions and the rate and period of stress application under the experimental wheel.

7) To compare 'VCLs' from (6) with apparent virgin compression lines and primary functions , for similar soil moisture conditions and rate and period of stress application,

obtained from disturbed and 'undisturbed' soils in laboratory tests.

D: Prediction of dry bulk density changes

8) To use the estimated values of in situ soil stresses and in situ stress/strain functions to develop a prediction model for the changes of dry bulk density beneath a wheel.

9) To test the model for the prediction of changes of dry bulk density with suitable field experimental data from additional experiments.

## 2.5 Preliminary Investigations

Before embarking on a large scale research program, it was necessary to test some of the ideas put forward in this chapter; notably the identification of apparent virgin compression lines from measurements of bulk density before and after wheel passage. Satisfactory data was available from long term cultivation experiments (Pidgeon and Soane, 1978). This was combined with estimates of stresses from much simplified forms of Söhne's equations. Linear clusters, as proposed in section 2.2.1, could be identified from graphs relating the logarithm of expected maximum stress to the bulk density after passage of a wheel. Further short term field tests also supported these findings.

# CHAPTER 3 - METHODS AND TECHNIQUES

The methods used to collect the data are now explained, as well as techniques used to compact the field soils.

## 3.1 Application of Stresses to Field Soils

A slowly moving, 'non-slipping' single tractor rear wheel was chosen as the most suitable means of applying compactive stresses in field experiments; Söhne's equations were designed to predict stresses beneath such wheels. Loaded plates of various sizes and shapes have been used in other research. The stresses they apply are easier to analyse but the results may be difficult to compare with those of a real wheel. Using a single tractor rear wheel avoided the complicating effects of the previous passage of a tractor front wheel.

The experimental wheel was provided by a three wheeled tractor (Nuffield Universal 4; 26.7 kW 3.28 tonnes[1]) shown in Fig.11. The distance of the front wheel track from the centre of the rear wheel tracks (1 m) isolated any effects of the front wheel upon the soil subsequently run over by the rear wheel. Tyre size was '12.5/11-36' 4PR; a commonly used size.

Rear wheel loading could be varied by altering the three-point linkage load. A rear mounted forklift (Chieftain Forge, weight 0.65 tonnes) was used for these load alterations. Table 3 describes the wheel loads used; maximum values were limited by tractor stability at low speeds (approx. 1 km/h).

---

1 Maximum load with water ballasted tyres.


Fig.11 The three wheeled Nuffield tractor. The front wheel running along a 'tramline' and the rear wheels running into an experimental plot.

TABLE 3 LOADS USED FOR EXPERIMENTAL REAR WHEEL

| Load on three-point linkage | Tractor front weights | Wheel load, tonnes |
|---|---|---|
| a. None - tractor alone | front frame weight | 0.89 |
| b. Rear mounted forklift | front frame weight + 6 x 45 kg | 1.21 |
| c. Rear mounted forklift + wooden pallet (50 kg) + 2 x 230 kg | front frame weight + 6 x 45 kg + 1 x 90 kg | 1.56 |
| d. As for c + 3 x 160 kg | " " " " " | 1.86 |

Maximum rated load + 40% for 12.4/11-36 tyre (4PR) = 1600 kg

A compressed air cylinder and pressure regulation equipment were used for variation of tyre inflation pressure during the field experiments. This provided four inflation pressures for each of the wheel loadings shown in Table 3. Minimum pressures were set by manufacturer's recommendations[1]. This precaution avoided extreme variation of tyre/soil contact stress caused by tyre wall stiffness effects at low inflation pressures (VandenBerg and Gill, 1962). Maximum wheel loadings were guided by manufacturer's recommendations of maximum rated load for 20 mph[2] plus 40 per cent additional load and 25 per cent additional tyre inflation pressure for slow speed and infrequent working. (Maximum 20 mph[2] rated load = 1135 kg)[3].

Tyre load and inflation pressure were examined in terms of tyre/soil contact area and mean surface pressure. Measurements of contact area were initially made on a rigid horizontal concrete surface. The influence of variations of soil surface strength was considered later. The areas and major axes (contact length) of the contact 'ellipsoids' are described in Table 4.

1. 12 psi (83 kPa).
2. 30 km/h.
3. Although loading d, Table 3, was beyond conventional recommended levels, its use was found to be safe over the short distances and very low speeds of the experimental runs.

TABLE 4 TYRE CONTACT AREAS AND LENGTHS OF ELLIPSES OF EXPERIMENTAL WHEELS ON A RIGID SURFACE WITH DIFFERENT LOADINGS AND TYRE INFLATION PRESSURES. (THE METHODS ARE EXPLAINED IN SECT.3.7.1)

| Wheel load, tonnes | 0.89 | 1.21 | 1.56 | 1.86 |
|---|---|---|---|---|
| Tyre inflation pressure, kPa,(psi) | | | | |
| 83 (12) | CA = 680) W1<br>CL = 40) | CA = 892<br>CL = 44 | CA = 1236<br>CL = 56 | |
| 110 (16) | CA = 646<br>CL = 42 | CA = 758) W2<br>CL = 47) | CA = 1076<br>CL = 52 | |
| 136 (20) | CA = 595<br>CL = 42 | CA = 732<br>CL = 44 | CA = 912) W3<br>CL = 48) | |
| 172 (25) | - | - | - | CA = 1052) W4<br>CL = 48) |
| | | Mean standard deviations<br>CA - 20.1<br>CL - 2.0 | | |

CA = contact area, $cm^2$ CL = contact length, cm

When different combinations of wheel load and tyre inflation pressure were used to apply stresses to field soils, it was preferred to have combinations with similar ellipse length A contact area with constant wheel forward speed and constant elipse length applied stresses to the soil for the same period of time. This avoided the influence of variation of time dependent effects on the compaction process. Thus four 'wheel treatments' referred to W1, W2, W3 and W4 were used forthe experiments. The wheel loads and inflation pressures of each treatment are indicated in Table 4.

The tyre lug pattern (Dunlop T100) was a commonly used form. The lugs were well worn, see Fig.11, which reduced their effect on the distribution of stresses at the tyre/soil interface. The

possibility of using a smooth, lugless tyre was not pursued because of possible traction problems on soft soil. Wheel forward speed was maintained as constant as possible during the experimental runs (1.0 km/h, 1st gear). Throughout the experiment, wheelslip was minimised by an absence of drawbar load and estimated as 4 per cent from field measurements.

## 3.2 In situ Measurements of Stresses

This was carried out by means of two deformable spherical stress transducers, developed for the project due to the problems of existing stress transducers for the measurement of soil stresses (Blackwell and Soane, 1978)[1]. The design of the transducers was based on a recent technical innovation by Verma et al. (1975), which considerably reduced the problems of unidirectionality and stiffness encountered by stress transducers (see Section 1.3). This innovation was a flexible, water-filled rubber ball enclosing a strain gauged pressure transducer.

The device transmitted soil stresses at the ball/soil interface to the internal water pressure transducer. Although this device had omnidirectionality and less uniaxial stiffness than previous devices, its use presented two main problems:

1. Any level of internal water pressure could be created by a number of combinations of forces at the ball/soil interface. Therefore, in general, interpretation of any signal from the device was difficult.
2. Individual instrumentation of each device would require a costly and complex electronic recording system when a large number of devices needed monitoring over a short period, e.g. Möller (1975).

1 A reprint is shown in Appendix 10

A solution to these problems demanded a better understanding of the behaviour of a water-filled rubber ball (WFRB) in a stress system and a modification of the instrumentation previously used.

3.2.1 Theory of behaviour of the transducers

When the system has all principal stresses equal, in pure hydrostatic stress, the internal ball pressure will be directly proportional to the hydrostatic stress as in Fig.12 line AB; this discounts any effects of wall stiffness. From any point on AB, e.g. C, a simple deviator stress can be applied where first principal stress $\sigma_1$ exceeds both second and third principal stresses $\sigma_2$ and $\sigma_3$. If $\sigma_2$ and $\sigma_3$ are reduced to keep the mean principal stress $\frac{\sigma_1 + \sigma_2 + \sigma_3}{3}$ constant, the path CD will be followed. Thus the same internal ball pressure (P) can be produced by a pure hydrostatic stress (as at point G) or a hydrostatic stress and a deviator stress (as at point D).

However, if the ball now experiences uniform increases of principal stresses a path DE will be followed, parallel to AB, as an increase of hydrostatic stress occurs. A similar uniform reduction would cause path DF to be followed. The theoretical procedure can be repeated to create a family of lines parallel to AB.

Thus in this simplified stress system ($\sigma_1 = \sigma_2$) the hydrostatic stress and deviator stress appear to define the internal pressure of the ball. Similar results were also found by Verma et al. (1975), during tests on their device. Thus if the internal pressure of the water filled rubber ball and one of the unknown stresses is measured (either hydrostatic or deviator) the

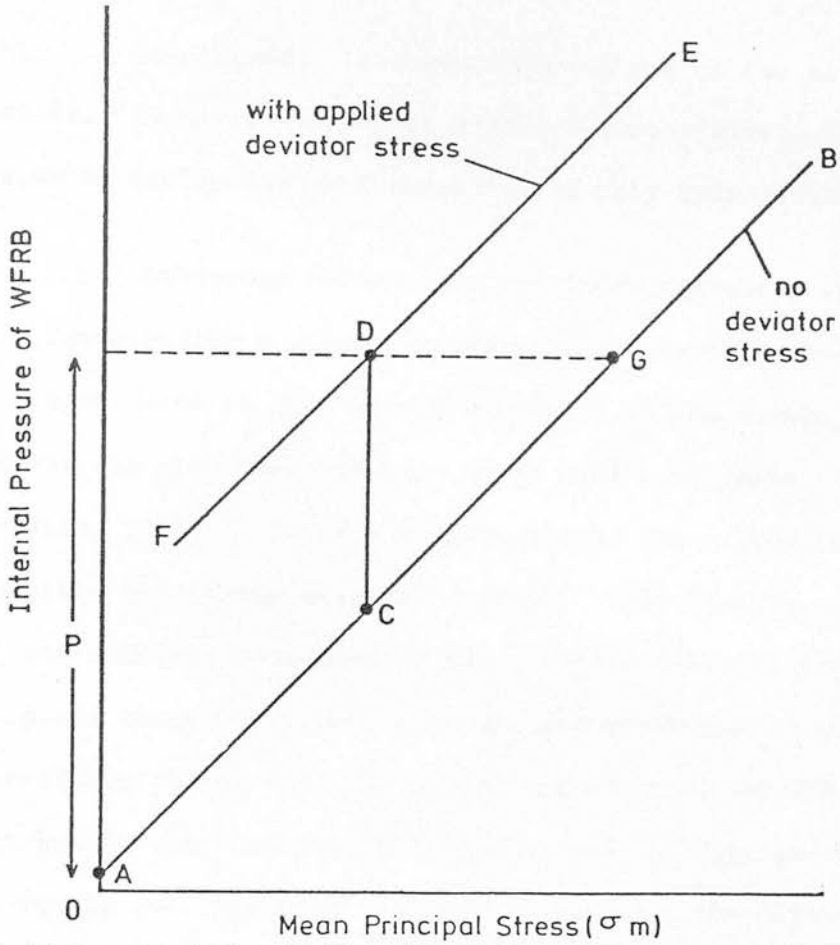


Fig.12 The expected relationship between the mean principal stress and the internal pressure of the water filled rubber ball (WFRB), with and without the application of a deviator stress.

Fig.13 The water filled rubber ball (WFRB), prototype 2.

other can be derived; this requires the use of two separate devices. A device to detect simple deviator stress appeared easier to design than one sensitive to only hydrostatic stress.

Any plastically deformable, yet incompressible, spherical body experiencing a stress system will deform to a shape which is a complement of the 'stress ellipsoid' of the system. This concept has also been referred to as Lamé's Ellipsoid (Folinenko-Borodich, 1965). It is a representation which geometrically describes the stress state at a point. The longest, shortest and intermediate semi-axes of the ellipsoid describe the first, third and second principal stresses respectively. Thus pure hydrostatic stress will not change the shape of the spherical body but deviator stress, when second and third principal stresses are equal, will generate a prolate spheroid; the direction of the minor axis being parallel to that of the major principal stress. The lengths of the axes of any spheroid formed will be proportional to the principal stresses of the stress system experienced, provided any elastic rebound of the material of which the spherical body is made can be ignored. It was considered that a 'mastic' material would have suitable properties of plastic and elastic behaviour for such a spherical body to detect simple deviator stress.

### 3.2.2. Design and instrumentation of the WFRB and mastic ball

The thin walled (2 mm) flexible silicone rubber hollow sphere used by Verma was very sensitive to soil stresses, but it was not considered rugged enough for field soils. Comparison was made between Verma's transducer and two prototypes of more rugged

design; both made from commercially available 'squash' balls. Comparative dimensions are given in Table 5 and prototype 2 is shown in Fig.13. A cyanocrylate glue was used for the bond between ball and tube.

TABLE 5 COMPARATIVE DIMENSIONS OF THE WATER FILLED BALLS

| Ball | Material | External Diameter, cm | Wall Thickness, mm |
|---|---|---|---|
| Verma et al. (1975) | Silicone rubber | 2.5 | 1.5 |
| Prototype 1 (modified 'squash'[1] ball) | Mixture of neoprene and natural rubbers | 3.2 | 2.0 |
| Prototype 2 (unmodified 'squash'[1] ball) | | 3.8 | 5.0 |

1 Dunlop red spot

Prototype 1 was prepared by sand-papering the outside to reduce the wall thickness. It was thought this would provide more sensitivity than the unmodified form and yet remained sufficiently rugged. Hydrostatic tests (as described later in section 3.2.3) were made on each prototype, (Fig.14) and results compared to the performance of Verma's balls. Although all three exhibited linear relationships between applied and detected pressures Verma's design wasmore sensitive than either prototype and prototype 2 least sensitive of all. However, since the unmodified form could still detect pressure differences as small as 0.1 bar within its level of variability, it was decided to pursue this, more practical, design. Problems of creating a reproducible wall thickness for prototype 1 also encouraged the choice of prototype 2.

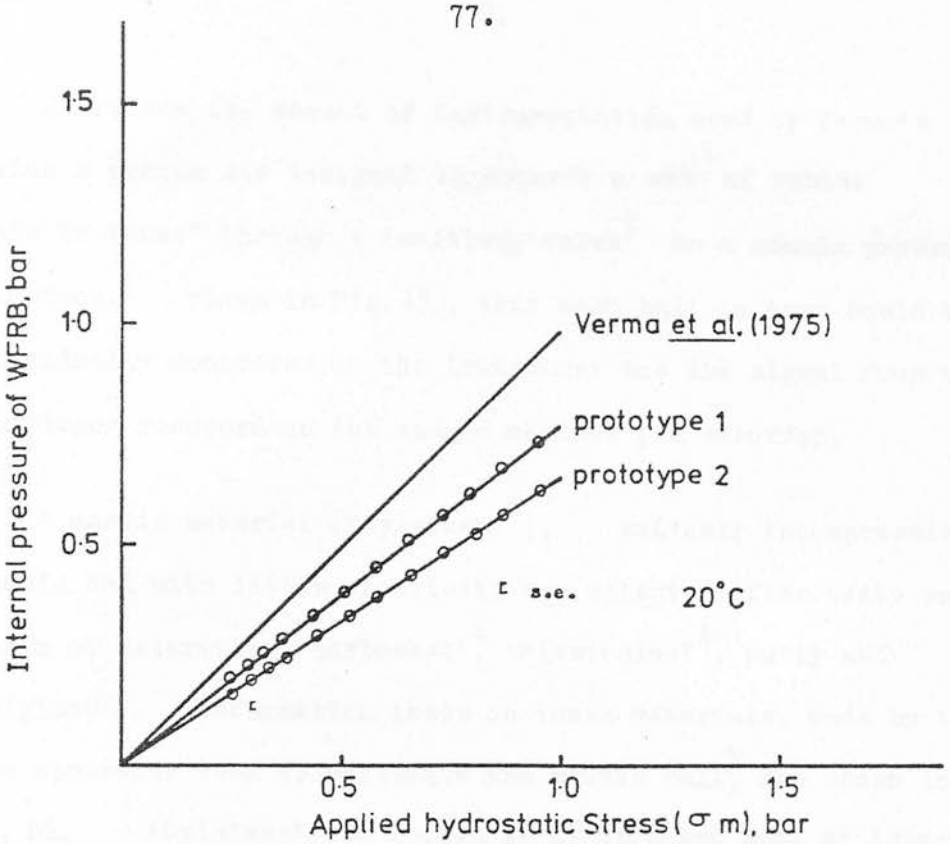


Fig.14 Comparison of the sensitivity of the prototype water filled rubber balls (WFRB) with the ball designed by Verma.

Fig.15 The water filled rubber ball and associated equipment for measurement of the internal water pressure.

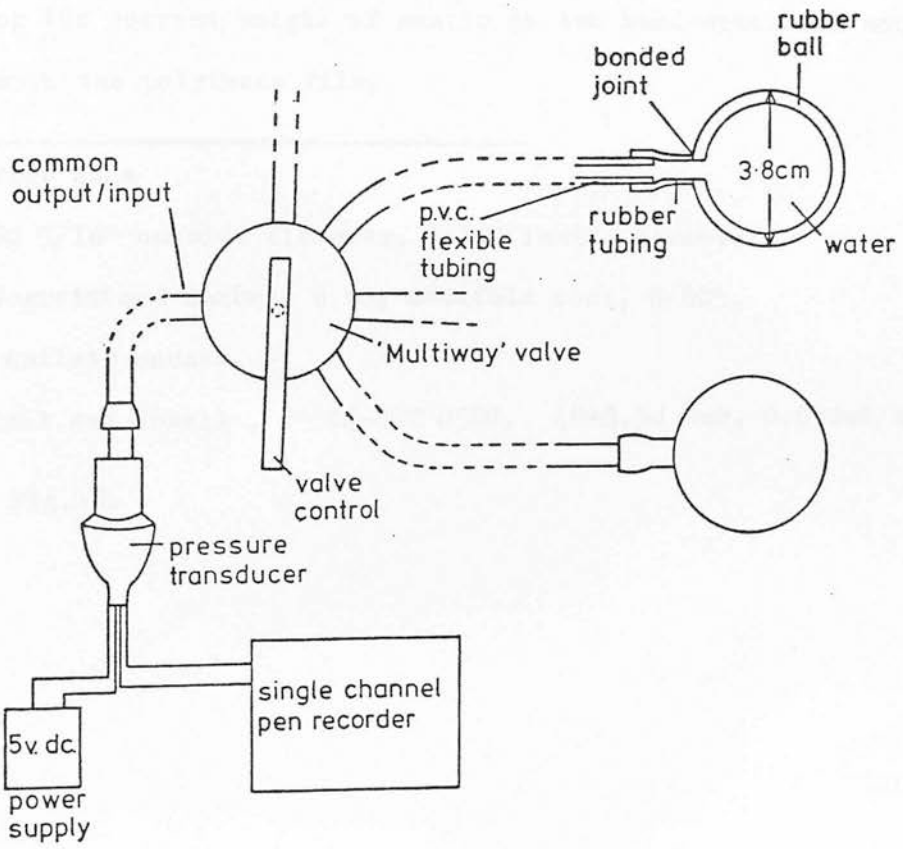

To reduce the amount of instrumentation used by Verma's device a system was designed to connect a set of rubber balls by tubes[2] through a 'multiway' valve[3] to a common pressure transducer[4] shown in Fig. 15 , thus each ball in turn could be individually connected to the transducer and the signal from the transducer recorded on the single channel pen recorder.

A mastic material ('Sylglass'[1]), suitably incompressible, plastic and with little elasticity was selected after tests on a number of materials; 'Arboseal'[1], 'Plastecine'[1], putty and 'Sylglass'[1]. Deformation tests on these materials, made by the same apparatus used to calibrate the mastic ball[5], are shown in Fig. 16. 'Sylglass' was chosen as it deformed well at lower temperatures (approx. 10°C) without extreme deformation at higher temperatures (approx. 20°C). As the mastic had a slightly volatile lubricant, the mastic spheres were covered by two hemispheres of thin flexible polythene film. The spheres were formed by pressing the correct weight of mastic in two hemi-spherical moulds lined with the polythene film.

---

1 Trade name

2 PVC 5/16" outside diameter, 3/16" inside diameter.

3 Negretti and Zambra 6 way manifold cock, G/805, 2 outlets unused.

4 Bell and Howell , 4-366-002 05HO. (0-3.54 bar, 0.052mV/bar)

5 See Fig.18.

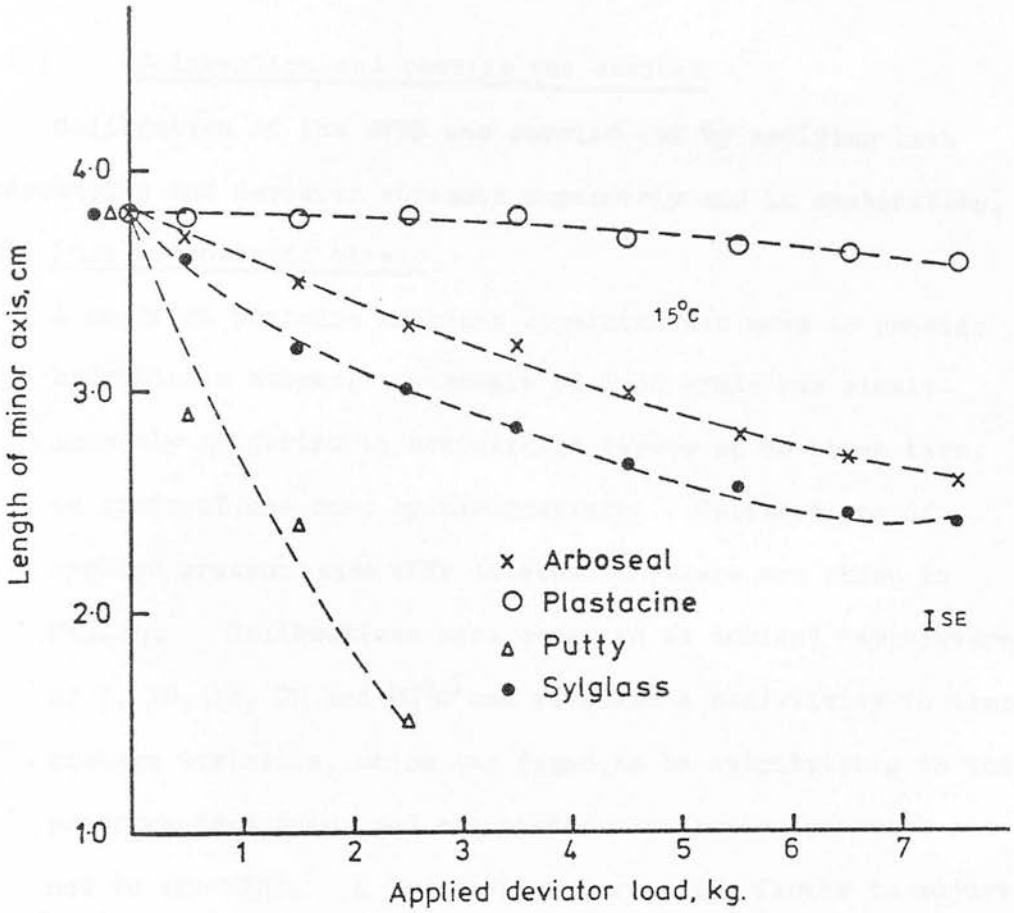


Fig.16 Deformation tests upon four materials of plastic behaviour (all at 15°C).

Fig.17 Calibration of the water filled rubber ball (WFRB) at different temperatures under hydrostatic stress.

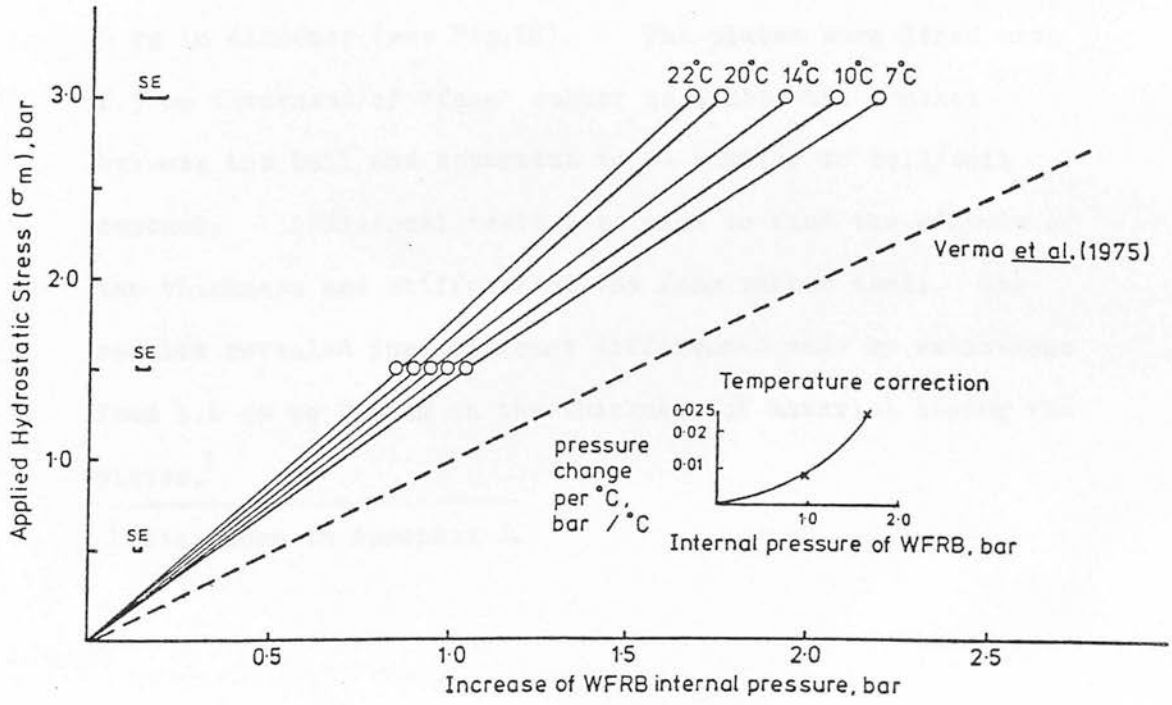

### 3.2.3 Calibration and testing the devices

Calibration of the WFRB was carried out by applying both hydrostatic and deviator stresses separately and in combination.

(a) Pure hydrostatic stress

A modified pressure membrane apparatus was used to provide hydrostatic stress. A sample of four WFRBs was simultaneously subjected to hydrostatic stress up to three bars, in steps of one bar, by air pressure. Calibrations of applied pressure with WFRB internal pressure are shown in Fig. 17. Calibrations were obtained at ambient temperatures of 7, 10, 14, 20 and 22°C[1] and revealed a sensitivity to temperature variation, which was found to be attributable to the pressure transducer and associated electronic apparatus and not to the WFRB. A temperature correction factor to adjust the estimated hydrostatic stress is also shown in Fig.17. Thus a measurement of air temperature adjacent to the recording equipment was required during fieldwork.

(b) Pure deviator stress

This was applied to the WFRB between parallel metal plates 5 cm in diameter (see Fig.18). The plates were lined with 2.5 cm thickness of 'foam' rubber to enable the contact between the ball and apparatus to be similar to ball/soil contact. Additional tests were made to find the effects of the thickness and stiffness of the foam rubber used. The results revealed insignificant differences made by variations from 1.0 cm to 2.5 cm in the thickness of material lining the plates.[1]

---

[1] Data shown in Appendix 1.

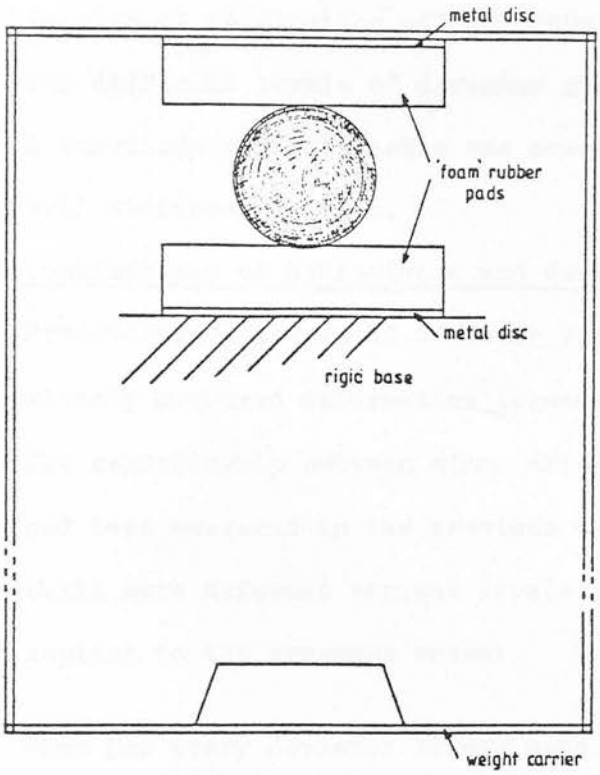


Fig.18 The apparatus for calibration of the balls under deviator loading.

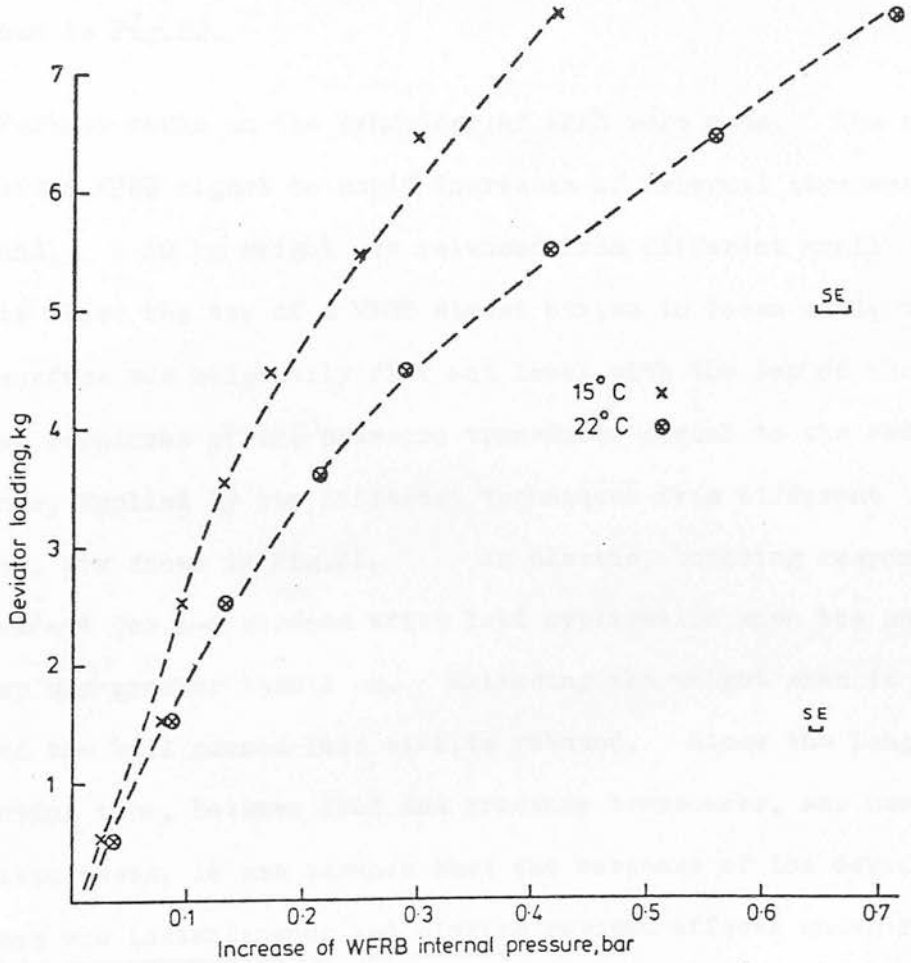


Fig.19 Calibration of the water filled rubber ball (WFRB) at two temperatures under deviator loading.

Results of calibration of the WFRBs at different temperatures for different levels of deviator stress[1] are shown in Fig.19. A curvilinear relationship was present, probably caused by wall stiffness effects.

(c) Combinations of hydrostatic and deviator stress

Predetermined levels of deviator stress were applied by previously measured deformation between the parallel plates. The relationship between minor axis length and deviator load had been measured in the previous tests (b). While the balls were deformed various levels of hydrostatic stress were applied to the pressure vessel.

Thus for every deviator stress used a calibration for varying hydrostatic stress was obtained. The resulting family of lines is shown in Fig.20.

Further tests on the behaviour of WFRB were made. The response rate of the WFRB signal to rapid increases of external stresses was examined. A 10 kg weight was released from different small heights above the top of a WFRB almost buried in loose sand; the sand surface was originally flat and level with the top of the WFRB. Typical responses of the pressure transducer signal to the sudden loadings, applied by two different techniques from different heights, are shown in Fig.21. An elastic, bouncing response was evident for 1-2 seconds after load application when the height of drop was greater than 1 cm. Releasing the weight when it touched the ball caused less elastic rebound. Since the longest connecting tube, between WFRB and pressure transducer, was used for these tests, it was assumed that the response of the devices to stresses was instantaneous and elastic rebound effects under rolling

1 Data shown in Appendix 1.

Fig.20 Calibration of the water filled rubber ball (WFRB) at 22°C under combinations of hydrostatic stress and deviator loading.

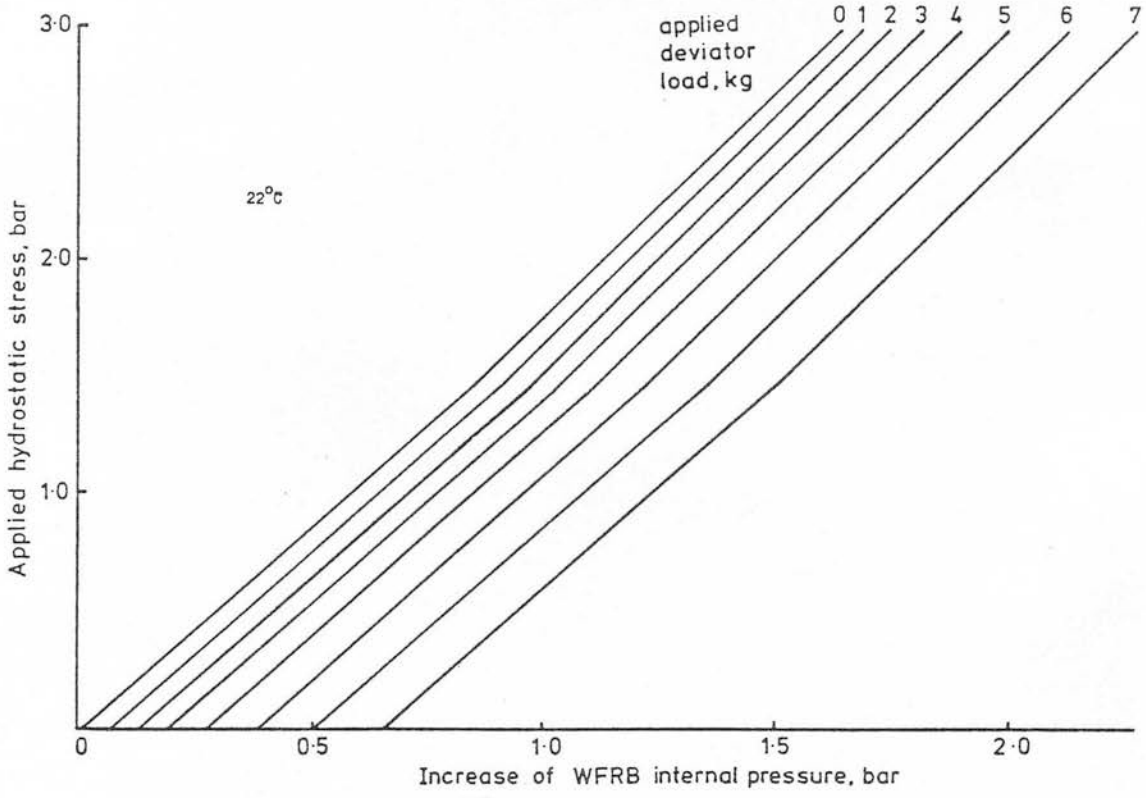


Fig.21 Dynamic responses of the water filled rubber ball to rapid increases of stress; a, d and e weight released from 2 cm above the ball; b and c weight released when touching the ball.

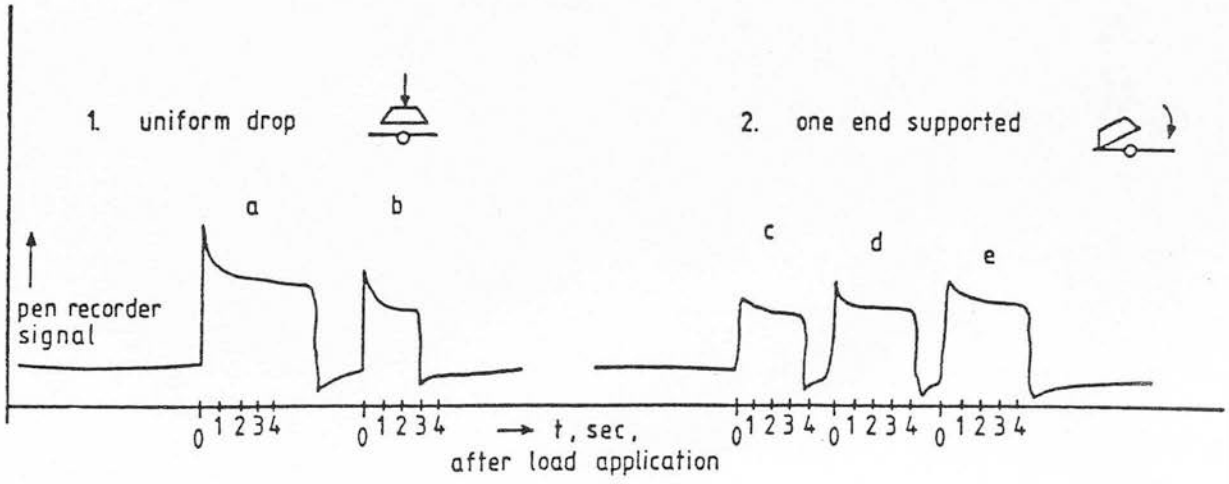

wheels with constant forward speed would be negligible.

The reliability of the WFRB was examined by subjecting a sample of six balls to repeated loadings in a modified 'Swedish' compaction apparatus, after Håkansson (1974). Of the total number of loadings (36) only 5 per cent showed signs of leakage at the ball/tube joints. This was considered reliable enough for field use.

The calibration of deformation of the mastic ball under deviator stress (see Fig.22 ) was carried out with the apparatus used to apply pure deviator stress to the WFRB.[1] The calibration curves for different temperatures are shown in Fig.23. Between each loading the balls were remoulded to their original shape, as in the field the balls would be spherical before loading. A recalibration after use in the field tests is shown also in Fig.23. These results reveal some changes of stiffness, presumably due to evaporation of the mastic's lubricant.

Thus, it was established that the two spherical devices could be used to identify compressive and shearing stresses and estimates of $\sigma_1$ and $\sigma_3$ could be derived from them in more simple stress systems (where $\sigma_2 \doteq \sigma_3$). The devices were also very inexpensive and easily constructed. The low cost and ease of construction made feasible the use of large numbers of devices, buried in field soils for long periods of time before or between tests.

## 3.3 Dry Bulk Density In Situ

Gamma-ray transmission, employing the equipment available at the SIAE[2] (Soane, 1977), was used to measure dry bulk density.[3] Compared to many other techniques of in situ measurement of bulk density, it

1. Data shown in Appendix 1. 2. Scottish Institute of Agricultural Engineering.
3. The equipment is shown in Fig.25a.

Fig.22 Mastic balls with and without deformation by deviator loads. left: no load; centre: 0.5 kg; right: 3.5 kg (all at 19°C).

Fig.23 Calibration of the minor axis length of the mastic ball at different temperatures under deviator loading, before and after the field tests.

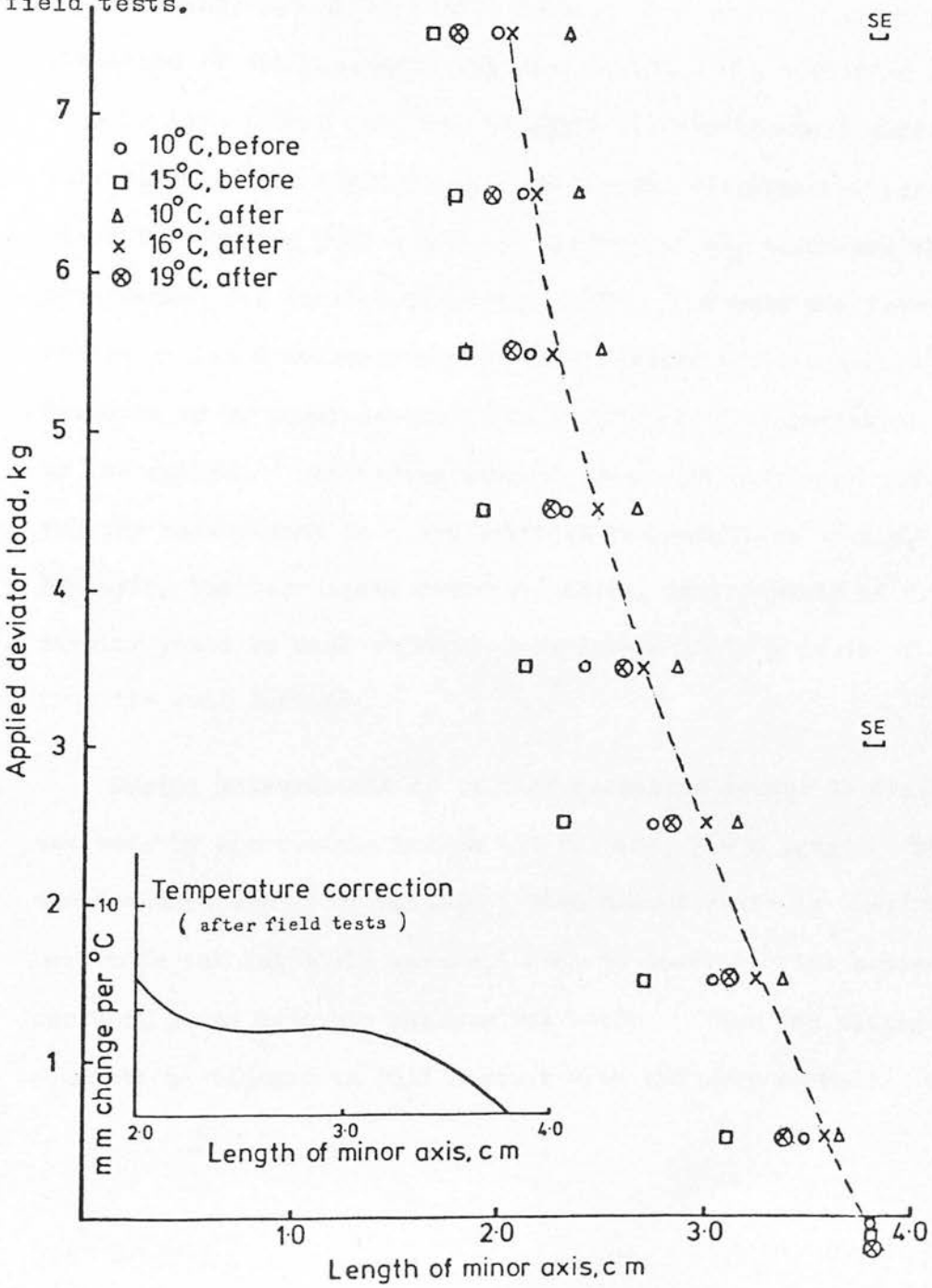

is less destructive and time-consuming (Soane et al. 1971). Possible inaccuracies caused by probe bending (Soane, 1977; Raghavan et al. 1976a) were reduced during later field work by using access holes of larger diameter (2.5 cm) than the probe tubes (2.1 cm). Errors from changes of sample thickness remained, but were of a smaller order than those created by probe bending changing the distance between the source and detector. Surface resolution was improved by keeping the alignment jig in position while the probes were inserted into the access holes. Soane (1974a) has shown that a surface absorber of similar construction to the alignment jig will maintain the variation of count rate to less than 5 per cent beyond 7 cm from the soil surface. Variations of the readings by random count fluctuations were minimised by counting 5000 gamma-ray interceptions, a maximum value recommended for field work (Soane, 1977). Stones can introduce errors in field measurements by interference between source and detector or by local decompaction following displacement of stones by the spikes. Discarding results from such positions and repeating the measurement in a new position reduced these errors. Employing the techniques described above, measurements of dry bulk density could be made at every 3 cm from 6 cm to a depth of 42 cm from the soil surface.

During measurements of initial densities access to field plots was made by lightweight bridge (50 cm wide, 2.8 m long). This avoided unnecessary trampling. When measurements in wheel tracks were made the lug marks were cut away to create a flat horizontal surface, level with the maximum rut depth. Thus the alignment jig could be positioned in full contact with the soil surface; the

depth from the original soil surface to the base of the jig was measured for each position.

## 3.4 Soil Moisture Conditions, In Situ

### 3.4.1 Soil moisture content

A gravimetric method, using oven drying at 105°C for 24 hours, was used. Samples were collected at 6 or 12 cm intervals to 36 cm depth, according to the field site. Access to the plots was provided by the bridge. Automatic weighing methods (Henshall, 1978) improved efficiency during later work.

### 3.4.2 Soil moisture tension

Two techniques were employed, according to the range of tensions present. Mercury manometer tensiometers measured the range 0–800 millibars and gypsum resistance blocks measured tensions above 800 millibars. Berryman et al. (1976) described the basic construction and use of the mercury manometer tensiometers; minor modifications were made to suit the particular needs of the experiment. The resistance of the Gypsum Blocks (Soil Moisture Equipment Corp. Cat. No.5200) changed according to soil moisture tension in the blocks. The resistance was measured by a 'Moisture Meter' (Soil Moisture Equipment Corp. Cat.No.5410). The blocks were calibrated as follows to check the manufacturer's specification.

A pressure plate apparatus, described by Richards (1965), was modified to accommodate the blocks and enable electric connections to be made. Three blocks, chosen randomly from the total number to be used in the experiment, were tested. Before the series of measurements the blocks were saturated and covered in saturated

kaolin ( < 2mm). Measurements of vessel pressure, bottle supply pressure, meter reading and volume of drained water were made every 12 or 24 hours. Results are shown in Table 6[1] and periods of equilibrium indicated. A correction to moisture meter readings was needed because of the differences between readings made by direct electrical connections and those made through the walls of the pressure vessel (see Table 6[1]). Equilibrium conditions were defined as two similar consecutive readings of the moisture meter and volume of drained water. For each equilibrium condition the block resistance is plotted against soil moisture tension in Fig.24.

Comparison of the measured calibration points with the manufacturer's calibration curve revealed that the measured calibration had greater variability and the measured calibration at 3 to 5 bar showed higher resistances than the manufacturer's curve.

The former observation may be explained by variations between dimensions of the manufactured blocks, the latter by air leakages at high pressures causing drying; evidence of leaks is provided by the drop in pressure of the compressed air supply bottles.

The correspondence between measured and manufacturer's calibration was considered close enough to use the manufacturer's calibration curve with a larger range between maximum and minimum readings at one moisture tension.

---

1 Appendix 2.

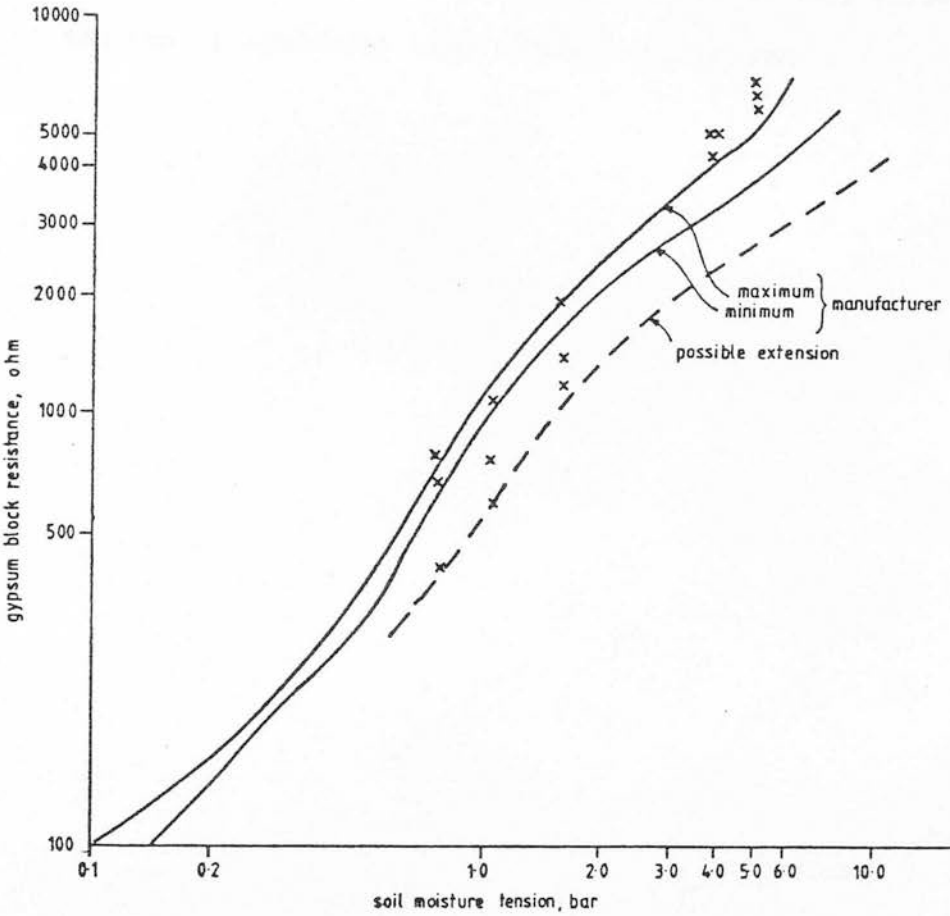


Fig.24 Comparison of the gypsum block calibration curve provided by the manufacturer with the 'equilibrium' conditions for each block tested in the pressure vessel. Each point represents an individual block at one 'equilibrium' condition.

When installed in the experimental plots the tensiometers were either all placed at 15 cm or at 10 cm intervals to 30 cm depth. The blocks were installed at 10 and 30 cm in a 'pocket' of silt to improve contact with the soil during soil shrinkage (Berryman et al. 1976). This gave measurements of soil moisture tension representative of the upper 30 cm of soil while avoiding the use of extremely large amounts of equipment.

## 3.5 Soil Strength, In Situ

### 3.5.1 Cone resistance

An electrically driven, constant velocity penetrometer using a 12.9 mm base, 30° cone (Brown and Anderson, 1975) mounted on a trailer especially designed for field use (Soane, 1974c) was used to measure cone resistance of the field plots. The wide track (2.8 m between wheel centres) of the trailer and the tractor used to manoeuvre it, avoided unnecessary trampling and trafficking of the plots. Analogue signals recording vertical load on the cone, displacement of the cone and soil surface level were collected by a tape recording system. The analogue record was later digitised and analysed by data handling programs using the PDP11 and ERCC Multiple Access computing systems available at SIAE. These techniques gave measurements of cone resistance at 3 cm intervals to a depth of 30 or 33 cm. Calibration of the electronic signal from the penetrometer load cell was made in the field before each occasion the penetrometer was used during 1977.

### 3.5.2 Shear strength

A hand-held shear vane using a 19 mm, four bladed vane (Soane et al. 1977) permitted measurement of vane shear strength at 9 cm intervals to 27 cm depth. The interference between adjacent shear strength measurements required a 9 cm interval between each depth at each location. Access to the plots was made either from adjacent ruts, or by the bridge previously described.

## 3.6 Intransient[1] Soil Factors

Particle size distribution, soil organic matter content, upper and lower plastic limits, Proctor compaction curves, optimum soil

1. As defined by Soane (1975)

moisture content and particle density were measured using standard laboratory tests available at SIAE (Soane and Campbell, 1970). Upper and lower plastic limits were measured by the Casagrande method. Drop-cone measurements (Campbell, 1976) were also made to examine the plastic limit for remoulded soil and the loose, aggregated soil (agg. diam$<$ 1 cm) used in the laboratory tests.

## 3.7 Tyre/Soil Contact Area

### 3.7.1 Direct measurement

The projection of the area of contact on to a horizontal plane for a stationary tyre was assumed to be essentially identical to that of a slowly moving tyre; measurement of the latter being much more difficult. Spray paint colouring the soil adjacent to the wheel was used to mark the edges of the contact zone, when the wheel was moved (preferably in reverse to avoid extra disturbance of the marks) the area within the coloured soil could be measured. A clear perspex sheet with a 4 cm square grid was placed over the contact zone and the area of the horizontal projection of the zone determined by square counting. The zone was traced out on the grid with an erasable marker and the number of whole and partial squares in the zone counted. Contact area ($cm^2$) was calculated from the expression

$$\text{Contact Area} = (\text{number of whole squares} + \text{number of partial squares}/2)) \times 16$$

In very soft soil conditions this measurement was less like the area of the true contact zone, especially in the forward part. In very hard soil conditions the measured area was principally that of lug/soil contact. When contact area was measured for a rigid surface the wheel was run onto a sheet of paper before spraying.

### 3.7.2 Indirect measurement

The inconvenience of direct contact area measurements during the field experiments, and their time-consuming nature, necessitated the design of a more convenient, indirect measurement. A relationship was expected between sinkage and contact area of each wheel treatment. Measurements of sinkage were derived from assessment of the cross-sectional shape of the rut. A relief-meter (Burwell et al. 1963) depicted in Fig.25b was a suitable instrument for this. The presence of a lug pattern in the wheel rut required the following systematic positioning of the meter. For each measurement of cross-sectional shape the meter was placed transverse to the centre-line. The first needle in sequence (from left to right) which fell inside the wheelmark was arranged to fall in a lug mark. This needle was always at the left hand edge of the wheelmark, looking in the direction of wheel motion. The soil surface adjacent to the rut was determined from the mean of five needle readings on either side of the rut. Thus surface depression at 5 cm intervals across the rut could be measured.

## 3.8 Other Wheel Factors

A vehicle weighbridge, available at SIAE, was used to measure the static load on the rear wheels used during the tests. This was assumed the same as the dynamic load as the tractor had no drawbar load. Tyre inflation pressure was measured with an accurate tyre pressure gauge. Wheel forward speed was measured by timing the wheel over a fixed distance. Wheelslip was measured by recording the distance covered by a fixed number of revolutions of the wheel, and comparison with the expected 'no slip' distance.

Fig.25a The gamma-ray transmission equipment. The auger for soil moisture samples, alignment jig and spikes, probes (22 cm spacing) and transport trolley with scaler are shown.

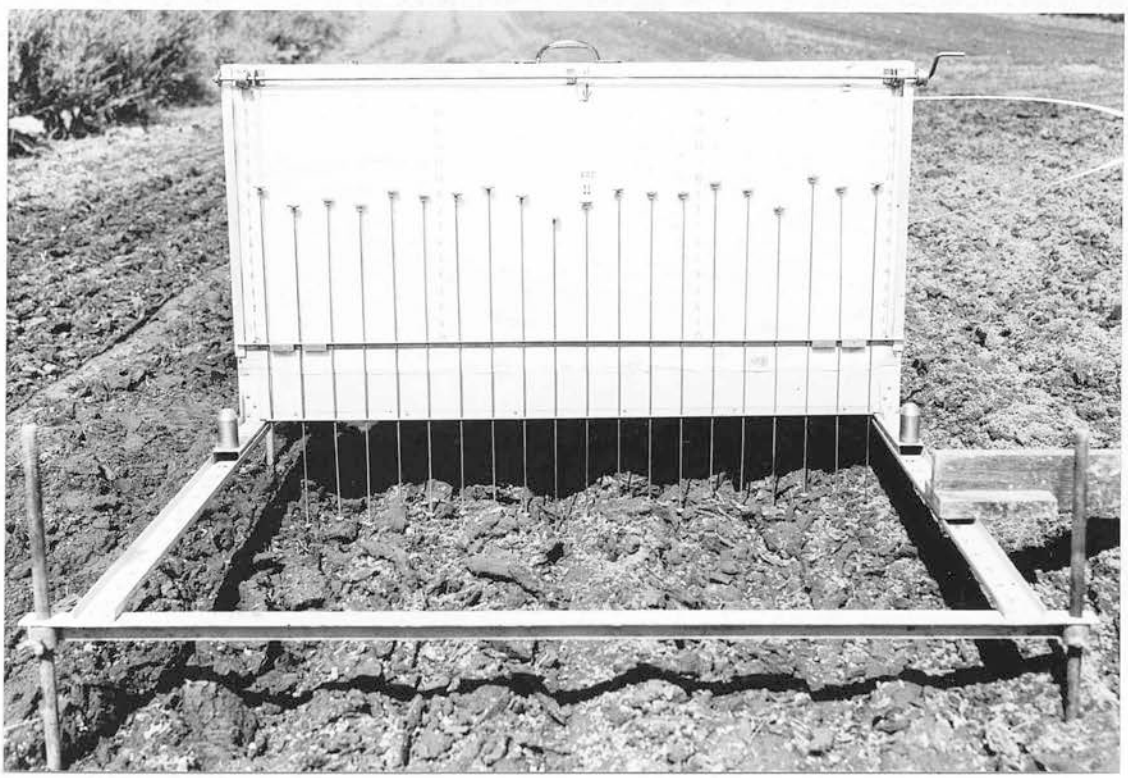

Fig.25b The needle reliefmeter used to describe transverse rut profiles.

## 3.9 Laboratory Measurement of Stresses and Strains of Disturbed and 'Undisturbed' Soil

A wheel with tyre/soil contact length of 50 cm and a forward speed of 1 km/h was estimated to be above any one part of the soil for approximately 2 seconds; simulation of this stress period was attempted in the laboratory.

### 3.9.1 Equipment for stress application

Spherical pressures (P) were applied using the parts of a Farnell triaxial machine able to apply different levels of hydrostatic stress to a sample. The pressure cell of the machine had an internal height of 48 cm, internal diameter of 22 cm and a recommended maximum cell pressure of 10 bar. A cross-section of the cell is shown in Fig.26a. Air from a compressed air cylinder was used for cell pressurisation, after Dexter and Tanner (1973). Sealing of air leaks from the cell base and between the rubber membrane and sample base was improved by a 2 to 3 cm depth of water over the bottom of the cell. Variation of cell pressure caused by sample deformation was corrected by allowing more air into the cell through tap 'A' or releasing air through air bleed tap 'C'. Cell pressures were increased in steps. Steps of approximately 0.03 bar were used below 0.1 bar; steps of 0.1 bar from 0.1 bar to 1 bar and steps of 1 bar above 1 bar. Often a measurement at 1.5 bar was also found convenient due to the use of a log-scale for P. Each step was applied at approximately 0.05 bar/s and maintained for approximately one minute by manual control of the inlet tap 'A' and the pressure regulators

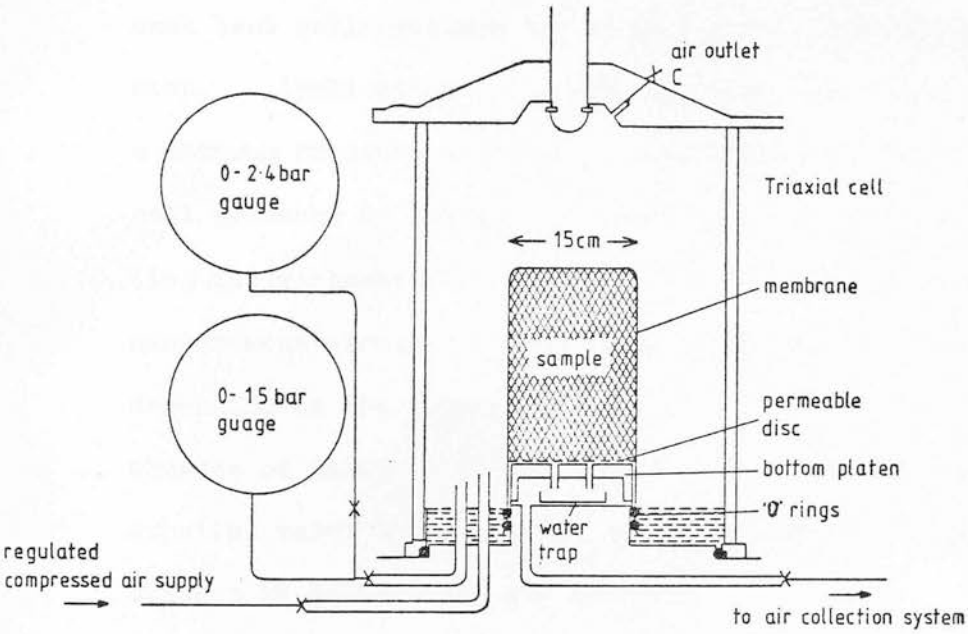


Fig.26a A cross section of the triaxial cell and a mounted sample of loose soil.

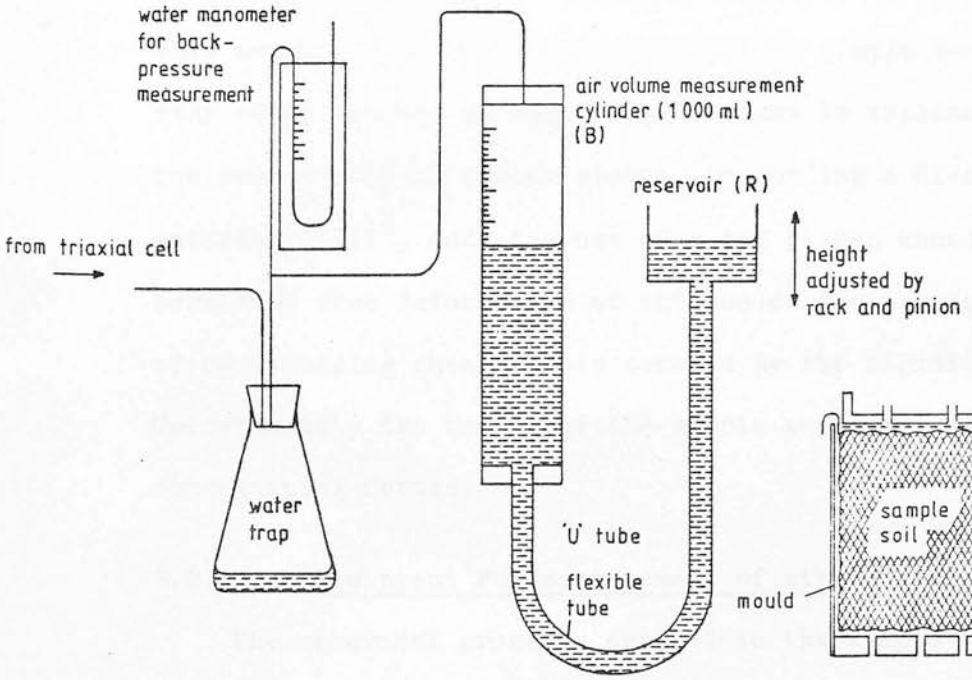


Fig.26b The apparatus for the collection of air expelled from the sample and measurement of the air volume.




Fig.26c The preparation of a loose soil sample for mounting in the triaxial machine

controlling the supply of compressed air. This allowed dissipation of sample pore air pressure at each pressure step. During each test cell pressure was reduced to 0.2 bar after the 1.0 bar step. Application of further pressure steps then continued until a maximum pressure was reached, followed by a final reduction of cell pressure to 0.2 bar. (This relaxed the sample without letting the membrane part from the sample and cause volume measurement errors.) The maximum pressure was 5.0 to 8.0 bar depending on the amount of sample deformation and the presence or absence of water in the air collection system; a large amount of expelled water would inhibit the measurement of sample volume changes by restricting air movement.

Stresses were applied to a 15 cm diameter, 15 cm high soil sample while confined in a rubber membrane, see Fig.26a. This membrane offered less constraint to sample deformation than many other methods of sample confinement in triaxial tests. Closing one end of a 15 cm rubber sleeve, by bonding a disc of the same material to it[1], made the use of a top platen unnecessary. This permitted free deformation of the top of the sample by an absence of constraining shear forces created by the rigidity of a platen. Unfortunately the bottom of the sample was still affected by such constraining forces.

### 3.9.2 Equipment for measurement of stress and strain

The spherical pressure applied to the sample was a constant function of cell pressure (P = cell pressure x $\sqrt{3}$). Cell pressure was measured by two Budenberg test gauges; one gauge covered the range 0 to 2.4 bar, the other 1 to 8 bar (each was

1. A cyanocrylate glue was used for the bond.

accurate to 1 per cent full-scale deflection). Thus each gauge had a different sensitivity and was more suitable for either high or low pressures.

Sample strain was measured as changes of sample volume. This change of volume was measured by the volume of air expelled from the soil and was converted to changes of dry bulk density using the mass and moisture content of the sample. The volume of air expelled during each pressure step passed through the permeable disc of fabric at the base of the sample, though the holes in the bottom platen and into the air collection tube, see Fig. 26b. A small tray under the bottom platen, and a water trap in the air line permitted the collection of any expelled water. The air collection system was a large scale, water-filled 'U' tube, designed after Bishop and Henkel (1967) and Davies et al. (1973b).

The expelled air depressed the meniscus in one arm of this U tube 'B' made from a graduated measuring cylinder. The volume change could be measured on the graduations to $\pm$ 5 ml. (This error lay within 5 per cent of the total sample volume.) Depression of the water surface in one arm of the U tube would create a back pressure in the air collection system. This change of pressure was monitored by a water manometer in the air collection system. Raising or lowering reservoir 'R', Fig. 26b., at the end of the U tube open to the atmosphere could correct the pressure in the air collection system to zero. A rack and pinion mechanism enabled a precise alteration of the height of the reservoir. Volume readings uncorrected for back pressure were taken 2 s and 30 s after the application of each pressure step, as well as the

water manometer reading of back pressure. Volume readings corrected for back pressure, by adjustment of reservoir 'R', were also taken after 30 s. As the back pressure remained very steady after approximately 1 s from pressure application, it was assumed that the 30 s volume correction for back pressure could be used to correct the 2 s volume reading.

Absolute values of dry bulk density of each sample required the determination of initial or final sample volume. Measurement of final sample volume by a wax coating method was more precise than an estimation of the initial volume from the sample shape before testing (approximately a cylinder). A 20 cm deep bath of molten paraffin wax, maintained between 55 and 60°C, accommodated the final compressed soil sample held in a wire basket. Two or three quick immersions were required to seal the sample surface, yet prevent heating and expansion of the remaining pore air. A 30 cm deep water displacement bath and a 2 litre measuring cylinder provided the volume of sample, basket and wax. Weighing of soil, basket and wax in the appropriate combinations enabled calculation of the final soil volume.

Table 7 is an example of a results sheet for one test. Computer programs, developed for a programmable calculator and stored on magnetic cards, were made for the calculation of corrected volumes and dry bulk densities at 2 and 30 seconds after each pressure step. The equations are described in Appendix 3.

### 3.9.3. Sample preparation

Disturbed samples for testing of loose soil were collected by spade while 'undisturbed' samples were removed by a method similar

TABLE 7 EXAMPLE OF LABORATORY TEST DATA

TRIAXIAL TESTING Date: 10.4.78 Operators: PSB, DS

SOIL: Macmerry S7 1387(2) Wax = 0.76 g/cm$^3$

INITIAL MOISTURE CONTENT: Tin No. = 379, Wet wt. = 263.76g, Dry wt. = 248.16 g, w (% w/w) = 8.82%

INITIAL MASS: Membrane + mould + fabric disc + 'O' rings + platen = 2201 g

Soil + " " " " " " = 4892 g, soil = 2691 g

Sample packing: loose, <1 cm

dry fabric = 10.74 g, wet fabric = 11.74 g. Dry tray = 23.72 g, wet tray = 23.72 g

FINAL VOLUME: basket = 247.98 g, basket + soil = 2934 g, basket + soil + wax = 3119 g

wax = 185 g, soil = 2686 g: Displaced water = 1960 cc − 39 cc (basket),

Volume of wax = 243 cc, Volume of soil = 1677.6 cc

| Cell pressure, bar | Air volume reading, cc 2s | 30s | Water manometer, cm | Air volume reading, cc corrected for back pressure 2s | 30s | Dbd, 30s g/cm$^3$ |
|---|---|---|---|---|---|---|
| 0 | 140 | 140 | 5.8 | 140 | 140 | 1.056 |
| 0.03 | 190 | 205 | 4.4 | 200 | 215 | 1.091 |
| 0.05 | 240 | 247.5 | 5.2 | 242.5 | 250 | 1.108 |
| 0.08 | 275 | 277.5 | 5.2 | 277.5 | 280 | 1.123 |
| 0.1 | 295 | 300 | 5.5 | 295 | 300 | 1.134 |
| 0.2 | 350 | 355 | 4.7 | 355 | 360 | 1.166 |
| 0.3 | 390 | 395 | 5.2 | 395 | 400 | 1.189 |
| 0.4 | 415 | 422.5 | 5.4 | 420 | 427.5 | 1.205 |
| 0.5 | 440 | 445 | 5.4 | 445 | 450 | 1.218 |
| 0.7 | 470 | 480 | 5.2 | 477.5 | 487.5 | 1.242 |
| 1.0 | 510 | 520 | 5.2 | 515 | 525 | 1.266 |
| 0.2 | relaxed to | | | 510 | 510 | 1.256 |
| 1.5 | 552.5 | 562.5 | 4.7 | 560 | 570 | 1.296 |
| 2.0 | 590 | 600 | 5.1 | 597.5 | 607.5 | 1.322 |
| 3.0 | 645 | 655 | 5.0 | 650 | 660 | 1.361 |
| 4.0 | 690 | 700 | 5.0 | 697.5 | 707.5 | 1.397 |
| 5.0 | 730 | 740 | 5.1 | 737.5 | 747.5 | 1.430 |
| 6.0 | 765 | 775 | 5.3 | 770 | 780 | 1.458 |
| 7.0 | 800 | 810 | 5.4 | 807.5 | 817.5 | 1.491 |
| 0.2 | relaxed to | | | 782.5 | 782.5 | 1.460 |

to that used by Yaacob (1976) with large cylindrical cores. The metal cylinders for the cores were 40 cm high, 45 cm internal diameter and made of 5 mm thick mild steel with a lower cutting edge tapered to displace soil outwards from the cylinder centre. When used, each cylinder was driven into the soil by hammering a wooden block on a round (50 cm diameter) 3 cm thick steel plate resting on the top of the cylinder. Approximately 5 cm of the cylinder remained above the soil surface after insertion. The whole cylinder and enclosed soil core was removed by digging away the soil around the outside of the cylinder, inserting a spade under the core and carefully levering the soil core away from the remaining field soil. The core was then cut square with the end of the cylinder, placed upright on a tray of loose soil and carefully transported to the laboratory. Fig. 27 shows a complete cylinder and core.

'Undisturbed' samples were taken without any adjustment of the soil moisture content. Disturbed samples were collected when the soil moisture content was near field capacity and allowed to dry while spread thinly on trays in the laboratory. When the weight of the soil and tray indicated a suitable moisture content the soil was sealed in bags for 24 h to allow even distribution of soil moisture.

Loose soil samples were sieved to 1 cm removing stones, vegetation and larger aggregates. Approximately 2 kg of this soil was poured into the membrane lining a mould, see Fig. 26c. After levelling with the top of the mould the loose soil was covered by a disc of permeable fabric and a detachable bottom platen put on

Fig.27 A complete soil core and cylinder soon after removal from the field.

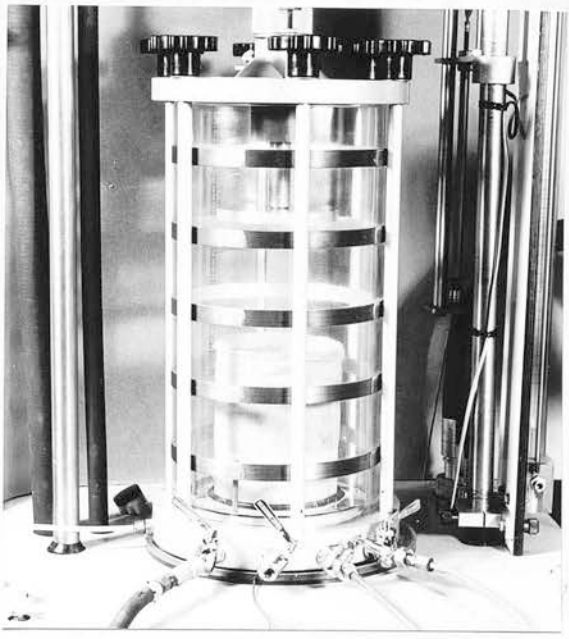

Fig.28 The triaxial compression cell with a sample of loose soil prepared for testing.

Fig.29 A soil core with the cylinder removed. Some loss of soil has occurred from the top, right-hand edge.

Fig.30 An 'undisturbed' soil core after being trimmed to 15 cm diameter.

the sample. The whole unit was weighed before careful inversion onto the pedestal of the triaxial machine and location of the two 'O' rings to seal the membrane. This technique caused very little disturbance of the initially loose soil. Fig.28 shows a loose sample prepared in the triaxial machine.

The large 'undisturbed' cores required trimming before mounting. The size of the field core enabled a central core of 15 cm diameter and 15 cm height to remain as little disturbed as possible. The cylinders were removed from the cores by carefully displacing a 5 mm annulus of soil adjacent to the inside of the cylinder with thin metal rods and flat lengths of wood 5 mm thick and 2 cm wide. The cylinder could then be lifted clear of the soil core. Fig.29 shows a soil core with the cylinder removed. Each core was then trimmed back from each outside edge using a sharp steel spatula until the remaining core was a close fit in a 23 cm length of plastic tubing of 15 cm internal diameter. Fig.30 shows a trimmed core. The 15 cm core was then covered by the membrane, cut square at 15 cm length and placed on the bottom platen in the triaxial machine.

### 3.9.4 Precision tests

Information was required on the variability inherent in the test process. A uniform, well remoulded Macmerry topsoil was used. After air drying, and mechanical mixing for one hour, the soil was sieved to 2 mm, wetted to a moisture content of 7 or 8.5 per cent (w/w) and sealed for 24 h. The results are shown in Fig.31. Virgin compression lines were more evident for the tests at a moisture content of 8.5 per cent (w/w). A mean slope of the

Fig.31 The results of tests upon the precision of the equipment for triaxial compression. Soil: Macmerry, aggregates < 2 mm diam.

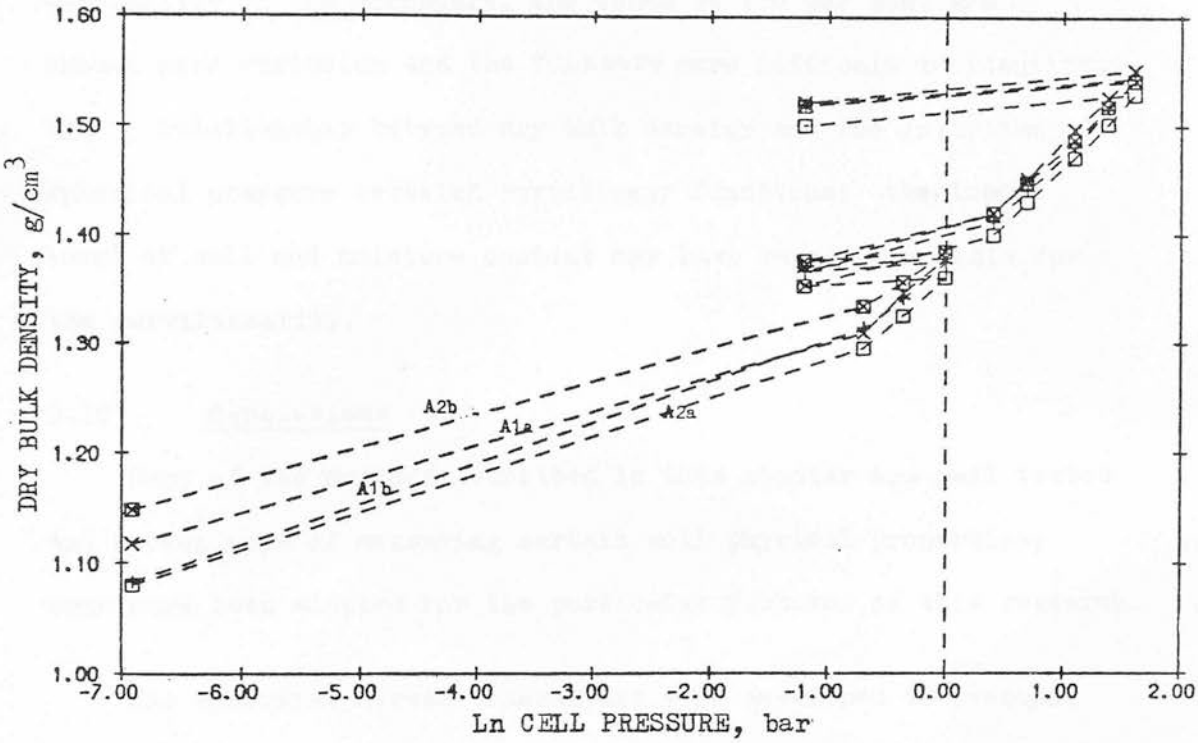


a. Mean soil moisture content 8%, w/w.

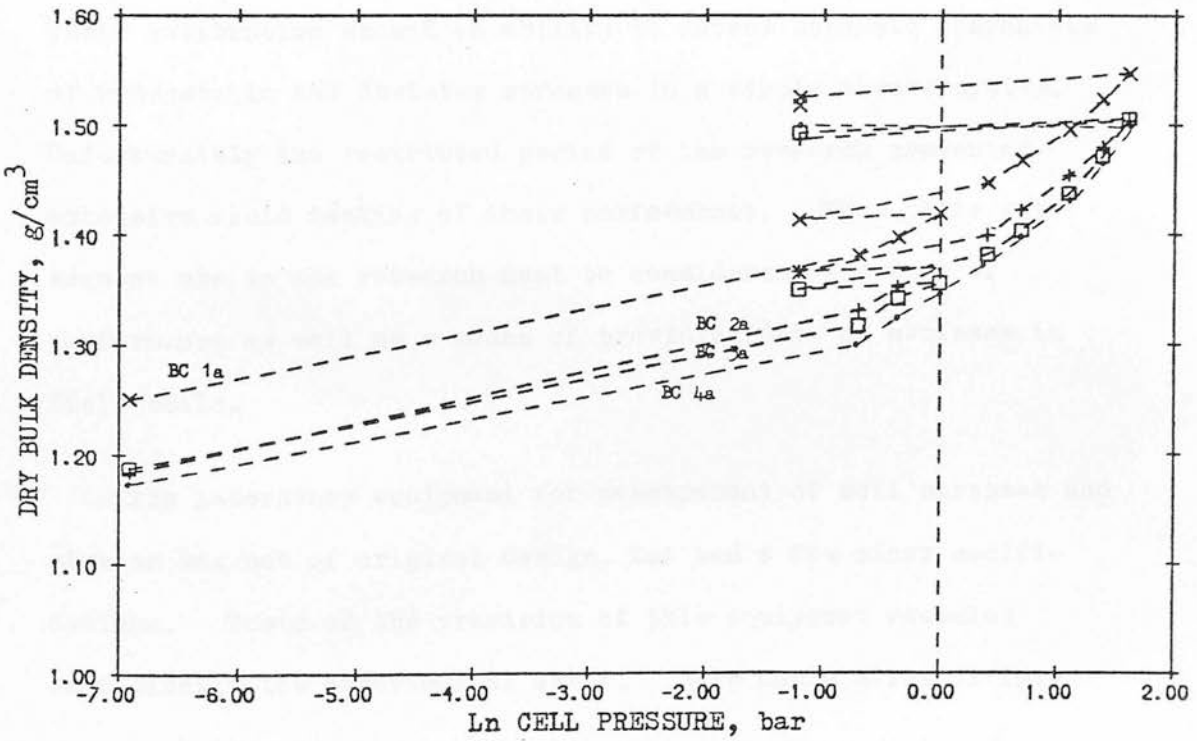


b. Mean soil moisture content 7%, w/w.

VCL of 0.233 $g/cm^3$ unit ln P and mean intercept of 1.428 $g/cm^3$ were found with standard deviations of 0.005 and 0.009 respectively. Although this was an acceptably low level of variability of the procedure, the tests at 7.0 per cent w/w showed more variation and the VCLs were more difficult to identify. The relationship between dry bulk density and the logarithm of spherical pressure revealed curvilinear functions; the lower level of soil and moisture content may have been responsible for the curvilinearity.

## 3.10 Conclusions

Many of the methods described in this chapter are well tested and proven ways of measuring certain soil physical properties; some have been adapted for the particular purposes of this research.

The spherical stress transducers were developed to overcome some problems associated with rigid strain gauged-diaphragm transducers and reduce the instrumentation costs of the research. Their calibration showed an ability to detect separate components of hydrostatic and deviator stresses in a simple stress system. Unfortunately the restricted period of the research prevented extensive field testing of their performance. Thus their subsequent use in the research must be considered as a test of performance as well as a means of providing data on stresses in field soils.

The laboratory equipment for measurement of soil stresses and strains was not of original design, but had a few minor modifications. Tests of the precision of this equipment revealed sufficiently low experimental error. This could allow differ-

ences between slopes and between intercept of virgin compression lines of 0.015 $g/cm^3$/unit lnP and 0.03 $g/cm^3$ respectively to be identified at $P < 0.05$ (three times the standard deviations of the precision tests).

# CHAPTER 4 - EXPERIMENTAL DESIGN

Satisfactory experimental design required the incorporation of the methods of measurement with the experimental aims in a way suitable for valid statistical analysis of the results. Three large scale field experiments for the measurement of *in situ* stresses and strains, one soil tank experiment for studies of tyre contact area, one laboratory experiment for measurement of soil stresses and strains and two field tests are described in this chapter.

## 4.1 Field Compaction Experiments (c.f. Sect.2.4 aim 5)

### 4.1.1 1976, SIAE, Section 7

The geographical location of the site was NT 243641. Soil of the Macmerry series, stoney phase, was present (Ragg and Futty, 1967). Measurements of intransient soil factors had been made for previous research (Soane and Campbell, 1967) and are presented in Chapter 5. Texture of the upper 30 cm was sandy loam, a suitable example of a coarser textured soil and one commonly used for cereal production in lowland Scotland.

Fig.32 shows the plan of the site. The sets of experimental runs were made on four different occasions, each with different soil moisture conditions. Each set of runs used one of the sets of blocks marked 'M'. Within each M block three different 'wheel treatments', described in Table 4[1], were used; marked as 'W' on the plan. The experimental wheel ran over soils of four different bulk density profiles. These were prepared in strips transverse to the direction of the experimental wheel; indicated as

1 Section 3.1 and Figs.45 and 46.

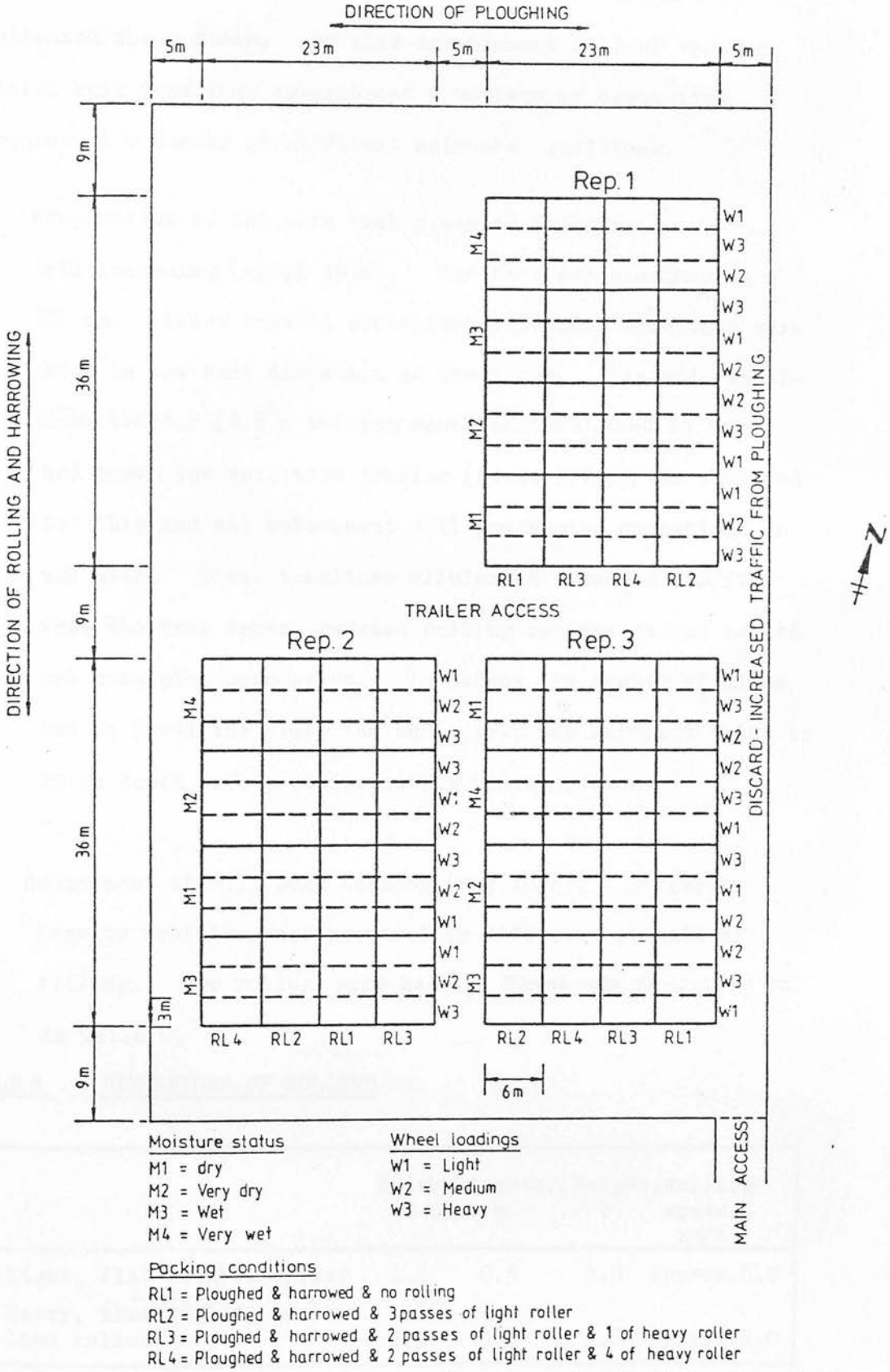


Fig.32 The field plan for the compaction experiment at Section 7, SIAE, 1976, Macmerry soil.

'RL' values on the plan. All experimental treatments were replicated three times. By this arrangement soil of various initial bulk densities experienced a variety of compacting stresses at a number of different moisture conditions.

Preparation of the site took place as follows:

1. Soil loosening (April 1976). The area was ploughed to 25 cm. After initial consolidation, access tramlines were made in the same direction as the slope. The wide wheel-track tractor (2.8 m between wheel centres), used to tow and power the soil test trailer (Soane, 1974c), was employed for this and all subsequent soil processing operations on the site. These tramlines eliminated unwanted traffic from the test areas, reduced rolling resistance and marked out some plot boundaries. To reduce the number of clods and to level the plots the whole area was harrowed twice to 25 cm depth with a reciprocating harrow (Vicon).

2. Adjustment of soil bulk density (May 1976). Different density profiles were prepared by different amounts of rolling. Two rollers were used. These are described in in Table 8.

TABLE 8 DIMENSIONS OF ROLLERS

| | Width, m | Diameter, m | Weight, t | Rolling speed, km/h |
|---|---|---|---|---|
| a. Light, flat seedbed roller | 2.6 | 0.5 | 0.8 | approx.8.0 |
| b. Heavy, sand filled, grass-land roller | 2.5 | 0.8 | 2.8 | approx.8.0 |

Trial runs made on discard areas allowed the numbers of passes of each roller to be decided for each of the required bulk density profiles. Loosest, very firm and two intermediate conditions were required. The amounts of rolling used to prepare each 'treatment' are described in Table 9 .

TABLE 9 INITIAL DRY BULK DENSITY, Section 7, 1976

| Soil Treatment | Mean bulk density, 0 - 30 cm | Amount of rolling |
|---|---|---|
| RL1 | 1.025 g/cm$^3$ | None |
| RL2 | 1.126 " | Three passes of light roller |
| RL3 | 1.235 " | 2 passes of light and 1 of heavy |
| RL4 | 1.297 " | 2 passes of light and 4 of heavy |

When the plots were rolled the soil moisture content (% w/w) at 10 and 20 cm were 22.0 and 24.5 per cent respectively, equivalent to a soil moisture tension of approximately 90 and 75 millibars. The soil surfaces after treatments RL1, RL3 and RL4 are shown in Figs.33,34 and 35. The corresponding bulk density profiles are shown in Fig.36.

3. Vegetation control. Soil moisture variation was provided by the processes of evaporation, precipitation and drainage in the absence of growing plants; a vegetation-free surface was much easier to maintain than a growing crop and avoided any effect the plant roots could have on soil strength. Regular applications of pre- and post-emergent herbicides were made to keep the plots weed-free. Fig.37 is a general view of the whole site soon after preparation.

Fig.33 Soil rolling treatment RL1 (no rolling), Macmerry soil, 30 cm ruler for scale.

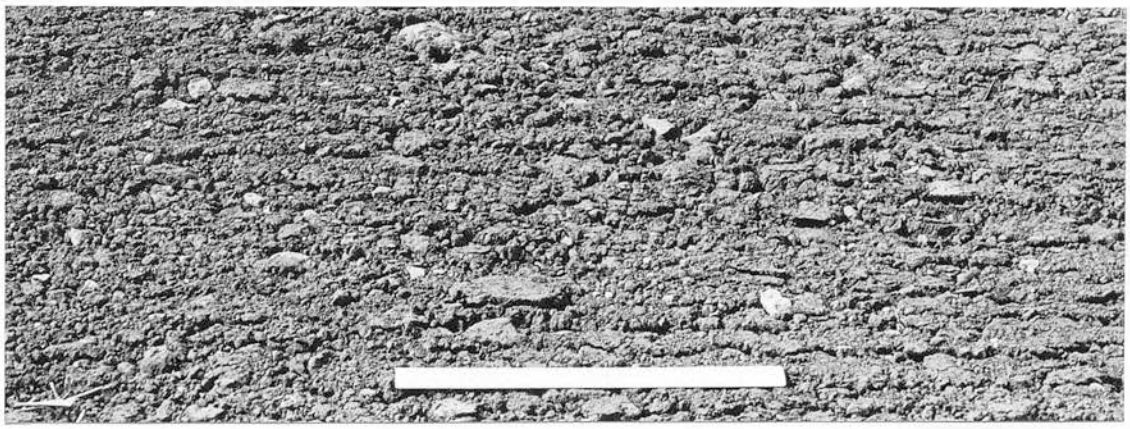

Fig.34 Soil rolling treatment RL3 (two passes of the light roller, one of the heavy roller), Macmerry soil, 30 cm ruler for scale.

Fig.35 Soil treatment RL4 (two passes of the light roller, four of the heavy), Macmerry soil. The same scale as Fig.34.

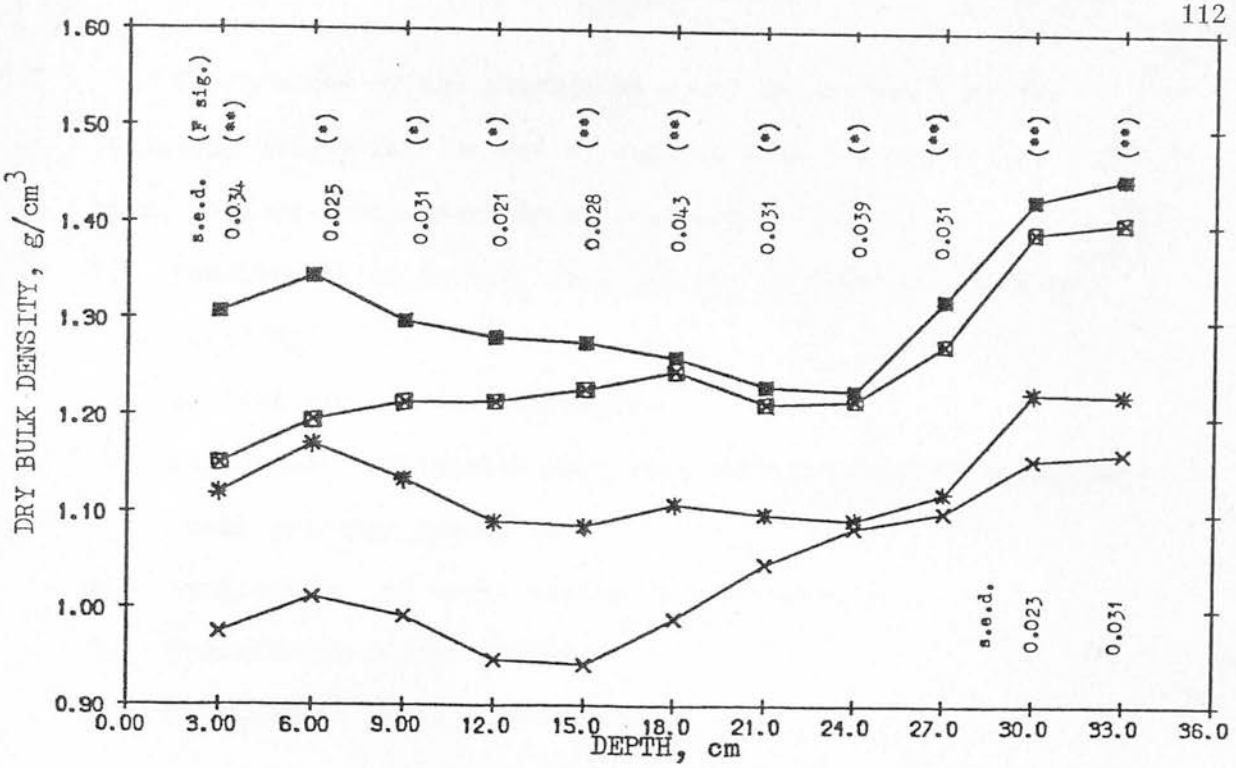


Fig.36 Profiles of initial dry bulk density for each soil treatment (RL), Macmerry soil, Section 7, 1976. Values at 3 cm depth are dubious due to the poor resolution of the gamma ray transmission equipment near the soil surface.

Fig.37 A general view of the experimental site at Section 7 soon after application of the soil rolling treatments.

The conduct of the experiment could be divided into the following stages for the set of runs in each M block of the field plan, used on each experimental occasion.

1. Measurement of initial bulk density profiles (12.5.76 to 8.6.76).
2. Installation of tensiometers.
3. Measurement of initial cone resistances, shear strengths and soil moisture contents.
4. Application of wheel treatments to sub-plots.
5. Measurement of rut profiles.
6. Measurement of final bulk densities.

The locations and numbers of these measurements are shown in Fig.38. Stages 1 and 6 were independent of soil moisture conditions and therefore could be carried out at any suitable time. Stage 2 took place one week before the runs and stages 3, 4 and 5 on the same day.

Dates and approximate field conditions for each M occasion are described in Table10.

TABLE 10 EXPERIMENTAL OCCASIONS, Section 7, 1976
WITH DESCRIPTIONS OF SOIL MOISTURE STATUS FOR EACH OCCASION

| Occasion | Soil moisture conditions | Mean moisture content, 0 - 30 cm (% w/w) | Date |
|---|---|---|---|
| M1 | 'Moist' ( 80) | 23.3 | 22.6.76 |
| M2 | 'Dry' (109) | 20.9 (18, 0 - 12 cm) | 5.8.76 |
| M3 | 'Wet' ( 67) | 25.25 | 12.10.76 |
| M4 | 'Very wet' ( 46) | 28.2 | 2.11.76 |

Mean soil moisture tension (millibars) at 15 cm shown in parentheses.

Fig.38 The location and number of the measurements made in each plot of the field compaction experiments.

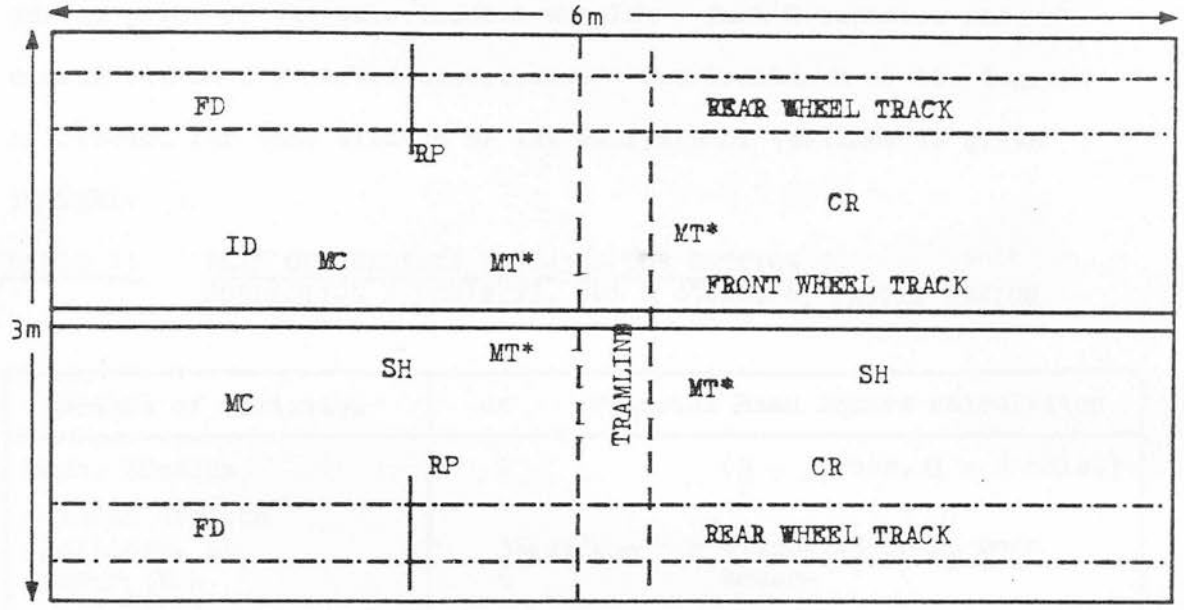


a. Section 7, 1976.

ID = Initial dry bulk density.

FD = Final dry bulk density.

MC = Moisture content, %, w/w.

CR = Initial cone resistance.

SH = Initial vane shear strength.

RP = Rut profile.

MT = Moisture tension.

* = not measured in every plot.

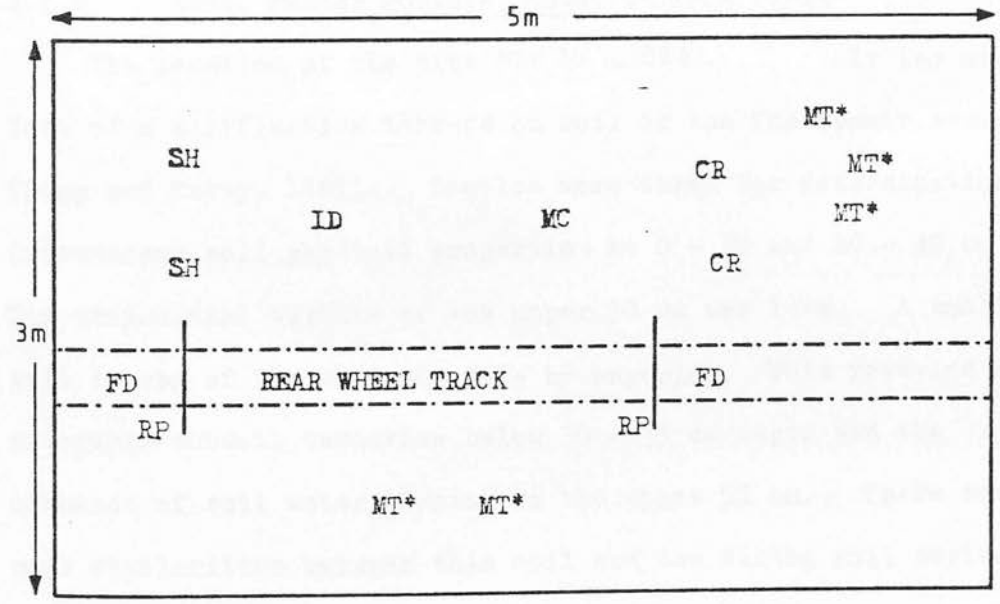


b. Lower Terrace field, 1977.

The layout of the experiment for statistical analysis of the results was based on a 'Tartan' design, strips of rolling running across paths of the experimental wheels. Each M occasion was considered as a separate experiment. The breakdown of the degrees of freedom for each stratum of the analysis of variance is given in Table 11.

TABLE 11 PLAN OF ANALYSIS VARIANCE FOR SECTION 7. COMPACTION EXPERIMENT, ONE M OCCASION, TARTAN DESIGN

| Source of variation | df | Expected Mean Square calculation |
|---|---|---|
| Reps. Stratum | 2 | ($\beta$ = 3 rows, $\alpha$ = 4 cols.) |
| Columns Stratum | | |
| Rollings, RL | 3 | $\beta\sigma_a^2 + \sigma_b^2 =$ [1] estimated by $E_1$ mean square |
| Error$_1$ ($E_1$) | 6 | |
| Sub-rows Stratum | | |
| Wheel treatments, W | 2 | $\alpha\sigma_b^2 + \sigma_c^2$ = estimated by $E_2$ mean square |
| Error$_2$ ($E_2$) | 4 | |
| Cols. x Sub-rows Stratum | | |
| RL x W | 6 | $\sigma_c^2$ = estimated by $E_3$ mean square |
| Error$_3$ ($E_3$) | 12 | |
| TOTAL | 35 | |

4.1.2 1977, Easter Howgate, Lower Terrace field

The location of the site was NT 238640. It lay at the foot of a solifluction terrace on soil of the Threipmuir series (Ragg and Futty, 1967). Samples were taken for determination of intransient soil physical properties at 0 - 20 and 20 - 40 cm depth. The predominant texture of the upper 30 cm was loam. A small scale soil survey of the site was made by augering. This revealed considerable subsoil variation below 30 - 35 cm depth and the presence of soil water gleying in the upper 50 cm. There are some similarities between this soil and the Winton soil series often used for cereal production in lowland Scotland.

1 $\sigma_a^2$, $\sigma_b^2$ & $\sigma_c^2$ are the variances due to rollings, wheels and individual plots respectively.

Fig.39 shows the field plan. Experimental runs were made on three occasions, each at different soil moisture conditions. M, RL and W have the same meaning as in the field plan for the 1976 experiment. The wheel treatments used are described in Table 4, Section 3.1. In this experiment the experimental wheels were run in the same direction as soil rolling; this enabled the soil stress experiment to be incorporated in the same field plan. Again three replications were made.

Preparation of the site took place as follows:

1. Improvement of site drainage (April 1977). A 1 m deep ditch was dug along the south-east side of the site and refilled after a 20 cm layer of gravel was spread at the bottom. This connected the existing field drains and improved site drainage. Measurements made by piezometers after ditch installation showed that sufficient water table movement occurred after heavy rain to allow the upper 50 cm to become unsaturated after two days.
2. Soil loosening (March, 1977). The same procedures as in 1976 were used.
3. Grass establishment (May, 1977). A fast growing grass ("Westergaard" annual rye grass, Lollium multiflorum (Lam.)) was chosen to improve drying of the fine textured soil.[1] Seed was broadcast and hand raked over the whole site, the plots being rolled once with the light roller to assist emergence. Some problems of uneven emergence and weed competition was encountered owing to a very dry period soon after sowing. Height of the grass was maintained at

1 It was recognised that the grass roots may also influence the soil strength.

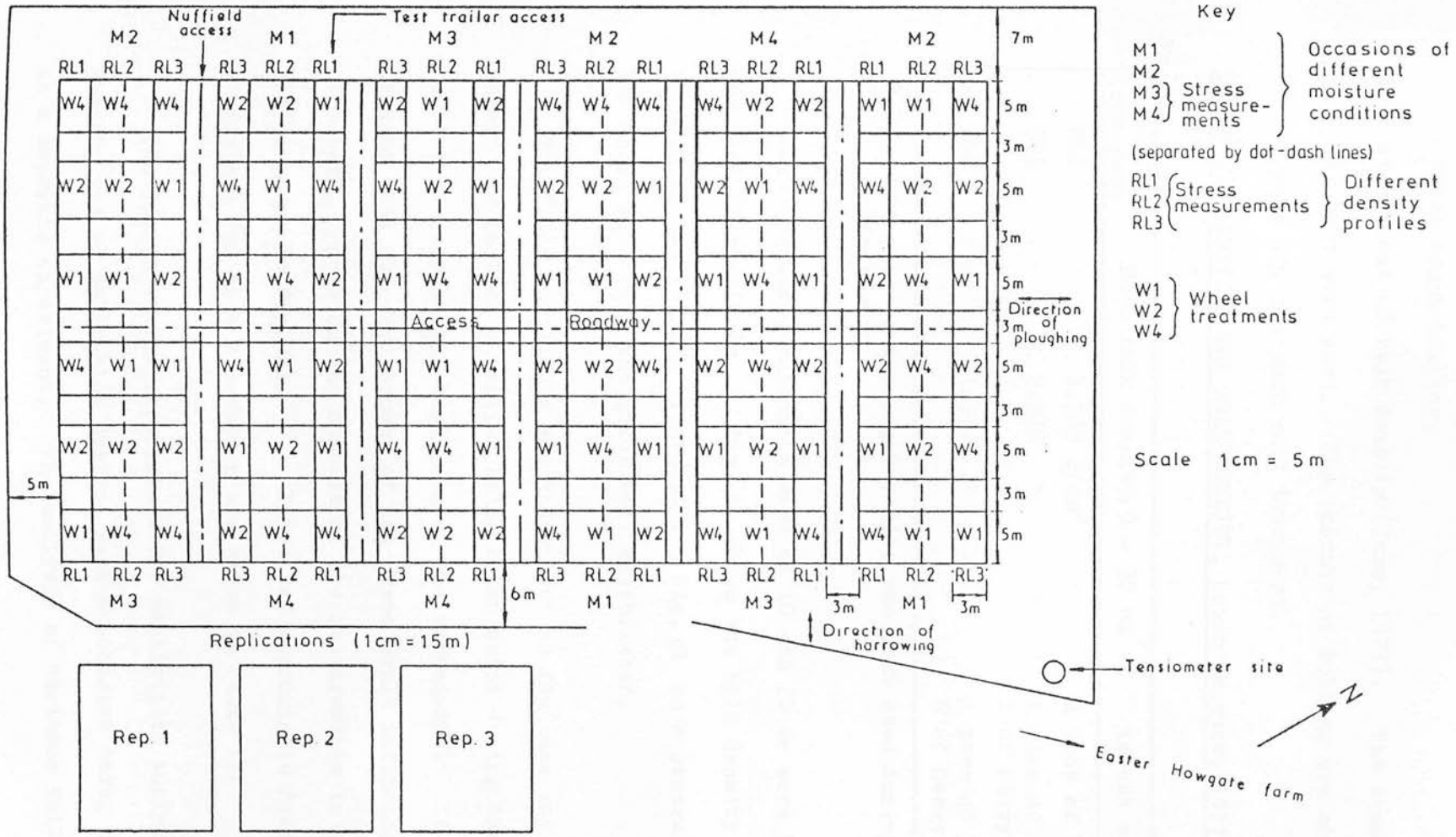


Fig.39 The field plan for the compaction experiment at Lower Terrace field, ESCA, 1977. Threipmuir soil.

approximately 20 cm by a rotary mower mounted on the wide wheel track tractor.

4. Adjustment of bulk density (June, 1977). The same methods as 1976 were used. The amounts of rolling are shown in Table 12, for each soil treatment.

TABLE 12 INITIAL DRY BULK DENSITY, Lower Terrace, 1977

| Soil Treatment | Mean bulk density, 0 - 30 cm | Amount of rolling |
|---|---|---|
| RL1 | 1.189 g/cm$^3$ | 1 pass of light roller |
| RL2 | 1.280 " | 1 pass of light roller, 1 of heavy |
| RL3 | 1.390 " | 1 pass of light roller, 6 of heavy |

N.B. The pass of the light roller was that used during grass sowing.

Soil moisture contents(% w/w) at 10 and 20 cm were 18 and 20 per cent respectively. Fig. 40 shows the bulk density profiles created by the rolling treatments. Fig. 41 is a general view of the whole site with the grass well established.

The field experiment was undertaken in the same way as in 1976 except for initial densities being taken twice during the season instead of only at the beginning of the experiment. It was thought that the development of the grass could influence soil structure. Location and numbers of the measurements in each sub-plot were as in Fig.38b. Dates and approximate field conditions for each M occasion are given in Table 13.

The layout of the experiments for statistical analysis of the results was as split-plot design, each M occasion being considered as a separate experiment. The analysis of variance followed con-

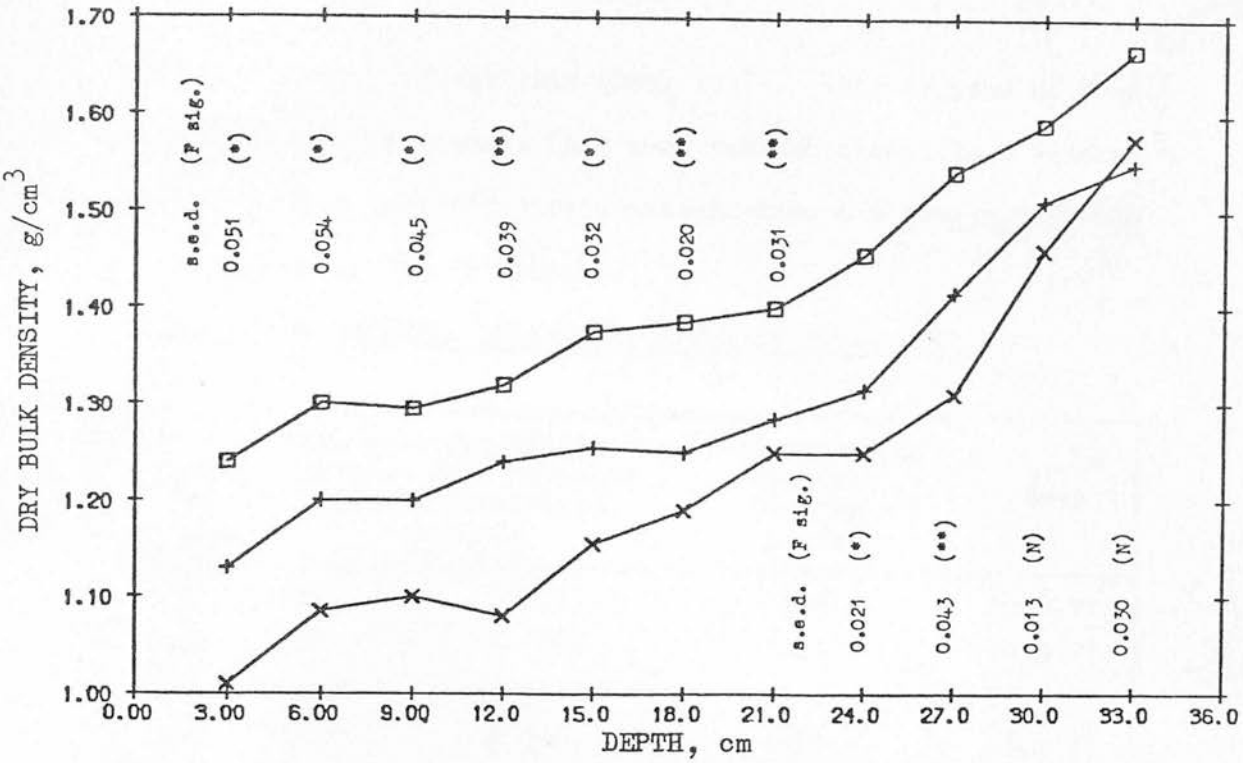


Fig.40 Profiles of initial dry bulk density for each soil treatment (RL), Lower Terrace field, 1977. Threipmuir soil. Values at 3 cm depth are dubious due to poor resolution of the gamma-ray transmission equipment near the soil surface. The profile for each treatment is a mean for all the occasions of measurement.

Fig.41 A general view of the experimental site at Lower Terrace field with the grass well established.

ventional split-plot analysis (Cox, 1958). The degrees of freedom of the main treatments (RL) were reduced from 2 to 1 because RL2 plots were used for stress measurements and always confined to the centre of the 'M' blocks.

TABLE 13 EXPERIMENTAL OCCASIONS, LOWER TERRACE, 1977

| Soil moisture status occasion | Soil moisture conditions and mean soil moisture tension (millibars) 0-20 cm | | Soil moisture content 0-20 cm (% w/w) | Date |
|---|---|---|---|---|
| M1 | Dry | (1556) | 13.6 | 18.8.77 |
| M2 | Wet | ( 90) | 23.0 | 1.9.77 |
| M3 | Moist | ( 181) | 20.6 | 22.9.77 |
| M4 | Moist | ( 330) | 18.8 | 8.8.77 |
| (Occasion M3 was only used for stress measurement while M4 was for compaction and stress measurements.) | | | | |

4.2 Soil stress measurement sites (c.f. Sect.2.4 aim 2)

These were located within the field experiment at Lower Terrace field. Fig.42 shows the location and design of the plots used. All stress measurements were made on soil bulk density profile RL2 and at similar soil moisture conditions.

Installation of the stress transducers was assisted by moulding a hemispherical cavity in the soil using a rigid sphere of the same diameter as the balls; this cavity accommodated the balls before they were covered. The technique improved the contact between the water-filled ball and the soil and reduced the unwanted deformation of the sensitive mastic ball; the mastic could be easily deformed during handling. Small access trenches were dug for the tubes attached to the WFRBs. Figs.43a and 43b depict the installed devices following partial excavation after the field tests. Depths of the weight WFRBs in each plot were

Fig.42 The location and design of the field plots for the measurement of stresses beneath tractor wheels.

a. Location of the plots (enclosed in thick lines) within the field plan for Lower Terrace field (see Fig.39).

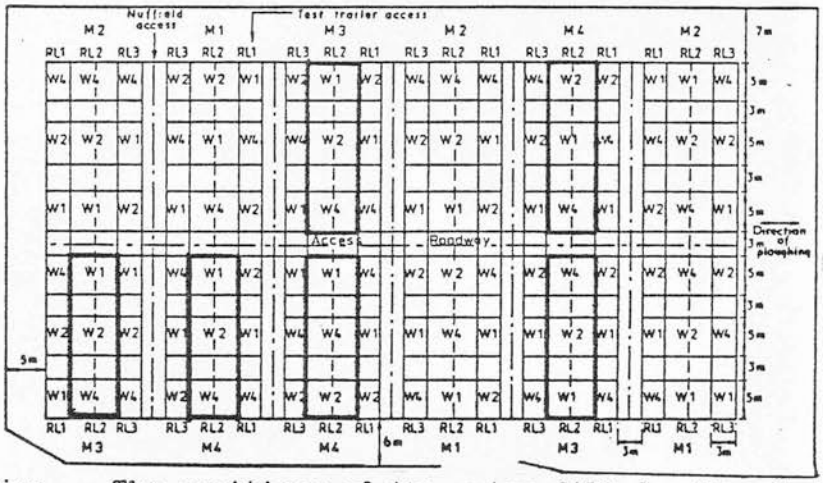


b. Plot design. The positions of the water filled rubber balls (WFRB) and Mastic balls are indicated.

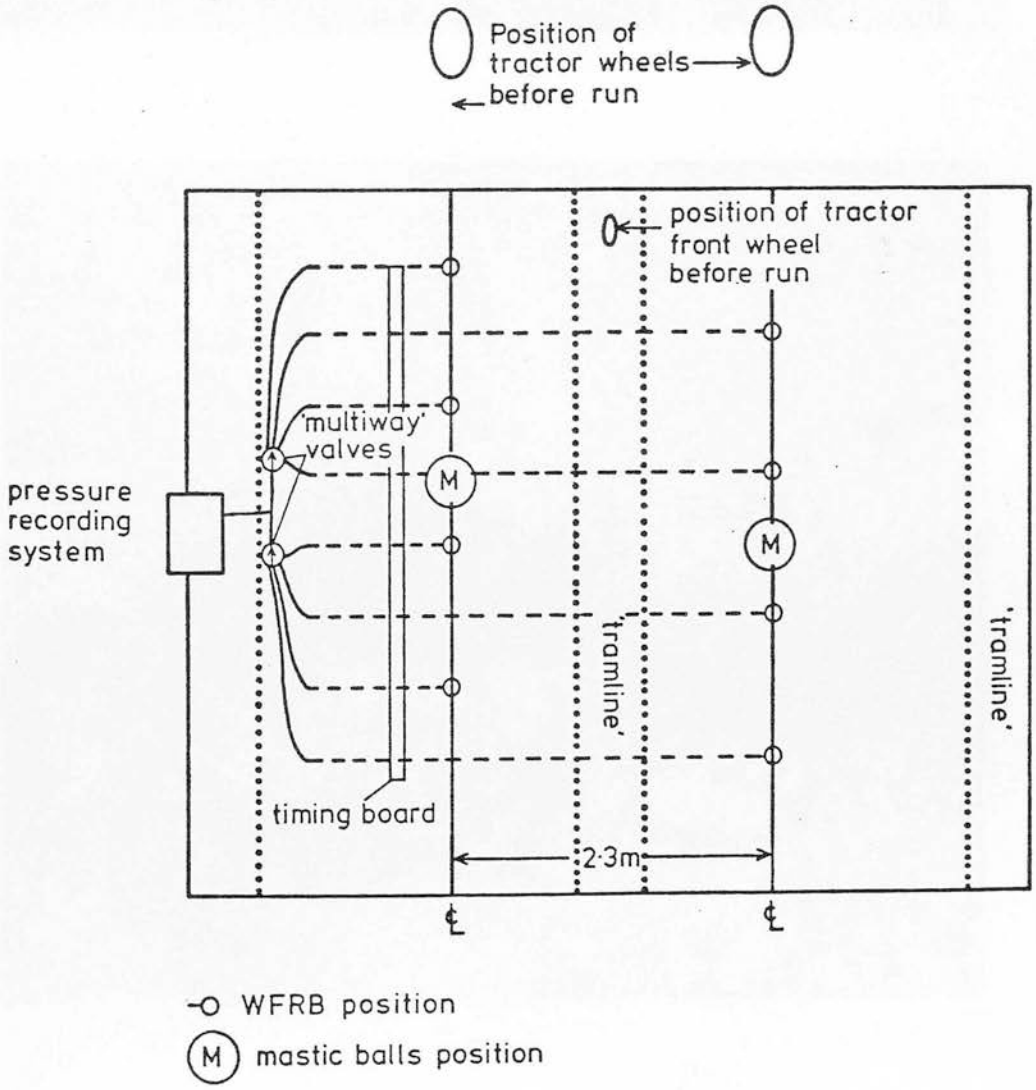

Fig.43a A water filled rubber ball following partial excavation after the field tests.

Fig.43b Mastic balls partially excavated after the field tests. The white layers of kaolin assisted their location.

randomly allocated. Nominal depths of 10, 20, 30 and 40 cm were used for all balls before the soil was rolled. Estimations of the depths of the devices after rolling were made by the measurement of displacement of soil 'markers' (short lengths of 1 cm O.D. plastic tubing). The markers were inserted into the walls of soil pits. The pits were back-filled before rolling and later excavated to measure the depths after rolling.

The procedure followed when running the experimental wheels over each plot was as follows:

1. Tubes from installed balls were connected to tubes from the multiway valve using PVC tube connectors with the help of a portable water bath.
2. The tractor was positioned at the end of the plot, the side wall of the front wheel touching the guiding string. A marked board, shown in Fig.42, was positioned and the tractor run forward at its predetermined speed (approx. 1 km/h). Steerage of the front wheel was assisted by an observer in front of the vehicle giving hand signals to the driver. The multiway valve was connected to each ball in sequence as the centre of the wheel passed over it. Estimation of the position of the wheel was assisted by the marked board.
4. Mercury thermometers were used to record temperatures at 10, 20 and 30 cm below the soil surface and adjacent to the WFRB pressure measurement equipment.
5. After wheel passage any deviations of the centre line of the wheel from its expected path were measured.

6. At a suitable time afterwards all the devices were excavated, a large access trench being dug alongside the position of the mastic balls. A vertical face was carefully cut back until one half of each ball was exposed. Outside calipers were used to measure the minor axis in situ , the ball being carefully removed for measurement of major and intermediate axes. Direction of the intermediate axis and depth below original soil surface were also measured.

4.3 Measurement of tyre contact area and sinkage (c.f. Sect.2.4 aim 3)

An empirical relationship between these two factors was derived by an experiment during October 1977 in the SIAE soil tank.[1] The tank has been described by other authors (Soane, et al. 1976). Control of the soil strength conditions was based on the same principles as the field experiments. The reciprocating harrow was modified for the soil tank width and used to loosen the soil between use to 25 cm depth with the harrow again powered by the wide wheeltrack tractor. Each experimental run used the wheels of the three-wheel tractor prepared in the same way as in the field experiments. One of its rear wheels was run on to soils of different surface hardness. Four hardnesses were used in each run, each hardness in a different quarter or 'plot' of the soil tank. The soil strength was increased by a self-propelled vibrating roller (Green and Thomas, PRV Mk.II). The different strength conditions are described in Table 14.

1 The tank contained soil of the Macmerry series.

TABLE 14 SURFACE SOIL STRENGTHS USED FOR THE SOIL TANK EXPERIMENT, 1977

| Soil strength condition | Description | Rolling |
|---|---|---|
| 1 | 'Very loose' | None |
| 2 | 'Soft' | 1 pass, no vibrator |
| 3 | 'Firm' | 2 passes, no vibrator |
| 4 | 'Hard' | 8 passes + vibrator |

Two measurements of contact area and rut profile were taken in each plot. The choice of wheel treatment, soil surface hardness and left or right wheel was randomised for each plot. The wheel treatments were W1, W2 and W4 as in the 1977 field experiment. Each run was replicated twice.

4.4 Laboratory tests (c.f. Sect.2.4 aim 7)

Disturbed samples were takenduring January and February 1978 from the upper 20 cm of soil at each field site. One bulked sample was made from four sub-samples for each replicate. The samples of Threipmuir soil were taken from the same surface soil used for the 1977 field experiment whereas the Macmerry soil had been ploughed twice since the 1976 field experiment. 'Undisturbed' samples were taken during March 1978 from four randomly chosen positions from the site of the field compaction experiment at Lower Terrace field.

As many 2 kg samples of loose soil as possible were obtained for each bulked sample. The lower limit of soil moisture conditions was set by air-dry values, the upper limit by near-saturation conditions when water was expelled at cell pressures of only one bar (see Section 3.9.1). Tests on

the 'undisturbed' samples were made as soon as possible after removal from the field, to prevent unwanted drying.

## 4.5 Field tests of the prediction model (c.f. Sect.2.4 aim 9)

### 4.5.1 Macmerry soil

Tests were made during September 1977 and on the same site as the 1976 field compaction experiment. Plots were chosen between the wheel tracks made by the combine harvester. Straw was cleared from the plots by hand. The field plan for the tests and the location and number of measurements are shown in Fig.44a. Initial soil measurements included dry bulk densities beneath the wheel track centre line and the profile of the wheel rut. All measurements were taken using the same maximum depths and depth intervals as used in the 1977 field compaction experiment at Lower Terrace field. All bulk density measurements were taken from the soil test trailer, the hydraulic jacking system being used to prepare the 2.5 cm wide access holes. Wheel treatments W3 and W4 were used for the tests.

### 4.5.2 Threipmuir soil

This experiment compared the compaction beneath a conventional tyre (12.4/11-36) with that beneath dual wide-section tyres (18.5-20). The tests were made during September 1977 on a site on Threipmuir soil adjacent to the field compaction experiment at Lower Terrace field (NT 237640). The layout of the plots is shown in Fig.44b. Four replications were made; each was divided into two plots with a central 'tram line'. The soil was prepared in the same way as in the field compaction experiments, but without any rolling. Dry bulk density, cone resistance, moisture content

Fig.44 The design of the plots for the field tests of the compaction model.

a. The location and number of measurements for each plot, Section 7, 1977. Macmerry soil.

A key to the symbols is shown in Fig.38.

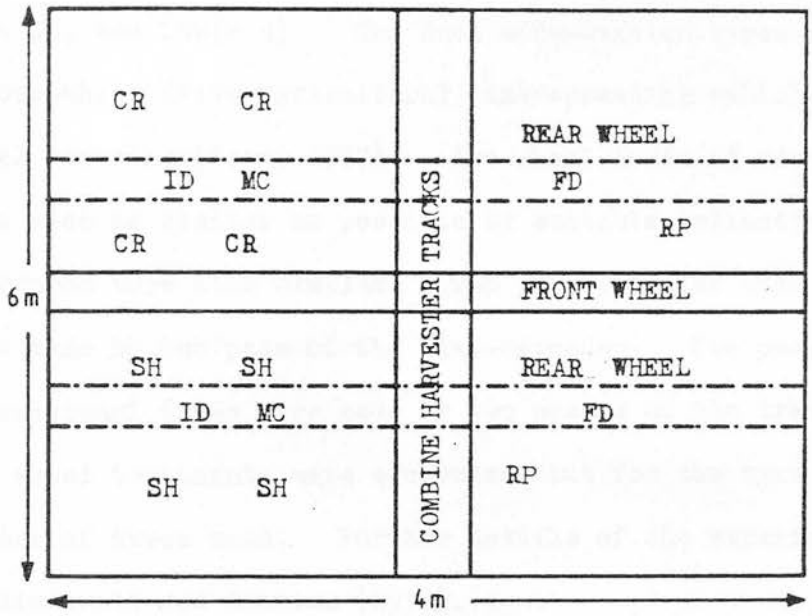


b. The design of the plots, Lower Terrace, 1977. Limespreader trials. Threipmuir soil.

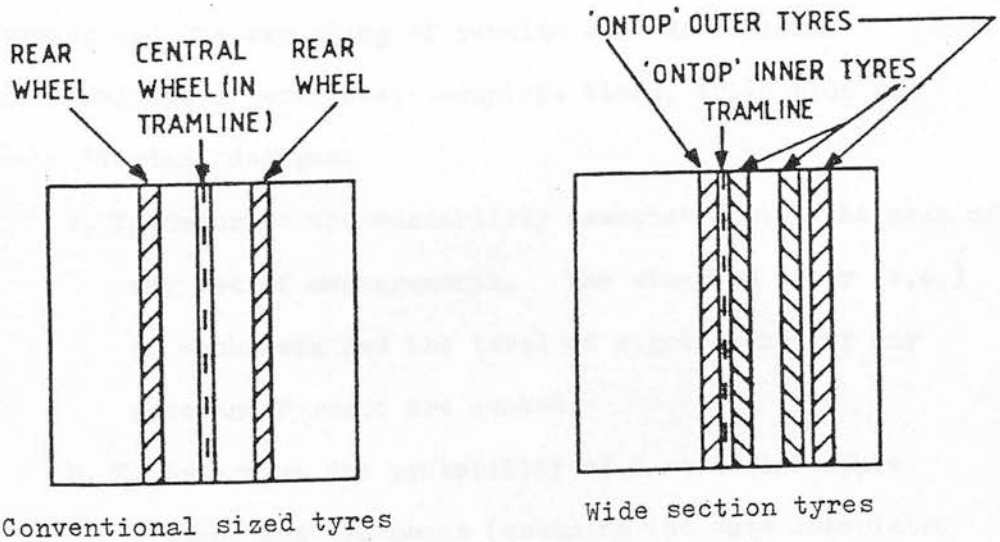

and vane shear strength measurements were made in each soil plot before and after the passage of the wheels, as well as the maximum rut depth and contact area of the tyres. The Nuffield three wheeled tractor provided the conventional tyre (using wheel treatment W4, see Table 4). The dual wide-section tyres were part of a four-wheel drive agricultural lime-spreading vehicle with four wheel steering (Howe, 1977). The wheel loads of each vehicle were made as similar as possible by suitable ballasting; inflation pressures were also similar. Two passes of the wide section tyres were made by one pass of the lime-spreader. Two passes of the conventional tyres were made by two passes of the tractor. Thus the wheel treatments were equivalent but for the tyre sizes and number of tyres used. Further details of the experiment are given by Blackwell and Dickson (1978).

## 4.6 The Use of Statistical Analyses

Investigation of much experimental data was assisted by various methods of statistical analysis.[1] These methods, their purpose and the reporting of results were as follows:

1. Analysis of variance; complete block, split plot and 'Tartan' designs.
   a. To describe the variability associated with the mean of any set of measurements. The standard error (s.e.) of each mean and the level of significance of any relevant F ratio are quoted.
   b. To determine the probability of a real difference between any two means (assuming the data associated with each mean is normally distributed). The standard error of the difference between the means (s.e.d.) and

1. Computer programs for some of these analyses are mentioned in Appendix 9.

the level of significance of the F ratio are quoted.

2. Linear andLeast-squares Regression.

   a. To describe the 'goodness of fit' of a linear regression, as well as the level of probability of the regression and the variability (s.e.) associated with each regression constant.

   b. To assess the goodness of fit of a set of data to a non-linear equation from the associated error mean square value.

3. Comparison of observed dry bulk density and that predicted by the model (Chap.8) by the 'standard deviation of prediction' (s.d.p.) and the linear regression of predicted against observed values.

Throughout the text the levels of significance of F ratios and regressions are denoted as follows:

* = $P < 0.05$ and $P > 0.01$; ** = $P < 0.01$ and $P > 0.001$;

*** = $P < 0.001$.

Absence of such a symbol, or the symbol 'N', indicates $P > 0.05$.

# CHAPTER 5 - EXPERIMENTAL RESULTS

## 5.1 In situ Measurements of Soil Strains and Soil Physical conditions during the Field Compaction Experiments

Data obtained from Section 7, 1976 and Lower Terrace Field, 1977, are described here.

### 5.1.1 Dry bulk density changes

The results from the experimental runs on each different occasion are shown in Figs.45a to 45p for Macmerry and Figs.46a to 46i for Threipmuir. Each figure is subdivided into separate graphs for each different original soil bulk density (RL treatment). Upon each of these graphs are shown the original Dbd profile, Dbd profile after wheel passage and the surface depression after wheel passage. The surface depression is the Maximum Rut Depth, as defined in Section 5.1.2. Thus the original and final dry bulk density profiles after each wheel treatment on the same original soil conditions can be compared. Standard errors of the differences between mean values at each depth are also shown. A computer program was developed to draw the graphs described above using the graph plotting facilities available at SIAE (Brown, 1972). Measurements at 3 cm depths were excluded due to inaccuracy of the equipment within 5 cm of the jig/soil interface (Soane, 1977).

It is evident from Figs.45a to 46i and their summary in Table 15 that the wheel treatments could be ranked in the following order of increasing effect on soil dry bulk density: W1 < W2 < W3 for Macmerry and W1 < W2 < W4 for Threipmuir. Statistical analysis

---

1. Measurements of dry bulk density after wheel passage are also shown in Appendix 4.

Fig.45a Dry bulk density profiles beneath the track centre before (----) and after (——) the wheel treatments for soil treatment RL 1, occasion M1, Macmerry soil.

45a

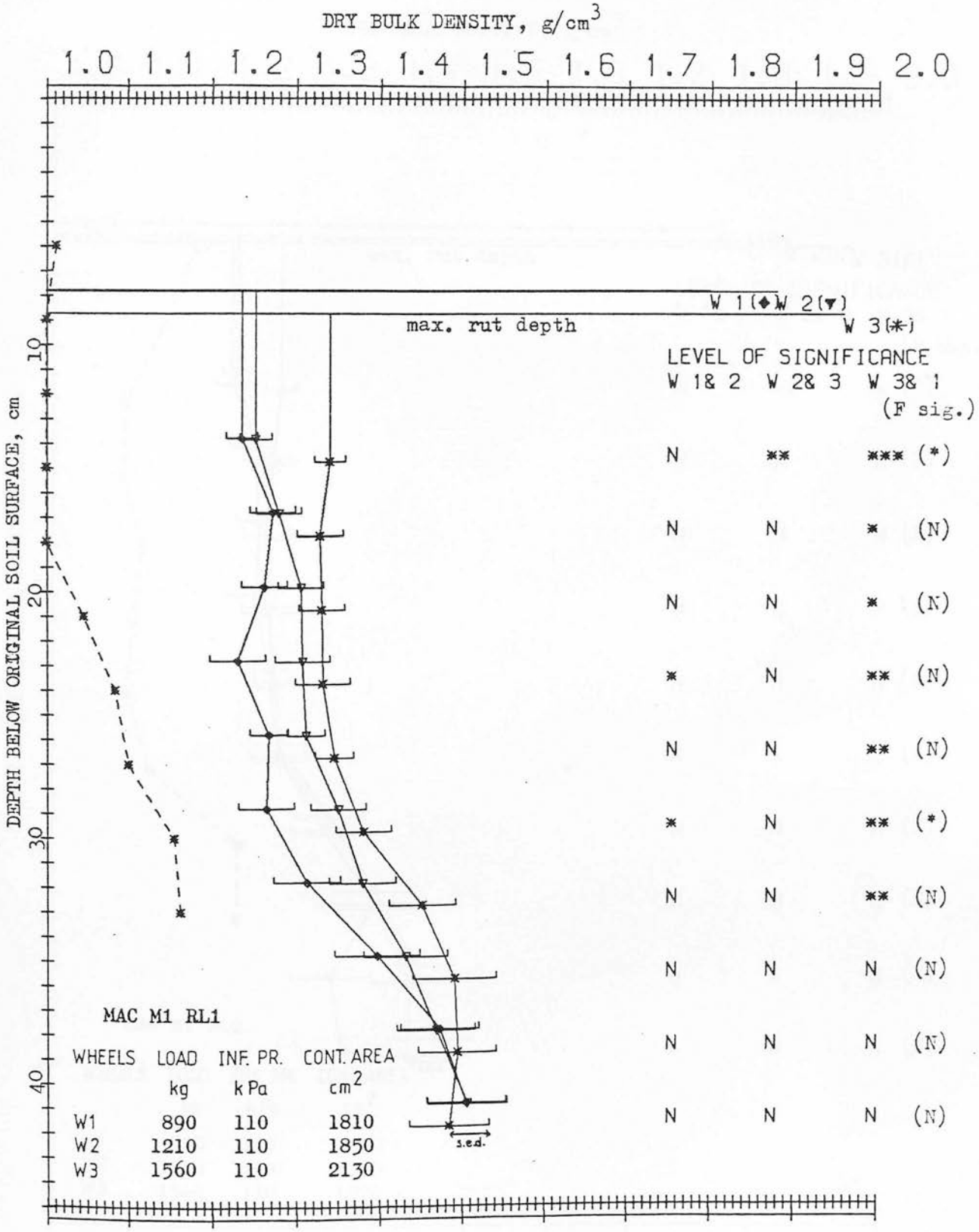

Fig.45b Dry bulk density profiles beneath the track centre before (----) and after (——) the wheel treatments for soil treatment RL 2, occasion M1, Macmerry soil.

45b

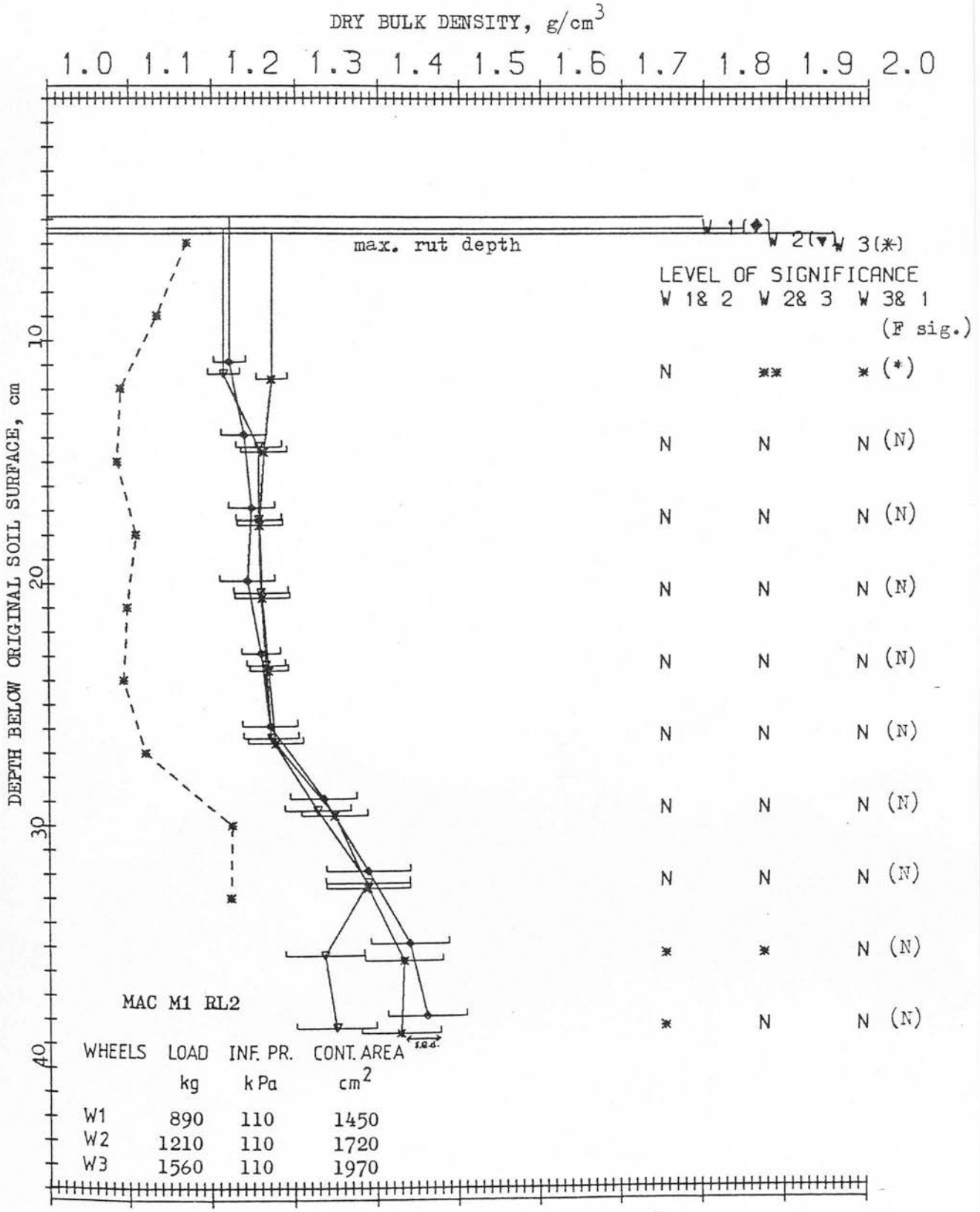

Fig.45c Dry bulk density profiles beneath the track centre before (---) and after (——) the wheel treatments for soil treatment RL 3, occasion M1, Macmerry soil.

45c

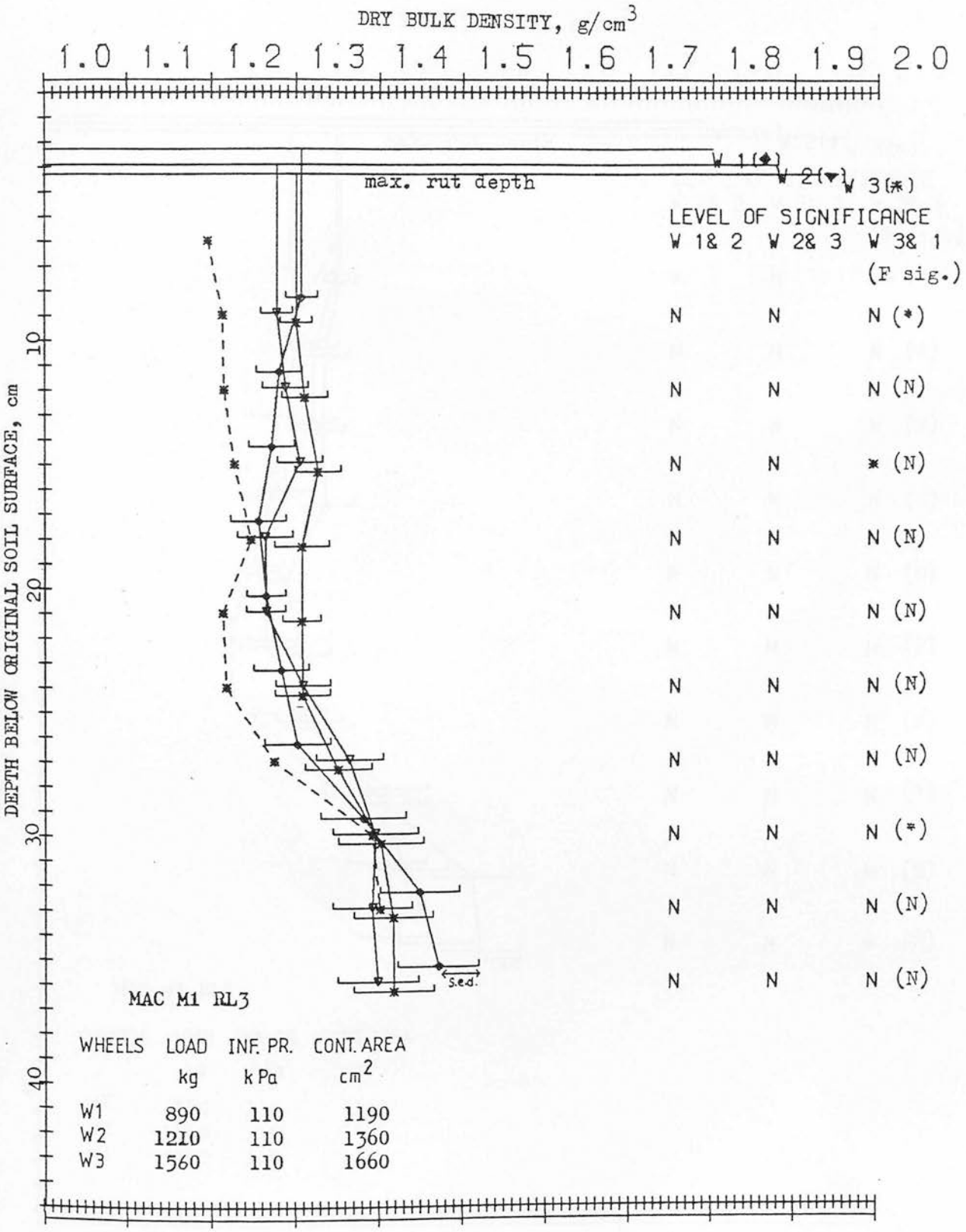

Fig.45d Drybulk density profiles beneath the track centre before (---) and after (——) the wheel treatments for soil treatment RL 4, occasion M1, Macmerry soil.

45d

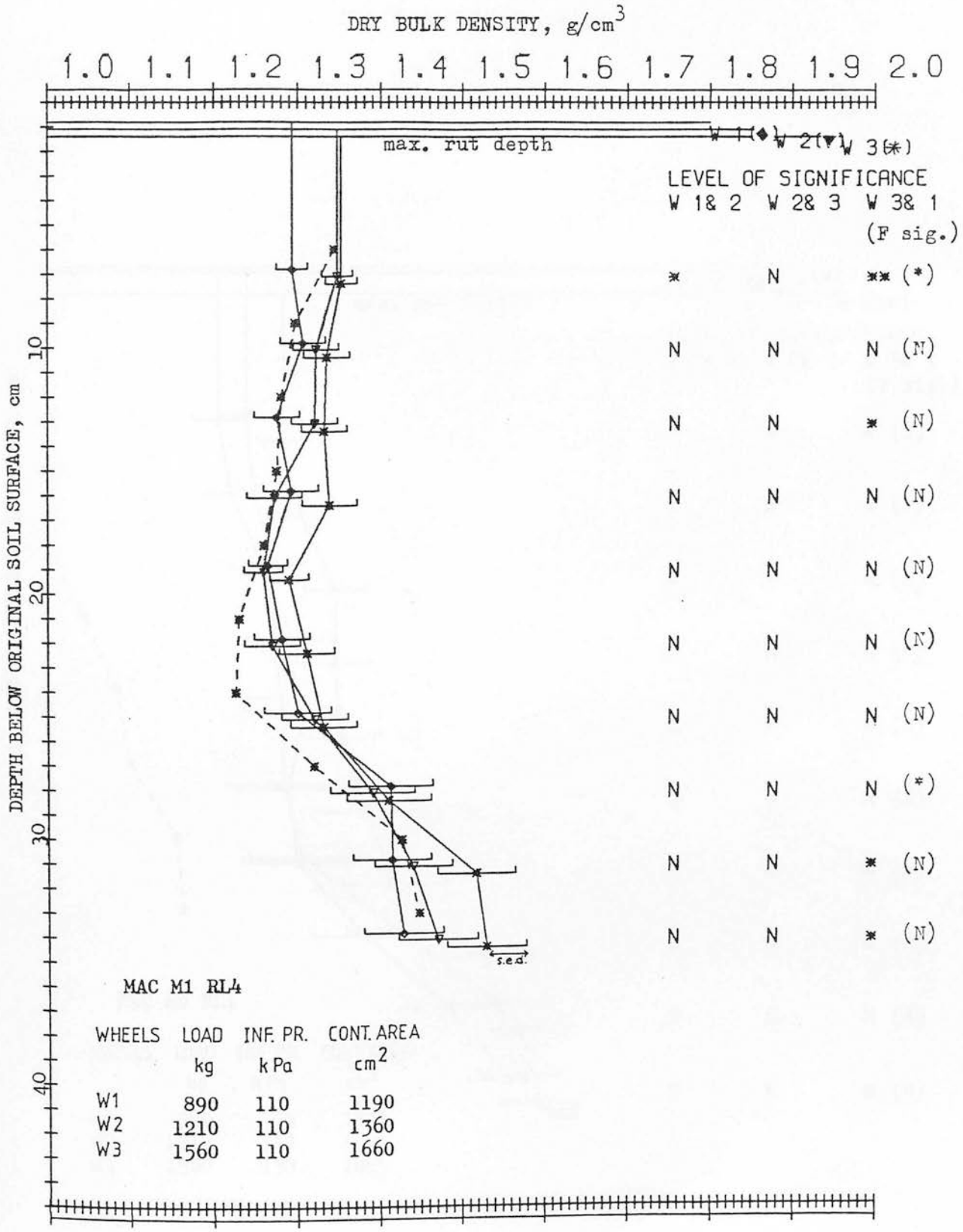

Fig.45e Dry bulk density profiles beneath the track centre before (----) and after (——) the wheel treatments for soil treatment RL 1, occasion M2, Macmerry soil.



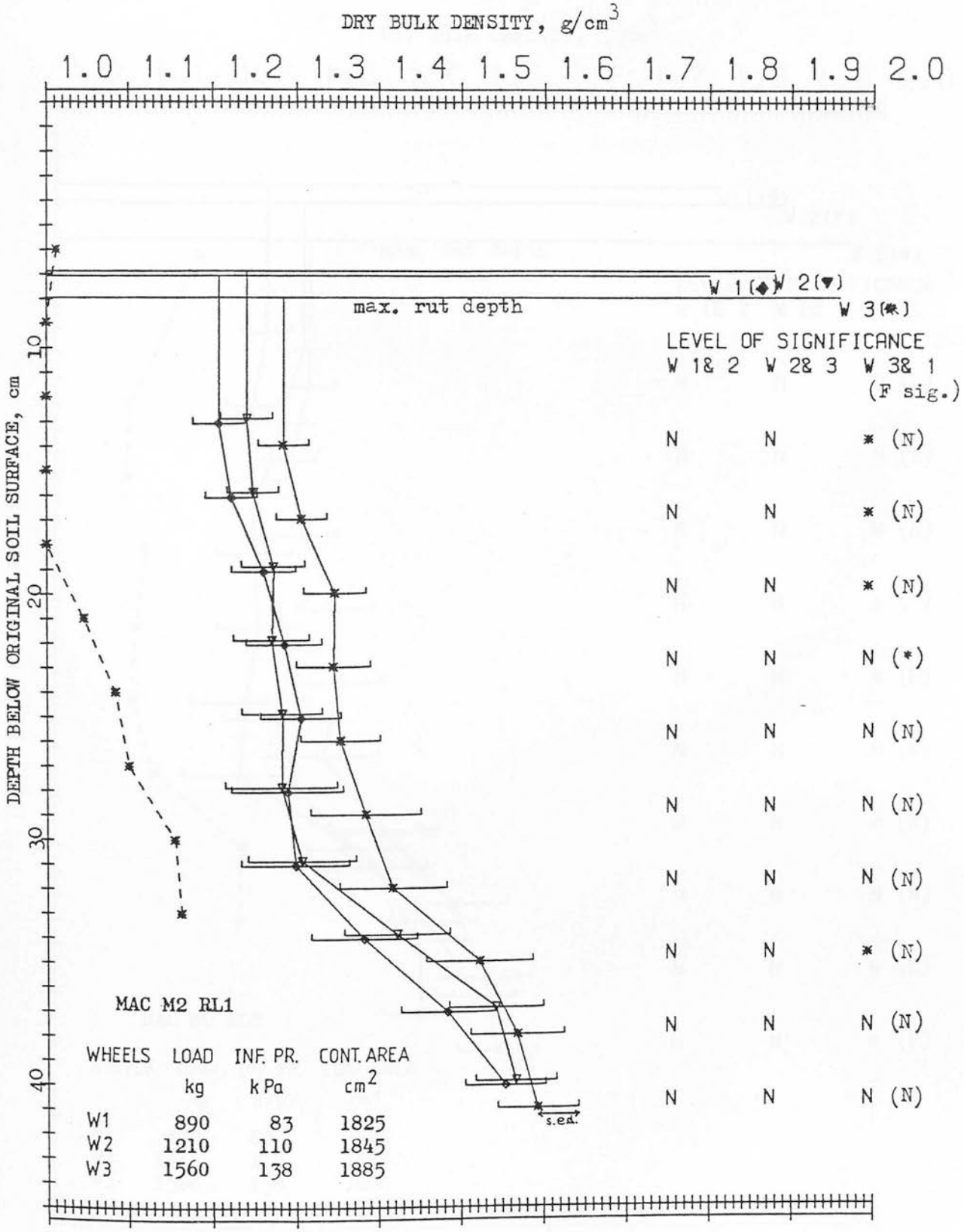

Fig.45f Dry bulk density profiles beneath the track centre before (----) and after (——) the wheel treatments for soil treatment RL 2, occasion M2, Macmerry soil.

45f

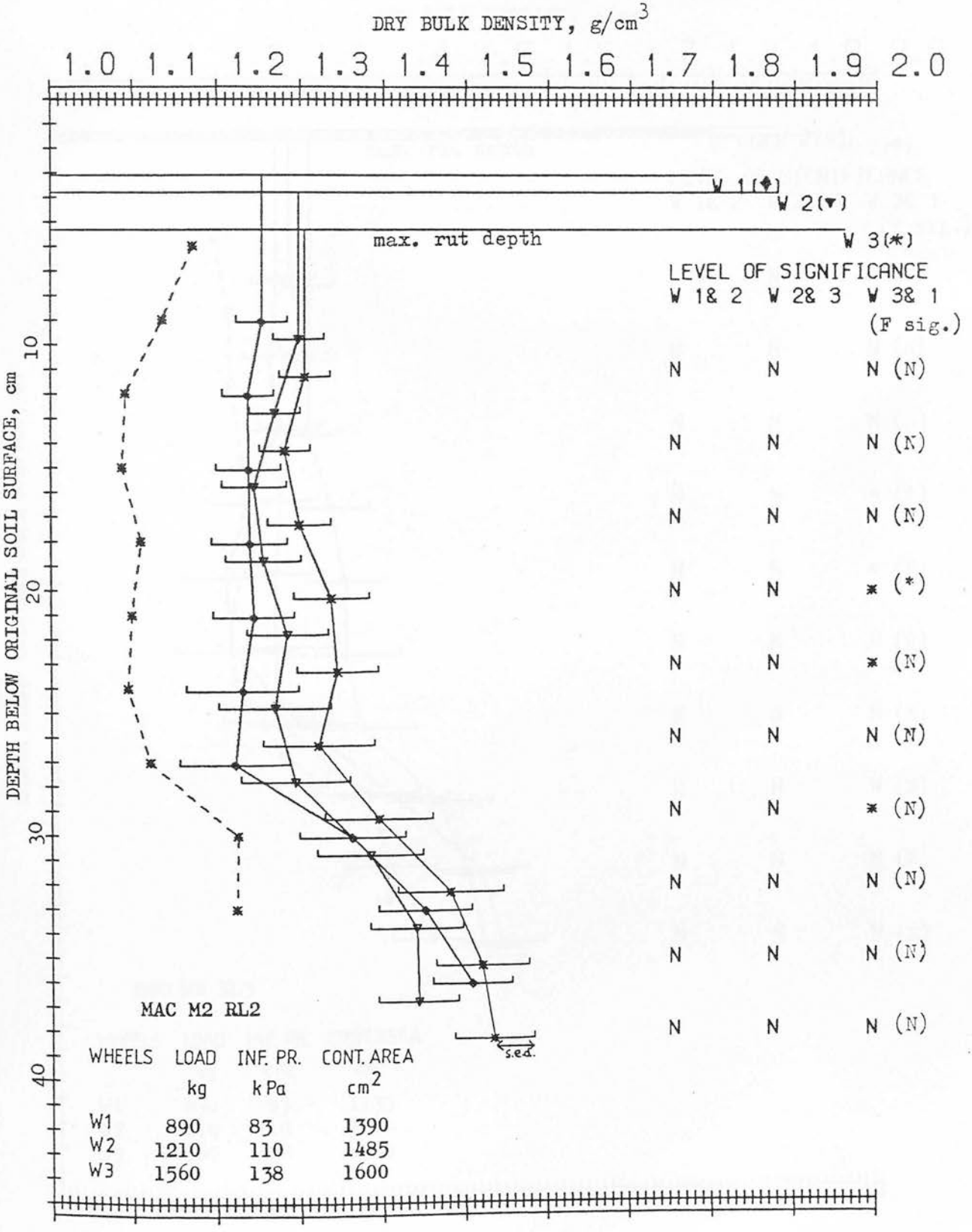

Fig.45g Dry bulk density profiles beneath the track centre before (----) and after (——) the wheel treatments for soil treatment RL 3, occasion M2, Macmerry soil.

45g

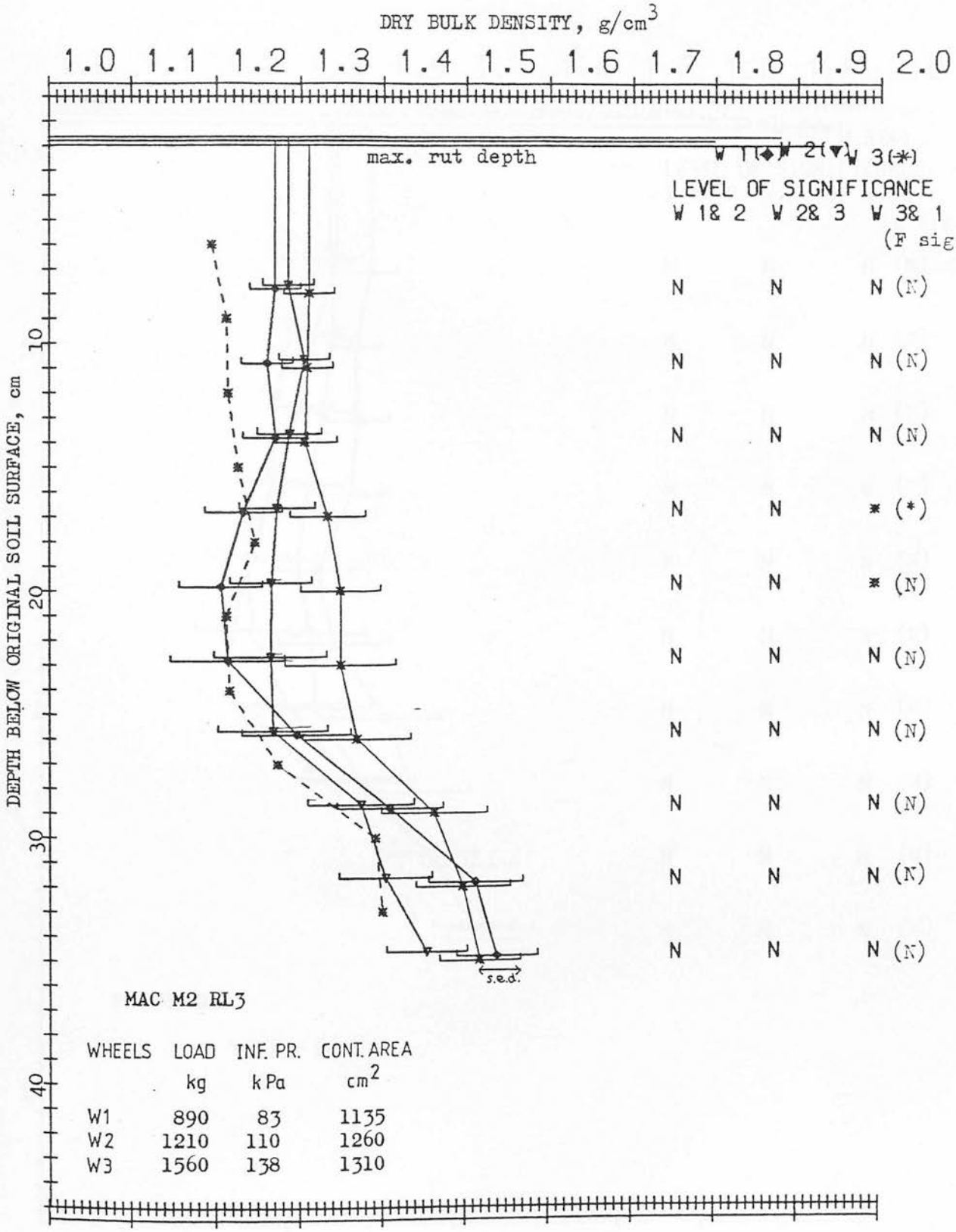

Fig.45h Dry bulk density profiles beneath the track centre before (----) and after (——) the wheel treatments for soil treatment RL 4, occasion M2, Macmerry soil.

45h

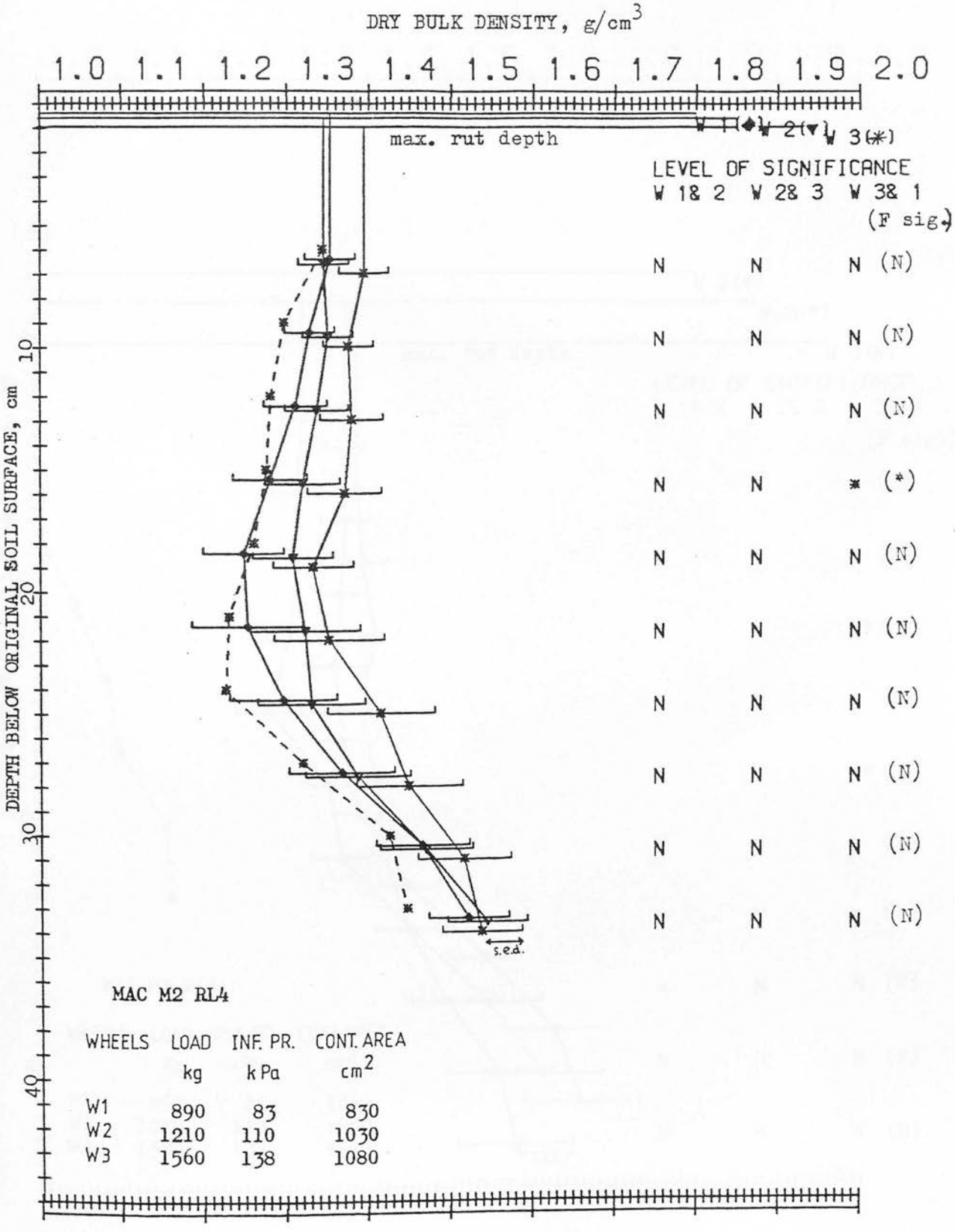

Fig.45i Dry bulk density profiles beneath the track centre before (----) and after (——) the wheel treatments for soil treatment RL 1, occasion M3, Macmerry soil.

45i

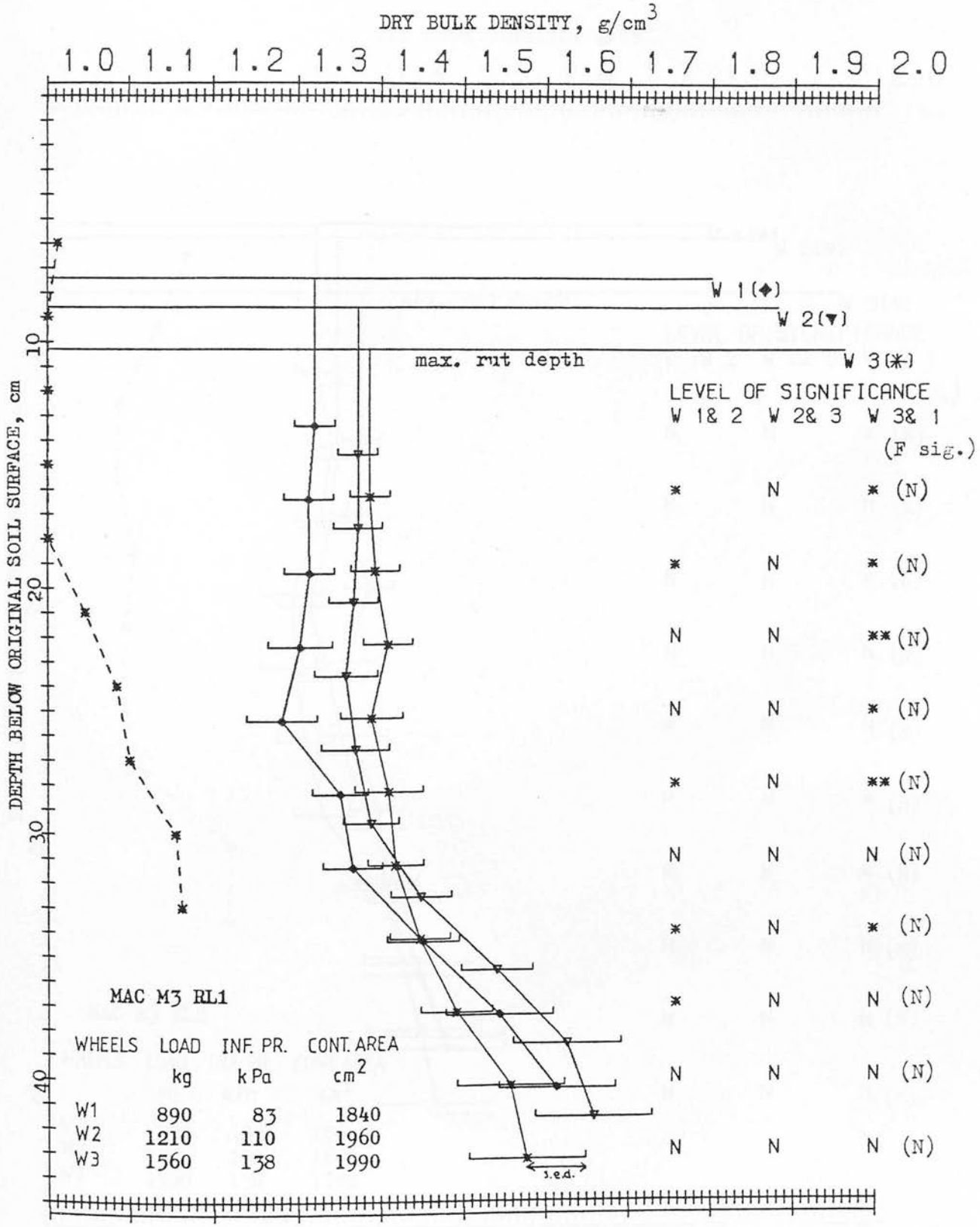

Fig.45j Dry bulk density profiles beneath the track centre before (----) and after (——) the wheel treatments for soil treatment RL 2, occasion M3, Macmerry soil.

45j

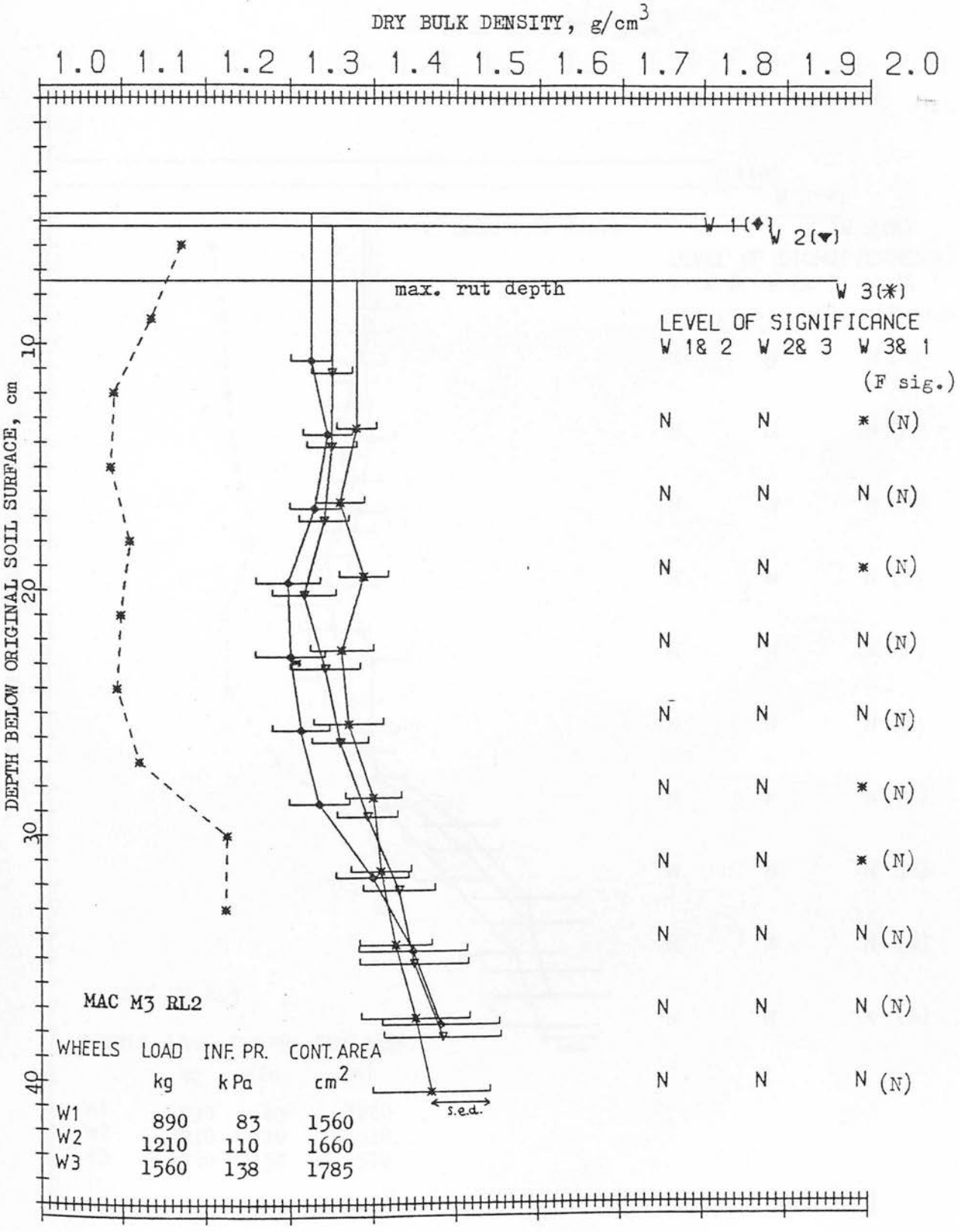

Fig.45k Dry bulk density profiles beneath the track centre before (----) and after (——) the wheel treatments for soil treatment RL 3, occasion M3, Macmerry soil.

45k

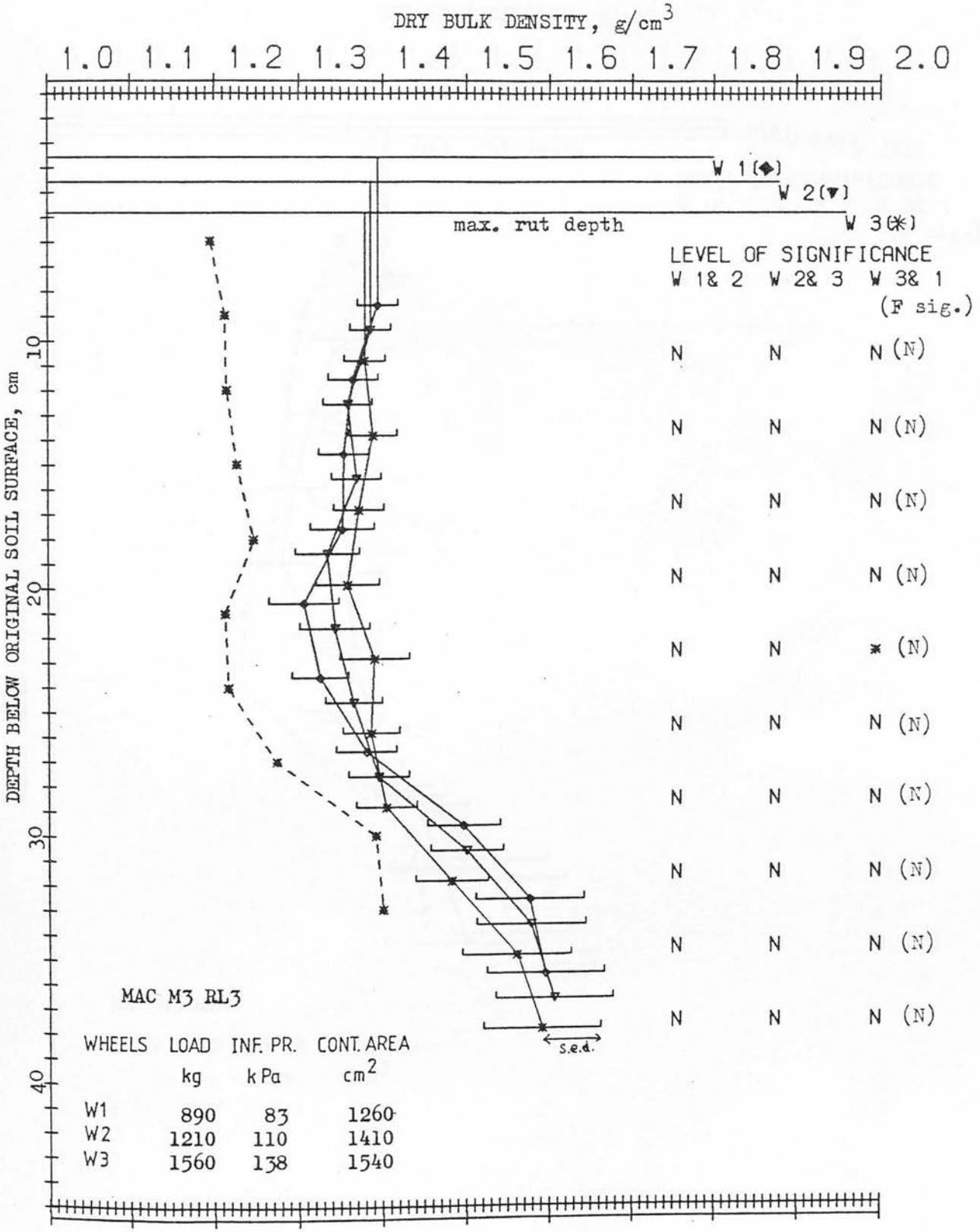

Fig.451 Dry bulk density profiles beneath the track centre before (----) and after (——) the wheel treatments for soil treatment RL 4, occasion M3, Macmerry soil.

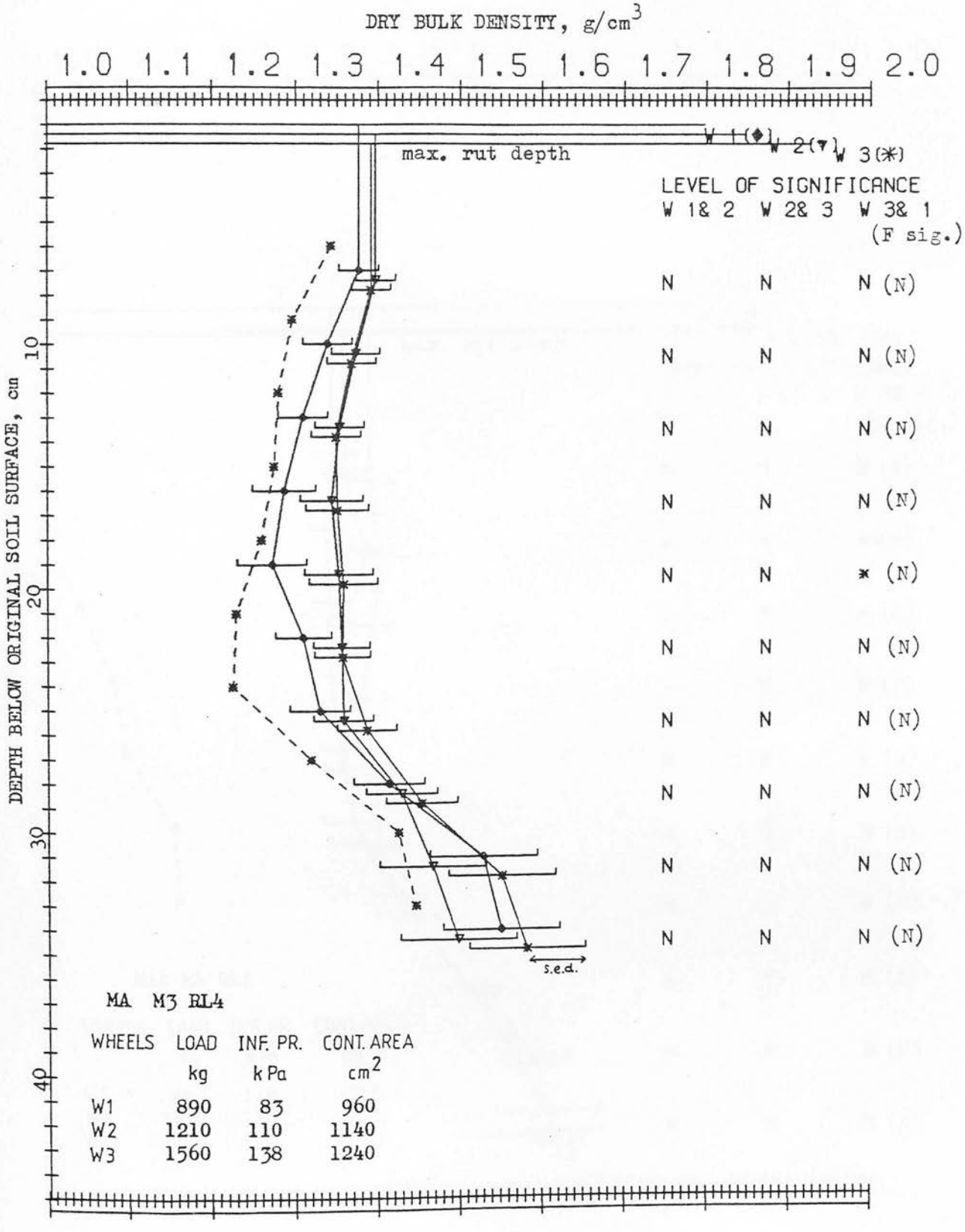

Fig.45m Dry bulk density profiles beneath the track centre before (----) and after (——) the wheel treatments for soil treatment RL 1, occasion M4, Macmerry soil.

45m

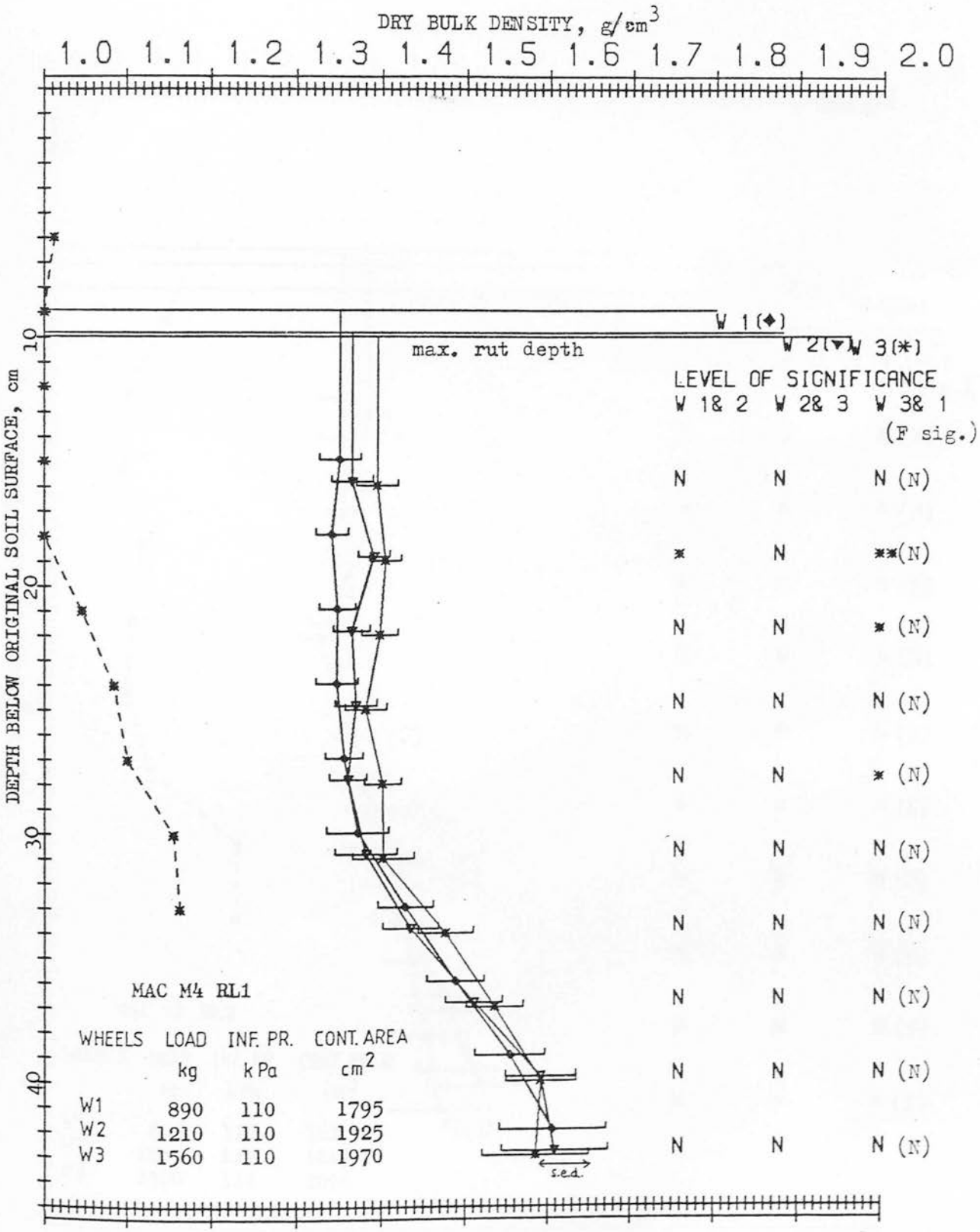

Fig.45n Dry bulk density profiles beneath the track centre before (----) and after (——) the wheel treatments for soil treatment RL 2, occasion M4, Macmerry soil.

45n

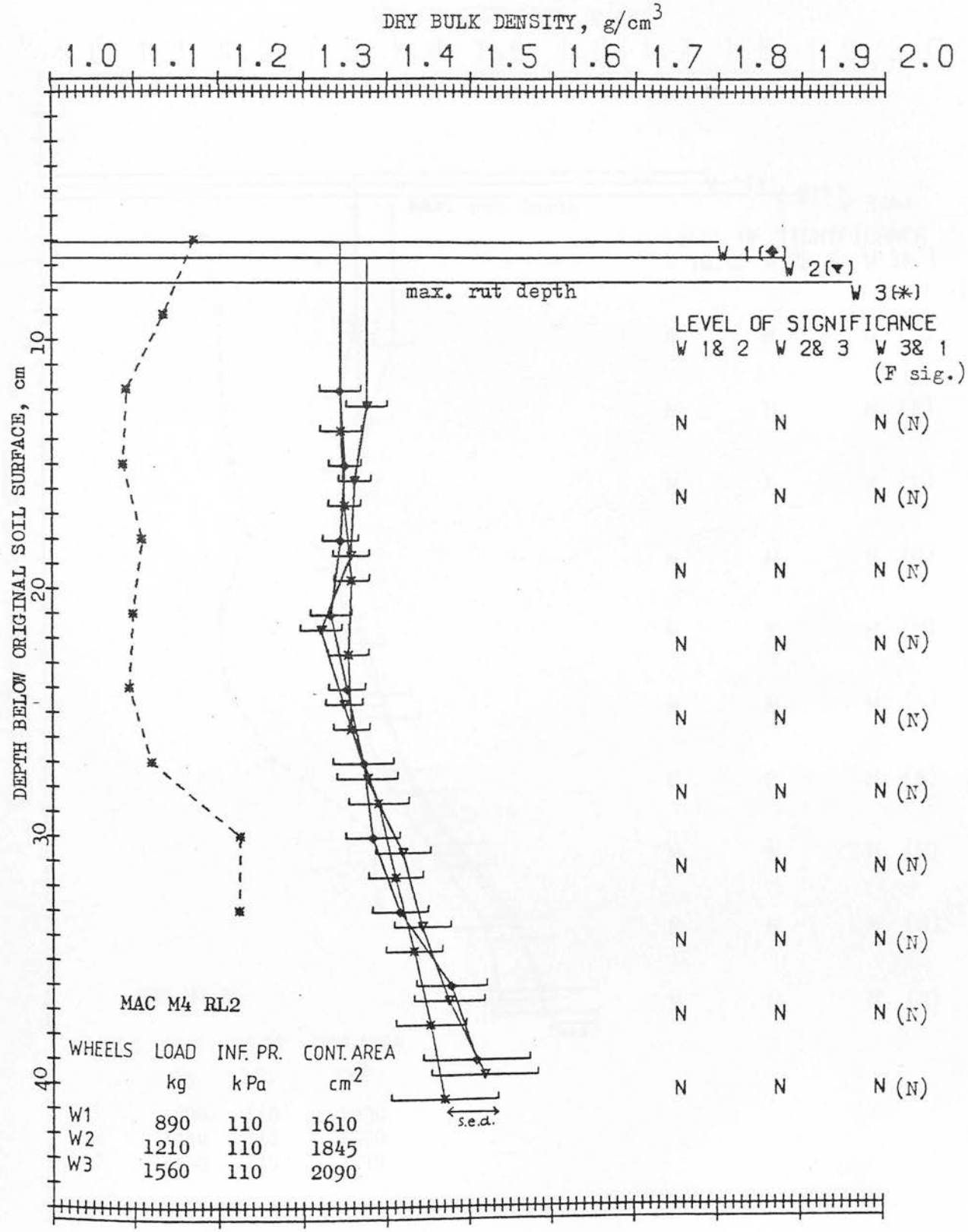

Fig.45o Dry bulk density profiles beneath the track centre before (----) and after (——) the wheel treatments for soil treatment RL 3, occasion M4, Macmerry soil.

45o

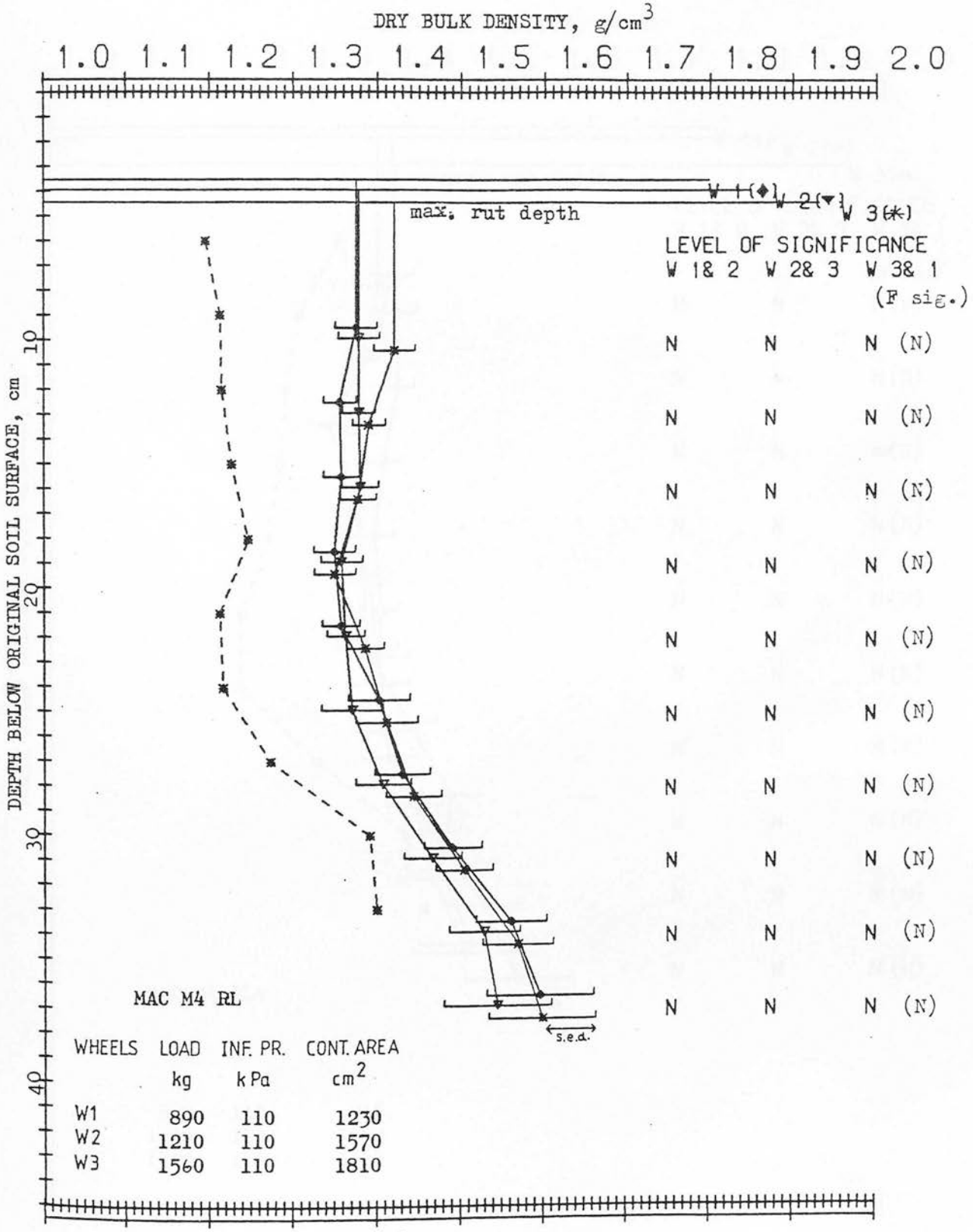

Fig.45p Dry bulk density profiles beneath the track centre before (----) and after (——) the wheel treatments for soil treatment RL 4, occasion M4, Macmerry soil.

45p

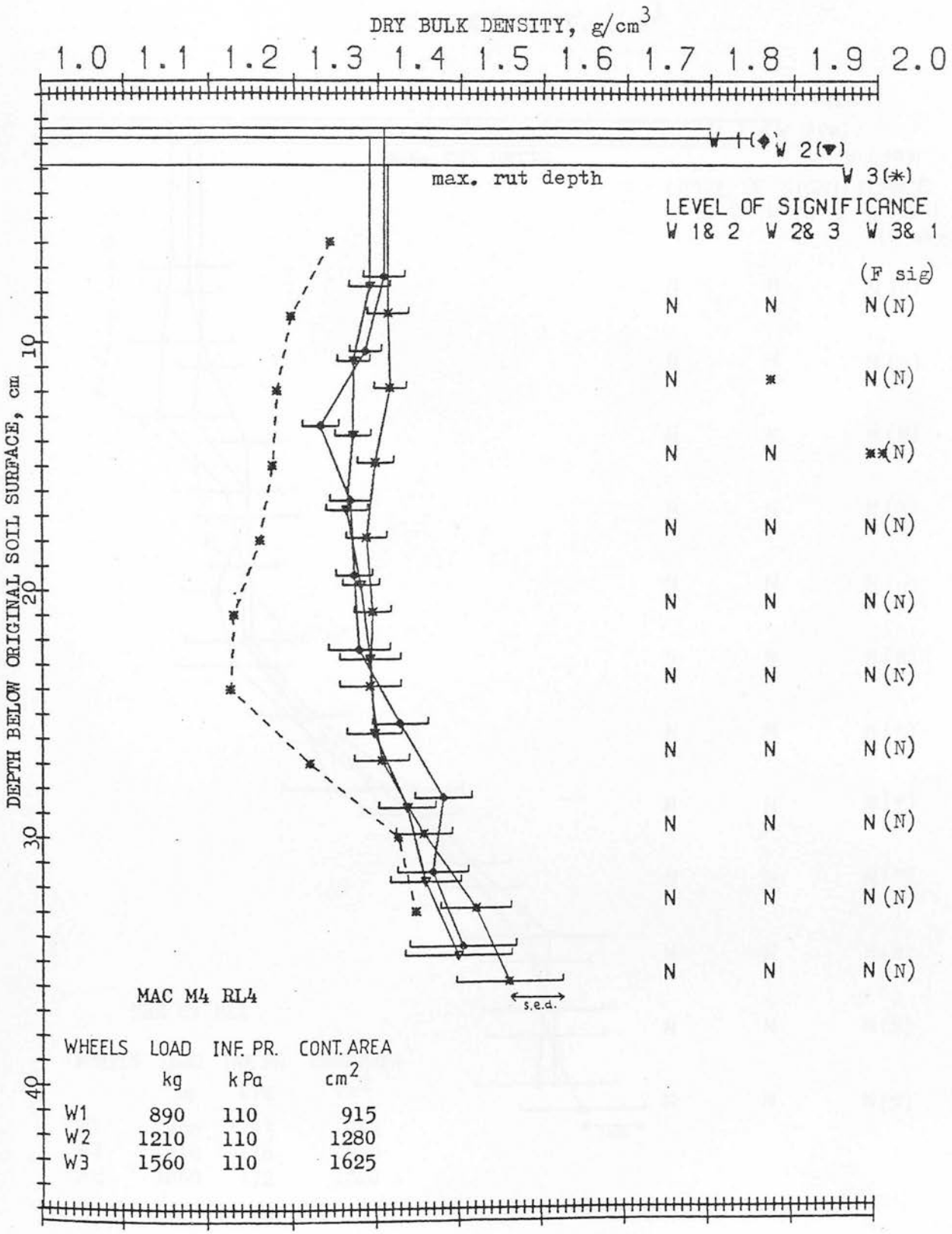

Fig.46a Dry bulk density profiles beneath the track centre before (---) and after (——) the wheel treatments for soil treatment RL 1, occasion M1, Threipmuir soil.

46a

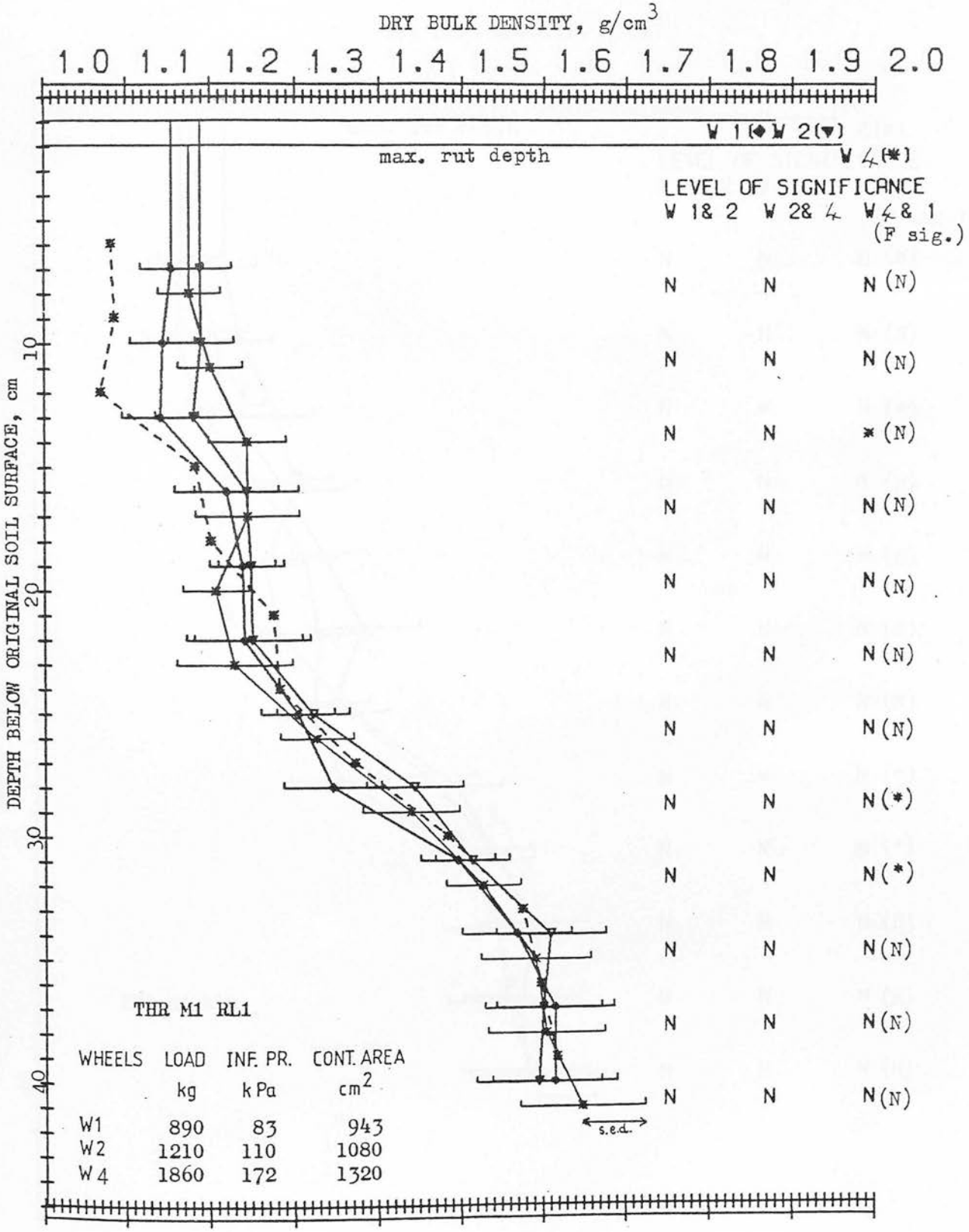

Fig.46b Dry bulk density profiles beneath the track centre before (----) and after (——) the wheel treatments for soil treatment RL 2, occasion M1, Threipmuir soil.

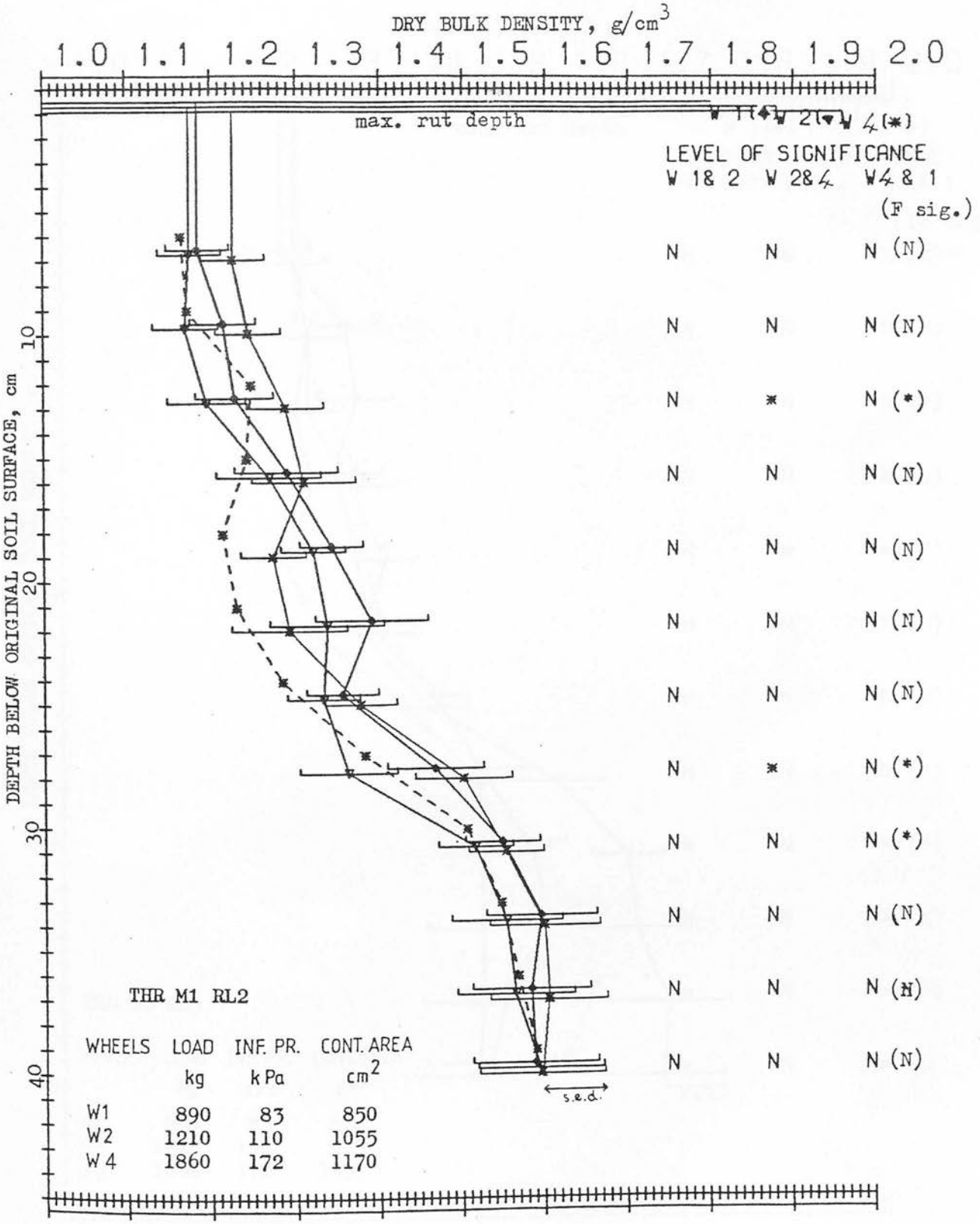

Fig.46c Dry bulk density profiles beneath the track centre before (---) and after (——) the wheel treatments for soil treatment RL 3, occasion M1, Threipmuir soil.

46c

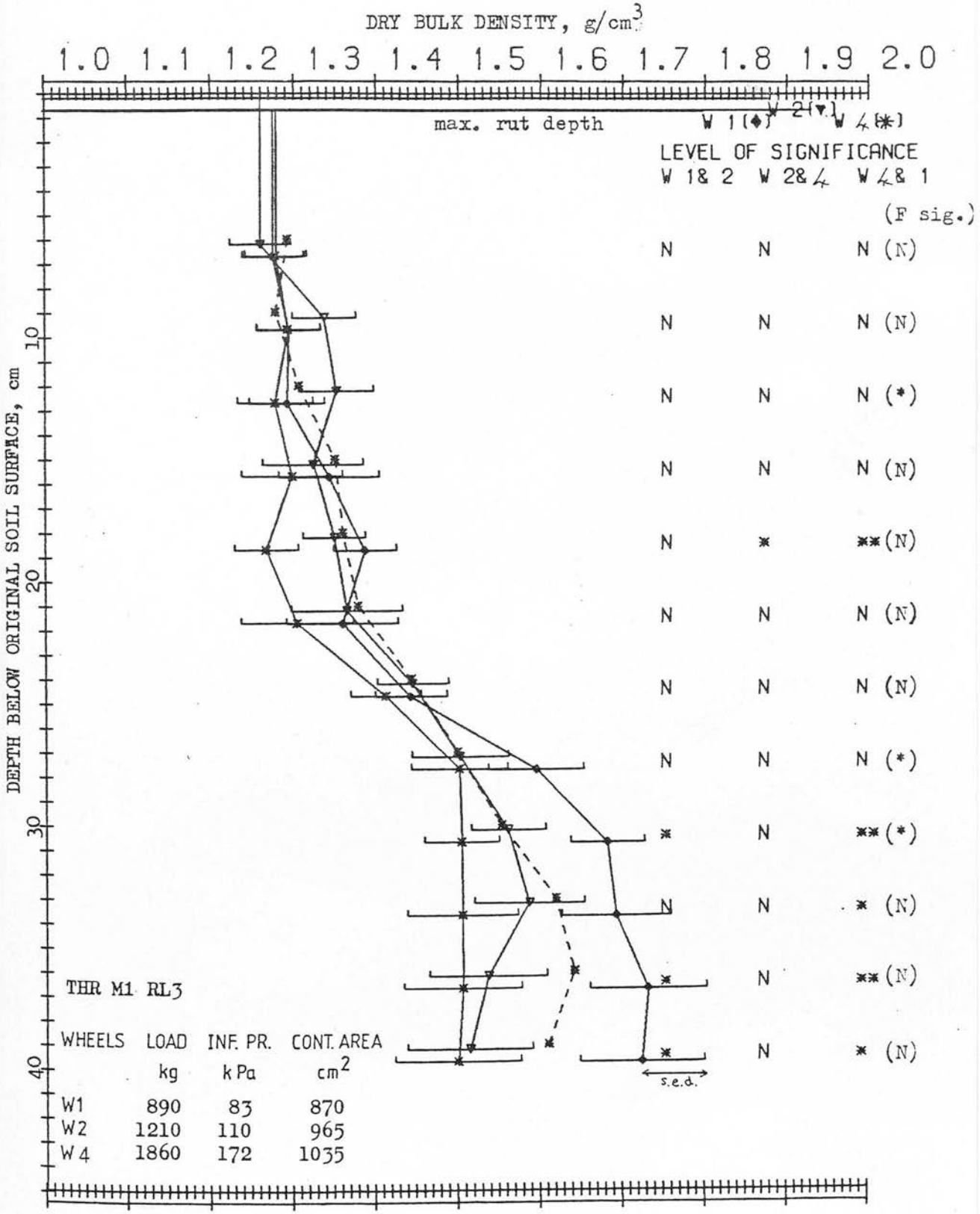

Fig.46d Dry bulk density profiles beneath the track centre before (---) and after (——) the wheel treatments for soil treatment RL 1, occasion M2, Threipmuir soil.

46d

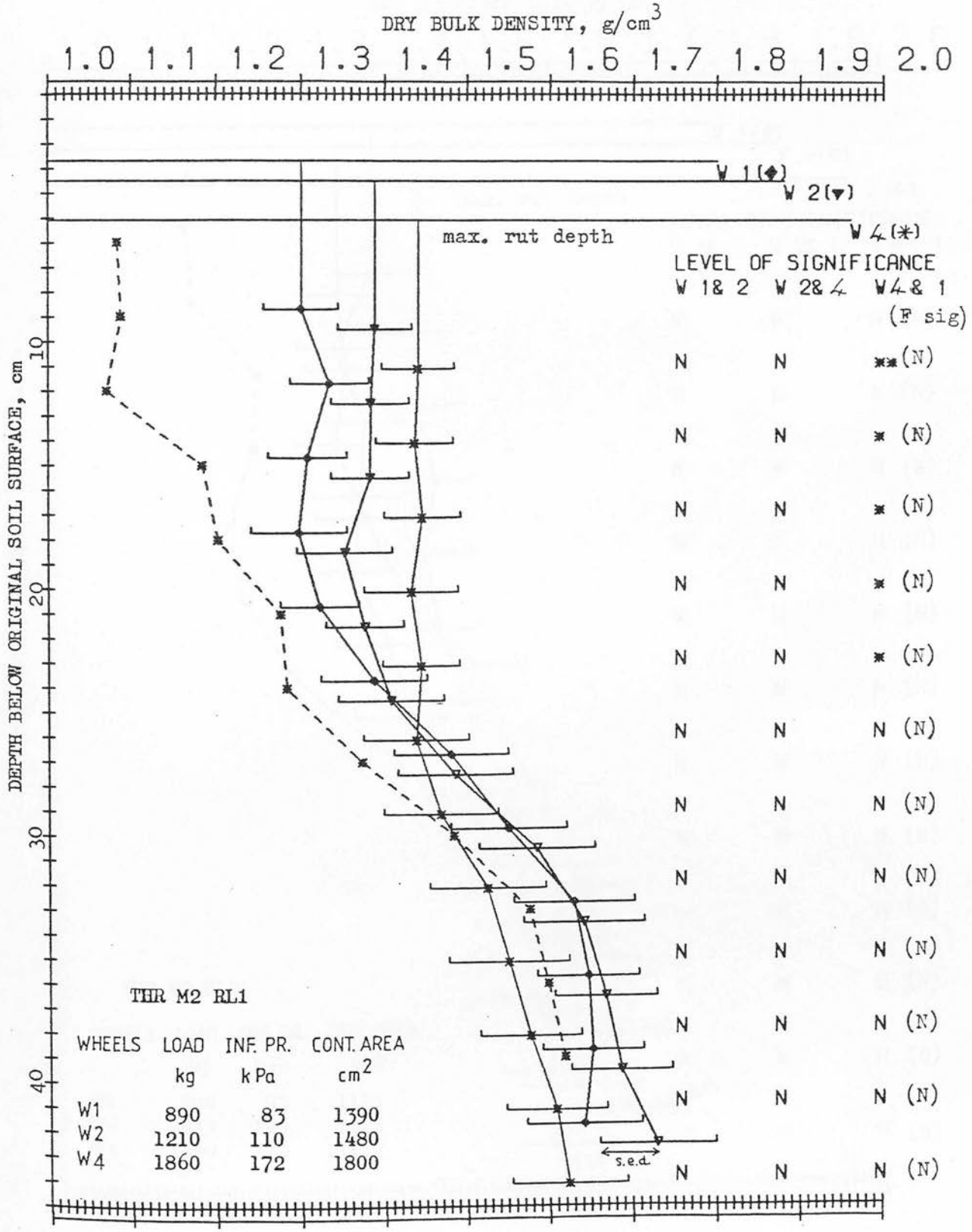

Fig.46e Dry bulk density profiles beneath the track centre before (---) and after (——) the wheel treatments for soil treatment RL 2, occasion M2, Threipmuir soil.



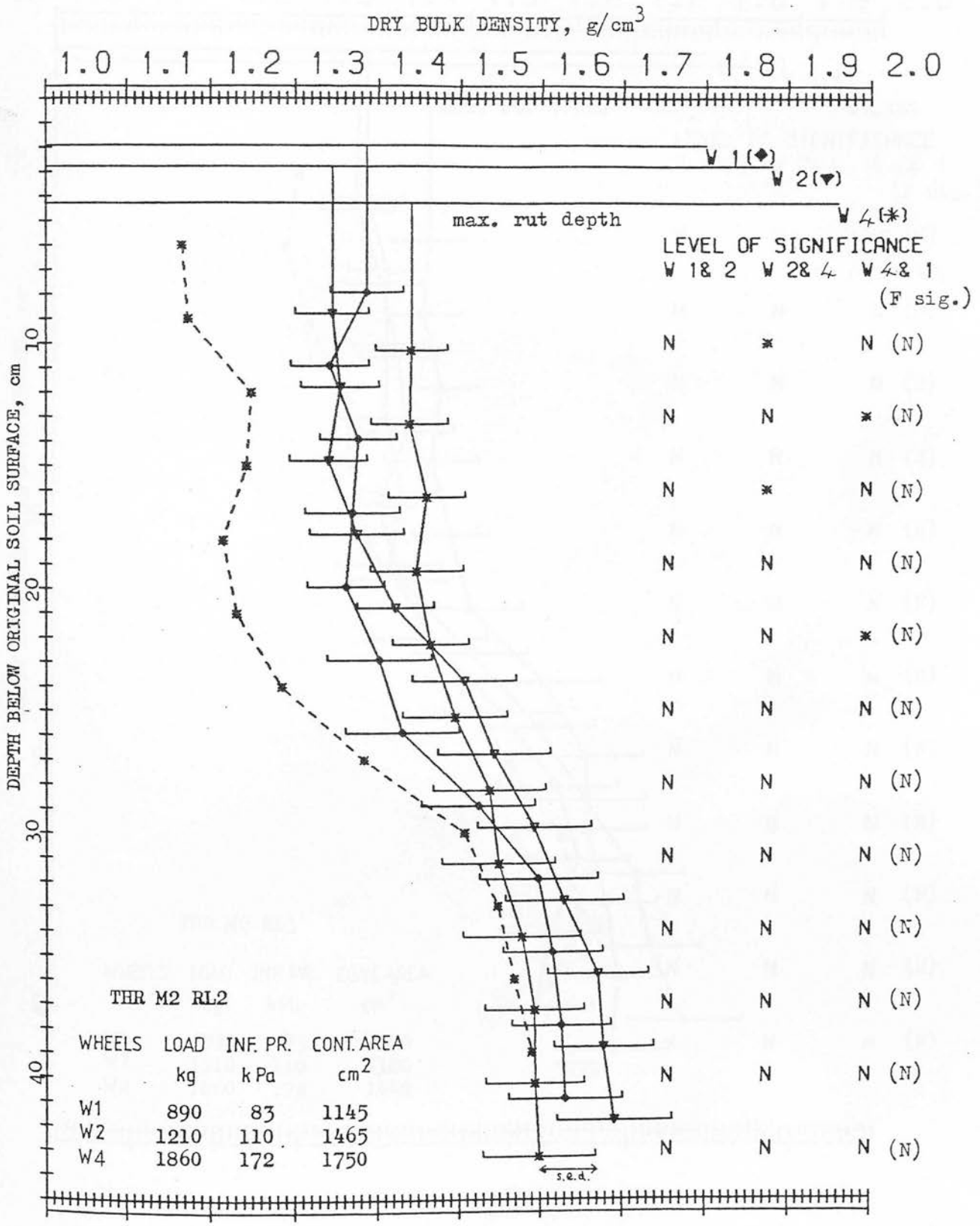

Fig.46f Dry bulk density profiles beneath the track centre before (---) and after (——) the wheel treatments for soil treatment RL 3, occasion M2, Threipmuir soil.

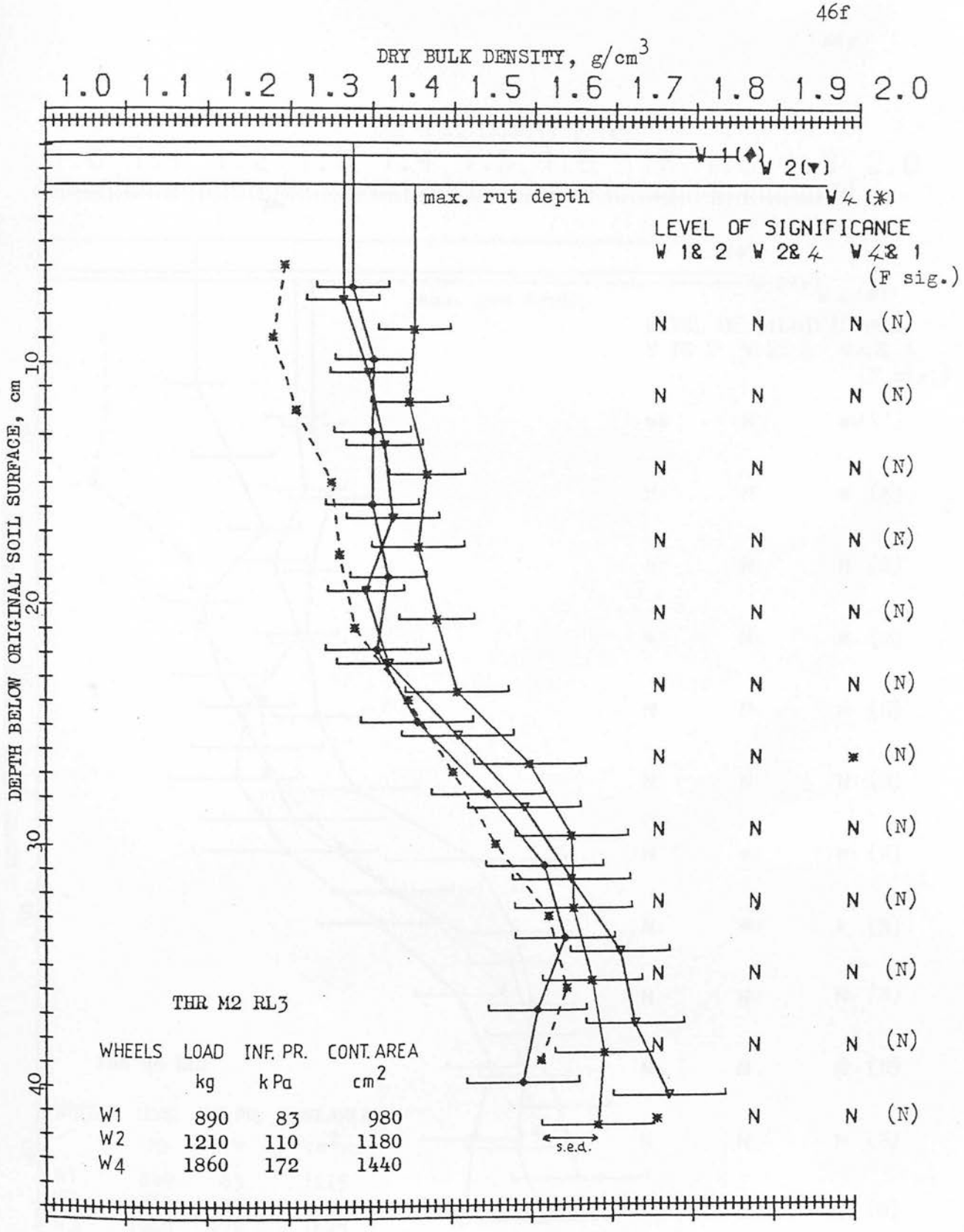

Fig.46g Dry bulk density profiles beneath the track centre before (- - -) and after (——) the wheel treatments for soil treatment RL 1, occasion M4, Threipmuir soil.

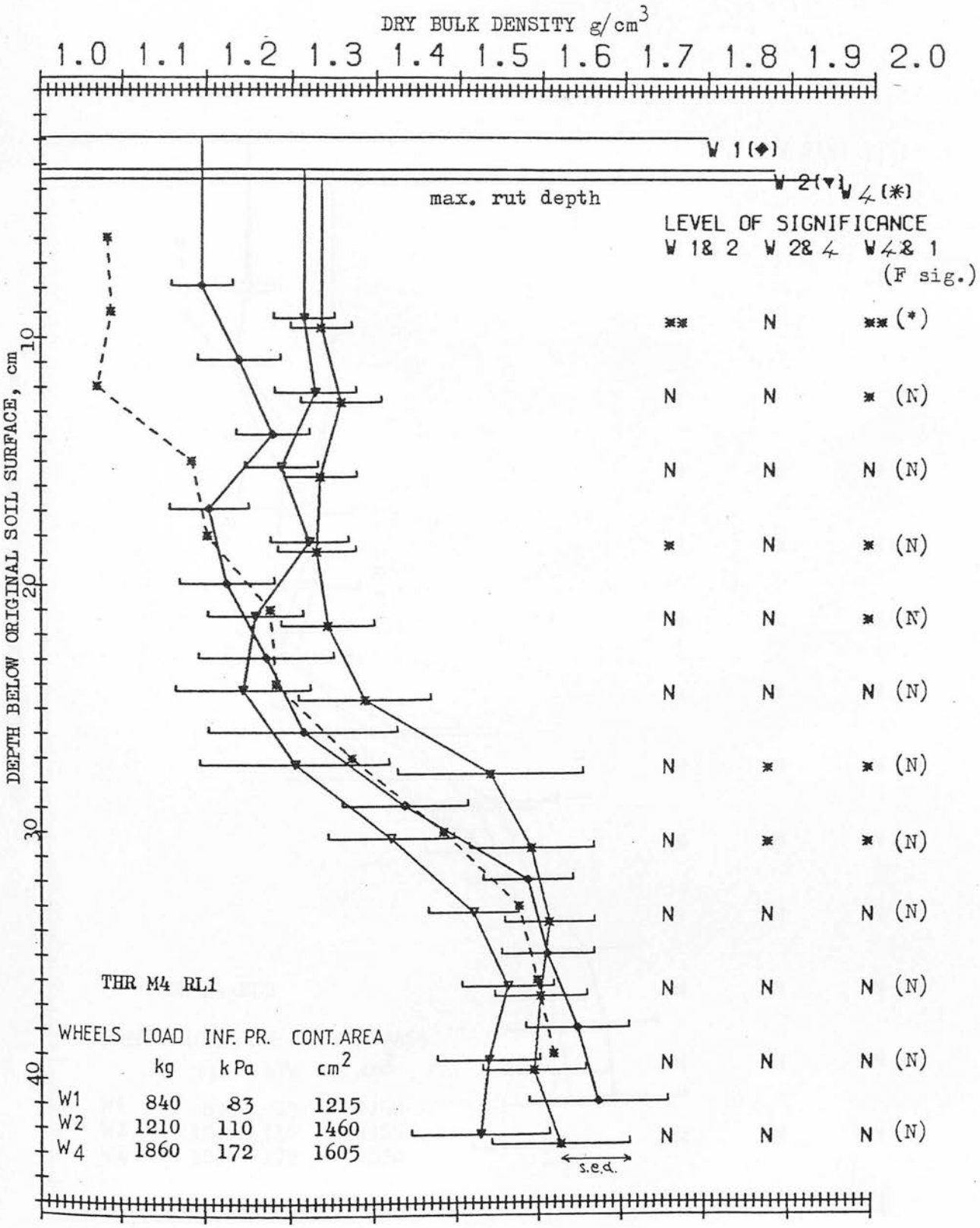

Fig.46h Dry bulk density profiles beneath the track centre before (- - -) and after (——) the wheel treatments for soil treatment RL 2, occasion M4, Threipmuir soil.

46h

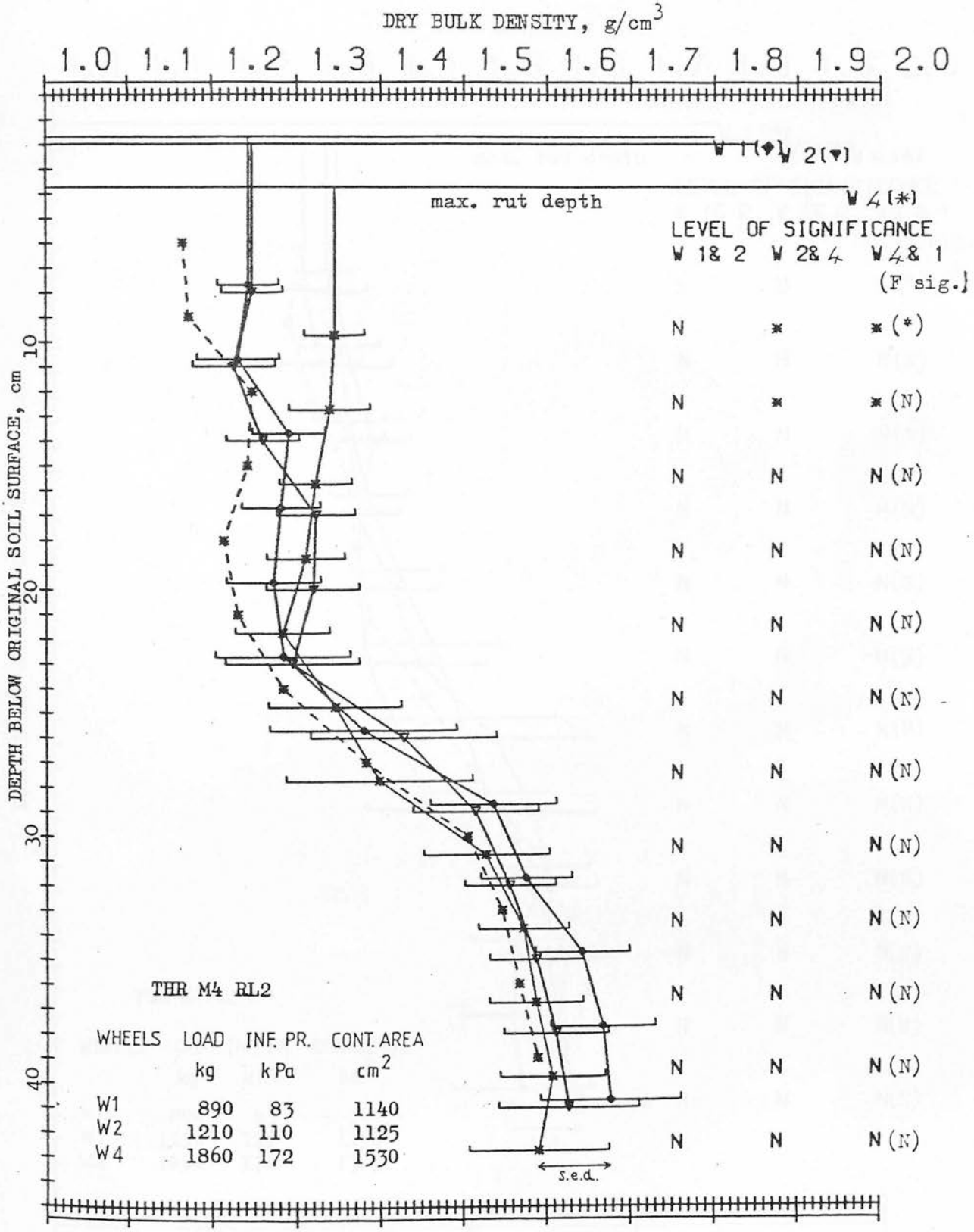

Fig.46i Dry bulk density profiles beneath the track centre before (- - -) and after (——) the wheel treatments for soil treatment RL 3, occasion M4, Threipmuir soil.

46i

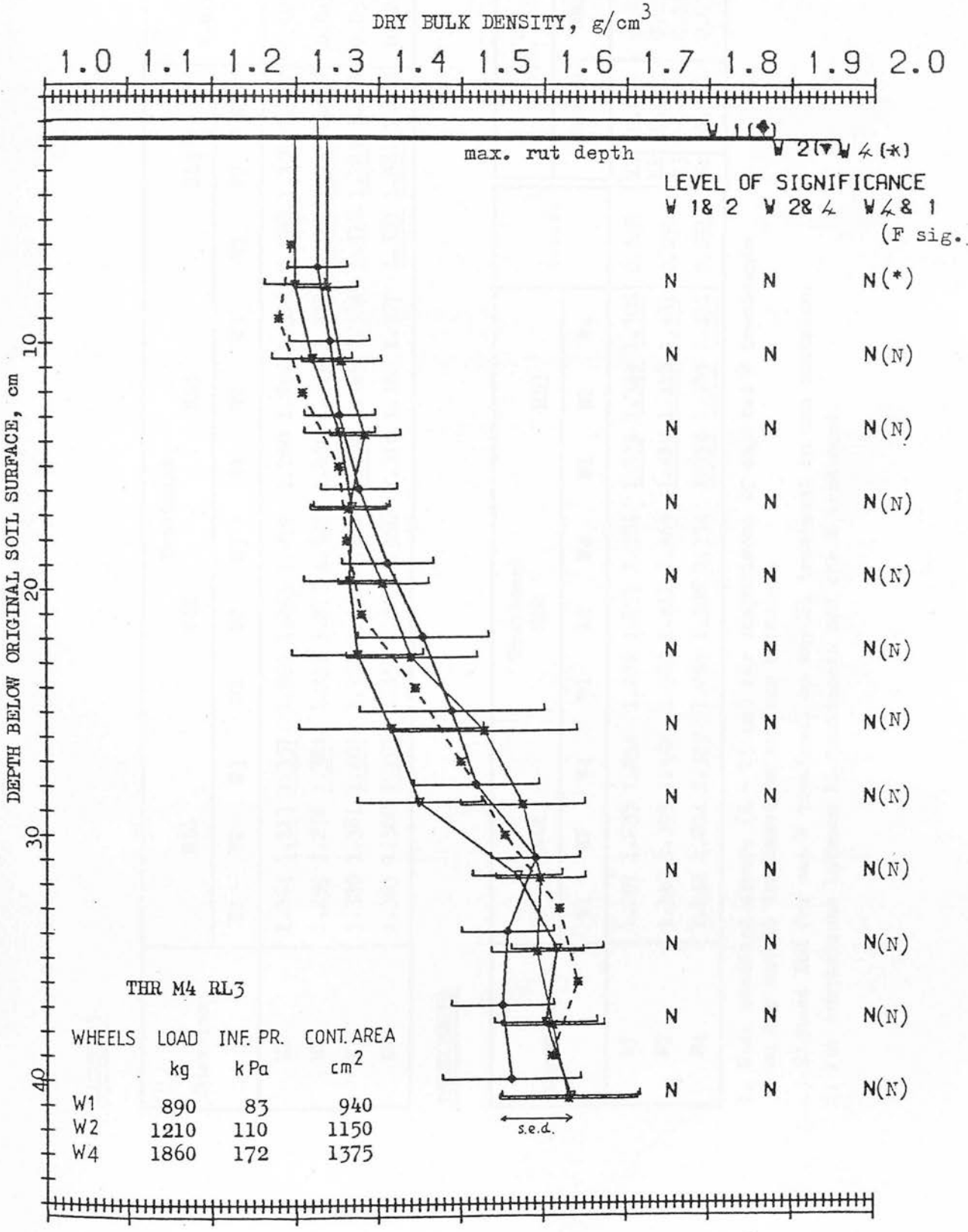

TABLE 15 MEAN DRY BULK DENSITY VALUES, $g/cm^3$, 6-25 cm BELOW RUT BOTTOM AFTER WHEEL TREATMENTS (W) ON DIFFERENT SOIL TREATMENTS (RL) AT DIFFERENT MOISTURE CONDITIONS (M) ON DIFFERENT OCCASIONS FOR EACH SOIL

MACMERRY

| Occasion | Treatment RL1 W1 | RL1 W2 | RL1 W3 | RL2 W1 | RL2 W2 | RL2 W3 | RL3 W1 | RL3 W2 | RL3 W3 | RL4 W1 | RL4 W2 | RL4 W3 | s.e.d.[1] |
|---|---|---|---|---|---|---|---|---|---|---|---|---|---|
| M1 | 1.264 | 1.313 | 1.357 | 1.260 | 1.265 | 1.279 | 1.280 | 1.296 | 1.316 | 1.288 | 1.301 | 1.327 | 0.029 |
| M2 | 1.259 | 1.276 | 1.384 | 1.237 | 1.273 | 1.325 | 1.250 | 1.279 | 1.332 | 1.296 | 1.331 | 1.376 | 0.047 |
| M3 | 1.320 | 1.381 | 1.407 | 1.326 | 1.350 | 1.382 | 1.354 | 1.365 | 1.384 | 1.316 | 1.393 | 1.368 | 0.033 |
| M4 | 1.363 | 1.380 | 1.407 | 1.353 | 1.365 | 1.366 | 1.376 | 1.377 | 1.397 | 1.382 | 1.381 | 1.401 | 0.026 |

THREIPMUIR

| Occasion | Treatment RL1 W1 | RL1 W2 | RL1 W4 | RL2 W1 | RL2 W2 | RL2 W4 | RL3 W1 | RL3 W2 | RL3 W4 | s.e.d.[1] |
|---|---|---|---|---|---|---|---|---|---|---|
| M1 | 1.207 | 1.233 | 1.234 | 1.286 | 1.257 | 1.284 | 1.339 | 1.349 | 1.306 | 0.048 |
| M2 | 1.340 | 1.395 | 1.442 | 1.380 | 1.411 | 1.469 | 1.410 | 1.418 | 1.487 | 0.051 |
| M4 | 1.246 | 1.294 | 1.375 | 1.283 | 1.306 | 1.334 | 1.394 | 1.385 | 1.411 | 0.051 |

| s.e.d.[2] | Threip. | Mac. |
|---|---|---|
| M1 | 0.048 | 0.034 |
| M2 | 0.043 | 0.042 |
| M3 | - | 0.030 |
| M4 | 0.056 | 0.033 |

1. Mean standard errors (6 - 25 cm) for comparisons of any two W treatments on any one RL treatment on any one occasion.

(——)=Highest Dbd for one W treatment on any RL treatment on one occasion.

2. For comparisons between RL treatments and one W treatment.

of the data revealed few significant differences (at $P < 0.05$) between the mean values at any one depth beneath the wheels, or the average mean values between 6 and 25 cm. However, there was a consistent trend of the higher bulk density following the passage of the wheel with highest mean surface pressure.

The statistical analysis of all field data of dry bulk density and rut dimensions after wheel passage used comparisons of split-plot treatments (W treatments) on any one main treatment (RL treatment). Differences between the means were assumed significant at $P < 0.05$ if greater than two standard errors of the differences. This was only a 'rule of thumb' technique as the t statistic would not be normally distributed for such comparisons.

For any one wheel treatment the largest bulk density increases were observed on the loosest and weakest original soil conditions, RL 1. Largest absolute values of Dbd of the upper 25 cm of soil after wheel passage on any one occasion were on either RL 1 or RL 4 for Macmerry and on RL 3 for Threipmuir. As seen from Table 15, the differences between final Dbd profiles were usually more significant between wheel treatments on the same RL treatment than between RL treatments for the same wheel treatment. Comparing different occasions, the wetter run M4 of Macmerry showed the highest resultant Dbd values (approx. 1.4 $g/cm^3$), the drier run M2 the lowest (approx. 1.24 $g/cm^3$); these differences were significant at $P < 0.05$. For Threipmuir the wetter run M2 caused the highest Dbd values (approx. 1.45 $g/cm^3$), the drier run M1 the lower (approx. 1.2 $g/cm^3$); these differences were significant at $P < 0.05$.

Examining the form of the Dbd profiles for the upper 20 cm, many showed highest values within 9 cm of rut bottom, but some showed highest Dbd between 10 and 15 cm depth, i.e. Macmerry, Fig.45c , W2; Fig.45c , W3; Fig.45d , W3; Fig.45f , W3; Fig.45i , W3 and Fig.45j , W3, and Threipmuir Fig.46b , W1; Fig.46g , W1 and Fig.46h , W2. However, such 'foci' of compaction were not very distinct. Assessment of Dbd changes of the Macmerry soil below 30 cm from the original soil surface was hindered by the insufficient depth of the original Dbd profile. Unfortunately the size of the standard errors below 30 cm for both soils suggests that soil variability below the depth of tillage would inhibit an accurate assessment of soil strains in such zones. The higher variability below 15 cm depth may have been due to bending of the radiation equipment probes (see Figs.46c and 46f ). It was also suspected that cracks developed between access holes during some measurements (Fig.46i ) while the steel spikes were being driven into the hard, dry soil at Lower Terrace field.

### 5.1.2 Wheel sinkages

Reliefmeter measurements provided data on surface sinkage at 5 cm intervals along the transverse cross-section of the rut. This data was used to derive the following parameters describing the cross-section:

1. Maximum rut depth (Max.RD): The greatest surface sinkage recorded along the cross-section.
2. Mean rut depth (MRD): The mean value of surface sinkage for all positions where sinkage occurred (i.e. n positions).
3. Simplified cross-sectional area of the rut (CSA): MRD x n x 5.

A computer program[1] was developed to handle data from the reliefmeter, calculate values of Max.RD, MRD and CSA and apply an analysis of variance to the results. The mean values and standard errors of Max.RD, MRD and CSA for all the experimental occasions are shown in Table 16. Figs.47a to 47z show the mean shape of the rut cross-sections after each wheel treatment on each RL treatment on each occasion for both soil types. It must be noted that the mean MRD value for any treatment combination is not equivalent to the average needle depth of the mean rut cross-sections, due to differences between the methods of computation.

The depth of the mean rut cross-sections after the wheel treatments could usually be ranked for any one RL treatment in the following order, W1 < W2 < W3 for Macmerry and W1 < W2 < W4 for Threipmuir; the deepest ruts caused by wheels of highest mean surface pressures. Sinkages of any one wheel treatment on any one occasion could be ranked according to the original soil conditions, i.e. RL1 > RL2 > RL3 > RL4. Deepest overall sinkages occurred on wettest occasions, shallowest on driest occasions, for the same W, RL treatments and soil types. Rut measurements on the strongest soil at the Lower Terrace site (M1, RL3 and M4, RL3, Figs47s &z) were obscured by the vegetation. This is reflected in the higher standard errors for M4 and 'negative sinkages' for M1, RL3 (Fig.47s). Tyre sidewall support may have become significant for W4 on Threipmuir. M4, RL3, W4 and M1, RL2, W4 show less sinkage at the rut centre and more at the rut edges than for treatments W1 and W2 on the same soils (Figs.47r and 47v).

---

1. See Appendix 9.

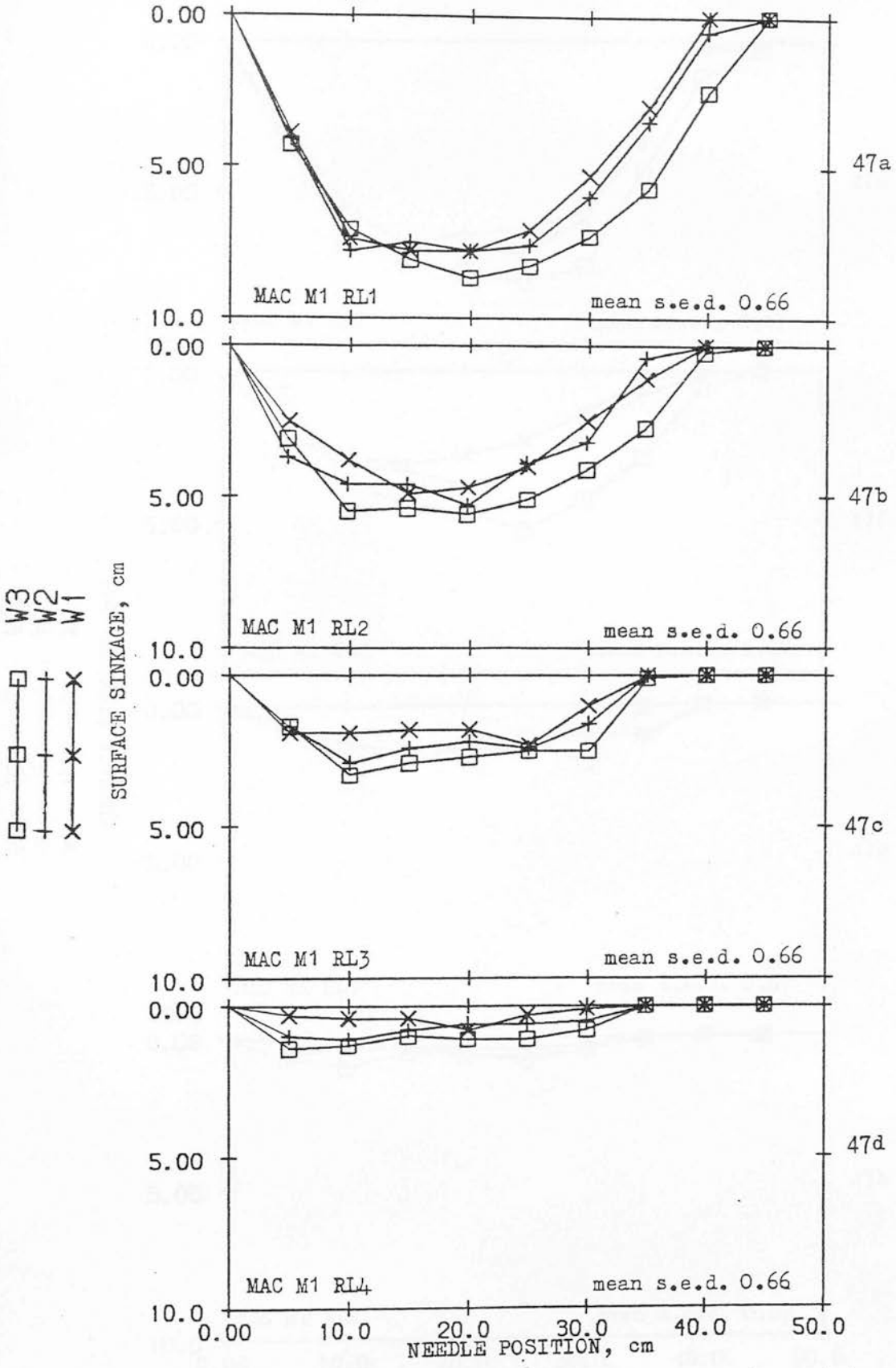


Fig.47 Transverse rut profiles described by the mean surface sinkage at each needle position of the reliefmeter. Each wheel treatment (W) on each soil treatment (RL) for occasion M1 (mean moisture content, 0-30 cm, 23.3%, w/w), Macmerry soil.

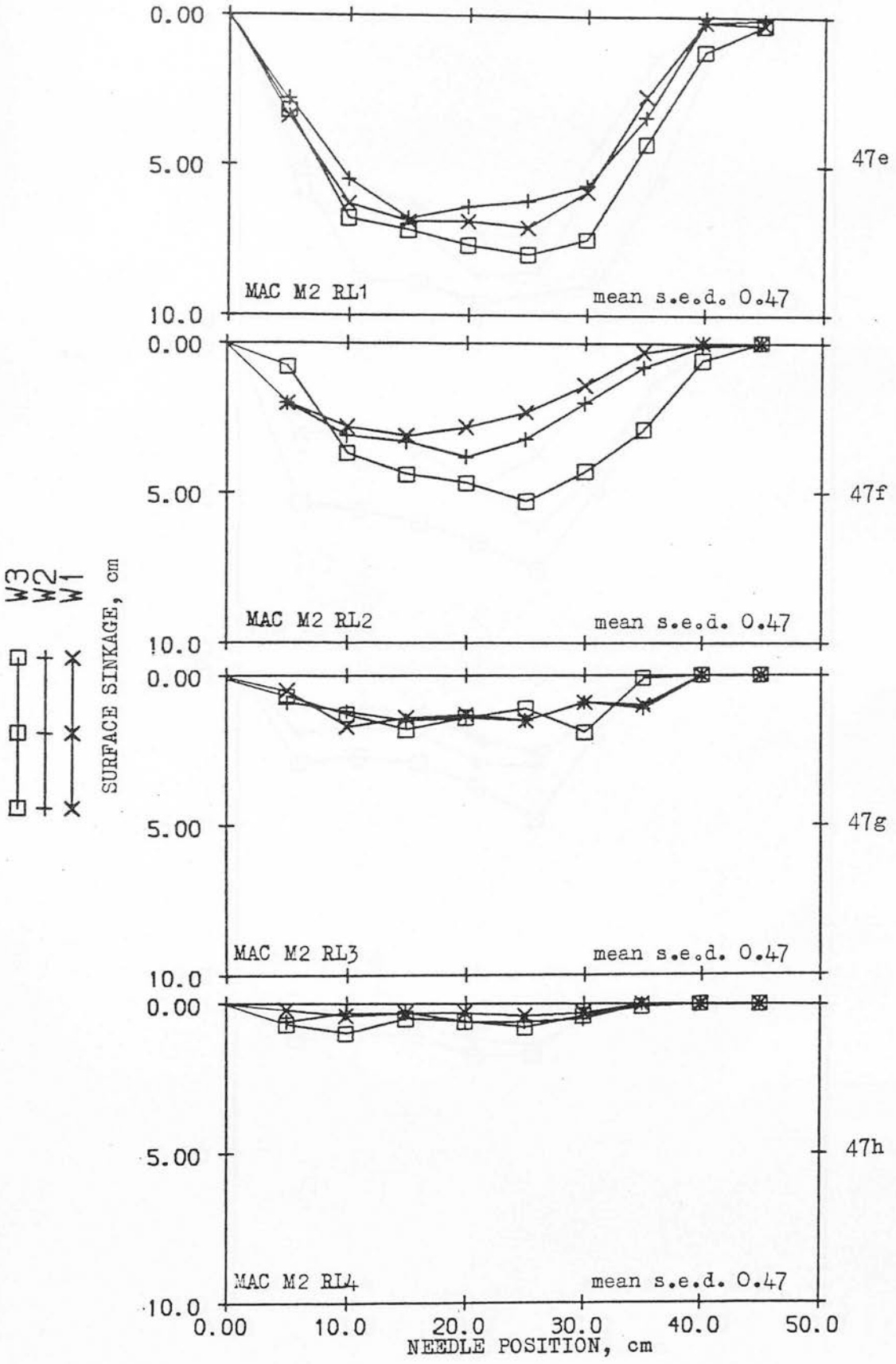


Fig.47 Transverse rut profiles described by the mean surface sinkage at each needle position of the reliefmeter. Each wheel treatment (W) on each soil treatment (RL) for occasion M2 (mean moisture content, 0-12 cm, 18.0%, w/w), Macmerry soil.

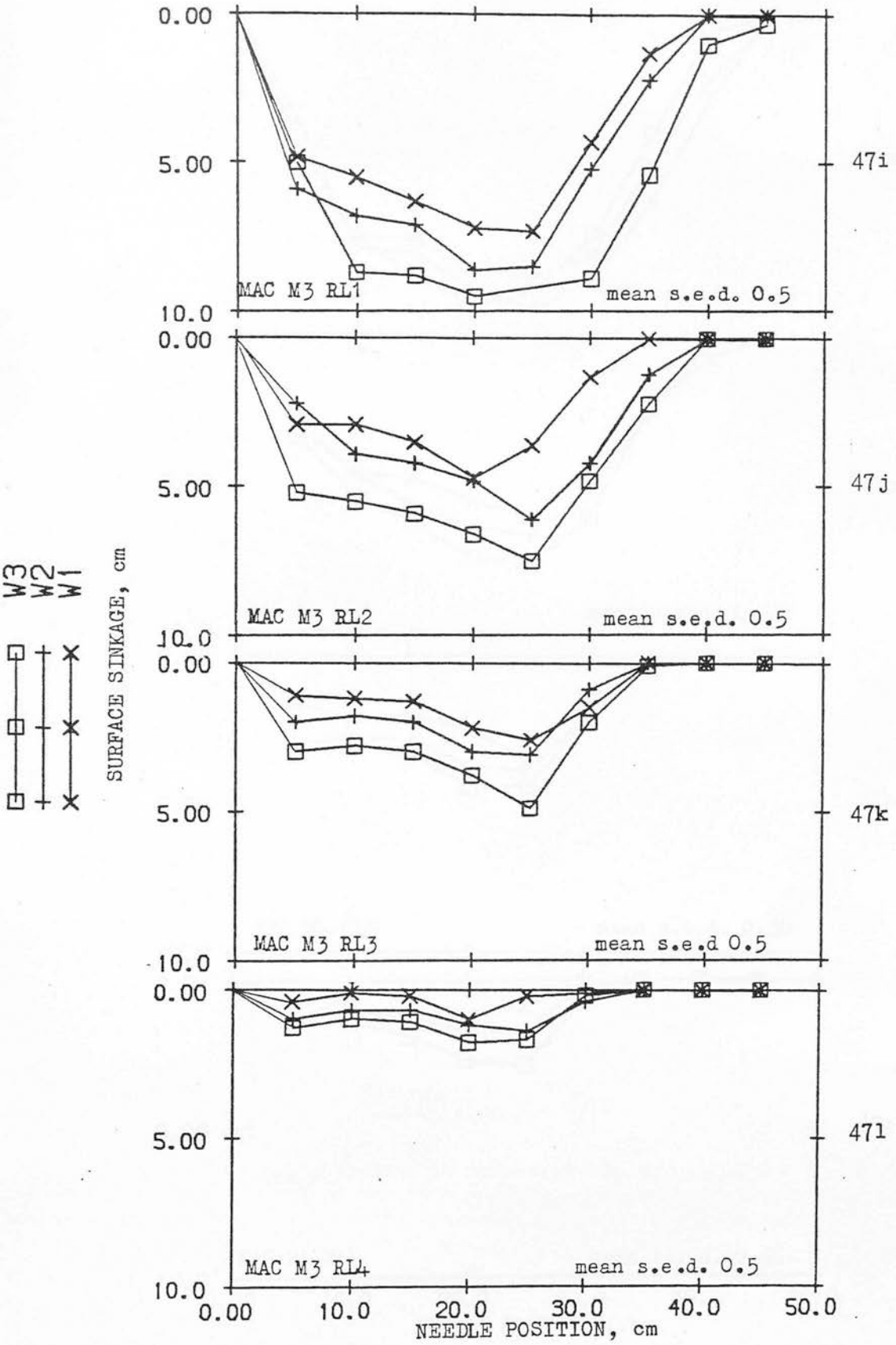


Fig.47 Transverse rut profiles described by the mean surface sinkage at each needle position of the reliefmeter. Each wheel treatment (W) on each soil treatment (RL) for occasion M3 (mean moisture content, 0-30 cm, 25.3%, w/w), Macmerry soil.

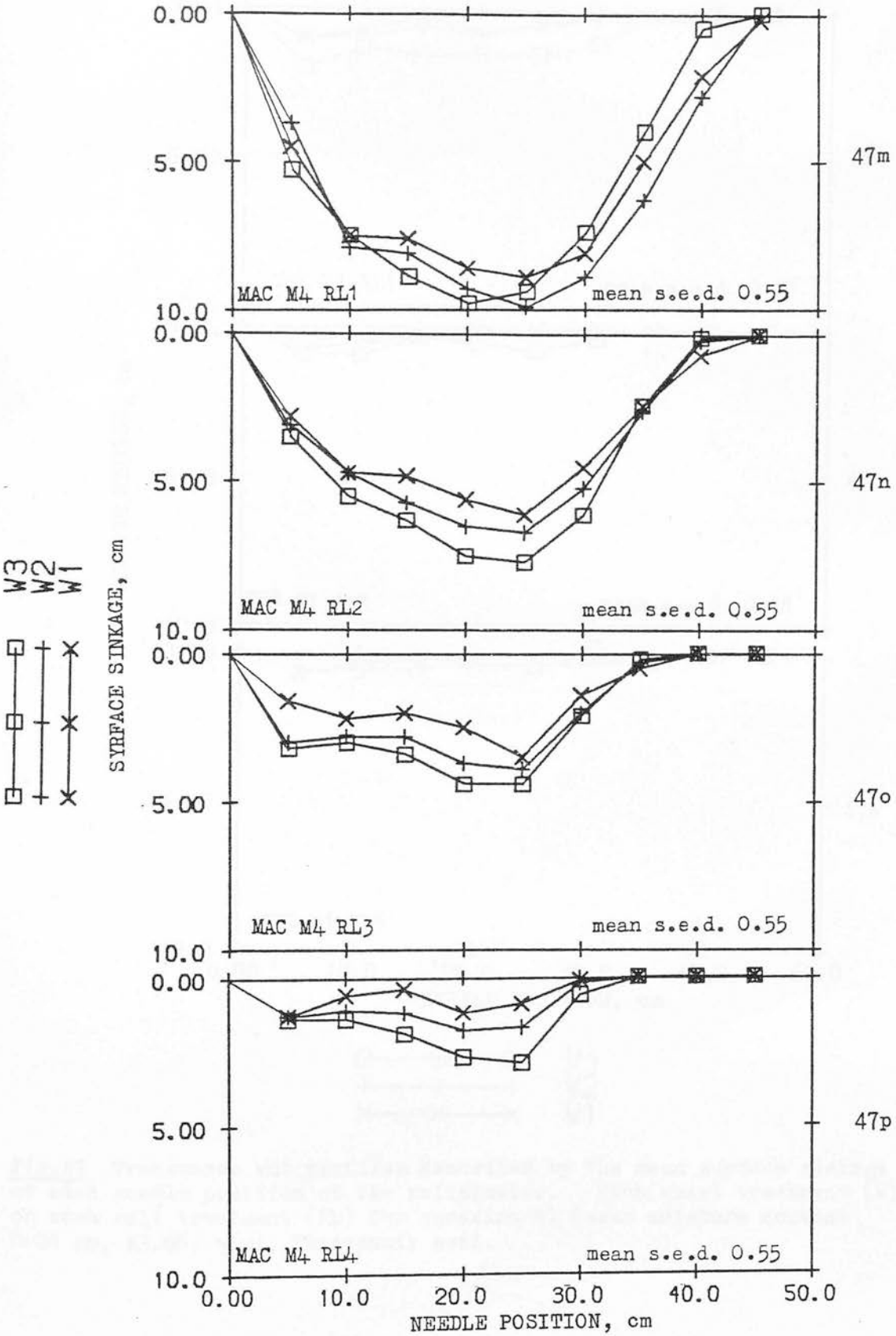


Fig.47 Transverse rut profiles described by the mean surface sinkage at each needle position of the reliefmeter. Each wheel treatment (W) on each soil treatment (RL) for occasion M4 (mean moisture content, 0-30 cm, 28.2%, w/w), Macmerry soil.

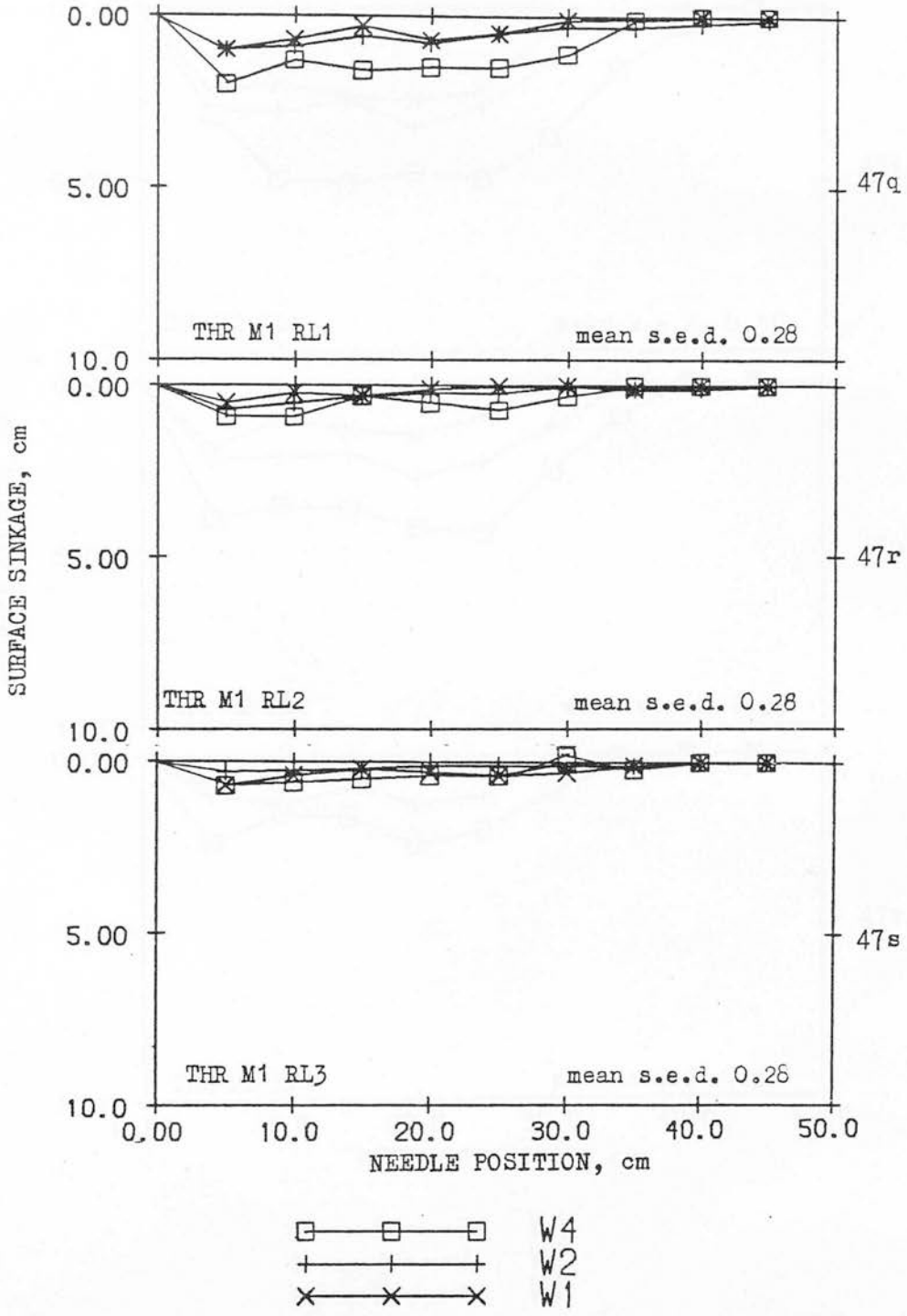


Fig.47 Transverse rut profiles described by the mean surface sinkage at each needle position of the reliefmeter. Each wheel treatment (W) on each soil treatment (RL) for occasion M1 (mean moisture content 0-20 cm, 13.6%, w/w), Threipmuir soil.

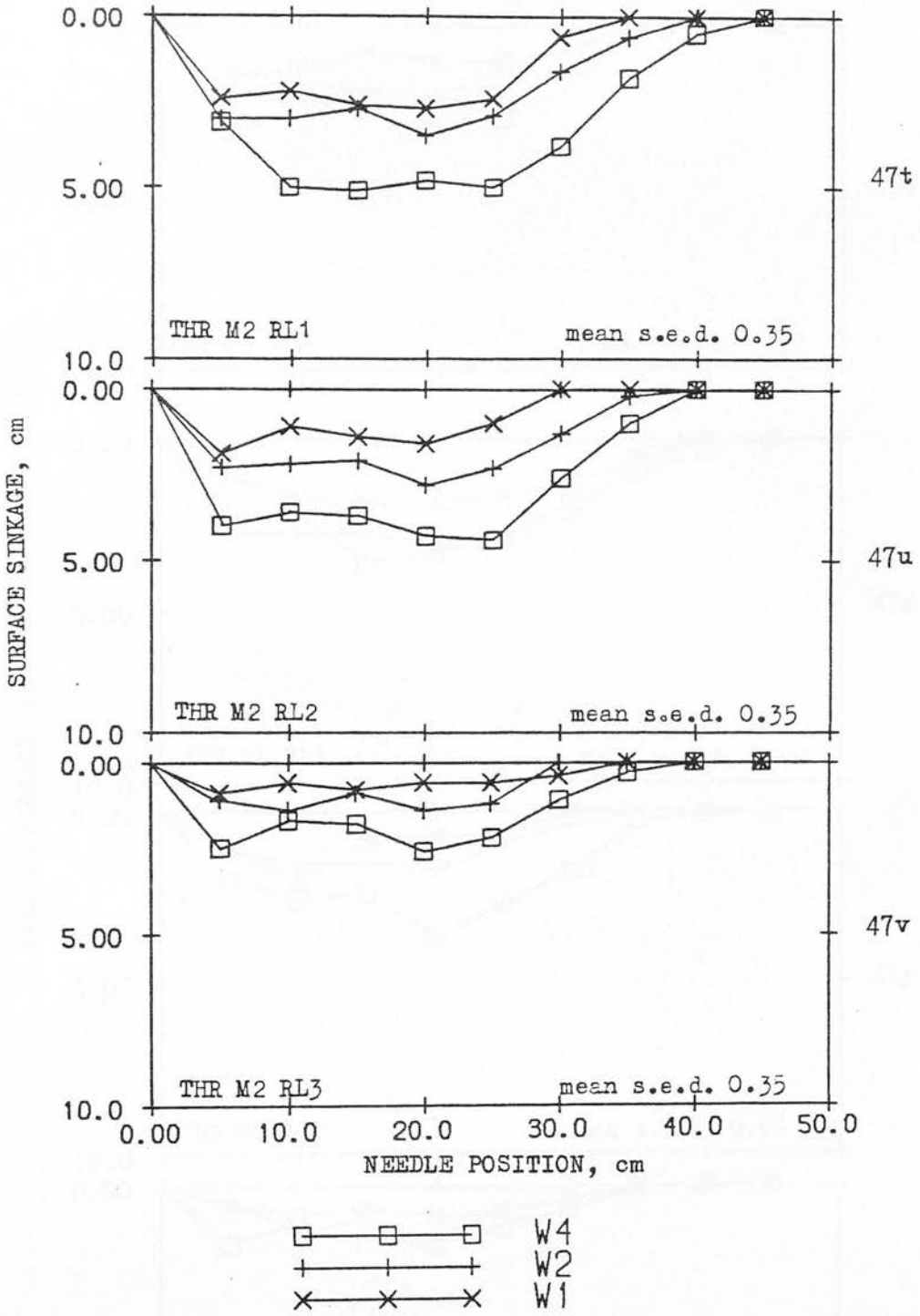


Fig.47 Transverse rut profiles described by the mean surface sinkage at each needle position of the reliefmeter. Each wheel treatment (W) on each soil treatment (RL) for occasion M2 (mean moisture content 0-20 cm, 23.0%, w/w), Threipmuir soil.

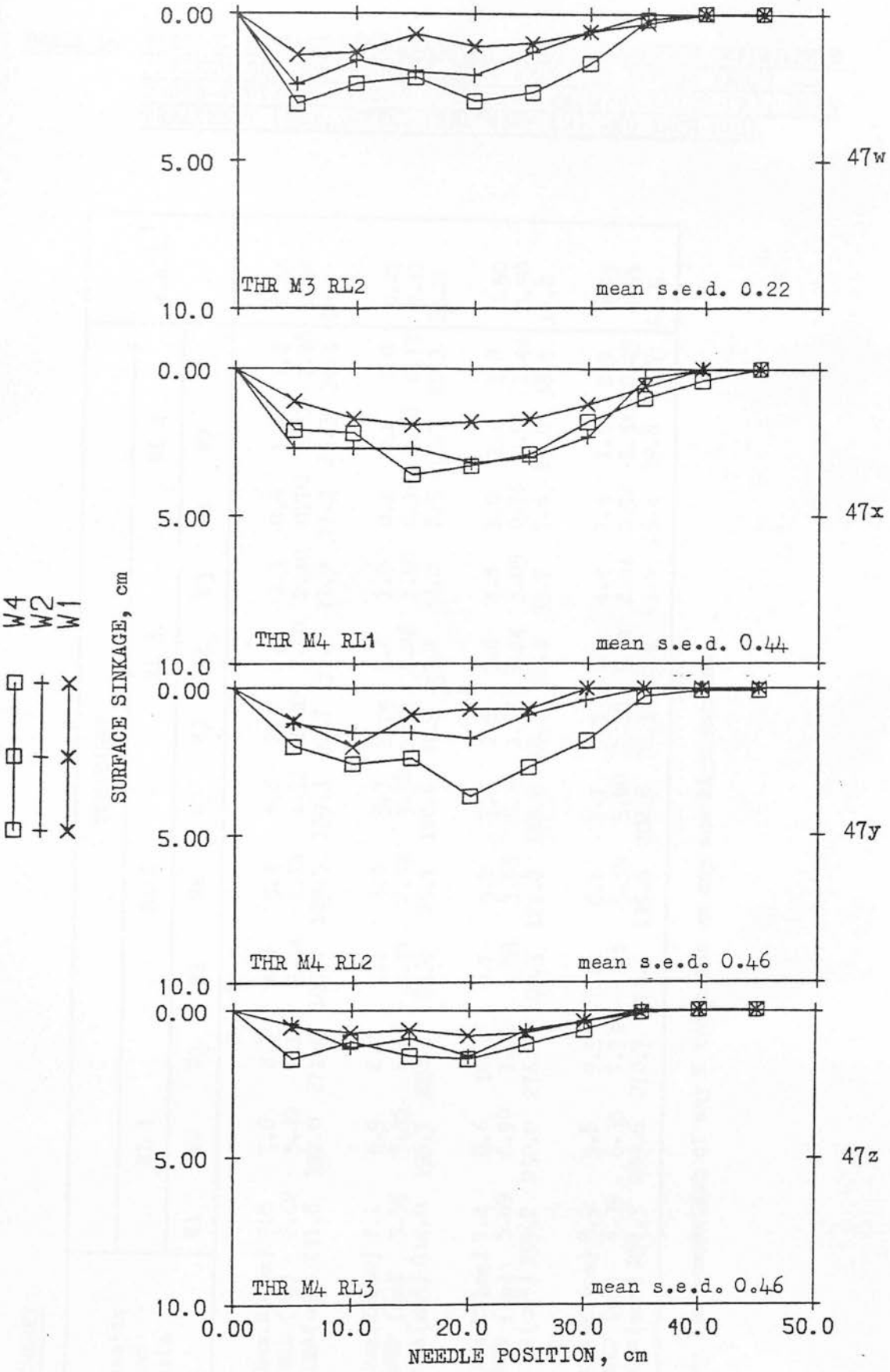


Fig.47 continued Transverse rut profiles described by the mean surface sinkage at each needle position of the reliefmeter. Each wheel treatment (W) on each soil treatment (RL) for occasion M3 (mean moisture content 0-20 cm, 20.6%, w/w) and occasion M4 (mean moisture content 0-20 cm, 18.8%, w/w), Threipmuir soil.

TABLE 16 SURFACE SINKAGE MEASUREMENTS, FIELD COMPACTION EXPERIMENTS
MAXIMUM RUT DEPTHS (MAX.RD), MEAN RUT DEPTHS (MRD) and
CROSS-SECTIONAL AREAS (CSA) FOR EACH OCCASION (M), SOIL
TREATMENT (RL), WHEEL TREATMENT (W) AND EACH SOIL

MACMERRY

| Occasion and data | TREATMENT | | | | | | | | | | | | s.e.d.[1] |
|---|---|---|---|---|---|---|---|---|---|---|---|---|---|
| | RL 1 | | | RL 2 | | | RL 3 | | | RL 4 | | | |
| | W1 | W2 | W3 | W1 | W2 | W3 | W1 | W2 | W3 | W1 | W2 | W3 | |
| M1 | | | | | | | | | | | | | |
| Max.RD(cm) | 7.8 | 7.8 | 8.7 | 4.9 | 5.4 | 5.6 | 2.3 | 2.9 | 3.3 | 0.8 | 1.1 | 1.4 | 0.66 |
| MRD (cm) | 6.62 | 5.49 | 7.11 | 3.34 | 4.14 | 4.31 | 2.00 | 1.90 | 2.40 | 0.70 | 0.81 | 1.28 | 0.66 |
| CSA($cm^2$) | 231.8 | 192.0 | 271.6 | 105.4 | 129.5 | 159.3 | 56.7 | 57.1 | 71.9 | 11.4 | 23.3 | 34.3 | 23.7 |
| M2 | | | | | | | | | | | | | |
| Max.RD(cm) | 7.1 | 6.9 | 8.0 | 3.1 | 3.8 | 5.3 | 1.75 | 1.6 | 1.9 | 0.4 | 0.6 | 1.0 | 0.47 |
| MRD (cm) | 5.55 | 5.35 | 5.55 | 2.47 | 2.53 | 3.38 | 1.37 | 1.46 | 1.50 | 0.36 | 0.58 | 0.73 | 0.47 |
| CSA($cm^2$) | 214.0 | 195.7 | 212.1 | 83.0 | 85.1 | 120.6 | 41.9 | 49.1 | 44.0 | 8.5 | 15.7 | 20.3 | 23.0 |
| M3 | | | | | | | | | | | | | |
| Max.RD(cm) | 7.4 | 8.6 | 10.3 | 4.7 | 5.2 | 7.4 | 2.6 | 3.6 | 4.8 | 1.0 | 1.4 | 1.8 | 0.50 |
| MRD (cm) | 5.69 | 6.90 | 7.91 | 3.53 | 3.65 | 5.39 | 1.87 | 2.14 | 3.05 | 0.76 | 0.97 | 1.44 | 0.50 |
| CSA($cm^2$) | 199.2 | 230.0 | 276.8 | 100.3 | 127.8 | 188.8 | 59.3 | 61.4 | 95.7 | 7.6 | 25.8 | 38.5 | 17.0 |
| M4 | | | | | | | | | | | | | |
| Max.RD(cm) | 8.9 | 9.8 | 9.9 | 6.1 | 6.7 | 7.7 | 3.5 | 3.9 | 4.4 | 1.4 | 1.8 | 2.9 | 0.55 |
| MRD (cm) | 6.39 | 6.35 | 7.73 | 4.46 | 5.35 | 5.80 | 2.19 | 3.04 | 2.94 | 0.94 | 1.34 | 2.45 | 0.55 |
| CSA($cm^2$) | 257.3 | 229.6 | 270.7 | 170.6 | 195.6 | 202.8 | 70.3 | 98.6 | 93.6 | 25.4 | 39.8 | 73.7 | 24.5 |

1. For comparison of any W treatment on any one RL treatment

TABLE 16 (continued)

THREIPMUIR

| Occasion and data | TREATMENT | | | | | | | | | s.e.d.[1] |
|---|---|---|---|---|---|---|---|---|---|---|
| | RL 1 | | | RL 2 | | | RL 3 | | | |
| | W1 | W2 | W4 | W1 | W2 | W4 | W1 | W2 | W4 | |
| M1 | | | | | | | | | | |
| Max.RD (cm) | 1.0 | 1.0 | 2.0 | 0.5 | 0.7 | 0.9 | 0.7 | 0.2 | 0.7 | 0.2 |
| MRD (cm) | 0.71 | 0.75 | 1.34 | 0.41 | 0.66 | 0.85 | 0.48 | 0.36 | 0.46 | 0.2 |
| CSA ($cm^2$) | 16.7 | 23.6 | 43.6 | 7.6 | 14.1 | 21.2 | 11.9 | 5.1 | 14.3 | 10.5 |
| M2 | | | | | | | | | | |
| Max.RD (cm) | 2.7 | 3.5 | 5.1 | 1.9 | 2.8 | 4.3 | 0.9 | 1.4 | 2.6 | 0.25 |
| MRD (cm) | 2.47 | 2.53 | 4.12 | 1.41 | 2.44 | 3.64 | 0.82 | 1.13 | 1.83 | 0.25 |
| CSA ($cm^2$) | 74.1 | 80.9 | 152.8 | 35.1 | 78.3 | 121.5 | 22.0 | 26.7 | 58.9 | 15.6 |
| M3 | | | | | | | | | | |
| Max.RD (cm) | - | - | - | 1.4 | 2.4 | 3.1 | - | - | - | 0.22 |
| MRD (cm) | - | - | - | 1.09 | 1.76 | 2.37 | - | - | - | 0.22 |
| CSA ($cm^2$) | - | - | - | 40.6 | 52.1 | 58.0 | - | - | - | 10.5 |
| M4 | | | | | | | | | | |
| Max.RD (cm) | 1.9 | 3.2 | 3.6 | 1.7 | 2.0 | 3.7 | 0.9 | 1.6 | 1.7 | 0.56 |
| MRD (cm) | 1.69 | 2.39 | 2.65 | 1.4 | 0.91 | 2.38 | 0.7 | 1.00 | 1.55 | 0.56 |
| CSA ($cm^2$) | 52.2 | 77.0 | 86.5 | 32.7 | 25.2 | 71.3 | 19.6 | 28.9 | 42.5 | 20.2 |

1. For comparison of any W treatments on any one RL treatment

### 5.1.3 Initial soil moisture conditions

#### 5.1.3.1 Soil moisture content

Mean soil moisture contents (% w/w) are shown in Table 17a for Macmerry and Table 17b for Threipmuir. Occasion M2 was the driest for Macmerry (overall mean 21 per cent); wettest was occasion M4 (overall mean 28.2 per cent). M1 was only significantly drier than M3 in the top 12 cm. A smaller range of moisture content variation was shown below 12 cm than above for these bare soil conditions; 10 per cent moisture content compared to 13 per cent moisture content. For the Threipmuir soil occasion M1 was the driest (overall mean 13.6 per cent) and M2 the wettest (overall mean 23 per cent). The variation of moisture content with depth was more uniform than at the Macmerry site; grass roots assisted moisture extraction from below 12 cm depth. Both the Macmerry and Threipmuir soils showed lowest moisture contents for the loosest soil conditions (RL1); however, differences within occasions rarely approached values significant at $P < 0.05$.

#### 5.1.3.2 Soil moisture tension

Mean soil moisture tension values are shown in Table 18 . An analysis of variance to account for missing values was used to calculate standard errors of the differences between the means (Cochran and Cox, 1960). Readings were occasionally lost during use of the tensiometers due to airlocks in the water column and poor pot/soil contact.

The measurements on occasion M1, Lower Terrace, using gypsum resistance blocks proved difficult to interpret. It appeared that some blocks dried very little and some extremely rapidly. These

TABLE 17a MEAN GRAVIMETRIC MOISTURE CONTENT, MACMERRY SOIL, SECTION 7 AT DIFFERENT DEPTHS (UNITS, % w/w)

| Occasions, depth | SOIL TREATMENTS RL 1 | RL 2 | RL 3 | RL 4 | s.e.d. |
|---|---|---|---|---|---|
| M1 6-12 cm | 19.4 | 22.4 | 21.8 | 22.1 | 1.2 |
| 24-30 cm | 28.2 | 27.5 | 26.8 | 26.4 | 1.5 |
| M2 6-12 cm | 15.1 | 18.4 | 18.6 | 19.9 | 1.2 |
| 24-30 cm | 23.6 | 22.5 | 24.4 | 24.7 | 1.5 |
| M3 6-12 cm | 24.2 | 23.9 | 25.9 | 24.7 | 1.2 |
| 24-30 cm | 25.5 | 24.9 | 27.6 | 25.5 | 1.5 |
| M4 6-12 cm | 26.9 | 25.4 | 27.6 | 27.9 | 1.2 |
| 24-30 cm | 28.9 | 28.0 | 30.1 | 31.2 | 1.5 |
| s.e.d. | | | | | |
| 6-12 cm | 1.2 | 1.2 | 1.2 | 1.2 | |
| 24-30 cm | 1.55 | 1.55 | 1.55 | 1.55 | |

TABLE 17b MEAN GRAVIMETRIC MOISTURE CONTENT, THREIPMUIR SOIL, LOWER TERRACE, AT DIFFERENT DEPTHS (UNITS, % w/w)

| Occasions, depth | SOIL TREATMENTS RL 1 | RL 2 | RL 3 | s.e.d. |
|---|---|---|---|---|
| M1 6-12 cm | 10.8 | 11.9 | 10.2 | 0.9 |
| 12-24 cm | 13.2 | 14.4 | 13.9 | 1.6 |
| 24-36 cm | 14.0 | 14.6 | 15.0 | 1.6 |
| M2 6-12 cm | 23.6 | 23.5 | 23.5 | 0.9 |
| 12-24 cm | 24.2 | 24.1 | 24.0 | 0.8 |
| 24-36 cm | 22.5 | 22.5 | 22.6 | 0.8 |
| M3 6-12 cm | - | 18.2 | - | 1.7 |
| 12-24 cm | - | 21.0 | - | 1.3 |
| 24-36 cm | - | 20.4 | - | 1.4 |
| M4 6-12 cm | 17.7 | 17.0 | 17.8 | 0.7 |
| 12-24 cm | 18.5 | 18.4 | 19.2 | 1.5 |
| 24-36 cm | 17.9 | 18.6 | 18.6 | 1.5 |

TABLE 18 VARIATION OF SOIL MOISTURE TENSION BETWEEN OCCASIONS, SOIL (RL) TREATMENTS AND DEPTHS, MILLIBARS

| MACMERRY | | | | | |
|---|---|---|---|---|---|
| Occasion, depth, | RL 1 | RL 2 | RL 3 | RL 4 | s.e.d. |
| M1 15 cm | 29.2 | 63.2 | 67.8 | 73.1 | 16.3 |
| M2 15 cm | 165.6 | 161.0 | 261.7 | 278.0 | " |
| M3 15 cm | 65.5 | - | 67.0 | 71.3 | " |
| M3/4 CR[1] 15 cm | 67.7 | - | 73.1 | - | " |
| M4 15 cm | 57.1 | - | - | 70.7 | " |
| s.e.d. | 16.4 | 16.4 | 16.4 | 16.4 | |

| THREIPMUIR | | | | |
|---|---|---|---|---|
| Occasion, depth, | RL 1 | RL 2 | RL 3 | s.e.d. |
| M1[2] 10 cm | 9500 (7500) | 18000 (1200) | 35000 (16000) | 16000 (3000) |
| 30 cm | 3400 (5000) | 1150 (5000) | 4900 ( 4500) | 2000 (1000) |
| M2 10 cm | 68.5 | - | 69.7 | 94 |
| 20 cm | 64.0 | - | 67.0 | 48 |
| 30 cm | 60.0 | - | 56.0 | 41 |
| M3 10 cm | 118.7 | - | 316.8 | 94 |
| 20 cm | 112.0 | - | 162.0 | 48 |
| 30 cm | 119.0 | - | 105.0 | 41 |
| M4 10 cm | 285.9 | - | 428.7 | 94 |
| 20 cm | 359.0 | - | 368.0 | 48 |
| 30 cm | 404.0 | - | 533.0 | 41 |

1. Measurement of cone resistance for M3 and M4.
2. means for selected blocks shown in parentheses

differences were assumed to be caused by either extreme isolation of the block from the soil by the silt pocket, or loss of block/soil contact respectively. An analysis of means of all groups for 10 occasions of measurement, excluding the blocks which dried very rapidly or not at all, is shown in Table 18.

The measurements of soil moisture tension showed a similar pattern of variation throughout the experiments as the measurements of soil moisture content.

### 5.1.4 Initial soil strength

#### 5.1.4.1 Cone resistance

Mean cone resistance values for each occasion and RL treatment are shown in Figs.48a to 48c for Macmerry and Figs.49a to 49c for Threipmuir.[1] Instrumentation problems prevented measurement of cone resistance on the same day as occasion M3, Macmerry. The values measured on an occasion with very similar moisture tension conditions, see Table 18, were considered representative of the cone resistance values for occasions M3 and M4, Macmerry. The similarity of cone shear strength for both these occasions also supported this assumption. Insufficient time prevented the measurement of cone resistance for occasion M3, Threipmuir.

Both soil types showed higher cone resistances for soil of higher bulk density, for the same occasion. In most cases any one RL treatment had a higher cone resistance at lower soil moisture contents and vice-versa. However, RL3 and RL4, Macmerry, showed some reduction of cone resistance for the driest conditions. This may have been caused by brittle failure of the soil and the formation of radial cracks, as observed by Mulqueen et al. (1976), as

1 And Appendix 4.

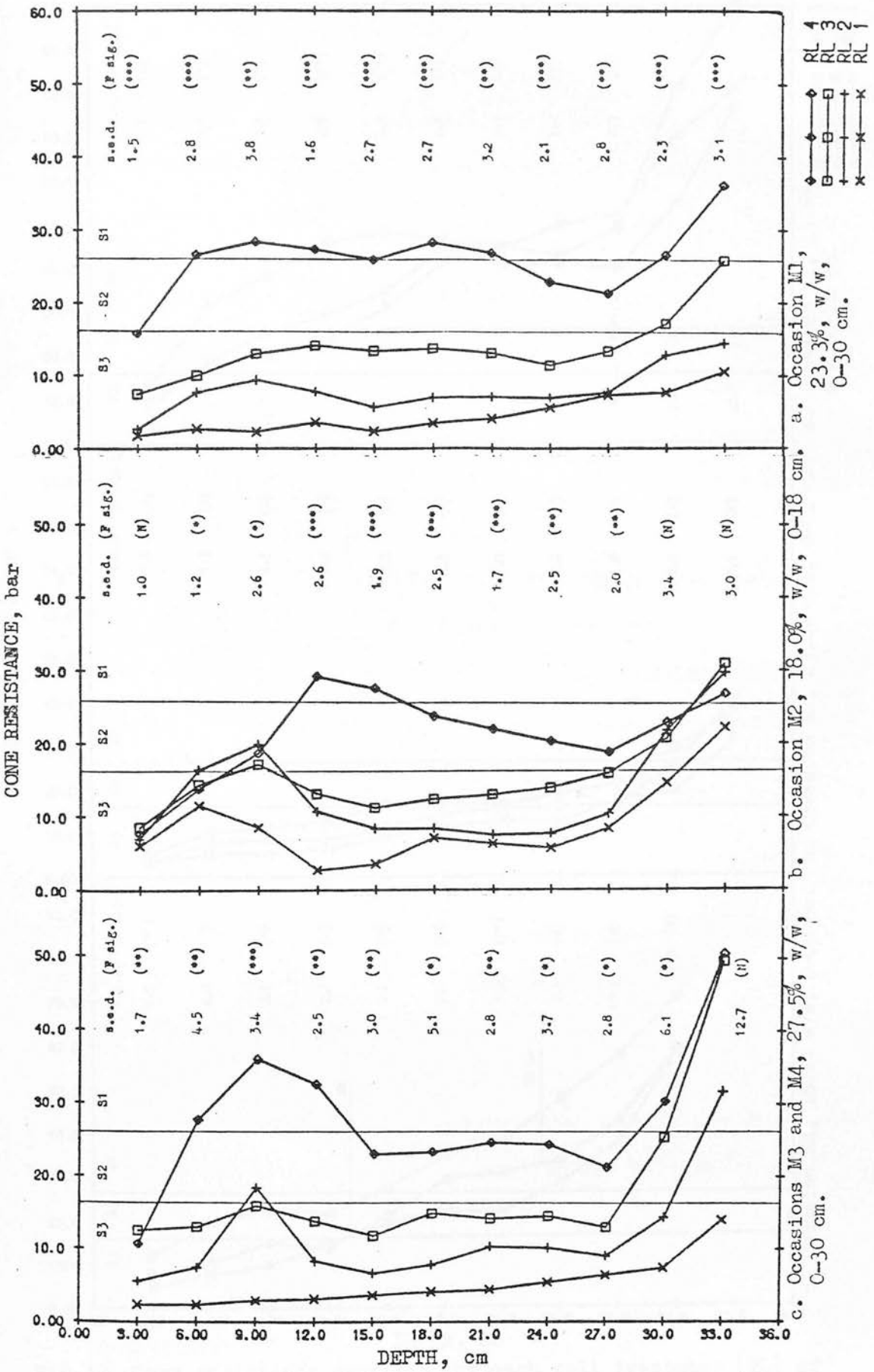


Fig.48 Cone resistance profiles for each soil treatment (RL) of the Macmerry soil on each occasion (M). The mean soil moisture conditions for each occasion are indicated.

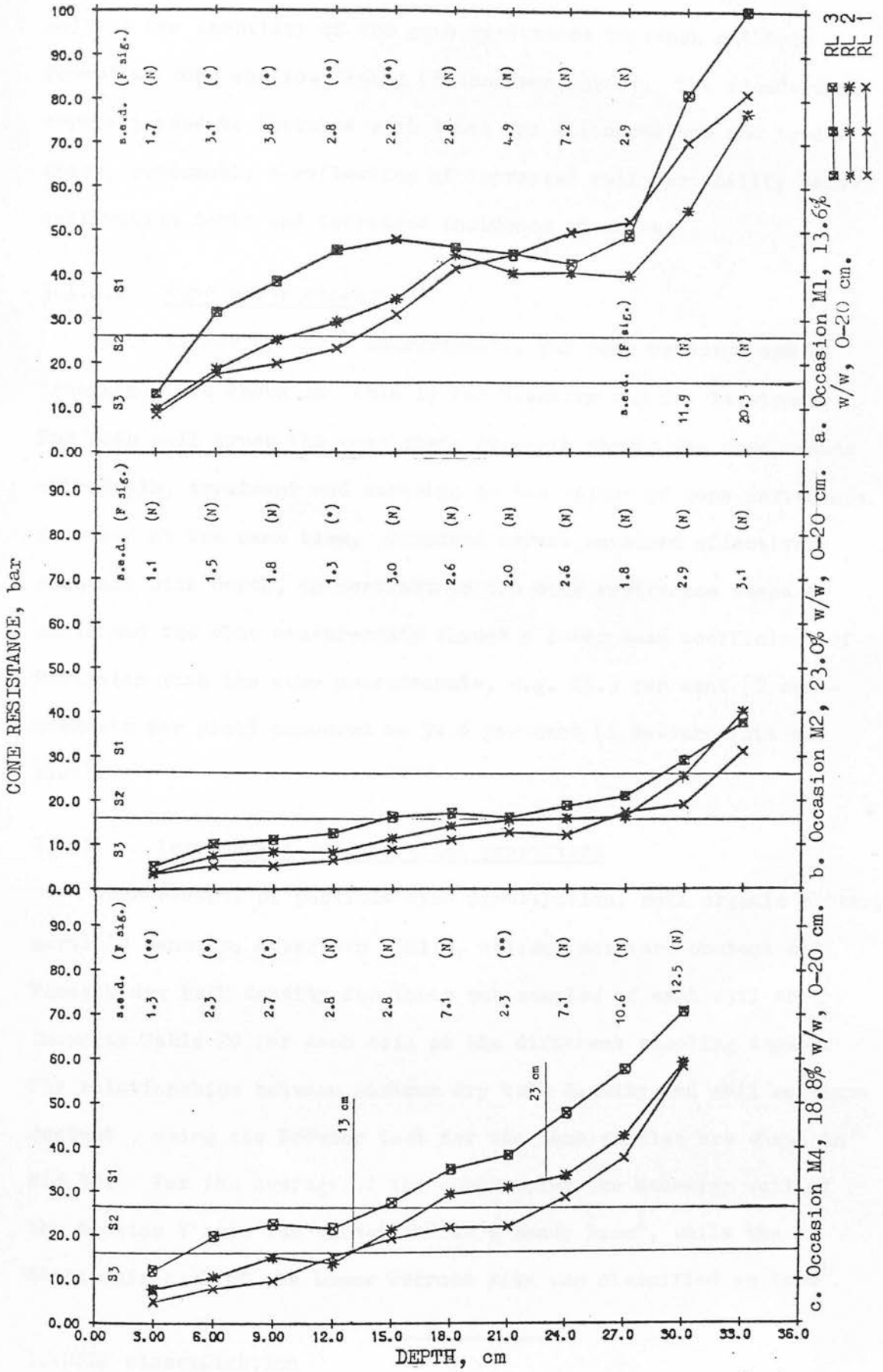


Fig.49 Cone resistance profiles for each soil treatment (RL) of the Threipmuir soil on each occasion (M). The mean soil moisture conditions for each occasion are indicated.

well as the inability of the cone resistance to reach a 'limit force' at such shallow depths (Richardson, 1969). The standard errors tended to increase with depth for all occasions and treatments, presumably a reflection of increased soil variability below cultivation depth and increased incidence of stones.

5.1.4.2 Vane shear strength

Mean values of these measurements, for each occasion and RL treatment, are shown in Table 19 for Macmerry and for Threipmuir. For both soil types the vane shear strength showed the same trends with depth, treatment and occasion as the values of cone resistance measured at the same time. Standard errors remained effectively constant with depth, in contrast to the cone resistance measurements and the vane measurements showed a lower mean coefficient of variation than the cone measurements, e.g. 25.3 per cent (2 measurements per plot) compared to 54.6 per cent (2 measurements per plot).

5.1.5 Intransient soil physical properties

Measurements of particle size distribution, soil organic matter, particle density, Atterberg limits, optimum moisture content and Proctor dry bulk density for three sub-samples of each soil are shown in Table 20 for each soil at the different sampling depths. The relationships between maximum dry bulk density and soil moisture content , using the Proctor test for the same samples are shown in Fig.50. For the average of the sub-samples the Macmerry soil of the Section 7 site was classified as a sandy loam[1], while the Threipmuir soil of the Lower Terrace site was classified as loam[1].

---

1. USDA classification

TABLE 19 MEAN VALUES OF INITIAL VANE SHEAR STRENGTH (kPa) AT DIFFERENT DEPTHS FOR EACH EXPERIMENTAL OCCASION (M), EACH SOIL TREATMENT (RL) AND EACH SOIL TYPE

| Soil type and Occasion | SOIL TREATMENT | | | | Mean (Fig) s.e.d. |
|---|---|---|---|---|---|
| | RL 1 | RL 2 | RL 3 | RL 4 | |
| Macmerry | | | | | |
| M1 | | | | | |
| depth, cm | | | | | |
| 9 | 9.0 | 14.6 | 27.4 | 36.7 | 1.4 (***) |
| 18 | 12.9 | 16.3 | 23.3 | 30.8 | 1.6 (***) |
| M2 | | | | | |
| depth, cm | | | | | |
| 9 | 8.1 | 20.3 | 32.7 | 39.9 | 3.1 (***) |
| 18 | 15.2 | 22.7 | 38.8 | 41.9 | 4.5 (***) |
| 27 | 17.7 | 24.8 | 48.4 | 59.7 | 7.1 (***) |
| M3 | | | | | |
| depth, cm | | | | | |
| 9 | 5.5 | 13.5 | 23.2 | 36.3 | 1.3 (***) |
| 18 | 10.75 | 14.3 | 26.3 | 33.0 | 2.0 (***) |
| 27 | 18.0 | 22.0 | 47.0 | 52.7 | 1.5 (***) |
| M4 | | | | | |
| depth, cm | | | | | |
| 9 | 6.9 | 12.9 | 22.1 | 34.3 | 1.8 (***) |
| 18 | 10.6 | 15.4 | 21.8 | 30.6 | 1.3 (***) |
| 27 | 14.8 | 15.1 | 33.2 | 42.0 | 2.7 (***) |
| Threipmuir | | | | | |
| M1 | | | | | |
| depth, cm | | | | | |
| 9 | 47.1 | 45.9 | 72.9 | | 7.8 (*) |
| 18 | 63.9 | 64.6 | 74.9 | | 6.4 |
| 27 | 92.7 | 104.4 | 102.1 | | 3.9 |
| M2 | | | | | |
| depth, cm | | | | | |
| 9 | 19.2 | 26.5 | 36.7 | | 3.5 (*) |
| 18 | 28.4 | 34.1 | 41.8 | | 5.2 |
| 27 | 55.0 | 62.7 | 72.6 | | 12.2 |
| M4 | | | | | |
| depth, cm | | | | | |
| 9 | 22.4 | 36.6 | 46.8 | | 4.3 (*) |
| 18 | 47.6 | 63.8 | 65.7 | | 2.8 (**) |
| 27 | 76.4 | 90.6 | 102.9 | | 8.8 |

TABLE 20 SOIL PHYSICAL ANALYSIS DATA

| Sample No. | Threipmuir: | | | 0–20 cm depth |
|---|---|---|---|---|
| | S/439 | S/441 | S/443 | Mean |
| Replication | 1 | 2 | 3 | |
| Size fraction(%) >37.5 mm | | | 6.8 | 2.26 |
| 37.5 – 20.0 mm | 1.9 | 1.2 | 1.5 | 1.53 |
| 20.0 – 10.0 mm | 2.5 | 4.9 | 3.7 | 3.7 |
| 10.0 – 5.0 mm | 3.8 | 3.4 | 3.3 | 3.5 |
| 5.0 – 2.0 mm | 3.7 | 3.8 | 3.6 | 3.7 |
| 2.0 – 0.6 mm | 5.1 | 4.7 | 4.7 | 4.83 |
| 0.6 – 0.2 mm | 15.4 | 13.9 | 13.2 | 14.17 |
| 0.2 – 0.060 mm | 25.7 | 24.3 | 22.9 | 24.3 |
| 0.060 – 0.020 mm | 15.5 | 16.5 | 14.7 | 15.47 |
| 0.020 – 0.006 mm | 7.8 | 7.9 | 6.9 | 7.53 |
| 0.006 – 0.002 mm | 5.3 | 6.0 | 5.7 | 5.67 |
| 0.002 – 0.000 mm | 13.2 | 13.4 | 12.9 | 13.7 |
| Grading coef.($Log_{10}$ (D75/D25) | 1.32 | 1.39 | 1.47 | 1.39 |
| Particle density ($g/cm^3$) Un0x | 2.576 | 2.574 | 2.578 | 2.576 |
| 0x | 2.652 | 2.661 | 2.659 | 2.657 |
| Proctor[4] max. dry bulk density | 1.646 | 1.648 | 1.675 | 1.656 |
| Optimum moisture | 17.0 | 15.9 | 17.1 | 16.7 |
| Atterberg liquid limit[3] (% w/w) | 33.4 | 35.6 | 34.2 | 34.4 |
| " plastic limit[3] (% w/w) | 26.9 | 26.2 | 25.0 | 26.03 |
| Plasticity Index | 6.5 | 9.4 | 9.3 | 8.4 |
| Loss on Oxidation (%) | 3.1 | 2.9 | 3.1 | 3.03 |
| Texture (U.S.D.A. 1951) | SaL | L | L | L |
| B.S.C.S. Group | SML | SMI | SML | SML |
| D.C. Plastic limit ( <425 µm )[1] | | | | 19 |
| D.C. Plastic limit ( <1 cm)[2] | | | | 20 |

1.Drop cone plastic limit (remoulded soil , % w/w)
2.Drop cone plastic limit (aggregate <1 cm diam, % w/w)

4.B.S. 2.5 kg rammer method, using separate samples

3.Casagrande method

TABLE 20 (continued)

| Threipmuir: 20–40 cm depth | | | | Macmerry: 0–15 cm depth | | | |
|---|---|---|---|---|---|---|---|
| S/440 | S/442 | S/444 | Mean | S/108 | S/109 | S/114 | Mean |
| 1 | 2 | 3 | | 2 | 3 | 1 | |
| 0.0 | 3.4 | 0.0 | | nil | nil | nil | |
| 0.3 | 1.2 | 7.6 | 3.0 | 6.9 | nil | 10.3 | 5.7 |
| 3.4 | 3.3 | 4.1 | 3.6 | 3.9 | 2.8 | 4.4 | 3.7 |
| 3.6 | 2.9 | 3.9 | 3.5 | 2.4 | 2.3 | 2.7 | 2.5 |
| 3.5 | 3.5 | 3.8 | 3.6 | 2.3 | 1.5 | 5.3 | 3.0 |
| 4.9 | 4.6 | 4.7 | 4.7 | 5.4 | 5.0 | 4.3 | 4.9 |
| 14.9 | 13.7 | 13.2 | 13.9 | 20.5 | 22.8 | 15.9 | 19.7 |
| 26.5 | 24.3 | 22.7 | 24.5 | 31.9 | 35.8 | 24.6 | 30.8 |
| 15.8 | 15.8 | 14.5 | 15.4 | 9.8 | 14.0 | 12.7 | 12.2 |
| 8.3 | 7.9 | 7.4 | 7.9 | 9.0 | 5.6 | 5.3 | 6.6 |
| 5.3 | 6.1 | 5.4 | 5.6 | 4.0 | 3.5 | 4.3 | 3.9 |
| 13.2 | 13.1 | 12.7 | 13.0 | 4.0 | 6.5 | 10.0 | 6.8 |
| 1.31 | 1.41 | 1.49 | 1.40 | 6.2 | 8.0 | 11.0 | 8.4 |
| 2.569 | 2.574 | 2.585 | 2.576 | 2.50 | 2.50 | 2.49 | 2.50 |
| 2.650 | 2.670 | 2.665 | 2.662 | 2.62 | 2.64 | 2.60 | 2.62 |
| 1.667 | 1.731 | 1.675 | 1.691 | 1.58 | 1.60 | 1.56 | 1.58 |
| 16.3 | 17.3 | 17.0 | 16.9 | 20.0 | 19.0 | 22.0 | 20.3 |
| 34.3 | 35.7 | 35.1 | 35.0 | 33.0 | 30.0 | 36.0 | 33.0 |
| 29.3 | 24.2 | 25.2 | 26.2 | 28.0 | 27.0 | 29.0 | 28.0 |
| 5.0 | 11.5 | 10.0 | 8.8 | 5.0 | 3.0 | 7.0 | 5.0 |
| 2.9 | 3.0 | 3.3 | 3.1 | 5.2 | 5.3 | 4.3 | 4.9 |
| L | L | L | L | SaL | Ls | SaL | SaL |
| SML | SCI | SMI | SML | ML | ML | MI | ML |
| | | | | | | | 20 |
| | | | | | | | 25 |

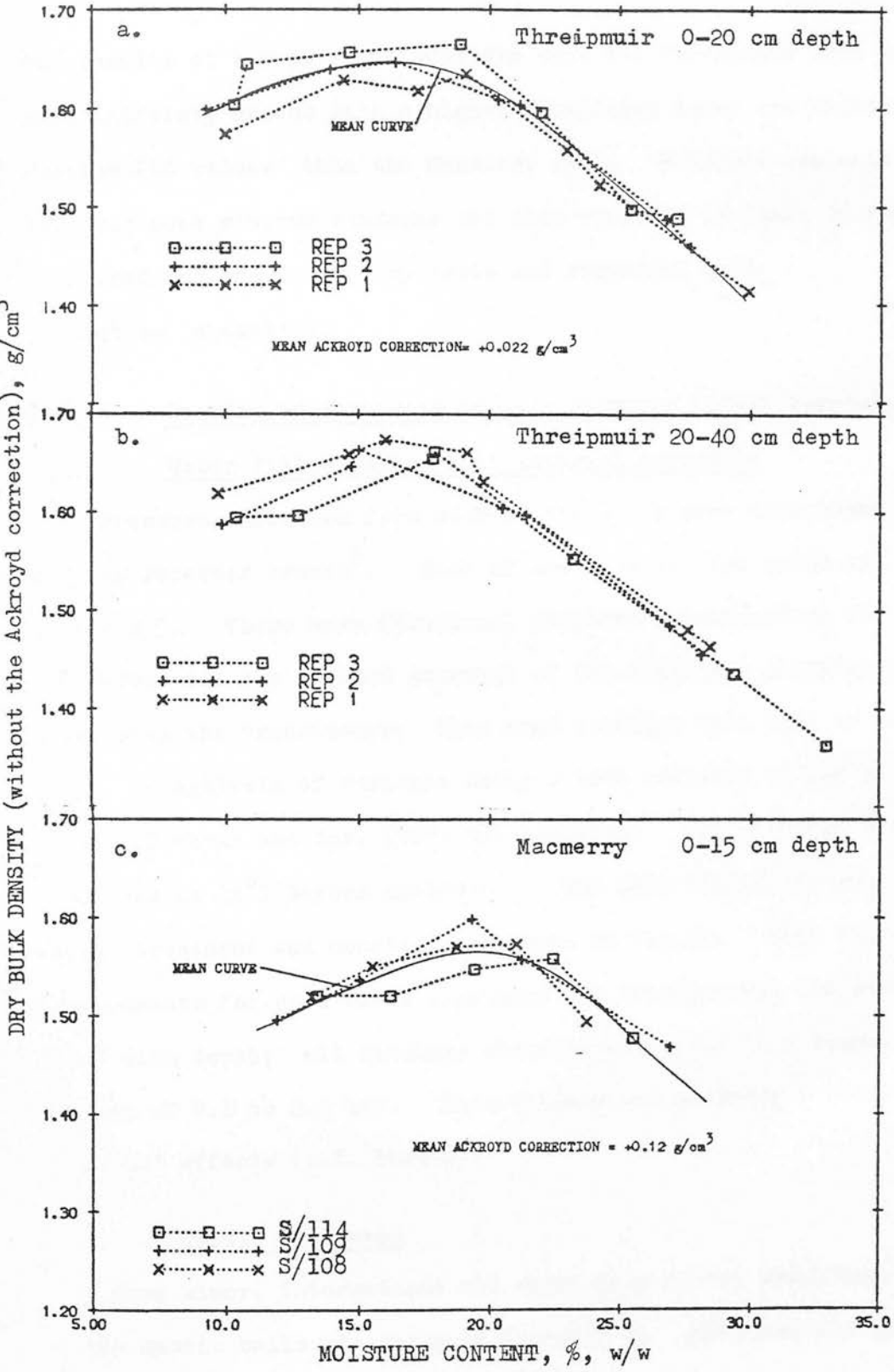


Fig.50 Proctor curves for bulked samples from the sites of the field experiments. Each sample is indicated by the sample number, or the replication block from which it was collected. Mean curves, fitted by eye, are shown for a and c.

The results of the physical analysis show the Threipmuir soil was more uniformly graded with a higher plasticity index and higher maximum Dbd values[1] than the Macmerry soil. Moisture contents for drop-cone minimum sinkages are also recorded in Table 20 for soil used for the laboratory tests and remoulded soil ( $< 425$ um diameter).

## 5.2 In situ Measurements of Soil Stresses (Lower Terrace,1977)

### 5.2.1 Water filled rubber ball internal pressures

Pressure increases from each of the balls were determined from the pen recorder traces[2]. Each of these values are given in Appendix 5. There were occasional problems co-ordinating the multi-way valve with the forward movement of the wheel and aligning the wheel with the transducers; thus some readings were lost or doubtful. An analysis of variance using a best estimate of the missing values (Cochran and Cox, 1960) was employed. All readings were corrected to 22°C before analysis[3]. The mean values for each depth, treatment and occasion are shown in Fig.51. Each set of measurements for each wheel treatment and occasion had the same trend with depth; all readings steadily decreased to a common minimum of 0.1 to 0.2 bar. This minimum was probably a result of 'arching' effects (c.f. Chap.6).

### 5.2.2 Mastic ball axes

Mean minor, intermediate and major axes of the resulting shapes of the mastic balls are shown in Appendix 5. Measurements were corrected to 16°C[3]. Damage to the balls during excavation caused 8 per cent of the minor axis measurements to be lost; thus analysis of variance with missing values was again used. Fig.52 shows the

1. Proctor
2. An example is shown in Fig.53.
3. Since most data was collected at air or soil temperatures near this value.

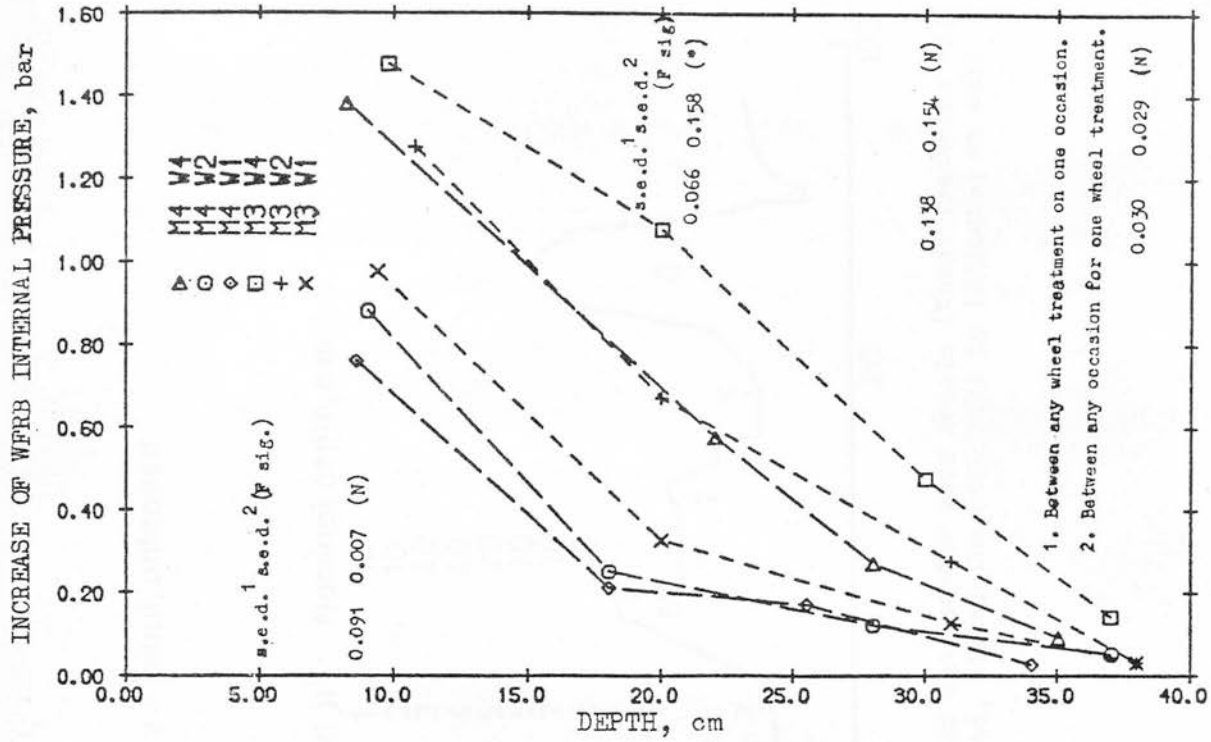


Fig.51 Variations of the mean increases of the internal pressure of the water filled rubber balls (WFRB) with depth below the original soil surface. Each experimental occasion (M) and wheel treatment (W) are indicated. All pressure increases were adjusted to their equivalent at 22°C.

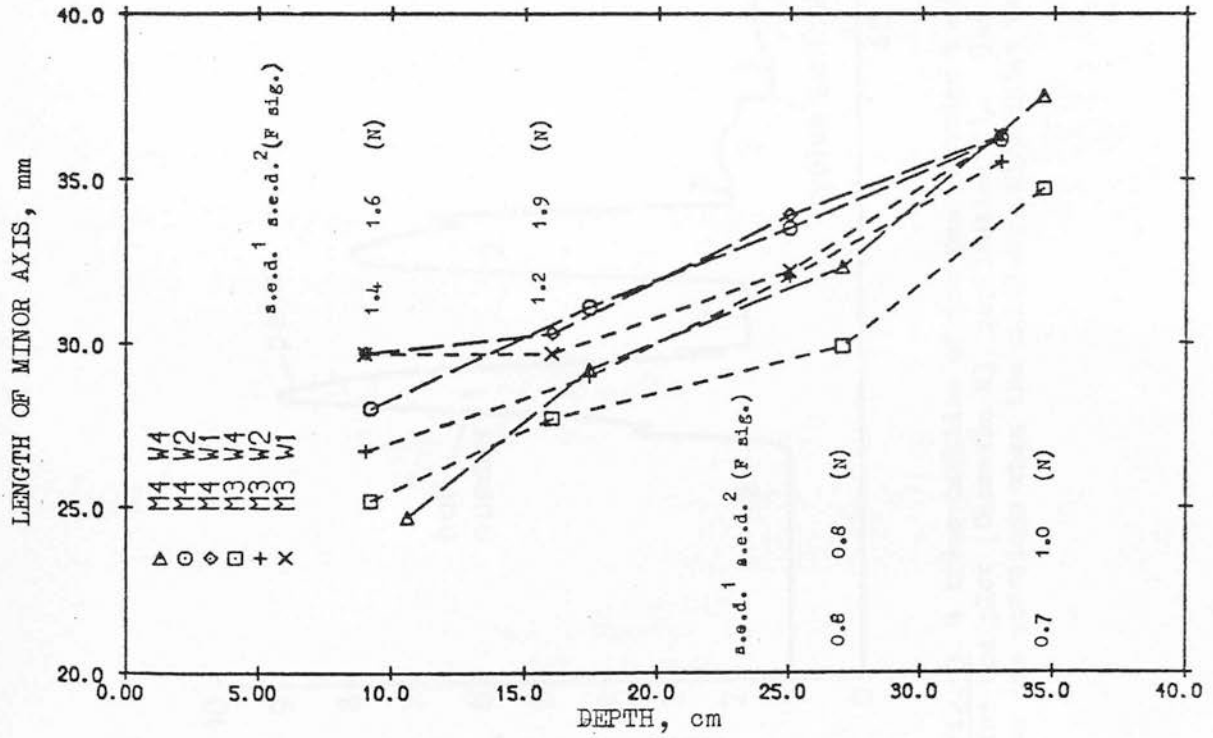


Fig.52 Variations of the mean lengths of the minor axes of the Mastic balls with the depth below the original soil surface. Each experimental occasion (M) and wheel treatment (W) are indicated. All axis lengths were adjusted to their equivalent at 16°C.

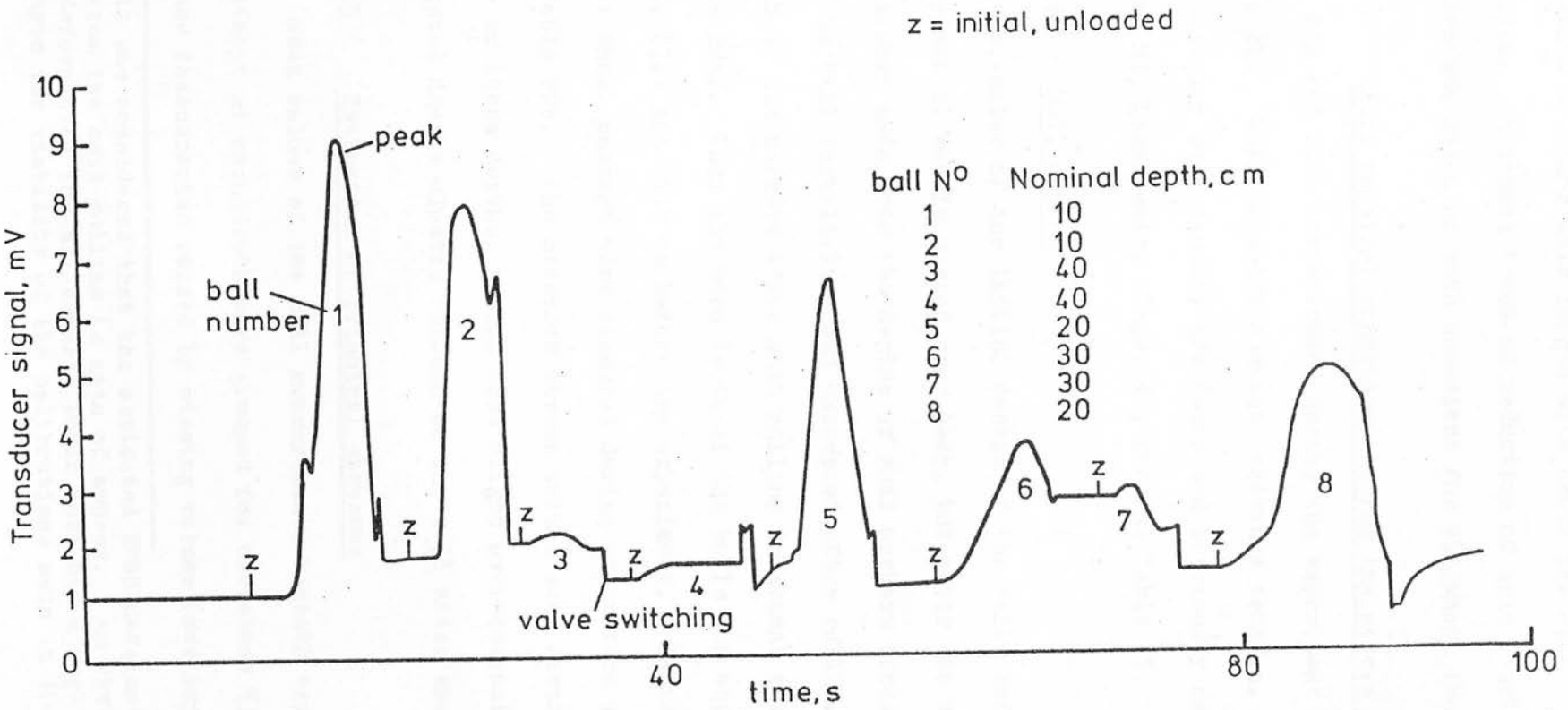


Fig.53 A transposition of the pen recorder trace from one run of the tractor rear wheels (Wheel treatment W2) for one plot (Occasion M3, replication 3). The initial, unloaded, signal for each ball is indicated as well as the occasions when the multiway valve inlet was changed.

variation of minor axis length with depth for each treatment and occasion. A common trend of reduction of axis length towards the surface was shown on both occasions for all wheel treatments.

5.2.3 Soil physical conditions during the stress measurements

Air and soil temperatures during the experiment are shown in Table 21. Soil moisture content, moisture tension, cone resistance and dry bulk density are described previously for occasions M3 and M4, Threipmuir; Figs.49c, 46c and Table 17.

5.2.4 Ball depths

Estimates of the initial depths of the balls before the experimental wheels passed over them, but after the rolling treatments were made from the depths of soil markers buried at the same time as ball installation and excavated after rolling. The mean depth of the markers after each rolling treatment are shown in Table 22a.[1] Thus the mean depth of the balls was estimated as 9.6, 18.4, 27.7 and 36.7 cm before the experiment. Depths of balls after wheel passage were measured during excavation and are shown in Table 22b. The measured stress values were assumed to have been at these depths, though some slight over-estimation was expected due to elastic rebound of the soil after wheel passage.

5.2.5 Estimation of principal stresses

Mean values of the ball measurements beneath each wheel treatment at each depth were grouped for occasions M3 and M4 to reduce inaccuracies caused by missing values (see Appendix 5).

1. It was considered that the estimated WFRB deformation resulting from the soil rolling (a mean of approx. 3 mm vertical axis deformation for all depths) would have had a negligible effect upon the viability of the calibrations made in the laboratory.

TABLE 21 RECORD OF AIR AND SOIL TEMPERATURES (°C) DURING IN SITU MEASUREMENTS OF SOIL STRESSES

| Wheel Treatment | Replication | 1 | | 2 | | 3 | |
|---|---|---|---|---|---|---|---|
| | Occasion | M4 | M3 | M4 | M3 | M4 | M3 |
| W1 air | | 24 | 11.5 | 16 | 11.5 | 23 | 11.5 |
| soil 10 cm depth | | 15 | 10.5 | 14 | 10.5 | 15 | 10.5 |
| 20 cm " | | 14 | 10.5 | 14 | 10.5 | 16 | 10.5 |
| 30 cm " | | 14 | 10.5 | 14 | 10.5 | 15 | 10.5 |
| W2 air | | 23 | 11.5 | 23 | 10.0 | 22 | 10.0 |
| soil 10 cm " | | 21 | 10.5 | 17 | 10.5 | 20 | 10.5 |
| 20 cm " | | 16 | 10.5 | 16 | 10.5 | 17 | 10.5 |
| 30 cm " | | 16 | 10.5 | 17 | 10.5 | 16 | 10.5 |
| W3 air | | 21 | 10.0 | 21 | 10.0 | 10 | 10.0 |
| soil 10 cm " | | 15 | 10.5 | 15 | 10.0 | 10.5 | 10.5 |
| 20 cm " | | 15 | 10.5 | 16 | 10.5 | 10.5 | 10.5 |
| 30 cm " | | 15 | 10.5 | 15 | 10.5 | 10.5 | 10.5 |

TABLE 22a MEAN DEPTH OF SOIL MARKERS AFTER ROLLING, cm
LOWER TERRACE FIELD, 1977

| Nominal original depth, cm | Rolling treatment, all 'M' blocks | | | Standard errors of means |
|---|---|---|---|---|
| | RL 1 (no rolling) | RL 2 1 pass, heavy roll | RL 3 5 passes, heavy roll | |
| 10 | 11.0 | 9.6 | 8.5 | 0.3 |
| 20 | 20.0 | 18.4 | 17.1 | 0.2 |
| 30 | 29.4 | 27.7 | 26.3 | 0.2 |
| 40 | 38.5 | 36.7 | 34.9 | 0.2 |

N.B: Markers planted after grass sown and rolled with light roller.

TABLE 22b MEAN DEPTH OF WFRBs AND MASTIC BALLS AFTER WHEEL PASSAGE, cm (FROM ORIGINAL SOIL SURFACE)

| Nominal original depth, cm | Wheel treatment, M3 and M4 combined | | | Standard errors of means |
|---|---|---|---|---|
| | W1 | W2 | W4 | |
| 10 | 9.0 | 9.7 | 9.6 | 0.55 |
| 20 | 18.4 | 18.8 | 20.3 | 0.88 |
| 30 | 27.1 | 28.1 | 28.3 | 1.55 |
| 40 | 34.9 | 36.2 | 35.9 | 0.64 |

5.2.5.1 Estimation of deviator load

Using the mastic ball calibration line for 16°C, determined immediately after excavation, the mean minor axis length was used to estimate the deviator load experienced at each depth beneath each W treatment. Table 23 shows mean axis lengths, estimated deviator loads and standard error of the estimates.

5.2.5.2 Estimation of first principal stress( $\sigma_1$ ) and third principal stress($\sigma_3$)

For each depth below each wheel the appropriate WFRB calibration line was chosen according to the deviator load and air temperature. It was convenient to adjust all WFRB readings to their equivalent at 22°C.[1] Thus the estimated value of $\sigma_3$ could be read from the WFRB calibration line knowing the corresponding value of WFRB peak pressure. These values and their standard errors are shown in Table 24 . Calculation of $\sigma_1$ was by addition of $\sigma_3$ and the deviator stress. Deviator stress was obtained by dividing the deviator load by the maximum vertical cross-sectional area of the mastic balls. The area was calculated using the average of the mean values of major, intermediate and minor axes for each depth beneath each experimental wheel; values of $\sigma_1$ are also given in Table 24 .

5.3 Tyre Contact Area and Wheel Sinkage Measurements (Soil Tank, 1977)

Data collected with the reliefmeter was used in section 5.1.2 to calculate Max. Rut Depth, Mean Rut Depth and Cross-sectional Area for each of the rut profiles measured for the soil tank experiment. These values and their corresponding contact areas

1. Since most of the field measurements were taken at ambient air temperatures near this value.

TABLE 23 MASTIC BALL FIELD RESULTS FOR THREE WHEEL TREATMENTS (ADJUSTED TO 16°C)

| Nominal depth, cm | Mean lengths of minor axes, cm | | | Standard error of means, cm | Estimated deviator loadings, kg | | | Standard error of estimate, kg |
|---|---|---|---|---|---|---|---|---|
| | W1 | W2 | W4 | | W1 | W2 | W4 | |
| 10 | 3.00 | 2.68 | 2.46 | 0.10 | 2.50 | 3.60 | 4.60 | 0.3 |
| 20 | 2.98 | 2.95 | 2.82 | 0.15 | 2.50 | 2.45 | 3.05 | 0.3 |
| 30 | 3.31 | 3.24 | 3.07 | 0.06 | 1.00 | 1.10 | 1.95 | 0.2 |
| 40 | 3.46 | 3.61 | 3.60 | 0.05 | 0.30 | 0.10 | 0.30 | 0.2 |

TABLE 24 ESTIMATED VALUES OF FIRST AND THIRD PRINCIPAL STRESS FROM WFRB AND MASTIC BALL RESULTS FOR THE FIELD (ADJUSTED TO 22°C)

TABLE 24 FIRST PRINCIPAL STRESS ($\sigma_1$) AND THIRD PRINCIPAL STRESS ($\sigma_3$)

| Nominal ball depth, cm | Estimated $\sigma_3$ from WFRB, bar | | | | Estimated deviator stress from mastic ball, bar | | | Estimated $\sigma_1$ ($\sigma_3$ + deviator stress), bar | | | |
|---|---|---|---|---|---|---|---|---|---|---|---|
| | W1 | W2 | W4 | s.e. est. | W1 | W2 | W4 | W1 | W2 | W4 | s.e. est. |
| 10 | 1.27 | 1.42 | 1.90 | 0.1 | 0.18 | 0.25 | 0.31 | 1.45 | 1.68 | 2.21 | 0.1 |
| 20 | 0.32 | 0.55 | 1.22 | 0.1 | 0.18 | 0.18 | 0.21 | 0.51 | 0.73 | 1.43 | 0.1 |
| 30 | 0.10 | 0.25 | 0.45 | 0.05 | 0.08 | 0.08 | 0.15 | 0.18 | 0.33 | 0.60 | 0.05 |
| 40 | 0.05 | 0.05 | 0.15 | 0.05 | 0.03 | 0.01 | 0.03 | 0.08 | 0.06 | 0.17 | 0.05 |

are shown in Appendix 5. Extra observations, with very large sinkage, were obtained from the mean of three field observations to extend the range of measurements.

## 5.4 Laboratory Measurements of Stresses and Strains (1977)

The fundamental data from each test, on each soil, are shown in Appendix 7. The data is represented graphically in Figs.54 to 56. This assists identification of the virgin compression lines, primary functions and maximum dry bulk density; for the convenience of drawing the graphs some points are interpolated. Very little difference (approx. 0.01 $g/cm^3$) was found between the Dbd values after 2 seconds and 30 seconds of stress application. Therefore the more reliable 30s data was used to construct the figures. Fig.57 shows four examples of soil samples after testing; part of the wax coating is removed to reveal the form of the soil sample surfaces; the differences between 'undisturbed' samples, aggregates $<$ 1 cm diam. and aggregates $<$ 2 mm diam. can clearly be seen.

## 5.5 Summary of the Experimental Results

Sets of data have been collected from two large field experiments on two soils of different texture (sandy loam and loam). These have described volumetric soil strains and surface sinkages beneath wheels of a range of mean tyre/soil contact pressures running over soils of a range of initial bulk densities and moisture conditions.

Sets of data have also been collected from the field to compare *in situ* measurements of soil stresses with those estimated by stress prediction equations.

Fig.54 The results of triaxial compression tests upon loose Macmerry soil in the laboratory. The soil aggregates are less than 1.0 cm diameter. The graphs show dry bulk density 30s after the application of step-wise increases of spherical pressure (P) to each sample. Various ranges of soil moisture content were used.

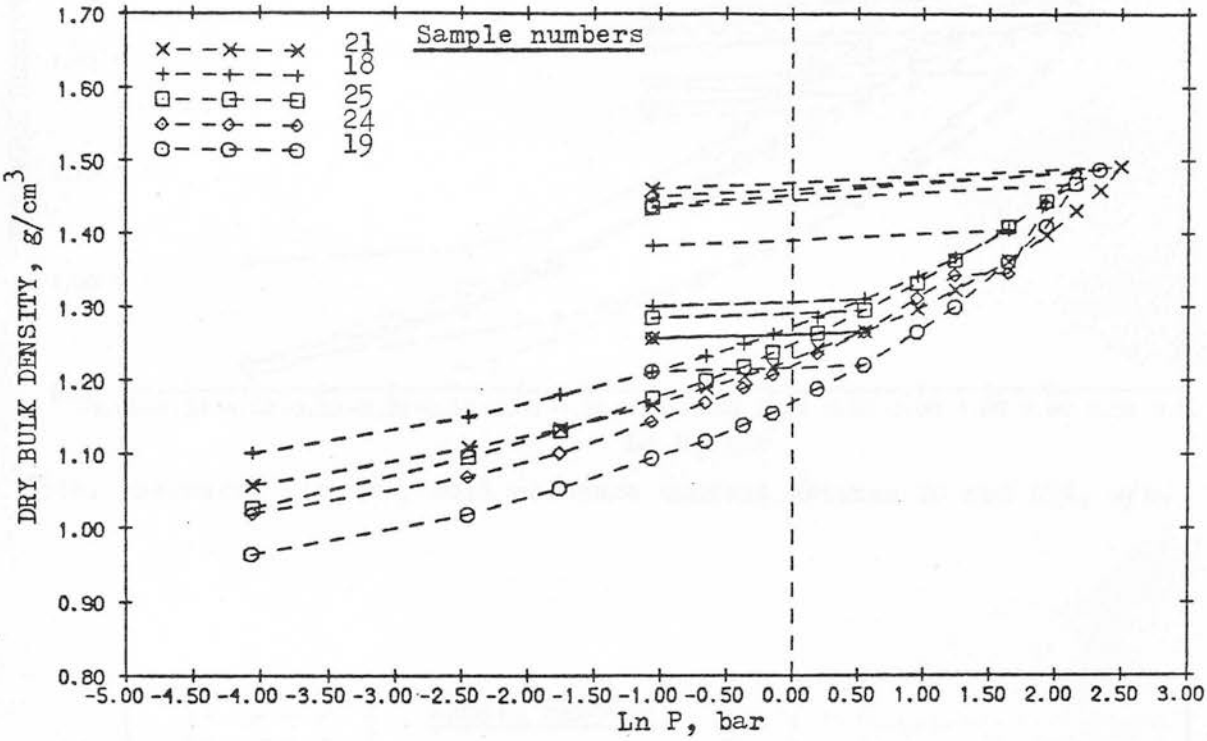


54a. Macmerry (loose), soil moisture content between 5 and 15%, w/w.

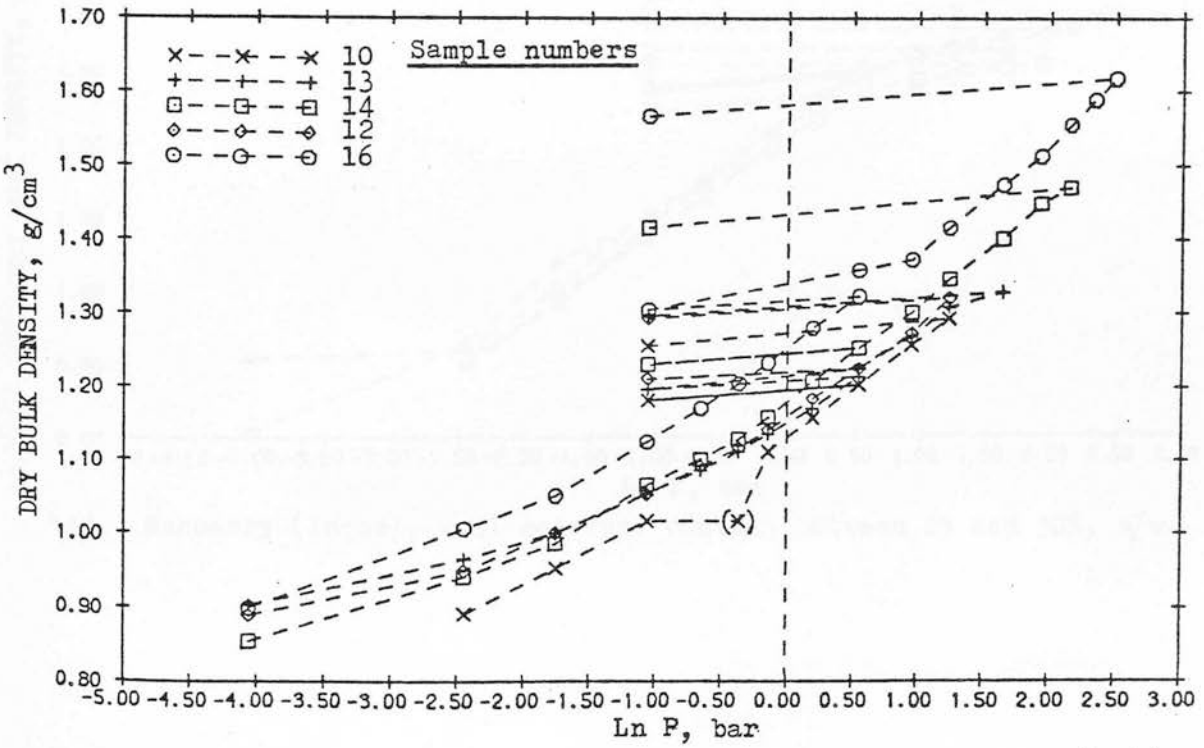


54b. Macmerry (loose), soil moisture content between 15 and 20%, w/w.

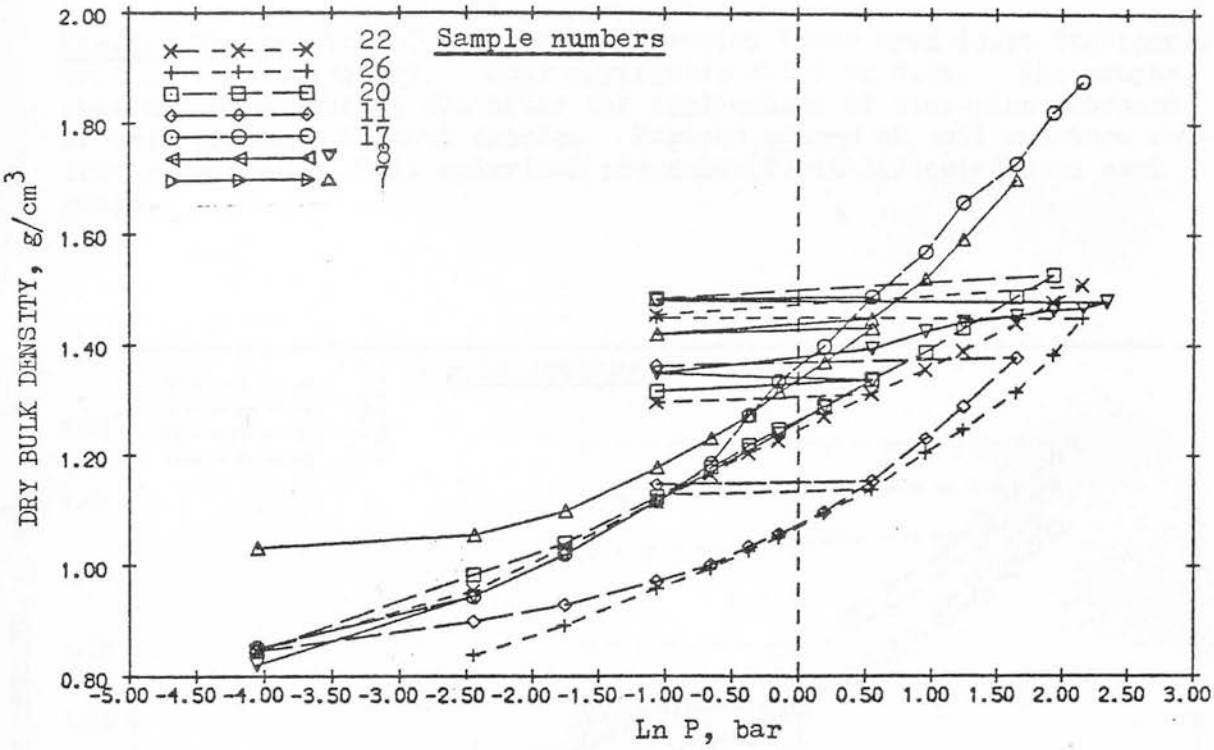


54c. Macmerry (loose), soil moisture content between 20 and 25%, w/w.

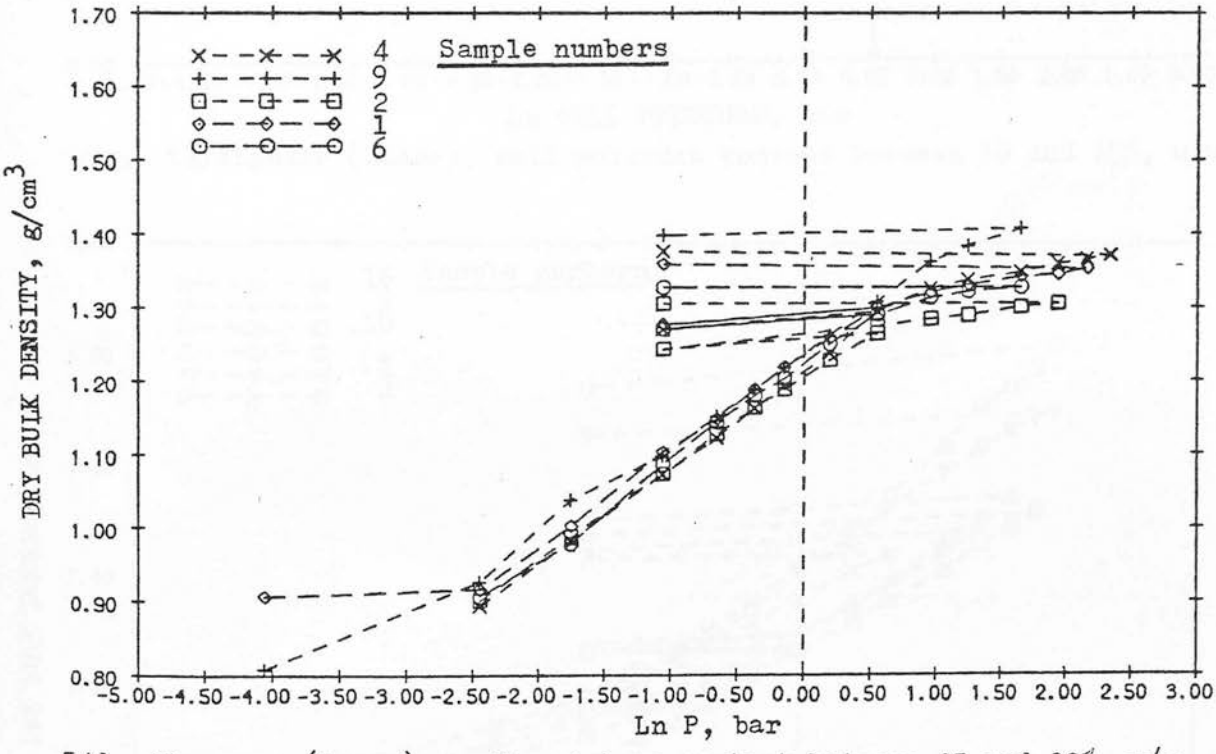


54d. Macmerry (loose), soil moisture content between 25 and 30%, w/w.

Fig.55 The results of triaxial compression tests upon loose Threipmuir soil in the laboratory. Soil aggregates $<1.0$ cm diam. The graphs show dry bulk density 30s after the application of step-wise increases of cell pressure to each sample. Various ranges of soil moisture content were used. Unit spherical pressure (P) is indicated upon each graph.

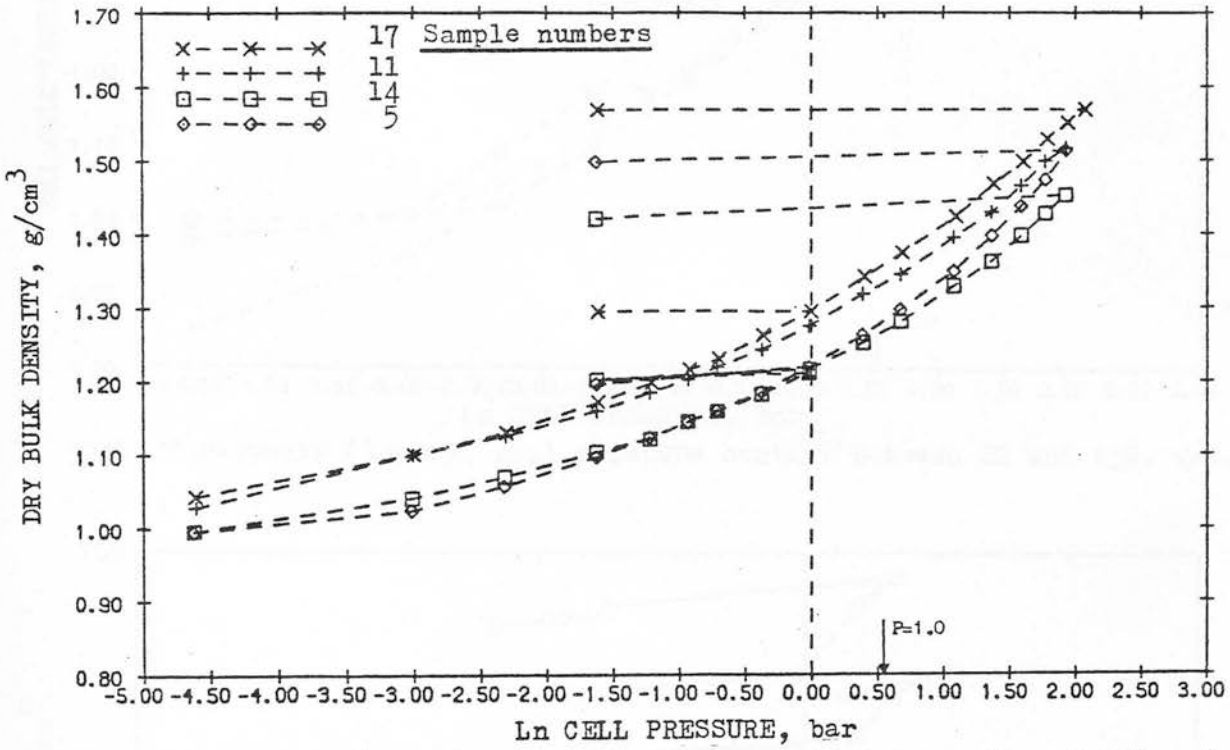


55a. Threipmuir (loose), soil moisture content between 10 and 15%, w/w.

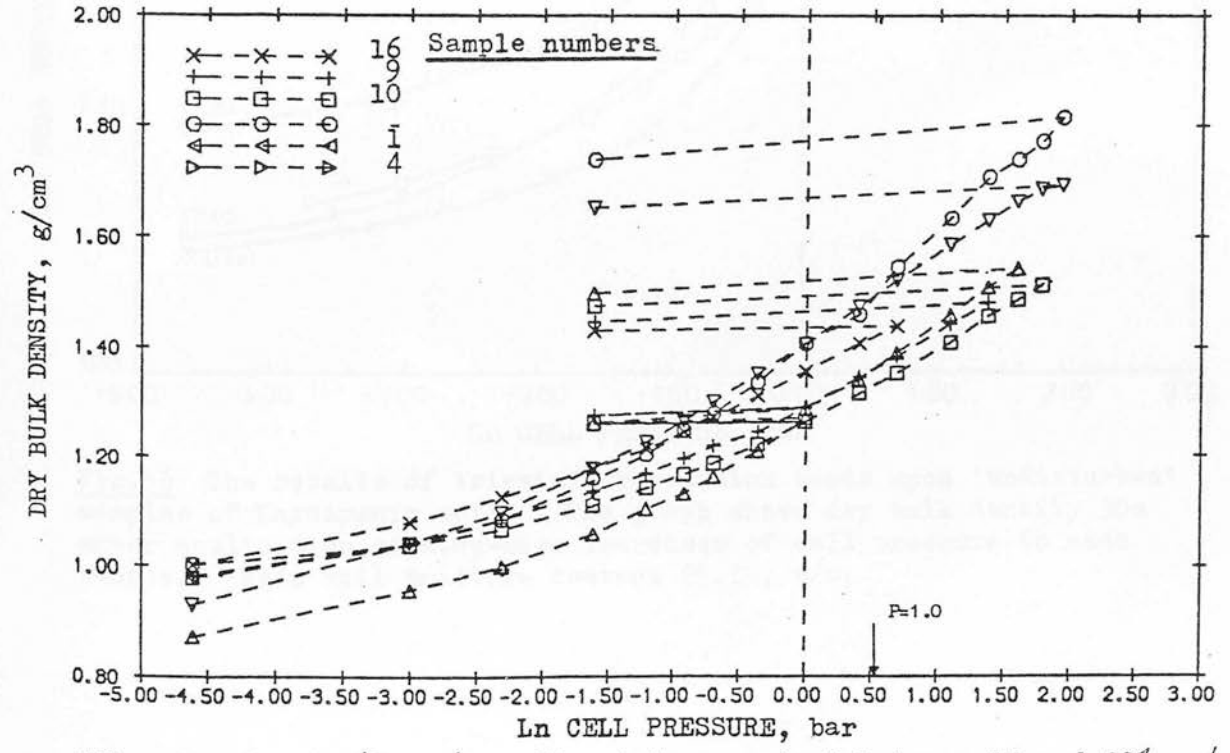


55b. Threipmuir (loose), soil moisture content between 15 and 20%, w/w.

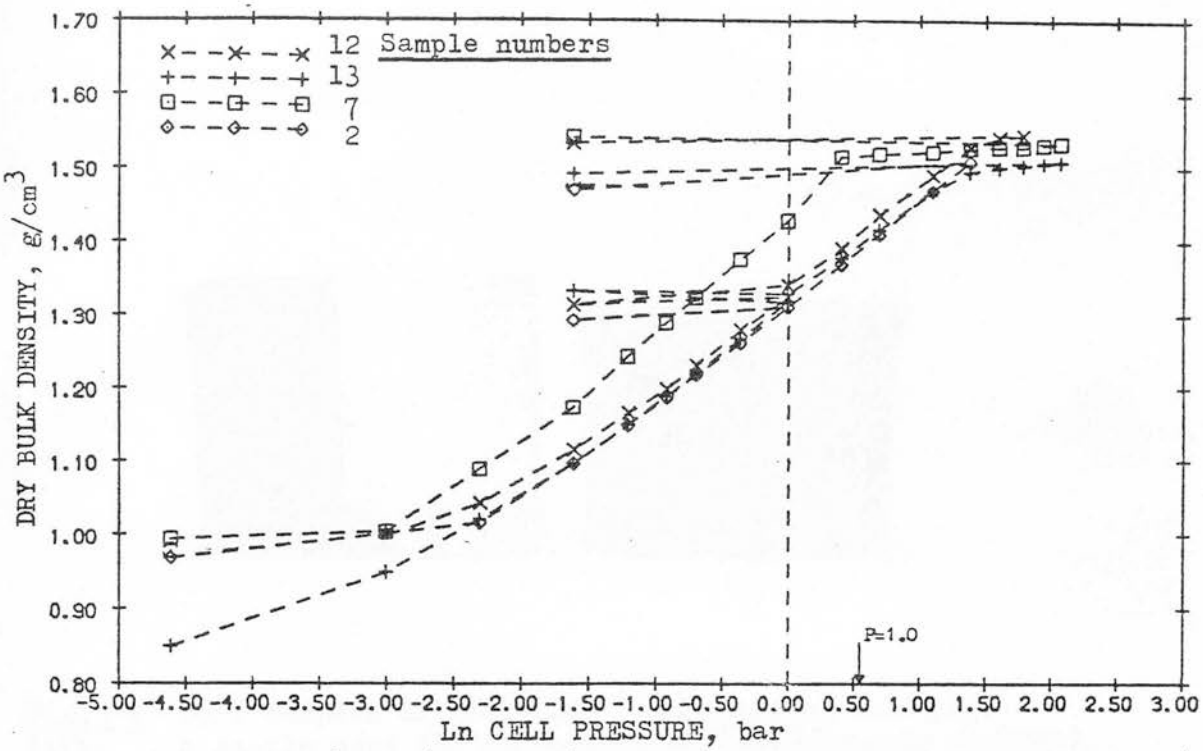


55c. Threipmuir (loose), soil moisture content between 20 and 25%, w/w.

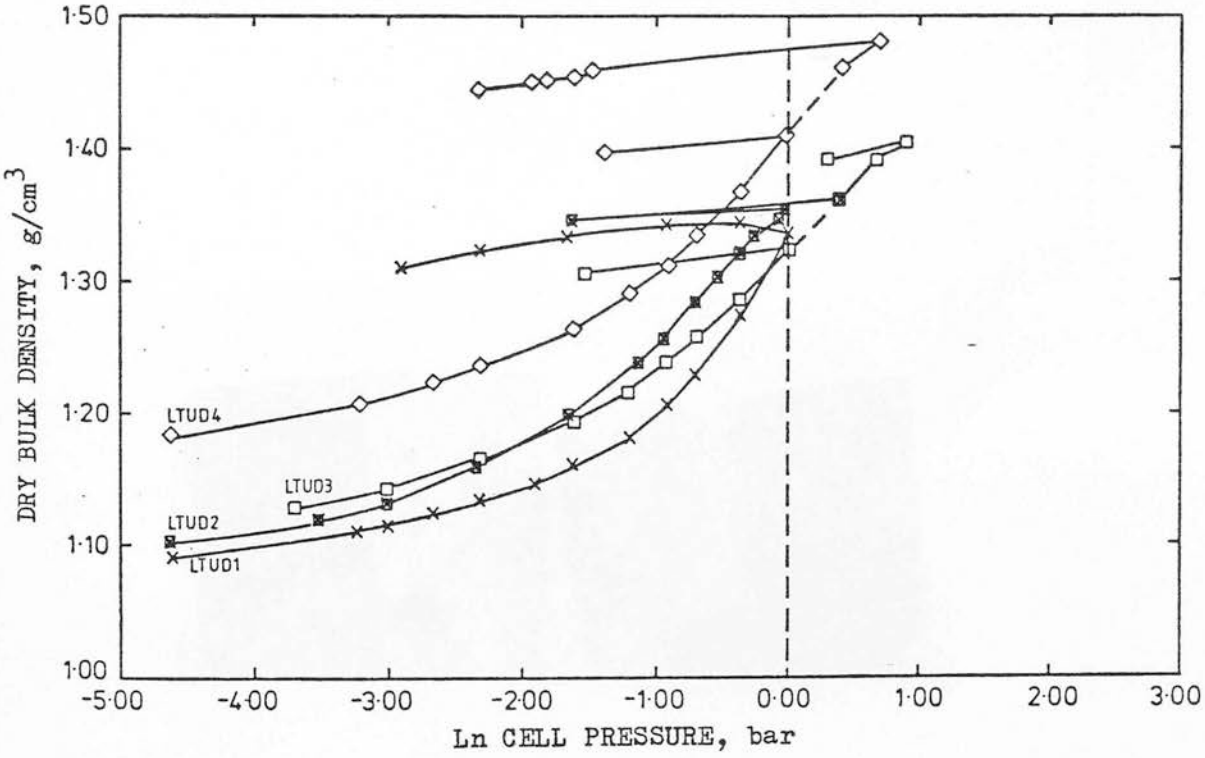


Fig.56 The results of triaxial compression tests upon 'undisturbed' samples of Threipmuir soil. The graph shows dry bulk density 30s after application of step-wise increases of cell pressure to each sample. Mean soil moisture content 25.7%, w/w.

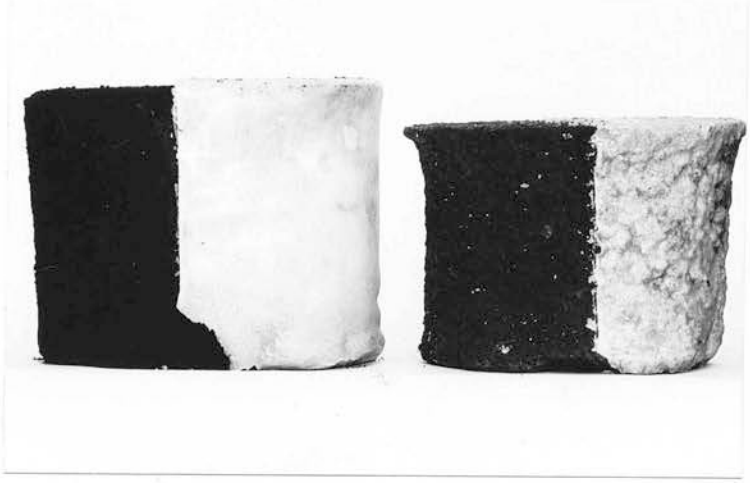

Fig.57a Soil samples after triaxial compression testing.
left: A sample used for the precision tests (sample no.BC4A), aggregates < 2 mm diam., moisture content 7.0% w/w.
right: A sample of Macmerry soil, aggregates < 1.0 cm diam., moisture content 21.2% w/w (sample no.26).

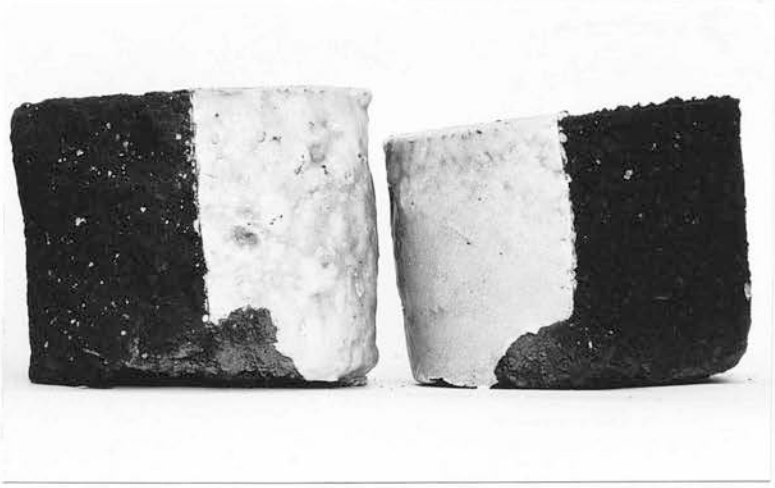

Fig.57b Soil samples after triaxial compression testing.
left: An 'undisturbed' sample of Threipmuir soil, moisture content 24.1% w/w (sample no.LTUD3).
right: A sample of Macmerry soil, aggregates < 1.0 cm diam., moisture content 7.7% w/w (sample no.23).

Supplementary data from a soil tank experiment were intended to relate tyre/soil contact area to wheel sinkage.

Laboratory measurements of soil stresses and strains were expected to indicate critical state functions to compare with similar functions derived from the relationships between the stresses and strains of field soils measured in situ.

# CHAPTER 6 - ANALYSES OF THE RESULTS

The data collected from the field and laboratory were used to identify parameters of Critical State functions of the soils (primary function, apparent virgin compression line and maximum dry bulk density[1]). These parameters could then provide the basis of a prediction method for dry bulk density changes beneath the wheels used in the experiments. The Critical State parameters were derived from *in situ* and laboratory measurements of stresses and strains. Before *in situ* stresses could be estimated, the stress prediction equations (Sect.2.1) required assessment by comparison of predicted and measured values of *in situ* stresses and measured soil strength conditions. Operation of the stress prediction equations needed an estimate of the tyre/soil contact area; estimation of these areas was the first step in the analysis of the results. Suitable estimates of *in situ* stresses could then be combined with *in situ* measurements of strains to identify the Critical State soil parameters and their variation with soil moisture conditions (described in Section 2.2). Similar parameters could also be derived for soils tests in the laboratory. These laboratory results, with corresponding results from 'undisturbed' soil samples could also help test the validity of the Critical State parameters derived *in situ*.

## 6.1 The Relationships between Tyre/Soil Contact Area and Wheel Sinkage

### 6.1.1 Regression of the data

Contact area is plotted against Mean Rut Depth (MRD) and Maximum Rut Depth (Max.RD) for three of wheel treatments in

1. See Section 2.2.

Figs.58a, b and c. Cross-sectional area of the rut was not considered as the very small variation of rut width made it almost directly dependent upon MRD. Least scatter about a best fit curve was given by tyre/soil contact area and MRD. Results from Söhne et al. (1962) are superimposed on Fig.58b. These show a similar trend between contact area and sinkage and a close correspondence between the data for wheel treatment W2 and data for a tyre of very similar size and load. Equations of the following form were used to obtain suitable non-linear regressions:

$$\text{Contact area (CA)} = A - Be^{-c.MRD} \quad \ldots\ldots\ldots\ldots (10)$$

(A, B and C are constants for each wheel treatment.)

The values of the constants giving minimum error mean square values and good correspondence with extreme points are shown in Table 25.

TABLE 25 VALUES OF CONSTANTS FROM NON-LINEAR CURVE FITTING OF CONTACT AREA AND MEAN RUT DEPTH

| Constant | A, $cm^2$ | B, $cm^2$ | c, $cm^{-1}$ | Error mean square |
|---|---|---|---|---|
| Treatment | | | | |
| W1 | 2200 | 1500 | 0.25 | 4606 |
| W2 | 2200 | 1350 | 0.25 | 7954 |
| W4 | 2100 | 1250 | 0.3507 | 15538 |

For wheel treatment W3 a curve was estimated between those for W2 and W4, see Fig.58c. It is interesting to note the considerable similarity between the non-linear functions for each wheel treatment. Therefore a common non-linear function for all wheel treatments could have been made, but this would have sacrificed the accuracy of contact area prediction for the extreme wheel treatments.

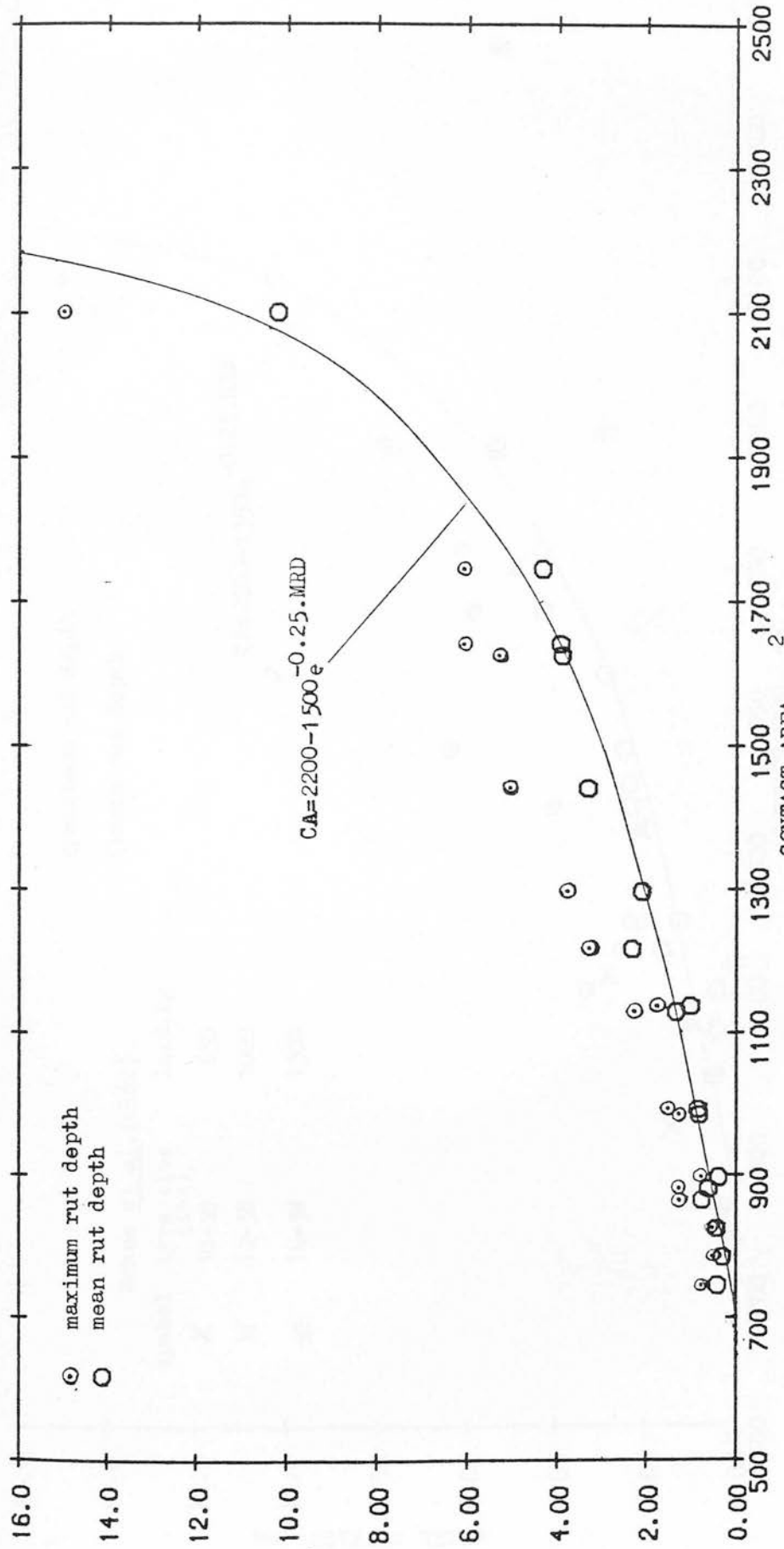


Fig.58a The relationships between wheel sinkage and tyre/soil contact area from the soil tank data for wheel treatment W1. The best fit non-linear function relating mean rut depth to contact area is superimposed.

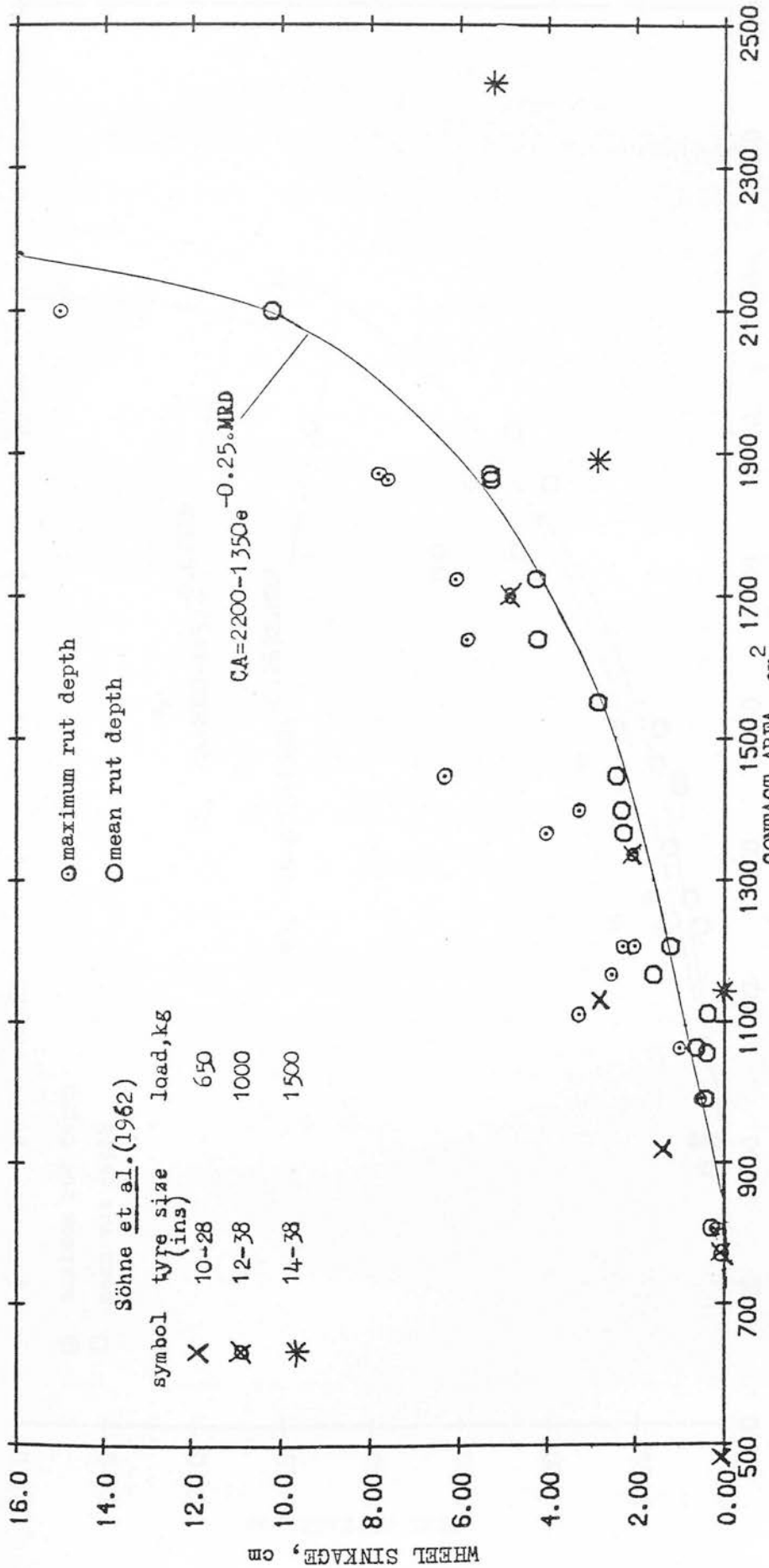


Fig.58b The relationships between wheel sinkage and tyre/soil contact area from the soil tank data for wheel treatment W2. The best fit non-linear function relating mean rut depth (MRD) to contact area is superimposed as well as similar measurements by Söhne et al. (1962).

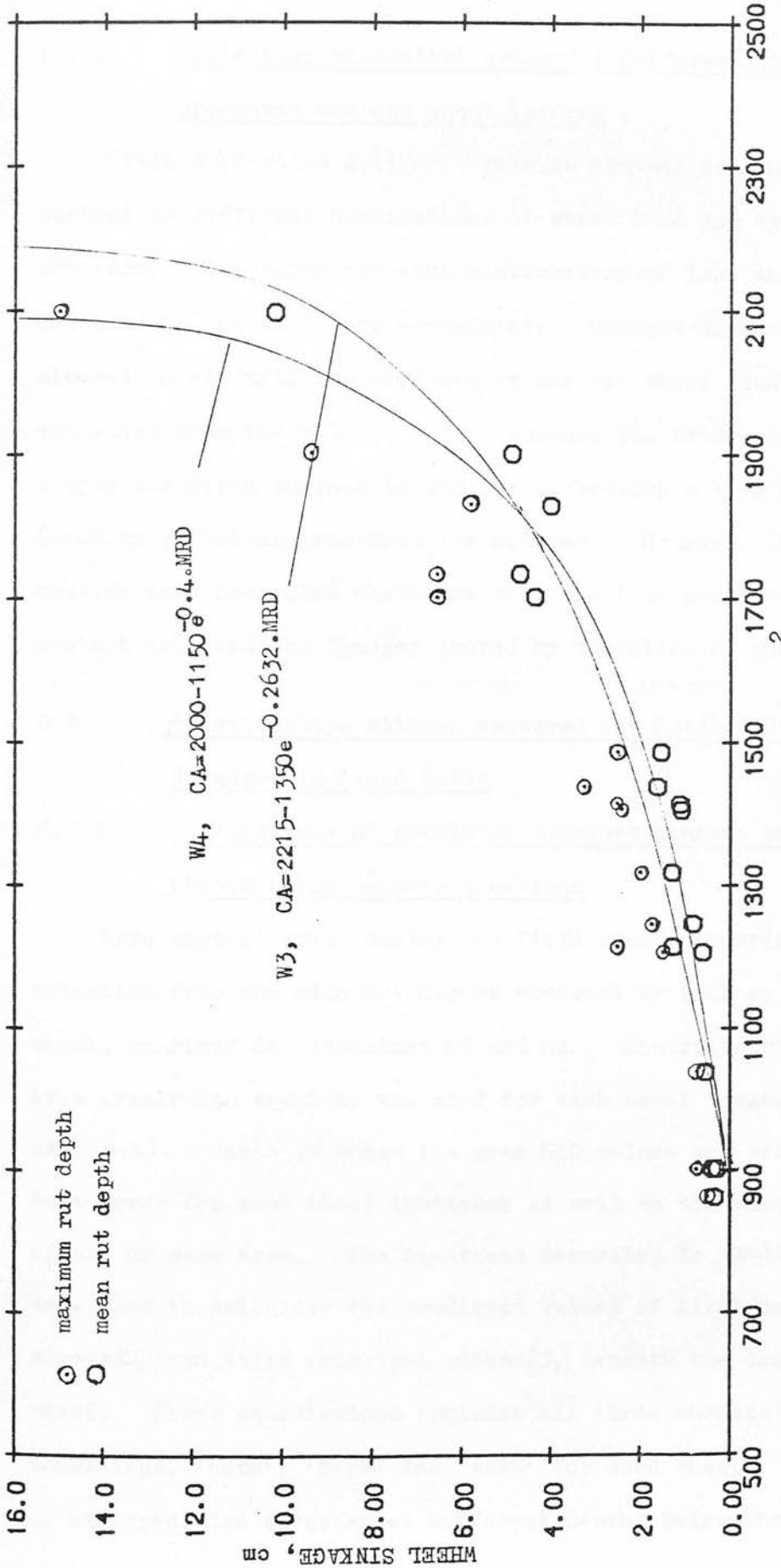


Fig.58c The relationships between wheel sinkage and tyre/soil contact area from the soil tank data for wheel treatment W4. The best fit non-linear, of the same type used for treatments W1 and W2, relating mean rut depth to contact area is superimposed. An estimated function for wheel treatment W3 is also shown.

### 6.1.2 Estimation of contact areas for different inflation pressures and one wheel loading

Table 4 (Section 4.1) relates contact area on a rigid surface to different combinations of wheel load and tyre inflation pressure. The table contains combinations of load and pressure not used in the soil tank experiment. Changes of contact area by alteration of inflation pressure at any one wheel loading can be estimated from the table. This assumes the interaction between a tyre and rigid surface is similar to between a tyre and soil when loads or inflation pressures are altered. However, the changes of contact area described above are very small in proportion to total contact area and the changes caused by variation of wheel load.

## 6.2 Relationships between Measured and Predicted Stresses in Field Soils

### 6.2.1 Calculations of predicted stresses beneath experimental wheels using Söhne's equations

Tyre contact areas during the field stress experiments were estimated from the mean rut depths produced by each experimental wheel, combined for occasions M3 and M4. The appropriate contact area prediction equation was used for each wheel treatment (c.f. sect. 6.1). Table 26 shows the mean MRD values and estimated contact areas for each wheel treatment as well as the diameter of the circle of same area. The equations described in section 2.1 were used to calculate the predicted values of first principal stress($\sigma_1$) and third principal stress($\sigma_3$) beneath the centre of each wheel. These calculations included all three surface strength conditions, 'hard', 'firm' and 'soft' for each wheel. The values of the predicted stresses at different depths below the wheels

are shown in Table 26.

6.2.2 Comparison of measured and predicted stresses

The mean values of measured and predicted $\sigma_1$ at different depths below the soil surface and grouped for occasions M3 and M4 are shown in Figs.59a, b and c. Between 10 and 15 cm depth measured values were generally similar to predicted values using equations S3 and S2. Below 15 cm measured values and predicted values from equation S1 were similar, although S1 was a noticeable underestimate beyond 25 cm depth. Bulk density changes of the upper 25 to 30 cm measured for the same occasions as some of the stress measurements revealed volumetric changes of approximately 10 per cent. Therefore despite the close agreement between measured and predicted stresses at some depths, the measured strains threw doubt on the applicability of Söhne's equations as they assumed volumetric strains in the order of 1 per cent (c.f. section 2.1).

The cone resistance profile for occasion M4, Fig.49c shows considerable variation of soil strength with depth. Therefore any one prediction equation, requiring a uniform soil strength with depth, would be unlikely to fit the observed values. Closest similarity was shown between observed values and values predicted for soft soil conditions where lower cone resistance values were measured; 10 cm depth for W1, W2 and W4 and 20 cm for W4. Correspondingly the observed values and values predicted for hard soil conditions were similar where higher cone resistance values had been measured. These observations suggested a quantitative correlation between the observed soil strength and the concentra-

TABLE 26 CALCULATION OF $\sigma_1$ AND $\sigma_3$ (BAR) BENEATH EXPERIMENTAL WHEELS, STRESS EXPERIMENT, LOWER TERRACE FIELD

| Estimation of tyre/soil Contact Area of Wheel Treatments (W1,W2,W4) | | | |
|---|---|---|---|
| | Mean MRD (M3 and M4), cm | Estimated Contact area, $cm^2$ | Diameter of equivalent circle, cm |
| W1 | 1.24 | 1101 | 37.4 |
| W2 | 1.33 | 1233 | 39.6 |
| W4 | 2.38 | 1557 | 44.5 |

| Maximum Stresses beneath Wheel treatment W1, Wheel load 890 kg, Mean surface pressure 0.824 bar | | | | | |
|---|---|---|---|---|---|
| Equation and stresses | S1 ($\sigma_1$) | S4 ($\sigma_3$) | S2 ($\sigma_1$) | S3 ($\sigma_1$) | S6 ($\sigma_3$) |
| depth, cm 3 | - | - | - | 1.627 | 0.452 |
| 6 | 0.817 | 0.428 | 1.217 | 1.565 | 0.541 |
| 12 | 0.754 | 0.437 | 1.087 | 1.339 | 0.668 |
| 18 | 0.634 | 0.416 | 0.879 | 1.062 | 0.630 |
| 24 | 0.506 | 0.381 | 0.681 | 0.817 | 0.520 |
| 30 | 0.397 | 0.347 | 0.524 | 0.628 | 0.412 |
| 36 | 0.314 | 0.319 | 0.408 | 0.489 | 0.324 |
| 42 | 0.251 | 0.297 | 0.323 | 0.387 | 0.258 |
| Maximum Stresses beneath Wheel treatment W2, Wheel load 1200 kg, Mean surface pressure 0.992 bar | | | | | |
| Equation and stresses | S1 ($\sigma_1$) | S4 ($\sigma_3$) | S2 ($\sigma_1$) | S3 ($\sigma_1$) | S6 ($\sigma_3$) |
| depth, cm 3 | - | - | - | 1.967 | 0.539 |
| 6 | 0.984 | 0.513 | 1.469 | 1.896 | 0.639 |
| 12 | 0.921 | 0.527 | 1.332 | 1.647 | 0.798 |
| 18 | 0.789 | 0.507 | 1.101 | 1.333 | 0.775 |
| 24 | 0.641 | 0.468 | 0.868 | 1.043 | 0.657 |
| 30 | 0.511 | 0.428 | 0.678 | 0.812 | 0.529 |
| 36 | 0.408 | 0.394 | 0.533 | 0.638 | 0.422 |
| 42 | 0.328 | 0.367 | 0.425 | 0.506 | 0.339 |
| Maximum Stresses beneath Wheel treatment W4, Wheel load 1860 kg, Mean surface pressure 1.218 bar | | | | | |
| Equation and stresses | S1 ($\sigma_1$) | S4 ($\sigma_3$) | S2 ($\sigma_1$) | S3 ($\sigma_1$) | S6 ($\sigma_3$) |
| depth, cm 6 | 1.212 | 0.627 | 1.811 | 2.348 | 0.755 |
| 12 | 1.156 | 0.647 | 1.687 | 2.100 | 0.955 |
| 18 | 1.028 | 0.634 | 1.450 | 1.764 | 0.981 |
| 24 | 0.866 | 0.597 | 1.187 | 1.429 | 0.876 |
| 30 | 0.712 | 0.552 | 0.954 | 1.144 | 0.734 |
| 36 | 0.581 | 0.511 | 0.766 | 0.918 | 0.602 |
| 42 | 0.476 | 0.474 | 0.620 | 0.743 | 0.492 |

Equations S1 to S6 are given in section 2.1.

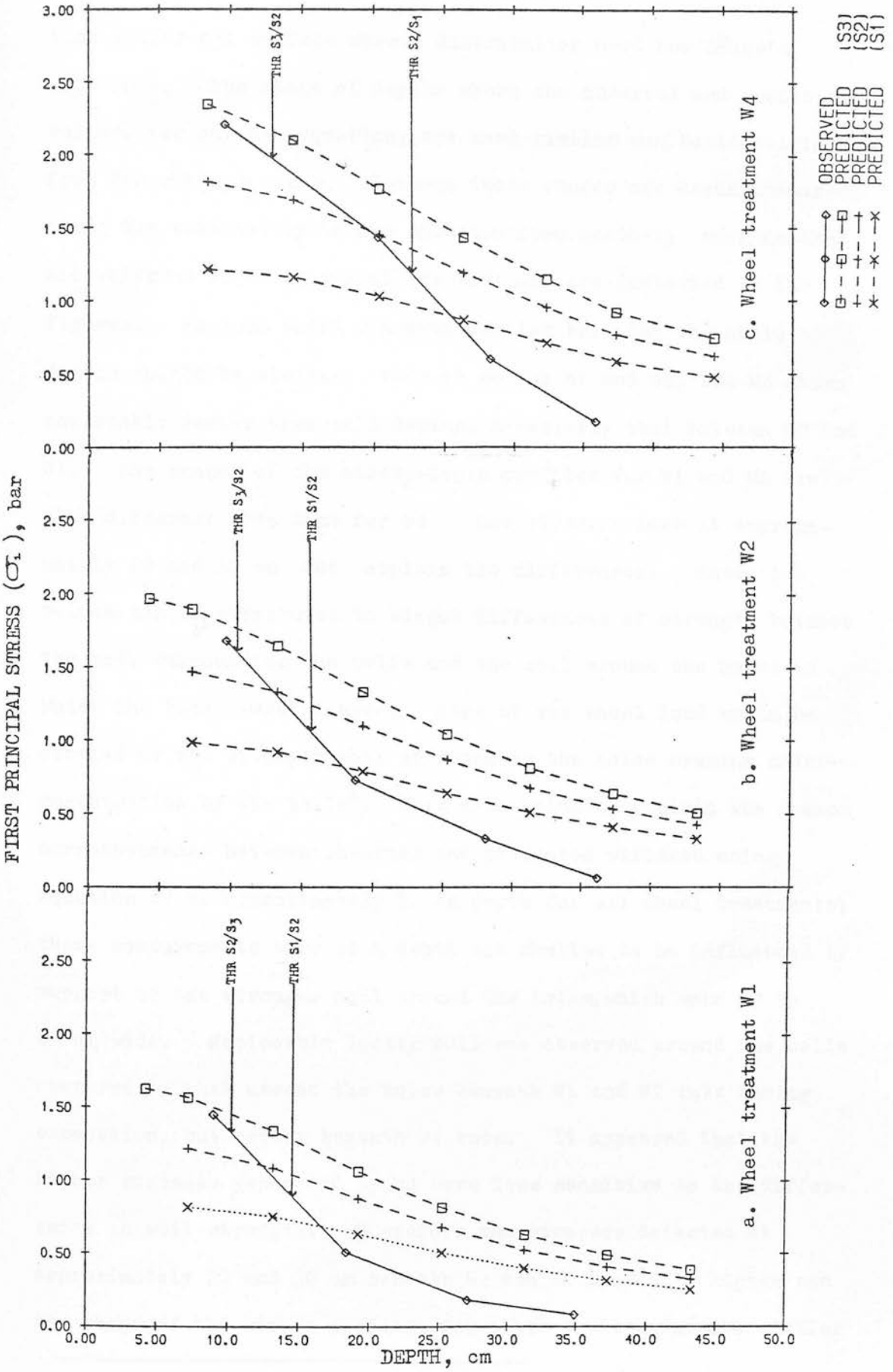


Fig.59 The variation of observed values of first principal stresses ($\sigma_1$) and predicted from Söhne's equations (S1, S2 and S3). Each wheel treatment is examined separately and the threshold depths (THR) are indicated.

tion factor and surface stress distribution used for Söhne's equations. The range of depths where the observed and predicted values, for any one equation, are most similar can be identified from Figs.59 a, b and c. Between these ranges are depths separating the suitability of one equation from another; such depths are referred to as 'threshold depths' and are indicated in the figures. As each wheel ran over similar soil the threshold depths should be similar; this is so for W1 and W2, but W4 shows noticeably deeper threshold depths, especially that between S2 and S1. The shapes of the stress-depth profiles for W1 and W2 are also different from that for W4. Low stress values at approximately 20 and 30 cm can explain the differences. These low values can be attributed to slight differences of strength between the soil surrounding the balls and the soil around the holes in which the balls were planted. More of the wheel load would be carried by the stronger soil surrounding the holes causing under-registration by the balls[1]. This also helps to explain the common correspondence between observed and predicted stresses using equation S3 at approximately 10 cm depth for all wheel treatments; these measurements were at a depth too shallow to be influenced by support of the stronger soil around the holes, which were 30 to 40 cm wide. Noticeably looser soil was observed around the balls compared to that around the holes beneath W1 and W2 ruts during excavation, but rarely beneath W4 ruts. It appeared that the higher stresses generated by W4 were less sensitive to the differences in soil strength. Therefore the stresses detected at approximately 20 and 30 cm beneath W2 and W1 should be higher and the shape of the stress profiles for these treatments more similar

1. An 'arching' effect, c.f. section 1.3.

to that of W4. The threshold depths of W1 and 2 would then correspond closer to those of W4. Therefore the cone resistance values at the threshold depths for treatment W4 were taken as the soil strength boundaries between the 'soft', 'firm' and 'hard' conditions proposed by Söhne for the selection of the prediction equations. This assumes that cone resistance values are not influenced by soil depth beyond the upper few centimetres where the cone resistance is approaching its 'limit' value (Mulqueen et al. 1976). It also assumes that the measured cone resistance of the soil in the experimental plots is representative of the soil around the balls.

Calculation of the cone resistance values at the threshold depths needed an estimation of cone resistance of the soil during occasion M3 at Lower Terrace. There were linear relationships between soil moisture content and cone resistance for the two threshold depths of the Threipmuir soil, although there were too few data for significant regressions[1]. Estimates of the values of cone resistance at the threshold depths for occasion M3 were made using the regressions and the mean cone resistance for occasions M3 and M4 at each threshold depth was calculated[1]. Thus the threshold value of cone resistance between equations S1 and S2 was approximately 26 bar and between equations S2 and S3 approximately 16 bar. From significant linear relationships between cone resistance and vane shear strength at 9 and 18 cm depth[1] the threshold values of cone resistance could be interpreted as 27 kPa and 34 kPa vane shear strength for S2/S3 and S1/S2 respectively.

---

1. See Appendix 6.

The measured and predicted values of $\sigma_3$ in Table 26 show little similarity of size or trend with depth. This lack of correspondence can be assigned to the dependence of equations S4 and S6 on an assumed and constant value of Poisson's ratio; this dependence is absent from equations S1, S2 and S3, as explained in Section 2.1. A more suitable estimate can be made from the ratio between the observed values of $\sigma_1$ and $\sigma_3$. These ratios are shown in Table 27.

TABLE 27 RATIOS BETWEEN OBSERVED VALUES OF FIRST AND THIRD PRINCIPAL STRESSES FOR EACH WHEEL TREATMENT AND DEPTH

| Nominal depth, cm | Treatment | W1 | W2 | W4 |
|---|---|---|---|---|
| 10 | | 1.138 | 1.161 | 1.147 |
| 20 | | 1.900* | 1.358* | 1.143 |
| 30 | | 1.800* | 1.333* | 1.331 |
| 40 | | 2.12 * | - | 1.220 |

The values indicated (*) can be discounted due to the soil strength differences, described previously, between soil adjacent to the balls and soil around the holes. The very large values at greatest depth below W1 and W2 are also ignored. The mean of the remaining more reliable values (1.19) could be used to estimate $\sigma_3$ for further calculations.

When second and third principal stresses were considered equal the values of spherical stress (P) and deviatoric stress (R) could be calculated using the observed ratio as follows:

$$\sigma_3 = \frac{\sigma_1}{1.19} \qquad \therefore \text{ from equations (1) and (2) (section 2.2)}$$

$$P = 1.55\sigma_1 \quad , \quad R = 0.13\sigma_1 \quad \text{and} \quad R = 0.08P$$

This very low value of R compared to P suggested deviatoric stress would have a negligible effect upon changes of dry bulk density. Although R would increase in proportion to P, its effect on volumetric strain of strain hardening soil would decrease as P increased (Schofield and Wroth, 1968). Increasing levels of confining stress require larger deviator stresses to achieve the same strain. Therefore for most of the field results the stress/strain path of the soil beneath the experimental wheels would be near the Dbd, lnP plane of the Dbd, lnP, lnR space (section 2.2). This simplified identification of the Critical State parameters as only the virgin compression lines needed to be considered, apart from the smaller influence of deviatoric stress.

## 6.3 Identification of the Stress/Strain Functions

### 6.3.1 The apparent virgin compression line, in situ

The threshold values of cone resistance which aided prediction of soil stresses for the Threipmuir soil were also applied to the Macmerry soil. Stress measurements had not been made in soils of cone resistance less than about 10 bar. Therefore there was some ignorance of the soil stresses at such low strengths and relatively unconfined conditions when deviatoric stresses may be much higher than those in soil above 10 bar cone resistance.

Mean Rut Depths of the field ruts enabled an estimation of the contact area of the experimental wheel making the rut,[1] using the appropriate contact area prediction equation. The initial cone resistance below 6 cm depth of the soil defined the choice of the prediction equation for $\sigma_1$, while avoiding cone resistance which had not reached a 'limit' value. Thus the estimated value of maxi-

1. These estimates of contact area are shown in Figs.45 and 46.

mum spherical pressure ($P_{max}$)[1] and final dry bulk density after wheel passage ($Dbd_f$) could be known for each 3 cm depth interval below the tyre/soil interface, excluding the first 3 cm depth.

$Dbd_f$ and $\ln P_{max}$ could now be related to each other. This examination of the data sometimes required separate consideration of the different parts of the soil profile. One part would be wetter than the other and the cone resistance values sometimes required different stress prediction equations from the other. The choices of stress prediction equations and division of the $Dbd_f$ profiles are shown in Table 28. The threshold values of cone resistance (c.f. section 6.2.2) are indicated on the graphs of initial cone resistance and depth for each of the soils and experimental occasions (Figs.48a to 49c). Graphs of $\ln P_{max}$ and $Dbd_f$ are shown in Figs.60a to 60y for Macmerry and Figs.61a to 61h for Threipmuir. Each figure examines a separate occasion, part of profile and RL treatment. $Dbd_f$ and $\ln P_{max}$ values are grouped from all W treatments on the same occasion and RL treatment. Thus soil of various initial dry bulk density values but similar moisture contents experienced a variety of values of $P_{max}$ under the experimental wheels. This interaction created a variety of $Dbd_f$ values. Thus the variation of initial $Dbd$, $P_{max}$ and $Dbd_f$ satisfied the requirements described in section 2.2.1 for the identification of the 'VCL' from in situ measurements.

Most of the graphs showed a linear cluster of points below which no other points occurred (as expected in section 2.2.1). 'Best fit' straight lines could be constructed through these clusters by linear regression. However, some subjective decision

1. Calculated from $P_{max} = 1.55\sigma_1$ (as in section 6.2.2).

TABLE 28 ALLOCATION OF STRESS PREDICTION EQUATIONS FOR FIELD COMPACTION EXPERIMENTS ACCORDING TO THE INITIAL CONE RESISTANCE OF THE SOIL (code for equations explained in Section 2.1)

MACMERRY

| Soil Treatment | | RL 1 | RL 2 | RL 3 | RL 4 |
|---|---|---|---|---|---|
| Occasion | Depth | | | | |
| M1 | 0 - 33 cm | S3 | S3 | S3 | S2 |
| M2 | 0 - 12 cm | S3 | S3 | S3 | S2 |
| M2 | 12 - 33 cm | S3 | S3 | S3 | S2 |
| M3 | 0 - 12 cm | S3 | S3 | S3 | S1 |
| M3 | 12 - 33 cm | S3 | S3 | S3 | S2 |
| M4 | 0 - 12 cm | S3 | S3 | S3 | S1 |
| M4 | 12 - 33 cm | S3 | S3 | S3 | S2 |

THREIPMUIR

| Soil Treatment | | RL 1 | RL 2 | RL 3 |
|---|---|---|---|---|
| Occasion | Depth | | | |
| M1 | 0 - 12 cm | S2 | S2 | S1 |
| M1 | 12 - 39 cm | S1 | S1 | S1 |
| M2 | 0 - 18 cm | S3 | S3 | S3 |
| M2 | 18 - 39 cm | S3 | S2 | S2 |
| M4 | 0 - 15 cm | S3 | S3 | S2 |
| M4 | 15 - 39 cm | S2 | S2 | S1 |

Figures 60 and 61 A collection of graphs relating dry bulk density after wheel passage to the natural logarithm of the expected maximum spherical pressure ($P_{max}$). The data is separated by soil type, Macmerry = MAC (Fig.60), Threipmuir = THR (Fig.61), experimental occasion (M), soil rolling treatment (RL), stress prediction equation (S) and the range of depths of the measurements. The points included in the linear clusters are indicated thus ( * ). The best fit straight line through each cluster is shown as well as the slope (M), intercept (C), correlation coefficient (R) and the significance of the analysis of regression for the line. The mean gravimetric moisture content for each set of data (W) is also indicated.

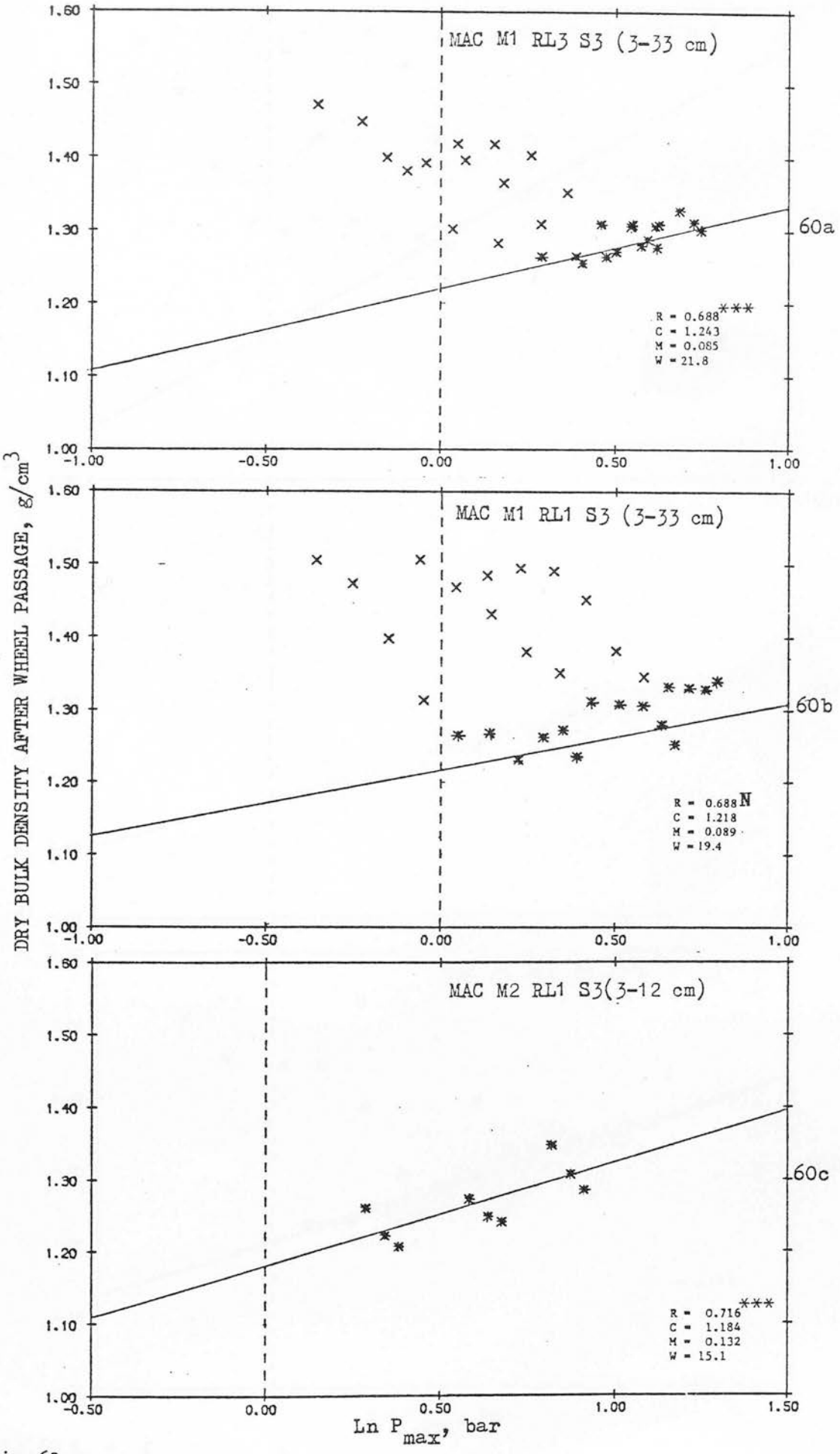
MAC M1 RL3 S3 (3-33 cm)
R = 0.688***
C = 1.243
M = 0.085
W = 21.8
60a
MAC M1 RL1 S3 (3-33 cm)
R = 0.688N
C = 1.218
M = 0.089
W = 19.4
60b
MAC M2 RL1 S3(3-12 cm)
R = 0.716***
C = 1.184
M = 0.132
W = 15.1
60c
DRY BULK DENSITY AFTER WHEEL PASSAGE, g/cm3
Ln Pmax, bar

Fig.60 a, b, c

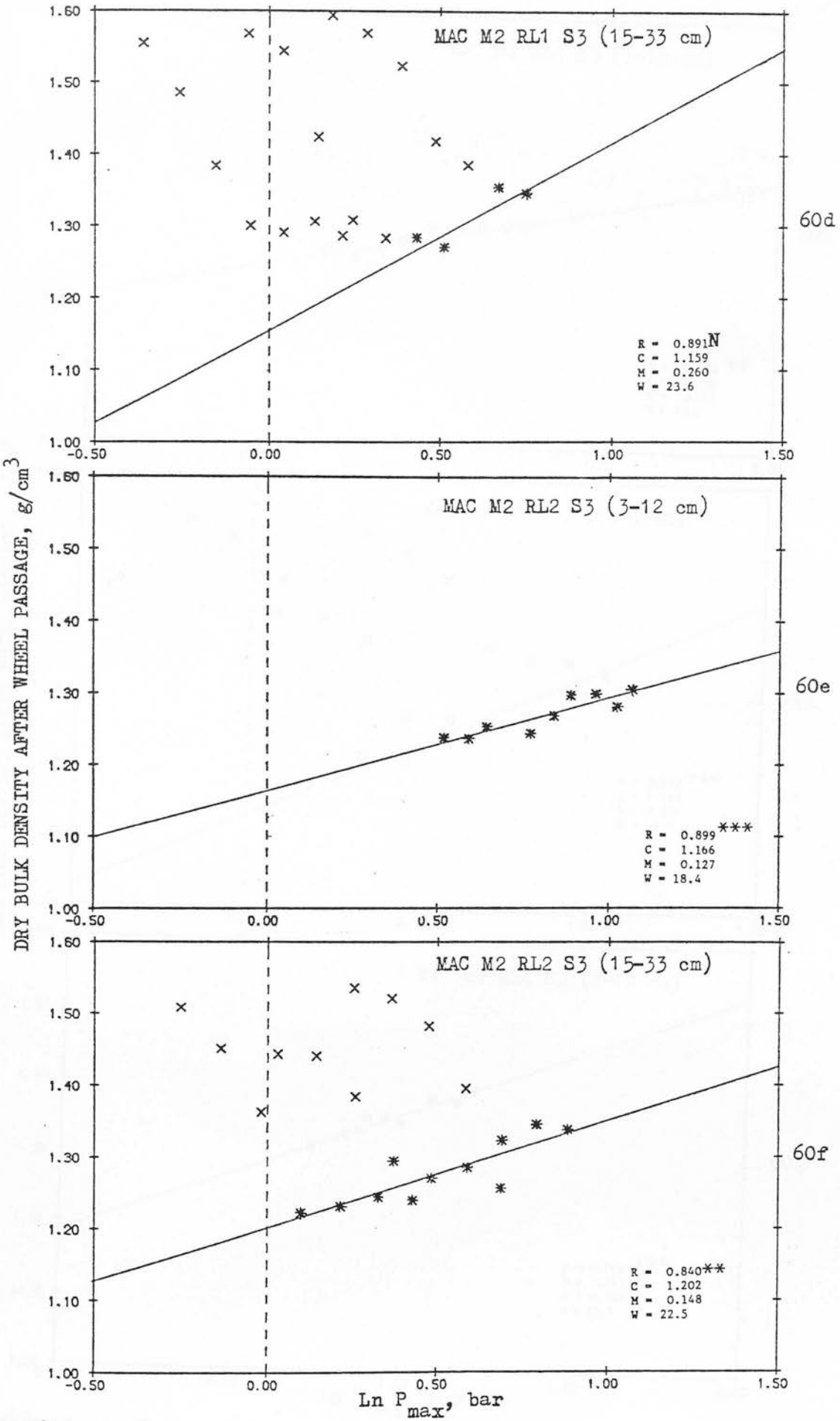
MAC M2 RL1 S3 (15-33 cm)
R = 0.891N
C = 1.159
M = 0.260
W = 23.6
60d
MAC M2 RL2 S3 (3-12 cm)
R = 0.899***
C = 1.166
M = 0.127
W = 18.4
60e
MAC M2 RL2 S3 (15-33 cm)
R = 0.840**
C = 1.202
M = 0.148
W = 22.5
60f
DRY BULK DENSITY AFTER WHEEL PASSAGE, g/cm3
Ln Pmax, bar
1.00
1.10
1.20
1.30
1.40
1.50
1.60
-0.50
0.00
0.50
1.00
1.50

Fig.60 d, e, f

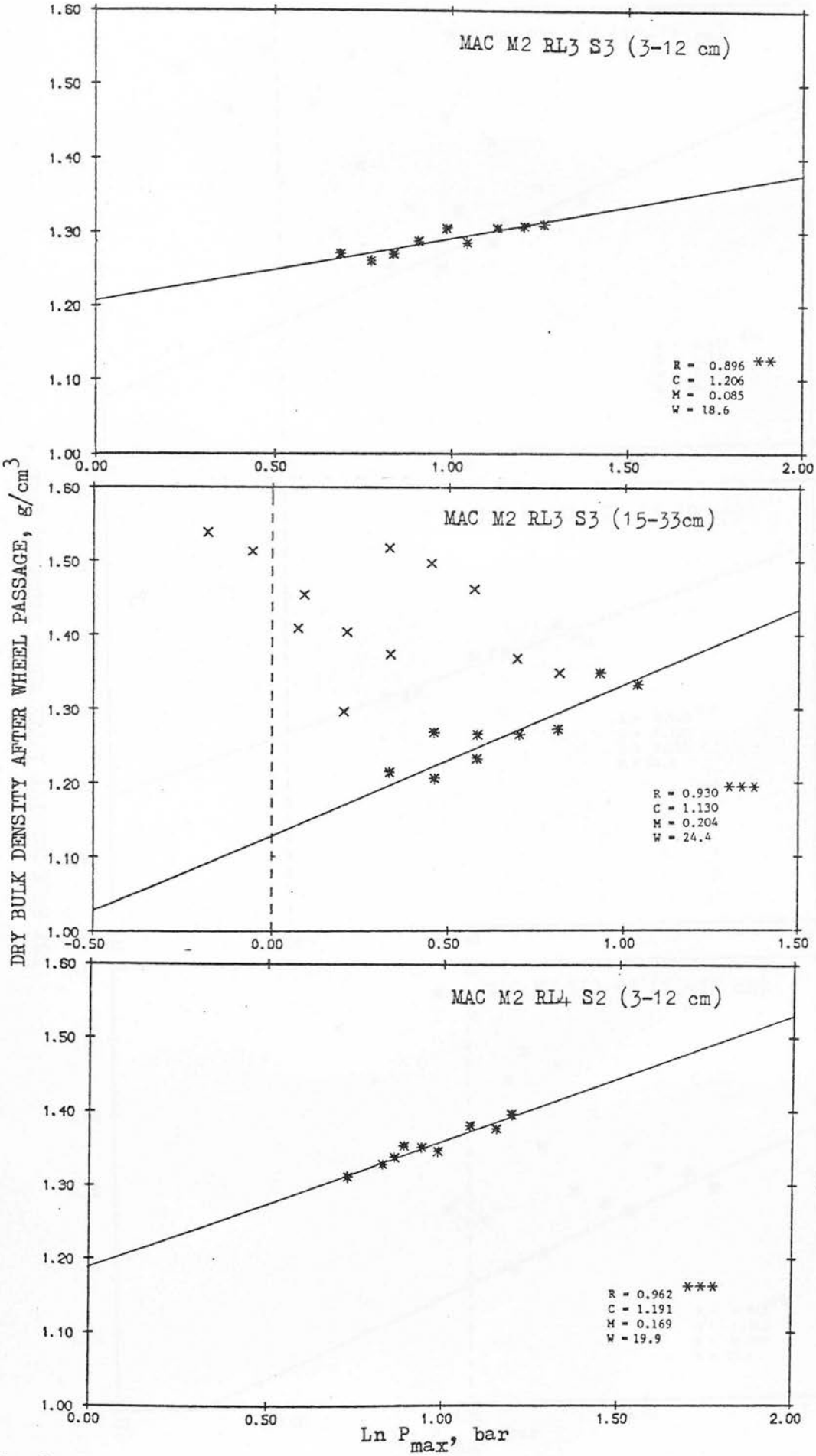
MAC M2 RL3 S3 (3-12 cm)
R = 0.896 **
C = 1.206
M = 0.085
W = 18.6
60h
MAC M2 RL3 S3 (15-33cm)
R = 0.930 ***
C = 1.130
M = 0.204
W = 24.4
60i
MAC M2 RL4 S2 (3-12 cm)
R = 0.962 ***
C = 1.191
M = 0.169
W = 19.9
60j
DRY BULK DENSITY AFTER WHEEL PASSAGE, g/cm3
Ln Pmax, bar

Fig.60h, i, j

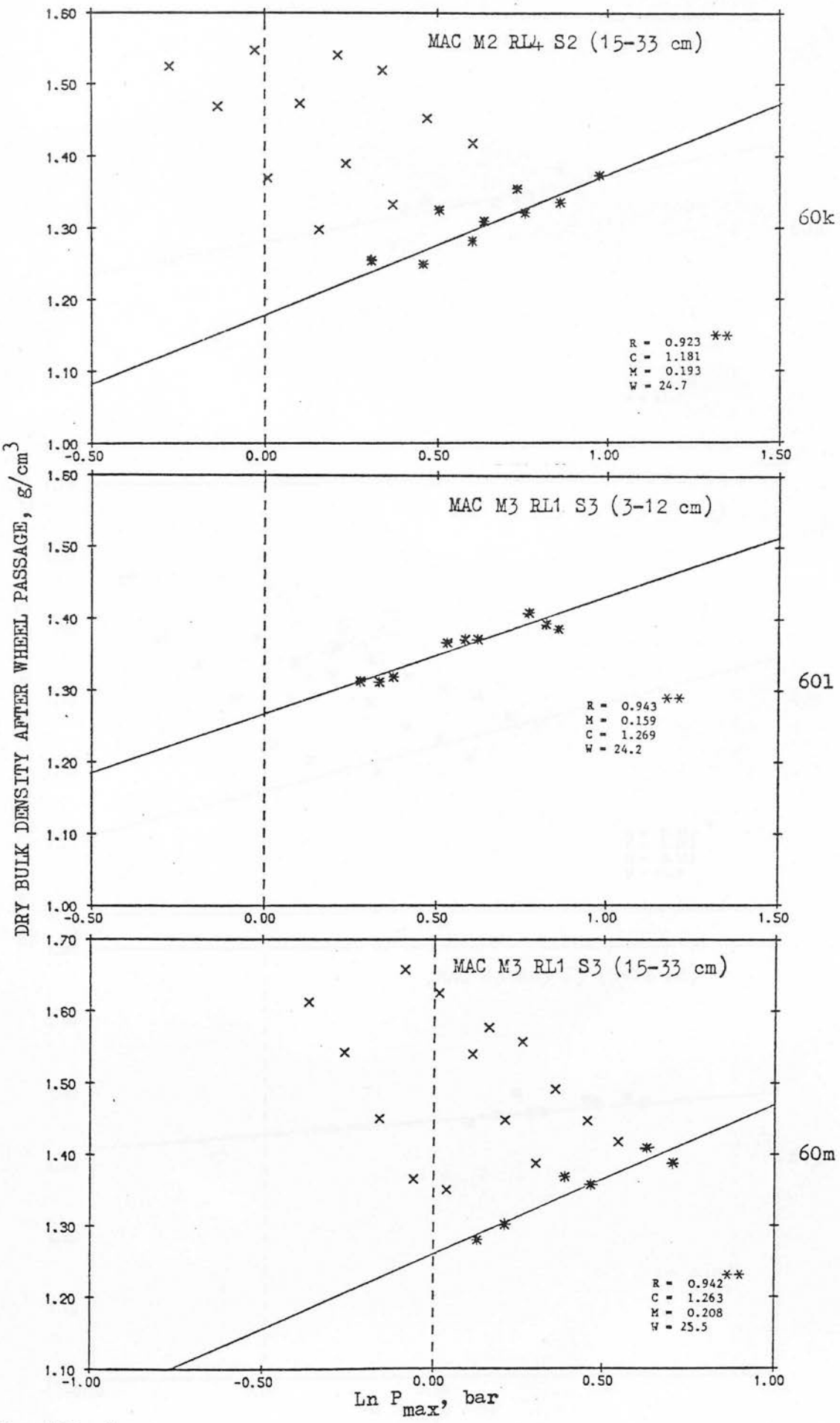
MAC M2 RL4 S2 (15-33 cm)
R = 0.923 **
C = 1.181
M = 0.193
W = 24.7
60k
MAC M3 RL1 S3 (3-12 cm)
R = 0.943 **
M = 0.159
C = 1.269
W = 24.2
601
MAC M3 RL1 S3 (15-33 cm)
R = 0.942 **
C = 1.263
M = 0.208
W = 25.5
60m
DRY BULK DENSITY AFTER WHEEL PASSAGE, g/cm3
Ln Pmax, bar

Fig.60 k, l, m

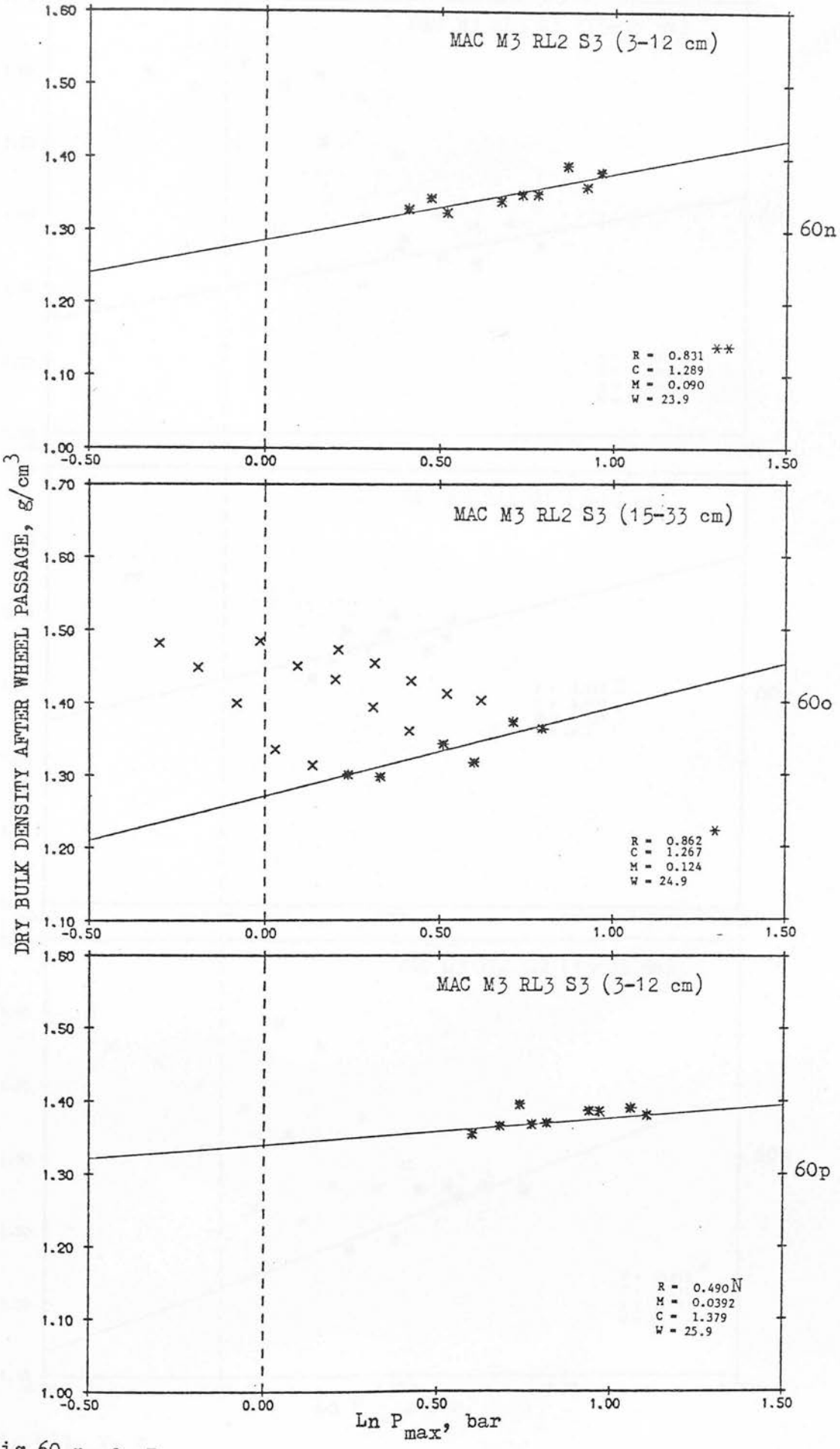
MAC M3 RL2 S3 (3-12 cm)
R = 0.831 **
C = 1.289
M = 0.090
W = 23.9
60n
MAC M3 RL2 S3 (15-33 cm)
R = 0.862 *
C = 1.267
M = 0.124
W = 24.9
60o
MAC M3 RL3 S3 (3-12 cm)
R = 0.490N
M = 0.0392
C = 1.379
W = 25.9
60p
DRY BULK DENSITY AFTER WHEEL PASSAGE, g/cm3
Ln Pmax, bar

Fig.60 n, o, p

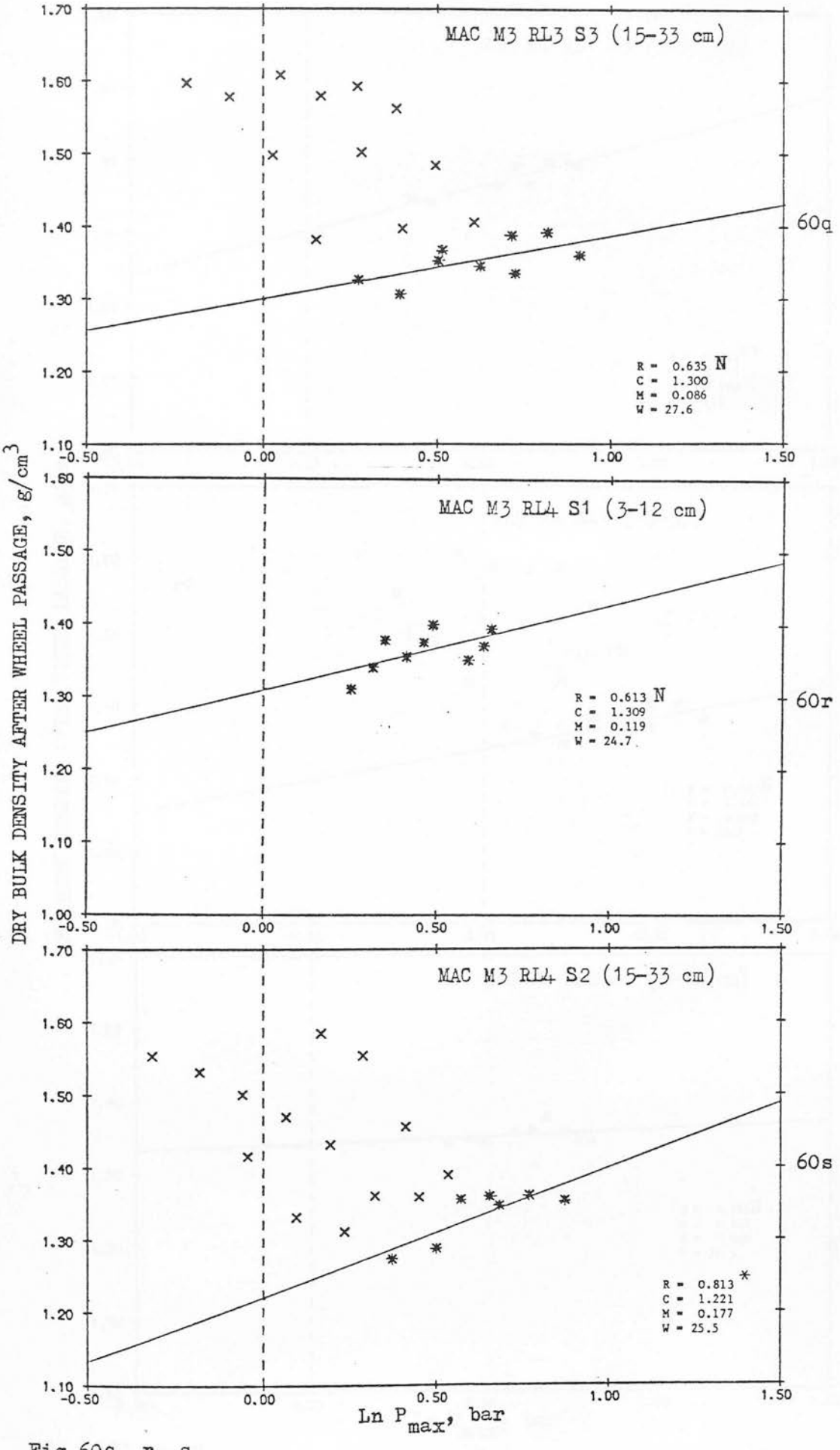
MAC M3 RL3 S3 (15-33 cm)
60q
R = 0.635 N
C = 1.300
M = 0.086
W = 27.6
MAC M3 RL4 S1 (3-12 cm)
60r
R = 0.613 N
C = 1.309
M = 0.119
W = 24.7
MAC M3 RL4 S2 (15-33 cm)
60s
R = 0.813 *
C = 1.221
M = 0.177
W = 25.5
DRY BULK DENSITY AFTER WHEEL PASSAGE, g/cm3
Ln Pmax, bar

Fig.60q, r, s

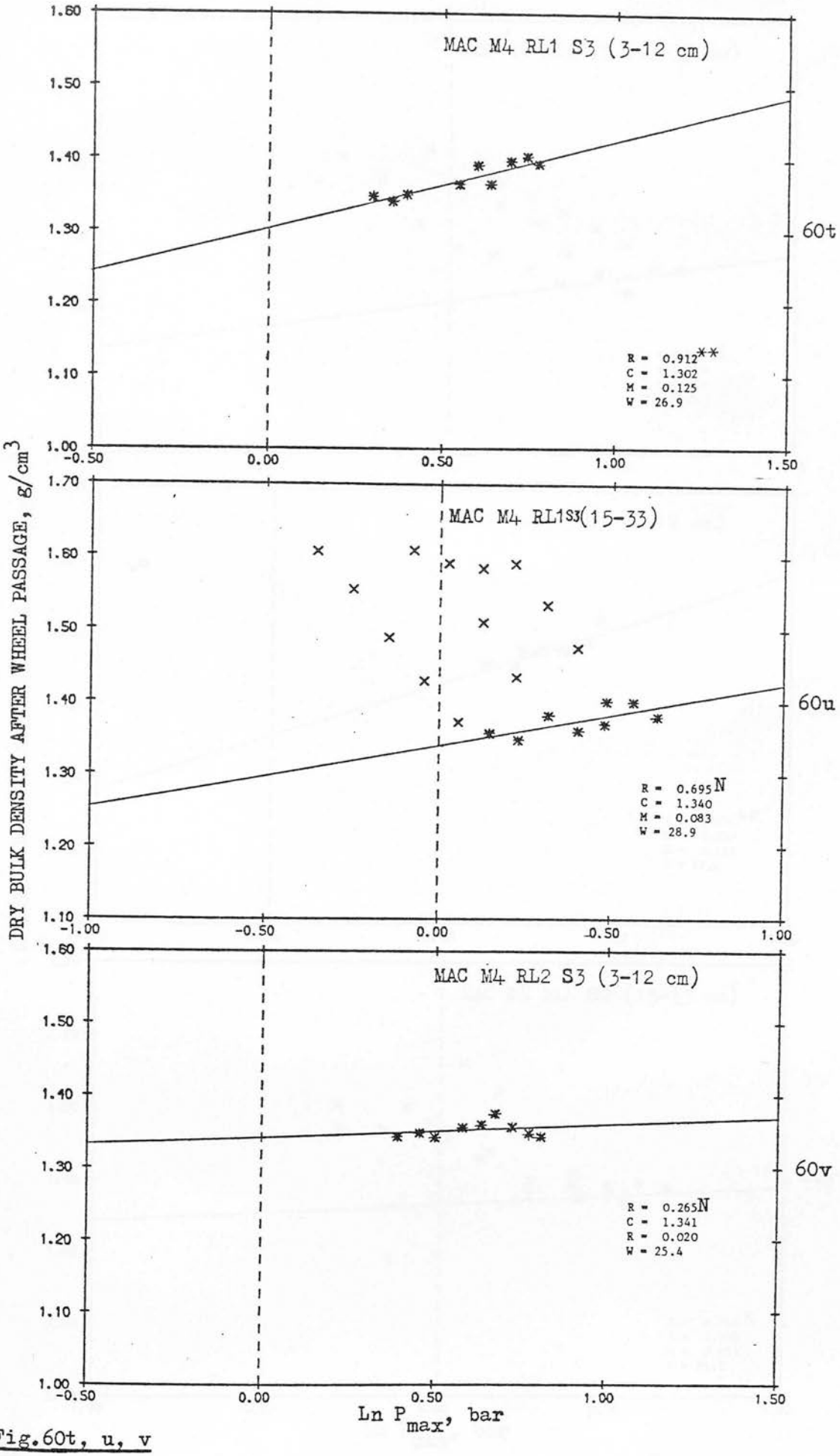
MAC M4 RL1 S3 (3-12 cm)
R = 0.912**
C = 1.302
M = 0.125
W = 26.9
60t
MAC M4 RL1S3(15-33)
R = 0.695N
C = 1.340
M = 0.083
W = 28.9
60u
MAC M4 RL2 S3 (3-12 cm)
R = 0.265N
C = 1.341
R = 0.020
W = 25.4
60v
DRY BULK DENSITY AFTER WHEEL PASSAGE, g/cm3
Ln Pmax, bar

Fig.60t, u, v

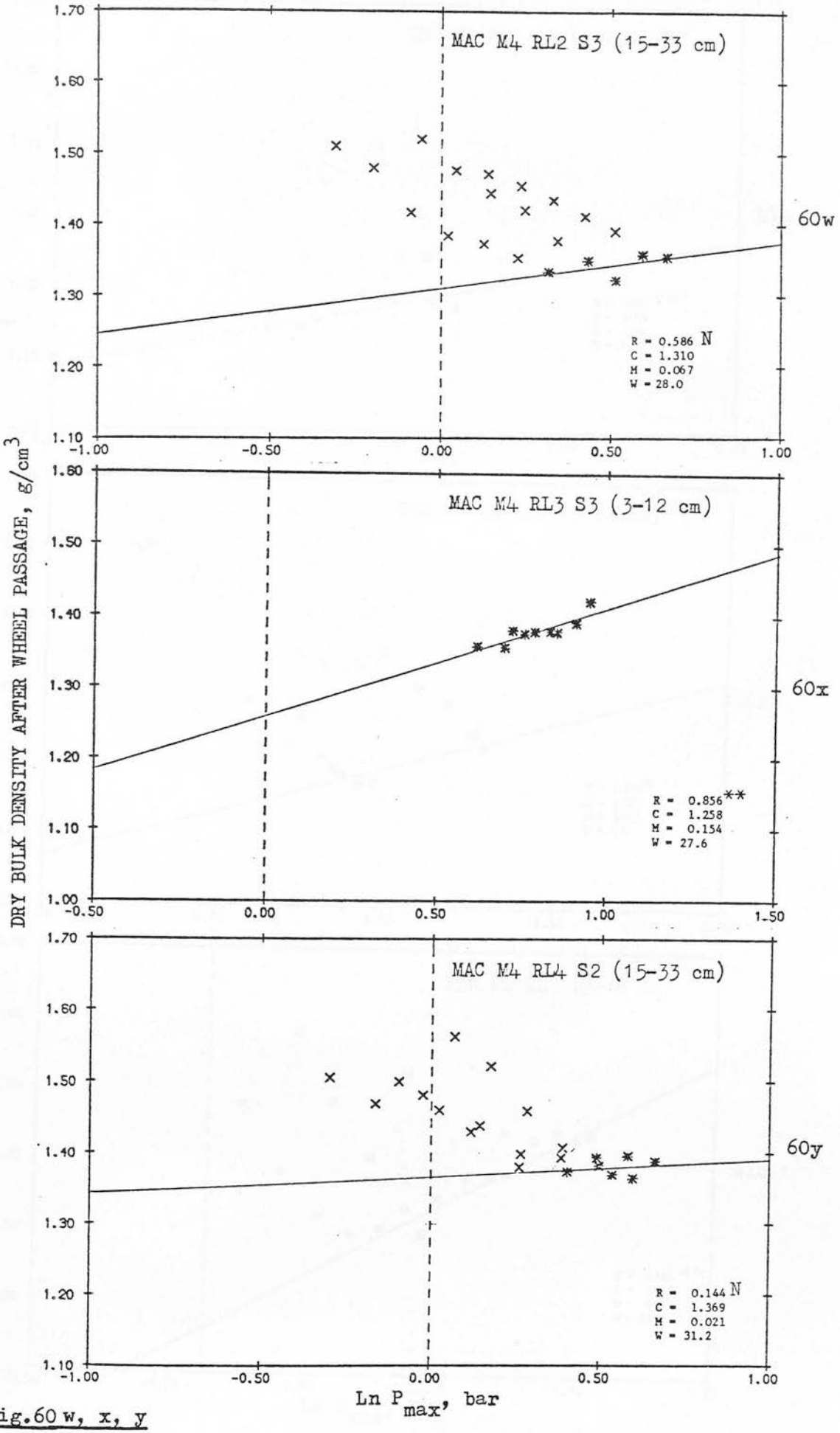
MAC M4 RL2 S3 (15-33 cm)
R = 0.586 N
C = 1.310
M = 0.067
W = 28.0
60w
MAC M4 RL3 S3 (3-12 cm)
R = 0.856**
C = 1.258
M = 0.154
W = 27.6
60x
MAC M4 RL4 S2 (15-33 cm)
R = 0.144 N
C = 1.369
M = 0.021
W = 31.2
60y
DRY BULK DENSITY AFTER WHEEL PASSAGE, g/cm3
Ln Pmax, bar

Fig.60 w, x, y

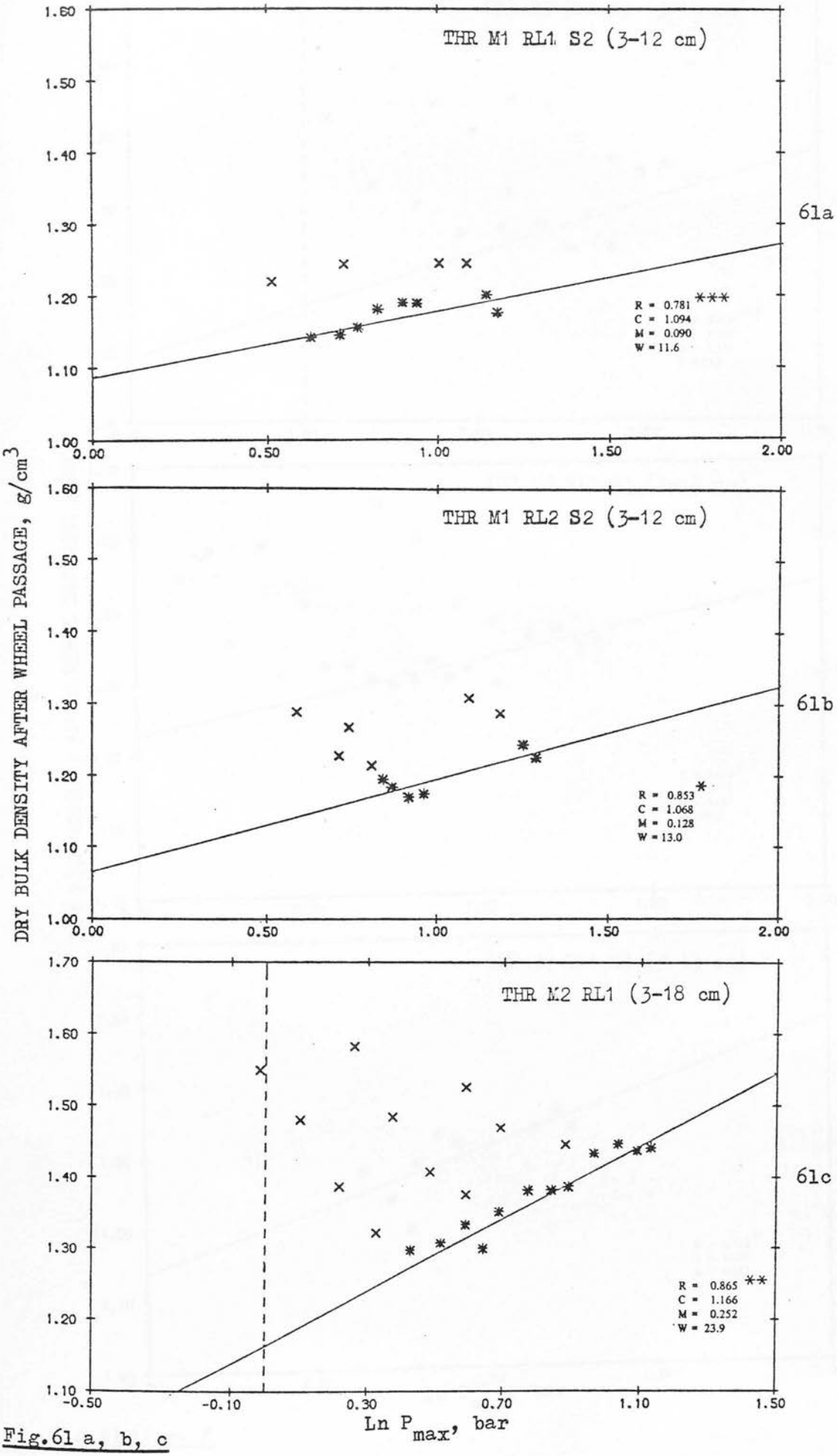
THR M1 RL1 S2 (3-12 cm)
R = 0.781 ***
C = 1.094
M = 0.090
W = 11.6
61a
THR M1 RL2 S2 (3-12 cm)
R = 0.853
C = 1.068
M = 0.128
W = 13.0
61b
THR M2 RL1 (3-18 cm)
R = 0.865 **
C = 1.166
M = 0.252
W = 23.9
61c
DRY BULK DENSITY AFTER WHEEL PASSAGE, g/cm3
Ln Pmax, bar

Fig.61 a, b, c

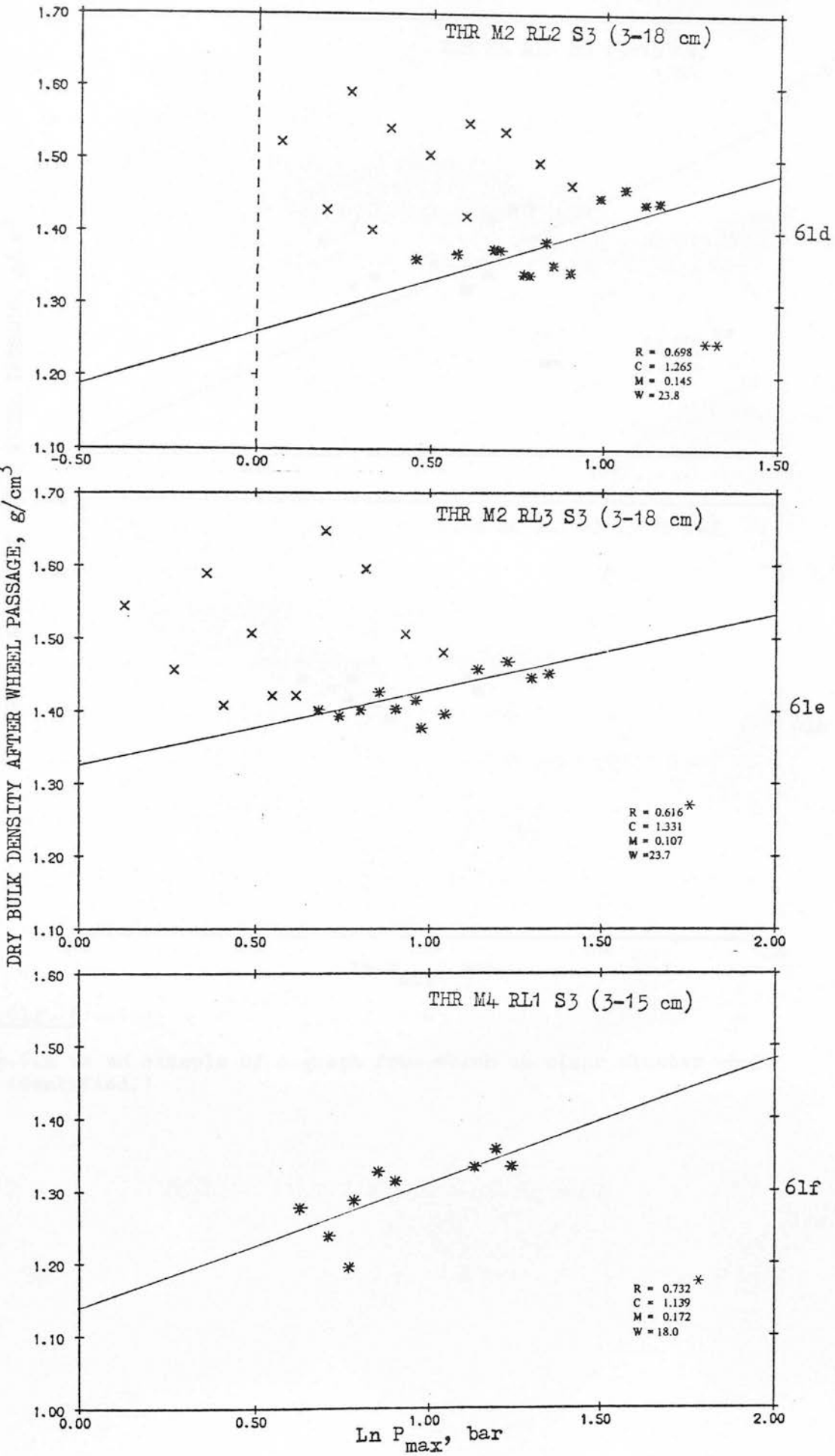
THR M2 RL2 S3 (3-18 cm)
R = 0.698 **
C = 1.265
M = 0.145
W = 23.8
61d
THR M2 RL3 S3 (3-18 cm)
R = 0.616 *
C = 1.331
M = 0.107
W = 23.7
61e
THR M4 RL1 S3 (3-15 cm)
R = 0.732 *
C = 1.139
M = 0.172
W = 18.0
61f
DRY BULK DENSITY AFTER WHEEL PASSAGE, g/cm3
Ln Pmax, bar

Fig.61d, e, f

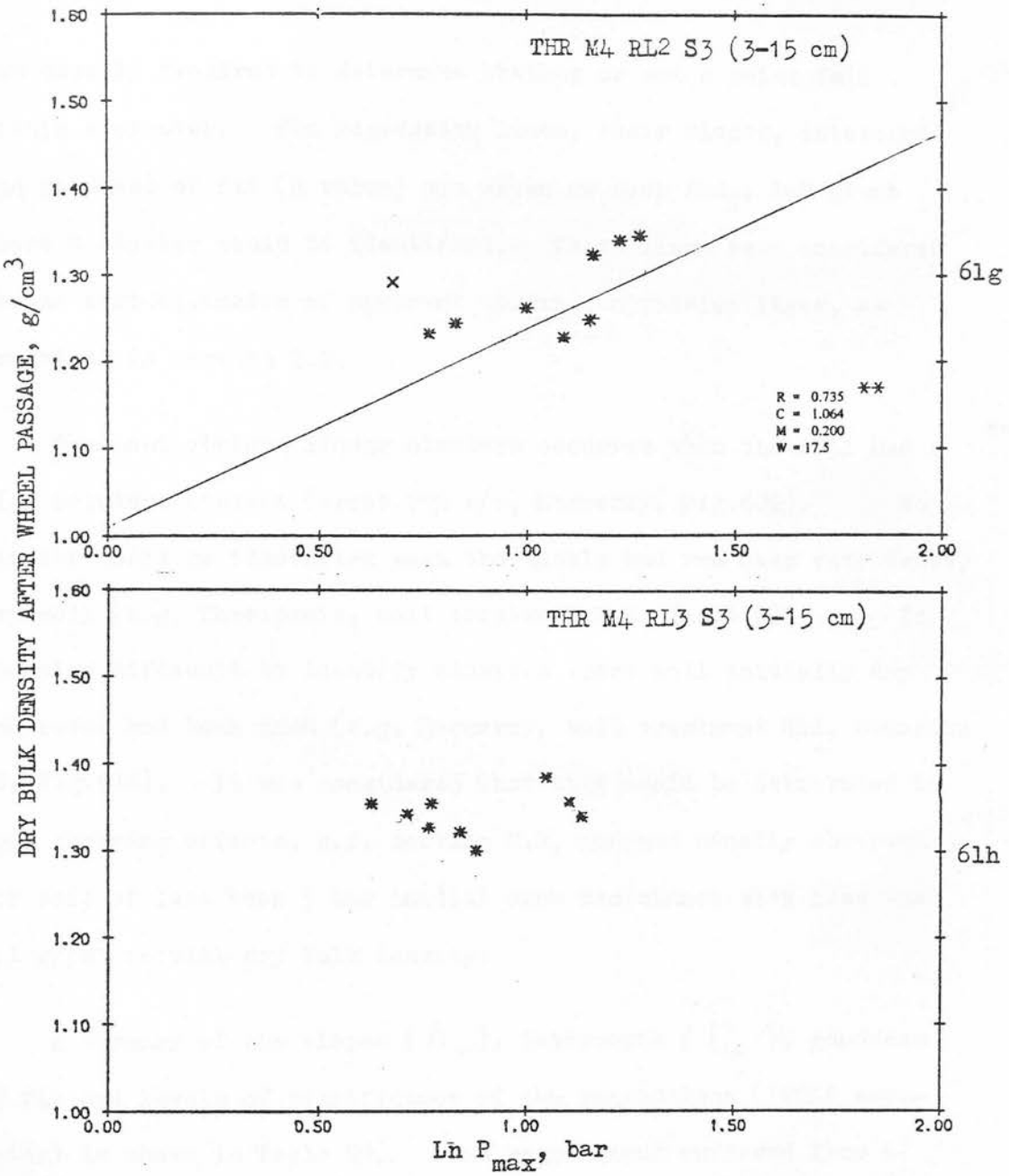


61g

61h

Fig.61g, h

(Fig.61h is an example of a graph from which no clear cluster could be identified.)

was usually required to determine whether or not a point fell within a cluster. The regression lines, their slopes, intercepts and goodness of fit (R value) are shown on each $Dbd_f$, lnP graph where a cluster could be identified. These lines were considered as the best estimates of apparent virgin compression lines, as explained in section 2.2.

The most obvious linear clusters occurred when the soil had a high moisture content (about 25% w/w, Macmerry, Fig.60k). No cluster could be identified when the wheels had run over very dense, dry soil (e.g. Threipmuir, soil treatment RL3, Fig.61h). It was also difficult to identify clusters where soil initially dry and loose had been used (e.g. Macmerry, soil treatment RL1, occasion M2, Fig.61d). It was considered that this could be attributed to soil shearing effects, c.f. section 2.2, and was usually observed for soil of less than 5 bar initial cone resistance with less than 1.1 $g/cm^3$ initial dry bulk density.

A summary of the slopes ( $\lambda_{v'}$ ), intercepts ( $\Gamma_{v'}$ ), goodness of fit and levels of significance of the regressions ('VCL' estimates) is shown in Table 29. Some regressions suffered from a poor clustering, or a shortage of data, but the majority of 'VCL' estimates were derived from significant regressions with a good fit to a straight line.

### 6.3.2 The apparent virgin compression line, from laboratory results

The real virgin compression line was readily identified from graphs of P and Dbd for the initially loose soil samples (agg. diam. $<$ 1 cm), see Figs.54 and 55. Some curvilinearity was observed

TABLE 29 ESTIMATES FROM GRAPHS OF $Dbd_f$ and $\ln P_{max}$ OF SLOPE AND INTERCEPT OF APPARENT VIRGIN COMPRESSION LINES, ORDERED BY VALUE OF MOISTURE CONTENT

MACMERRY — Regression coefficient (R) indicated

| Occasion and soil Treatment | Depths, cm | Stress prediction equation | Moisture content, % w/w | 'VCL' Slope, g/cm³/unit ln P | 'VCL' Intercept, g/cm³ | R | Sig. level |
|---|---|---|---|---|---|---|---|
| M2 RL 1 | 3-12 | S3 | 15.1 | 0.132 | 1.184 | 0.716 | ** |
| M2 RL 2 | 3-12 | S3 | 18.4 | 0.127 | 1.166 | 0.899 | *** |
| M2 RL 3 | 3-12 | S3 | 18.6 | 0.085 | 1.206 | 0.896 | ** |
| M1 RL 1 | 3-33 | S3 | 19.4 | 0.246 | 1.218 | 0.688 | |
| M2 RL 4 | 3-12 | S2 | 19.9 | 0.169 | 1.191 | 0.962 | *** |
| M1 RL 3 | 3-33 | S3 | 21.8 | 0.085 | 1.243 | 0.688 | *** |
| M1 RL 4 | 3-33 | S2 | 22.1 | 0.176 | 1.171 | 0.816 | *** |
| M2 RL 2 | 15-33 | S3 | 22.5 | 0.148 | 1.202 | 0.840 | ** |
| M2 RL 1 | 15-33 | S3 | 23.6 | 0.260 | 1.159 | 0.891 | |
| M3 RL 2 | 3-12 | S3 | 23.9 | 0.090 | 1.289 | 0.831 | ** |
| M3 RL 1 | 3-12 | S3 | 24.2 | 0.159 | 1.269 | 0.943 | ** |
| M2 RL 3 | 15-33 | S3 | 24.4 | 0.204 | 1.130 | 0.930 | *** |
| M3 RL 4 | 3-12 | S1 | 24.7 | 0.119 | 1.309 | 0.613 | |
| M2 RL 4 | 15-33 | S2 | 24.7 | 0.193 | 1.181 | 0.923 | ** |
| M3 RL 2 | 15-33 | S3 | 24.9 | 0.124 | 1.267 | 0.862 | * |
| M4 RL 2 | 3-12 | S3 | 25.4 | 0.020 | 1.341 | 0.265 | |
| M3 RL 1 | 15-33 | S3 | 25.5 | 0.208 | 1.263 | 0.942 | ** |
| M3 RL 4 | 15-33 | S2 | 25.5 | 0.177 | 1.221 | 0.813 | * |
| M3 RL 3 | 3-12 | S3 | 25.9 | 0.039 | 1.340 | 0.490 | |
| M4 RL 1 | 3-12 | S3 | 26.9 | 0.125 | 1.302 | 0.912 | ** |
| M4 RL 3 | 3-12 | S3 | 27.6 | 0.154 | 1.258 | 0.856 | ** |
| M3 RL 3 | 15-33 | S3 | 27.6 | 0.086 | 1.300 | 0.635 | |
| M4 RL 2 | 15-33 | S3 | 28.0 | 0.067 | 1.310 | 0.586 | |
| M4 RL 1 | 15-33 | S3 | 28.9 | 0.083 | 1.340 | 0.695 | |
| M4 RL 3 | 15-33 | S3 | 30.1 | 0.005 | 1.360 | 0.052 | |
| M4 RL 4 | 15-33 | S2 | 31.2 | 0.021 | 1.369 | 0.144 | |
| | | | mean s.e. | 0.039 | 0.035 | | |

THREIPMUIR

| | | | | | | | |
|---|---|---|---|---|---|---|---|
| M1 RL 1 | 3-12 | S2 | 11.6 | 0.090 | 1.094 | 0.781 | *** |
| M1 RL 2 | 3-12 | S2 | 13.0 | 0.128 | 1.068 | 0.853 | * |
| M4 RL 2 | 3-15 | S3 | 17.5 | 0.200 | 1.064 | 0.735 | ** |
| M4 RL 1 | 3-15 | S3 | 18.0 | 0.172 | 1.140 | 0.732 | * |
| M2 RL 3 | 3-18 | S3 | 23.7 | 0.107 | 1.331 | 0.616 | * |
| M2 RL 2 | 3-18 | S3 | 23.8 | 0.145 | 1.265 | 0.698 | ** |
| M2 RL 1 | 3-18 | S3 | 23.9 | 0.252 | 1.166 | 0.865 | ** |
| | | | mean s.e. | 0.048 | 0.038 | | |

TABLE 30 VCL, SWELLING AND RELAXATION PARAMETERS FROM TRIAXIAL TESTS, 1978

MACMERRY

| Sample No. | Moisture content, %, w/w | 'VCL' slope g/cm³/unit ln P | 'VCL' intercept g/cm³ | Slope of swelling line g/cm³/unit ln P | Slope of relaxation line, g/cm³/unit ln P at 1 bar | Slope of relaxation line, g/cm³/unit ln P at end test |
|---|---|---|---|---|---|---|
| 21 | 8.8 | 0.319 | 1.265 | 0.036<br>0.035+ | 0.015 | 0.015 |
| 18 | 9.1 | 0.205 | 1.330 | 0.037<br>0.035+ | 0.015 | 0.0175 |
| 25 | 11.4 | 0.212 | 1.325 | 0.048<br>0.046+ | - | 0.02 |
| 24 | 12.4 | 0.326 | 1.300 | 0.041<br>0.037+ | 0.015 | 0.02 |
| 19 | 12.6 | 0.373 | 1.270 | 0.043<br>0.040+ | 0.01 | 0.0175 |
| 10 | 16.9 | 0.251 | 1.242 | - | 0.03 | 0.035 |
| 13 | 19.0 | 0.276 | 1.260 | - | 0.025 | 0.03 |
| 14 | 19.0 | 0.276 | 1.375 | - | 0.025 | 0.035 |
| 12 | 19.1 | 0.328 | 1.275 | - | 0.02 | 0.02 |
| 16 | 20.0 | 0.266 | 1.295 | - | 0.03 | 0.04 |
| 22 | 20.9 | 0.237 | 1.355 | - | 0.02 | 0.035 |
| 20 | 21.5 | 0.288 | 1.385 | - | 0.03 | 0.03 |
| 11 | 23.1 | 0.482 | 1.264 | 0.041<br>0.038+ | 0.010 | 0.015 |
| 17 | 23.4 | 0.543 | 1.59 | - | 0.03 | 1 |
| 8 | 23.9 | 0.543 | 1.555 | - | 0.02 | 0.025 |
| 7 | 23.9 | 0.299 | 1.39 | - | 0.04 | E |
| 4 | 25.7 | 0.299 | 1.345 | - | 0.03 | E |

KEY

+ = regression line constrained through P = 0.01 bar

1 = leaking

E = 'end point' reached, very little strain at end of test

UD = 'undisturbed'

TABLE 30 (continued)

MACMERRY (continued)

| Sample No. | Moisture content, %, w/w | 'VCL' slope g/cm³/unit ln P | 'VCL' intercept g/cm³ | Slope of swelling line g/cm³/unit ln P | Slope of relaxation line, g/cm³/unit ln P at 1 bar | Slope of relaxation line, g/cm³/unit ln P at end test |
|---|---|---|---|---|---|---|
| 9 | 26.1 | 0.276 | 1.360 | - | - | E |
| 5 | 26.2 | 0.237 | 1.290 | - | - | 1 |
| 2 | 26.8 | 0.251 | 1.305 | (0.025) | 0.03 | 1 |
| 1 | 26.8 | 0.299 | 1.374 | - | 0.035 | 1 |
| 6 | 27.3 | 0.299 | 1.345 | - | 0.03 | E |
| 3 | 28.5 | 0.266 | 1.285 | - | - | E |
| | | | Mean | 0.041 (0.004) | 0.024 | 0.035 |
| | | | (s.d.) | 0.038+ (0.004) | (0.009) | (0.08) |

KEY

| | |
|---|---|
| + | = regression line constrained through P = 0.01 bar |
| 1 | = leaking |
| E | = 'end point' reached, very little strain at end of test |
| UD | = 'undisturbed' |

TABLE 30 (continued)

THREIPMUIR

| Sample No. | Moisture content, % w/w | 'VCL' slope g/cm³/unit ln P | 'VCL' intercept g/cm³ | Slope of swelling line g/cm³/unit ln P | Slope of relaxation line, g/cm³/unit ln P | |
|---|---|---|---|---|---|---|
| | | | | | at 1 bar | at end test |
| 11 | 11.7 | 0.246 | 1.325 | - | 0.01 | 1 |
| 14 | 11.8 | 0.237 | 1.264 | 0.037<br>0.034+ | 0.02 | 0.02 |
| 17 | 12.3 | 0.299 | 1.350 | 0.044<br>0.041+ | 0.025 | 0.02 |
| 15 | 13.6 | 0.255 | 1.340 | 0.042<br>0.038+ | 0.0175 | 0.0275 |
| 5 | 14.0 | 0.326 | 1.284 | - | 0.035 | 0.015 |
| 10 | 15.4 | 0.306 | 1.324 | 0.041<br>0.039+ | 0.02 | 0.025 |
| 9 | 15.8 | 0.293 | 1.350 | 0.051<br>0.047+ | 0.02 | 0.03 |
| 16 | 15.8 | 0.255 | 1.398 | 0.059<br>0.055+ | - | 0.035 |
| 1 | 17.5 | 0.312 | 1.330 | - | 0.015 | 0.03 |
| 4 | 19.0 | 0.340 | 1.460 | - | 0.03 | 0.03 |
| 12 | 20.0 | 0.299 | 1.395 | - | 0.02 | 0.01 |
| 2 | 20.6 | 0.312 | 1.375 | - | 0.03 | 0.03 |
| 13 | 20.6 | 0.340 | 1.420 | - | - | 0.015 |
| 19 | 23.3 | 0.319 | 1.478 | - | 0.025 | 1 |
| 7 | 23.3 | 0.340 | 1.420 | - | 0.03 | E |

KEY

+ = regression line constrained through P = 0.01 bar

1 = leaking

E = 'end point' reached, very little strain at end of test

UD = 'undisturbed'

TABLE 30 (continued)

THREIPMUIR ('undisturbed' samples)

| Sample No. | Moisture content, %, w/w | 'VCL' slope g/cm³/unit-lnP | 'VCL' intercept g/cm³ | Slope of swelling line g/cm³/unit-lnP | Slope of relaxation line, g/cm³/unit-lnP at 1 bar | Slope of relaxation line, g/cm³/unit-lnP at end test |
|---|---|---|---|---|---|---|
| LT UD1 | 27.0 | 0.325 | 1.37 | 0.022<br>0.019+ | - | 0.0175 |
| LT UD2 | 26.1 | 0.235 | 1.40 | 0.032<br>0.027+ | - | 0.0175 |
| LT UD3 | 24.1 | 0.214 | 1.37 | 0.026<br>0.024+ | - | 0.01 |
| LT UD4 | 25.6 | 0.220 | 1.44 | 0.027<br>0.024+ | - | 0.0175 |
| | | | Mean Dist. | 0.046<br>0.042+ | 0.023<br>(0.007) | 0.024<br>(0.008) |
| | | | UD (s.d.) | 0.027<br>(0.004)<br>0.023+<br>(0.003) | - | 0.016<br>(0.004) |

KEY

| | |
|---|---|
| + | = regression line constrained through P = 0.01 bar |
| l | = leaking |
| E | = 'end point' reached, very little strain at end of test |
| UD | = 'undisturbed' |

for soil less than approximately 15 per cent w/w. Estimation of a virgin compression line was then made for the stress/strain path above P = 1.0 bar. The apparent virgin compression line could be constructed by geometry, using the relaxation path, as in Fig.5. The slopes and intercepts of the 'VCL's and the moisture content of the soils are recorded in Table 30 for each test. The 'VCL's identified from tests on the 'undisturbed' samples are also recorded in Table 30, as are the swelling slopes and relaxation slopes at one bar and at the end of the tests.

6.3.3 The relationships between the 'VCL' and soil moisture content

Slope and intercept of the 'VCL's estimated in situ are related to field moisture content (w) in Fig.62 for Macmerry and Fig.63 for Threipmuir. Superimposed upon the scatter of individual observations for Macmerry are the mean values for each 2 per cent interval of w, from 15 per cent, and their respective standard deviations, as well as the mean standard error of the regression coefficients. The Macmerry data showed a peaked curvilinear trend between w and 'VCL' slope and a rising, almost linear trend between w and 'VCL' intercept. However, a 't' test upon the values near the peak showed a difference insignificant at $P < 0.05$. Fewer data were available to relate the 'VCL' to soil moisture content for the Threipmuir soil. A peaked trend between w and 'VCL' slope and a rising trend between w and 'VCL' intercept were suggested from the mean values of the standard errors of the regression coefficients, but a more accurate definition of the relationship required more data.

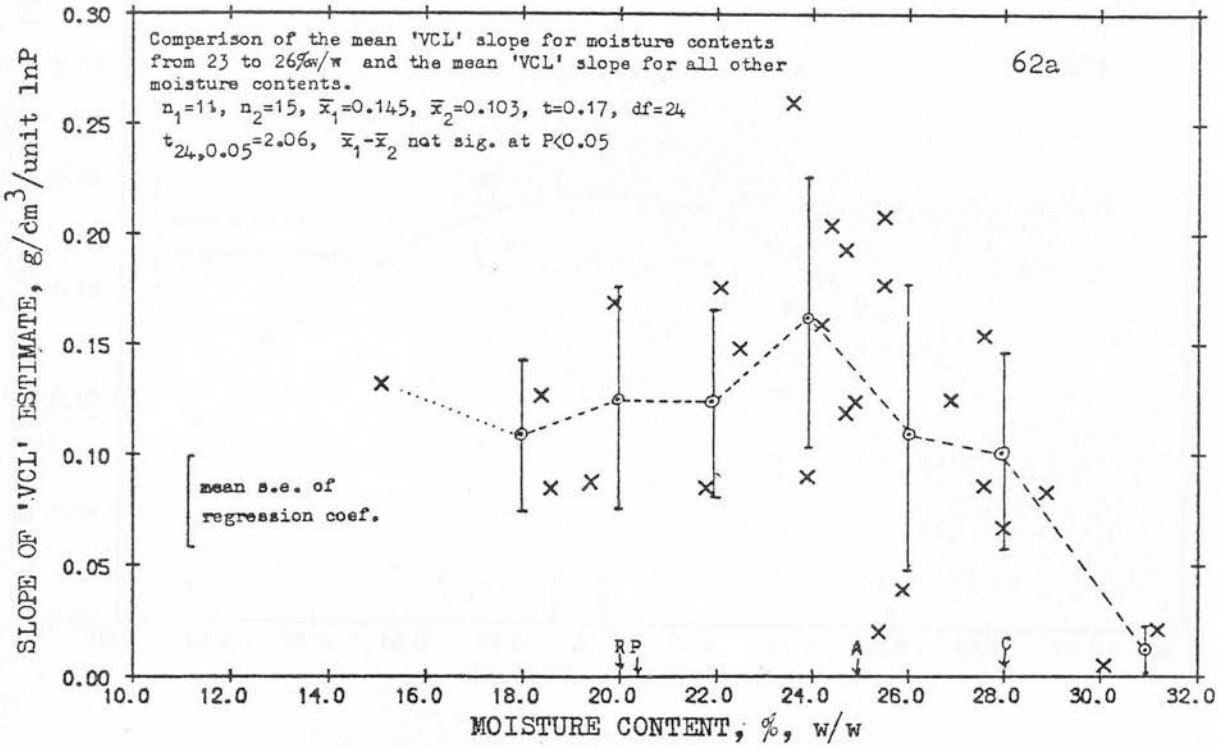


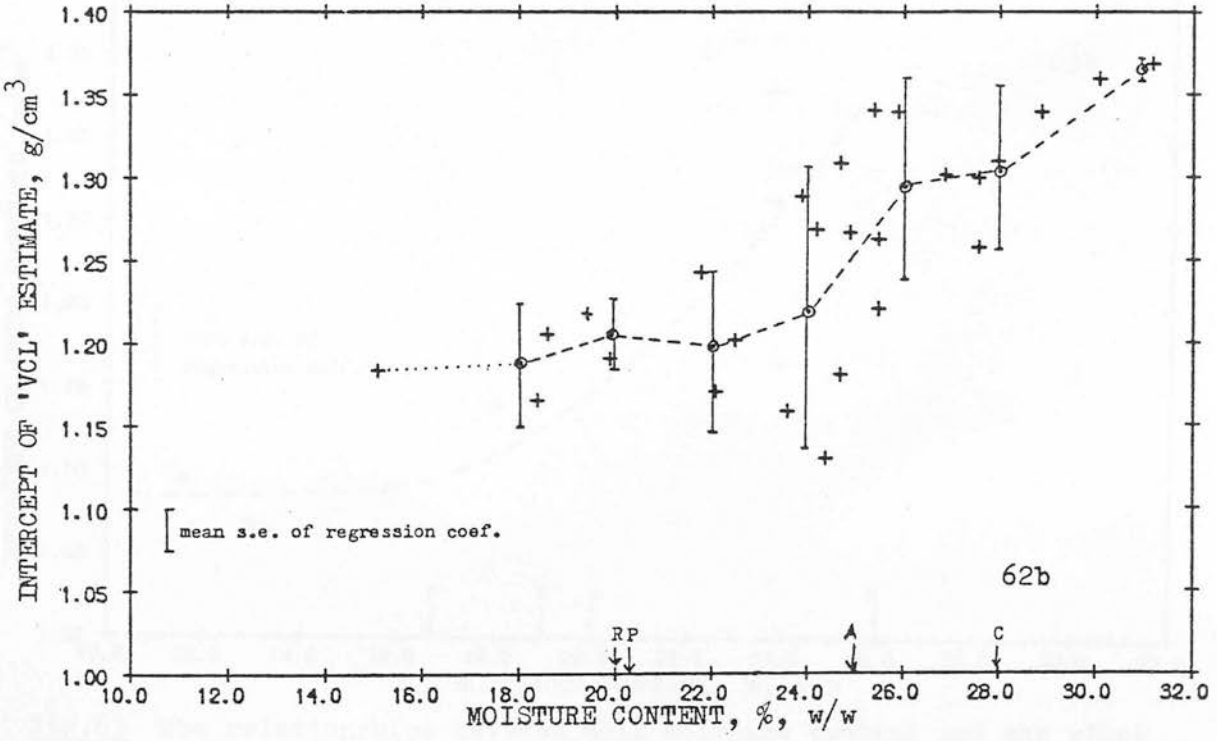


Fig.62 The relationships between soil moisture content and the slope (62a) and the intercept (62b) of the estimates of the apparent virgin compression line from in situ measurements of Macmerry soil. Means and standard deviations for each 2% interval of moisture content are shown as well as the mean standard error from the linear regressions through the clusters in Figs.60 and 61. The various lower plastic limits of the soil are indicated (C = Casagrande method; R = drop-cone method, remoulded soil; A = drop-cone method, aggregates < 1.0 cm diameter). P = Proctor 'optimum' moisture content.

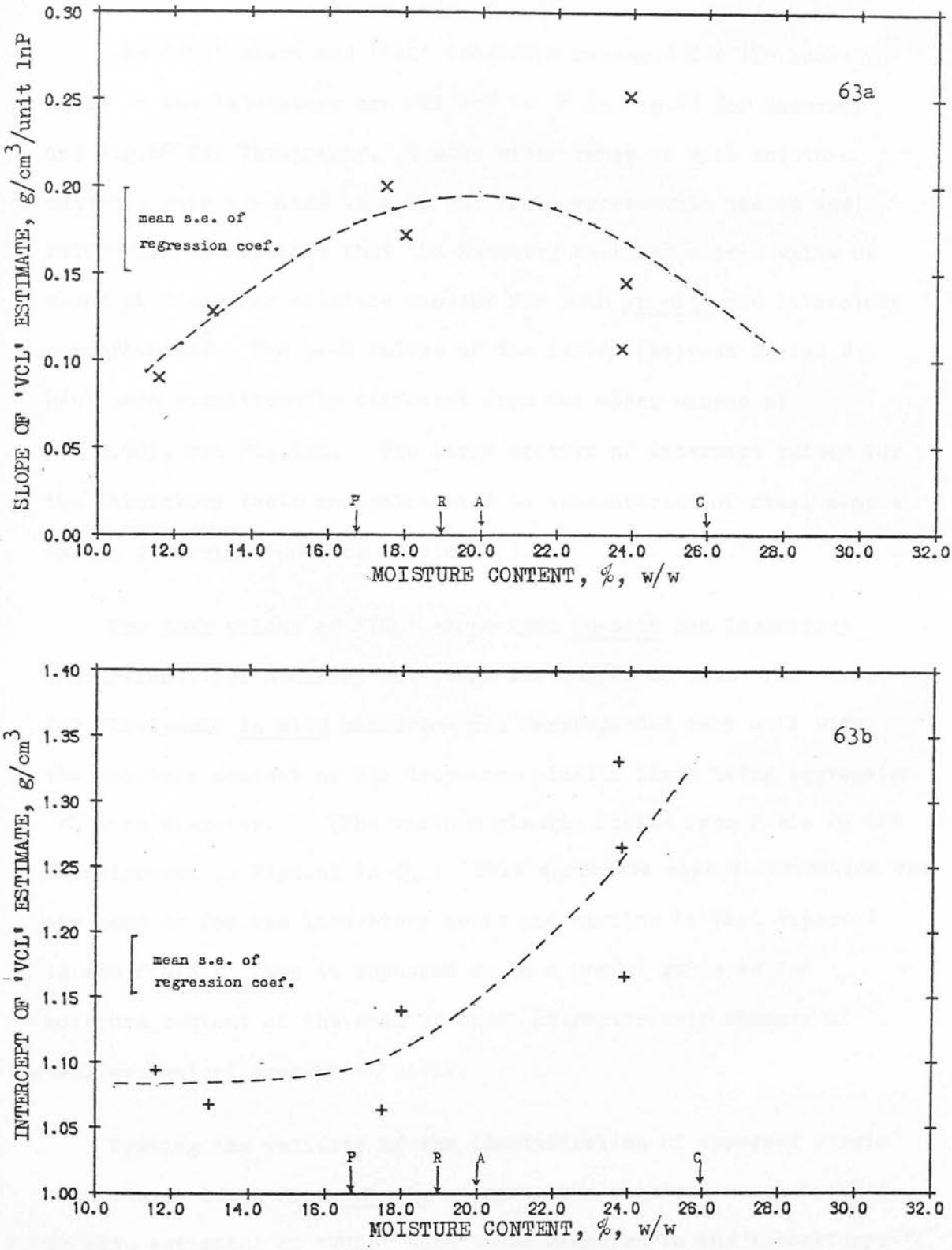


Fig.63 The relationships between soil moisture content and the slope (63a) and the intercept (63b) of the estimates of the apparent virgin compression line ('VCL'), from in situ measurements of Threipmuir soil. 'Best fit' curves fitted by eye between the points are shown as well as the mean standard errors of the linear regressions and the various plastic limits and the Proctor 'optimum' moisture content (as in Fig.62).

The 'VCL' slope and 'VCL' intercept measured for the loose soils in the laboratory are related to **w** in Fig.64 for Macmerry and Fig.65 for Threipmuir. A much wider range of soil moisture contents were examined than in the field experiments and it was interesting to observe that the Macmerry soil had a peak value of slope at a similar moisture content for both in situ and laboratory measurements.[1] The peak values of the latter (between 22 and 24% w/w) were significantly different from the other slopes at $P < 0.001$, see Fig.64a. The large scatter of intercept values for the laboratory tests was attributed to inaccuracies of final sample volume determination (see section 3.9.4).

The peak values of 'VCL' slope from in situ and laboratory measurements for Macmerry soil, and the suggested peak 'VCL' slope for Threipmuir in situ measurements, corresponded very well with the moisture content of the drop-cone plastic limit using aggregates $<$ 1 cm diameter. (The various plastic limits from Table 20 are superimposed on Figs.62 to 65.) This aggregate size distribution was the same as for the laboratory tests and similar to that expected in the field. Thus it appeared to be a useful guide to the moisture content of the soil at which characteristic changes of soil mechanical properties occur.

Testing the validity of the identification of apparent virgin compression lines from in situ measurements required comparison of in situ estimates of 'VCLs' with those measured in the laboratory. A more detailed comparison was made by separating 'VCLs' measured at moisture contents above the drop-cone plastic limit ( $<$ 1 cm agg.diam.) with those below this moisture content. Table 31a

1. No distinct peak was observed for Threipmuir.

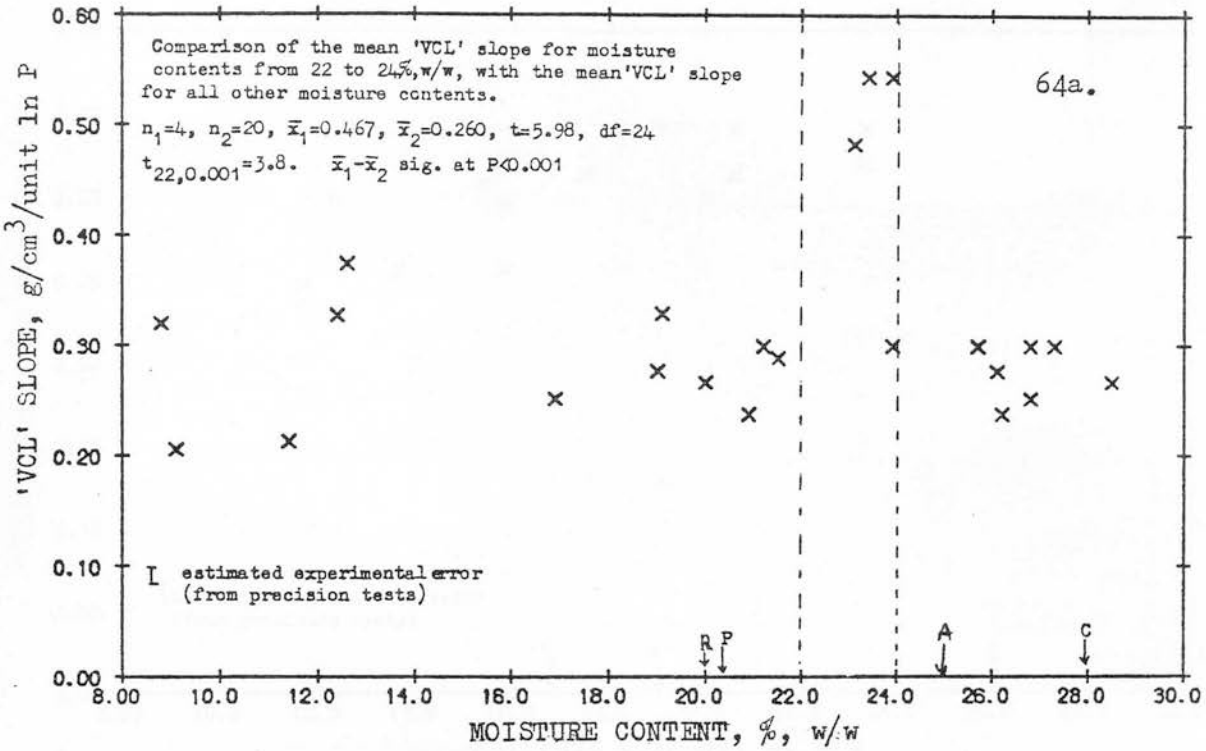


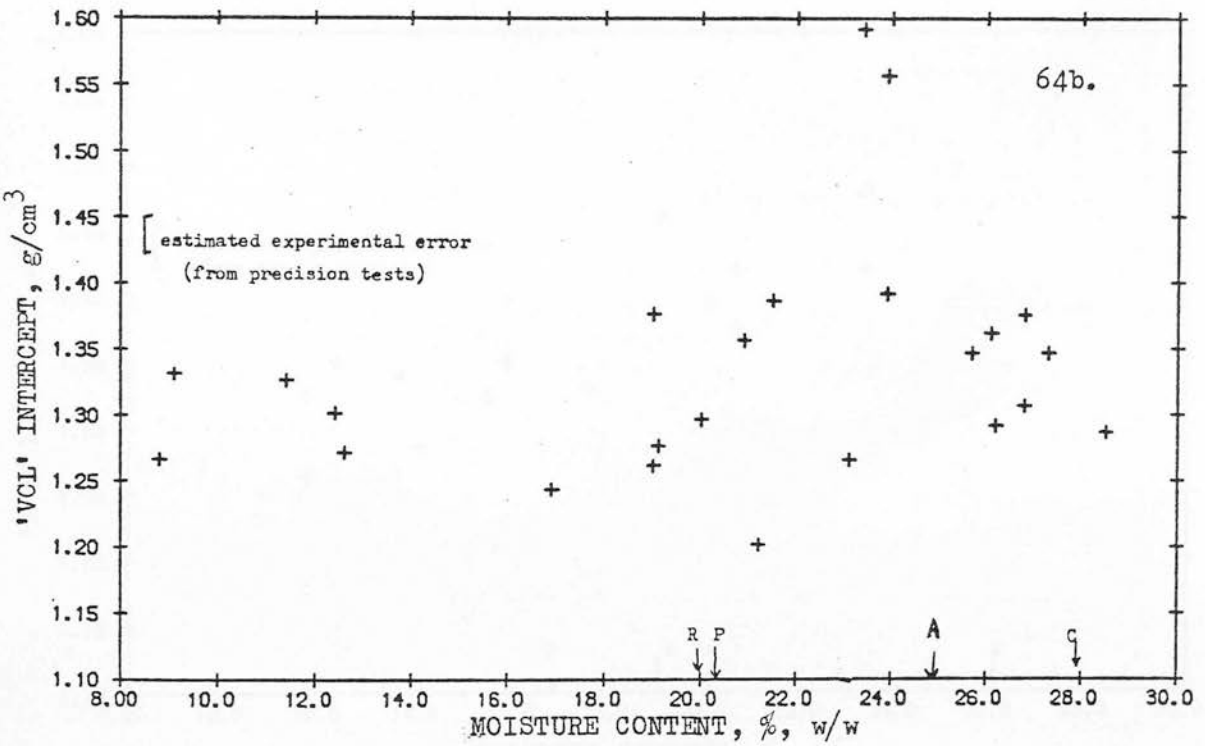


Fig.64 The relationships between soil moisture content and the slope (64a) and intercept (64b) of the apparent virgin compression lines ('VCL') derived from triaxial compression tests upon loose Macmerry soil (aggregates < 1.0 cm diam.) The expected levels of experimental error are indicated as well as the lower plastic limits and the Proctor 'optimum' moisture content (as in Fig.62).

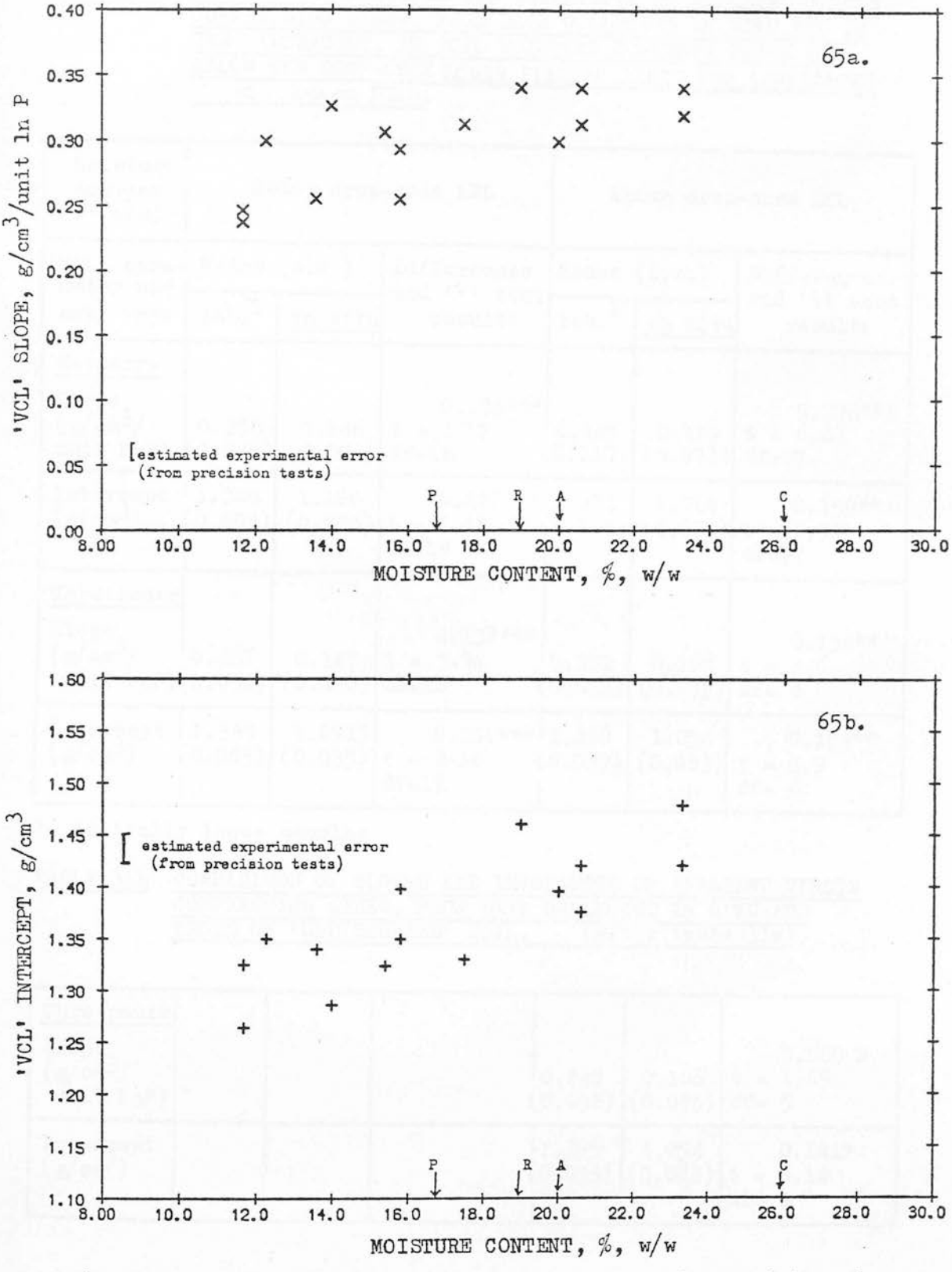


Fig.65 The relationships between soil moisture content and the slope (65a) and intercept (65b) of the apparent virgin compression line ('VCL') derived from triaxial compression tests upon loose Threipmuir soil (aggregates < 1.0 cm diam.) The expected levels of experimental error are indicated as well as the various plastic limits and the Proctor 'optimum' moisture content (as in Fig.62).

TABLE 31a COMPARISON OF SLOPES AND INTERCEPTS OF APPARENT VIRGIN COMPRESSION LINES, FROM DATA COLLECTED IN SITU AND IN THE LABORATORY, AT SOIL MOISTURE CONTENTS ABOVE AND BELOW THE DROP-CONE LOWER PLASTIC LIMIT FOR AGGREGATES < 1.0 cm DIAM.

| Moisture content (% w/w) | Below drop-cone LPL | | | Above drop-cone LPL | | |
|---|---|---|---|---|---|---|
| 'VCL' parameter and soil type | Means (s.e.) lab.[1] | Means (s.e.) in situ | Differences and 't' test results | Means (s.e.) lab.[1] | Means (s.e.) in situ | Differences and 't' test results |
| Macmerry | | | | | | |
| Slope ($g/cm^3$/unit lnP) | 0.280 (0.048) | 0.146 (0.053) | 0.136*** t = 5.72 df=18 | 0.345 (0.117) | 0.119 (0.073) | 0.226*** t = 6.43 df=27 |
| Intercept ($g/cm^3$) | 1.306 (0.054) | 1.186 (0.034) | 0.120*** t = 6.18 df=18 | 1.373 (0.106) | 1.214 (0.279) | 0.159** t = 2.93 df=27 |
| Threipmuir | | | | | | |
| Slope ($g/cm^3$/unit lnP) | 0.287 (0.034) | 0.147 (0.048) | 0.139*** t = 5.96 df=12 | 0.322 (0.018) | 0.168 (0.075) | 0.154** t = 4.6 df= 6 |
| Intercept ($g/cm^3$) | 1.343 (0.065) | 1.0915 (0.035) | 0.251*** t = 8.34 df=12 | 1.418 (0.039) | 1.254 (0.083) | 0.164** t = 3.9 df= 6 |

1. initially loose samples

TABLE 31b COMPARISON OF SLOPES AND INTERCEPTS OF APPARENT VIRGIN COMPRESSION LINES, FROM DATA COLLECTED IN SITU AND TESTS ON 'UNDISTURBED' SOIL. (After table 31a)

| | | | | | | |
|---|---|---|---|---|---|---|
| Threipmuir | | | | | | |
| Slope ($g/cm^3$/unit lnP) | | | | 0.248 (0.052) | 0.168 (0.075) | 0.080 N t = 1.69 df= 5 |
| Intercept ($g/cm^3$) | | | | 1.395 (0.033) | 1.254 (0.083) | 0.141* t = 3.16 df= 5 |

shows the outcome of the analyses. Means of 'VCL' slopes and intercepts from in situ and laboratory data, above or below the drop-cone plastic limit, for the two soils, were compared using the 't' statistic. This revealed differences between laboratory and in situ values significant at least at $P < 0.01$; 'VCL' slopes and intercepts derived from laboratory data being consistently higher than those derived in situ.

The higher intercepts from laboratory data were expected in section 2.3.2, since the viscous response of the soil would attenuate soil deformation beneath a moving wheel. The reduction of slope by viscous responses was not expected. This may indicate a different change of viscous response to changes of initial packing state from that put forward in section 2.3.2, Fig.8a, or more intense shearing processes where low levels of spherical pressure were expected. (This would 'raise' the left part of the cluster shown in Fig.6a, section 2.2.1.)

Validity of the 'VCL' identification from in situ measurements could be examined more closely by comparison of the tests on 'undisturbed' samples in the laboratory with in situ measurements made on the same soil at similar moisture contents; as in Table 31b. There were small and insignificant differences of slope between the in situ and 'undisturbed' measurements, but only a small number of measurements could be compared. The larger intercept from the 'undisturbed' tests may have been caused by the step-wise increases of stresses, unlike those beneath a moving wheel. Thus the comparison of in situ estimations of virgin compression lines, and measurements of the same function in the

laboratory suggest, for the limited range of soil conditions examined, that the two functions are very similar. Therefore the method of identification of apparent virgin compression lines from in situ measurements may have been successful, but the method has not been definitely proven.

### 6.3.4 The relationships between the 'VCL' and soil moisture tension(in situ)

Measurement of soil moisture tension of the Macmerry soil was neither as comprehensive nor as satisfactory as for the Threipmuir soil. The relationships between soil moisture content (w) and the logarithm of soil moisture tension measurements at the same depths and occasions are shown in Figs.66a for Threipmuir and 66b for Macmerry.

These graphs were a reflection of the 'characteristic curve' of the field moisture conditions. The lines may give reliable prediction of soil moisture tension from certain values of w Unfortunately the soil with the most reliable moisture characteristics (Threipmuir) was that with the least sufficient amount of data on the slope and intercept of the 'VCL'. Therefore no attempt was made to relate soil moisture tension to the stress/strain relationships of the soil, apart from a general observation that the peaks of the relationship between soil moisture content and 'VCL' slope for Macmerry and Threipmuir were equivalent to approximately 76[1] and 210 millibar respectively.

---

1. This figure is associated with some doubt, since the in situ soil moisture characteristic from which it was derived (Fig.66b) was subject to much variability of moisture tension readings.

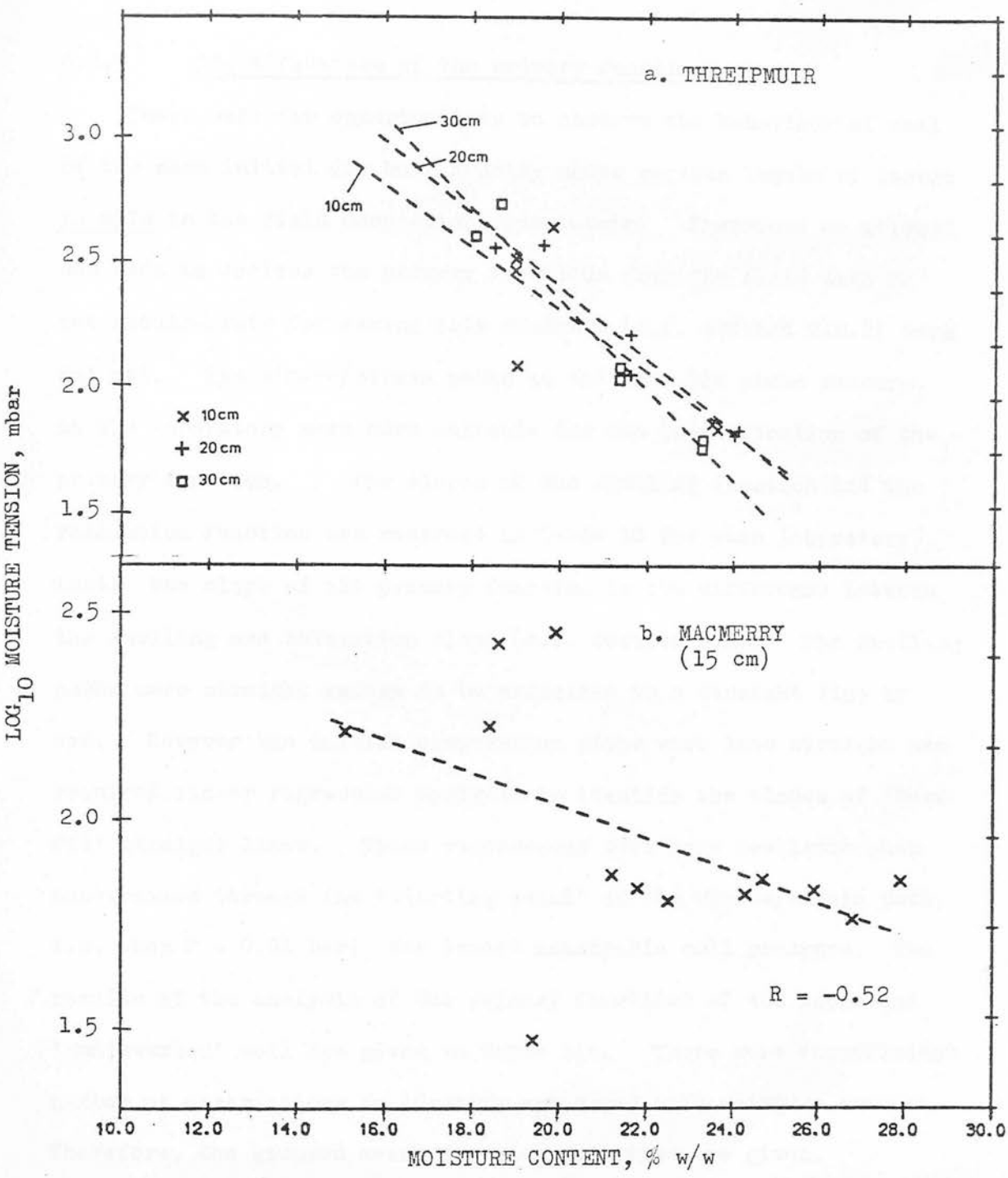


Fig.66 The relationships between in situ measurements of moisture content and moisture tension for each of the soil types.

### 6.3.5 Identification of the primary functions

There were few opportunities to observe the behaviour of soil of the same initial dry bulk density under various levels of stress *in situ* in the field compaction experiments. Therefore no attempt was made to analyse the primary functions from the field data as the requirements for making this analysis (c.f. Section 2.2.2) were not met. The stress/strain paths in the lnP, Dbd plane measured in the laboratory were more suitable for the identification of the primary function. The slopes of the swelling function and the relaxation function are recorded in Table 30 for each laboratory test; the slope of the primary function is the difference between the swelling and relaxation slope (c.f. Section 2.2). The swelling paths were straight enough to be estimated to a straight line by eye. However the initial compression paths were less straight and required linear regression analyses to identify the slopes of 'best fit' straight lines. These regressions were more realistic when constrained through the 'starting point' of the stress/strain path, i.e. when P = 0.01 bar; the lowest measurable cell pressure. The results of the analysis of the primary functions of the loose and 'undisturbed' soil are given in Table 31c. There were insufficient number of observations to identify any trend with moisture content. Therefore, the grouped means for each soil type are given.

TABLE 31c MEAN SLOPES OF SWELLING, RELAXATION AND PRIMARY FUNCTIONS FROM LABORATORY TESTS ON BOTH SOILS, $g/cm^3$/unit lnP

| Soil condition | Function | Macmerry | Threipmuir |
|---|---|---|---|
| disturbed | swelling | 0.038 (0.004) | 0.042 (0.004) |
| | relaxation | 0.0245(0.0085) | 0.0235(0.0075) |
| 'undisturbed' | swelling | - | 0.027 (0.004) |
| | relaxation | - | 0.016 (0.004) |
| disturbed | primary | 0.0135(0.007) | 0.0185(0.005) |
| 'undisturbed' | primary | 0.008 - estimated | 0.011 (0.004) |

N.B: Mean standard deviations in parenthesis

It appears that the primary function of the 'undisturbed' soil had a 60 per cent smaller slope than that of the disturbed soil. This may have been due to the structure of the soil developed during the season or the presence of plant roots, or both.

### 6.3.6 Maximum dry bulk density ($Dbd_{max}$)

It can be seen from Figs.54 to 56 that some of the laboratory tests brought the soil close to a maximum dry bulk density (c.f. section 2.2). However the variability associated with determination of final volume of the samples prevented any clear conclusions about the levels of this maximum dry bulk density for different levels of soil moisture content. The results of the Proctor tests provided another estimate of maximum dry bulk density for different levels of soil moisture content. Although the ranges of these Proctor values were similar to the $Dbd_{max}$ from the triaxial tests (approx.1.3-1.6 $g/cm^3$ for Macmerry), their use as an absolute guide to the maximum soil deformation presented problems. The values of Proctor dry bulk density at any one moisture content are dependent

upon the technique used in the Proctor test, e.g. the weight of the hammer.

## 6.4 Summary of the Analyses of the Results

1. Exponential relationships exist between tyre/soil contact area and mean rut depth of the tyre; a separate relationship is suggested for each combination of wheel load and tyre inflation pressure. Prediction of contact area from these relationships can assist the use of prediction equations for stresses beneath wheels.

2. Quantitative soil strength limits have been suggested for the use of Söhne's equations to predict first principal stresses beneath the experimental wheels, for soils of strength greater than about 10 bar cone resistance. An estimate of third principal stress was suggested from an empirical ratio observed between measurements of $\sigma_1$ and $\sigma_3$ . However, some problems of soil 'arching' could be detected from the measurements of stresses in situ.

3. Graphs relating dry bulk density after wheel passage and estimated maximum spherical pressure at different depths beneath the experimental wheels, could be constructed from the field data. Some estimates of apparent virgin compression lines ('VCL') could be made by linear regressions through characteristic clusters of points on these graphs. Soil shearing effects appeared to obscure such clusters for soil of less than 5 bar cone resistance and less than 1.1 $g/cm^3$ initial dry bulk density.

4. Apparent virgin compression lines could also be measured for disturbed and undisturbed soils tested in the laboratory, as well as slopes of primary functions.

5. Slopes and intercepts of the 'VCLs' measured *in situ* and in the laboratory could be related to soil moisture content. Characteristic peak slopes and changes of intercept occurred near the drop-cone plastic limit for soil of similar aggregate size ( $<$ 1.0 cm diam.)

6. Slopes and intercepts of loose soil tested in the laboratory were consistently and significantly higher than those estimated from *in situ* measurements.

7. 'VCLs' measured from tests on 'undisturbed' soil cores were very similar to 'VCLs' estimated from the same soil at similar moisture content *in situ*. This suggested some validity of the method of estimating 'VCLs' from field measurements before and after the passage of a wheel.

# CHAPTER 7 - CONSTRUCTION OF THE MODEL

Analyses of the experimental results provided information about the stress/strain behaviour of two field soils at various soil strengths and moisture contents. The stress/strain behaviour was described by the primary function, apparent virgin compression line and maximum dry bulk density.[1] These functions were used to construct a model to predict soil compaction based on the mechanical behaviour of soil beneath some agricultural wheels.

Although Finite Element methods appeared most suitable for compaction models (c.f. Section 1.6) their use in this research was restricted because:-

1) Detailed knowledge of the stresses at the tyre/soil interface was absent. Only the general hypotheses of Söhne (1953, 1958) were available. These hypotheses did not seem suitable for Finite Element methods. The stress distributions used applied to a hypothetical circle, of larger diameter than wheel width, and the form of the distribution changed in discrete steps as the soil surface strength changed (see Section 2.1).

2) The Finite Element method divides the soil into discrete elements with a simple geometric shape, e.g. square or triangle. These elements are described in two or three dimensions and form a network of nodes and boundaries between the elements. The use of a Finite Element network in a vertical plane requires a 'Plane Strain' solution of stresses and strains, where the strains in one

1. See Section 2.2

of the three dimensions are considered negigible (Smith, 1971). The use of a three dimensional network is too time-consuming for most computational methods currently available. The two-dimensional plane strain solution is unrealistic for compaction beneath moving wheels, since strain occurs in all three dimensions. Since Söhne's equations use all three dimensions, when calculating stresses they appear more appropriate.

A model, using a column of elements beneath the centre line of the wheel, of similar construction to some Finite Element models, appeared suitable. Confining the model to beneath the centre line was compatible with Söhne's stress prediction equations and examined the soil zones usually most influenced by soil compaction. The use of Söhne's stress prediction equations avoided detailed knowledge of the tyre/soil interface stresses and calculated stresses in three dimensions.

## 7.1 Geometry and input factors

The geometry of the model is shown in Fig.67. Cubical elements of soil, each with original dimensions of approximately 3 cm were used; these dimensions closely corresponded to the scale of measurements often made for field soils. A column of these elements, the centre of each beneath the centre line of the wheel, experienced stresses from a simplified tyre/soil contact zone. The zone was simplified to a flat eliptical surface (c.f. section 2.1). Each element was also described for each soil type by an initial element height, depth of centre below

Fig.67 The geometry used for the model to predict dry bulk density after wheel passage. A transverse section across the centre of the tyre/soil contact area is shown.

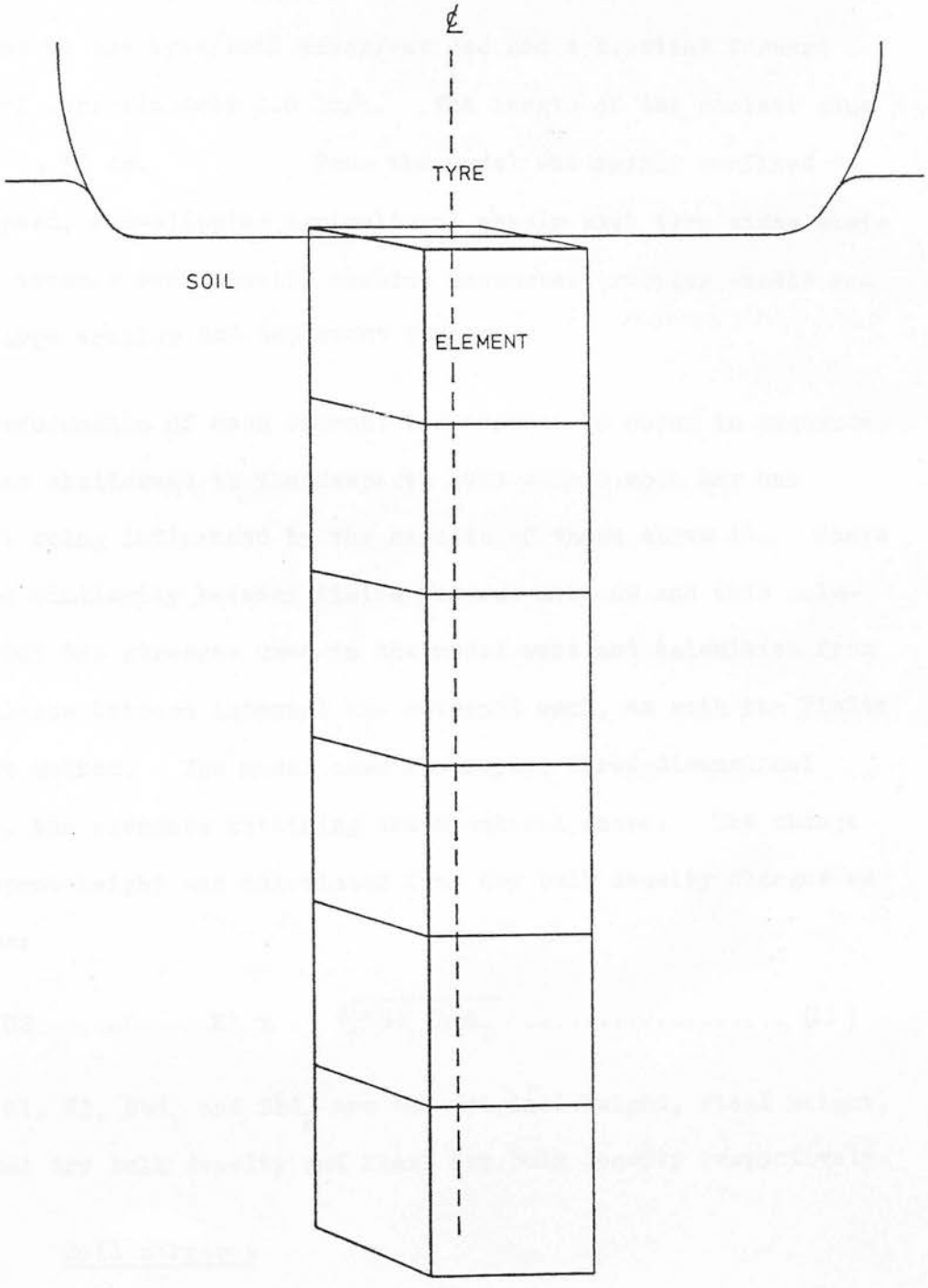

the tyre/soil interface, dry bulk density, cone resistance and gravimetric moisture content.

## 7.2 Wheel dynamics and soil strains

The contact zone used for the model only applied vertical stresses to the tyre/soil interface and had a constant forward speed of approximately 1.0 km/h. The length of the contact zone was 40 to 50 cm. Thus the model was mainly confined to slow speed, non-slipping agricultural wheels with tyre sizes similar to tractor rear wheels, combine harvester traction wheels and some large trailer and implement wheels.

Deformation of each element was assumed to occur in sequence, from the shallowest to the deepest; the stress upon any one element being influenced by the strains of those above it. There is some similarity between Finite Element methods and this solution, but the stresses used in the model were not calculated from the balance between internal and external work, as with the Finite Element method. The model used isotropic, three-dimensional strain, the elements retaining their cubical shape. The change of element height was calculated from dry bulk density changes as follows:

$$H2 = H1 \times \sqrt[3]{Dbd_1/Dbd_2} \quad \ldots\ldots\ldots\ldots\ldots\ldots (11)$$

where H1, H2, $Dbd_1$ and $Dbd_2$ are the original height, final height, original dry bulk density and final dry bulk density respectively.

## 7.3 Soil stresses

Maximum stresses expected beneath the wheel centre line were calculated from Söhne's stress prediction equations (c.f. section

2.1). The tyre/soil contact area could either be predicted from wheel load, tyre inflation pressure and mean rut depth for a '12.4/11-36' tyre (c.f. section 6.1) or put directly into the model. The contact area and wheel load, either estimated or directly measured were used in the appropriate stress prediction equation. The appropriate equation was selected according to the strength of the soil, measured by cone resistance or vane shear strength (c.f. section 6.2). The stress prediction equation gave values of expected maximum first principal stresses beneath the wheel centre line. The corresponding third principal stress was estimated as $\sigma_1/1.19$ (from the empirical field observations) and equivalent spherical pressures (P) and deviatoric stresses (R) were calculated assuming equality of second and third principal stresses (c.f. Section 6.2). The predicted values of stresses were considered appropriate until the volumetric strain of the element exceeded one per cent (after Froelich, 1934). For larger strains the model recalculated the element depth and the maximum expected values of P and R. This often occurred up to ten times for each element before final strain was achieved.

## 7.4 Stress/strain functions

Unless the soil was very loose, (i.e. cone resistance $<$ approx. 5 bar, vane shear strength $<$ approx. 15 kPa)[1] deviatoric stress was assumed to have a negligible effect. Therefore the stress/strain paths of the elements during wheel passage were assumed to be confined to the Dbd-lnP plane (c.f. section 2.2). The primary function, apparent virgin compression line ('VCL') and maximum dry bulk density ($Dbd_{max}$) controlled the progress of the stress/strain path as the value of spherical pressure (P) approached the expected

1. And initial Dbd $<$ 1.1 g/cm$^3$ (sandy loam)

maximum value ($P_{max}$). The slope of the primary function was independent of soil moisture content and chosen according to soil type , soil looseness and abundance of roots (c.f. section 6.3.5 Table 31c). 'Undisturbed' soil, not recently cultivated and loose, with plant roots from a growing crop, was estimated to have a primary function slope 40 per cent smaller than that for a loose, recently cultivated soil with no roots. The slope and intercept of the 'VCL' of the field soils was determined by the soil type and the nearest unit percentage gravimetric soil moisture content (c.f. Chap.6, Figs.62 and 63). $Dbd_{max}$ was assumed to be approximately equal to the Proctor dry bulk density (hammer weight of 2.5 kg) for the nearest unit percentage gravimetric soil moisture content (c.f. Chap.6 , Figs.50a and c). The Proctor dry bulk densities were adjusted by the'Ackroyd' correction (Ackroyd, 1964) to apply the results to all the size fractions of the soil, including those $>$ 1.91 cm ($\frac{3}{4}$") in diameter.

Each element beginning a stress/strain path had an initial value of $P_{max}$ calculated. This determined the expected end of the path. P was increased from the nominal zero (0.01 bar) in small increments of lnP (e.g. 0.05). A new value of Dbd was calculated after each increment, according to the appropriate function. This process halted when either $P_{max}$ was reached or volumetric strain since the calculation of $P_{max}$ became greater than 1 per cent. The latter case required a recalculation of $P_{max}$ before step-wise increase of P could be resumed. The end-point of the stress/strain path was determined by the convergence of P and $P_{max}$. The final values of Dbd, element height and depth could then be calculated. Once the final values for each

had been computed the sum of the vertical strains of the elements provided an estimate of surface sinkage beneath the wheel.

## 7.5 Computer program

A program was developed to assist the operation of the model. A flow-chart of the program, based on the procedures described in the preceding sections, is shown in Fig.68. The program code and operation are described in Appendix 8. The input and output of the program are shown in Table 32.

TABLE 32 INPUT AND OUTPUT FACTORS OF THE COMPUTER PROGRAM FOR THE DRY BULK DENSITY PREDICTION MODEL

| Factor | Input | Output |
|---|---|---|
| Wheel | 1. Wheel load<br>2a. Tyre/soil contact area<br>or<br>2b. Tyre inflation pressure and mean rut depth (for '12.4/11-36' tyre) | (1) Tyre/soil contact area (if input 2b). |
| Soil | 1. Number of elements<br>for each element<br>2. Initial Dbd<br>3. Initial cone resistance<br>4. Initial soil moisture content<br>5. Soil type | For each element:<br>1. Final element height<br>2. " " depth below tyre/soil interface<br>3. Final element Dbd<br>4. Final maximum spherical pressure<br>5. Final maximum deviatoric stress |

The program also included a facility for comparing the predicted Dbd values with any observed Dbd values at the same depth (by interpolation of the observed Dbd profile) and calculating a standard deviation between predicted values ($Dbd_p$) and observed values ($Dbd_o$):

Standard deviation of prediction for n elements (s.d.p.) $= \left[ \frac{\sum \left( Dbd_p - Dbd_o \right)^2}{n} \right]^{\frac{1}{2}}$

Fig.68 The flow chart of the computer program used to operate the model for predicting dry bulk density after wheel passage. The names of the program variables are shown in parentheses.

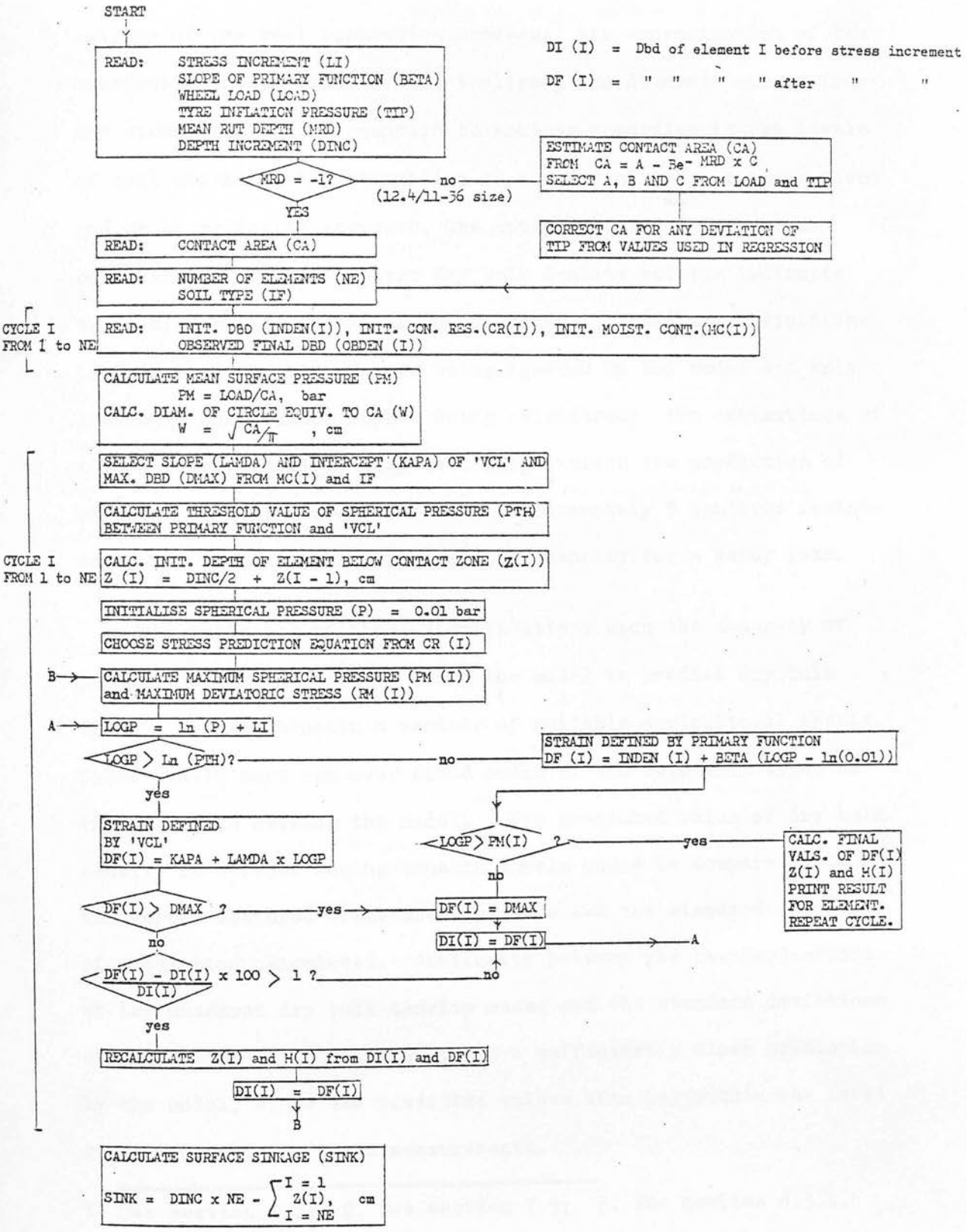

# CHAPTER 8 - TESTING THE MODEL

The bulk density prediction model used a number of simplifications of the real compaction process; the approximation of the tyre/soil contact zone to a flat elipse, the discrete change from one stress prediction equation to another according to the levels of soil strength, the assumption of a constant ratio between first and third principal stresses, the approximation of maximum dry bulk density[1] to the Proctor dry bulk density and the isotropic three-dimensional strain of the elements. These simplifications lead to soil shearing forces being ignored by the model and only isotropic compression forces being considered; the estimations of soil stresses in situ[3] suggested this limited the prediction of stresses to soils of greater than approximately 5 bar cone resistance, and greater than 1.1 $g/cm^3$ bulk density for a sandy loam.

The influence of these simplfications upon the accuracy of prediction was assessed by using the model to predict dry bulk density changes beneath a variety of suitable agricultural wheels. These wheels were run over field soils of the same soil types as those used to develop the model. The predicted value of dry bulk density at various depths beneath wheels could be compared with the values measured after wheel passage and the standard deviation of prediction[2] calculated. Similarity between the standard errors of the measured dry bulk density means and the standard deviations of prediction was considered to be a sufficiently close prediction by the model, since the predicted values then lay within the level of accuracy of the field measurements.

---

1. See section 2.2; 2. See section 7.5; 3. See section 6.3.1.

8.1 SIAE, Section 7, October 1977 (Macmerry soil)

The conduct of the experiment has been described previously (section 4.5.1). The measurement of initial cone resistance and moisture content of the soil and mean rut depths are shown in Table 33. This data, with information about wheel load and tyre inflation pressure, provided the input for the model for each wheel treatment. Initial Dbd, observed final Dbd and predicted Dbd profiles are shown in Figs.69a and 69b for wheel treatments W3 and W4 respectively. The unexpected measured bulk density decreases after wheel passage were attributed to problems of access hole preparation. Two different spike diameters were used (2.4 cm for initial measurements, 2.1 cm for final measurements). The stronger soil encountered during the final measurements made this necessary due to insufficient penetration by the wider spikes.

The predicted final Dbd profile for treatment W4 had a standard deviation of prediction of 0.059 $g/cm^3$ and underestimated observed values between 3 and 15 cm while overestimating below 27 cm. The standard error of the means of the field measurements of dry bulk density was approximately 0.04 $g/cm^3$, almost 60 per cent of the standard error of prediction.

The doubtful validity of the field measurements for the Section 7 model test was further reflected in the prediction for wheel treatment W3. The standard deviation of prediction was very high (0.08 $g/cm^3$), but the form of the predicted profile in relation to the initial profile looks similar to profile changes observed by wheels running over strong soils, e.g. section 5.1.1. Fig.45 Thus the observed Dbd profiles are less convin-

TABLE 33 INITIAL SOIL PHYSICAL CONDITIONS AND MEAN RUT DEPTHS. MODEL TEST, SECTION 7, 1977

W = moisture content, CR = cone resistance

| Depth, cm | Wheel Treatment W3 | | W4 | |
|---|---|---|---|---|
| | Init. W, % w/w | Init. CR, bar | Init. W, % w/w | Init. CR, bar |
| 3 | 27.9 | 5.0 | 27.9 | 6.5 |
| 6 | 26.8 | 8.2 | 27.3 | 11.5 |
| 9 | 25.8 | 11.9 | 26.7 | 11.8 |
| 12 | 26.5 | 12.6 | 26.4 | 12.9 |
| 15 | 27.2 | 12.9 | 26.1 | 12.9 |
| 18 | 27.2 | 12.8 | 26.9 | 12.0 |
| 21 | 27.2 | 12.6 | 27.7 | 12.7 |
| 24 | 27.0 | 12.5 | 27.0 | 11.3 |
| 27 | 26.8 | 14.6 | 26.4 | 17.4 |
| 30 | 25.7 | 17.7 | 26.3 | 22.9 |
| 33 | 24.6 | 26.0 | 26.3 | 28.5 |
| 36 | 25.0 | 28.0 | 24.2 | 30.0 |
| 39 | 25.7 | 28.0 | 22.1 | 30.0 |
| Mean rut depth | 1.49 cm | | 1.56 cm | |

TABLE 34 WHEEL DATA AND INITIAL SOIL PHYSICAL CONDITIONS. MODEL TEST, LOWER TERRACE, 1977

| Wheel Treatment: | Conventional, single | Wide-section, dual |
|---|---|---|
| Tyre size: | 12.4/11-36 | 18-22.5 F |
| Wheel load: | 1.86 t | 1.875 t |
| Tyre inflation pressure: | 1.724 bar | 1.724 bar |
| Tyre contact area: | 2 090 $cm^2$ | 4 480 $cm^2$ |

| Depth, cm | Init. Moisture content, % w/w | Init. cone resistance, bar |
|---|---|---|
| 3 | 16.1 | 1.1 |
| 6 | 18.3 | 1.3 |
| 9 | 20.4 | 1.2 |
| 12 | 20.9 | 1.6 |
| 15 | 21.4 | 2.2 |
| 18 | 21.4 | 2.6 |
| 21 | 21.3 | 2.8 |
| 24 | 22.1 | 4.9 |
| 27 | 23.0 | 6.0 |
| 30 | 22.9 | 11.5 |
| 33 | 20.9 | 17.9 |
| 36 | 20.9* | 23.6 |
| 39 | 20.9* | 28.8 |

* estimated

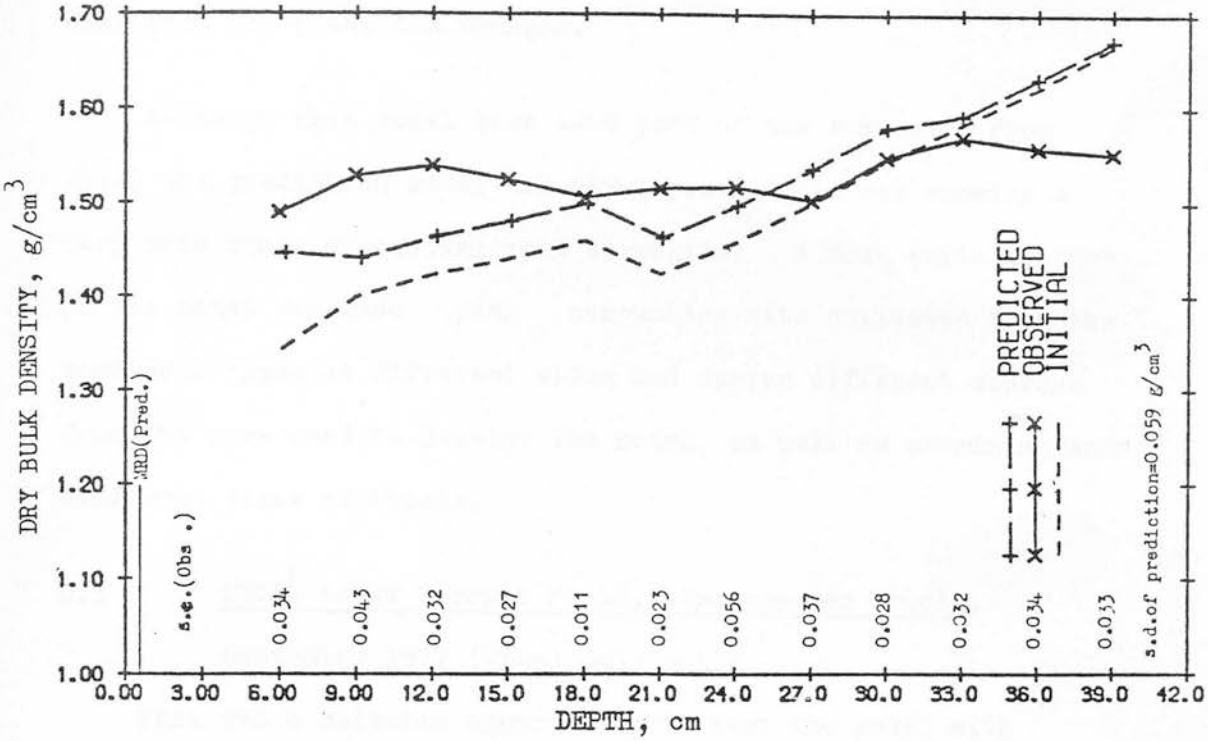


a. Wheel treatment W4.

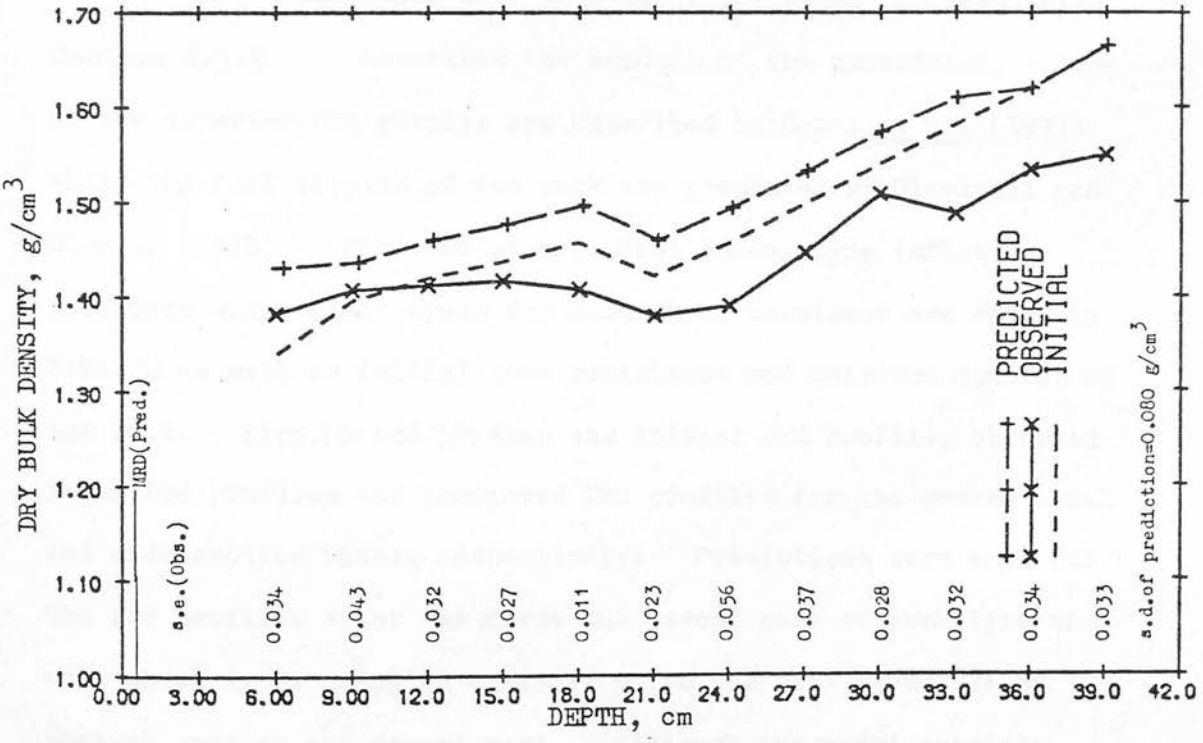


b. Wheel treatment W3.

Fig.69 Model testing, Section 7, SIAE, 1977. Standard errors of the measured means and the predicted mean rut depth (MRD) are shown.

cing than the predicted changes.

Although this model test used part of the same site from which the prediction model was developed, it did not examine a very wide range of initial soil strengths. A more suitable test of the model was made with compaction data collected from the same soil types at different sites and during different seasons from the ones used to develop the model, as well as examining some different sizes of wheels.

## 8.2 ESCA[1], Lower Terrace Field, Limespreader Trials, September 1977 (Threipmuir soil)

This was a suitable opportunity to test the model with Threipmuir soil using looser initial soil conditions and wider section tyres than those used to develop the model for that soil. Section 6.5.2 describes the conduct of the experiment. Some of the experimental results are described by Soane et al. (1977) while the full details of the work are presented by Blackwell and Dickson (1978). The tyre sizes, wheel loads, tyre inflation pressures and contact areas for each wheel treatment are shown in Table 34 as well as initial cone resistance and moisture content of the soil. Figs.70a and 70b show the initial Dbd profile, observed final Dbd profiles and predicted Dbd profiles for the conventional and wide section wheels respectively. Predictions were made for the Dbd profiles after the first and second pass of each tyre of each wheel type, using an estimate of 10 per cent reduction of contact area on the second pass. Although the model predicts higher Dbd values after conventional wheel passage than after passage of the wide section tyres, the values predicted for both

1. East of Scotland College of Agriculture

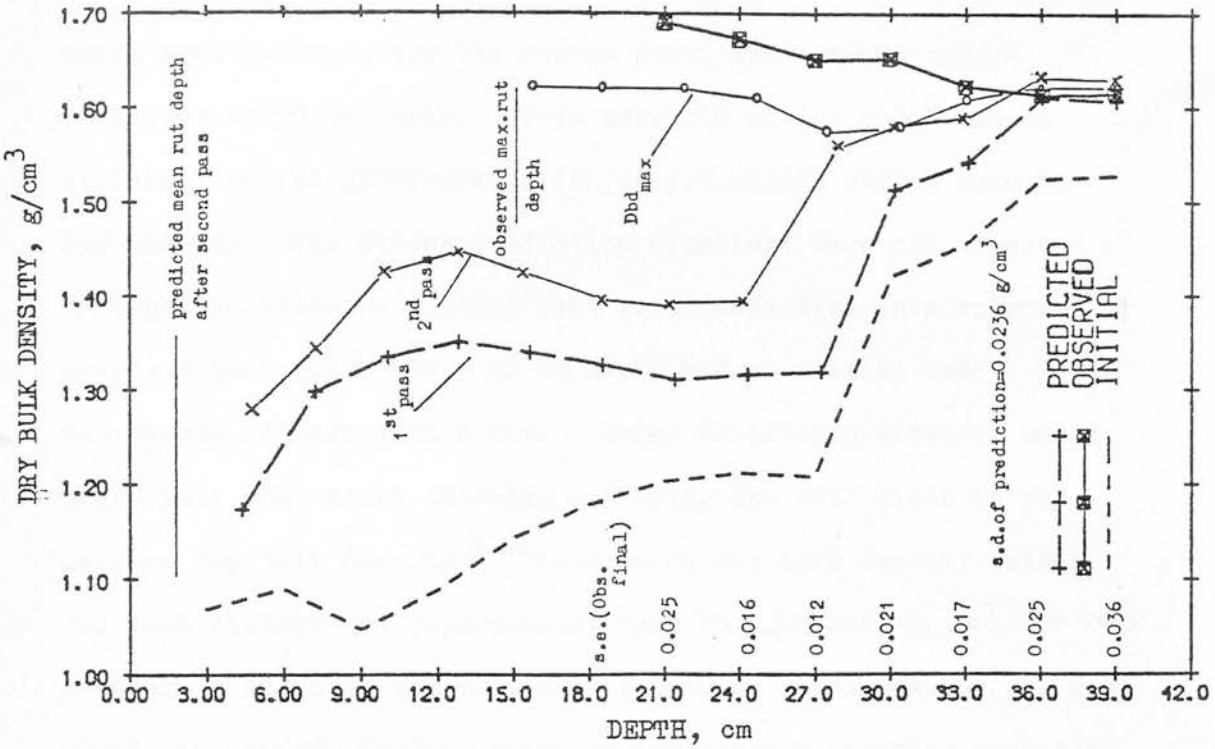


a. Conventional sized tyres, 12.4/11-36.

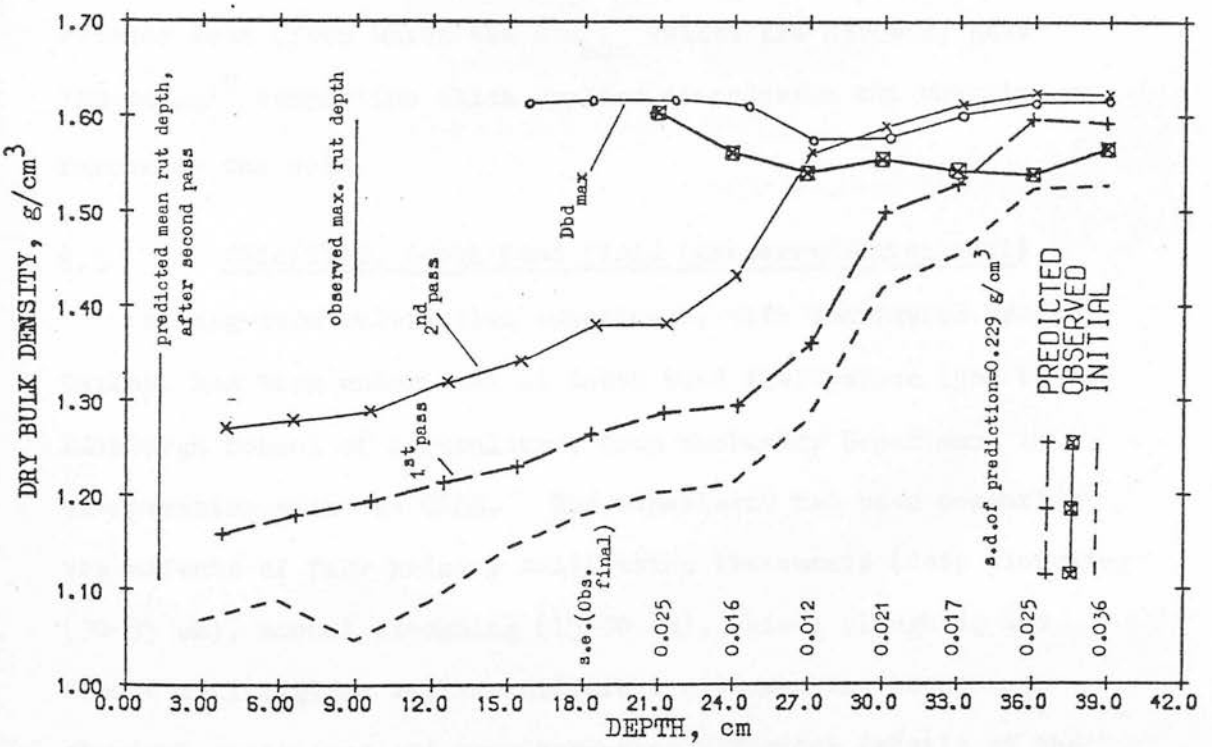


b. Wide section tyres, dual 18.5-20.

Fig.70 Model testing, Lower Terrace field limespreader trials, 1977. Standard errors of the measured final bulk densities and the predicted mean rut depths are shown, as well as the expected levels of maximum dry bulk density ($Dbd_{max}$) from the Proctor curves.

wheel treatments, after the second pass, are extreme under-estimates to 30 cm depth. This poor fit of the model can be explained by the under-prediction of deviatoric stress beneath the wheels. The stress prediction equations were not expected to apply to soils of initial cone resistance less than approximately 5 bar; soil above 30 cm depth had an initial cone resistance of less than 6 bar. Large deviatoric stresses would cause more compactive shearing and bring the soil close to the maximum dry bulk density.[1] The Proctor dry bulk density values[3] for each element are superimposed upon Figs.70a and 70b and are very similar to the observed values of Dbd after wheel passage. This similarity offers further evidence for extreme shearing processes occurring as the wheels ran over the loose, weak soil since the Proctor test (from which the $Dbd_{max}$ values are derived) uses 'kneading'[2] compaction which applies compression and shearing forces to the soil.

## 8.3 ESCA/SIAE, South Road field (Macmerry/Winton soil)

A long-term cultivation experiment, with continuous spring barley, had been undertaken at South Road field since 1968 by Edinburgh School of Agriculture, Crop Husbandry Department in co-operation with the SIAE. The experiment had been comparing the effects of four primary cultivation treatments (deep ploughing (30-35 cm), normal ploughing (15-20 cm), chisel ploughing and direct drilling) as well as different nitrogen levels on soil physical conditions and crop responses. Further details of the experiment, for various periods between 1968 and 1975, are given by Holmes and Lockhart (1970), Soane et al. (1970), Soane (1976) and Pidgeon and Soane (1978). In many seasons, shortly after

1. See section 2.2. 2. See section 1.4.1. 3. With Ackroyd correction.

harvest, some soil physical properties had been measured in and out of the front wheel tracks made by the combine harvester. Seventy-five per cent of the experimental area was occupied by Macmerry soil and on some occasions only the measurements taken on Macmerry soil had been selected. The different cultivation treatments provided a variety of initial dry bulk density profiles which were a good test of the versatility of the model.

In some years, notably 1971, 1973 and 1974, the soil physical measurements at different depths in and out of the combine track included dry bulk density, cone resistance and moisture content using almost the same methods as described in Chap. 3. The 'in' track measurements had been made in the centre-line of the wheel track and the 'out' measurements at a lateral distance of approximately 1 m from an 'in' measurement. Thus this data was compatible with the form of the input of the dry bulk density prediction model. Wheel loads of the combine harvesters were able to be estimated from the manufacturers' specifications and an estimate of the amount of grain and fuel being carried when the wheel tracks were made. Tyre inflation pressures and tyre contact areas were estimated from tyre manufacturers' specifications of rated loads, inflation pressures and ellipse contact areas[1]. The ellipse contact areas corresponded to a mean rut depth of 0.5 cm using the functions for wheel treatment 'W2' derived for a '12.4/11-36' .4PR tyre (Section 6.1); treatment W2 was closest to the rated load and inflation pressure for the size of tyre. This correspondence allowed the curvilinear function relating contact area to mean rut depth to be adopted

---

1. The best fit ellipse enclosing the tyre tread pattern in contact with a rigid surface (Inns and Kilgour, 1978).

for different sizes of tyre according to the ellipse contact area. The intercept of the function was changed to allow the ellipse area to correspond to a mean rut depth of 0.5 cm. The mean rut depth for each wheel track was estimated from field observations.

8.3.1 1971 harvest

An International 8-41 harvester had been used. Wheel loadings were estimated for a half full grain tank[2] and are shown in Table 35, as well as the estimated contact areas and initial soil moisture contents and cone resistances for each cultivation treatment. The soil physical measurements are fully described by Soane (1976). The initial Dbd profile, observed final Dbd profile and results of each prediction are shown in Figs.71a, b, c and d for each cultivation treatment. The standard deviation was very close to the standard error of the means for all but the direct drilling treatment. However, the measurements of very low bulk density changes near the surface and larger changes at depth for the direct drilling treatment appeared highly anomalous.

8.3.2. 1973 harvest

A Ransome 801 combine harvester, modified to carry experimental threshing equipment, was used. Wheel loadings were estimated for a half full grain tank[2] and are shown in Table 36 with the contact areas, initial moisture contents and cone resistances for each cultivation treatment.[1] The initial Dbd profile, observed final Dbd profile and results of each prediction for each main cultivation treatment are shown in Figs.72 a, b, c and d. The prediction for the chisel ploughing and direct drilling treatments was close to the observed values while the deep ploughing

1. Soil physical data is taken from Pidgeon (1975).
2. And half full fuel tank.

TABLE 35 WHEEL DATA AND INITIAL SOIL PHYSICAL CONDITIONS, SOUTH ROAD HARVEST, 1971

Estimated wheel load with half-full grain and fuel tanks - 2.05 t
Tyre size - 16.9/14-25, 6PR: ellipse area at rated load and infl. press. (2.4 t, 1.6 bar) = 1.675 $cm^2$
MRD = mean rut depth, CA = contact area

| Depth, cm | Deep ploughing treatment Est. MRD = 2.0 cm Est. CA = 2 115 $cm^2$ | | Normal ploughing treatment Est. MRD = 2.0 cm Est. CA = 2 115 $cm^2$ | |
|---|---|---|---|---|
| | Init. moisture cont., % w/w | Init. cone res., bar | Init. moisture cont., % w/w | Init. cone res., bar |
| 3 | 25.7 | 7.6 | 27.8 | 7.2 |
| 6 | 25.4 | 10.2 | 27.5 | 8.9 |
| 9 | 25.0 | 12.8 | 27.2 | 8.6 |
| 12 | 24.5 | 13.0 | 27.2 | 11.6 |
| 15 | 23.9 | 13.2 | 27.1 | 12.6 |
| 18 | 24.1 | 13.1 | 26.4 | 15.1 |
| 21 | 24.2 | 12.9 | 25.6 | 17.6 |
| 24 | 24.5 | 16.5 | 24.1 | 21.3 |
| 27 | 24.7 | 20.0 | 22.6 | 25.0 |
| 30 | 24.1 | 22.5 | 21.5 | 26.6 |
| 33 | 23.4 | 25.0 | 20.4 | 27.0 |
| Depth, cm | Chisel ploughing treatment Est. MRD = 1.5 cm Est. CA = 2 015 $cm^2$ | | Direct drilling treatment Est. MRD = 1.0 cm Est. CA = 1 865 $cm^2$ | |
| | Init. moisture cont., % w/w | Init. cone res., bar | Init. moisture cont., % w/w | Init. cone res., bar |
| 3 | 27.4 | 8.0 | 28.4 | 12.0 |
| 6 | 27.2 | 10.7 | 27.2 | 14.2 |
| 9 | 27.0 | 13.4 | 25.9 | 16.4 |
| 12 | 26.4 | 13.2 | 25.9 | 15.7 |
| 15 | 25.8 | 13.0 | 25.8 | 14.9 |
| 18 | 25.4 | 14.7 | 25.0 | 15.7 |
| 21 | 24.9 | 16.5 | 24.8 | 16.4 |
| 24 | 23.4 | 19.2 | 23.2 | 20.7 |
| 27 | 21.8 | 22.0 | 21.6 | 25.0 |
| 30 | 23.0 | 24.5 | 21.2 | 26.0 |
| 33 | 20.9 | 27.0 | 20.8 | 27.0 |

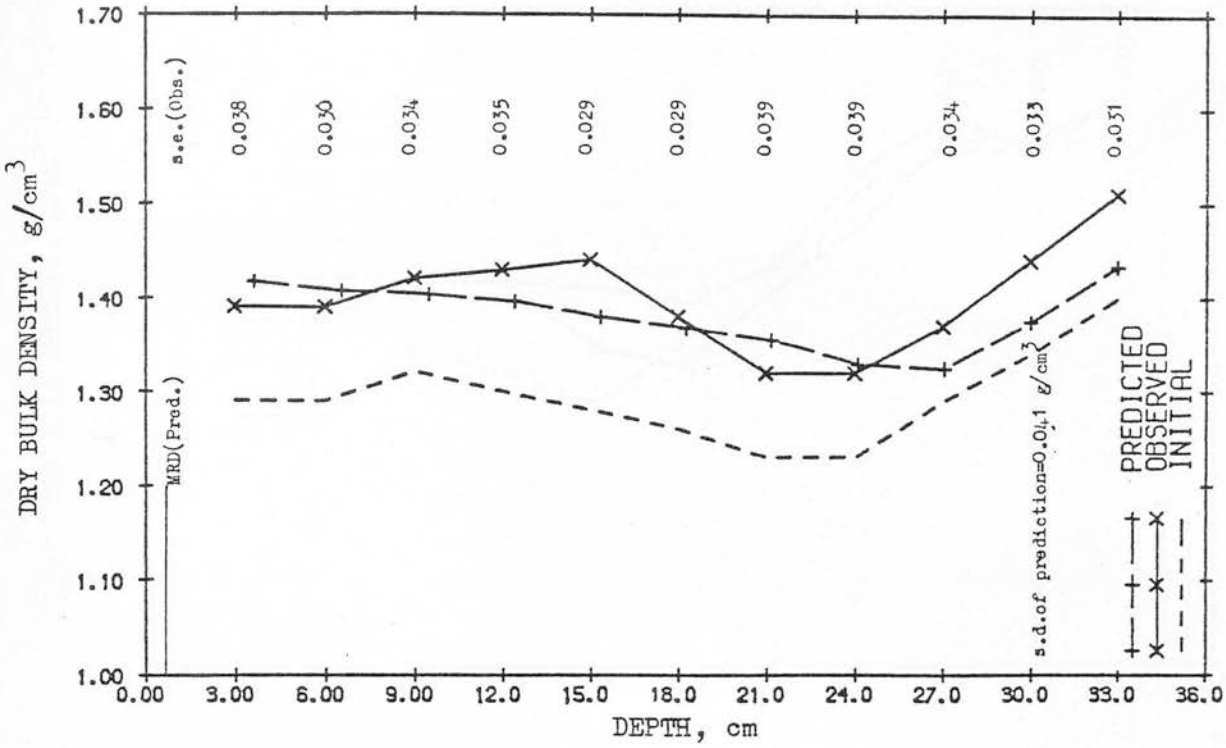


a. Deep ploughing treatment.

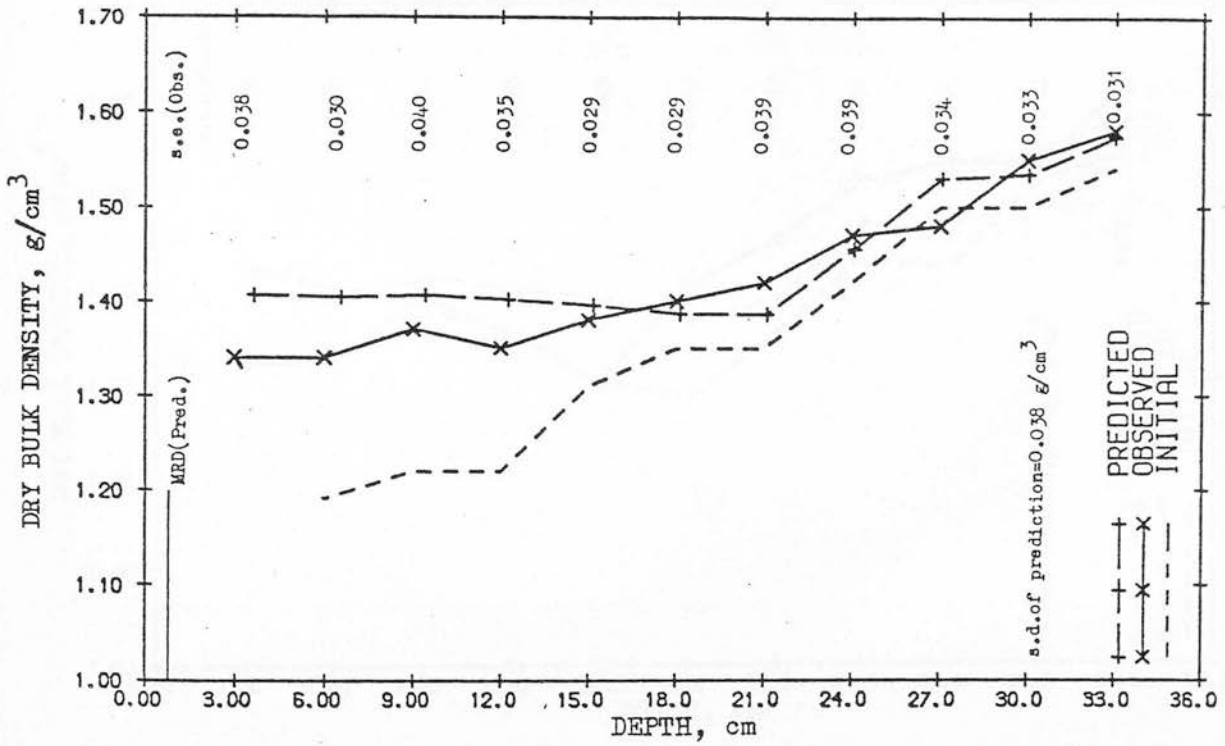


b. Normal ploughing treatment.

Fig.71 Model testing, South Road field, 1971 harvest. Dry bulk density before and after passage of the combine harvester wheel over the soils with different cultivation treatments. Standard errors of the measurements and the predicted mean rut depth (MRD) are shown.

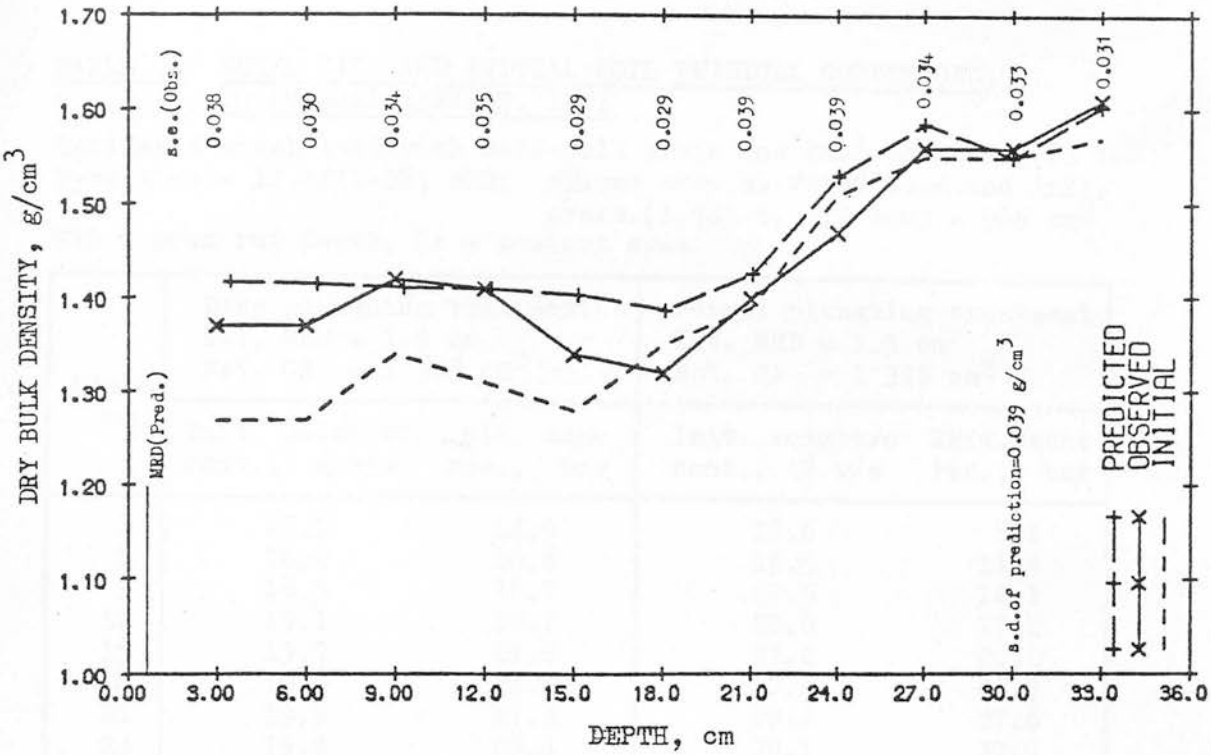


c. Chisel ploughing treatment.

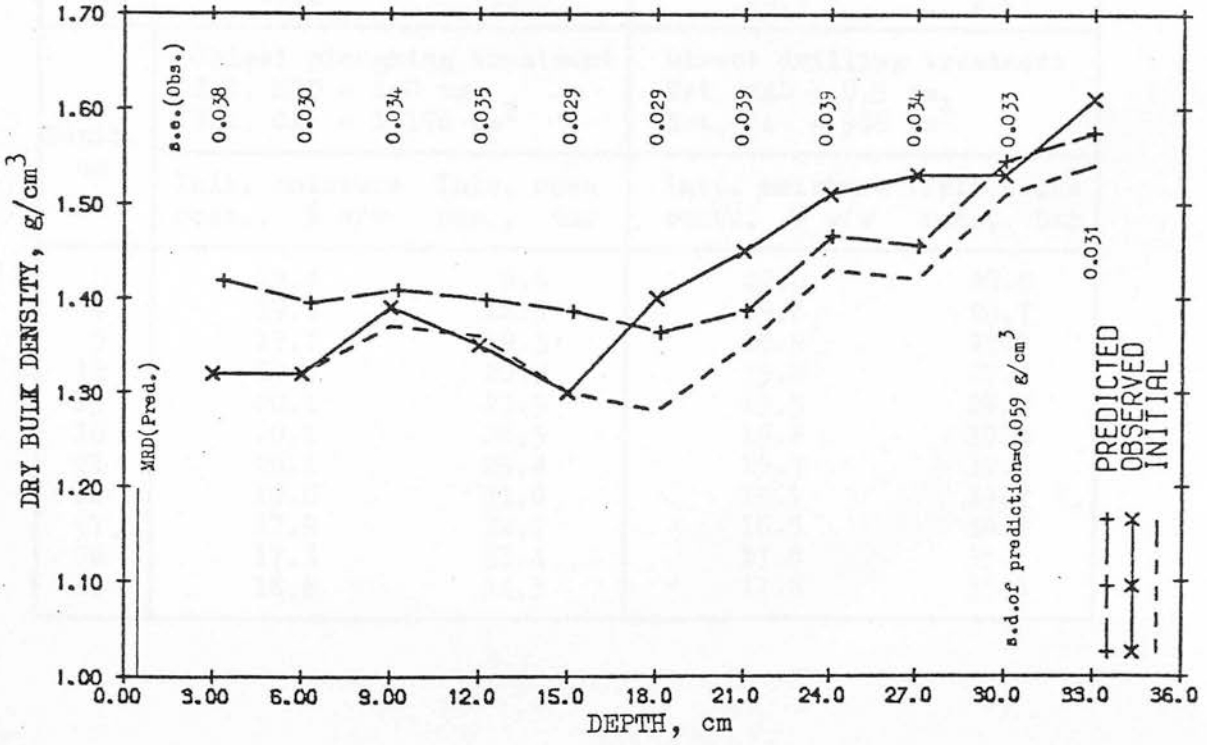


d. Direct drilling treatment.

Fig.71 continued

TABLE 36 WHEEL DATA AND INITIAL SOIL PHYSICAL CONDITIONS, SOUTH ROAD HARVEST, 1973

Estimated wheel load with half-full grain and fuel tanks - 1.83 t
Tyre size - 12.4/11-28, 6PR; ellipse area at rated load and infl. press.(1.785 t, 2.0 bar) = 986 $cm^2$
MRD = mean rut depth, CA = contact area

| Depth, cm | Deep ploughing treatment Est. MRD = 1.5 cm Est. CA = 1 326 $cm^2$ | | Normal ploughing treatment Est. MRD = 1.5 cm Est. CA = 1 326 $cm^2$ | |
|---|---|---|---|---|
| | Init. moisture cont., % w/w | Init. cone res., bar | Init. moisture cont., % w/w | Init. cone res., bar |
| 3 | 17.9 | 14.5 | 18.6 | 8.1 |
| 6 | 18.2 | 16.6 | 19.5 | 11.1 |
| 9 | 18.5 | 18.7 | 20.5 | 14.1 |
| 12 | 19.1 | 20.2 | 20.8 | 17.1 |
| 15 | 19.7 | 21.6 | 21.2 | 20.2 |
| 18 | 19.8 | 24.5 | 20.8 | 23.9 |
| 21 | 19.9 | 27.3 | 20.4 | 27.6 |
| 24 | 19.6 | 28.8 | 20.1 | 30.0 |
| 27 | 19.3 | 30.2 | 19.8 | 32.3 |
| 30 | 19.3 | 31.9 | 19.2 | 33.0 |
| 33 | 19.2 | 33.3 | 18.6 | 33.7 |
| Depth, cm | Chisel ploughing treatment Est. MRD = 1.0 cm, Est. CA = 1 176 $cm^2$ | | Direct drilling treatment Est. MRD = 0.5 cm, Est. CA = 986 $cm^2$ | |
| | Init. moisture cont., % w/w | Init. cone res., bar | Init. moisture cont., % w/w | Init. cone res., bar |
| 3 | 19.4 | 9.6 | 20.6 | 20.5 |
| 6 | 19.6 | 14.5 | 19.8 | 23.7 |
| 9 | 19.7 | 19.3 | 18.9 | 27.0 |
| 12 | 19.9 | 20.9 | 19.2 | 27.6 |
| 15 | 20.1 | 23.5 | 19.5 | 28.2 |
| 18 | 20.1 | 26.5 | 19.6 | 30.4 |
| 21 | 20.1 | 29.4 | 19.7 | 32.5 |
| 24 | 19.0 | 31.0 | 19.1 | 33.7 |
| 27 | 17.9 | 32.7 | 18.5 | 34.9 |
| 30 | 17.3 | 33.4 | 17.8 | 35.3 |
| 33 | 16.6 | 34.3 | 17.2 | 35.6 |

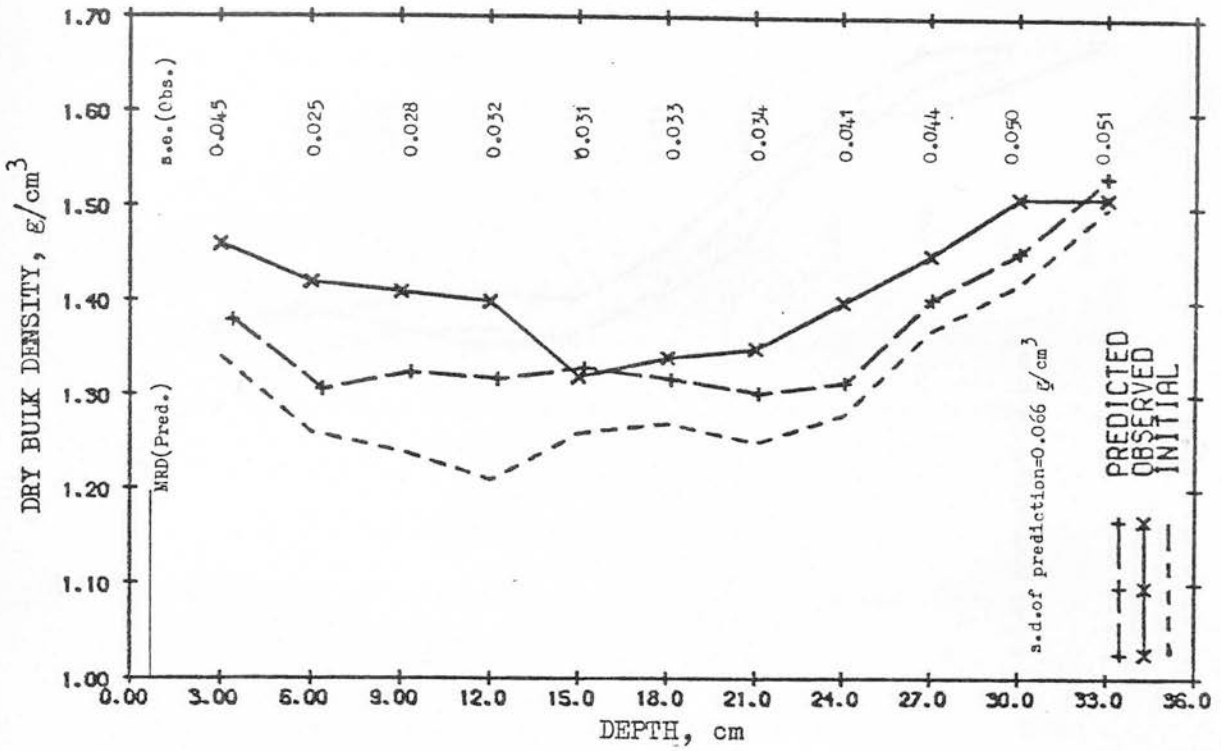


a. Deep ploughing treatment.

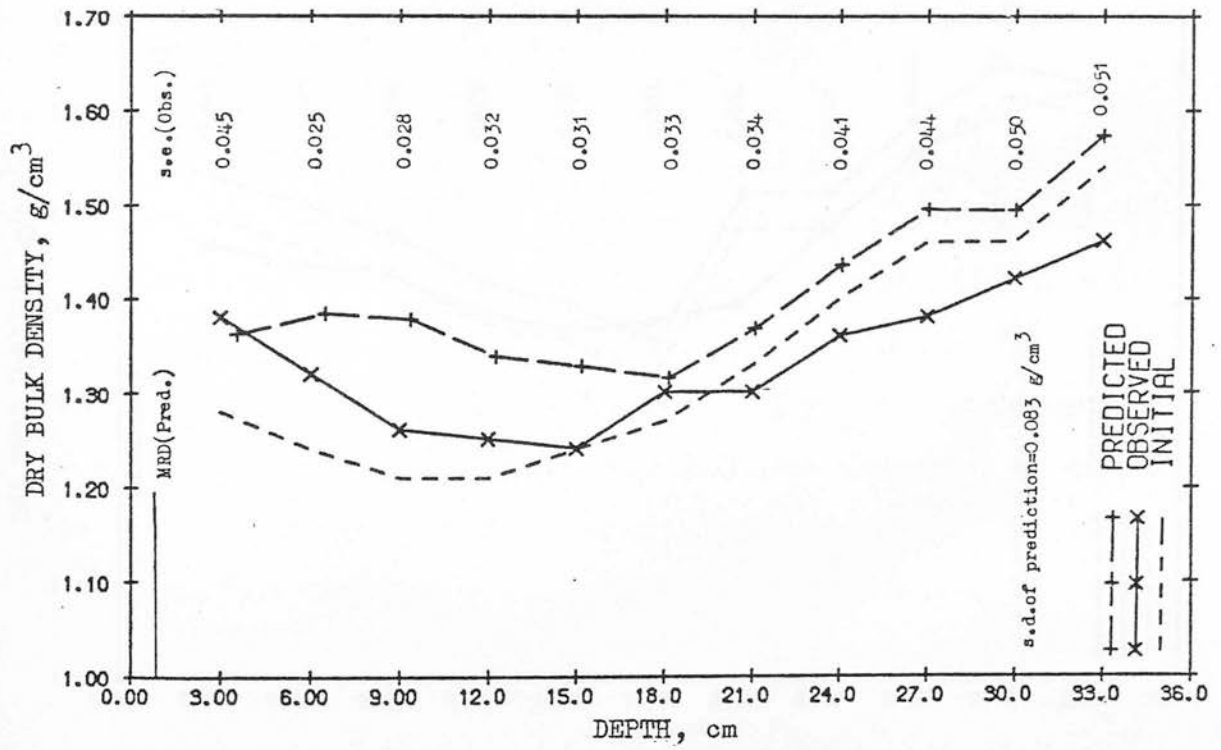


b. Normal ploughing treatment.

Fig.72 Model testing, South Road field, 1973 harvest. Dry bulk density before and after passage of the combine harvester wheel over the soils with different cultivation treatments. Standard errors of the measurements and the predicted mean rut depth (MRD) are shown.

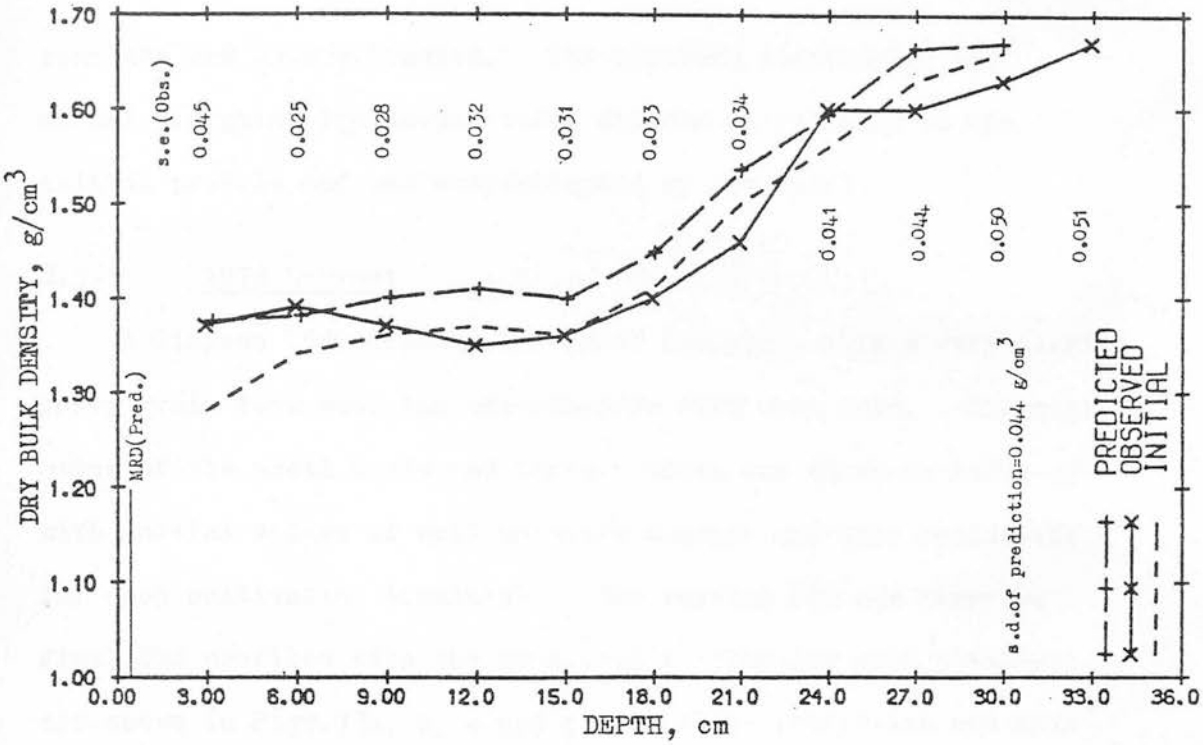


c. Chisel ploughing treatment.

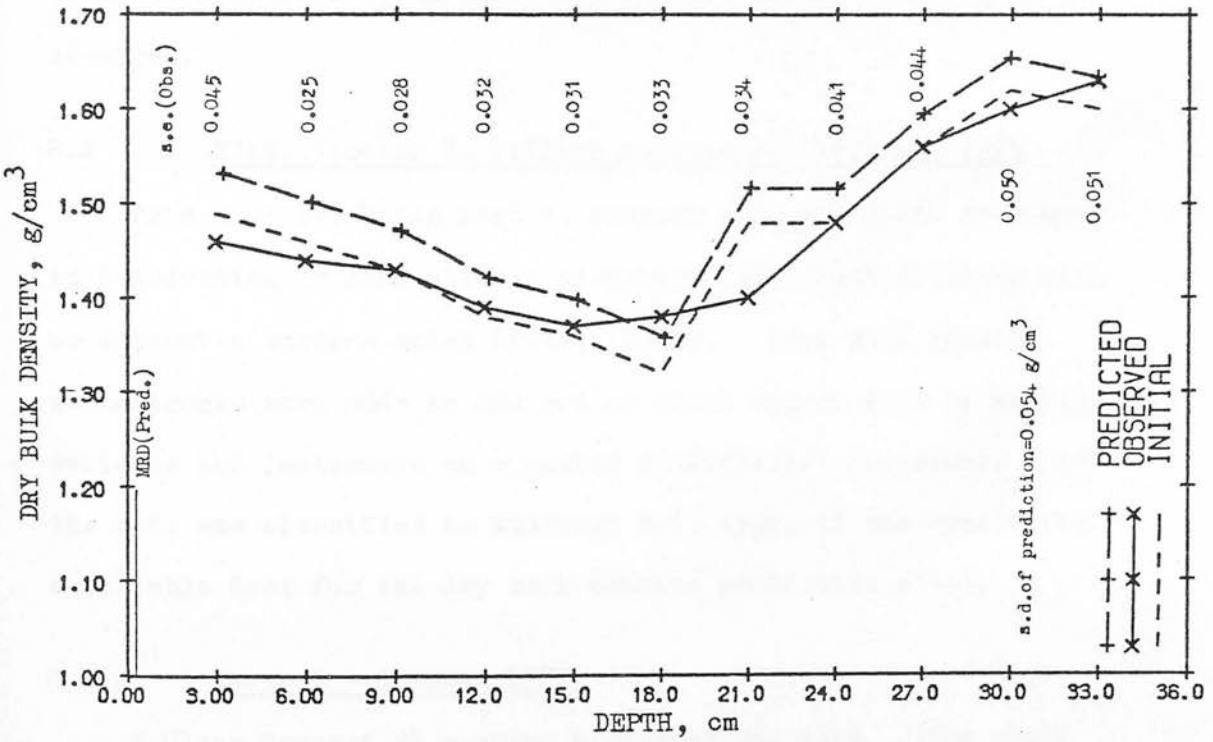


d. Direct drilling treatment.

Fig.72 continued

response was underestimated. The observed response of the normal ploughing treatment looked dubious in relation to the initial profile and was overestimated by the model.

### 8.3.3 1974 harvest

A Clayson 1540 combine harvester was used, with a very nearly empty grain tank when the experimental ruts were made. The estimates of the wheel loads and contact areas are shown in Table 37 with initial values of soil moisture content and cone resistance for each cultivation treatment. The initial Dbd and observed final Dbd profiles with the predicted profile for each treatment are shown in Figs. 73a, b, c and d. Close prediction was made for all but the normal ploughing treatment, where large underestimation at 9 to 15 cm depth and overestimation at 21 to 30 cm occurred.

## 8.4 SIAE, Section 8, Tillage experiment, 1977 and 1978

This site was being used to compare soil and plant responses to cultivation by conventional ploughing and direct drilling with or without a surface mulch (Vila, 1978). Some soil physical measurements were made in and out of wheel tracks made by various vehicles and implements on a number of different occasions. As the soil was classified as Macmerry soil type, it was considered a suitable test for the dry bulk density prediction model.

### 8.4.1 Harvest - October 1977

A Claas Compact 25 combine harvester was used. The grain tank was observed to have filled and emptied a number of times during the harvest. Therefore, a half-full tank was used to estimate the wheel loads. Estimates of contact area and wheel

TABLE 37 WHEEL DATA AND INITIAL SOIL PHYSICAL CONDITIONS FOR MACMERRY SOIL ONLY, SOUTH ROAD HARVEST, 1974

Estimated wheel load with almost empty grain tank* = 2.854 t
Tyre size - 18.4/15-26, ellipse area at rated load and infl. pres. (2.520 t, 2.1 bar) = 1 970 $cm^2$
MRD = mean rut depth, CA = contact area

| Depth, cm | Deep ploughing treatment Est. MRD = 2.0 cm Est. CA = 2 410 $cm^2$ | | Normal ploughing treatment Est. MRD = 2.0 cm Est. CA = 2 410 $cm^2$ | |
|---|---|---|---|---|
| | Init. moisture cont., % w/w | Init. cone res., bar | Init. moisture cont., % w/w | Init. cone res., bar |
| 3 | 25.5 | 4.1 | 28.8 | 3.9 |
| 6 | 25.7 | 5.8 | 27.6 | 5.6 |
| 9 | 25.9 | 7.5 | 27.6 | 7.2 |
| 12 | 25.6 | 9.2 | 26.8 | 8.7 |
| 15 | 25.2 | 10.8 | 26.8 | 10.1 |
| 18 | 25.1 | 12.3 | 26.4 | 12.0 |
| 21 | 25.0 | 13.7 | 25.9 | 13.8 |
| 24 | 24.9 | 15.2 | 24.6 | 15.5 |
| 27 | 24.7 | 16.6 | 23.3 | 17.1 |
| 30 | 23.6 | 20.8 | 22.5 | 21.7 |
| 33 | 23.1 | 24.9 | 21.6 | 26.2 |
| Depth, cm | Chisel ploughing treatment Est. MRD = 1.5 cm Est. CA = 2 310 $cm^2$ | | Direct drilling treatment Est. MRD = 1.0 cm Est. CA = 2 160 $cm^2$ | |
| | Init. moisture cont., % w/w | Init. cone res., bar | Init. moisture cont., % w/w | Init. cone res., bar |
| 3 | 28.4 | 4.8 | 29.2 | 6.4 |
| 6 | 26.9 | 6.8 | 27.1 | 8.9 |
| 9 | 25.4 | 8.7 | 25.0 | 11.3 |
| 12 | 24.8 | 10.3 | 24.9 | 13.7 |
| 15 | 24.3 | 11.9 | 24.8 | 16.0 |
| 18 | 24.3 | 14.1 | 25.0 | 17.6 |
| 21 | 24.2 | 16.3 | 25.1 | 19.1 |
| 24 | 22.5 | 18.1 | 24.6 | 20.5 |
| 27 | 22.6 | 19.9 | 22.8 | 21.9 |
| 30 | 21.6 | 24.2 | 22.0 | 25.7 |
| 33 | 20.6 | 28.5 | 21.2 | 29.5 |

* as observed when experimental ruts made.

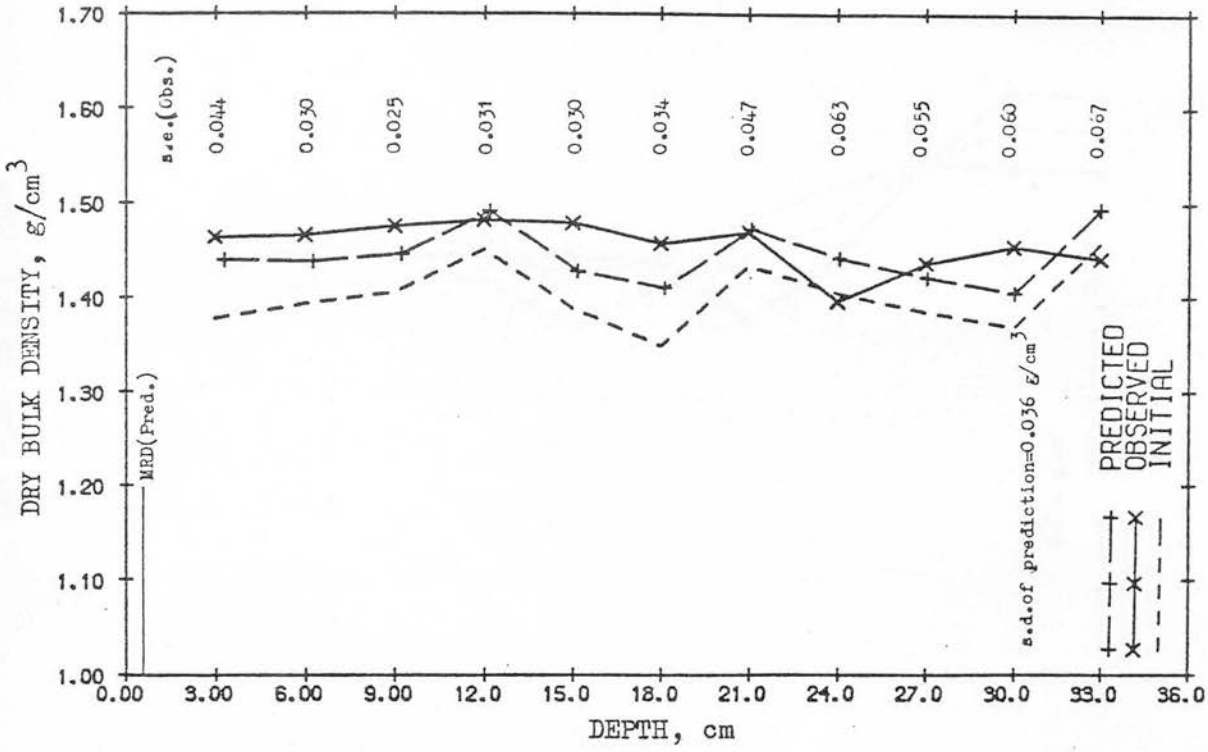


a. Deep ploughing treatment.

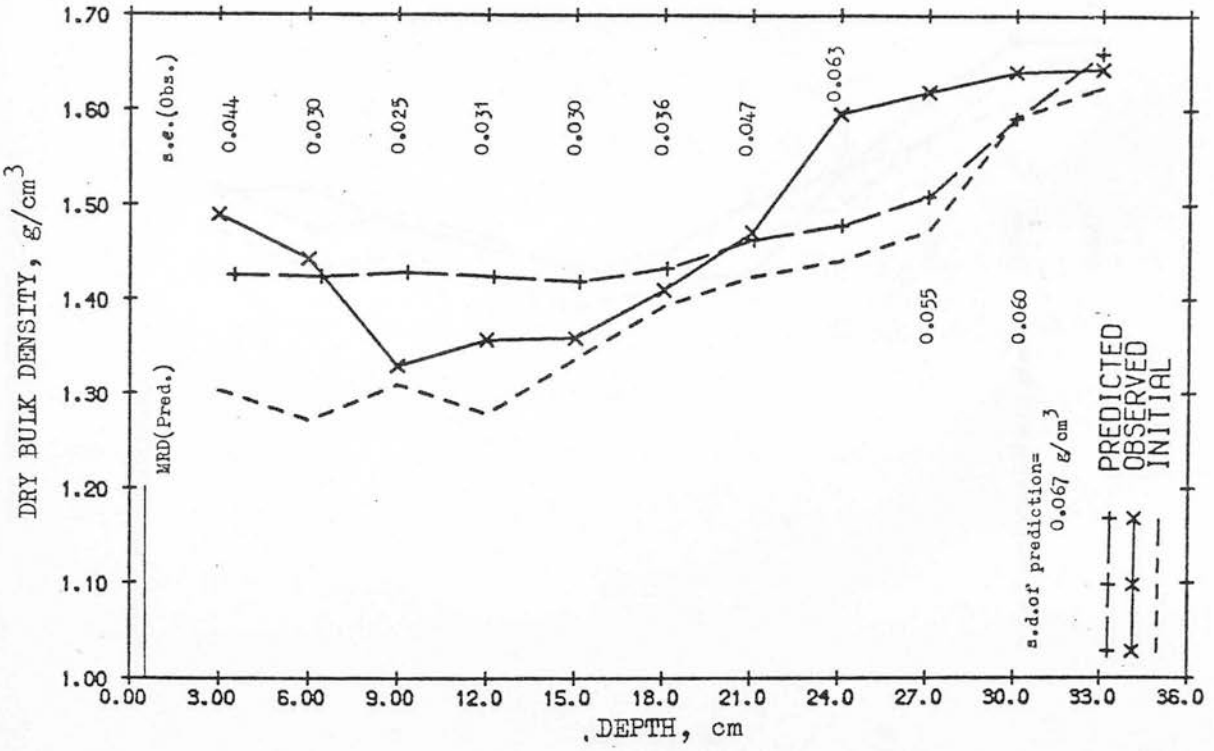


b. Normal ploughing treatment.

Fig.73 Model testing, South Road field, 1974 harvest. Dry bulk density before and after passage of the combine harvester wheel over the soils with different cultivation treatments. Standard errors of the measurements and the predicted mean rut depths (MRD) are shown.

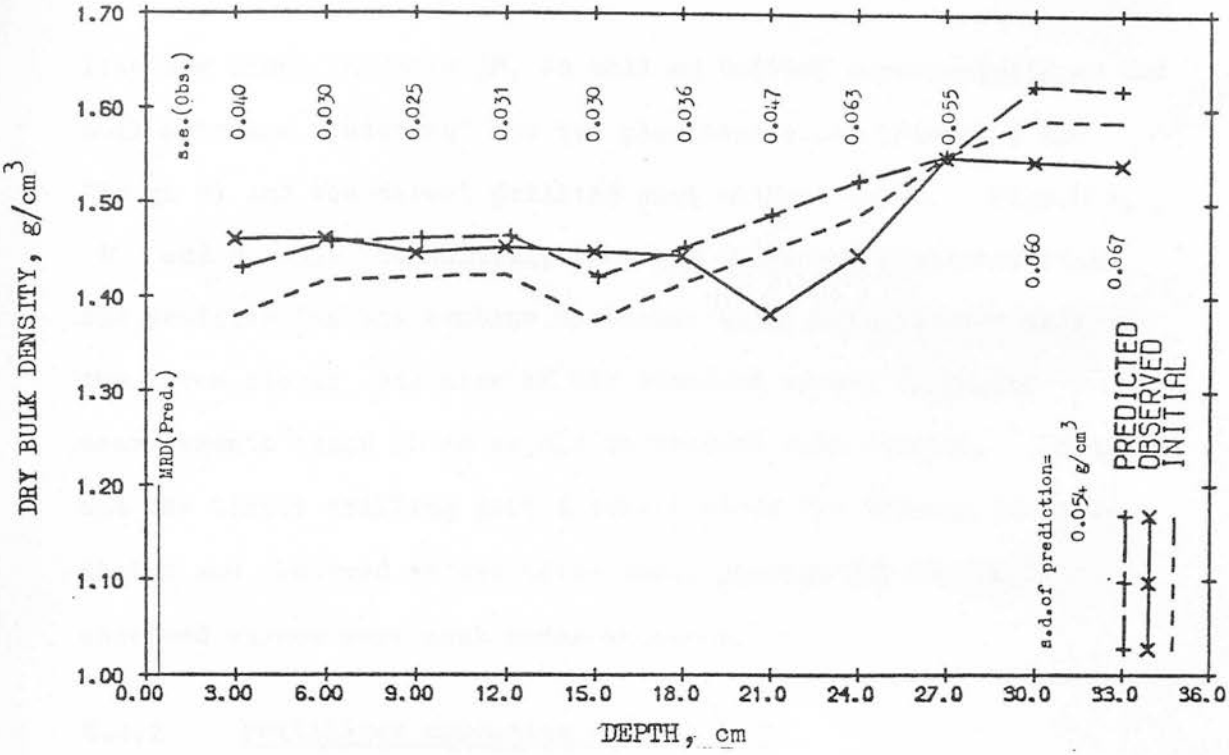


c. Chisel ploughing treatment.

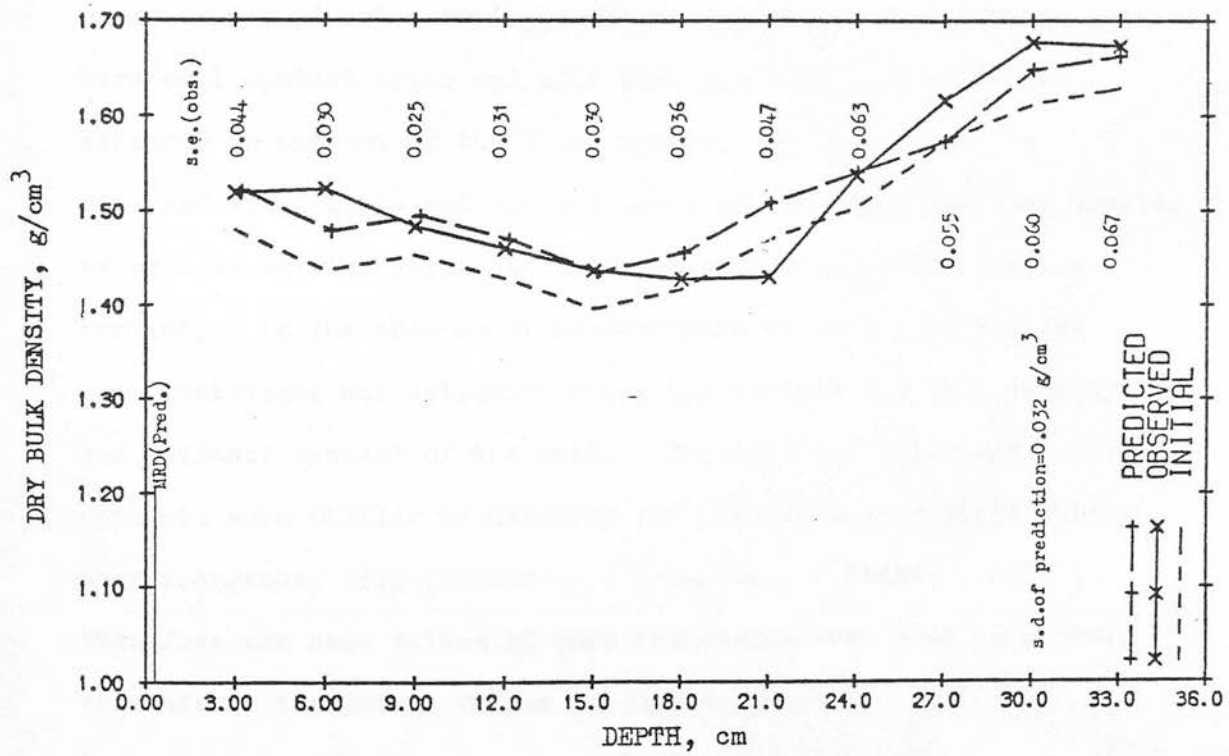


d. Direct drilling treatment.

Fig.73 continued

load are shown in Table 38, as well as initial cone resistances and soil moisture contents of the two ploughing plots (Plough 1 and Plough 2) and the direct drilling plot without mulch. Figs.74 a, b and c show the initial, observed final and predicted final Dbd profiles for the combine harvester wheel running over each of the three plots; the size of the standard errors suggested measurements below 30 cm should be treated with caution. Plough 2 and the direct drilling plot showed a close fit between the predicted and observed values after wheel passage but Plough 1 observed values were much underestimated.

8.4.2 Fertiliser spreading - March 1978

An International Harvester 454 (total weight 1.65 t, 31.7 kW rated engine power) carrying a Vicon centrifugal spreader was used. Tyre/soil contact areas and some soil physical properties were measured in and out of the wheel tracks. Table 39 shows the measured wheel loads and contact areas of the front and rear wheels, as well as initial values of cone resistance and soil moisture content. In the absence of measurements of soil strength the cone resistance was estimated using the initial dry bulk density and moisture content of the soil. The bulk densities and moisture contents were similar to Macmerry soil at South Road field during crop emergence, 1973 (Tables 31, 32 and 34; Pidgeon, 1975); therefore the same values of cone resistance were used as a best estimate of the actual values at Section 8.

Initial Dbd profiles and predicted Dbd profile for the passage of each wheel are shown in Figs.75a and b for the direct drilling plot without mulch and the second ploughing plot. A close fit

TABLE 38 WHEEL DATA AND INITIAL SOIL PHYSICAL CONDITIONS, HARVEST 1977, SECTION 8

Estimated wheel load for half-full grain tank - 1.5 t
Tyre size - 11.5/80-15, 6PR: ellipse area at rated load and infl. press. (1.41 t, 2.0 bar) = 660 $cm^2$

| Depth, cm | Ploughing Plot (Plough 1) Est. MRD = 1.5 cm Est. CA = 975 $cm^2$ | | Ploughing Plot (Plough 2) Est. MRD = 1.5 cm Est. CA = 975 $cm^2$ | | Direct drilling without mulch Est. MRD = 0.5 cm Est. CA = 660 $cm^2$ | |
|---|---|---|---|---|---|---|
| | Initial moisture content, % w/w | Initial cone res., bar | Initial moisture content, % w/w | Initial cone res., bar | Initial moisture content, % w/w | Initial cone res., bar |
| 5 | 21.0 | 9.9 | 21.8 | 10.3 | 26.4 | 15.2 |
| 10 | 28.0 | 16.0 | 21.7 | 14.4 | 22.5 | 22.4 |
| 15 | 21.4 | 19.7 | 22.7 | 13.3 | 22.3 | 20.6 |
| 20 | 23.6 | 15.3 | 22.7 | 17.5 | 22.7 | 20.3 |
| 25 | 21.7 | 33.3 | 23.6 | 32.3 | 23.9 | 32.4 |
| 30 | 21.5 | 48.5 | 23.4 | 39.1 | 24.0 | 42.6 |
| 35 | 21.3 | 46.8 | 21.5 | 46.7 | 21.1 | 48.2 |
| 40 | 19.7 | 48.3 | 21.4 | 42.4 | 20.3 | 50.0 |
| 45 | 19.3 | 48.3[1] | 20.4 | 42.4[1] | 20.6 | 50.0[1] |

TABLE 39 WHEEL DATA AND INITIAL SOIL PHYSICAL CONDITIONS, FERTILISER SPREADING 1978, SECTION 8

Wheel loads: front (f) - 0.41 t, rear (r) - 0.97 t
Tyre sizes: front - 9.1-16, rear - 12.4/11-32

| Depth, cm | Ploughing Plot (Plough 1) contact areas = 1 232 $cm^2$ (f) 1 992 $cm^2$ (r) | | Ploughing Plot (Plough 2) contact areas = as Plough 1 | | Direct drilling without mulch contact areas = 520 $cm^2$ (f) 960 $cm^2$ (r) | |
|---|---|---|---|---|---|---|
| | Initial moisture content, % w/w | Initial cone res., bar | Initial moisture content, % w/w | Initial cone res., bar | Initial moisture content, % w/w | Initial cone res., bar |
| 5 | 16.6 | 2.0 | 11.7 | 2.0 | 23.4 | 6.0 |
| 10 | 21.3 | 5.4 | 19.2 | 5.4 | 23.3 | 11.7 |
| 15 | 22.3 | 7.9 | 21.4 | 7.9 | 23.8 | 13.0 |
| 20 | 25.7 | 9.3[1] | 32.3 | 9.3[1] | 24.0 | 15.4[1] |
| 25 | 26.8 | 11.2 | 19.7 | 11.2 | 24.3 | 18.3 |
| 30 | 26.1 | 13.1 | 24.7 | 13.1 | 24.5 | 21.2 |
| 35 | 23.7 | 15.0 | 27.1 | 15.0 | 24.6 | 30.0 |
| 40 | 21.1 | 20.0 + | 24.1 | 20.0 + | 22.2 | 30.0+ |
| 45 | 21.5 | 20.0 + | 21.7 | 20.0 + | 22.1 | 30.0+ |

1. by estimation. + guessed.

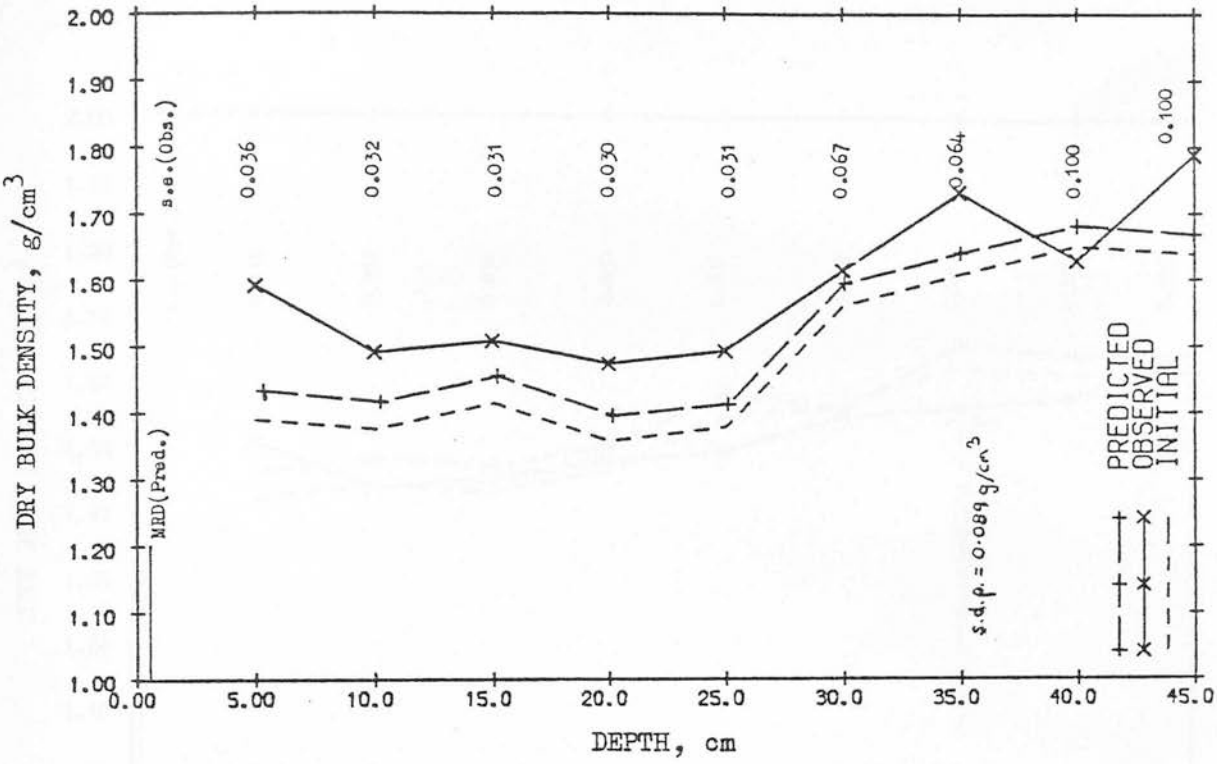


a. Ploughing plot 1.

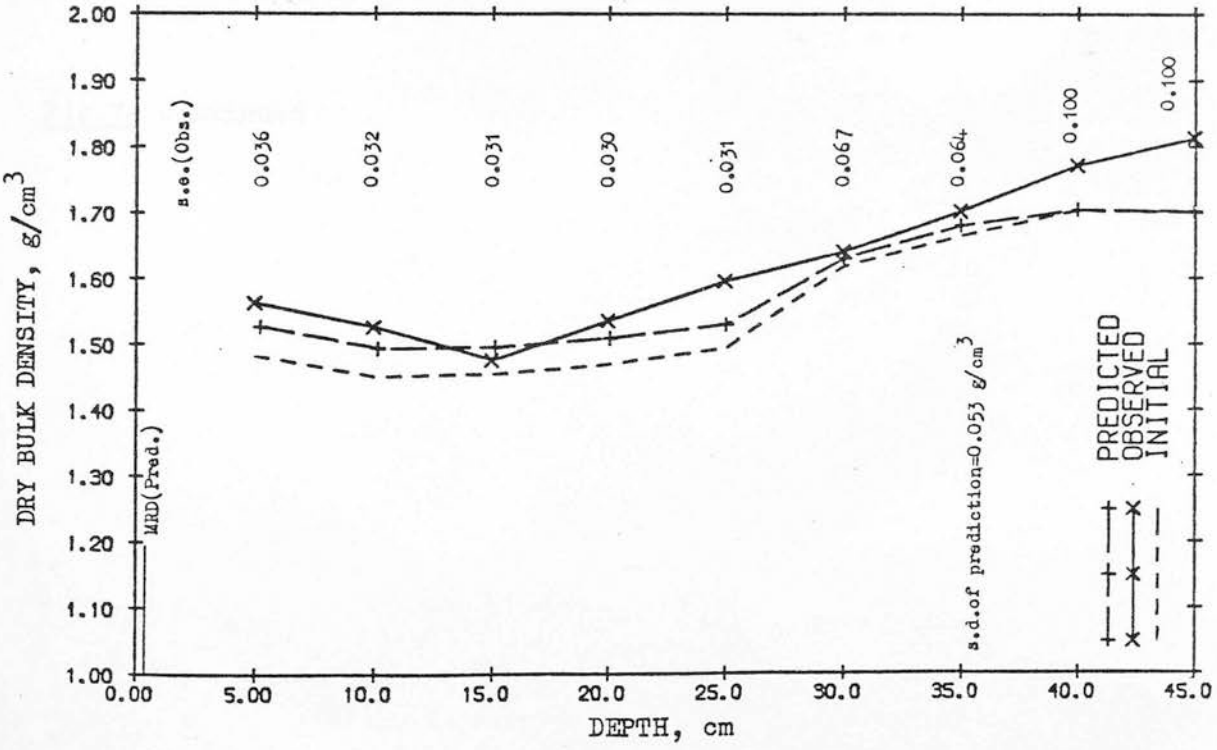


b. Ploughing plot 2.

Fig.74 Model testing, Section 8, SIAE, 1977 harvest. Dry bulk density before and after passage of the combine harvester wheel over the plots with different cultivation treatments. Standard errors of the measurements and the predicted mean rut depths (MRD) are shown.

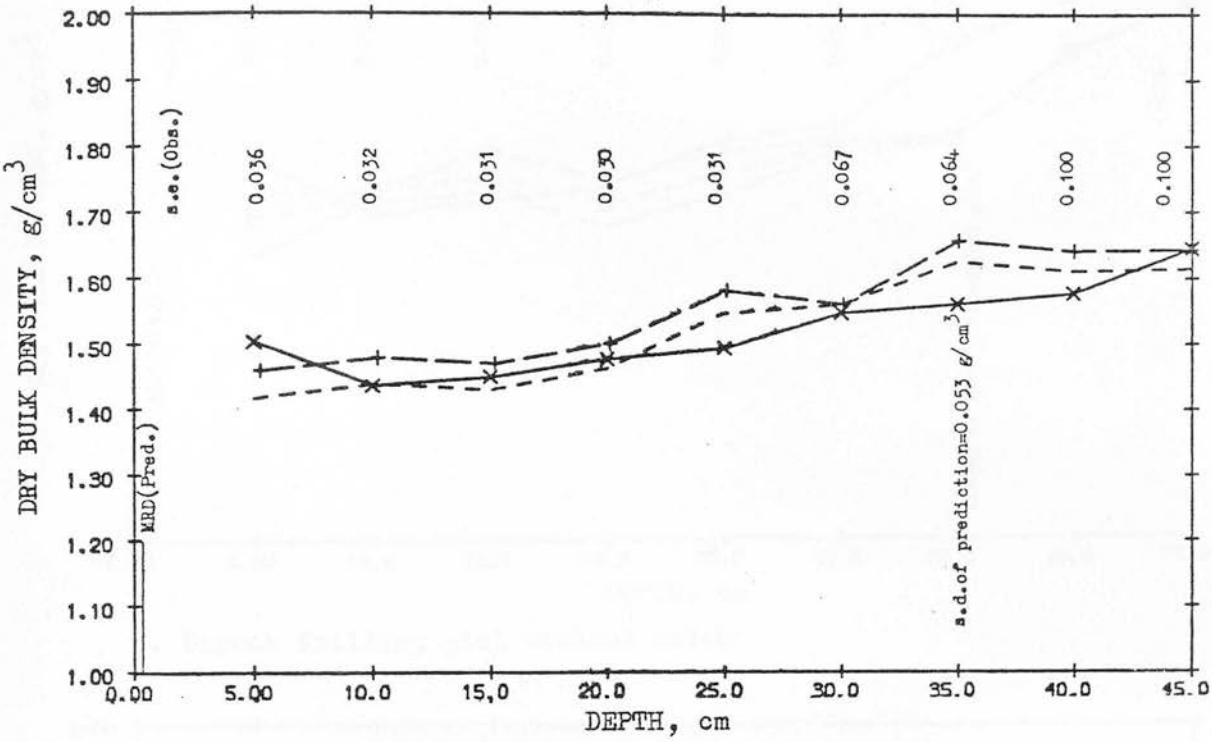


c. Direct drilling plot without mulch.

Fig.74 continued

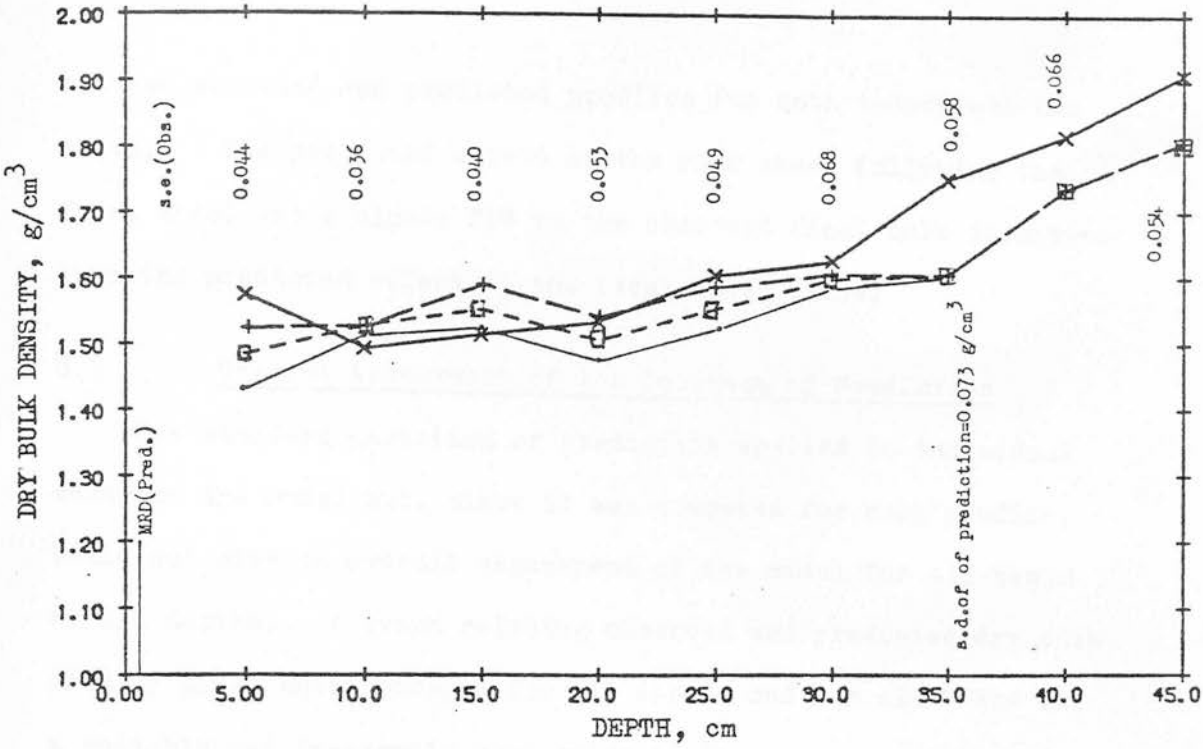


a. Direct drilling plot without mulch

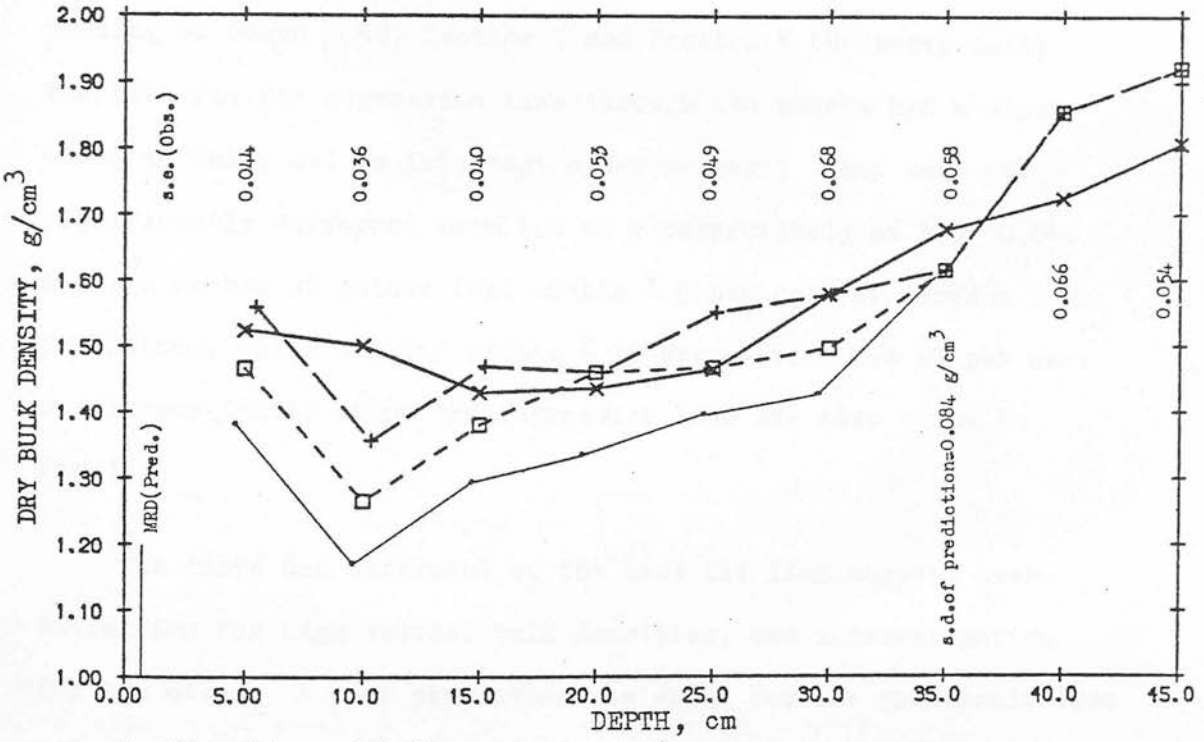


b. Ploughing plot 2.

Fig.75 Model testing, Section 8, SIAE, Fertiliser spreading, 1978. Dry bulk densities before and after passage of the front and back wheels of the tractor carrying the spreader. Standard errors of the measurements and the predicted mean rut depths (MRD) are shown.

Predicted dry bulk density after front wheel.
Observed dry bulk density after front and back wheel.
Predicted dry bulk density after front and back wheel.
Observed initial dry bulk density.

between observed and predicted profiles for both treatments was shown. The predicted effect of the rear wheel following the front wheel was a closer fit to the observed final bulk densities than the predicted effect of the front wheel alone.

## 8.5 General Assessment of the Goodness of Prediction

The standard deviation of prediction applied to individual tests of the model but, since it was computed for each profile, could not give an overall assessment of the model for all tests at all depths. A graph relating observed and predicted dry bulk density after wheel passage for all depths and for all tests was a suitable and frequently used guide to the goodness of prediction (Gee-Clough et al. 1977). This is shown in Fig.76 for model testing at South Road, Section 7 and Section 8 (Macmerry soil). The best fit for regression line through the points had a slope close to unity and an intercept close to zero; they were not significantly different from 1.0 or 0 respectively at $P < 0.05$. A large number of points fell within $\pm$ 5 per cent of perfect prediction, while all lay within $\pm$ 10 per cent. The 95 per cent confidence limits about the regression line are also shown in Fig.76.

The slope and intercept of the best fit line suggest over-estimation for high initial bulk densities, and underestimation for low cases. A poor prediction was shown for the Threipmuir test using very low initial bulk density. This suggested soil of initial cone resistance of less than about 5 bar and initial dry bulk density less than about 1.1 $g/cm^3$ (loam or sandy loam) was unsuitable for the model. Some soil with initial cone resistance lower than 5 bar

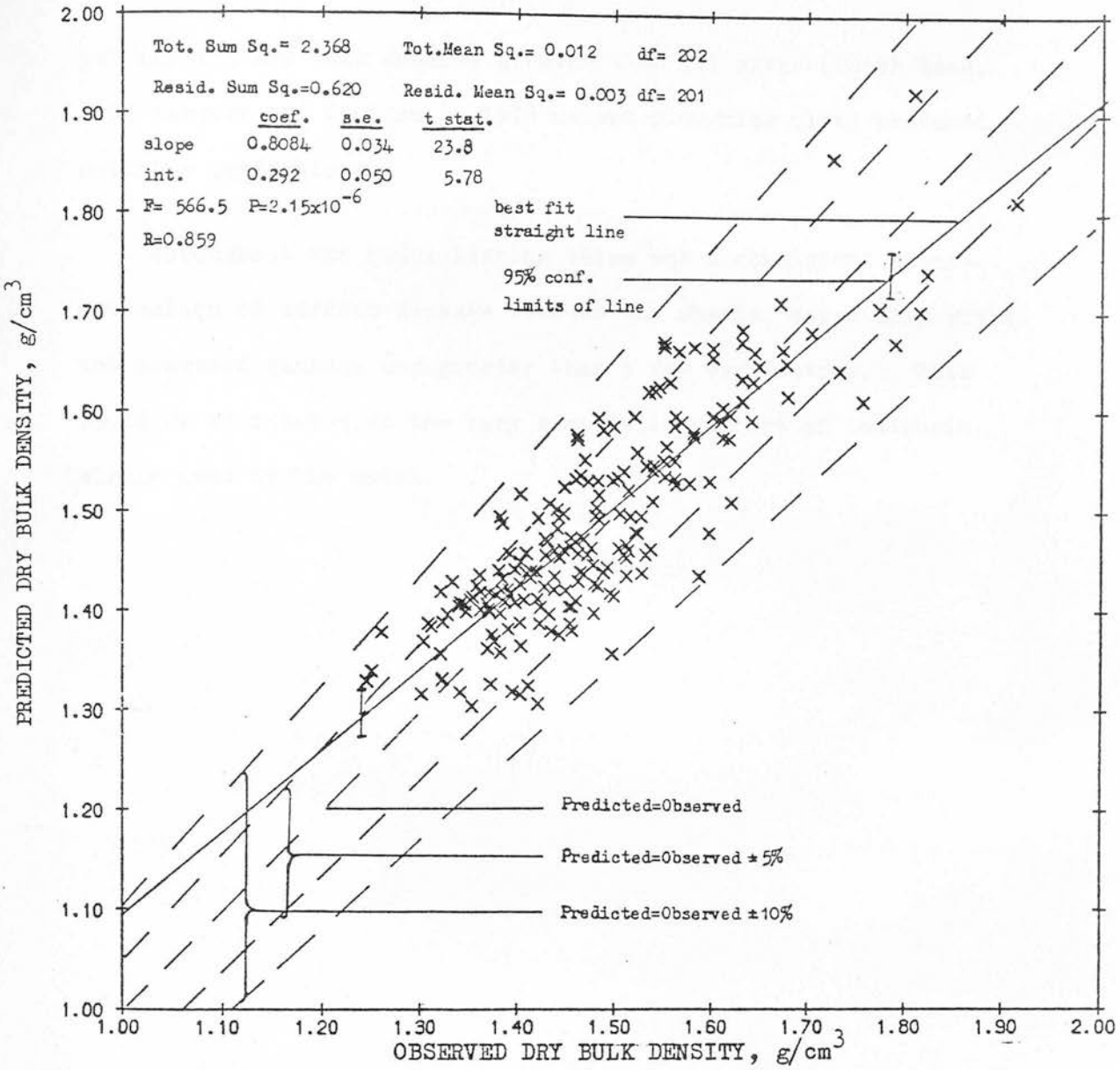


Fig.76 The relationship between observed and predicted dry bulk density at different depths beneath the original soil surface, for all the model tests on Macmerry soil (Section 7 and Section 8, SIAE and South Road field). The outcome of a linear regression analysis is shown as are the 95% confidence limits about the regression line and lines showing ± 5% and ± 10% deviation from exact prediction.

The ranges of wheel load, tyre size and tyre/soil contact area used for these tests were as follows:

| | Maximum | Minimum |
|---|---|---|
| Wheel load, kg | 2854 | 410 |
| Tyre size, ins (code) | 18.4/15-26 | 9.1-16 |
| Tyre/soil contact area, $cm^2$ | 2418 | 520 |

yet initial dry bulk density greater than 1.1 g/cm$^3$ (South Road, 1974 harvest and Section 8, 1978 second ploughing plot) produced suitable predictions.

Throughout the model testing there was a consistent under-estimation of surface sinkage beneath the wheels, especially where the measured sinkage was greater than a few centimetres. This could be attributed to the very simplistic concept of isotropic strain used by the model.

# CHAPTER 9 - DISCUSSION

The research has examined relationships between many soil and machinery factors influencing compaction of agricultural soils, as well as incorporating some relationships between these factors into a simplified prediction model of soil compaction. Each stage of the research can now be discussed.

## 9.1 Suitability of the Soil Mechanical Theories

Soil mechanical theories have been employed to predict stresses beneath wheels and to assist the understanding of relationships between soil stresses and strains. The simplistic assumptions of Söhne's stress prediction equations (Söhne, 1953, 1958) can be readily criticised. Their dependence upon an assumed and constant value of Poisson's ratio to compute second and third principal stresses appears to be their major handicap. Improvements may be achieved by replacing the loaded circular area by a more rectangular form, similar to the shape of the tyre/soil contact zone, as attempted by Yoshida and Kaku (1976). There are also large discrete changes of predicted stresses between equations designed for the three different soil strengths ('soft', 'firm' and 'hard') for the same depth beneath the same wheel. The prediction would therefore be more versatile if a greater number of soil strength conditions and a corresponding number of prediction equations, could be used to reduce these large changes due to differences of soil strength.[1]

The theory of Critical State soil mechanics has been used to interpret some influences of stresses upon soil packing state. However the application of the theory to agricultural soil has not yet been convincingly tested. Critical State theory requires that,

1. Derivation of a continuous function relating stress to soil strength would be a further improvement.

"The mechanical behaviour of soil depends only on the effective stress, the presence or absence of pore pressures or tensions has no effect, except insofar as they alter the effective stresses." (Kurtay and Reece, 1970). Calculation of effective stress is very difficult since measurement of the stresses in the water phase of unsaturated soil presents many problems (Larson and Allmaras, 1971). However the variation of such Critical State functions as the virgin compression line can be related to soil moisture status when 'non-effective' stresses are used which ignore the contribution of soil water forces.

The concepts of apparent virgin compression line ('VCL') and primary function, which avoid the use of relaxation functions, can be derived from Critical State theory. These appear to be useful tools for an analysis of stress/strain relationships since it seems possible to derive them from discrete field measurements made before and after application of stresses. However, it is unfortunate that the identification of 'VCL' and primary functions was so often obscured by shearing processes in 'loose' field soils. The identification was also handicapped by an insufficiently accurate prediction of stresses in field soils. The use of Söhne's equations for stress prediction caused large, discrete changes of stress from one soil strength condition to another. Such changes can influence the variability of estimates of the 'VCL'.

The 'VCL's identified from laboratory measurements in this study help to justify the application of Critical State theory of soil mechanics to agricultural soils. However, some of the laboratory results for 'dry' soil (moisture content 5-10 per cent w/w) revealed non-linear log-normal relationships between spherical

pressure and dry bulk density. The form of these functions is more similar to the stress/deformation functions found by Dexter (1975) for ideal brittle tilths, than to virgin compression lines. Thus some modification of Critical State theory may be required to explain the behaviour of dry, brittle aggregates.

Other soil mechanical observations of this work may generally assist a further understanding of the behaviour of Critical State functions with changes of soil moisture content. This requires setting aside the 'effective stress' concept described above. Relationships between the slope and intercept of the apparent virgin compression line and soil moisture content could be identified from the measurements of stresses and strains in the laboratory and estimations of stresses and strains from field data. These relationships were similar to those expected from examination of research into the effect of stresses on field soils at different soil moisture contents (c.f. section 2.3.1). The moisture content at maximum 'VCL' slope corresponded better to the lower plastic limit, measured by the drop-cone method (using aggregates $< 1$ cm diam.), than the Proctor 'optimum' moisture content or the lower plastic limit measured by the Casagrande method. The aggregate size distribution of less than 1 cm used for the drop-cone test was similar to that of much of the field soil after loosening and harrowing. Thus laboratory tests upon soil with a field aggregate size distribution appear more relevant to the mechanical behaviour of field soils than tests made upon remoulded, highly disturbed soil.

The virgin compression line and the projection of the critical state line upon the plane, describing changes of packing state with

spherical pressure (c.f. section 2.2, Fig.4b), appear to remain almost parallel during changes of soil moisture content (Potamias, 1976). Therefore measured changes of one line indicate some similar changes of the other. The critical state line should thus exhibit a maximum slope at the drop-cone lower plastic limit for the same soil.

The variation of slope and intercept of the virgin compression and critical state lines may assist the assessment of soil workability. Godwin and Spoor (1977) have suggested that soil becomes unworkable[1] when the moisture content is above approximately the lower plastic limit as large amounts of smearing and puddling occur. The maximum slopes of the virgin compression and critical state lines indicate maximum deformation by unit increases of stresses on loose soil. The rate of increase of the intercepts of the lines with changes of soil moisture content also indicates changes of the absolute value of packing state for a given level of stress. Therefore loose field soil becomes more sensitive to increases of stresses near the drop-cone plastic limit (for field aggregate size distribution). As well as this change of sensitivity, the absolute values of bulk density, caused by the same level of soil stresses, will steadily increase at moisture contents above this plastic limit. This shows that loose soil is more susceptible to compaction and probably more likely to puddle and smear, hence less workable and trafficable, at moisture contents near and above the drop-cone plastic limit, determined with soil of similar aggregate size distribution.

An influence of viscous responses upon the slope and intercept of the apparent virgin compression line ('VCL') was proposed from

1. Workability being defined as the ability to break clods during seedbed preparation without causing structural damage.

examination of time dependent responses of soil to applications of stress (c.f. sect.2.3.2). Reduction of the period of stress application was expected to reduce the intercept and increase the slope of the 'VCL'. Unfortunately this could not be fully tested since the technique of stress application in the field was unlike that in the laboratory. The laboratory tests used a stepwise method of increasing stress; any one level of stress being preceded by the previous lower step. However the maximum levels of stress expected at any one depth under a wheel in the field were preceded by almost zero stresses, the change of stress at this depth during wheel passage being much more rapid than for the laboratory tests. These differences of stress regimes prevented any direct quantitative comparisons of 'VCL's obtained from field and laboratory results, since more soil deformation was expected by the progressive, stepwise increases of stresses in the laboratory than for the same level of stress in the field.

## 9.2 Precision, Accuracy and Suitability of the Methods

Soil physics has a persistent but narrowing dichotomy between more realistic but less precise field measurements and more artificial but more precise laboratory measurements. This research reflects both sides of this conflict. The estimates of the slopes of the virgin compression lines from field data show much more variation than corresponding estimates from laboratory data and are derived from less precise measurements; compare Figs.62a and 64a. However, the laboratory results derive from methods of stress application unlike that of a wheel running over field soil and are a less accurate simulation of compaction under wheels than the field experiments.

Soil mechanical theories have principally developed from laboratory observations. These have a level of precision acceptable to many mathematical methods of analysis. However, the variability of field soil is inherent and unavoidable, irrespective of the precision of the measurement techniques, and theories derived in the laboratory are ultimately intended to predict the behaviour of field soils, despite the high levels of variation under field conditions.

The variability associated with the means of the field measurements was reduced by replication and sub-sampling. Thus techniques used for field measurements usually proved satisfactory for the collection of sufficient data in the time available. However a larger number of replications of the field experiments would have permitted a greater number of degrees of freedom in the analyses of variance. This could have allowed differences between means of field measurements to be detected at a higher probability of significance than in the analyses made of the field data.

The errors associated with most of the measurement techniques have been discussed by other authors (Freitag, 1971). The new spherical transducers for measuring soil stresses appeared successful, for applied stresses up to about three bar, but improvements could be made to reduce sources of error. The multiway valve reduced the numbers of pressure transducers, but created errors during valve changes. Using the valves to connect balls between plots rather than within them, could have reduced these errors. Since the calibration and use of the Water Filled Rubber Ball, a commercially available hollow rubber sphere with a thinner wall

(3.8 mm) has been obtained. This should be more sensitive to soil stresses than the 'squash' ball. Reduction of the transducer signal by soil 'arching' could be detected from the field measurements beneath some wheel treatments. Such errors associated with the installation of the devices could also be reduced if the installation immediately followed initial soil loosening. The information provided by the two spherical transducers could be increased if the dynamic measurements of the internal pressure of the Water Filled Rubber Ball could be complemented by dynamic measurements of the Mastic Ball axes; small displacement transducers embedded in the mastic may achieve this.

The laboratory methods of measuring stresses and volumetric strains of soil appear suitable for measurement of some Critical State parameters. The sample size is larger than that used in similar research (Potomias, 1976) and there is less constraint by rigid platens. The large sample size also allows large aggregates ( $<1$ cm diameter) to be tested without reducing the precision of sample volume measurement within 95 per cent of the real value. Although the apparatus was only used for isotropic compression, little modification is required to apply suitable deviator stresses to identify Critical State lines. However considerable modification of the apparatus is required to apply stresses at rates and over periods similar to those beneath a moving wheel. Corresponding modifications would also be needed to allow rapid explusion of soil fluid and measurement of changes of packing state. Continuous monitoring by radioactive transmission, after Fekete et al. (1975) may offer a suitable solution.

Using the Proctor dry bulk density as an estimate of the dry bulk density at critical state was convenient but unsatisfactory since the stresses applied by the Proctor test could not be described very quantitatively. More suitable 'standard compaction' tests would use combinations of known spherical pressure and deviatoric stress to bring the soil to its 'critical state' at various soil moisture conditions.

Single tractor rear wheels with controlled loads and inflation pressures have been used relatively successfully in this research, using a tractor with a single front wheel. However there was a suspicion of the wheel treatment W4 (Table 4) being so heavily loaded that the influence of tyre wall stiffness would considerably affect the stress distribution over the tyre/soil contact zone. Such effects have been observed by Abeels and Declerque (1977). The pen recorder trace of the internal pressure of the water filled rubber ball reduced these suspicions for the longitudinal axis of the contact zone. Single, rather than multiple, peak pressures were usually observed at 10 cm below treatment W4 (see Fig.63). However larger sinkages were sometimes measured near the rut edges than at the rut centres for this heavily loaded wheel treatment (Fig.47). This suggests that tyre wall stiffness may have had more influence on the stress distribution at the tyre/soil interface in the direction transverse to wheel motion.

## 9.3 Sufficiency of the Experimental Results

All the field measurements, except those from the gypsum blocks, showed equal or smaller variability than those for the same or similar methods used in other research, Soane (1975). Occas-

ional high levels of variability of dry bulk density measurements below 30 cm depth (s.e. $> 0.05$ g/cm$^3$) could be attributed to sub-soil variation and instrumentation problems.

The problems of unreliability and variability with the methods and results of soil moisture tension measurements were not unique to this research. Curtis and Trudgill (1974) describe similar problems. Despite these handicaps, the data relating field moisture tension and moisture content of the Threipmuir soil exhibit clear soil moisture characteristics for each depth (Fig.66a).

A useful comparison can be made between the dry bulk density profiles and rut profiles as methods of assessing different wheel treatments. Rut profile data could distinguish differences between wheel treatments at a lower level of probability (often $P < 0.05$) than dry bulk density profiles for the same wheel treatments. Thus the rut profile measurements were the more sensitive comparison, presumably as surface sinkage differences are an integration of numerous small bulk density changes of the soil beneath the wheels.

The close correlation between measurements of cone resistance and vane shear strength of the field soils (Appendix 6) suggests both techniques provide measurements of similar aspects of soil strength; the lower coefficients of variation of the field measurements of vane shear strength are an advantage over field measurements of cone resistance.

The virgin compression lines (VCL) for each soil moisture condition should be readily identified from the data of the laboratory measurements of stress and strain; however, the occasional unreliability of final sample volume measurement contributed to errors in the determination of the VCL intercepts.

## 9.4 Analyses of results

Söhne's stress prediction equations have been tested for field soils by comparing predicted and measured values of stresses. Application of the prediction equations required the estimation of tyre/soil contact area. The mean rut depth, as defined in section 5.1.2, appears a suitable parameter for the estimation of the horizontal projection of the tyre/soil contact area post facto. The empirical exponential functions relating mean rut depth to tyre/soil contact area seem applicable to a wide range of agricultural tyres. The strength of the upper soil layers (approximately 0-20 cm depth) measured by cone or vane may provide a parameter for estimating contact area before the tyre runs onto the soil, since wheel sinkage appears to show a correlation with initial soil strength (see Fig.47).

Comparison of measured and predicted stresses revealed a relationship between soil strength and the soil 'hardness' associated with each stress prediction equation. However the range of soil strength conditions examined was not as extensive as that commonly found in field soils and assumptions were made of stress predictions made for one soil texture (loam) applying to a soil of another texture (sandy loam). No stress measurements were made in soil of less than approximately 10 bar cone resistance, there-

fore the stress prediction equations developed by Söhne were used with caution below this limit. Subsequent analyses of the data (section 6.3.1) and testing of the compaction prediction model suggested this limit could be dropped to about 5 bar cone resistance, with a soil dry bulk density of at least 1.1 $g/cm^3$.

Many of the graphs relating final dry bulk density after wheel passage ($Dbd_f$) and the expected maximum spherical pressure ($P_{max}$) showed the pattern expected from the interpretation of Critical State soil mechanics in Chapter 2. Clear boundaries usually separated possible combinations of $Dbd_f$ and $P_{max}$ from those combinations not possible (i.e. very low $Dbd_f$ following very high $P_{max}$). A linear cluster of points lay approximately along the boundaries and best estimates of the apparent virgin compression lines ('VCL') could be fitted through these clusters. However the occurrence of soil shearing and plant roots (e.g. grass at Lower Terrace site) appeared to easily obscure the patterns of the clusters.

A comparison of 'VCL' estimations from field data with 'VCLs' from laboratory data revealed consistently and significantly higher 'VCL' slopes and intercepts from laboratory tests on loose soil than from the field data. The difference of intercept could be attributed to the shorter periods for viscous responses of soil deformation beneath a moving wheel than for the laboratory tests. A smaller number of laboratory tests on 'undisturbed' field soil samples showed very similar 'VCL' slopes to those estimated from field data from the same soil at similar moisture contents. Thus there is some evidence that apparent virgin compression lines can

be identified from measurements made in situ before and after the passage of a wheel over a field soil. However, more extensive testing of this method of identification is required.

The problems caused by an insufficient range of field measurements, due to a shortage of time and resources, are reflected by comparing the sets of data collected from Section 7 (1976) and Lower Terrace (1977). The more uniform soil moisture profiles and few soil (RL) treatments at Lower Terrace resulted in insufficient data to closely examine the variation of 'VCL' slope and intercept with soil moisture content.

The information relating 'VCL' parameters to soil moisture content of the two soils, discussed in section 9.1, is complementary to other similar research into soil mechanical properties. Bertilsson (1971) measured virgin compression lines for soil aggregates at different moisture contents by laboratory methods. The trends observed were similar to those by this research; maximum values of slope occurred near the plastic limit (Casagrande method) and the intercept increased steadily with moisture content. Observations by Potamias (1976) of changes of the slope and intercept of critical state lines also showed some similar trends.

Slopes of primary functions could be identified from the differences between swelling and relaxation slopes from the laboratory data. However, the same shortcomings of the stress regimes of the laboratory tests, which hinder interpretation of laboratory VCLs, imply that some caution is needed when applying such primary function slopes to field soils.

## 9.5 The Model

The general assessment of how well the compaction model predicts dry bulk density values created by the passage of agricultural wheels over field soils is shown in Fig.76. The close correspondence between predicted and observed values shows the model can predict resultant dry bulk density values after wheel passage within five to ten per cent of the real value, but the following qualifications must be considered:

a) The operation of the model is designed specifically for soil types whose soil mechanical behaviour is well documented; in this research Macmerry (sandy loam) and Threipmuir (loam).

b) Very loose initial soil conditions (less than approximately 5 bar cone resistance and less than approximately 1.1 $g/cm^3$ dry bulk density, for a loam or sandy loam) cannot be considered by this form of the model due to insufficient knowledge of the soil stresses developed beneath tyres in such conditions. Soil shearing and the development of extensive failure planes are expected to occur in such weak soils. These processes could lead to the formation of 'failure wedges' beneath wheels and the focussing of compaction at some depth beneath the wheel, as suggested by Bekker (1961). Such processes seem less likely in stronger soils with higher strength than the limits quoted here since compaction of such soil was usually greatest next to the surface.

c) Levels of wheelslip or skid greater than approximately 5 per cent[1] may introduce errors into the predicted values, especially near the soil surface.

d) The prediction of surface sinkage is very poor since isotropic soil strain was used for each element of soil used by the model.

e) Impact loading, vibration and forward speed greater than a few km/h have not been considered, but their effect is usually small in proportion to the major factors of wheel load and contact area.

f) A range of wheel loading of approximately one to three tonnes has been tested. Much higher loads must be used with caution.

g) Application of the model is as yet restricted to beneath the tyre centre line.

These restrictions limit the model to 'after sowing' and 'before ploughing' operations with wheels of low levels of slip or skid; however this still includes a very large number of opportunities for application of the model.

Further experimental work is required to improve the model by investigating stresses beneath wheels on very loose soils and extending the critical state relationships to consider higher levels of deviatoric stress. The application of the model could also be improved by extending the geometry to a plane transverse to the direction of wheel motion, as done by Bowen (1975) and examining the development of failure planes within the soil.

---

1. The slip of the experimental wheel was 4 per cent (section 3.1).

The model can be compared with existing methods of predicting compaction. These can be approximately divided into:

a) Soil mechanical models: mathematical expressions of compaction are explained with varying degrees of refinement from soil mechanical principles and analytical techniques such as Finite Element Analysis, e.g. Yong and Fattah (1976) and Yong et al. (1978).

b) Empirical models: large quantities of field data are related to simplified expressions of the major factors of the compaction processes. The relationships derived, such as from multiple linear regressions, are used to predict further situations, e.g. Raghavan and McKyes (1977) and Ericksson et al. (1974).

The prediction method described by this research appears to fall somewhere between these two extremes and has many similarities to that of Bowen (1975) and Amir et al. (1976). The model does not depend on a large amount of empirical data to explain each situation while its construction and operation is not so detailed as to make it unwieldy, expensive and difficult to use. The testing of the model against suitable field data from other research has been more extensive than for many other prediction methods; this must also be considered when comparisons are made between this model and others.

Satisfactory testing of the model suggested that it could be used to simulate soil compaction. Such simulation may help to indicate soil responses to changes of some factors influencing soil compaction; within the constraints of the model described above. Danfors (1977) and Raghavan and McKyes (1977) have discussed the benefits of reducing mean tyre/soil contact pressure. They expect lowest contact pressures to result in the least soil compaction.

The result of using the model for four different wheels running over a hypothetical topsoil, with uniform initial dry bulk density to 25 cm depth, is shown in Fig.77. Initial soil strenghts and moisture contents are also shown in the figure.

The four wheels have combinations of two different loads and two different contact areas arranged to give three different mean contact pressures. Each two values of load and contact area are different by a factor of two. Most compaction beneath the tyre centre line is caused by wheel 'D', with the highest contact pressure. Least compaction is caused by wheel 'A' with the lowest contact pressure. This agrees with the conclusions of Raghavan and McKyes (1977). However they do not distinguish between the influence of contact area and wheel load on contact pressure.

Wheels 'B' and 'C' have the same contact pressure and cause the same amount of compaction in the upper 10 cm depth of the 'topsoil', but not between 20 and 25 cm depth. The wheel carrying the higher load, 'C', causes more compaction in the deeper parts of the topsoil. Therefore information on contact pressure needs supplementing with data on wheel load and tyre/soil contact area to

Fig.77 Simulation by the dry bulk density prediction model of the compaction of a hypothetical soil by the passage of four different wheels.

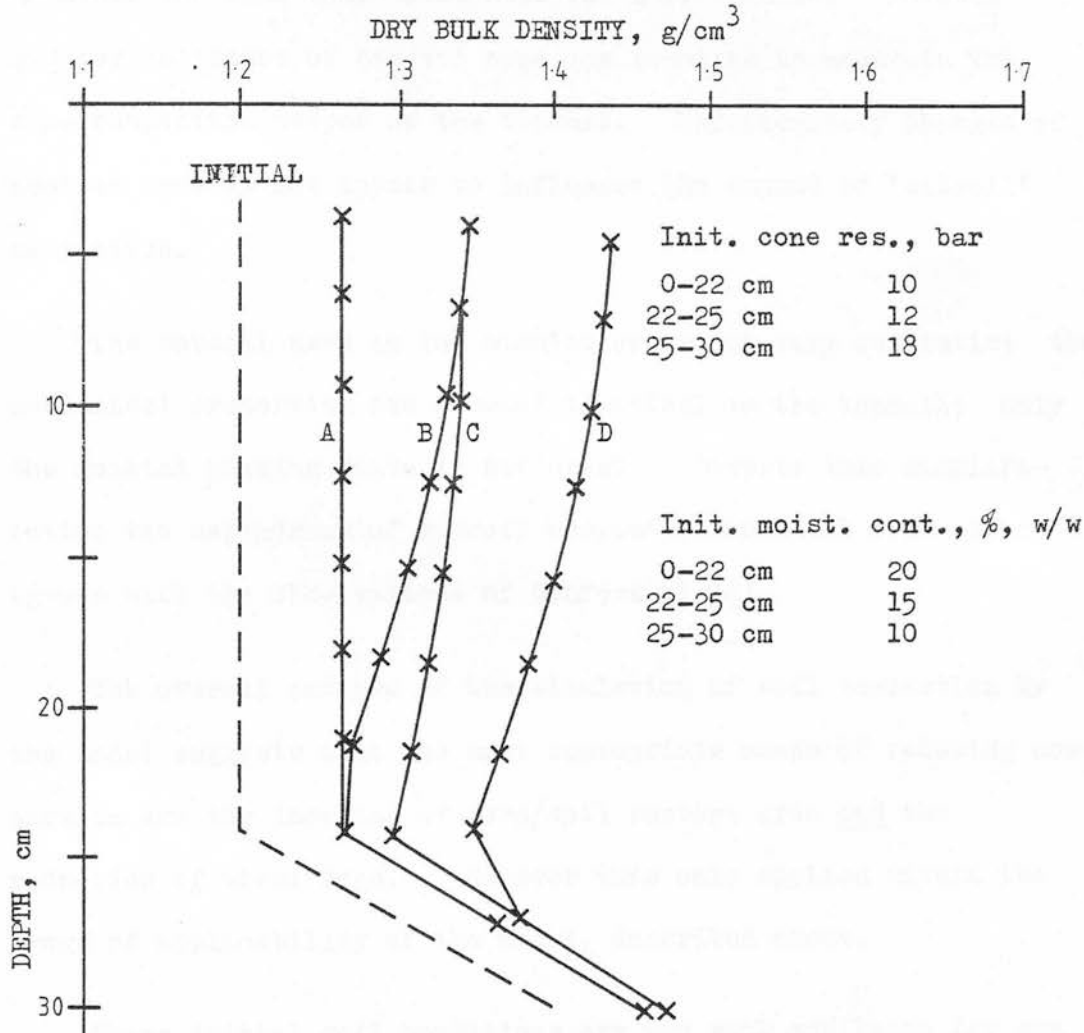


| WHEEL | WHEEL LOAD, kg | TYRE/SOIL CONTACT AREA, $cm^2$ | MEAN CONTACT PRESSURE, $kg/cm^2$ (kPa) |
|---|---|---|---|
| A | 1000 | 2000 | 0.5 (0.51) |
| B | 1000 | 1000 | 1.0 (1.02) |
| C | 2000 | 2000 | 1.0 (1.02) |
| D | 2000 | 1000 | 2.0 (2.04) |

distinguish between compaction at different depths in the topsoil.

The influences of wheel load and contact area on compaction, shown by the simulation, reveal that a two-fold increase of wheel load can be compensated by a two-fold increase of contact area to maintain the same compaction near the soil surface. However greater increases of contact area are required to maintain the same compaction deeper in the topsoil. Unfortunately changes of contact area do not appear to influence the amount of 'subsoil' compaction.

The subsoil used in the simulation is not very realistic; the mechanical properties are assumed identical to the topsoil; only the initial packing state is different. Despite this simplification the dependence of subsoil compaction on wheel load alone agrees with the observations of Danfors (1974).

The overall outcome of the simulation of soil compaction by the model suggests that the most appropriate means of reducing compaction are the increase of tyre/soil contact area and the reduction of wheel load. However this only applies within the range of applicability of the model, described above.

Where initial soil conditions are too weak and loose for use of the compaction model, empirical observations from field experiments used in this research may assist prediction. These observations are restricted to qualitative comparisons. Examination of the same wheel treatment to soils of different initial strength, during the compaction experiment at Section 7, reveals higher resultant bulk densities from wheels running over loose soil

than over firm soil (section 5.1.1). Similar conclusions can be drawn from the results of the model testing on Threipmuir soil (section 8.2) since the compaction model, designed for firm soil, predicts less compaction than occurred in the loose soil used for the test. An example from the field data of the same wheel leaving different dry bulk density profiles after running over soils of two different strengths is shown in Fig.78.

Fig.78 An example of compaction by the same wheel running over soils of two different initial strengths. Occasion M1 Macmerry soil. The mean cone resistance of the upper 20 cm was approximately three and seven bar for soils RL1 and RL2 respectively (wheel load 1560 kg, tyre inflation pressure 138 kPa, tyre size 12.4/11-36).

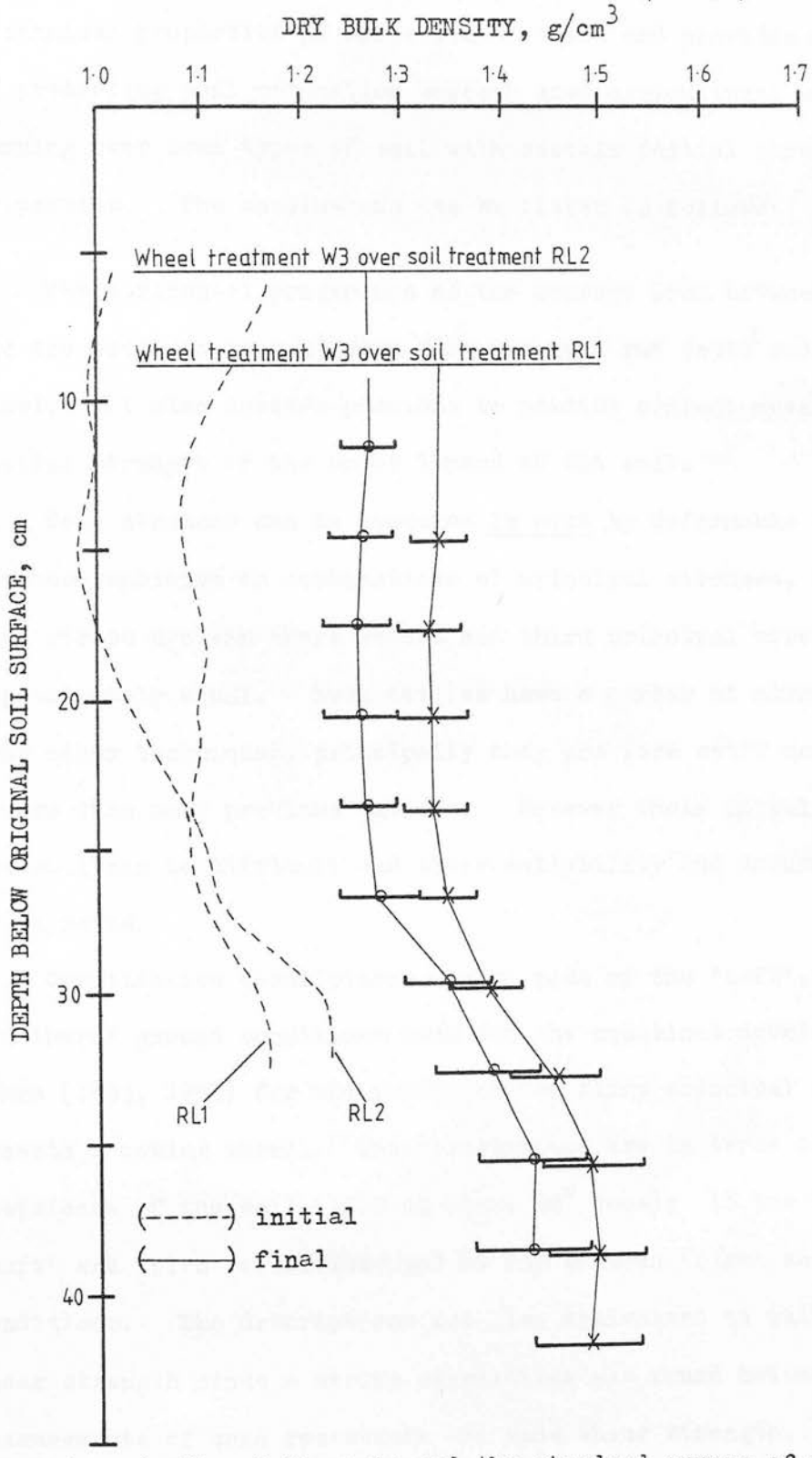


The maximum depths of the ruts and the standard errors of the differences between the means are also indicated.

# CHAPTER 10 - CONCLUSIONS

This research appears to assist the understanding of some mechanical properties of agricultural soils and provides a method of predicting soil compaction beneath some agricultural wheels running over some types of soil with certain initial physical properties. The conclusions can be listed as follows:

1. The horizontal projection of the contact area between a tyre and the soil can be estimated from the mean rut depth[1] made by the wheel. It also appears possible to predict contact area from the initial strength of the upper layers of the soil.

2. Soil stresses can be measured in situ by deformable spherical devices sensitive to combinations of principal stresses, in simplified stress systems where second and third principal stresses are approximately equal. Such devices have a number of advantages over other techniques, principally they are less stiff under axial stress than many previous devices. However their installation in the soil can be difficult and their reliability and accuracy could be improved.

3. Quantitative descriptions can be made of the 'soft', 'firm' and 'hard' ground conditions used for the equations developed by Söhne (1953, 1958) for the prediction of first principal stresses beneath a moving wheel. The descriptions are in terms of cone resistance of the soil (12.9 mm diam. 30° cone); 16 bar between 'soft' and 'firm' conditions and 26 bar between 'firm' and 'hard' conditions. The descriptions are also equivalent to values of vane shear strength since a strong correlation was found between field measurements of cone resistance and vane shear strength.

---

1. As defined in section 5.1.2.

4. Further evidence has been found for application of the Critical State theory of soil mechanics to the behaviour of unsaturated, structured agricultural soils. Virgin compression lines and relaxation functions could be identified from laboratory tests on soil aggregates less than one centimetre diameter and 'undisturbed' samples of field soils. Similar functions were evident from estimations of stress/strain relationships from field soil data collected in situ. However, some modification of Critical State theory is suggested for loose soil consisting of dry, brittle aggregates.

5. The number of Critical State functions required to describe the effects of stresses upon soil packing state can be reduced if attention is confined to packing conditions before and after the application of stresses, and the maximum levels of stresses applied. Critical State functions can thus be reduced to a 'primary function' and an 'apparent virgin compression line', when deviatoric stresses have a low or insignificant value.

6. Identification of the apparent virgin compression line ('VCL') seems possible from measurements of soil packing state taken before and after the passage of a wheel. Some evidence has been found for the validity of this technique, but further, more conclusive, proof is required. Since such a technique can be applied to field soils in situ, it may enable effects of field soil structure to be included in the stress/strain relationships derived from field measurements.

Identification of the 'VCL' was attempted from in situ measurements since no suitable laboratory technique was available. More information about soil mechanical properties can be collected from laboratory measurements than from field measurements, especially if soil samples are removed from the field with as little disturbance as possible. Unfortunately there appears to be, as yet, no laboratory equipment able to apply stresses at the rates and over the periods found beneath a moving wheel, as well as simultaneously measuring the large soil strains which can occur. The availability of such equipment would greatly enhance and expand the measurement of useful soil mechanical properties.

7. The changes of slope and intercept of the virgin compression line, and by implication the critical state line, with variation of the moisture content of the soil may further clarify and define the concepts of soil workability and trafficability. Maximum values of the slopes of the lines seem to occur at soil moisture contents corresponding to the lower plastic limit, measured by the drop-cone technique using an aggregate size distribution similar to that in the field. Intercepts of the lines seem to increase rapidly at moisture contents above this limit.

These changes of slope and intercept imply greater sensitivity of the soil to compaction. Thus soil may be defined as more workable and trafficable at moisture contents below the drop-cone lower plastic limit of the soil, in such an aggregate condition, than at moisture contents above such a limit.

8. A simplified model of soil compaction can be constructed using the techniques of stress prediction developed by Söhne and the Critical State functions of apparent virgin compression line and

primary function. The model relates spherical pressure to volumetric strain. This can predict the dry bulk density of a 'firm' field soil following the passage of an agricultural wheel with low levels of slip or skid; the model is, as yet, confined to the soil beneath the centre line of the wheel track.

9. Investigation of the soil stresses beneath wheels running over firm soils revealed the major principal stress as almost a constant ratio of the minor principal stresses, for the wheels and soil conditions studied. Testing of the prediction model suggested the ratio changed considerably when the soil was very loose and the effect of shearing stress became more evident. These observations assist the discussion of which soil stresses best correlate with compaction. Some research has found that in most circumstances major principal stress is best correlated (Chancellor, 1971; Kitani and Persson, 1967). However, there has been evidence that this is not always the case (Vanden Berg, 1966; Greacan, 1960). The research described in this thesis suggests that the major principal stress can correlate well with compaction for soil not initially loose and for wheels with low wheelslip (about 5 per cent). In these conditions compaction is mainly controlled by spherical pressure, which was shown to be proportional to the major principal stress when a constant ratio between major and minor principal stresses occurred. When the soil is looser and less confined, or wheelslip is greater than about 5 per cent, one can expect shearing forces to become more dominant and compaction will correlate better with a combination of mean principal stress and maximum shear stress, or strain (e.g. Vanden Berg, 1966). Additional measurements of stresses by the spherical transducers could

further clarify this.

10. It now seems possible to use the prediction model to foresee some compaction effects which have hitherto only been conjecture. With soil of suitable known mechanical properties one can use appropriate information about vehicle wheels and initial soil conditions to predict, within the limits of the model, the resultant dry bulk densities after the passage of various wheels. Different agricultural operations over soils of suitable initial soil conditions could be considered. Compaction of very loose soil may be possible using the model developed by Raghavan and McKyes (1977) for bulk density changes beneath wheels running over recently cultivated soils. Compaction expected during harvest, and the subsequent sowing of winter crops in relation to the date of return to field capacity, would be valuable information; especially in relation to the 'optimum' dry bulk densities for soil moisture availability proposed by Hall et al. (1977) and when applied to direct drilling operations in Scotland (Pidgeon and Ragg, 1979). Further use of the model, within its limitations, could also help to distinguish between the compaction beneath different tyre and wheel systems, and different vehicles, in a similar way to that of Danfors (1977). Such comparisons may assist the design of future agricultural machinery.

A simulation, by the prediction model, of compaction beneath different agricultural wheels and examination of data from the field experiments revealed the following:

1. Wheels with highest contact pressure caused the greatest compaction of the upper 'topsoil'.

2. Of two wheels with equal contact pressure, the one with highest wheel load caused the greater compaction of the lower topsoil.
3. Wheels carrying the highest load caused the greater compaction of the 'subsoil'. Variation of contact area had no effect on subsoil compaction.
4. Loose, weak soil (cone resistance $<$ 5 bar (12.9 mm, 30° cone), and dry bulk density $<$ 1.1 g/cm$^3$, sandy loam, or loam) compacted to higher dry bulk densities than stronger soil when the same wheel is ran over both soils.

Therefore it appears that the most suitable means of reducing soil compaction under a wheel may be the reduction of wheel load and an increase of tyre/soil contact area , as well as minimising traffic upon loose, weak soil. However it must be emphasised that all these statements made from the implications of the model of soil compaction are restricted to the ranges of soil and wheel parameters within which the model has been successfully tested. These ranges can be broadly described as wheels of low speed, with little slip or skid, running over loam or sandy loam soil before ploughing and after sowing operations.

It is hoped that this research has improved the understanding of the compaction of field soils by agricultural wheels and may assist the design of agricultural operations and agricultural vehicles.

# TABLE OF REFERENCES


ABEELS, P. & DECLERQUE, D. (1977). La locomotion tout terrain, la compaction du sol. (Off-road locomotion and soil compaction.) Revue Agric. 1977 (1), 131-150.

ACKROYD, T.N.W. (1964) Laboratory testing in soil engineering. London : Soil Mechanics Ltd.

AMIR, I., RAGHAVAN, G.S.V., McKYES, E. & BROUGHTON, R.S. (1976). Soil compaction as a function of contact pressure and soil moisture content. Can. J. agric. Engng, 18 (1), 54-57.

ANDERSSON, S. & WIKLERT, P. (1970). Soil physical studies in cultivated soils, XX. Studies of some soil profiles in Naarland. Grundförbättring, 23 (1-2), 3-76.

AREF, K.S., CHANCELLOR, W.J. & NIELSEN, D.R. (1974). Dynamic shear strength properties of unsaturated soils. Am. Soc. agric. Engrs paper 74-1013 (presented at ann. meeting ASAE, Oklahoma).

BAGANZ, K. & KUNATH, L. (1963). Some measurements of stress and compaction under tractor wheels and tracks. Dt. Agratech. 13 (4), 180-182.

BAILEY, A.C. (1971). Compaction and shear in compacted soils. Trans. Am. Soc. agric. Engrs 14 (1), 201-205.

BAVER, L.D., GARDNER, W.H. & GARDNER, W.R. (1972). Soil Physics. New York : Wiley.

BEKKER, M.G. (1956). Theory of land locomotion: the mechanics of vehicle mobility. ANN ARBOR : Univ. Michigan Press.

BEKKER, M.G. (1961). Mechanical properties of soil and soil compaction. Trans. Am. Soc. agric. Engrs 4, 231-234.

BERRYMAN, C., THORBURN, A. & TRAFFORD, B.D. (1976). Soil water tensiometers. Field Drainage Experimental Unit Tech. Bull. 76-7. M.A.F.F., A.D.A.S.

BERTILSSON, G. (1971). Topsoil reaction to mechanical pressure. Swed. J. agric. Res. 1 (13), 179-189.

BISHOP, A.W. & HENKEL, D.J. (1967). The measurement of soil properties in the triaxial test. 2nd ed. London: Edward Arnold.

BLACKWELL, P.S. & DEXTER, A.R. (1971). An evaluation of inductance gauges for dynamic measurement of soil strain. Natn. Inst. agric. Engng, Dept. Note DN/ER/184/1162. Silsoe : NIAE (unpub.)

BLACKWELL, P.S. & DICKSON, J.W. (1978). Comparison of soil compaction under conventional and dual wide section tyres carrying the same load over loose soil. Scot. Inst. agric. Engng, Dept. Note SIN/254 Penicuik : SIAE (unpublished).

BLACKWELL, P.S. & SOANE, B.D. (1978). Deformable spherical devices to measure stresses within field soils. J. Terramechanics (In press).

BOUSSINESQ, J. (1885). Application des pontiels a'l'etude de l'e'quilibre et du mouvment des solides e'lastiques. Paris : Gautheir Villard.

BOWEN, H.D. (1975). Simulation of soil compaction under tractor-implement traffic. Am. Soc. agric. Engrs paper 75-1569 (presented at Winter meeting, Chicago).

BROWN, K.T. and ANDERSON, G. (1975). Control and recording equipment for a soil penetrometer. Scot. Inst. agric. Engng, Dept. Note SSN/185, Penicuik : SIAE (unpublished).

BROWN, M.D. (1972). 370/155 Graph plotting reference manual. Edinburgh : Edinburgh Regional Computing Centre.

BURWELL, R.E., ALLMARAS, R.R. & AMEMIYA, M. (1963). A field measurement of total porosity and surface microrelief of soils. Proc. Soil Sci. Soc. Am. 27, 697-700.

BUTSON, M.J. (1977). A general graph-plotting routine for use with IMP programs. Scot. Inst. agric. Engng, Dept. Note SSN/231, Penicuik : SIAE (unpublished).

CAMPBELL, D.J. (1976). Plastic limit determination using a drop-cone penetrometer. J. Soil Sci. 27 (3), 295-300.

CANNELL, R.Q., DAVIES, D.B., MACKNEY, D. & PIDGEON, J.D. (1978). The suitability of soils for sequential direct drilling of combine-harvested crops in Britain:- a provisional classification. Outlook in Agriculture, Special Number, 1978.

CHANCELLOR, W.J. (1966). Combined hypothesis for anticipating soil strains beneath surface impressions. Trans. Am. Soc. agric. Engrs 9 (6), 887-895.

CHANCELLOR, W.J. (1971). Effects of compaction on soil strength. Am. Soc. agric. Engrs Monograph 'Compaction of Agricultural Soils', p 190-212. St. Joseph, Michigan : ASAE.

CHANCELLOR, W.J. (1976). Compaction of soil by agricultural equipment. Bull. 1881, Div. ag. Sciences, Univ. California, Davies.

CHANCELLOR, W.J. & SCHMIDT, R.H. (1961). Study of soil deformation under surface loads. Am. Soc. agric. Engrs paper 61-121, (presented at ASAE meeting, Iowa, 1961).

CHESNESS, J.L., EFRAIN, E.R. & COBB, C. (1970). Quantitative description of soil compaction in peach orchards utilizing portable penetrometer. Am. Soc. agric. Engrs paper 70-143 (presented at ASAE Summer meeting).

CHILINGARIAN, G.V. & WOLF, K.K. (1975). Compaction of coarse grained sediments, I. Developments in Sedimentology, 18A. New York : Elsevier Sci. Pub. Co.

CHRISTOV, I. (1969). 'Niektoré pozantky získané meraním napätia pôdy pod traktorovými kolesami'. (Some information obtained by measurement of soil stresses under tractor wheels.) Acta. Tech. Ag. IV. Univ. Ag. Nittra, Czech.

CHUNG, T.J. & LEE, J.K. (1975). Dynamics of viscoelastoplastic soil under a moving wheel. J. Terramechanics, 12 (1), 15-31.

COCHRAN, W.G. & COX, G.M. (1960). Experimental Designs, 2nd edition. New York : Wiley.

COOPER, A.W., VANDEN BERG, G.E., McCOLLY, H.F. & ERICKSON, A.E. (1957). Strain gauge cell measures soil pressure. Agric. Engng, 38 (4), 232-237.

COX, D.R. (1958). Planning of experiments. New York : Wiley.

CURTIS, L.F., COURTNEY, M.F. & TRUDGILL, S.T. (1976). Soils in the British Isles. London : Longman.

CURTIS, L.F. & TRUDGILL, S. (1974). The measurement of soil moisture. Tech. Bull. 13 of Brit. Geomorph. Res. Group. : Geoabstracts.

DANFORS, B. (1974). Packning i alven. (Compaction in the subsoil). Special paper 24. Swed. Inst. agric. Engng, Uppsala.

DANFORS, B. (1977). Jordpackning - hjulustrustning. (Soil compaction - wheel equipment). Bull.368. Swed. Inst. agric. Engng, Uppsala.

DAVIES, D.B., EAGLE, D.J. & FINNEY, J.B. (1972). Soil management. Ipswich : Farming Press.

DAVIES, D.B., FINNEY, J.B. & RICHARDSON, S.J. (1973a). Relative effect of tractor weight and wheelslip in causing compaction. J. Soil Sci. 24 (3), 399-409.

DAVIES, P.F., DEXTER, A.R. & TANNER, D.W. (1973b). Isotropic compression of hypothetical and synthetic brittle tilths. J. Terramechanics, 10 (4), 21-34.

DAY, P.R. & HOLMGREN, G.C. (1952). Microscopic changes in soil structure during compression. Proc. Soil Sci. Soc. Am. 16, 73-77.

DEXTER, A.R. (1973). A review of soil mechanical properties. Proc. Natn. Inst. agric. Engng Subject day. 'The Mechanical Behaviour of Agricultural Soils'. Silsoe : NIAE.

DEXTER, A.R. (1975). Uniaxial compression of ideal brittle tilths. J. Terramechanics, 12 (1), 3-14.

DEXTER, A.R. & TANNER, D.W. (1971). Packing density of ternary mixtures of spheres. Nature London Phys. Sci. 230 (16), 177-179.

DEXTER, A.R. & TANNER, D.W. (1973). The response of unsaturated soils to isotropic stress. J. Soil Sci. 24 (4), 491-502.

DEXTER, A.R. & TANNER, D.W. (1974). Time dependence of compressibility for remoulded and undisturbed soils. J. Soil Sci. 25 (2), 153-164.

DOMZAL, M. & SLOWINSKA-JURKIEWICZ, A. (1975). Effect of pressure on structure of pores and on water capacity of soils. Roczniki Glebozn 26 (1), 49-60.

DUNLAP, W.H. & WEBER, J.A. (1971). Compaction of unsaturated soil under a general state of stress. Trans. Am. Soc. agric. Engrs 14 (4), 601-607.

DWYER, M.J. (1970). Compaction problems on Agricultural Soils. Natn. Inst. agric. Engng, Dept. Note DN/TE/ 011/1450. Silsoe : NIAE (unpublished).

ERIKSSON, J., DANFORS, B. & HÅKANSSON, I. (1974). The effect of soil compaction on soil structure and crop yields. Bull.354 Swed. Inst. agric. Engng, Uppsala, Engl. trans.

FAURE, A. & FIES, J.C. (1972). (Experimental study of the susceptibility of loose materials to compaction in relation to their particle size distribution.) Annls Agron. 23 (3),317-332.

FEKETE, A. (1972). Estimation of the effect of tyres on soil density. Mezög. Gépes. tanulmányuk, 1972 (4), 16-18.

FEKETE, A., BAGANZ, K. & HELBIG, W. (1975). Some observations on soil compaction under a tyre. J. Terramechanics 12 (3/4), 217-223.

FOLINENKO-BORODICH, M. (1965). Theory of Elasticity. New York : Dover Publications.

FOUNTAINE, E.R. & PAYNE, P.J. (1952). Effect of tractors on volume weight and other soil properties. Natn. Inst. agric. Engng, Case Study 17. Silsoe : NIAE.

FRANKLIN, A.G., OROZCO, L.F. & SEMRAU, R. (1973). Compaction and strength of slightly organic soils. J. of Soil Mech. Fdns. Div. Am. Soc. civ. Engrs 99, 451-557.

FREDLUND, D.G. & MORGENSTERN, N.R. (1977). Stress state variables for unsaturated soils. Proc. Am. Soc. civ. Engrs, J. of Geotech. Engng Div. 103 (5), 447-466.

FREE, G.R., LAMBE, J. & CARLETON, E.A. (1947). Compactibility of certain soils as related to organic matter. J. Am. Soc. Agron. 39, 1068-1076.

FREITAG, D.R. (1971). Methods of measuring soil compaction. in 'Compaction of agricultural soils'. Am. Soc. agric. Engrs monograph,47-105. St. Joseph, Michigan : ASAE.

FROELICH, O.K. (1934). Druckveteilung im baugrunde. Vienna, 1934.

GARDNER, W.H., CAMPBELL, G.S. & CALISSENDORFF, C. (1972). Systematic and random errors in dual energy soil bulk density and water content measurements. Proc. Soil Sci. Soc. Am. 36, 393-486.

GEE-CLOUGH, D. (1976). The Bekker theory of rolling resistance amended to take account of skid and deep sinkage. J. Terramechanics 13 (2), 87-105.

GEE-CLOUGH, D., McALLISTER, M., PEARSON, G. & EVERNDEN, D.W. (1977). The empirical prediction of tractor-implement field performance. Natn. Inst. agric. Engng, Dept. Note DN/T/809/01006. Silsoe : NIAE (unpublished).

GILL, W.R. (1971). Economic assessment of soil compaction. 431-458 in Am. Soc. agric. Engrs monograph 'Compaction of agricultural soils'. St. Joseph, Michigan : ASAE.

GILL, W.R. & REAVES, C.A. (1956). Compaction patterns of smooth rubber tyres. Agric. Engng 37 (10), 677-680.

GODWIN, R.J. & SPOOR, G. (1977). Soil factors influencing workdays. Agric. Engr 32 (4), 87-90.

GRAECEN, E.L. (1960). Water content and soil strength. J. Soil Sci. 11 (2), 313-333.

HAKÅNSSON, I. (1973). The sensitivity of different crops to soil compaction. Proc. 6th Int. Conf. Soil Tillage Res. (ISTRO) 14:1-3, Wageningen, Neth.

HAKÅNSSON, I. (1974). Technical note in 'The effect of soil compaction on soil structure and crop yields'. Eriksson et al. 1974.

HALL, D.G.M., REEVE, M.J., THOMASSON, A.J. & WRIGHT, V.F. (1977). Water retention, porosity and density of field soils. Soil Survey Technical Monograph No.9. Harpenden : Soil Survey of England and Wales.

HEGEDUS, E. (1965). Pressure distribution under rigid wheels. Trans. Am. Soc. agric. Engrs 8 (3), 305-308, 311.

HENSHALL, J.K. (1978). The performance of an automatic recording balance system for use in soil testing. Scot. Inst. agric. Engng, Dept. Note SIN/246, Penicuik : SIAE (unpublished).

HETTIARATCHI, D.R.P. & REECE, A.R. (1975). Boundary wedges in two dimensional passive soil failure. Géotechnique 25 (2), 197-220.

HOLMS, J.C. & LOCKHART, D.A.S. (1970). Cultivations in relation to continuous barley growing. I. Crop growth and development. Proc. Int. Conf. Tillage Res. Methods (Silsoe, 1970), 46-57.

HOVANESIAN, J.D. & BUCHELE, W.F. (1959). Development of a recording volumetric transducer for studying effects of soil parameters on compaction. Trans. Am. Soc. agric. Engrs, 2 (1), 78-81.

HOWE, S. (1977). 'On top of the job'. Power Farming, August 1977, 53.

INNS, F.M. & KILGOUR, J. (1978). Agricultural tyres. London : Dunlop Ltd.

ISHII, K. & TOKUGANA, Y. (1967). (Soil compaction caused by tractor traffic. 1. Effect of soil moisture contents.) J. Sci. Soil and Manure, Tokyo, 38, 36 72.

ISHII, K. & TOKUGANA, Y. (1972). Soil compaction caused by tractor traffic. 5. Distribution of pressure produced. J. Sci. Soil and Manure, Tokyo, 43 (1), 1-7.

JURGENSON, L. (1934). The application of theories of elasticity and plasticity to foundation problems. J. Boston Soc. civil Engrs 21 (3), 206-241.

KAWANO, Y. & HOLMS, W.E. (1958). Compaction tests as a means of soil structure evaluation. Proc. Soil Sci. Soc. Am. 22 (5), 369-372.

KHAMIDOV, A. (1960). (Use of gamma rays in the study of the effects of wheels on the soil.) (Trudy. VIM 1960 (28), 94-107.) Trans. in J. agric. Engng Res. 6 (2), 147-152.

KITANI, O & PERSSON, P.E. (1967). Stress strain relationships for soil with variable lateral strain. Trans. Am. Soc. agric. Engrs 10, 738-741.

KOLOBOV, G.G. (1966). Soil pressure measurement beneath tractor wheels. J. Terramechanics 3 (4), 9-15.

KOOLEN, A.J. (1974). A method for soil compactibility determination. J. Agric. Engng Res. 19, 271-278.

KRICK, G. (1969). Radial and shear stress distribution under rigid wheels and pneumatic tyres operating on yielding soils with consideration of tyre deformation. J. Terramechanics 6 (3), 73-98.

KUIPERS, H. (1959). Confined compression tests on soil aggregate samples. Meded. LandbHoogesch. OpzoekStns. Gent. 24, 349-357.

KUMAR, L. & WEBER, J.A. (1974). Compaction of unsaturated soils by different stress paths. Trans. Am. Soc. agric. Engrs 17, 1064-1069, 1072.

KUNIN, N.F. & BUSHMIN, A.P. (1967). 'The mechanics of compacting soils' from 'Collected works of agricultural mechanics', Vol.7, 206-211. Machine Construction Publishing House. (Natn. Inst. agric. Engng translation, Silsoe : NIAE).

KURTAY, T. & REECE, A.R. (1970). Plasticity theory and Critical State soil mechanics. J. Terramechanics 7 (3 & 4), 23-56.

LAMBE, W.T. (1958). The engineering behaviour of compacted clay. Proc. Am. Soc. civ. Engrs, J. Soil. Mech. and Found. Div., SM2, Paper 1655, 1-35.

LARSON, W.E. & ALLMARAS, R.R. (1971). Management factors and natural forces as related to compaction, in Am. Soc. agric. Engnrs 'Compaction of Agricultural Soils', 367-427. St. Joseph, Michigan : ASAE.

M.A.F.F. (Agricultural Advisory Council) (1970). Modern farming and the soil. London : H.M.S.O.

M.A.F.F. (1976). Selection, care and use of agricultural tyres. A.D.A.S. Mechanization leaflet 30. M.A.F.F. : H.M.S.O.

M.A.F.F. (1978). Statistical information : December, 1977 agricultural returns for England and Wales. Supplement to Press Notice No.68 (Machinery items). (Stats.198/78) M.A.F.F. Press office.

McKIBBEN, E.G. (1971). Introduction to 'Compaction of Agricultural Soils'. Am. Soc. agric. Engrs monograph. St. Joseph, Michigan : ASAE.

McLEOD, H.E., REED, I.F. & GILL, W.R. (1966). Draft, Power, Efficiency and Soil compaction characteristics of single, dual and low pressure tyres. Trans. Am. Soc. agric. Engrs 9, 41-44.

McMURDIE, J.L. & DAY, P.R. (1958). Compression of soil by isotropic stress. Proc. Soil Sci. Soc. Am. 22, 18-21.

MAJIDZADEH, K. & GUIRGUIS, H.R. (1973). Fundamentals of soil compaction and performance. In Highway Research Record 438. "Soil compaction and corrugations".

MÖLLER, N. (1975). A data collection system for engineering measurements in tillage research. Swed. J. agric. Res. 5, 101-111.

MULQUEEN, J., STAFFORD, J.V. & TANNER, D.W. (1976). Evaluation of penetrometers for measuring soil strength. Natn. Inst. agric. Engng, Dept. Note DN/T/738/1162. Silsoe : NIAE(unpub.)

NAGAHORI, K. & SATO, K. (1974). (Subsoil characteristics in a paddy field as affected by the passage of a bulldozer. Soil compaction in a sloping clayey paddy field.) Science reports of the Faculty of Agriculture, Okayama Univ. 43, 85-93.

NICHOLS, M.L. (1937). Models of research in soil dynamics as applied to implement design. Bull.229. Alabama exp. st. Alabama Polytech. Inst., Auburn, Alabama.

ONAFEKO, O. & REECE, A.R. (1967). Soil stresses and deformations beneath rigid wheels. J. Terramechanics 4 (1), 59-80.

PERDOK, U.D. (1976). Soil workability and stability to vehicular traffic. Landbouk. Tijdscht 88 (6), 173-178.

PERUMPRAL, J.V., LILJEDAHL, J.B. & PERLOFF, W.H. (1969). The finite element method for predicting stresses and soil deformation under a tractive device. Am. Soc. agric. Engrs paper 69-680, (presented at An. meeting ASAE, Chicago).

PERUMPRAL, J.V., LILJEDAHL, J.B. & PERLOFF, W.H. (1971). A numerical model for predicting stresses and soil deformation under a tractor wheel. J. Terramechanics, 8 (1), 9-22.

PIDGEON, J.D. (1975). Soil responses to reduced cultivations and direct drilling for continuous barley at South Road, 1973. Scot. Inst. agric. Engng Dept. Note SIN/198. Penicuik:SIAE(unpub.)

PIDGEON, J.D. & RAGG, J.M. (1978). Soil, climatic and management options fordirect drilling cereals in Scotland. Outlook in Agriculture. Special number, 1978.

PIDGEON, J.D. and SOANE, B.D. (1978). Soil structure and strength relations following tillage, zero tillage and wheel traffic in Scotland. p 371-378 in 'Modification of Soil Structure' Ed. Emerson, W.W. et al. John Wiley and Sons, 1978.

POHJAKAS, K. (1966). The effect of soluble salts on the compactability of four Saskatchewan soils. Can. J. Soil Sci. 46, 47-52.

POTOMIAS, C. (1976). Critical state parameters of unsaturated soils. M.Sc. thesis Univ. Newcastle upon Tyne. Dept. agric. Engng, May 1976.

POULOS, H.G. & DAVIES, E.H. (1974). Elastic solutions for soil and rock mechanics. New York : Wiley.

PROCTOR, R.R. (1933). Fundamental principles of soil compaction. Engng News Rec. 111, 245-248, 286-289, 348-351.

RAGG, J.M. & FUTTY, D.W. (1967). Soils of the country around Haddington and Eyemouth. Mem. Soil Survey of Grt. Britain, Edinburgh : H.M.S.O.

RAGHAVAN, G.S.V., McKYES, E., BEAULIEU, B., MÉRINEAU, F. & AMIR, I. (1976a). Study of traction and compaction problems on Eastern Canadian agricultural soils. II. Report to Agriculture Canada. Engng Res. Services.Serial OSW 5-0010. Dept. Ag.Engng, McGill University, Canada.

RAGHAVAN, G.S.V., McKYES, E., AMIR, I., CHASSÉ, M. & BROUGHTON,R.S. (1976b). Prediction of compaction due to off-road vehicle traffic. Trans. Am. Soc. agric. Engrs 19 (4), 107-115.

RAGHAVAN, G.S.V. & McKYES, E. (1977a). Study of traction and compaction problems on Eastern Canadian Soils III. Report to Agriculture Canada. Engng Res. Services.OSW 76-00030. Dept. Agric. Engng, McGill University, Canada. (Also partly reported in Raghavan & McKyes, 1978. Statistical models for predicting compaction generated by off-road vehicular traffic on different soil types. J. Terramechanics 15 (1), 1-14.)

RAGHAVAN, G.S.V., McKYES, E. & CHASSÉ, M. (1977b). Effect of wheel slip on soil compaction. J. agric. Engng Res. 22, 79-83.

RANEY, W.A. & EDMINSTER, T.W. (1961). Approaches to soil compaction research. Trans. Am. Soc. agric. Engrs 4 (2),246-248.

REAVES, I.F. & COOPER, A.W. (1960). Stress distribution in soil under tractor loads. Agric. Engng 41 (1), 20-21, 31.

REAVES, C.A. & NICHOLS, M.L. (1955). Soil surface reaction to pressure. Ag. Engng 36, 813-820.

REECE, A.R. (1976). Compaction, loosening and the cultivation of soil. Proc. 8th Int. Conf. ag. Mechnization (F.I.M.A.), Zaragoza, 5, 1-20. Spain, 1976.

REECE, A.R. (1977). Soil mechanics of agricultural soils. Soil Sci. 123 (5), 332-337.

REED, I.F., COOPER, A.W. & REAVES, C.A. (1959). Effect of 2 wheel and tandem drives on traction and soil compacting stresses. Trans. Am. Soc. agric. Engrs 2 (1), 22-25.

RICHARDS, L.A. (1965). Physical condition of water in soil.in 'Methods of Soil Analysis. Pt. 1 Physical and Minereological Properties', Ed. Black, C.A. (1965). Agronomy monograph No.9, Am. Soc. Agronomists. Maddison, Wisconsin.

RICHARDSON, R.C.D. (1969). The wear of metal shares in agricultural soil. Ph.D. Thesis. Univ. London, 1969.

RIECHMANN, E. (1965). (Determination of soil compaction due to travel of soil of tractors and farm machinery.) Mittbund vers Aust. Landw. Masch. Wieselburg 11 (4), 229-325.

ROSCOE, K.H., SCHOFIELD, A.N. & WROTH, C.P. (1958). On the yielding of soils. Geotechnique 8, 22-53.

SACK, H. (1962). (On the causes of soil compaction in the furrow bottom, and how to avoid it.) Grundl. Landtech. 1962 (15), 5-10. (Natn. Inst. agric. Engng translation 129) Silsoe : NIAE.

SCHOFIELD, A. & WROTH, P. (1968). Critical state soil mechanics. New York : McGraw-Hill.

SCOTT BLAIR, G.W. (1937). Compressibility curves as a quantitative measure of soil tilth. J. agric. Sci. 27 (4),541-556.

SELIG, E.T. & GRANGAARD, O.M. (1970). A new technique for soil strain measurement. Mat. Res. and Standards, MTRSA, 10 (10), 19-21.

SITKEI, G. & FEKETE, A. (1974). Bodenverdichtung unter Schlepper und Ackerwagenreifen. Budapest : Uppsato.

SMART, P. (1975). Experimental stress-strain curves. Civ. Engng, August 1975, 39.

SMITH, G.N. (1971). An introduction to matrix and finite element methods in civil engineering. London : Applied Science.

SOANE, B.D. (1967). Double energy gamma ray transmission and density measurement in soil tillage studies. Int. Soil Water Symp. Int. Comm. on Irrig. and drainage. Prague : Disc.I : 197-205.

SOANE, B.D. (1970). The effect of traffic and implements on soil compaction. J. Proc. Instn. agric. Engrs 25 (3), 115-126.

SOANE, B.D. (1973). Review of cultivation and compaction research. Paper No.2.Proc. Natn. Inst. agric. Engng Subject day. 'Mechanical behaviour of agricultural soils'. Silsoe : NIAE.

SOANE, B.D. (1974a). Effect of probe spacing on the performance of soil density gamma ray transmission equipment with a geiger muller detector. Scot. Inst. agric. Engng,Dept. Note SSN/171. Penicuik : SIAE (unpublished).

SOANE, B.D. (1974b). Insertion of narrow bore gamma ray transmission probes by hydraulic jacking. Scot. Inst. agric. Engng Dept. Note SSN/170. Penicuik : SIAE (unpublished).

SOANE, B.D. (1974c). A test vehicle for the rapid determination of soil physical properties in the field. Trans. 10th Int. Cong. Int. Soil Sci. Soc., Moscow, 1974, I : 363-368.

SOANE, B.D. (1975). Studies in some soil physical properties in relation to cultivations and traffic. p 160-183 in 'Soil physical conditions and crop production'. M.A.F.F. Tech. Bull.29. London : H.M.S.O.

SOANE, B.D. (1976a). Soil responses to reduced cultivation and direct drilling for continuous barley at South Road: preliminary studies, 1967. Scot. Inst. agric. Engng,Dept. Note SIN/196. Penicuik : SIAE (unpublished).

SOANE, B.D. (1976b). Soil responses to reduced cultivation and direct drilling for continuous barley at South Road, 1971 and 1972. Scot. Inst. agric. Engng,Dept. Note SIN/197. Penicuik : SIAE (unpublished).

SOANE, B.D. (1977). Gamma ray transmission systems for the *in situ* measurement of packing state - review paper. In Biennial report of Scot. Inst. agric. Engng 1977, 59-86. Edinburgh : SIAE.

SOANE, B.D. & CAMPBELL, D.J. (1967). The effect of conventional and rotary ploughing in autumn and spring on some physical properties of the soil. Scot. Inst. agric. Engng, Soils Lab. int. rept. 18. Penicuik : SIAE (unpublished).

SOANE, B.D. & CAMPBELL, D.J. (1970). Standard methods for determination of mechanical properties of soil. Scot. Inst. agric. Engng, Dept. Note SSN.59. Penicuik : SIAE (unpublished).

SOANE, B.D., CAMPBELL, D.J. & HERKES, S.M. (1970). Cultivations in relation to continuous barley growing. II. Soil physical conditions. Proc. Inst. Conf. Tillage Res. Methods. Silsoe, 1970, 58-76.

SOANE, B.D., CAMPBELL, D.J. & HERKES, S.M. (1971). Hand held gamma ray transmission equipment for the measurement of bulk density of field soils. J. ag. Engng Res. 16, 146-156.

SOANE, B.D., CAMPBELL, D.J. & HERKES, S.M. (1972). Characterization of some Scottish arable topsoils by agricultural and engineering methods. J. Soil Sci. 23 (1), 93-104.

SOANE, B.D., KENWORTHY, G. & PIDGEON, J.D. (1976). Soil tank and field studies of compaction under wheels. Proc. 7th Inst. Soil Tillage Res. Stockholm, Sweden, 48: 1-6.

SOANE, B.D., PIDGEON, J.D., BLACKWELL, P.S. & DICKSON, J.W. (1977). Compaction under wheels - a note on research in progress at the Scottish Institute of Agricultural Engineering. Soil and Water, 5 (4), 2-6.

SÖHNE, W. (1953). Pressure distribution in the soil and soil deformation under tractor tyres. Grundl. Landtech. 5, 49-63.

SÖHNE, W. (1958). Fundamentals of pressure distribution and soil deformation under tractor tyres. Ag. Engng 39 (5), 276-286,290.

SÖHNE, W., CHANCELLOR, W.J. & SCHMIDT, R.H. (1962). Investigation of the compactability of some California soils. Univ. California, Davis, unpublished.

SOMMER, C., STOINEV, K. & ALTEMÜLLER, H.J. (1972). (The behaviour of four different model soils under vertical pressure). Landbforsch-Völkenrode 22 (1), 45-56.

SPOTTS, J.W. & BROWN, K.W. (1975). A technique for installing induction coils in a soil profile with a minimum of disturbance. Proc. Soil Sci. Soc. Am. 39, 1006-1007.

STEINHARDT, R. (1974). Evaluating penetration resistance and wheel sinkage response to soil water suction changes in draining clay soils. Proc. Soil Sci. Soc. Am. 38(3),518-522.

STEINHARDT, R. & TRAFFORD, B.D. (1974). Some effects of subsurface drainage and ploughing on the structure and compactability of clay soil. J. Soil Sci. 25 (2), 138-152.

STUPICA, T. (1974). (Soil compaction and pore size distribution as affected by soil cultivation.) Zbornik Biotechniske Fakultete Univerze v Ljubljani, Kmetijstvo, 23, 35-55.

TAYLOR, H.M. & VOMOCIL, J.A. (1959). Changes of soil compressibility associated with poly electrolyte treatment. Proc. Soil Sci. Soc. Am. 23 (3), 181-183.

THADDEN, T.J. (1962). Operating characteristics of radial-ply tractor tyres. Trans. Am. Soc. agric. Engrs 5 (1), 109-110.

TRABBIC, G.W., LASK, K.V. & BUCHELLE, W.F. (1959). Measurement of soil-tyre interface pressures. Ag. Engng 40 (11), 678-681.

TROUSE, A.C. (1971). Soil conditions as they affect plant establishment, root development and yield. A. Present knowledge and need for research. 225-276 in Am. Soc. agric. Engrs monograph 'Compaction of agricultural soils'. St. Joseph, Michigan : ASAE.

VANDEN BERG, G.E. (1966). Triaxial measurements of shear strain and compaction in unsaturated soils. Trans. Am. Soc. agric. Engrs 9, 460-467.

VANDEN BERG, G.E. & GILL, W.R. (1962). Pressure distribution between a smooth tyre and soil. Trans. Am. Soc. agric. Engrs 5 (2), 105-107.

VANDEN BERG, G.E., REED, I.F. & COOPER, A.W. (1961). Evaluating and improving performance of traction devices. Proc. 1st Int. Conf. on Soil Vehicle Systems. Turin, 402-411.

VERMA, B.P., BAILEY, A.C., SCHAFER, R.R. & FUTRAL, J.G. (1975). A pressure transducer in soil compaction study. Am. Soc. agric. Engrs paper 75-1034. (Ann. Meeting ASAE, Davies, Calif.)

VERMA, B.P. & FUTRAL, J.H. (1975). A pressure transducer for deforming media. Am. Soc. agric. Engrs paper 75-5009. (Ann. Meeting ASAE, Davies, Calif.)

VILA, J.J. (1978). The effect of tillage and zero tillage on soil water properties. M. Phil. thesis, Univ. Edinburgh, in preparation, 1978.

VOMOCIL, J.A., FOUNTAINE, E.R. & REGINATO, R.J. (1958). Influence of drawbar load on the compacting effect of wheeled tractors. Proc. Soil Sci. Soc. Am. 22, 178.

WEAVER, H.A. & JAMISON, V.C. (1951). Effects of moisture on tractor tyre compaction of soil. Soil Sci. 71, 15-23.

WINDISCH, E. & YONG, R.N. (1970). The determination of strain-rate behaviour beneath a moving wheel. J. Terramechanics 7, 55-67.

WONG, J. & REECE, A.R. (1967). Prediction of rigid wheel performance, based on the analysis of soil-wheel stresses. 1. Performance of driven rigid wheels. J. Terramechanics 4 (1), 81-98.

YAACOB, O. (1976). Field techniques for obtaining a large number of undisturbed soil cores. Malaysian agric. Res. 5 (1), 83-85.

YONG, R.N. (1973). Predictive requirements for physical performance of mobility. J. Terramechanics 10 (4), 47-60.

YONG, R.N. & FATTAH, E.A. (1976). Prediction of wheel-soil interaction and performance using the finite element method. J. Terramechanics 13 (4), 227-240.

YONG, R.N., FATTAH, E.A. & BOONSINSUK, P. (1978). Analysis and prediction of tyre-soil interaction and performance using finite elements. J. Terramechanics 15 (1), 43-63.

YOSHIDA, I. & KAKU, K. (1976). Study of the vertical stress distributions in artificial soil grounds. Agric. Bull. Saga. Univ. 41, 55-64.

ZIENCEWICH, O.C. (1971). The finite element method in engineering science. New York : McGraw-Hill.

APPENDIX 1 TABLE A — CALIBRATION OF THE INTERNAL PRESSURE (BAR) OF THE WATER FILLED RUBBER BALL, UNDER AIR PRESSURE, AT DIFFERENT TEMPERATURES. EACH VALUE IS A MEAN OF TWO READINGS FROM FOUR DIFFERENT BALLS. STANDARD ERRORS SHOWN IN PARENTHESES

| Temp. °C | Applied air pressure, bar | | | | | | |
|---|---|---|---|---|---|---|---|
| | 0 | 0.5 | 1.0 | 1.5 | 2.0 | 2.5 | 3.0 |
| 7 | 0.128 (0) | | | 1.152 (0.04) | | | 2.29 (0.058) |
| 10 | 0.146 (0) | | | 1.138 (0.035) | | | 2.19 (0.066) |
| 14 | 0.169 (0.017) | 0.466 (0.038) | 0.786 (0.047) | 1.106 (0.047) | 1.403 (0.07) | 1.725 (0.018) | 2.03 (0.091) |
| 20 | 0.164 (0.015) | | | 1.074 (0.043) | | | 1.90 (0.0895) |
| 22 | 0.165 (0.015) | | | 1.050 (0.05) | | | 1.81 (0.09) |

TABLE B — CALIBRATION OF THE INCREASE OF INTERNAL PRESSURE (BAR) OF THE WATER FILLED RUBBER BALL, UNDER DEVIATOR LOADING AT DIFFERENT TEMPERATURES. EACH VALUE IS A MEAN OF EIGHT READINGS. STANDARD ERRORS ARE SHOWN IN PARENTHESES

| | | Applied deviator load, kg | | | | | |
|---|---|---|---|---|---|---|---|
| | 0 | 0.5 | 1.5 | 2.5 | 3.5 | 5.5 | 7.5 |
| deflection* | 68 | 63 | 54 | 47 | 45 | 40 | 37 |
| Temp., °C | | | | | | | |
| 15 | 0.0 | 0.025 (0.020) | 0.080 (0.035) | 0.098 (0.050) | 0.130 (0.065) | 0.280 (0.010) | 0.460 (0.010) |
| 22 | 0.0 | 0.030 (0.001) | 0.082 (0.010) | 0.142 (0.009) | 0.210 (0.011) | 0.423 (0.009) | 0.708 (0.004) |

* distance between outer surfaces of parallel plates, mm.

APPENDIX 1 TABLE C — CALIBRATION OF MINOR AXIS OF MASTIC BALLS (mm) AGAINST DIFFERENT LEVELS OF DEVIATOR LOAD AT DIFFERENT TEMPERATURES BEFORE AND AFTER FIELD TESTS. EACH VALUE IS A MEAN OF TWO READINGS FROM FOUR DIFFERENT BALLS. MEAN STANDARD DEVIATIONS SHOWN IN PARENTHESES

| Temp., °C | Deviator load, kg | | | | | | | Mean s.e. |
|---|---|---|---|---|---|---|---|---|
| | 0 | 0.5 | 1.5 | 2.5 | 3.5 | 5.5 | 7.5 | |
| Before field tests | | | | | | | | |
| 10°C | 38 | 34.5 | 30.5 | 27.5 | 24.0 | 22.0 | 20.0 | 1.5 |
| 15°C | 38 | 31.5 | 27.0 | 23.2 | 21.0 | 22.0 | 20.0 | 1.3 |
| After field tests | | | | | | | | |
| 16°C | 38 | 36.0 | 32.5 | 30.0 | 27.2 | 22.8 | 19.8 | 0.9 |
| 19°C | 38 | 34.0 | 30.0 | 26.5 | 25.5 | 20.5 | 17.3 | 0.9 |

APPENDIX 1

TABLE D

THE EFFECT OF 'FOAM' RUBBER PAD THICKNESS UPON THE RESPONSE OF THE WATER FILLED BALL TO DEVIATOR LOADING (c.f. SECTION 3.2.3), 13°C

| Deviator load, kg | Mean signal from pressure transducer, mV | | | s.e. |
|---|---|---|---|---|
| | No pad | 1.0 cm pad | 2.5 cm pad | |
| 0 | 1.0 | 0.95 | 0.9 | 0.1 |
| 0.5 | 1.1 | 1.0 | 1.0 | 0.1 |
| 1.5 | 1.4 | 1.3 | 1.25 | 0.1 |
| 2.5 | 1.9 | 1.6 | 1.5 | 0.1 |
| 3.5 | 2.4 | 2.0 | 1.9 | 0.15 |
| 4.5 | 3.0 | 2.4 | 2.3 | 0.1 |
| 5.5 | 3.6 | 2.9 | 2.7 | 0.1 |
| 6.5 | 4.1 | 3.2 | 3.0 | 0.15 |
| 7.5 | 4.5 | 3.5 | 3.35 | 0.15 |

APPENDIX 2 (TABLE 6)

DATA FROM THE CALIBRATION OF THE GYPSUM RESISTANCE BLOCKS

All moisture meter data in moisture meter units, at 18-20°C. * = equilibrium condition

| Date | Time | Moisture block no. 1 | 2 | 3 | Vessel pressure, bar | Bottle pressure, kg/cm$^2$ | Burette reading, cc |
|---|---|---|---|---|---|---|---|
| 1.5.77 | 9.00 | 80 | 62 | 65 | 1.40 | 120 | max. |
| 2.5.77 | 9.00 | 50 | 38 | 46 | 1.70 | 110 | " |
| 2.5.77 | 17.00 | 59 | 40 | 49 | 1.40 | 110 | " |
| 3.5.77 | 9.00 | 52 | 39 | 46 | 1.55 | 110 | 49 |
| 3.5.77 | 12.00 | 51 | 38 | 46 | 1.60 | 110 | 49 |
| 3.5.77 | 20.00 | 50 | 37 | 46 | 1.60 | 110 | 49* |
| 4.5.77 | 9.00 | 83 | 70 | 77 | 1.0 | 105 | 44 |
| 5.5.77 | 9.00 | 71 | 54 | 63 | 1.05 | 100 | 43.5 |
| 5.5.77 | 12.00 | 71 | 54 | 63 | 1.00 | 100 | 43.5* |
| 6.5.77 | 9.00 | 78 | 62 | 72 | 0.70 | 100 | 44.0 |
| 6.5.77 | 17.00 | 82 | 70 | 76 | 0.60 | 100 | 45.5 |
| 7.5.77 | 14.00 | 76 | 60 | 69 | 0.75 | 100 | 44 |
| 8.5.77 | 14.00 | 76 | 58 | 67 | 0.80 | 95 | 44* |
| 9.5.77 | 8.00 | 74 | 56 | 64 | 1.00 | 95 | 44 |
| 9.5.77 | 12.00 | 48 | 36 | 40 | 3.15 | 90 | 35.6 |
| 9.5.77 | 18.00 | 37 | 31 | 33 | 3.45 | 90 | 25.5 |
| 10.5.77 | 9.00 | 26 | 22 | 26 | 3.05 | 84 | 47.5 |
| 10.5.77 | 14.00 | 22 | 20 | 22 | 3.5 | 80 | 44 |
| 10.5.77 | 20.00 | 22 | 20 | 20 | 3.9 | 80 | 43* |
| 11.5.77 | 8.00 | 14 | 18 | 13 | 4.5 | 70 | 40 |
| 12.5.77 | 14.00 | 16 | 14 | 15 | 5.0 | 20 | 32.5* |
| 12.5.77 | 14.00 | 8 | 7 | 13 | direct connection to blocks | | |

## APPENDIX 3 CALCULATION OF THE DRY BULK DENSITY OF SOIL SAMPLES BEING TESTED IN THE LABORATORY

The dry bulk density of the soil sample during any part of the test was calculated by the following formula:

$$Dbd_x = \frac{M}{SV + FV - x} \left(1 - \frac{w}{100}\right), \quad g/cm^3$$

where $Dbd_x$ = dry bulk density corresponding to a reading of x cc of the air volume measurement cylinder

$x$ = reading from the air volume measurement cylinder, cc (30s after stress application and corrected for back pressure)[2]

$M$ = wet mass of soil, g

$SV$ = final sample volume, measured by wax coating method, cc

$FV$ = final reading from the air volume measurement cylinder (total volume of soil air outside the sample at the end of the test[1]), cc

$W$ = gravimetric moisture content of the sample, % w/w

---

1. If the water meniscus in the cylinder had been raised during the test, when the capacity of the cylinder had been reached, the actual readings taken after raising the meniscus would need correcting for thevolume of air already collected.
2. If the dry bulk density after 2 s. was required x became the air volume cylinder reading after 2 s., corrected for back pressure.

## APPENDIX 4 FIELD MEASUREMENTS OF DRY BULK DENSITY AND INITIAL CONE RESISTANCE

The following tables show the mean dry bulk density values at each depth measured beneath the centre line of the wheel treatments on each soil treatment for each occasion and each soil. All depths are measured from the maximum rut depth.

The abbreviations used in the tables are as follows:

M = experimental occasion of different soil moisture status, see Tables 10 and 13, Chap.4.

RL = soil treatment, of different initial dry bulk density, see Tables 9 and 12, Chap.4.

W = wheel treatment, see Table 4, Chap.3.

Table A. Section 7, 1976, Macmerry Soil.

Table B. Lower Terrace field, 1977, Threipmuir Soil.

TABLE A DRY BULK DENSITY MEASUREMENTS AT 3 cm INTERVALS BELOW MAXIMUM RUT DEPTH. EACH FIGURE IS A MEAN OF 6, UNITS g/cm3 MACMERRY

| Occasion | depth, cm | TREATMENTS RL1 W1 | RL1 W2 | RL1 W3 | RL2 W1 | RL2 W2 | RL2 W3 |
|---|---|---|---|---|---|---|---|
| M1 | 3 | 1.062 | 1.122 | 1.266 | 1.172 | 1.910 | 1.155 |
| | 6 | 1.235 | 1.252 | 1.340 | 1.223 | 1.216 | 1.273 |
| | 9 | 1.272 | 1.279 | 1.328 | 1.240 | 1.258 | 1.264 |
| | 12 | 1.262 | 1.306 | 1.330 | 1.249 | 1.257 | 1.259 |
| | 15 | 1.231 | 1.308 | 1.332 | 1.244 | 1.260 | 1.261 |
| | 18 | 1.268 | 1.312 | 1.346 | 1.260 | 1.266 | 1.269 |
| | 21 | 1.265 | 1.351 | 1.381 | 1.271 | 1.272 | 1.278 |
| | 24 | 1.313 | 1.380 | 1.451 | 1.335 | 1.328 | 1.348 |
| | 27 | 1.398 | 1.432 | 1.491 | 1.389 | 1.389 | 1.389 |
| | 30 | 1.473 | 1.468 | 1.495 | 1.440 | 1.336 | 1.433 |
| | 33 | 1.505 | 1.506 | 1.485 | 1.461 | 1.351 | 1.429 |
| M2 | 3 | 0.999 | 1.112 | 1.223 | 1.166 | 1.305 | 1.112 |
| | 6 | 1.207 | 1.241 | 1.285 | 1.253 | 1.297 | 1.305 |
| | 9 | 1.222 | 1.248 | 1.306 | 1.236 | 1.269 | 1.281 |
| | 12 | 1.260 | 1.272 | 1.347 | 1.237 | 1.244 | 1.298 |
| | 15 | 1.286 | 1.270 | 1.345 | 1.239 | 1.255 | 1.337 |
| | 18 | 1.306 | 1.283 | 1.353 | 1.244 | 1.284 | 1.344 |
| | 21 | 1.290 | 1.282 | 1.384 | 1.231 | 1.269 | 1.322 |
| | 24 | 1.299 | 1.307 | 1.417 | 1.222 | 1.294 | 1.394 |
| | 27 | 1.383 | 1.423 | 1.522 | 1.362 | 1.384 | 1.481 |
| | 30 | 1.484 | 1.543 | 1.568 | 1.450 | 1.440 | 1.520 |
| | 33 | 1.554 | 1.567 | 1.593 | 1.508 | 1.442 | 1.535 |
| M3 | 3 | 1.279 | 1.307 | 1.347 | 1.281 | 1.321 | 1.385 |
| | 6 | 1.319 | 1.371 | 1.386 | 1.324 | 1.350 | 1.380 |
| | 9 | 1.312 | 1.371 | 1.392 | 1.344 | 1.350 | 1.360 |
| | 12 | 1.313 | 1.366 | 1.408 | 1.329 | 1.340 | 1.389 |
| | 15 | 1.301 | 1.357 | 1.388 | 1.297 | 1.317 | 1.363 |
| | 18 | 1.280 | 1.368 | 1.409 | 1.300 | 1.342 | 1.372 |
| | 21 | 1.350 | 1.387 | 1.417 | 1.313 | 1.360 | 1.402 |
| | 24 | 1.365 | 1.448 | 1.447 | 1.335 | 1.393 | 1.411 |
| | 27 | 1.450 | 1.540 | 1.491 | 1.399 | 1.431 | 1.429 |
| | 30 | 1.543 | 1.625 | 1.557 | 1.448 | 1.449 | 1.453 |
| | 33 | 1.613 | 1.658 | 1.577 | 1.481 | 1.484 | 1.472 |
| M4 | 3 | 1.377 | 1.246 | 1.339 | 1.289 | 1.346 | 1.303 |
| | 6 | 1.350 | 1.365 | 1.303 | 1.343 | 1.376 | 1.344 |
| | 9 | 1.341 | 1.391 | 1.403 | 1.349 | 1.361 | 1.349 |
| | 12 | 1.347 | 1.364 | 1.396 | 1.344 | 1.356 | 1.357 |
| | 15 | 1.347 | 1.369 | 1.380 | 1.333 | 1.321 | 1.353 |
| | 18 | 1.355 | 1.359 | 1.400 | 1.352 | 1.348 | 1.357 |
| | 21 | 1.372 | 1.381 | 1.401 | 1.372 | 1.376 | 1.390 |
| | 24 | 1.422 | 1.434 | 1.475 | 1.383 | 1.419 | 1.411 |
| | 27 | 1.488 | 1.510 | 1.534 | 1.416 | 1.443 | 1.433 |
| | 30 | 1.554 | 1.591 | 1.590 | 1.478 | 1.475 | 1.453 |
| | 33 | 1.606 | 1.608 | 1.584 | 1.509 | 1.519 | 1.470 |

| Occasion | depth, cm | TREATMENTS | | | | | |
|---|---|---|---|---|---|---|---|
| | | RL3 | | | RL4 | | |
| | | W1 | W2 | W3 | W1 | W2 | W3 |
| M1 | 3 | 1.157 | 1.261 | 1.265 | 1.260 | 1.237 | 1.265 |
| | 6 | 1.306 | 1.277 | 1.300 | 1.293 | 1.347 | 1.352 |
| | 9 | 1.279 | 1.288 | 1.311 | 1.307 | 1.321 | 1.334 |
| | 12 | 1.271 | 1.305 | 1.327 | 1.275 | 1.320 | 1.331 |
| | 15 | 1.255 | 1.264 | 1.308 | 1.293 | 1.272 | 1.338 |
| | 18 | 1.264 | 1.265 | 1.308 | 1.265 | 1.259 | 1.289 |
| | 21 | 1.283 | 1.309 | 1.309 | 1.282 | 1.269 | 1.311 |
| | 24 | 1.302 | 1.365 | 1.352 | 1.300 | 1.320 | 1.331 |
| | 27 | 1.381 | 1.396 | 1.403 | 1.412 | 1.389 | 1.409 |
| | 30 | 1.449 | 1.392 | 1.418 | 1.414 | 1.439 | 1.516 |
| | 33 | 1.471 | 1.399 | 1.418 | 1.428 | 1.470 | 1.529 |
| M2 | 3 | 1.230 | 1.202 | 1.298 | 1.302 | 1.152 | 1.348 |
| | 6 | 1.270 | 1.286 | 1.310 | 1.353 | 1.346 | 1.396 |
| | 9 | 1.261 | 1.305 | 1.308 | 1.328 | 1.351 | 1.377 |
| | 12 | 1.271 | 1.287 | 1.305 | 1.311 | 1.338 | 1.381 |
| | 15 | 1.233 | 1.273 | 1.333 | 1.281 | 1.320 | 1.372 |
| | 18 | 1.206 | 1.266 | 1.349 | 1.249 | 1.309 | 1.334 |
| | 21 | 1.214 | 1.265 | 1.349 | 1.254 | 1.324 | 1.354 |
| | 24 | 1.296 | 1.268 | 1.368 | 1.297 | 1.332 | 1.417 |
| | 27 | 1.409 | 1.374 | 1.462 | 1.369 | 1.389 | 1.451 |
| | 30 | 1.513 | 1.404 | 1.497 | 1.467 | 1.472 | 1.518 |
| | 33 | 1.539 | 1.454 | 1.518 | 1.523 | 1.546 | 1.539 |
| M3 | 3 | 1.367 | 1.325 | 1.365 | 1.367 | 1.397 | 1.423 |
| | 6 | 1.394 | 1.386 | 1.380 | 1.378 | 1.400 | 1.394 |
| | 9 | 1.365 | 1.359 | 1.389 | 1.340 | 1.375 | 1.370 |
| | 12 | 1.354 | 1.369 | 1.373 | 1.311 | 1.356 | 1.351 |
| | 15 | 1.352 | 1.334 | 1.359 | 1.288 | 1.346 | 1.353 |
| | 18 | 1.306 | 1.344 | 1.391 | 1.274 | 1.355 | 1.361 |
| | 21 | 1.326 | 1.366 | 1.387 | 1.311 | 1.358 | 1.359 |
| | 24 | 1.381 | 1.396 | 1.406 | 1.331 | 1.360 | 1.389 |
| | 27 | 1.497 | 1.501 | 1.484 | 1.415 | 1.431 | 1.458 |
| | 30 | 1.577 | 1.607 | 1.592 | 1.531 | 1.469 | 1.553 |
| | 33 | 1.595 | 1.607 | 1.592 | 1.553 | 1.500 | 1.584 |
| M4 | 3 | 1.347 | 1.370 | 1.366 | 1.392 | 1.370 | 1.389 |
| | 6 | 1.376 | 1.379 | 1.421 | 1.408 | 1.391 | 1.414 |
| | 9 | 1.356 | 1.379 | 1.390 | 1.386 | 1.372 | 1.416 |
| | 12 | 1.358 | 1.380 | 1.378 | 1.333 | 1.371 | 1.398 |
| | 15 | 1.350 | 1.359 | 1.350 | 1.369 | 1.364 | 1.388 |
| | 18 | 1.358 | 1.364 | 1.387 | 1.373 | 1.381 | 1.395 |
| | 21 | 1.403 | 1.371 | 1.412 | 1.379 | 1.393 | 1.393 |
| | 24 | 1.431 | 1.408 | 1.444 | 1.429 | 1.398 | 1.406 |
| | 27 | 1.491 | 1.467 | 1.505 | 1.480 | 1.437 | 1.458 |
| | 30 | 1.561 | 1.529 | 1.570 | 1.468 | 1.459 | 1.521 |
| | 33 | 1.596 | 1.545 | 1.600 | 1.505 | 1.499 | 1.562 |

TABLE B DRY BULK DENSITY MEASUREMENTS AT 3 cm INTERVALS BELOW MAXIMUM RUT DEPTH. EACH FIGURE IS A MEAN OF 6, UNITS $g/cm^3$ THREIPMUIR

| Occasion | depth, cm | TREATMENTS | | | | | | | | |
|---|---|---|---|---|---|---|---|---|---|---|
| | | RL1 | | | RL2 | | | RL3 | | |
| | | W1 | W2 | W3 | W1 | W2 | W3 | W1 | W2 | W3 |
| M1 | 3 | 1.148 | 1.214 | 1.168 | 1.181 | 1.188 | 1.256 | 1.272 | 1.224 | 1.301 |
| | 6 | 1.156 | 1.190 | 1.177 | 1.185 | 1.175 | 1.226 | 1.277 | 1.261 | 1.280 |
| | 9 | 1.145 | 1.191 | 1.202 | 1.214 | 1.170 | 1.244 | 1.296 | 1.339 | 1.295 |
| | 12 | 1.142 | 1.181 | 1.245 | 1.228 | 1.195 | 1.287 | 1.294 | 1.354 | 1.279 |
| | 15 | 1.220 | 1.244 | 1.240 | 1.289 | 1.268 | 1.309 | 1.345 | 1.325 | 1.300 |
| | 18 | 1.239 | 1.249 | 1.208 | 1.342 | 1.320 | 1.273 | 1.389 | 1.350 | 1.268 |
| | 21 | 1.242 | 1.251 | 1.230 | 1.390 | 1.336 | 1.292 | 1.361 | 1.366 | 1.306 |
| | 24 | 1.304 | 1.322 | 1.327 | 1.355 | 1.332 | 1.377 | 1.444 | 1.446 | 1.413 |
| | 27 | 1.346 | 1.444 | 1.440 | 1.466 | 1.362 | 1.501 | 1.596 | 1.503 | 1.502 |
| | 30 | 1.496 | 1.514 | 1.527 | 1.547 | 1.514 | 1.552 | 1.683 | 1.561 | 1.505 |
| | 33 | 1.568 | 1.609 | 1.591 | 1.594 | 1.552 | 1.599 | 1.694 | 1.587 | 1.506 |
| | 36 | 1.614 | 1.600 | 1.604 | 1.582 | 1.564 | 1.605 | 1.732 | 1.537 | 1.507 |
| | 39 | 1.614 | 1.595 | 1.648 | 1.588 | 1.594 | 1.597 | 1.725 | 1.515 | 1.501 |
| M4 | 3 | 1.258 | 1.259 | 1.242 | 1.188 | 1.250 | 1.299 | 1.283 | 1.276 | 1.308 |
| | 6 | 1.195 | 1.314 | 1.334 | 1.243 | 1.247 | 1.344 | 1.327 | 1.300 | 1.339 |
| | 9 | 1.238 | 1.327 | 1.358 | 1.231 | 1.226 | 1.338 | 1.341 | 1.321 | 1.356 |
| | 12 | 1.278 | 1.288 | 1.333 | 1.291 | 1.260 | 1.321 | 1.353 | 1.354 | 1.385 |
| | 15 | 1.203 | 1.321 | 1.329 | 1.281 | 1.323 | 1.310 | 1.378 | 1.369 | 1.365 |
| | 18 | 1.224 | 1.258 | 1.343 | 1.273 | 1.319 | 1.283 | 1.412 | 1.366 | 1.407 |
| | 21 | 1.270 | 1.243 | 1.387 | 1.284 | 1.295 | 1.345 | 1.455 | 1.376 | 1.442 |
| | 24 | 1.315 | 1.304 | 1.539 | 1.380 | 1.428 | 1.399 | 1.490 | 1.417 | 1.530 |
| | 27 | 1.436 | 1.419 | 1.589 | 1.536 | 1.514 | 1.527 | 1.520 | 1.451 | 1.576 |
| | 30 | 1.585 | 1.519 | 1.611 | 1.575 | 1.556 | 1.572 | 1.592 | 1.570 | 1.598 |
| | 33 | 1.609 | 1.561 | 1.601 | 1.642 | 1.588 | 1.587 | 1.558 | 1.618 | 1.594 |
| | 36 | 1.645 | 1.538 | 1.593 | 1.667 | 1.611 | 1.607 | 1.552 | 1.605 | 1.613 |
| | 39 | 1.671 | 1.528 | 1.626 | 1.677 | 1.627 | 1.590 | 1.563 | 1.635 | 1.633 |
| M2 | 3 | 1.206 | 1.249 | 1.236 | 1.218 | 1.222 | 1.282 | 1.173 | 1.177 | 1.343 |
| | 6 | 1.299 | 1.386 | 1.438 | 1.386 | 1.344 | 1.440 | 1.377 | 1.365 | 1.452 |
| | 9 | 1.333 | 1.381 | 1.434 | 1.341 | 1.353 | 1.438 | 1.403 | 1.396 | 1.446 |
| | 12 | 1.307 | 1.381 | 1.444 | 1.375 | 1.339 | 1.459 | 1.401 | 1.416 | 1.468 |
| | 15 | 1.297 | 1.351 | 1.431 | 1.368 | 1.374 | 1.447 | 1.401 | 1.426 | 1.458 |
| | 18 | 1.322 | 1.375 | 1.443 | 1.361 | 1.421 | 1.464 | 1.421 | 1.393 | 1.481 |
| | 21 | 1.386 | 1.407 | 1.437 | 1.402 | 1.505 | 1.495 | 1.408 | 1.422 | 1.506 |
| | 24 | 1.479 | 1.484 | 1.467 | 1.430 | 1.542 | 1.537 | 1.456 | 1.507 | 1.596 |
| | 27 | 1.549 | 1.582 | 1.523 | 1.523 | 1.629 | 1.578 | 1.544 | 1.589 | 1.648 |
| | 30 | 1.628 | 1.639 | 1.549 | 1.615 | 1.670 | 1.593 | 1.615 | 1.648 | 1.651 |
| | 33 | 1.645 | 1.666 | 1.575 | 1.626 | 1.677 | 1.594 | 1.640 | 1.708 | 1.674 |
| | 36 | 1.651 | 1.685 | 1.607 | 1.631 | 1.691 | 1.600 | 1.606 | 1.728 | 1.689 |

TABLE C CONE RESISTANCE MEASUREMENTS AT 3 cm INTERVALS BELOW THE ORIGINAL SOIL SURFACE. UNITS, bar. MACMERRY

| Occasion | depth, cm | TREATMENT RL 1 | RL 2 | RL 3 | RL 4 |
|---|---|---|---|---|---|
| M1 | 3 | 1.75 | 3.57 | 7.39 | 15.67 |
| | 6 | 2.62 | 7.59 | 9.88 | 26.51 |
| | 9 | 2.18 | 9.33 | 12.87 | 28.33 |
| | 12 | 3.49 | 7.68 | 14.13 | 27.31 |
| | 15 | 2.33 | 5.82 | 13.39 | 25.93 |
| | 18 | 3.39 | 6.88 | 13.68 | 28.16 |
| | 21 | 4.03 | 7.04 | 13.10 | 26.81 |
| | 24 | 5.50 | 6.68 | 11.39 | 22.78 |
| | 27 | 7.26 | 7.76 | 13.31 | 21.19 |
| | 30 | 7.74 | 12.78 | 17.09 | 26.55 |
| | 33 | 10.53 | 14.40 | 25.73 | 36.08 |
| M2 | 3 | 6.03 | 6.98 | 8.63 | 7.63 |
| | 6 | 11.53 | 16.43 | 14.44 | 13.66 |
| | 9 | 8.45 | 19.85 | 17.21 | 18.55 |
| | 12 | 2.73 | 10.66 | 13.14 | 29.09 |
| | 15 | 3.47 | 8.37 | 11.18 | 27.53 |
| | 18 | 7.07 | 8.41 | 12.40 | 23.71 |
| | 21 | 6.29 | 7.50 | 13.00 | 21.89 |
| | 24 | 5.77 | 7.67 | 13.92 | 20.25 |
| | 27 | 8.37 | 10.36 | 15.91 | 18.68 |
| | 30 | 14.57 | 21.81 | 20.72 | 22.76 |
| | 33 | 22.15 | 29.74 | 30.87 | 26.70 |
| M3/4 | 3 | 2.29 | 5.49 | 12.51 | 10.64 |
| | 6 | 2.31 | 7.36 | 12.98 | 27.60 |
| | 9 | 2.86 | 8.40 | 15.92 | 35.92 |
| | 12 | 3.09 | 8.30 | 13.81 | 32.51 |
| | 15 | 3.66 | 6.63 | 11.81 | 22.97 |
| | 18 | 4.08 | 7.75 | 13.92 | 23.25 |
| | 21 | 4.42 | 10.27 | 14.15 | 24.63 |
| | 24 | 5.38 | 10.12 | 14.51 | 24.35 |
| | 27 | 6.45 | 9.00 | 13.00 | 21.22 |
| | 30 | 7.39 | 14.41 | 25.41 | 30.28 |
| | 33 | 14.02 | 31.73 | 49.58 | 50.62 |

TABLE C (Continued) CONE RESISTANCE MEASUREMENTS AT 3 cm INTERVALS BELOW THE ORIGINAL SOIL SURFACE. UNITS, bar. THREIPMUIR

| Occasion | depth, cm | TREATMENT RL 1 | RL 2 | RL 3 |
|---|---|---|---|---|
| M1 | 3 | 8.24 | 9.46 | 12.94 |
| | 6 | 17.32 | 18.32 | 31.26 |
| | 9 | 19.64 | 24.24 | 38.12 |
| | 12 | 23.16 | 29.15 | 45.29 |
| | 15 | 30.94 | 34.45 | 47.83 |
| | 18 | 45.91 | 44.32 | 41.07 |
| | 21 | 44.64 | 40.21 | 44.45 |
| | 24 | 42.32 | 40.40 | 49.56 |
| | 27 | 39.70 | 48.88 | 51.91 |
| | 30 | 54.42 | 80.96 | 69.93 |
| | 33 | 76.74 | 99.65 | 81.03 |
| M2 | 3 | 3.32 | 3.62 | 5.02 |
| | 6 | 5.13 | 7.38 | 10.00 |
| | 9 | 5.16 | 8.38 | 11.10 |
| | 12 | 6.35 | 8.16 | 12.48 |
| | 15 | 8.84 | 11.35 | 16.32 |
| | 18 | 11.02 | 14.16 | 17.16 |
| | 21 | 12.75 | 15.56 | 16.21 |
| | 24 | 12.13 | 15.89 | 18.86 |
| | 27 | 17.35 | 16.32 | 21.10 |
| | 30 | 19.13 | 25.67 | 29.10 |
| | 33 | 31.18 | 40.15 | 37.80 |
| M4 | 3 | 4.81 | 5.94 | 12.43 |
| | 6 | 7.94 | 10.54 | 19.86 |
| | 9 | 9.75 | 15.02 | 22.59 |
| | 12 | 13.67 | 15.29 | 21.60 |
| | 15 | 19.24 | 21.27 | 27.45 |
| | 18 | 21.86 | 29.62 | 35.07 |
| | 21 | 22.05 | 30.97 | 38.34 |
| | 24 | 28.64 | 33.61 | 47.75 |
| | 27 | 37.64 | 42.60 | 57.70 |
| | 30 | 58.37 | 59.29 | 70.80 |

APPENDIX 5 FIELD MEASUREMENTS OF PRESSURE AND DEFORMATION OF THE SPHERICAL STRESS TRANSDUCERS. LOWER TERRACE, 1977

1. Maximum internal pressures of water filled balls, bars. All values corrected to equivalent at 22°C; * denotes missing value.

| Replication | Occasion | Wheel Treatment | Nominal depth, cm 10 | 20 | 30 | 40 |
|---|---|---|---|---|---|---|
| 1 | M4 | W1 | 0.710 | 0.180 | 0.110 | 0.000 |
| 1 | M4 | W1 | 0.695 | * | * | 0.020 |
| 2 | M4 | W1 | 1.080 | 0.220 | 0.040 | 0.000 |
| 2 | M4 | W1 | 0.640 | 0.180 | 0.040 | 0.202 |
| 3 | M4 | W1 | * | 0.200 | * | 0.020 |
| 3 | M4 | W1 | * | 0.270 | * | * |
| 1 | M3 | W1 | * | * | * | * |
| 1 | M3 | W1 | * | * | * | * |
| 2 | M3 | W1 | 1.100 | 0.450 | 0.160 | 0.020 |
| 2 | M3 | W1 | 1.000 | * | 0.160 | 0.070 |
| 3 | M3 | W1 | 0.830 | 0.540 | 0.180 | 0.020 |
| 3 | M3 | W1 | 1.050 | 0.490 | 0.030 | 0.030 |
| 1 | M4 | W2 | 0.600 | * | * | 0.020 |
| 1 | M4 | W2 | 0.800 | 0.220 | 0.100 | 0.000 |
| 2 | M4 | W2 | 0.990 | 0.270 | 0.180 | 0.000 |
| 2 | M4 | W2 | 1.060 | 0.160 | 0.100 | * |
| 3 | M4 | W2 | 0.710 | * | 0.100 | 0.050 |
| 3 | M4 | W2 | 1.220 | 0.220 | 0.120 | 0.040 |
| 1 | M3 | W2 | 1.270 | 0.430 | 0.130 | 0.050 |
| 1 | M3 | W2 | 1.210 | 0.450 | 0.180 | 0.030 |
| 2 | M3 | W2 | * | 0.880 | 0.450 | 0.000 |
| 2 | M3 | W2 | 1.350 | 0.500 | 0.220 | 0.040 |
| 3 | M3 | W2 | * | 0.830 | 0.430 | 0.040 |
| 3 | M3 | W2 | * | * | 0.290 | 0.090 |
| 1 | M4 | W4 | 1.550 | * | * | * |
| 1 | M4 | W4 | 1.260 | 0.530 | 0.040 | 0.070 |
| 2 | M4 | W4 | * | * | 0.050 | * |
| 2 | M4 | W4 | * | * | 0.150 | 0.110 |
| 3 | M4 | W4 | 0.910 | 0.570 | 0.640 | 0.110 |
| 3 | M4 | W4 | 1.550 | 0.660 | * | 0.100 |
| 1 | M3 | W4 | 1.380 | 0.660 | 0.600 | 0.180 |
| 1 | M3 | W4 | 1.500 | * | 0.600 | 0.110 |
| 2 | M3 | W4 | 1.550 | 1.230 | 0.730 | 0.090 |
| 2 | M3 | W4 | * | 1.350 | 0.200 | 0.027 |
| 3 | M3 | W4 | 1.430 | 1.300 | 0.350 | 0.219 |
| 3 | M3 | W4 | 1.450 | * | * | * |

APPENDIX 5 (continued)

2. Lengths of minor axes of Mastic balls upon excavation, mm. All values corrected to 16°C; * denotes missing value.

Mean major axes shown in parentheses.

| Replication | Occasion | Wheel Treatment | Nominal depth, cm 10 | 20 | 30 | 40 |
|---|---|---|---|---|---|---|
| 1 | M4 | W1 | 10(43) | 32(42) | 34(41) | 37(38) |
| 1 | M4 | W1 | 28(41) | 30(41) | 34(41) | 36(37) |
| 2 | M4 | W1 | 31(43) | 29 * | 33 * | * * |
| 2 | M4 | W1 | 32(42) | 32(42) | 36(42) | 38(42) |
| 3 | M4 | W1 | 30(41) | 31(43) | 33(42) | 34(43) |
| 3 | M4 | W1 | 25(48) | 28(45) | 33(41) | 35(40) |
| 1 | M3 | W1 | 28(42) | 30(40) | 33(39) | 33(39) |
| 1 | M3 | W1 | 35(41) | 30(41) | 32(41) | 33(39) |
| 2 | M3 | W1 | 27(42) | 33(41) | 32(41) | 35(38) |
| 2 | M3 | W1 | 30(42) | 32(41) | 33(37) | 36(39) |
| 3 | M3 | W1 | * * | 27(41) | 32(42) | 36(41) |
| 3 | M3 | W1 | 29(42) | 26(43) | 31(40) | 28(41) |
| 1 | M4 | W2 | 28(42) | 32(41) | 35(39) | 37(38) |
| 1 | M4 | W2 | 30(43) | 32(43) | 34(41) | 38(38) |
| 2 | M4 | W2 | 32(42) | 32(44) | 37(39) | 38(38) |
| 2 | M4 | W2 | 30(42) | 34(43) | 35(42) | 35(42) |
| 3 | M4 | W2 | 24(45) | 28(45) | 32(42) | 36(40) |
| 3 | M4 | W2 | * * | 29(44) | 32(43) | 33(41) |
| 1 | M3 | W2 | 28(43) | 31(41) | 33(40) | 34(40) |
| 1 | M3 | W2 | 28(40) | 31(40) | 35(40) | 35(38) |
| 2 | M3 | W2 | 26(45) | 30(42) | 32(41) | 38(39) |
| 2 | M3 | W2 | 26(44) | 26(43) | 31(40) | 38(38) |
| 3 | M3 | W2 | 25(44) | 29(42) | 32(40) | 35(38) |
| 3 | M3 | W2 | 27(45) | 27(42) | 29(41) | 32(41) |
| 1 | M4 | W4 | 20(30) | 27(43) | 33(41) | 37(39) |
| 1 | M4 | W4 | 26(41) | 28(40) | 35(40) | 37(38) |
| 2 | M4 | W4 | * * | * * | * * | * * |
| 2 | M4 | W4 | * * | * * | * * | * * |
| 3 | M4 | W4 | 22(45) | 32(44) | 32(45) | 37(38) |
| 3 | M4 | W4 | 26(44) | 30(44) | 29(43) | * * |
| 1 | M3 | W4 | 26(44) | 28(44) | 29(41) | 33(39) |
| 1 | M3 | W4 | 26(45) | 28(43) | 31(38) | 35(38) |
| 2 | M3 | W4 | 28(43) | 28(45) | 32(44) | 38(39) |
| 2 | M3 | W4 | 27(45) | 27(44) | 30(41) | 38(39) |
| 3 | M3 | W4 | 22(46) | 28(45) | 28(42) | 33(41) |
| 3 | M3 | W4 | * * | 27(43) | 28(40) | 31(42) |

APPENDIX 5 (continued) THE RESULTS OF ANALYSES OF THE LENGTHS OF THE MINOR AXIS OF THE MASTIC BALLS AT DIFFERENT, NOMINAL DEPTHS. (Axis length measured in millimetres)

| Source of variation | df (missing values) | Sum of squares | Mean squares | F ratio |
|---|---|---|---|---|
| 10 cm nominal depth | | | | |
| Replications | 2 | 215.3 | 3.3770 | 5.731 |
| Rep. Occasions | | | | |
| Occasions | 1 | 2.4 | 0.0767 | 0.065(N) |
| Residual | 2 | 74.8 | 1.1729 | 1.990 |
| Total | 3 | 77.2 | 0.8075 | 1.370 |
| Rep. Occ. Wheel Treatments | | | | |
| Wheel Treatments | 2 | 427.7 | 6.7085 | 10.704(**) |
| Occ. Wheel | 2 | 16.6 | 0.2598 | 0.414(N) |
| Residual | 7(1) | 139.9 | 0.6267 | 1.064 |
| Total | 11 | 584.2 | 1.6658 | 2.827 |
| Rep. Occ. Wheel.Point | 14(4) | 263.0 | 0.5893 | |
| Grand Total | 30 | 1139.7 | | |
| Estimated Grand Mean | 27.31 | | | |
| Total number of observations | 36 | | | |
| Number of missing values | 5 | | | |
| Maximum number of iterations | 4 | | | |

| Treatment code | Estimated value |
|---|---|
| M4 W4 | 27.13 |
| M4 W4 | 27.13 |
| M4 W2 | 24.00 |
| M3 W1 | 29.00 |
| M3 W4 | 22.00 |

| Source of variation | df (missing values) | Sum of squares | Mean squares | F ratio |
|---|---|---|---|---|
| 20 cm nominal depth, minor axis length, mm | | | | |
| Replications | 2 | 81.0 | 0.7976 | 3.988 |
| Rep. Occasions | | | | |
| Occasions | 1 | 209.1 | 4.1204 | 6.37(N) |
| Residual | 2 | 65.6 | 0.6468 | 3.234 |
| Total | 3 | 274.7 | 1.8047 | 9.023 |
| Rep. Occ. Wheel Treatments | | | | |
| Wheel Treatments | 2 | 14.0 | 0.1376 | 0.107(N) |
| Occ. Wheel | 2 | 64.9 | 0.6392 | 0.499(N) |
| Residual | 7(1) | 455.3 | 1.2817 | 6.409 |
| Total | 11 | 534.2 | 0.9569 | 4.785 |
| Rep. Occ. Wheel.point | 17(1) | 172.5 | 0.2000 | |
| Grand Total | 33 | 1062.4 | | |
| Estimated Grand Mean | 29.85 | | | |
| Total number of observations | 36 | | | |
| Number of missing values | 2 | | | |
| Maximum number of iterations | 1 | | | |

| Treatment code | Estimated value |
|---|---|
| M4 W4 | 32.26 |
| M4 W4 | 32.26 |

| Source of variation | df (missing values) | Sum of squares | Mean squares | F ratio |
|---|---|---|---|---|
| 30 cm nominal depth, minor axis length, mm | | | | |
| Replications | 2 | 269.2 | 2.1233 | 13.883 |
| Rep. Occasions | | | | |
| Occasions | 1 | 314.3 | 4.9590 | 29.340(*) |
| Residual | 2 | 21.4 | 0.1690 | 1.105 |
| Total | 3 | 335.8 | 1.7657 | 11.545 |
| Rep. Occ. Wheel Treatments | | | | |
| Wheel Treatments | 2 | 159.2 | 1.2562 | 6.547(*) |
| Occ. Wheel | 2 | 23.5 | 0.1857 | 0.968 |
| Residual | 7(1) | 85.1 | 0.1919 | 1.254(N) |
| Total | 11 | 267.9 | 0.3842 | 2.512 |
| Rep. Occ. Wheel.Point | 17(1) | 164.8 | 0.1529 | |
| Grand Total | 33 | 1037.6 | | |
| Estimated Grand Mean | 32.45 | | | |
| Total number of observations | 36 | | | |
| Total number of missing values | 2 | | | |
| Maximum number of iterations | 4 | | | |

| Treatment code | Estimated value |
|---|---|
| M4 W4 | 34.13 |
| M4 W4 | 34.13 |

| Source of variation | df (missing values) | Sum of squares | Mean squares | F ratio |
|---|---|---|---|---|
| 40 cm nominal depth, minor axis length, mm | | | | |
| Replications | 2 | 407.4 | 3.6843 | 10.33 |
| Rep. Occasions | | | | |
| Occasions | 1 | 221.6 | 4.0089 | 6.830(N) |
| Residual | 2 | 64.9 | 0.5869 | 1.646 |
| Total | 3 | 286.5 | 1.7276 | 4.844 |
| Rep. Occ. Wheel Treatments | | | | |
| Wheel Treatments | 2 | 50.0 | 0.4623 | 3.00(N) |
| Occ. Wheel | 2 | 51.9 | 0.4691 | 3.111(N) |
| Residual | 7(1) | 58.4 | 0.1508 | 0.423 |
| Total | 11 | 160.2 | 0.2635 | 0.739 |
| Rep. Occ. Wheel.point | 15(3) | 295.8 | 0.3567 | |
| Grand Total | 31 | 1149.9 | | |
| Estimated Grand Mean | 35.61 | | | |
| Total number of observations | 36 | | | |
| Number of missing values | 4 | | | |
| Maximum number of iterations | 3 | | | |

| Treatment code | Estimated value |
|---|---|
| M4 W1 | 38.0 |
| M4 W4 | 38.5 |
| M4 W4 | 38.5 |
| M4 W4 | 37.0 |

APPENDIX 5 (continued) THE RESULTS OF ANALYSES OF VARIANCE OF THE INCREASES OF INTERNAL PRESSURE OF THE WATER FILLED RUBBER BALLS AT DIFFERENT NOMINAL DEPTHS. (Pressure measured in bar.)

| Source of variation | df (missing values) | Sum of squares | Mean squares | F ratio |
|---|---|---|---|---|
| 10 cm nominal depth | | | | |
| Replications | 2 | 6.66 | 0.07904 | 1.774 |
| Rep. Occasions | | | | |
| Occasions | 1 | 20.47 | 0.48579 | 106.102(**) |
| Residual | 2 | 0.39 | 0.00459 | 0.103 |
| Total | 3 | 20.86 | 0.16498 | 3.703 |
| Rep. Occ. Wheel Treatments | | | | |
| Wheel Treatments | 2 | 79.32 | 0.94105 | 38.191(**) |
| Occ. Wheel | 2 | 4.92 | 0.05834 | 2.367(N) |
| Residual | 4(4) | 4.15 | 0.02464 | 0.553 |
| Total | 8 | 88.39 | 0.26212 | |
| Rep. Occ. Wheel.point | 12(6) | 22.53 | 0.04453 | |
| Grand Total | 25 | 138.44 | | |
| Estimated Grand Mean | 1.127 | | | |
| Total number of observations | 36 | | | |
| Number of missing values | 10 | | | |
| Maximum number of iterations | 7 | | | |

| Treatment code | Estimated value |
|---|---|
| M4 W4 | 1.487 |
| M4 W4 | 1.487 |
| M4 W1 | 0.725 |
| M4 W1 | 0.725 |
| M3 W1 | 0.940 |
| M3 W1 | 0.940 |
| M3 W2 | 1.350 |
| M3 W4 | 1.550 |
| M3 W2 | 1.240 |
| M3 W2 | 1.240 |

| Source of variation | df (missing values) | Sum of squares | Mean squares | F ratio |
|---|---|---|---|---|
| 20 cm nominal depth, pressure increase, bar | | | | |
| Replications | 2 | 18.15 | 0.26699 | 22.674 |
| Rep. Occasions | | | | |
| Occasions | 1 | 38.64 | 1.13719 | 5.690(N) |
| Residual | 2 | 13.58 | 0.19984 | 16.972 |
| Total | 3 | 52.23 | 0.51229 | 43.507 |
| Rep. Occ. Wheel Treatments | | | | |
| Wheel Treatments | 2 | 67.81 | 0.99768 | 76.366(**) |
| Occ. Wheel | 2 | 8.90 | 0.13097 | 10.025(*) |
| Residual | 6(2) | 2.66 | 0.01306 | 1.110 |
| Total | 10 | 78.37 | 0.23357 | 19.836 |
| Rep. Occ. Wheel.point | 8(10) | 3.2 | 0.01177 | |
| Grand Total | 23 | 152.95 | | |
| Estimated Grand Mean | 0.509 | | | |
| Total number of observations | 36 | | | |
| Number of missing values | 12 | | | |
| Maximum number of iterations | 4 | | | |

| Treatment code | Estimated value |
|---|---|
| M4 W1 | 0.180 |
| M4 W2 | 0.220 |
| M4 W4 | 0.530 |
| M4 W4 | 0.566 |
| M4 W4 | 0.566 |
| M4 W2 | 0.220 |
| M3 W1 | 0.005 |
| M3 W1 | 0.005 |
| M3 W4 | 0.660 |
| M3 W1 | 0.450 |
| M3 W2 | 0.830 |
| M3 W4 | 1.300 |

| Source of variation | df (missing values) | Sum of squares | Mean squares | F ratio |
|---|---|---|---|---|
| 30 cm nominal depth, pressure increase, bar | | | | |
| Replications | 2 | 11.05 | 0.06020 | 3.351 |
| Rep. Occasions | | | | |
| Occasions | 1 | 10.78 | 0.11751 | 1.172(N) |
| Residual | 2 | 18.40 | 0.10026 | 5.581 |
| Total | 3 | 29.18 | 0.10601 | 5.901 |
| Rep. Occ. Wheel Treatments | | | | |
| Wheel Treatments | 2 | 27.99 | 0.15255 | 2.671(N) |
| Occ. Wheel | 2 | 9.54 | 0.05201 | 0.911(N) |
| Residual | 6(2) | 31.45 | 0.05712 | 3.180 |
| Total | 10 | 68.99 | 0.07518 | 4.185 |
| Rep.Occ. Wheel.point | 11(7) | 18.13 | 0.01796 | |
| Grand Total | 26 | 127.35 | | |
| Estimated Grand Mean | 0.239 | | | |
| Total number of observations | 36 | | | |
| Number of missing values | 9 | | | |
| Maximum number of iterations | 3 | | | |

| Treatment code | Estimated value |
|---|---|
| M4 W1 | 0.110 |
| M4 W2 | 0.100 |
| M4 W4 | 0.040 |
| M4 W1 | 0.355 |
| M4 W1 | 0.355 |
| M4 W4 | 0.640 |
| M3 W1 | 0.133 |
| M3 W1 | 0.133 |
| M3 W4 | 0.350 |

| Source of variation | df (missing values) | Sum of Squares | Mean Squares | F ratio |
|---|---|---|---|---|
| 40 cm nominal depth, pressure increase, bar | | | | |
| Replications | 2 | 11.96 | 0.0048899 | 6.757 |
| Rep. Occasions | | | | |
| Occasions | 1 | 10.25 | 0.008377 | 4.316(N) |
| Residual | 2 | 4.75 | 0.0019411 | 2.682 |
| Total | 3 | 15.00 | 0.0040864 | 5.646 |
| Rep. Occ. Wheel Treatments | | | | |
| Wheel Treatments | 2 | 80.65 | 0.0329644 | 12.24(*) |
| Occ. Wheel | 2 | 1.29 | 0.0005290 | 0.196(N) |
| Residual | 7(1) | 23.06 | 0.0026932 | 3.721 |
| Total | 11 | 105.01 | 0.0078036 | 10.783 |
| Rep. Occ. Wheel.point | 12(6) | 10.62 | 0.0007237 | |
| Grand Total | 28 | 142.6 | | |
| Estimated Grand Mean | 0.0575 | | | |
| Total number of observations | 36 | | | |
| Number of missing values | 7 | | | |
| Maximum number of iterations | 3 | | | |

| Treatment code | Estimated value |
|---|---|
| M4 W4 | 0.0700 |
| M4 W2 | 0.0000 |
| M4 W1 | 0.1100 |
| M3 W1 | 0.0371 |
| M3 W1 | 0.0371 |
| M3 W4 | 0.2190 |

TABLE 3 TYRE/SOIL CONTACT AREAS AND WHEEL SINKAGE MEASUREMENTS (SOIL TANK)

| Replicate | Wheel Treatment | Contact area, $cm^2$ | Mean rut depth, cm | Max. rut depth, cm | Cross sectional area, $cm^2$ | Soil hardness treatment[1] |
|---|---|---|---|---|---|---|
| 2 | W1 | 1440 | 3.35 | 5.08 | 100.3 | 1 |
| 2 | W1 | 1624 | 3.45 | 5.33 | 127.5 | 1 |
| 1 | W1 | 1640 | 3.89 | 6.10 | 135.9 | 1 |
| 1 | W1 | 1744 | 4.01 | 6.10 | 120.7 | 1 |
| 2 | W1 | 984 | 0.81 | 1.27 | 16.5 | 2 |
| 2 | W1 | 992 | 0.84 | 1.52 | 25.4 | 2 |
| 1 | W1 | 1296 | 2.11 | 3.81 | 63.5 | 2 |
| 1 | W1 | 1216 | 2.34 | 3.30 | 58.4 | 2 |
| 2 | W1 | 880 | 0.61 | 1.25 | 15.2 | 3 |
| 2 | W1 | 864 | 0.76 | 1.27 | 19.1 | 3 |
| 1 | W1 | 1136 | 1.02 | 1.78 | 30.5 | 3 |
| 1 | W1 | 1128 | 1.53 | 2.29 | 40.6 | 3 |
| 2 | W1 | 744 | 0.41 | 0.76 | 10.2 | 4 |
| 2 | W1 | 784 | 0.30 | 0.51 | 7.6 | 4 |
| 1 | W1 | 824 | 0.38 | 0.51 | 11.4 | 4 |
| 1 | W1 | 896 | 0.38 | 0.75 | 11.4 | 4 |
| 1 | W2 | 1560 | 4.24 | 6.10 | 147.3 | 1 |
| 1 | W2 | 1640 | 4.24 | 5.84 | 148.6 | 1 |
| 2 | W2 | 1864 | 5.28 | 7.62 | 185.4 | 1 |
| 2 | W2 | 1720 | 5.33 | 7.87 | 186.7 | 1 |
| 1 | W2 | 1168 | 1.73 | 2.54 | 48.3 | 2 |
| 1 | W2 | 1208 | 0.81 | 2.29 | 11.4 | 2 |
| 2 | W2 | 1448 | 2.46 | 6.35 | 73.7 | 2 |
| 2 | W2 | 1552 | 1.91 | 3.05 | 57.2 | 2 |
| 1 | W2 | 1064 | 0.64 | 1.02 | 19.1 | 3 |
| 1 | W2 | 1208 | 1.22 | 2.03 | 36.8 | 3 |
| 2 | W2 | 1400 | 2.34 | 3.30 | 69.8 | 3 |
| 2 | W2 | 1968 | 2.29 | 4.06 | 68.6 | 3 |
| 1 | W2 | 992 | 0.44 | 0.51 | 8.9 | 4 |
| 1 | W2 | 808 | 0.30 | 0.51 | 7.6 | 4 |
| 2 | W2 | 1112 | 0.38 | 3.30 | 7.6 | 4 |
| 2 | W2 | 1056 | 0.41 | 0.51 | 10.2 | 4 |

1. see section 4.3.

TABLE 3 (continued)

| Replicate | Wheel Treatment | Contact area, $cm^2$ | Mean rut depth, cm | Max. rut depth, cm | Cross sectional area, $cm^2$ | Soil hardness treatment[1] |
|---|---|---|---|---|---|---|
| 2 | W4 | 1736 | 4.42 | 6.60 | 172.7 | 1 |
| 2 | W4 | 1704 | 4.42 | 6.60 | 177.8 | 1 |
| 1 | W4 | 1832 | 4.06 | 5.84 | 142.3 | 1 |
| 1 | W4 | 1904 | 4.93 | 9.40 | 172.2 | 1 |
| 2 | W4 | 1440 | 1.65 | 3.30 | 49.5 | 2 |
| 2 | W4 | 1488 | 1.57 | 2.54 | 47.0 | 2 |
| 1 | W4 | 1416 | 1.17 | 2.54 | 40.6 | 2 |
| 1 | W4 | 1408 | 1.12 | 2.54 | 39.7 | 2 |
| 2 | W4 | 1216 | 1.31 | 2.54 | 45.7 | 3 |
| 2 | W4 | 1320 | 1.32 | 2.03 | 33.0 | 3 |
| 1 | W4 | 1208 | 0.64 | 1.52 | 19.0 | 3 |
| 1 | W4 | 1248 | 0.84 | 1.78 | 25.4 | 3 |
| 2 | W4 | 1040 | 0.56 | 0.76 | 14.0 | 4 |
| 2 | W4 | 904 | 0.41 | 0.76 | 10.2 | 4 |
| 1 | W4 | 904 | 0.30 | 0.51 | 7.6 | 4 |
| 1 | W4 | 864 | 0.36 | 0.51 | 8.9 | 4 |

## APPENDIX 6 REGRESSIONS USED FOR ANALYSES OF THE RESULTS

a) Cone resistance (CR) and soil moisture content (MC) at threshold depths, soil treatment RL2, Lower Terrace field, 1977.

13 cm depth

| Degree of freedom | Total sum of squares | Total mean square | Residual sum of squares | Residual mean squares | R | F | P |
|---|---|---|---|---|---|---|---|
| 2 | 240.5 | 120.2 | | | | | |
| 1 | | | 21.2 | 21.2 | 0.955 | 10.33 | 0.192 |

| | coef. | s.e. | t. stat. |
|---|---|---|---|
| slope | - 2.193 | 0.68 | - 3.21 |
| int.(CR) | 59.65 | 13.08 | 4.56 |

for MC = 20.1% (w/w) (occasion M3) CR = 15.6 bar

mean CR for occasion M4 (16 bar) and M3= 15.8 bar

23 cm depth

| Degree of freedom | Total sum of squares | Total mean square | Residual sum of squares | Residual mean squares | R | F | P |
|---|---|---|---|---|---|---|---|
| 2 | 343.5 | 171.7 | | | | | |
| 1 | | | 7.03 | 7.03 | 0.9897 | 47.9 | 0.0914 |

| | coef. | s.e. | t. stat. |
|---|---|---|---|
| slope | - 2.99 | 0.432 | - 6.92 |
| int.(CR) | 84.00 | 8.0 | 10.47 |

for MC = 21.5% (w/w) (occasion M3) CR = 19.97 bar

mean CR for occasion M4 (33 bar) and M3= 26.4 bar

b) Vane shear strength (SH) and cone resistance (CR), 9 and 18 cm depths, Lower Terrace field, 1977.

| Degree of freedom | Total sum of squares | Total mean square | Residual sum of squares | Residual mean squares | R | F | P |
|---|---|---|---|---|---|---|---|
| 17 | 5217.5 | 306.9 | | | | | |
| | | | 568.8 | 35.6 | 0.944 | 130.8 | $4 \times 10^{-9}$ |

| | coef. | s.e. | t. stat. |
|---|---|---|---|
| slope | 0.616 | 0.054 | 11.43 |
| int.(SH) | 17.47 | 2.9 | 6.0 |

## APPENDIX 7 LABORATORY MEASUREMENTS OF STRESS AND DRY BULK DENSITY

The following tables show the data for each test on each soil at different moisture contents and initial packing conditions.

Each test is documented as follows:

| | | |
|---|---|---|
| S | = | sample number |
| R | = | replicate number |
| Cell P | = | cell pressure, bar |
| Dbd | = | dry bulk density, 30s after stress application, $g/cm^3$ |
| W | = | soil moisture content, % w/w |

TABLE A RESULTS OF TRIAXIAL TESTING

SOIL: Macmerry

| S.1 | | S.2 | | S.3 | | S.4 | | S.5 | | S.6 | | S.7 | |
|---|---|---|---|---|---|---|---|---|---|---|---|---|---|
| CellP | Dbd | CellP | Dbd | CellP | Dbd | CellP | Dbd | CellP | Dbd | CellP | Dbd | CellP | Dbd |
| 0. | 0.903 | 0 | 0.760 | 0 | 0.797 | 0 | 0.753 | 0 | 0.746 | 0 | 0.763 | 0 | 0.812 |
| 0.01 | 0.908 | 0.01 | 0.748 | 0.01 | 0.821 | 0.01 | 0.785 | 0.3 | 1.067 | 0.01 | 0.797 | 0.02 | 0.875 |
| 0.045 | 0.918 | 0.015 | 0.807 | 0.045 | 0.861 | 0.045 | 0.884 | 1.0 | 1.206 | 0.025 | 0.854 | 0.045 | 0.936 |
| 0.07 | 0,058 | 0.025 | 0.837 | 0.13 | 0.966 | 0.08 | 0.957 | 1.5 | 1.250 | 0.05 | 0.909 | 0.095 | 1.015 |
| 0.1 | 1.004 | 0.035 | 0.878 | 0.38 | 1.104 | 0.15 | 1.042 | 2.0 | 1.267 | 0.09 | 0.978 | 0.148 | 1.075 |
| 0.14 | 1.046 | 0.05 | 0.903 | 1.0 | 1.228 | 0.124 | 1097 | 3.0 | 1.281 | 0.2 | 1.089 | 0.27 | 1.157 |
| 0.21 | 1.109 | 0.075 | 0.950 | 2.0 | 1.268 | 0.47 | 1.188 | 4.0 | 1.296 | | 1.096 | | 1.162 |
| 0.27 | 1.135 | 0.1 | 0.990 | 3.0 | 1.296 | 0.73 | 1.248 | 5.0 | 1.308 | 0.54 | 1.217 | 0.459 | 1.230 |
| 0.35 | 1.172 | 0.055 | 0.987 | 0.2 | 1.291 | 1.05 | 1.297 | 6.0 | 1.327 | 0.81 | 1.268 | 0.778 | 1.303 |
| 0.48 | 1.213 | 0.15 | 1.040 | | | 0.23 | 1.272 | 7.0 | 1.346 | 1.0 | 1.292 | 1.0 | 1.338 |
| 0.80 | 1.278 | 0.22 | 1.086 | w=28.4 | | 1.5 | 1.328 | 0.045 | 1.360 | 0.24 | 1.273 | 0.21 | 1.313 |
| 1.0 | 1.301 | 0.32 | 1.141 | | | 2.0 | 1.339 | w=26.2 | | 1.5 | 1.315 | 1.0 | 1.351 |
| 0.2 | 1.278 | 0.49 | 1.186 | | | 3.0 | 1.350 | | | 2.0 | 1.323 | 1.5 | 1.394 |
| 1.55 | 1.322 | 0.74 | 1.238 | | | 4.0 | 1.361 | | | 3.0 | 1.329 | 2.0 | 1.426 |
| 2.0 | 1.332 | 1.0 | 1.266 | | | 5.0 | 1.367 | | | 0.27 | 1.329 | 3.0 | 1.443 |
| 3.0 | 1.343 | 0.2 | 1.245 | | | 6.0 | 1.372 | | | w=27.3 | | 4.0 | 1.455 |
| 4.0 | 1.346 | 1.0 | 1.276 | | | 0.46 | 1.381 | | | | | 5.0 | 1.465 |
| 5.0 | 1.354 | 1.5 | 1.286 | | | w=25,7 | | | | | | 6.0 | 1.468 |
| 0.43 | 1.360 | 2.0 | 1.291 | | | | | | | | | 7.0 | 1.48 |
| w=26.8 | | 3.0 | 1.302 | | | | | | | | | 0.62 | 1.48 |
| | | 4.0 | 1.307 | | | | | | | | | w=23.9 | |
| | | 0.42 | 1.307 | | | | | | | | | | |
| | | w=26.8 | | | | | | | | | | | |

CellP = cell pressure, bar  Dbd = calculated dry bulk density, $g/cm^3$

S = sample number

| S.21 | | S.22 | | S.23 | | S.24 | | S.25 | | S.26 | |
|---|---|---|---|---|---|---|---|---|---|---|---|
| CellP | Dbd | CellP | Dbd | CellP | Dbd | CellP | Dbd | CellP | Dbd | CellP | Dbd |
| 0 | 1.056 | 0 | 0.848 | 0 | 0.946 | 0 | 1.018 | 0 | 1.026 | 0 | 0.755 |
| 0.03 | 1.091 | 0.03 | 0.918 | 0.04 | 0.989 | 0.05 | 1.068 | 0.05 | 1.095 | 0.03 | 0.800 |
| 0.05 | 1.108 | 0.05 | 0.957 | 0.08 | 1.010 | 0.07 | 1.083 | 0.07 | 1.110 | 0.06 | 0.854 |
| 0.08 | 1.123 | 0.1 | 1.036 | 0.1 | 1.018 | 0.1 | 1.101 | 0.1 | 1.131 | 0.1 | 0.894 |
| 0.1 | 1.134 | 0.2 | 1.118 | 0.2 | 1.046 | 0.2 | 1.143 | 0.2 | 1.175 | 0.15 | 0.933 |
| 0.2 | 1.166 | 0.3 | 1.168 | 0.3 | 1.061 | 0.3 | 1.169 | 0.3 | 1.198 | 0.2 | 0.960 |
| 0.3 | 1.189 | 0.4 | 1.207 | 0.4 | 1.075 | 0.4 | 1.189 | 0.4 | 1.218 | 0.3 | 0.997 |
| 0.4 | 1.205 | 0.5 | 1.229 | 0.5 | 1.088 | 0.5 | 1.207 | 0.5 | 1.238 | 0.4 | 1.029 |
| 0.5 | 1.218 | 0.7 | 1.274 | 0.7 | 1.107 | 0.7 | 1.236 | 0.7 | 1.264 | 0.5 | 1.054 |
| 0.7 | 1.242 | 1.0 | 1.315 | 1.0 | 1.130 | 1.0 | 1.265 | 1.0 | 1.295 | 0.7 | 1.097 |
| 1.0 | 1.266 | 0.2 | 1.299 | 0.2 | 1.120 | 0.2 | 1.257 | 0.2 | 1.284 | 1.0 | 1.141 |
| 0.2 | 1.256 | 1.5 | 1.359 | 1.5 | 1.159 | 1.5 | 1.311 | 1.5 | 1.331 | 0.1 | 1.124 |
| 1.5 | 1.296 | 2.0 | 1.393 | 2.0 | 1.182 | 2.0 | 1.342 | 2.0 | 1.362 | 1.5 | 1.208 |
| 2.0 | 1.322 | 3.0 | 1.443 | 3.0 | 1.228 | 3.0 | 1.345 | 3.0 | 1.408 | 2.0 | 1.251 |
| 3.0 | 1.361 | 4.0 | 1.481 | 4.1 | 1.281 | 4.0 | 1.439 | 4.0 | 1.443 | 3.0 | 1.318 |
| 4.0 | 1.397 | 5.0 | 1.512 | 5.0 | 1.336 | 5.0 | 1.482 | 5.0 | 1.467 | 4.0 | 1.386 |
| 5.0 | 1.430 | 0.2 | 1.457 | 6.0 | 1.411 | 0.2 | 1.449 | 0.2 | 1.434 | 5.0 | 1.455 |
| 6.0 | 1.458 | 2=21.0 | | 7.0 | 1.487 | | | | | 0.2 | 1.452 |
| 7.0 | 1.491 | | | | 1.464 | 2=12.4 | | W=11.4 | | W=21.2 | |
| 0.2 | 1.460 | | | W=7.7 | | | | | | | |
| W=8.2 | | | | | | | | | | | |

| S.8 | | S.9 | | S.10 | | S.11 | | S.12 | | S.13 | | S.14 | |
|---|---|---|---|---|---|---|---|---|---|---|---|---|---|
| CellP | Dbd | CellP | Dbd | CellP | Dbd | CellP | Dbd | CellP | Dbd | CellP | Dbd | CellP | Dbd |
| 0 | 1.032 | 0 | 0.810 | 0 | 0.787 | 0 | 0.846 | 0 | 0.888 | 0 | 0.902 | 0 | 0.898 |
| 0.075 | 1.073 | 0.02 | 0.854 | 0.02 | 0.818 | 0.04 | 0.891 | 0.04 | 0.948 | 0.04 | 0.951 | 0.02 | 0.932 |
| 0.11 | 1.111 | 0.05 | 0.929 | 0.035 | 0.859 | 0.1 | 0.930 | 0.1 | 0.999 | 0.05 | 0.964 | 0.04 | 0.968 |
| 0.19 | 1.170 | 0.095 | 0.998 | 0.1 | 0.952 | 0.2 | 0.973 | 0.2 | 1.052 | 0.1 | 0.999 | 0.07 | 1.015 |
| 0.36 | 1.258 | 0.19 | 1.093 | 0.2 | 1.016 | 0.3 | 1.003 | 0.3 | 1.090 | 0.2 | 1.053 | 0.1 | 1.050 |
| 0.48 | 1.309 | 0.32 | 1.165 | 0.4 | 1.091 | 0.4 | 1.036 | 0.4 | 1.116 | 0.3 | 1.085 | 0.2 | 1.124 |
| 0.77 | 1.387 | 0.59 | 1.242 | 0.5 | 1.111 | 0.5 | 1.059 | 0.5 | 1.140 | 0.4 | 1.111 | 0.3 | 1.170 |
| 0.98 | 1.432 | 1.0 | 1.310 | 0.7 | 1.157 | 0.7 | 1.099 | 0.7 | 1.183 | 0.5 | 1.135 | 0.4 | 1.204 |
| 0.28 | 1.420 | 1.5 | 1.364 | 1.0 | 1.202 | 1.0 | 1.155 | 1.0 | 1.224 | 0.6 | 1.154 | 0.5 | 1.232 |
| 0.99 | 1.449 | 2.0 | 1.385 | 0.2 | 1.181 | 0.15 | 1.148 | 0.2 | 1.210 | 0.8 | 1.186 | 0.7 | 1.279 |
| 1.5 | 1.521 | 3.0 | 1.409 | 1.5 | 1.256 | 1.5 | 1.233 | 1.5 | 1.272 | 1.0 | 1.213 | 1.0 | 1.322 |
| 2.0 | 1.593 | 0.59 | 1.404 | 2.0 | 1.292 | 2.0 | 1.292 | 2.0 | 1.320 | 0.155 | 1.194 | 0.2 | 1.304 |
| 3.0 | 1.701 | w=26.1 | | 2.4 | 1.315 | 2.4 | 1.346 | 2.4 | 1.345 | 1.0 | 1.224 | 1.0 | 1.358 |
| 0.54 | 1.684 | | | 0.2 | 1.278 | 0.15 | 1.330 | 0.2 | 1.316 | 1.5 | 1.268 | 1.5 | 1.372 |
| w=23.9 | | | | w=16.9 | | w=23.1 | | w=19.1 | | 1.5 | 1.274 | 2.0 | 1.415 |
| | | | | | | | | | | 2.0 | 1.307 | 3.0 | 1.473 |
| | | | | | | | | | | 2.4 | 1.328 | 4.0 | 1.512 |
| | | | | | | | | | | 0.2 | 1.295 | 5.0 | 1.554 |
| | | | | | | | | | | w=19.0 | | 6.0 | 1.588 |
| | | | | | | | | | | | | 7.0 | 1.617 |
| | | | | | | | | | | | | 0.2 | 1.566 |
| | | | | | | | | | | | | w=19.0 | |

| S.15 | | S.16 | | S.17 | | S.18 | | S.19 | | S.20 | |
|---|---|---|---|---|---|---|---|---|---|---|---|
| CellP | Dbd | CellP | Dbd | CellP | Dbd | CellP | Dbd | CellP | Dbd | CellP | Dbd |
| 0 | 0.781 | 0 | 0.853 | 0 | 0.826 | 0 | 1.100 | 0 | 0.963 | 0 | 0.846 |
| 0.02 | 0.806 | 0.02 | 0.880 | 0.01 | 0.852 | 0.035 | 1.138 | 0.05 | 1.017 | 0.03 | 0.900 |
| 0.05 | 0.826 | 0.05 | 0.940 | 0.05 | 0.945 | 0.06 | 1.158 | 0.07 | 1.039 | 0.05 | 0.948 |
| 0.1 | 0.869 | 0.1 | 0.985 | 0.1 | 1.023 | 0.08 | 1.170 | 0.1 | 1.053 | 0.1 | 1.043 |
| 0.2 | 0.939 | 0.2 | 1.065 | 0.2 | 1.118 | 0.1 | 1.180 | 0.15 | 1.078 | 0.2 | 1.126 |
| 0.4 | 0.975 | 0.4 | 1.128 | 0.3 | 1.186 | 0.15 | 1.198 | 0.2 | 1.094 | 0.3 | 1.179 |
| 0.5 | 0.993 | 0.5 | 1.158 | | 1.193 | 0.2 | 1.210 | 0.3 | 1.117 | 0.4 | 1.220 |
| 0.7 | 1.023 | 0.7 | 1.205 | 0.4 | 1.275 | 0.3 | 1.232 | 0.4 | 1.139 | 0.5 | 1.250 |
| 1.0 | 1.059 | 1.0 | 1.252 | 0.5 | 1.337 | 0.4 | 1.249 | 0.5 | 1.156 | 0.7 | 1.289 |
| 0.9 | 1.066 | | | 0.7 | 1.399 | 0.5 | 1.263 | 0.7 | 1.188 | 1.0 | 1.340 |
| 0.8 | 1.066 | | | 1.0 | 1.489 | 0.7 | 1.286 | 1.0 | 1.220 | 0.2 | 1.318 |
| 0.7 | 1.066 | | | 0.2 | 1.484 | 1.0 | 1.310 | 0.3 | 1.215 | 1.5 | 1.390 |
| 0.6 | 1.066 | | | 1.5 | 1.570 | 0.2 | 1.300 | 0.2 | 1.211 | 2.0 | 1.433 |
| 0.5 | 1.066 | | | 2.0 | 1.661 | 1.5 | 1.340 | 1.5 | 1.265 | 3.1 | 1.493 |
| 0.4 | 1.066 | | | 3.0 | 1.731 | 2.0 | 1.366 | 2.0 | 1.299 | 4.0 | 1.529 |
| 0.3 | 1.066 | | | 4.0 | 1.824 | 3.0 | 1.404 | 3.0 | 1.360 | | 1.484 |
| 0.2 | 1.062 | | | 5.0 | 1.879 | 0.2 | 1.382 | 4.0 | 1.409 | | |
| 1.5 | 1.122 | 0.2 | 1.230 | w=23.4 | | w=9.1 | | 5.0 | 1.467 | w=21.5 | |
| 2.0 | 1.180 | 1.5 | 1.3 | | | | | 5.0 | 1.487 | | |
| 3.0 | 1.304 | 2.0 | 1.346 | | | | | | | | |
| 4.0 | 1.458 | 3.0 | 1.40 | | | | | | | | |
| 0.08 | 1.445 | 4.0 | 1.447 | | | | | 0.2 | 1.437 | | |
| w=19.0 | | 5.0 | 1.469 | | | | | w=12.6 | | | |
| | | 0.03 | 1.367 | | | | | | | | |
| | | w=19.0 | | | | | | | | | |

TABLE B RESULTS OF TRIAXIAL TESTING

SOIL: Threipmuir

| S1 | | S2 | | S3 | | S4 | | S5 | | S6 | | S7 | |
|---|---|---|---|---|---|---|---|---|---|---|---|---|---|
| Cell Pres. | Dbd | Cell Pres. | Dbd | Cell Pres. | Dbd | Cell Pres. | Dbd | Cell Pres. | Dbd | Cell Pres. | Dbd | Cell Pres. | Dbd |
| 0 | 0.825 | 0.03 | 0.927 | 0 | 0.791 | 0 | 0.913 | 0 | 0.936 | 0 | 0.893 | 0.02 | 0.963 |
| 0.01 | 0.870 | 0.105 | 1.018 | 0.015 | 0.814 | 0.01 | 0.929 | 0.01 | 0.963 | 0.01 | 0.914 | 0.035 | 0.990 |
| 0.02 | 0.913 | 0.195 | 1.094 | 0.032 | 0.842 | 0.02 | 0.975 | 0.03 | 1.004 | 0.022 | 0.940 | 0.06 | 1.009 |
| 0.03 | 0.932 | 0.119 | 1.092 | 0.057 | 0.871 | 0.062 | 1.051 | 0.07 | 1.039 | 0.07 | 0.968 | 0.08 | 1.068 |
| 0.04 | 0.947 | 0.238 | 1.117 | 0.1 | 0.908 | 0.108 | 1.104 | 0.124 | 1.070 | 0.132 | 0.996 | 0.151 | 1.131 |
| 0.05 | 0.955 | 0.397 | 1.187 | 0.154 | 0.947 | 0.189 | 1.168 | 0.227 | 1.105 | 0.254 | 1.027 | 0.227 | 1.196 |
| 0.07 | 0.968 | 0.6 | 1.242 | 0.289 | 1.003 | 0.357 | 1.248 | 0.386 | 1.142 | 0.459 | 1.063 | 0.432 | 1.304 |
| 0.09 | 0.982 | 1.0 | 1.313 | 0.451 | 1.046 | 0.622 | 1.334 | 0.662 | 1.182 | 0.762 | 1.102 | 0.692 | 1.374 |
| 0.108 | 0.998 | 0.243 | 1.297 | 0.622 | 1.076 | 1.046 | 1.411 | 1.0 | 1.221 | 1.0 | 1.124 | 0.851 | 1.354 |
| 0.2 | 1.056 | 4.0 | 1.510 | 0.956 | 1.111 | 0.208 | 1.388 | 0.254 | 1.212 | 0.257 | 1.117 | 1.041 | 1.426 |
| 0.295 | 1.102 | 0.473 | 1.483 | 0.222 | 1.111 | 1.7 | 1.494 | 1.05 | 1.229 | 1.5 | 1.176 | 0.184 | 1.400 |
| 0.4 | 1.130 | | | 1.45 | 1.176 | 2.5 | 1.557 | 1.5 | 1.264 | 2.0 | 1.219 | 1.5 | 1.462 |
| | | w = 20.6 | | 2.0 | 1.204 | 4.0 | 1.628 | 2.0 | 1.298 | 3.0 | 1.280 | 2.0 | 1.466 |
| 0.6 | 1.188 | | | 3.0 | 1.251 | 5.0 | 1.662 | 3.0 | 1.350 | 4.0 | 1.341 | 3.0 | 1.469 |
| | | | | 4.0 | 1.292 | 6.0 | 1.684 | 4.0 | 1.398 | 5.0 | 1.480 | 4.0 | 1.474 |
| 0.795 | 1.229 | | | 5.0 | 1.318 | 7.0 | 1.691 | 5.0 | 1.438 | 6.0 | 1.462 | 5.0 | 1.476 |
| 0.9 | 1.251 | | | 6.0 | 1.366 | 0.562 | 1.662 | 6.0 | 1.474 | 7.0 | 1.517 | 6.0 | 1.476 |
| 1.0 | 1.269 | | | 7.0 | 1.413 | | | 7.0 | 1.514 | 0.514 | 1.512 | 7.0 | 1.479 |
| 0.159 | 1.259 | | | 8.0 | 1.460 | w = 19.0 | | 0.559 | 1.502 | | | 8.0 | 1.481 |
| 1.0 | 1.287 | | | | 1.476 | | | | | w = 14.0 | | 0.465 | 1.487 |
| 1.5 | 1.341 | | | 0.23 | | | | w = 14.0 | | | | | |
| 2.0 | 1.389 | | | | | | | | | | | w = 23.3 | |
| 3.0 | | | | w = 20.1 | | | | | | | | | |
| 4.0 | 1.508 | | | | | | | | | | | | |
| 5.0 | 1.541 | | | | | | | | | | | | |
| 0.186 | 1.495 | | | | | | | | | | | | |

w = 17.5

| S8 | | S9 | | S10 | | S11 | | S12 | | S13 | | S14 | |
|---|---|---|---|---|---|---|---|---|---|---|---|---|---|
| Cell Pres. | Dbd | Cell Pres. | Dbd | Cell Pres. | Dbd | Cell Pres. | Dbd | Cell Pres. | Dbd | Cell Pres. | Dbd | Cell Pres. | Dbd |
| 0 | 0.957 | 0 | 0.926 | 0 | 0.957 | 0 | 1.029 | 0 | 0.903 | 0.02 | 0.884 | 0 | 0.981 |
| 0.02 | 1.002 | 0.01 | 0.980 | 0.02 | 1.002 | 0.02 | 1.066 | 0.02 | 0.932 | 0.04 | 0.931 | 0.03 | 1.029 |
| 0.06 | 1.045 | 0.05 | 1.038 | 0.06 | 1.045 | 0.033 | 1.084 | 0.035 | 0.963 | 0.07 | 0.984 | 0.05 | 1.042 |
| 0.1 | 1.067 | 0.13 | 1.100 | 0.1 | 1.067 | 0.06 | 1.107 | 0.06 | 1.002 | 0.1 | 1.022 | 0.08 | 1.062 |
| 0.23 | 1.199 | 0.32 | 1.173 | 0.23 | 1.119 | 0.09 | 1.123 | 0.1 | 1.044 | 0.057 | 1.018 | 0.1 | 1.071 |
| 0.4 | 1.167 | 0.55 | 1.231 | 0.4 | 1.167 | 0.11 | 1.130 | 0.18 | 1.103 | 0.105 | 1.032 | 0.04 | 1.066 |
| 0.64 | 1.212 | 0.69 | 1.245 | 0.64 | 1.212 | 0.035 | 1.126 | 0.26 | 1.149 | 0.208 | 1.102 | 0.1 | 1.074 |
| 1.1 | 1.275 | 1.0 | 1.290 | 1.1 | 1.275 | 0.1 | 1.131 | 0.38 | 1.194 | 0.297 | 1.151 | 0.2 | 1.105 |
| 0.3 | 1.264 | 0.28 | 1.279 | 0.3 | 1.264 | 0.2 | 1.161 | 0.43 | 1.215 | 0.4 | 1.190 | 0.35 | 1.129 |
| 1.5 | 1.317 | 1.5 | 1.345 | 1.5 | 1.317 | 0.4 | 1.204 | 0.57 | 1.251 | 0.5 | 1.221 | 0.4 | 1.146 |
| 2.0 | 1.354 | 2.0 | 1.383 | 2.0 | 1.354 | 0.069 | 1.245 | 0.81 | 1.302 | 0.7 | 1.269 | 0.7 | 1.184 |
| 3.0 | 1.410 | 3.0 | 1.442 | 3.0 | 1.410 | 1.0 | 1.277 | 1.0 | 1.327 | 1.0 | 1.319 | 1.0 | 1.213 |
| 4.0 | 1.457 | 4.0 | 1.481 | 4.0 | 1.457 | 1.5 | 1.315 | 0.32 | 1.318 | 0.2 | 1.334 | 0.23 | 1.205 |
| 5.0 | 1.487 | 0.53 | 1.457 | 5.0 | 1.487 | 0.24 | 1.309 | 1.0 | 1.342 | 1.0 | 1.330 | 1.0 | 1.218 |
| 6.0 | 1.512 | | | 6.0 | 1.512 | 1.5 | 1.321 | 1.5 | 1.393 | 1.5 | 1.379 | 1.5 | 1.254 |
| 0.6 | 1.487 | w = 15.8 | | 0.6 | 1.487 | 2.0 | 1.346 | 2.0 | 1.437 | 2.0 | 1.417 | 2.0 | 1.282 |
| w = 17.1 | | | | w = 15.4 | | 4.0 | 1.430 | 3.0 | 1.491 | 4.0 | 1.496 | 3.0 | 1.330 |
| | | | | | | 6.0 | 1.499 | 4.0 | 1.529 | 6.0 | 1.505 | 5.0 | 1.398 |
| | | | | | | w = 11.7 | | 5.0 | 1.543 | 8.0 | 1.510 | 7.0 | 1.453 |
| | | | | | | | | 6.0 | 1.546 | 0.15 | 1.490 | 0.38 | 1.428 |
| | | | | | | | | 0.56 | 1.538 | w = 20.6 | | w = 11.7 | |
| | | | | | | | | w = 20.0 | | | | | |

| S15 | | S16 | | S17 | | S18 | | S19 | |
|---|---|---|---|---|---|---|---|---|---|
| Cell Pres. | Dbd | Cell Pres. | Dbd | Cell Pres. | Dbd | Cell Pres. | Dbd | Cell Pres. | Dbd |
| 0 | 1.016 | 0 | 1.001 | 0 | 1.043 | 0 | 0.969 | 0 | 0.847 |
| 0.02 | 1.047 | 0.04 | 1.065 | 0.045 | 1.095 | 0.02 | 1.062 | 0.01 | 0.863 |
| 0.035 | 1.090 | 0.065 | 1.097 | 0.07 | 1.116 | 0.03 | 1.113 | 0.02 | 0.897 |
| 0.05 | 1.099 | 0.15 | 1.154 | 0.09 | 1.119 | 0.01 | 0.981 | 0.04 | 0.937 |
| 0.067 | 1.109 | 0.2 | 1.177 | 0.15 | 1.129 | 0.04 | 1.022 | 0.07 | 0.985 |
| 0.085 | 1.120 | 0.295 | 1.213 | 0.07 | 1.121 | 0.095 | 1.077 | 0.130 | 1.064 |
| 0.1 | 1.160 | 0.49 | 1.270 | 0.19 | 1.168 | 0.192 | 1.147 | 0.178 | 1.119 |
| 0.2 | 1.191 | 0.795 | 1.328 | 0.05 | 1.231 | 0.292 | 1.198 | 0.222 | 1.15 |
| 0.4 | 1.227 | 1.0 | 1.357 | 1.0 | 1.295 | 0.397 | 1.246 | 0.343 | 1.209 |
| 0.073 | 1.215 | 1.27 | 1.388 | 0.3 | 1.295 | 0.497 | 1.276 | 0.562 | 1.287 |
| 0.5 | 1.234 | 2.0 | 1.438 | 1.0 | 1.308 | 0.595 | 1.307 | 0.986 | 1.368 |
| 0.7 | 1.254 | 2.4 | 1.462 | 1.5 | 1.341 | 0.7 | 1.335 | 0.259 | 1.350 |
| 0.9 | 1.283 | 0.25 | 1.433 | 2.0 | 1.374 | 0.803 | 1.359 | 1.5 | 1.430 |
| 0.08 | 1.293 | w = 15.8 | | 3.0 | 1.423 | 0.9 | 1.379 | 2.0 | 1.445 |
| 1.0 | 1.370 | | | 4.0 | 1.467 | 1.0 | 1.405 | 3.0 | 1.450 |
| 2.0 | 1.373 | | | 5.0 | 1.467 | 2.0 | 1.544 | 4.0 | 1.458 |
| 3.0 | 1.422 | | | 6.0 | 1.528 | 3.0 | 1.631 | 5.0 | 1.461 |
| 5.0 | 1.492 | | | 7.0 | 1.550 | 5.0 | 1.737 | 6.0 | 1.471 |
| 7.0 | 1.534 | | | 8.0 | 1.568 | 7.0 | 1.813 | 6.7 | 1.477 |
| 0.19 | 1.498 | | | 0.34 | 1.543 | 0.21 | 1.737 | 0.211 | 1.493 |
| w = 13.6 | | | | w = 12.35 | | w = 17.8 | | w = 23.3 | |

## APPENDIX 8 A COMPUTER PROGRAM TO OPERATE THE PREDICTION MODEL OF DRY BULK DENSITY AFTER WHEEL PASSAGE

The program has been written in IMP language to run on the Edinburgh Multiple Access System (EMAS) operated by the Edinburgh Regional Computing Centre. The format of the input and output of the program, and the program code, are described in this appendix.

### 1. Input format

An example of the format of the input data file is given below. Each box represents a data position. The meaning and units of each data item are described in the key to the program code in the following section.

| F | LI | BETA | LOAD | TIP |
|---|---|---|---|---|
| MRD | CA | NE | IF | |
| INDEN | CR | MC | OBDEN | ) repeated for each element |

If CA $\neq$ 0 MRD = -1 and TIP can be any value.

If F = 1 all output made, if F = 2, selected output made. Input of this data as a file precedes an interactive 'prompt' for the input of 'DINC'.

### 2. Program code

A flowchart of the program is shown in Fig.68. The program code and a brief description of each section is shown on the following pages, as well as a key for the identification of each variable and other items used in the program.

## KEY TO THE PROGRAM VARIABLES

| | |
|---|---|
| ALPHA | Half the angle subtended by the lines joining opposite edges of the contact 'circle' with the centre of the element, radians. |
| BETA | Slope of the primary function, $g/cm^3$/unit ln P. |
| CA | Horizontal projection of the tyre/soil contact area, $cm^2$. |
| CR (1 to NE) | Array of initial cone resistances of the elements, bar. |
| DI (1 to NE) | Array of dry bulk densities before each stress increment, $g/cm^3$. |
| DIN | Depth interval between the centres of soil elements, cm. |
| DF (1 to NE) | Dry bulk densities after each stress increment, $g/cm^3$. |
| DMAX | Maximum dry bulk density (from Proctor curve), $g/cm^3$. |
| F | Output format control. |
| FR | Counter distinguishing between stress prediction equations S1, S2 and S3. |
| J | Switch variable. |
| GAMA | Intercept of 'VCL', $g/cm^3$. |
| GOA (10 to 32) | |
| GOB (10 to 30) | Switch arrays for the allocation of Critical State parameters. |
| H (1 to NE) | Array of heights of the elements, cm. |
| IF | Soil type (1 = Macmerry, 2 = Threipmuir). |

INDEN (1 to NE) Array of initial dry bulk densities of the elements, $g/cm^3$.

LAMDA Slope of the 'VCL', $g/cm^3$/unit ln P.

LI Stress (load) increment for each cycle of stress increase, ln (bar).

LOAD Wheel load.

LOGP The current value of the natural logarithm of spherical pressure, ln (bar).

MC (1 to NE) Array of gravimetric moisture contents of the elements, %, w/w.

MRD Mean rut depth, cm.

MSD Variable for calculation of the standard deviation of prediction.

NE Number of elements.

OBDEN (1 to NE) Array of observed final dry bulk densities, $g/cm^3$.

PIN Counter for the cycles of pressure increase.

PM (1 to NE) Array of maximum spherical pressures for each element, bar.

PMS Mean surface pressure, bar.

PTH Threshold spherical pressure, bar.

Q Cosine of ALPHA

RM (1 to NE) Array of maximum deviatoric stresses, bar.

S Tangent of ALPHA.

SKIP Flag indicating the use of either the 'VCL' (SKIP = 1) or primary function (SKIP = 0).

STIN Counter for the cycles of strain increase.

TIP Tyre inflation pressure.

V First principal stress, bar

| | |
|---|---|
| W | Width of the circle of same area as CA, cm. |
| Z (1 to NE) | Array of depths of element centres from the tyre/soil interface, cm. |

```
! MODPROG :A PROGRAM PREDICTING DRY BULK DENSITY
!           CHANGES BENEATH TRACTOR WHEELS      PAUL S. BLACKWELL


%BEGIN
%EXTERNALROUTINESPEC PROMPT(%STRING (15) S )
%SWITCH GOA(1:40), GOB(1:40)
%REAL LOAD, TIP, MRD, A, B, C, PMS, W, ALPHA, Q, LOGP, GAMA, LAMDA, PTH, S, V, CA, LI, DIN
%REAL BETA, DMAX, MSD
%INTEGER IF, NE, J, I, STIN, FR, PIN, SKIP, F
%REALARRAY INDEN(1:20), CR(1:20), MC(1:20), Z(1:20), DI(1:20), OBDEN(1:20)
%REALARRAY H(1:20), PM(1:20), RM(1:20), DF(1:20)
%ROUTINESPEC STRAIN
PROMPT('D.INC?: ')
NEWLINE
READ(DIN)



SELECTINPUT(5); SELECTOUTPUT(6)


! INPUT OF PROGRAM CONTROL VARIABLES, SLOPE OF PRIMARY FUNCTION
! AND WHEEL INPUT FACTORS

READ(F); READ(LI); READ(BETA)
READ(LOAD); READ(TIP); READ(MRD)
%PRINTTEXT' LOAD= '; PRINT(LOAD, 4, 2); %PRINTTEXT' TIP= '
PRINT(TIP, 2, 2); %PRINTTEXT' MRD= '; PRINT(MRD, 2, 1)
%PRINTTEXT' BETA= '; PRINT(BETA, 2, 4)
NEWLINE

%IF MRD<0 %THEN ->CADONE


! CALCULATION OF CONTACT AREA FROM FUNCTIONS USING MRD
! FOR 12.4/11-36 TYRE

CA=0

%IF LOAD<1.1 %AND LOAD>0.8 %THEN ->A
%IF LOAD<1.35 %AND LOAD>1.1 %THEN ->B
%IF LOAD<1.6 %AND LOAD>1.35 %THEN ->C
%IF LOAD<1.9 %AND LOAD>1.6 %THEN ->D
A: A=2200  ; B=1500 ; C=-0.25 ; %IF TIP≠12 %THEN %START
%IF TIP=16 %THEN CA=CA-80
%IF TIP=20 %THEN CA=CA-85
%IF TIP>20 %THEN CA=CA-100
%FINISH
->CACAL
B: A=2200  ; B=1500  ; C=-0.25; %IF TIP≠16 %THEN %START
%IF TIP=12 %THEN CA=CA+125
%IF TIP=20 %THEN CA=CA-35
%IF TIP>20 %THEN CA=CA-50
%FINISH
->CACAL
C: A=2215  ; B=1350  ; C=-0.2632; %IF TIP≠ 20 %THEN %START
%IF TIP=12 %THEN CA=CA+328
%IF TIP=16 %THEN CA=CA+164
%IF TIP>20 %THEN CA=CA-20
%FINISH
->CACAL
```

```
D: A=2000; B=1150; C=-0.4; %IF TIP≠25 %THEN %START
%IF TIP=12 %THEN CA=CA+500
%IF TIP=16 %THEN CA=CA+200
%IF TIP=20 %THEN CA=CA+100
%FINISH
CACAL: CA=CA+ A-EXP(LOG(B)+(C*MRD))
-> START


CADONE: READ(CA)


!  INPUT OF SOIL INPUT FACTORS FOR EACH ELEMENT

START: READ(NE); READ(IF)
%PRINTTEXT' CA= '; PRINT(CA, 3, 1); %PRINTTEXT' NE= '; WRITE(NE, 2)
%PRINTTEXT' IF= '; WRITE(IF, 1); %PRINTTEXT' LOAD INC= '; PRINT(LI, 1, 4)
NEWLINE
%CYCLE J=1, 1, NE; READ(INDEN(J)); READ(CR(J)); READ(MC(J))
READ(OBDEN(J)); %REPEAT


!  CALCULATION OF MEAN SURFACE PRESSURE AND WIDTH OF EQUIVALENT CIRCLE

PMS=(LOAD*1000)/(CA*1.0196) ; Z(1)=DIN; W=2*(SQRT(CA/3.14159))
NEWLINE; %PRINTTEXT' PMS= '; PRINT(PMS, 2, 2); %PRINTTEXT' W= '; PRINT(W, 2, 2)
NEWLINES(2)


!  CALCULATION OF STRESSES AND STRAINS FOR EACH ELEMENT



%CYCLE I=1, 1, NE
SKIP=0; DI(I)=INDEN(I); H(I)=DIN; LOGP=LOG(0.01); STIN=0; PIN=0


!  ALLOCATION OF MAXIMUM DRY BULK DENSITY , SLOPE AND INTERCEPT OF
!  'VOL' ACCORDING TO GRAVIMETRIC MOISTURE CONTENT OF EACH ELEMENT.
!  (NEAREST INTEGER VALUE)

%IF IF=2 %THEN -> LOWTER
J=INT(MC(I))
-> GOA(J)
GOA(10): LAMDA=0.1; GAMA=1.184; DMAX=1.59
-> TINC
GOA(11): LAMDA=0.1; GAMA=1.184; DMAX=1.60
-> TINC
GOA(12): LAMDA=0.1; GAMA=1.184; DMAX=1.62
-> TINC
GOA(13): LAMDA=0.1; GAMA=1.184; DMAX=1.63
-> TINC
GOA(14): LAMDA=0.1; GAMA=1.184; DMAX=1.64
-> TINC
GOA(15): LAMDA=0.132; GAMA=1.184; DMAX=1.65
-> TINC
GOA(16): LAMDA=0.132; GAMA=1.184; DMAX=1.66
-> TINC
GOA(17): LAMDA=0.119; GAMA=1.185; DMAX=1.67
-> TINC
GOA(18): LAMDA=0.106; GAMA=1.186; DMAX=1.68
-> TINC
GOA(19): LAMDA=0.117; GAMA=1.195; DMAX=1.69
-> TINC
```

```
GOTO(20):LAMDA=0.129;GAMA=1.204;DMAX=1.69
-> TINC
GOTO(21):LAMDA=0.136;GAMA=1.195;DMAX=1.68
-> TINC
GOTO(22):LAMDA=0.143;GAMA=1.186;DMAX=1.67
-> TINC
GOTO(23):LAMDA=0.165;GAMA=1.208;DMAX=1.53
-> TINC
GOTO(24):LAMDA=0.164;GAMA=1.229;DMAX=1.63
-> TINC
GOTO(25):LAMDA=0.139;GAMA=1.261;DMAX=1.61
-> TINC
GOTO(26):LAMDA=0.114;GAMA=1.294;DMAX=1.59
-> TINC
GOTO(27):LAMDA=0.106;GAMA=1.298;DMAX=1.56
-> TINC
GOTO(28):LAMDA=0.097;GAMA=1.302;DMAX=1.54
-> TINC
GOTO(29):LAMDA=0.069;GAMA=1.323;DMAX=1.52
-> TINC
GOTO(30):LAMDA=0.041;GAMA=1.344;DMAX=1.50
-> TINC
GOTO(31):LAMDA=0.013;GAMA=1.485;DMAX=1.36
-> TINC
GOTO(32):LAMDA=0.021;GAMA=1.936;DMAX=1.46
-> TINC
LOWTER:
J=INT(MC(I))
-> GOTO(J)
GOTO(10):LAMDA=0.67;GAMA=0.80;DMAX=1.62
-> TINC
GOTO(11):LAMDA=0.86;GAMA=0.80;DMAX=1.63
-> TINC
GOTO(12):LAMDA=0.105;GAMA=0.80;DMAX=1.65
-> TINC
GOTO(13):LAMDA=0.123;GAMA=0.85;DMAX=1.66
-> TINC
GOTO(14):LAMDA=0.140;GAMA=0.85;DMAX=1.66
-> TINC
GOTO(15):LAMDA=0.156;GAMA=0.88;DMAX=1.66
-> TINC
GOTO(16):LAMDA=0.170;GAMA=0.95;DMAX=1.66
-> TINC
GOTO(17):LAMDA=0.180;GAMA=1.1;DMAX=1.66
-> TINC
GOTO(18):LAMDA=0.190;GAMA=1.11;DMAX=1.66
-> TINC
GOTO(19):LAMDA=0.195;GAMA=1.128;DMAX=1.65
-> TINC
GOTO(20):LAMDA=0.198;GAMA=1.145;DMAX=1.64
-> TINC
GOTO(21):LAMDA=0.195;GAMA=1.174;DMAX=1.62
-> TINC
GOTO(22):LAMDA=0.190;GAMA=1.20;DMAX=1.61
-> TINC
GOTO(23):LAMDA=0.180;GAMA=1.225;DMAX=1.58
-> TINC
GOTO(24):LAMDA=0.170;GAMA=1.260;DMAX=1.56
-> TINC
GOTO(25):LAMDA=0.153;GAMA=1.30;DMAX=1.54
-> TINC
GOTO(26):LAMDA=0.137;GAMA=1.345;DMAX=1.52
-> TINC
GOTO(27):LAMDA=0.123;GAMA=1.375;DMAX=1.51
-> TINC
GOTO(28):LAMDA=0.123;GAMA=1.375;DMAX=1.47
-> TINC
GOTO(29):LAMDA=0.123;GAMA=1.375;DMAX=1.45
```

```
-> TINC
GOB(30):LAMDA=0.123;GAMA=1.375;DMAX=1.43


!  CALCULATION OF THRESHOLD SPHERICAL PRESSURE (PTH) BETWEEN PRIMARY
!  FUNCTION AND 'VCL'

TINC:  PTH=(INDEN(I)-GAMA-BETA*LOG(0.01))/(LAMDA-BETA)


%PRINTTEXT' EL.NO. ';WRITE(I,1);NEWLINE;%PRINTTEXT' MC= '
PRINT(MC(I),2,1);%PRINTTEXT' LAMDA= ';PRINT(LAMDA,2,4);%PRINTTEXT' GAMA= '
PRINT(GAMA,1,3);%PRINTTEXT' LOG PTH= ';PRINT(PTH,2,2);%PRINTTEXT' DMAX= '
PRINT(DMAX,1,3);%PRINTTEXT' CR= ';PRINT(CR(I),3,1);NEWLINE



!  STRAIN INCREMENT CYCLE. CALCULATION OF EXPECTED MAXIMUM STRESSES
!  FOR CURRENT ELEMENT SHAPE

STINC:  ALPHA=ARCTAN(Z(I),W/2);Q=COS(ALPHA);STIN=STIN+1;S=TAN(ALPHA)
%PRINTTEXT' STINC CYCLE ';WRITE(STIN,3);NEWLINE
%PRINTTEXT' Z= ';PRINT(Z(I),3,2);%PRINTTEXT' H= '
PRINT(H(I),2,1);%PRINTTEXT' ALPHA= ';PRINT(ALPHA,2,4)
%PRINTTEXT' DBD= ';PRINT(DI(I),2,3)
%PRINTTEXT' LOGP= ';PRINT(LOGP,2,3)


!  CHOICE OF STRESS PREDICTION EQUATION FROM THE INITIAL CONE
! RESISTANCE OF EACH ELEMENT  (ONLY  FIRST STRAIN CYCLE OF EACH ELEMENT)

%IF STIN#1 %THEN %START
%IF FR=1 %THEN ->G
%IF FR=2 %THEN ->F
%IF FR=3 %THEN ->E
%FINISH
%IF CR(I)> 0 %AND CR(I)< 16 %THEN ->E
%IF CR(I)> 16 %AND CR(I)< 26 %THEN ->F
%IF CR(I)> 26 %AND CR(I)< 100 %THEN ->G



!  CALCULATION OF PMAX AND RMAX

E: V=2*PMS*(1-(Q**6)-(1/S**2)*(0.5-((3/2)*Q**4)+Q**6))
 PM(I)=1.54769*V
   RM(I)=0.13*V
FR=3
->INC
F: V=1.5*PMS*(1-(Q**5)-((1/S**4)*((8/3)-(5*Q)+((10/3)*Q**3)-Q**5)))
 PM(I)=1.54769*V
   RM(I)=0.13*V
FR=2
->INC
G: V=PMS*(1-Q**4)
 PM(I)=1.54769*V
   RM(I)=0.13*V
FR=1
INC:%PRINTTEXT' FR= ';WRITE(FR,1);%PRINTTEXT' PMAX= ';PRINT(PM(I),2,5)
NEWLINE


!  STRESS INCREMENT CYCLE. CALCULATION OF THE DRY BULK DENSITY OF EACH
!  ELEMENT FOR EACH INCREMENT OF THE CURRENT VALUE OF   LN P  (LOGP)

PINC:  LOGP= LOGP+LI;PIN=PIN+1
%IF F=2 %THEN ->ROUND1
%PRINTTEXT' PINC CYCLE ';WRITE(PIN,3);%PRINTTEXT' LOGP= '
PRINT(LOGP,2,3);%PRINTTEXT' SKIP= ';WRITE(SKIP,1)
NEWLINE;ROUND1:
```

```
! COMPARISON OF LOGP,PTH AND PMAX

%IF LOGP>=LOG(PM(I)) %THEN -> OUT
%IF LOGP<PTH %THEN %START


! CALCULATION OF DBD USING PRIMARY FUNCTION

DF(I)=INDEN(I)+BETA*(LOGP-LOG(0.01))
-> DCH; %FINISH


! CALCULATION OF DBD USING 'VOL'

SKIP=1 ; DF(I)=GAMA+LAMDA*LOGP


! CHECK ON PRESENCE OF DMAX

DCH: %IF DF(I)>DMAX %THEN DF(I)=DMAX
%IF INDEN(I)>=DMAX %THEN DF(I)=INDEN(I)
%IF F=2 %THEN ->ROUND2
 %PRINTTEXT'DI= ' ; PRINT(DI(I),2,3); %PRINTTEXT'DF= '
PRINT(DF(I),2,3);NEWLINE
ROUND2:


! CHECK ON VOLUMETRIC STRAIN

%IF ((DF(I)-DI(I))/DI(I))*100<1 %THEN ->PINC
STRAIN
-> STINC


! CALCULATION OF FINAL STRAIN OF EACH ELEMENT

OUT: %IF SKIP =1 %THEN DF(I)=GAMA+LAMDA*LOG(PM(I)) %AND ->LCH
DF(I)=INDEN(I)+BETA*(LOG(PM(I))-LOG(0.01))
LCH: %IF DF(I) >DMAX %THEN DF(I)=DMAX
%IF INDEN(I)>=DMAX %THEN DF(I)=INDEN(I)
STRAIN
%PRINTTEXT' FINAL VALUES EL. NO. '
WRITE(I,2); %PRINTTEXT' INDEN= '; PRINT(INDEN(I),1,4); %PRINTTEXT' OBDEN= '
PRINT(OBDEN(I),1,4)
%PRINTTEXT' PREDEN= '; PRINT(DF(I),1,4); %PRINTTEXT' Z= '; PRINT(Z(I),2,2)
%PRINTTEXT' H= '; PRINT(H(I),2,2)
%PRINTTEXT' SIG1= '; PRINT(V,2,5)
%PRINTTEXT' PMAX= '; PRINT(PM(I),2,5)
NEWLINES(2)


! CALCULATION OF INITIAL DEPTH OF EACH ELEMENT

Z(I+1)=Z(I)+(DIN/2)+H(I)/2
%REPEAT

! CALCULATION OF SURFACE SINKAGE AND OUTPUT OF FINAL CONDITION OF EACH
ELEMENT

NEWLINES(2)
%PRINTTEXT'SINKAGE= '; PRINT((NE*DIN)-Z(NE),2,2);NEWLINE
%PRINTTEXT' Z        H        P        R        INDEN     PREDEN   OBDEN
CM       CM       BAR      BAR     G/CC      G/CC     G/CC '
NEWLINE
%CYCLE I=1,1,NE
PRINT(Z(I)+(NE*DIN)-Z(NE),2,2); SPACES(1); PRINT(H(I),1,2); SPACES(2)
PRINT(PM(I),1,4); SPACES(1); PRINT(RM(I),1,4); SPACES(1)
%PRINTTEXT' 0        '; SPACES(1); PRINT(DF(I),1,4); SPACES(1)
%PRINTTEXT' 0      '
NEWLINE
PRINT(I*DIN,2,0); %PRINTTEXT'       0        0        0    '
PRINT(INDEN(I),1,4)
```

```
%PRINTTEXT'       0     '
PRINT(ØBDEN(I),1,5)
NEWLINE
%REPEAT


! ØUTPUT ØF PREDICTEDAND FINAL VALUES AT THE SAME DEPTH

NEWLINES(2)
%PRINTTEXT'    Z    PREDEN    ØBDEN (ADJUSTED FØR DEPTH DIFFERENCES)'
NEWLINE
%CYCLE I=1,1,NE-1
ØBDEN(I)=ØBDEN(I)+((ØBDEN(I+1)-ØBDEN(I))/DIN)*((NE-I)*DIN-Z(NE)+Z(I))
%REPEAT
%CYCLE I=1,1,NE;PRINT(Z(I),2,1);SPACES(1)
PRINT(DF(I),1,4);SPACES(2);PRINT(ØBDEN(I),1,4);NEWLINE
%REPEAT


! CALCULATIØN ØF THE STANDARD DEVIATIØN ØF THE PREDICTED DRY BULK DENSI
TY
! VALUES FRØM THE ØBSERVED VALUES

MSD=0;%CYCLE I=1,1,NE
MSD=MSD+(ØBDEN(I)-DF(I))**2
%REPEAT
MSD=SQRT(MSD/NE)
NEWLINES(2)
%PRINTTEXT' STANDARD DEVIATIØN  ØF PREDICTIØN = ';PRINT(MSD,2,4)
%STØP


! RØUTINE TØ CALCULATE STRAINS ØF ELEMENTS FRØM CHANGES ØF
! DRY BULK DENSITY

%RØUTINE STRAIN
Z(I)=Z(I)-(H(I)/2)
H(I)=EXP(LØG(H(I))+(LØG(DI(I))-LØG(DF(I)))*0.333)
Z(I)=Z(I)+(H(I)/2)
DI(I)=DF(I)
%END


%ENDØFPRØGRAM
```

3. Output format

This is shown below. Use of option 2 for the output format (variable F) will omit the parts of the output indicated by underlining.

LOAD = TIP = MRD = BETA =

CA = NE = IF = LOAD INC = (LI)

PMS = W =

EL. NO.1

MC = LAMDA = GAMA = LOG PTH = DMAX = CR =

STINC (strain increase) CYCLE ( n )

Z = H = ALPHA = DBD(DF) = LOGP = FR = PMAX =

PINC (pressure increase) CYCLE ( n )

LOGP = SKIP =

DI = DF =

FINAL VALUES EL. NO ( n )

INDEN = OBDEN = PREDEN = Z =

SIG1 (v) = PMAX =

- after the analysis of all elements

SINKAGE =

- a table of final values of z, H, PM, RM, INDEN, PREDEN, OBDEN for each element.
- a table of values of PREDEN and OBDEN for the same values of Z.
- the standard deviation of prediction.

## APPENDIX 9 COMPUTER PROGRAMS USED FOR THE RESEARCH (Operated on lines LIAE01 and LIAE02 of the Edinburgh Multiple Access System)

| Name | Purpose |
|---|---|
| AVGAMMD)<br>AVGAMMG)<br>PBGAMM )<br>PBGAMMG) | The conversion of count rate and soil moisture content data to dry bulk density data and an analysis of variance of the bulk density data. |
| JKHMOTT | Calculation of soil moisture content from tin weighing data generated by the automatic balance system. |
| GRAPHDEN | Construction of graphs of dry bulk density before and after wheel passage, using the output from PBGAMM or PBGAMMG. |
| RUTANAL | Conversion of reliefmeter data into mean rut depth, maximum rut depth and mean cross-sectional area and mean rut profiles. |
| PLOTPDM | Construction of graphs relating dry bulk density after wheel passage to predicted maximum spherical pressure, using output from PBGAMM or PBGAMMG and wheel data. |
| GPLOT | Construction of various graphs for documentation of the data. |
| AVCOME)<br>AVCOMF) | Analysis of variance of data from experiments with complete block, or split plot design. |
| GENSTAT | Analysis of variance of data from experiments with 'tartan' design and data with missing values. |
| MULTREG | Linear regression analysis of two variables. |
| BMD07R | Non-linear regression. |

APPENDIX 10 "DEFORMABLE SPHERICAL DEVICES TO MEASURE STRESSES WITHIN FIELD SOILS"

P.S. BLACKWELL and B.D. SOANE

Submitted to Journal of Terramechanics in March 1978

*Journal of Terramechanics*, 1978, Vol. 15, No. 2, pp. 00 to 00. 0022–4898/78/0601–6081 $02.00/0


# DEFORMABLE SPHERICAL DEVICES TO MEASURE STRESSES WITHIN FIELD SOILS

P. S. BLACKWELL* and B. D. SOANE*

**Summary**—The design, calibration and use of two deformable spherical stress transducers are described. They are suitable for detecting principal stresses in deforming media such as soil and have major advantages over many rigid transducers previously used in such situations. One of the transducers is a water-filled rubber ball (WFRB) sensitive to hydrostatic and deviator stresses, the other is a mastic ball which deforms plastically and is sensitive to only deviator stresses. When the two devices are used at similar depths under a surface load, e.g. a wheel, the combined measurements of internal pressure of the WFRB and axial deformation of the mastic ball can be used to derive values for first and third principal stresses (assuming second and third principal stresses are equal). Calibration of the transducers at different temperatures is described.

Field measurements made with the transducer under loaded wheels are compared with predicted values at first principal stresses using equations developed by Söhne. Close correspondence between predicted and measured values was observed, when the existing soil strength conditions were taken into account.

The transducers promise to be useful in the measurement of stresses in field soils.

## INTRODUCTION

UNDERSTANDING and predicting the deformation behaviour of soils in field situations largely depends upon quantitative information about the stresses occurring in any part of the soil. Numerous workers [1, 2, 3, 4, 5, 6, 7] have described the construction and use of equipment to measure forces within field soils. Most of these techniques have suffered from the following shortcomings:

(a) Unidirectionality: Transducers using flexible diaphragms detect forces perpendicular to the diaphragm plane, thus these transducers must be orientated in the appropriate direction before use and any rotation of such a transducer during soil straining will alter the direction of the force being detected. Such rotations are very difficult to monitor and this uncertainty as to the direction of the detected stress is a considerable disadvantage when large soil deformations occur.

(b) Stiffness: The devices used have usually had a rigidity much greater than the surrounding soil leading to 'arching' problems, diversion of stresses from the device and misregistration. This problem can only be reduced if the mechanical properties of the device are similar to those of the surrounding soil.

A recent development by Verma *et al.* [8, 9] has considerably reduced the problems described above. A flexible, water-filled rubber ball was used to transmit soil stresses at the ball/soil interface to an internal water pressure transducer. Although this device had omnidirectionality and less uniaxial stiffness than previous devices its use presented two main problems.

*Scottish Institute of Agricultural Engineering, Bush Estate, Penicuik, Midlothian, Scotland.

(1) Any level of internal water pressure could be created by a number of combinations of forces at the ball/soil interface. Therefore, in general, interpretation of any signal from the device was difficult.
(2) Individual instrumentation of each device could require a costly and complex electronic recording system when a large number of devices needed monitoring over a short period, e.g. Möller [10].

A solution to these problems demanded a better understanding of the behaviour of a water-filled rubber ball (WFRB) in a stress system and a modification of the instrumentation previously used.

## THEORY OF BEHAVIOUR

*The water-filled rubber ball in a simplified stress system*

When the system has all principal stresses equal, in pure hydrostatic stress, the internal ball pressure will be directly proportional to the hydrostatic stress as in Fig. 1, line AB; this discounts any effects of wall stiffness. From any point on AB,

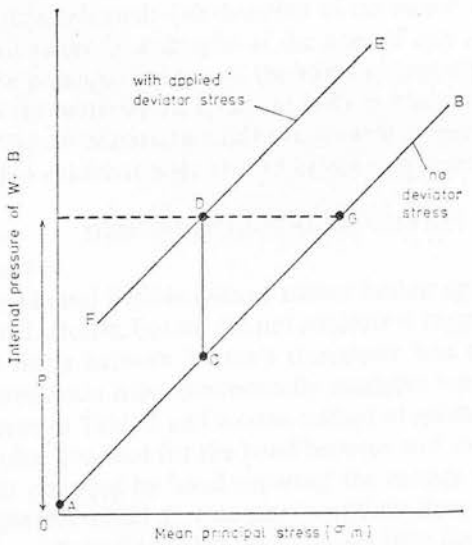


FIG. 1. Behaviour of water-filled rubber ball (theory).

e.g. C, a simple deviator stress can be applied where $\sigma_1$ exceeds both $\sigma_2$ and $\sigma_3$. If $\sigma_2$ and $\sigma_3$ are reduced to keep the mean principal stress $\sigma_1 + \sigma_2 + \sigma_3/3$ constant, the path $CD$ would be followed. Thus the same internal ball pressure ($P$) can be produced by a pure hydrostatic stress (as at point $G$) or a hydrostatic stress and a deviator stress (as at point $D$).

However, if the ball now experiences uniform increases of principal stresses a path $DE$ would be followed, parallel to $AB$, as an increase of hydrostatic stress occurs. A similar uniform reduction would cause path $DF$ to be followed. The theoretical procedure can be repeated to create a 'family' of lines parallel to $AB$.

Thus in this simplified stress system ($\sigma_2 = \sigma_3$) the hydrostatic stress and deviator stress appear to define the internal pressure of the ball. Similar results were also found by Verma *et al.* [8, 9] during tests on their device. Thus if the internal pressure of the water-filled rubber ball and one of the unknown stresses is measured (either hydrostatic or deviator) the other can be derived; this requires the use of two separate devices. A device to detect simple deviator stress appeared easier to design than one sensitive to only hydrostatic stress.

*Detection of simple deviator stress*

Any plastically deformable, yet incompressible, spherical body experiencing a stress system will deform to a shape which is a complement of the 'stress elipsoid' of the system. This concept has also been referred to as Lamé's Elipsoid [11]. It is a representation which geometrically describes the stress state at a point. The longest, shortest and intermediate semi-axes of the elipsoid describe the first, third and second principal stresses respectively. Thus pure hydrostatic stress will not change the shape of the spherical body but deviator stress, when second and third principal stresses are equal, will generate a prolate spheroid. The direction of the minor axis is parallel to that of the major principal stress. The lengths of the axes of any spheroid formed will be proportional to the principal stresses of the stress system experienced, provided any elastic rebound of the material the spherical body is made of can be ignored. It was considered that a 'mastic' material would have suitable properties of plastic and elastic behaviour for such a spherical body able to detect simple deviator stress.

## DESIGN AND INSTRUMENTATION

*Water-filled rubber ball*

The thin walled (2 mm) flexible silicone rubber hollow sphere used by Verma was very sensitive to soil stresses, but we did not consider it rugged enough for field soils. Comparison was made between Verma's transducer and two prototypes of more rugged design; both made from commercially available 'squash' balls. Comparative dimensions are given in Table 1 and a cross section of prototype 2 is given in Fig. 2. A cyanoacrylate glue was used for the bond between ball and tube.

Prototype 1 was prepared by 'sand papering' the outside to reduce the wall thickness. It was thought this would provide more sensitivity than the unmodified form and yet would remain sufficiently rugged. Hydrostatic tests (as described later in 'calibration') were made on each prototype, (Fig. 3) and results compared to the performance of Verma's ball. Although all three exhibit linear relationships between

TABLE 1. COMPARATIVE DIMENSIONS OF THE WATER-FILLED BALLS

| Ball | Material | O.D. cm | Wall thickness mm |
|---|---|---|---|
| Verma *et al.* [9] | Silicone rubber | 2.5 | 1.5 |
| Prototype 1 (modified 'squash' *ball) | Mixture of neoprene and Natural rubbers | 3.2 | 2.0 |
| Prototype 2 (unmodified 'squash' ball) | | 3.8 | 5.0 |

*Dunlop red spot.

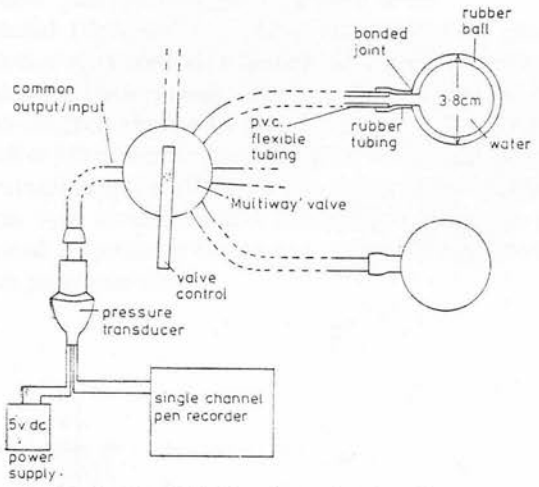


FIG. 2. The WFRB and associated equipment.

applied and detected pressures Verma's design is more sensitive than either prototype and prototype 2 is least sensitive of all. However, since the unmodified form could still detect pressure differences as small as 0.1 bar within its level of variability it was decided to pursue this, more practical, design. Problems of creating a reproducible wall thickness for prototype 1 also encouraged the choice of prototype 2.

To reduce the amount of instrumentation used by Verma's device a system was designed which could connect a set of rubber balls by tubes through a 'multiway' valve to a common pressure transducer shown in Fig. 2, thus each ball in turn could be individually connected to the transducer and the signal from the transducer recorded on the single channel pen recorder.

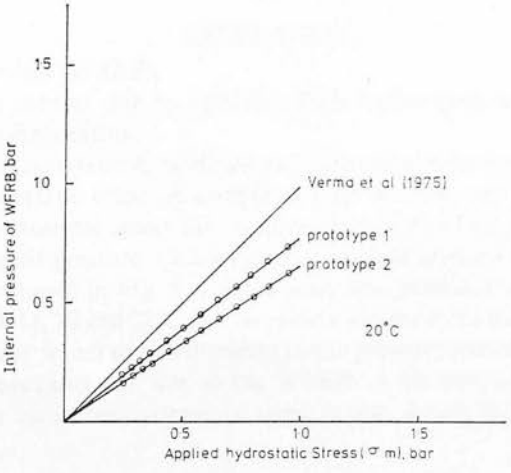


FIG. 3. Comparison of prototype WFRBs with design of Verma *et al.* (1975).

*Design of the 'mastic' ball for detection of deviator stress*

A mastic material ('Sylglass'*), suitably incompressible, plastic and with little elasticity was selected after tests on a number of materials; 'Arboseal', 'Plastecine'*, putty and 'Sylglass'*. Deformation tests on these materials, made by the same apparatus used to calibrate the mastic ball, are shown in Fig. 4. 'Sylglass' was chosen as it deformed well at lower temperatures (approx. 10°C) without extreme deformation at higher temperatures (approx. 20°C). As the mastic had a slightly volatile lubricant, the mastic spheres were covered by two hemispheres of flexible polythene film. The spheres were formed by pressing the correct weight of mastic in two hemispherical moulds lined with polythene film.

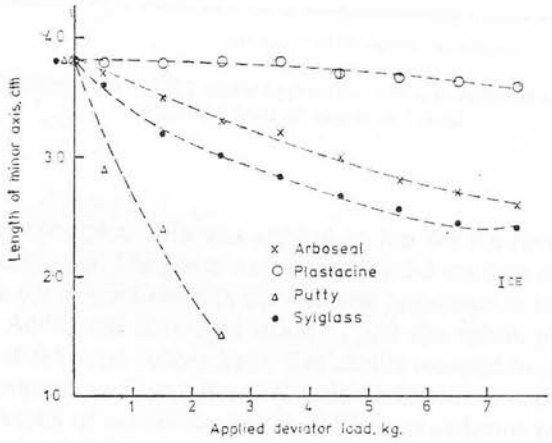


FIG. 4. Comparison of axial deformation of spheres of different materials.

## CALIBRATION

*Water-filled rubber ball (WFRB)*

Calibration was carried out by applying both hydrostatic and deviator stresses separately and in combination.

(a) Pure hydrostatic stress. A modified pressure membrane apparatus was used to provide hydrostatic stress. A sample of four WFRBs was simultaneously subjected to hydrostatic stress up to three bars (300 kPa), in steps of one bar (100 kPa) by air pressure. Calibrations of applied pressure and WFRB internal pressure are shown in Fig. 5. Calibrations were obtained at ambient temperatures of 7, 10, 14, 20 and 22°C and revealed a sensitivity to temperature variation, which was later found to be attributed to the pressure transducer and associated electronic apparatus and not to the WFRB. A temperature correction factor to adjust the estimated hydrostatic stress is also shown in Fig. 5.

*Trade name.

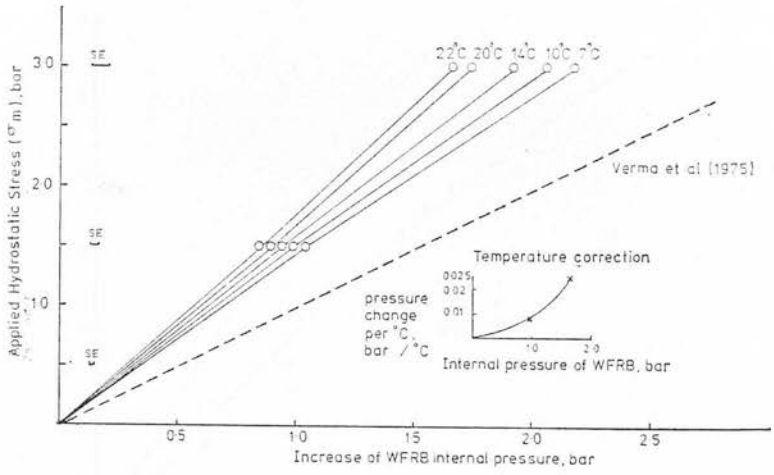


FIG. 5. Calibration of WFRB under hydrostatic stress at different temperatures with standard error of means indicated.

(b) Pure deviator stress. This was applied to the WFRB between parallel metal plates 5 cm in dia. The plates were lined with 2.5 cm thickness of 'foam' rubber to enable the contact between the ball and apparatus to be similar to ball/soil contact. Additional tests were made to find the effects of the thickness and stiffness of the foam rubber used. The results revealed insignificant differences made by variations from 1.0 cm—2.5 cm in the thickness of material lining the plates. Results of calibration of the WFRBs at different temperatures for different levels of deviator stress are shown in Fig. 6. A curvilinear relationship was present, probably caused by wall stiffness effects.

(c) Combinations of hydrostatic and deviator stress. Predetermined levels of deviator stress were applied by measured deformation between the parallel plates. The relationship between minor axis length and deviator load had been measured in the previous tests (b). While the balls were deformed various levels of hydrostatic stress were applied to the pressure vessel.

Thus for every deviator stress used a calibration for varying hydrostatic stress was obtained. The resulting 'family' of lines is shown in Fig. 7.

*Mastic Ball*

The calibration of deformation and deviator stress of the mastic ball was carried out with the apparatus used to apply pure deviator stress to the WFRB. The calibration curves for different temperatures are shown in Fig. 8. Between each loading the balls were remoulded to their original shape, as in the field the balls would be spherical before loading. A recalibration after use in the field tests is shown also in Fig. 8, these results reveal some changes of stiffness, presumably due to evaporation of the mastic's lubricant.

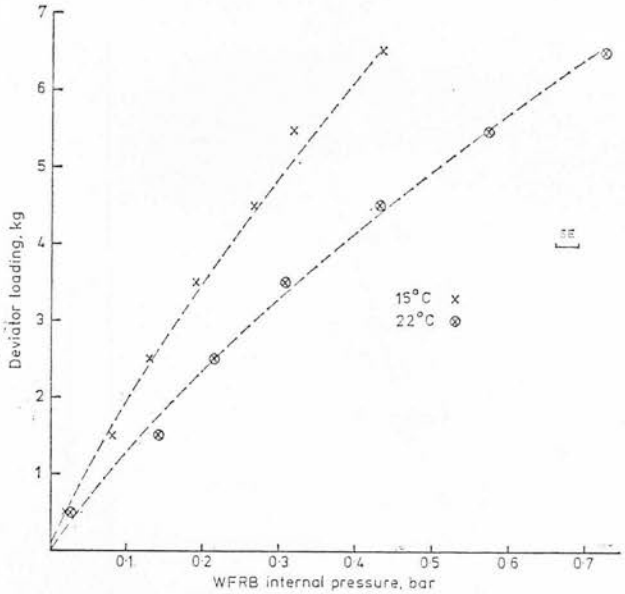


FIG. 6. Calibration of WFRB under deviator load with standard error of all means indicated.

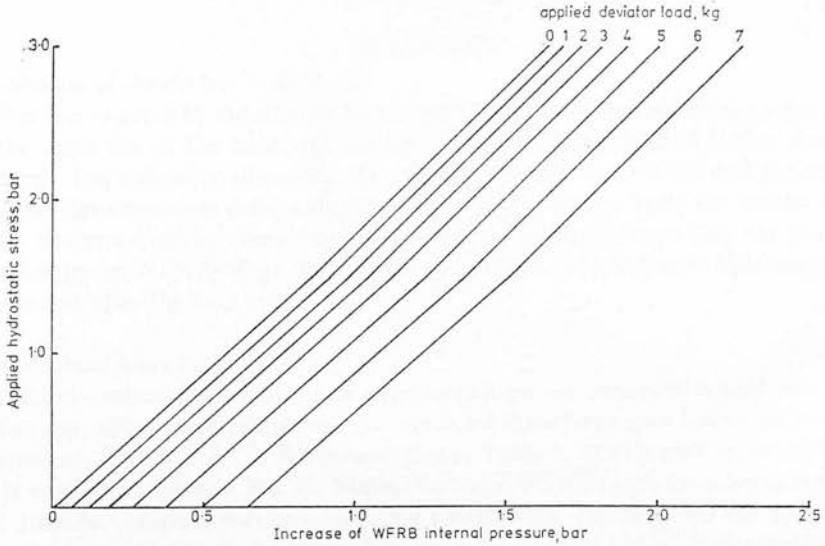


FIG. 7. Calibration of WFRB under hydrostatic and deviator stress at 22°C.

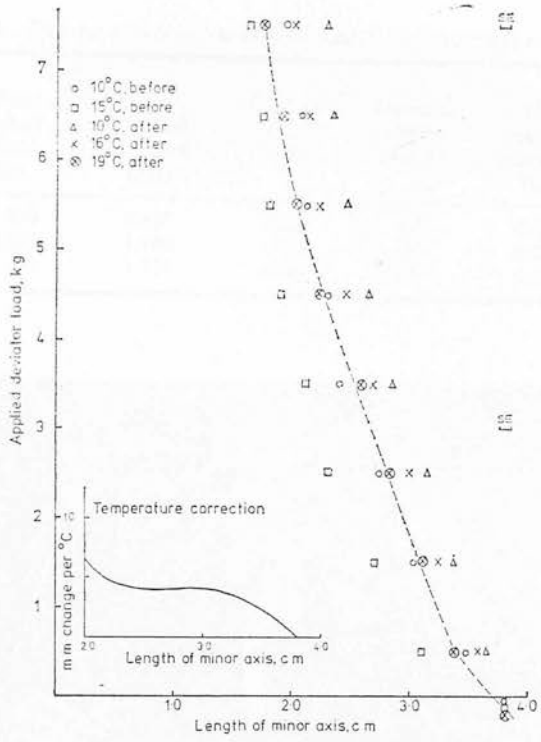


FIG. 8. Calibration of mastic ball, before and after field test, 'best fit' line used for field tests is indicated with standard errors of means.

## FIELD TESTS

*Installation of the devices in field soils*

This was assisted by moulding a hemispherical cavity in the soil using a rigid sphere of the same dia as the balls; this cavity accommodated the balls before they were covered. The technique improved the contact between the WFRB and the soil and reduced the unwanted deformation of the sensitive mastic ball; the mastic can be easily deformed during handling. Small access 'trenches' were dug for the tubes attached to the WFRBs. Figs. 9(a) and (b) depict the installed devices following partial excavation after the field tests.

*Experimental procedure*

The field measurements of stress were carried out by means of a field experiment using three different 'wheel treatments' replicated three times on a loam soil; the wheel treatments ($W1$, $W2$ and $W3$) are described in Table 2. Within each replication three plots were prepared as in Fig. 10. Mastic balls and WFRBs were installed during May and June before grass was sown and the plots rolled. This enabled the disturbance caused by installation to be reduced by consolidation and biological activity. Each plot was designed for eight mastic balls and eight WFRBs. The latter were installed in two 'staggered' lines, one metre between balls and 2.3 m (distance between wheel

TABLE 2. DETAILS OF WHEEL TREATMENTS USING 11 × 36 TYRES IN FIELD TESTS

| Treatment | Rear wheel load (kg) | Tyre inflation pressure (bar) | Contact area ($cm^2$) | Forward speed (km/h) | Mean surface pressure (bar) | Dia. of equivalent circle to contact area (cm) |
|---|---|---|---|---|---|---|
| W1 | 890 | 0.827 | 1000 | 1.0 | 0.873 | 35.7 |
| W2 | 1200 | 1.103 | 1250 | 1.0 | 0.951 | 39.9 |
| W3 | 1860 | 1.724 | 1600 | 1.0 | 1.138 | 45.1 |

FIG. 9. (a) WFRB partly excavated after field tests.

FIG. 9. (b) Mastic balls partly excavated after field tests.

centres of rear wheels of experimental tractor) between lines. The depth of each WFRB was randomly selected as 10, 20, 30 and 40 cm below the original soil surface before rolling. Mastic balls were set at the same depths used for WFRB installation at one position along each wheel line before rolling. Measurements of soil deformation caused by rolling were made using buried soil markers, thus the final depths of the balls were known before the experimental wheels ran over them.

Rear wheels of a Nuffield three-wheeled tractor were used to apply the wheel treatments, the alteration of load and inflation pressures enabled different contact areas and different 'mean surface pressures' to be obtained. The contact area was

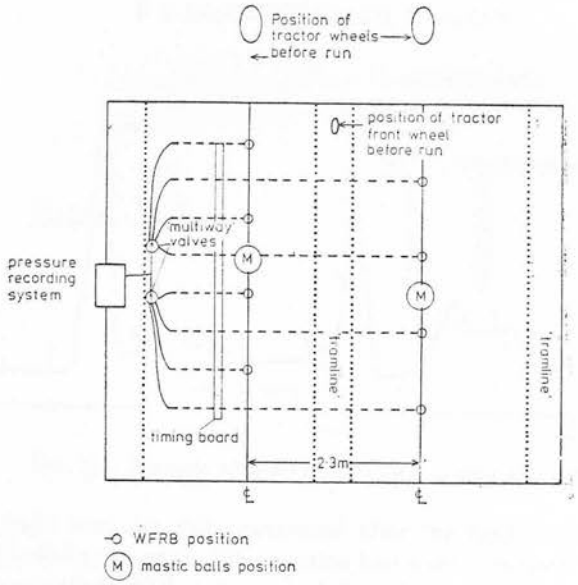


FIG. 10. Layout of the stress transducers in a single field plot with access 'tramlines' and centre lines of tractor wheel tracks indicated.

estimated from measurements of wheel sinkage and a known relationship between contact area and wheel sinkage derived from soil tank experiments.

Cone resistance of the experimental plots were made on the same day as the field tests. An electrically driven constant velocity penetrometer [12] (with a 13 mm base dia, 30° cone) provided measurements of cone resistance between the soil surface and 30 cm depth at 3 cm intervals.

Before the wheels were run over the plots the centre-line track for the front wheel was marked and the tubes from the WFRBs were connected to an 8-way valve and the pressure recording system. A strip of wood, marked at 0.5 m intervals, was placed alongside the path of the rear wheel nearest the valve operator. This had its first mark at a point opposite the position of the first WFRB to be run over; this 'time board' enabled more accurate estimation of the position of the wheel and timing of the valve changes by the valve operator.

As the tractor ran forward very slowly (approx. 1.0 km/h) the operator used the valve to connect the appropriate WFRB to the pressure recording system; pauses between ball positions were made if necessary. Measurements of air temperature and soil temperature at 10, 20 and 30 cm were made to correct the calibration.

Figure 11 is an example of a trace from the single-channel pen recorder used to monitor the WFRB signal. Peak pressures and zero-levels are shown; points where the valve was switched from one ball to another are also indicated. It was not necessary to account for the 'pressure head' effect caused by the different height of transducer and WFRB; all pressure measurements were defined as an increase from an 'unloaded' arbitrary zero.

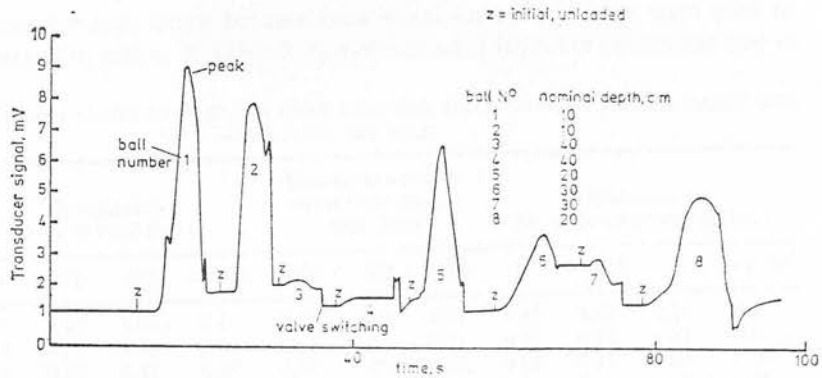


FIG. 11. Example of signal from WFRBs during field tests.

All mastic balls were carefully excavated after the field tests so that each ball remained *in situ* while two axes of its revealed half were measured. Minor, major and intermediate axes of the balls were recorded to the nearest 0.5 mm using 'outside' calipers; measurement of the latter two axes proved difficult due to irregularities of ball shape. Depth from the original soil surface and actual distance from the vertical plane through the centre-line of the wheel track were also recorded for both WFRBs and mastic balls upon excavation. Mastic balls removed after the tests were recalibrated within 24 hrs (Fig. 9) these calibrations were used for the actual computation of stresses.

*Results*

WFRB results are shown in Table 3; mastic ball results in Table 4. Means and

TABLE 3. WFRB FIELD RESULTS FOR THE THREE WHEEL W1, W2, W3 TREATMENTS DESCRIBED IN TABLE 2

| Nominal ball depth (when planted before rolling) (cm) | Real ball depth (as measured after rolling and wheel passage) (cm) | Mean WFRB internal pressures (bar) max. | | | Standard error of means (bar) |
|---|---|---|---|---|---|
| | | *W*1 | *W*2 | *W*3 | |
| 10 | 9.3 | 0.89 | 1.05 | 1.40 | 0.06 |
| 20 | 19.9 | 0.32 | 0.45 | 0.90 | 0.05 |
| 30 | 28.9 | 0.14 | 0.21 | 0.37 | 0.10 |
| 40 | 36.6 | 0.02 | 0.02 | 0.10 | 0.02 |

TABLE 4. MASTIC BALL FIELD RESULTS FOR THREE WHEEL TREATMENTS DESCRIBED IN TABLE 2

| Real ball depth (cm) | Mean lengths of minor axes (cm) | | | Standard error of means (cm) | Estimated deviator loadings (kg) | | | Standard error of estimate (kg) |
|---|---|---|---|---|---|---|---|---|
| | *W*1 | *W*2 | *W*3 | | *W*1 | *W*2 | *W*3 | |
| 9.3 | 3.00 | 2.68 | 2.46 | 0.10 | 2.50 | 3.60 | 4.60 | 0.3 |
| 19.9 | 2.98 | 2.95 | 2.82 | 0.15 | 2.50 | 2.45 | 3.05 | 0.3 |
| 28.9 | 3.31 | 3.24 | 3.07 | 0.06 | 1.00 | 1.10 | 1.95 | 0.2 |
| 36.6 | 3.46 | 3.61 | 3.60 | 0.05 | 0.30 | 0.10 | 0.30 | 0.2 |

standard errors for each depth beneath each wheel for all replicates were used to compute values of $\sigma_1$ and $\sigma_3$ in Table 5. $\sigma_3$ was estimated from the calibration line in

TABLE 5. ESTIMATED VALUES OF FIRST AND THIRD PRINCIPAL STRESS FROM WFRB AND MASTIC BALL RESULTS FOR THE FIELD

| Real ball depth (cm) | Estimated $\sigma_3$ from WFRB (bar) | | | | Estimated deviator stress from mastic ball (bar) | | | Estimated $\sigma_1$ ($\sigma_3$ + deviator stress) (bar) | | | |
|---|---|---|---|---|---|---|---|---|---|---|---|
| | *W*1 | *W*2 | *W*3 | s.e. est. | *W*1 | *W*2 | *W*3 | *W*1 | *W*2 | *W*3 | s.e. est. |
| 9.3 | 1.27 | 1.42 | 1.90 | 0.1 | 0.18 | 0.25 | 0.31 | 1.45 | 1.68 | 2.21 | 0.1 |
| 19.9 | 0.32 | 0.55 | 1.22 | 0.1 | 0.18 | 0.18 | 0.21 | 0.51 | 0.73 | 1.43 | 0.1 |
| 28.9 | 0.10 | 0.25 | 0.45 | 0.05 | 0.08 | 0.08 | 0.15 | 0.18 | 0.33 | 0.60 | 0.05 |
| 36.6 | 0.05 | 0.05 | 0.15 | 0.05 | 0.03 | 0.01 | 0.03 | 0.08 | 0.06 | 0.17 | 0.05 |

Fig. 7, corresponding to the deviator load at the same depth. $\sigma_1$ is the sum of $\sigma_3$ and deviator stress. Deviator stress was calculated using deviator load and maximum horizontal cross sectional area of the mastic ball. The cross-sectional area was calculated from the average of the appropriate major and intermediate axes of the mastic balls; on excavation these axes appeared essentially horizontal.

These measured values were compared with calculated values of $\sigma_1$ under the centre of a loaded circular area using equations developed by Söhne [13] (Fig. 12). Söhne's equations are described below.

$$\sigma_{1(z)} = Pm\,(1 - \cos^4 \alpha) \quad S1 \text{ (using } \nu = 4)$$

$$\sigma_{1(z)} = 1.5\,Pm\,(1\cos^5 \alpha - \cot^4 \alpha\,(^8/_3 - 5\cos \alpha + {}^{10}/_3 \cos^3 \alpha - \cos^5 \alpha)) \quad S2 \text{ (using } \nu = 5)$$

$$\sigma_{1(z)} = 2.0\,Pm\,(1 - \cos^6 \alpha - \cot^2 \alpha\,(\tfrac{1}{2} - {}^3/_2 \cos^4 \alpha + \cos^6 \alpha)) \quad S3 \text{ (using } \nu = 6)$$

$Pm$ = mean pressure at surface. $\alpha$ = half the angle formed by edges of contact area (assumed circular) and point at depth $z$, $\sigma_{1(z)} = \sigma_1$ at depth $z$. The concentration factors ($\nu$) were applied according to 'hardness' of ground, i.e. 4 = 'hard'; 5 = 'soft' and 6 = 'very soft'.

The three equations apply to different soil strength conditions and different distributions of surface pressure; equal, parabolic (power 4) and parabolic (power 2) for *S*1, *S*2 and *S*3 respectively. These different surface stress distributions have been observed beneath smooth tractor tyres by Vanden Berg and Gill [14].

## DISCUSSION OF FIELD RESULTS

When the measured and calculated values of $\sigma_1$ are examined both show a reduction with depth beneath the wheels. A systematic relationship between the measured values and the concentration factor ($\nu$) used in Söhne's equations can be identified. Stresses measured near 10 cm depth and 20 cm depth are similar to those calculated when $\nu = 5$ (*W*1 and *W*2) or $\nu = 6$ (*W*3). Measured stresses near to 30 and 40 cm

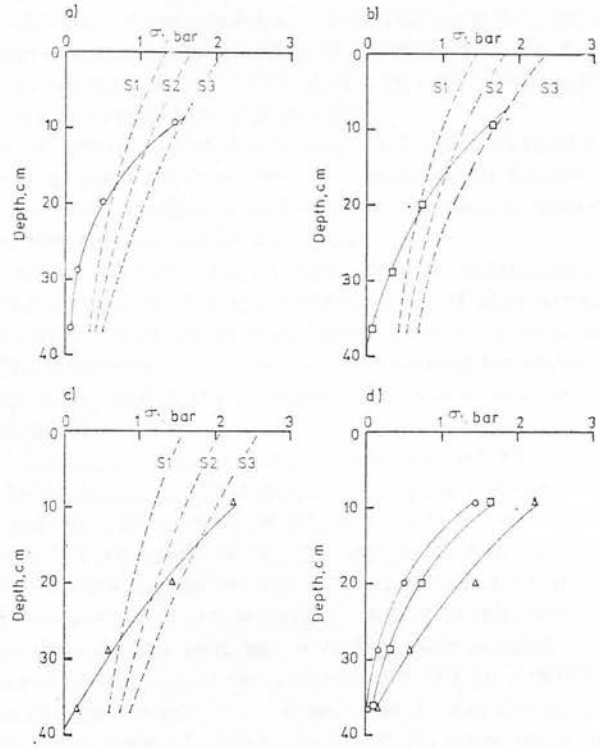


FIG. 12. Comparison of observed stresses (solid lines) and those calculated from Söhne's equations (broken lines). (a) Wheel treatment $W1$, ○ = observed; (b) Wheel treatment $W2$, □ = observed; (c) Wheel treatment $W3$, △ = observed; (d) Comparison of all observed values. The equations $S1$, $S2$ and $S3$ are referred to in the text.

depths are closest to those calculated when $\nu = 4$, but have much smaller values in some cases e.g. $W1$, 30 and 40 cm; $W2$, 40 cm; $W3$, 40 cm.

The lower concentration factors in Söhne's equations are applicable to soils of high elasticity constants; i.e. high soil 'strength'. Conversely the higher concentration factors apply to soils of low 'strength'. Relating these characteristics of the equations to the measured stress values it appears the soil is behaving as if it has low strength near the surface and greatly increased strength with depth. This suggested increase of soil strength with depth is confirmed by the measurements of cone resistance made at the field site. Cone resistance values increased steadily from 11 bar (1100 kPa) at 10 cm depth to 25 bar (2500 kPa) at 20 cm depth and then rapidly from 47 bar (4700 kPa) at 30 cm depth to an estimated 60 bar (6000 kPa) at 40 cm depth. From these observations one can deduce that the transducers are detecting stresses which relate well to the measured soil strength conditions.

## CONCLUSIONS

The devices have certain advantages when used to measure stresses in field soils.

The balls will adjust themselves to the direction of the principal stresses experienced and it is unnecessary to set the orientation of the device before use.

The devices are much less rigid than other devices previously used. Their mechanical properties are therefore more similar to the surrounding soil, this reduces problems of under or over-registration by 'arching' processes in the adjacent soil.

The devices are directly sensitive to $\sigma_1$ and $\sigma_3$ in conditions where the intermediate and minor principal stresses have similar value.

The low cost of materials and simple instrumentation provides a much lower cost per transducer than many other systems. This increases the feasibility of leaving large numbers of transducers installed in field sites for long periods, thus reducing the effect of interference with the soil during installation.

However, certain problems are evident. Despite omnidirectional response the mastic balls cannot provide dynamic measurements of their orientation. Therefore, knowledge of transducer re-orientation during rotation by large soil deformation is still limited. The elastic rebound of the soil surrounding the mastic ball must also be considered, this may confuse the estimation of deviator load as it is not accounted for in the calibration.

Switching the pressure detection system from one WFRB to another by hand as used in these field tests can be very time consuming and difficult. When measurements in locations closer than 0.5 m or under wheels moving at speeds greater than 1.0 km/h are needed each WFRB needs additional instrumentation. A water pressure transducer inside the WFRB, as used by Verma [9] may be suitable in such cases, but this would greatly increase instrumentation costs. A compromise between Verma's design and the system used in these field tests would be more suitable.

Despite their short-comings these devices are based on a better understanding of the response of deformable spheres to stresses. The devices also have advantages of less expensive and more simple instrumentation than many other stress transducers. When the devices were used in the field credible values of first principal stresses were measured beneath loaded wheels. These measured values correlated well to values derived from simplified stress predictions equations, with respect to measured soil strength values.

It is felt that further development and use of these devices could provide useful information on stress distribution in field soils, especially beneath wheels of agricultural vehicles.

## REFERENCES

[1] A. W. Cooper, G. E. Vanden Berg, H. F. McColly and A. E. Erickson, Strain gauge cell measures soil pressure, *Agric. Engng.* **38**, 232–237 (1975).

[2] I. F. Reed, A. W. Cooper and C. A. Reaves, Effect of two wheel and tandem drives on traction and soil compaction stresses, *Trans. ASAE* **2**, 22 (1959).

[3] G. E. Vanden Berg, A. W. Cooper, A. E. Erickson and W. M. Carlton, Soil pressure distribution under tractor and implement traffic, *Agric. Engng.* **38**, 845–855 (1957).

[4] R. E. McLeod, I. F. Reed, W. H. Johnson and W. R. Gill, Draft, power, efficiency and soil compaction characteristics of single, dual and low pressure tyres, *Trans. ASAE* **9**, 41–44 (1966).

[5] I. Christov, *Niektoré Poznatky Ziskane Meranim Napätia Pôdy Pod Traxtorovymi Kolesami*, (Some information obtained by soil stress measurements under tractor wheels), *Acta Tech. Ag. IV Univ. Mitra. Czech* (1969).

[6] I. F. Reed and A. W. Cooper, Stress distribution under tractor loads, *Agric. Engng.* **41**, 20–21 (1960).

[7] K. Baganz and L. Kunath, Some measurements of stresses and compaction under tractor wheels and tracks, *Dt. Agratech.* **13**, 4, 180–182 (1963).

[8] B. P. VERMA and J. G. FUTRAL, *A pressure transducer for deforming media*, *ASAE paper* **75**, 5009 (1975).
[9] B. P. VERMA, A. C. BAILEY, R. L. SCHAFER and J. G. FUTRAL, *A pressure transducer in soil compaction study*, *ASAE paper* **75**, 1034 (1975).
[10] N. MÖLLER, A data collection system for engineering measurements in tillage research, *Swedish J. Agric. Res.* **5**, 101–111 (1975).
[11] M. FOLINENKO-BORODICH, *Theory of Elasticity*, Dover Publications, New York (1965).
[12] K. T. BROWN and G. ANDERSON, Control and recording equipment for a soil penetrometer. *Scottish Institute of Agricultural Engineering*. Dept. Note SSN/185 Unpublished report (1975).
[13] W. H. SÖHNE, Fundamentals of pressure distribution and soil compaction under tractor tyres, *Agric. Engng.* **39**, 276–281, 290–291 (1958).
[14] G. E. VANDEN BERG and W. R. GILL. Pressure distribution beneath a smooth tire and soil. *Trans. ASAE* **5(2)**, 105–107 (1962).